biomedicines

Special Issue Reprint

Cardiovascular and Metabolic Disease

New Treatment and Future Directions

Edited by
Alfredo Caturano and Raffaele Galiero

www.mdpi.com/journal/biomedicines

MDPI

Cardiovascular and Metabolic Disease: New Treatment and Future Directions

Cardiovascular and Metabolic Disease: New Treatment and Future Directions

Editors

Alfredo Caturano
Raffaele Galiero

MDPI • Basel • Beijing • Wuhan • Barcelona • Belgrade • Manchester • Tokyo • Cluj • Tianjin

Editors

Alfredo Caturano
Department of Advanced
Medical and Surgical Sciences
University of Campania Luigi
Vanvitelli
Naples
Italy

Raffaele Galiero
Department of Advanced
Medical and Surgical Sciences
University of Campania Luigi
Vanvitelli
Naples
Italy

Editorial Office
MDPI
St. Alban-Anlage 66
4052 Basel, Switzerland

This is a reprint of articles from the Special Issue published online in the open access journal *Biomedicines* (ISSN 2227-9059) (available at: www.mdpi.com/journal/biomedicines/special_issues/Cardiovascular_Metabolic).

For citation purposes, cite each article independently as indicated on the article page online and as indicated below:

LastName, A.A.; LastName, B.B.; LastName, C.C. Article Title. *Journal Name* **Year**, *Volume Number*, Page Range.

ISBN 978-3-0365-7879-8 (Hbk)
ISBN 978-3-0365-7878-1 (PDF)

Contents

About the Editors

Alfredo Caturano

Alfredo Caturano, MD, graduated in Medicine and Surgery from Second University of Naples (SUN) in 2016. He achieved the Specialization Degree in Internal Medicine in 2021 at University of Campania "Luigi Vanvitelli". His specialization thesis, concerning the impact of glycaemic control on cardiovascular outcomes and mortality in a cohort of patients with type 2 diabetes mellitus in a multifactorial randomized controlled trial, was awarded the Annapaola Braggio prize by the Italian Society of Diabetology as the best specialization thesis on topics related to insulin resistance discussed in 2021 in Italy. He presently serves as PhD attendant at University of Campania "Luigi Vanvitelli" and has been supported with multiple grants from both Italian and European scientific societies.

Raffaele Galiero

Raffaele Galiero, MD, graduated in Medicine and Surgery at the University of Campania "Luigi Vanvitelli", Naples, in 2013. He achieved the Specialization Degree in Internal Medicine in 2020 at the University of Campania "Luigi Vanvitelli", Naples. At this time, he serves as PhD attendant at University of Campania "Luigi Vanvitelli", Naples.

Preface to "Cardiovascular and Metabolic Disease: New Treatment and Future Directions"

Cardiovascular diseases (CVDs) are the leading cause of death worldwide. In 2019, it has been estimated that 17.9 million people died from CVDs (32% of all global deaths). Of these deaths, 85% were due to heart attack and stroke. These data are usually powered by the coexistence of metabolic diseases, in particular diabetes. In fact, about 422 million people worldwide have diabetes, the majority living in low- and middle-income countries, and 1.5 million deaths are directly attributed to diabetes each year. It is vital to detect CVDs and metabolic disease as early as possible, as most cases can be prevented by addressing behavioral risk factors, such as tobacco use, unhealthy diet and obesity, physical inactivity, and harmful use of alcohol. Moreover, we are the main actors and observers of the innovations in every field of CVDs and metabolic disease treatment, from the pharmacological approach, with the advent of sodium glucose cotransporter 2 inhibitors for both heart failure and diabetes, to the improvement of new less-invasive and invasive techniques, such as immediate revascularization in both heart and brain infarction and new methods of mechanical cardiac support and multi-organ transplantation for the most advanced forms of heart failure. Given the complexity of this topic and its impact on clinical practice and public health, *Biomedicines* is launching a Special Issue entitled "Cardiovascular and Metabolic Disease: New Treatments and Future Directions" with the aim of gathering accurate and up-to-date scientific information on all aspects of new and upcoming treatment opportunities for CVDs and metabolic diseases.

The published articles not only report on the pathophysiological mechanisms underpinning this association, but also describe the results of latest clinical research about cardiovascular and metabolic diseases and offer a comprehensive overview of the recent advances in understanding pharmacological interventions to prevent cardiovascular events.

Alfredo Caturano and Raffaele Galiero
Editors

biomedicines

MDPI

Article

Ldlr-Deficient Mice with an Atherosclerosis-Resistant Background Develop Severe Hyperglycemia and Type 2 Diabetes on a Western-Type Diet

Weibin Shi [1,*], Jing Li [1], Kelly Bao [1], Mei-Hua Chen [1] and Zhenqi Liu [2]

[1] Department of Radiology and Medical Imaging, University of Virginia, Charlottesville, VA 22908, USA; jjeileen2006@hotmail.com (J.L.); kqb2j@virginia.edu (K.B.); mc2xc@hscmail.mcc.virginia.edu (M.-H.C.)
[2] Department of Medicine, University of Virginia, Charlottesville, VA 22908, USA; zl3e@hscmail.mcc.virginia.edu
* Correspondence: ws4v@virginia.edu; Tel.: +1-(434)-243-9420; Fax: +1-(434)-982-5680

Abstract: *Apoe*$^{-/-}$ and *Ldlr*$^{-/-}$ mice are two animal models extensively used for atherosclerosis research. We previously reported that *Apoe*$^{-/-}$ mice on certain genetic backgrounds, including C3H/HeJ (C3H), develop type 2 diabetes when fed a Western diet. We sought to characterize diabetes-related traits in C3H-*Ldlr*$^{-/-}$ mice through comparing with C3H-*Apoe*$^{-/-}$ mice. On a chow diet, *Ldlr*$^{-/-}$ mice had lower plasma total and non-HDL cholesterol levels but higher HDL levels than *Apoe*$^{-/-}$ mice. Fasting plasma glucose was much lower in *Ldlr*$^{-/-}$ than *Apoe*$^{-/-}$ mice (male: 122.5 ± 5.9 vs. 229.4 ± 17.5 mg/dL; female: 144.1 ± 12.4 vs. 232.7 ± 6.4 mg/dL). When fed a Western diet, *Ldlr*$^{-/-}$ and *Apoe*$^{-/-}$ mice developed severe hypercholesterolemia and also hyperglycemia with fasting plasma glucose levels exceeding 250 mg/dL. Both knockouts had similar non-HDL cholesterol and triglyceride levels, and their fasting glucose levels were also similar. Male *Ldlr*$^{-/-}$ mice exhibited greater glucose tolerance and insulin sensitivity compared to their *Apoe*$^{-/-}$ counterpart. Female mice showed similar glucose tolerance and insulin sensitivity though *Ldlr*$^{-/-}$ mice had higher non-fasting glucose levels. Male *Ldlr*$^{-/-}$ and *Apoe*$^{-/-}$ mice developed moderate obesity on the Western diet, but female mice did not. These results indicate that the Western diet and ensuing hyperlipidemia lead to the development of type 2 diabetes, irrespective of underlying genetic causes.

Keywords: low-density lipoprotein receptor; apolipoprotein E; hyperglycemia; type 2 diabetes; Western diet

Citation: Shi, W.; Li, J.; Bao, K.; Chen, M.-H.; Liu, Z. *Ldlr*-Deficient Mice with an Atherosclerosis-Resistant Background Develop Severe Hyperglycemia and Type 2 Diabetes on a Western-Type Diet. *Biomedicines* **2022**, *10*, 1429. https://doi.org/10.3390/biomedicines10061429

Academic Editors: Alfredo Caturano and Raffaele Galiero

Received: 9 May 2022
Accepted: 14 June 2022
Published: 16 June 2022

1. Introduction

Diabetes is a chronic health condition featured by fasting hyperglycemia (elevations in blood sugar). Type 2 diabetes (T2D) is the major form of diabetes accounting for 90–95% of all diabetes and constitutes one of the major public health problems in the U.S. and globally. Thirty-five million (13.5%) Americans aged 18 years or older are believed to have T2D [1]. Globally, 463 million adults are estimated to be living with T2D [2]. Additionally, 92 million American adults (37.6%) have prediabetes [1], a condition that carries the risk of contracting T2D. Diabetic patients experience increased rates of macrovascular complications, including more than twice the rates of coronary artery disease and stroke [3,4], and microvascular retinopathy and chronic kidney disease [5,6].

Dyslipidemia, which comprises elevated triglyceride and LDL cholesterol levels and reduced HDL cholesterol levels, often occurs together with hyperglycemia as integral components of T2D and the metabolic syndrome, with the latter also including abdominal obesity and hypertension. Accumulating evidence suggests that dyslipidemia may play a causal role in the pathogenesis of T2D. Prospective studies show that individuals with high triglyceride and LDL cholesterol levels have an increased risk of developing T2D [7–10].

Strong correlations between plasma lipid and glucose levels have been observed in segregating F2 populations derived from *Apoe*$^{-/-}$ mouse strains [11–13]. The strong evidence supporting a causal role for dyslipidemia in diabetes comes from genetic studies of rare mutations in *ABCA1* [14], LIPE [15], *LPL* [16], and *LRP6* [17], showing that these lipid genes are also linked to hyperglycemia or diabetes. However, contradictory findings concerning the relationship between dyslipidemia and diabetes are also noted: Hyperlipidemic patients receiving lipid-lowering therapy with PCSK9 inhibitory antibodies or statins show an increased incidence of new-onset diabetes [18–20]. Patients with heterozygous familial hypercholesterolemia caused by mutations in *LDLR*, *APOB*, *APOE,* and *PCSK9* are less vulnerable to diabetes [21,22].

Apoe$^{-/-}$ and *Ldlr*$^{-/-}$ mice are two widely used rodent models of dyslipidemia and atherosclerosis. On a chow diet, *Apoe*$^{-/-}$ mice have total plasma cholesterol levels of 300 to 500 mg/dL mainly from elevations of VLDL and chylomicron remnants, and *Ldlr*$^{-/-}$ mice have cholesterol levels of 200 to 300 mg/mL due to an accumulation of LDL [23–26]. When fed a Western diet, both *Apoe*$^{-/-}$ and *Ldlr*$^{-/-}$ mice develop severe hypercholesterolemia, with total cholesterol levels of ~1000 mg/dL [23,25,26]. We found that *Apoe*$^{-/-}$ mice on certain genetic backgrounds such as C57BL/6 (B6), C3H/HeJ (C3H), and SWR/J develop significant hyperglycemia and T2D with fasting plasma glucose exceeding 250 mg/dL when fed a Western-type diet [27,28]. Thus, we reasoned that *Ldlr*$^{-/-}$ mice would develop hyperglycemia and diabetes on a Western diet due to the ensuing severe dyslipidemia. To test this hypothesis, we characterized diabetes-related phenotypes in *Ldlr*$^{-/-}$ mice by comparing with *Apoe*$^{-/-}$ mice.

2. Materials and Methods

2.1. Mice

C3H-*Apoe*$^{-/-}$ mice and C3H-*Ldlr*$^{-/-}$ mice at N10 or more backcrossed generations were generated in our laboratory using the classical congenic breeding strategy [28]. Mice of both sexes were weaned at 3 weeks of age onto a chow diet containing 19% protein, 5% fat, 5% crude fiber, and 58% of the calories from carbohydrates (Teklad LM-485, Envigo, Indianapolis, IN, USA). At 6 weeks of age, one group was switched onto a Western diet containing 21% fat, 34.1% sucrose, 0.15% cholesterol, and 19.5% casein by weight (TD 88137, Envigo) and maintained on the diet for 12 weeks. The other group remained on a rodent chow diet throughout the entire experimental period. The animals were housed in a pathogen-free facility with a 12 h light–12 h dark cycle, consistent temperature (22 °C), and 50% humidity. Animal care and experimentation were carried out according to the current National Institutes of Health guidelines and approved by the University of Virginia Animal Care and Use Committee (Protocol # 3109). The reporting in this study follows the recommendations in the ARRIVE guidelines.

2.2. Measurements of Plasma Lipids, Glucose and Insulin

Mice were bled twice: once before and once at the end of the Western diet feeding. The animals were fasted overnight before retro-orbital blood was collected under isoflurane anesthesia. Plasma levels of total cholesterol, HDL cholesterol, and triglyceride were measured using cholesterol reagent from Stanbio Laboratory, HDL precipitating reagent from FUJIFILM Wako Diagnostics, and triglyceride reagent from Thermo DMA (Louisville, CO, USA) as reported in [11]. Plasma was diluted 3x with H_2O for measurement of total cholesterol concentrations in mice fed the Western diet. Plasma glucose concentrations were determined using a Sigma assay kit (Cat. # GAHK20) as reported in [11]. Plasma was diluted 3x for mice fed the Western diet but not diluted for chow-fed mice. Plasma insulin concentrations were measured with an ultra-sensitive ELISA kit from Crystal Chem INC (Elk Grove Village, IL; Cat. # 90080) according to the manufacturer's instructions.

2.3. Glucose Tolerance Test (GTT) and Insulin Tolerance Test (ITT)

GTT and ITT were performed as we described [27,28]. Briefly, overnight-fasted mice were injected intraperitoneally (IP) with 1 mg of glucose in 0.9% saline per gram of body weight in a volume of <0.3 mL. Blood glucose levels were measured with an UltraTouch glucometer using blood taken from cut tail tip at 0, 10, 20, 30, 60, 90, and 120 min after injection. ITT was performed under a non-fasting condition by IP injection with 0.75 U insulin in 0.9% saline per kg of body weight. Blood glucose was measured as above at 0, 15, 30, 45, and 60 min after insulin injection.

2.4. Statistical Analysis

Values were expressed as means ± SE, with *n* indicating the number of animals. The distributions of trait values were assessed for normality by examining skewness, kurtosis, and Q–Q plot as reported in [29]. Student's t test and ANOVA (Analysis of Variance) were used for determining statistical significance between two or more groups. When the *p*-value for ANOVA was statistically significant, Dunnett's correction was applied. Differences were considered statistically significant at $p < 0.05$.

3. Results

3.1. Fasting Plasma Lipid Levels

Both C3H-*Apoe*$^{-/-}$ and C3H-*Ldlr*$^{-/-}$ mice developed spontaneous hypercholesterolemia on a chow diet, and it was more severe in the former (Figure 1). Total cholesterol levels of C3H-*Ldlr*$^{-/-}$ mice were significantly lower than those of C3H-*Apoe*$^{-/-}$ mice (male: 285.8 ± 10.1 vs. 344.1 ± 24.6 mg/dL; female: 302.4 ± 14.6 vs. 419.2 ± 11.8 mg/dL; $p \leq 0.013$; n = 11 to 29). On the Western diet, both genotypes developed severe hypercholesterolemia. The total cholesterol level was significantly lower in male C3H-*Ldlr*$^{-/-}$ mice than in the C3H-*Apoe*$^{-/-}$ counterparts (719.1 ± 46.2 vs. 917.0 ± 43.1 mg/dL; $p = 0.035$; n = 4 to 12). Female C3H-*Ldlr*$^{-/-}$ mice did not differ significantly in total cholesterol level from the C3H-*Apoe*$^{-/-}$ counterparts (904.2 ± 41.3 vs. 1075.3 ±106.5 mg/dL; $p = 0.09$; n = 6 to 11).

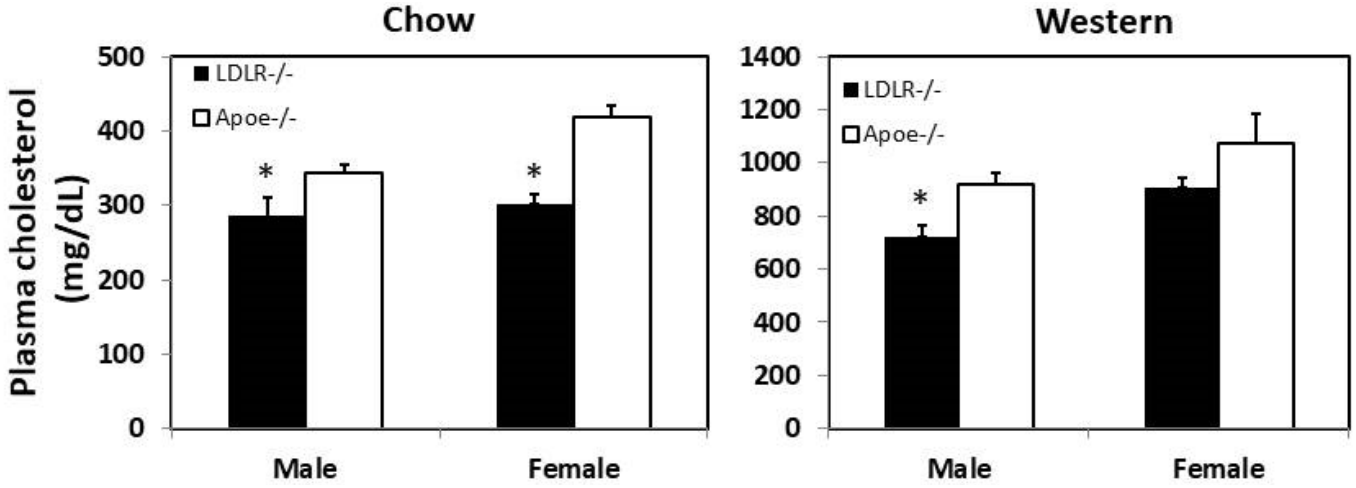

Figure 1. Fasting plasma levels of total cholesterol in male and female C3H-*Apoe*$^{-/-}$ and C3H-*Ldlr*$^{-/-}$ mice when fed a chow (left panel) or Western diet (right panel). Results are means ± SE of 4 to 29 mice per group. * $p < 0.05$ vs. *Apoe*$^{-/-}$ mice.

Male C3H-*Ldlr*$^{-/-}$ mice had significantly higher HDL cholesterol levels than the C3H-*Apoe*$^{-/-}$ counterparts on both chow (99.1 ± 5.6 vs. 57.0 ± 2.1 mg/dL; $p = 0.0023$; n = 11 to 29) and Western diets (94.7 ± 5.4 vs. 50.1 ± 4.3 mg/dL; $p = 0.00057$; n = 4 to 12) (Figure 2). Though statistically insignificant, female C3H-*Ldlr*$^{-/-}$ mice also had higher HDL cholesterol levels than female C3H-*Apoe*$^{-/-}$ mice on either chow (76.9 ± 2.1 vs. 53.0 ± 7.1 mg/dL; $p = 0.058$; n = 11 to 29) or the Western diet (44.5 ± 6.6 vs. 31.6 ± 2.1 mg/dL; $p = 0.10$; n = 6 to 11).

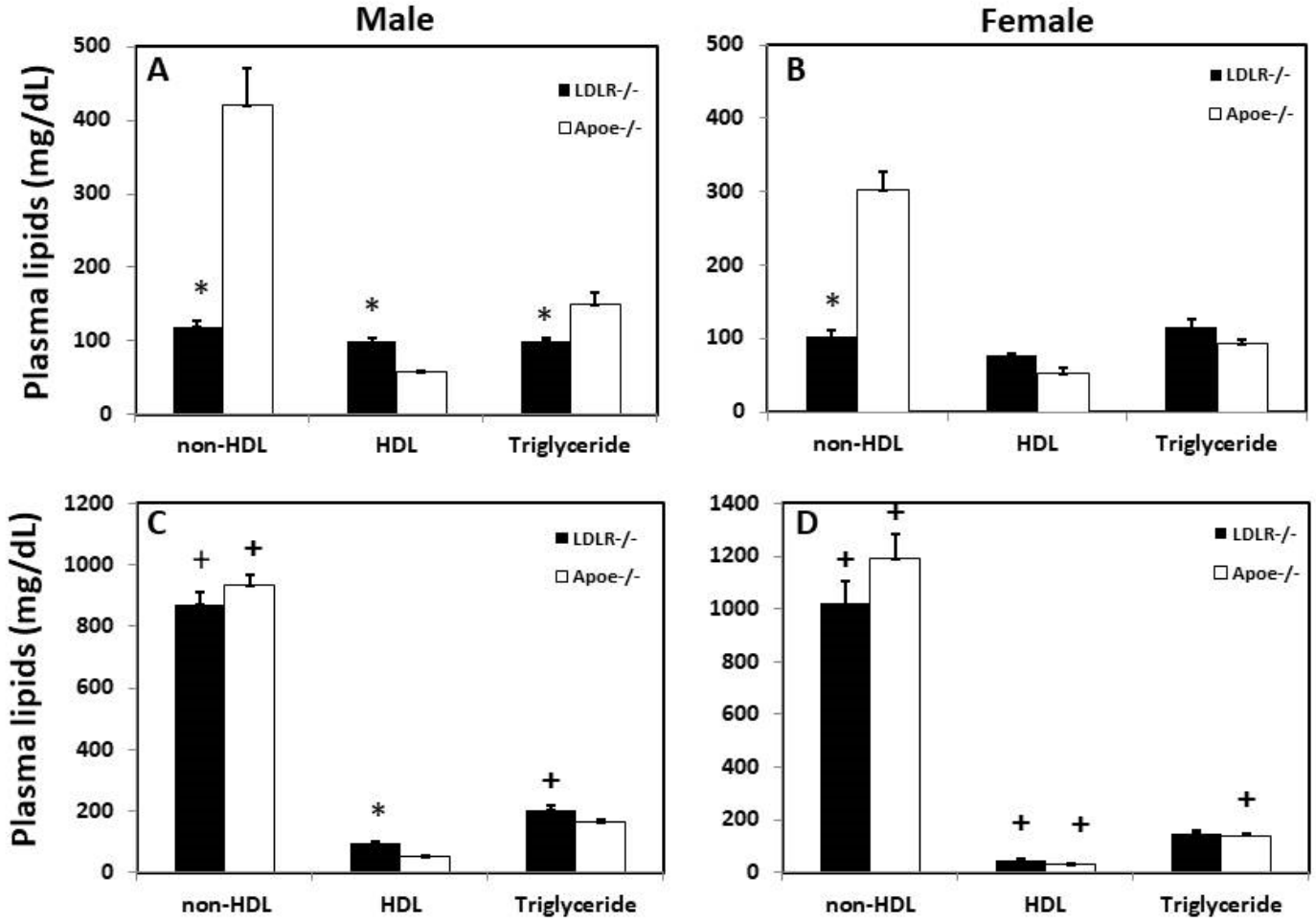

Figure 2. Fasting plasma levels of non-HDL, HDL cholesterol, and triglyceride in male and female C3H-*Apoe*$^{-/-}$ and C3H-*Ldlr*$^{-/-}$ mice fed a chow (**A**,**B**) or Western diet (**C**,**D**). Results are means ± SE of 4 to 29 mice per group. * $p < 0.05$ vs. *Apoe*$^{-/-}$ mice; + $p < 0.05$ vs. chow diet.

Non-HDL cholesterol levels of *Ldlr*$^{-/-}$ mice were significantly lower than those of the *Apoe*$^{-/-}$ counterparts on the chow diet for both males (119.2 ± 8.7 vs. 420.1 ± 50.1 mg/dL; $p = 0.0096$; $n = 4$ to 18) and females (102.5 ± 8.7 vs. 303.6 ± 24.4 mg/dL; $p = 0.0002$; $n = 4$–9) (Figure 2A,B). On the Western diet, non-HDL levels were dramatically elevated in *Ldlr*$^{-/-}$ and *Apoe*$^{-/-}$ mice of both sexes, exceeding 800 mg/dL (Figure 2C,D). No significant difference was found between the two knockouts ($p > 0.2$).

C3H-*Ldlr*$^{-/-}$ and C3H-*Apoe*$^{-/-}$ mice had similar plasma triglyceride levels except for males on the chow diet, with the former being significantly lower (100.1 ± 4.2 vs. 150.4 ± 15.3 mg/dL; $p = 0.00018$; $n = 4$ to 29).

3.2. Fasting Plasma Glucose Levels

On the chow diet, both male and female C3H-*Ldlr*$^{-/-}$ mice had 40~50% lower fasting glucose levels than the C3H-*Apoe*$^{-/-}$ counterparts (male: 122.5 ± 5.9 vs. 229.4 ± 17.5 mg/dL; $p = 2.0 \times 10^{-8}$; female: 144.1 ± 12.4 vs. 232.7 ± 6.4 mg/dL; $p = 1.6 \times 10^{-6}$; $n = 11$ to 29) (Figure 3). On the Western diet, both C3H-*Ldlr*$^{-/-}$ and C3H-*Apoe*$^{-/-}$ mice developed significant hyperglycemia, with fasting glucose levels exceeding 250 mg/dL. Male C3H-*Ldlr*$^{-/-}$ mice had a lower plasma glucose level (304.7 ± 21.8 vs. 398.1 ± 46.4 mg/dL; $p = 0.061$; $n = 4$ to 13), while female C3H-*Ldlr*$^{-/-}$ mice had a higher plasma glucose level when compared to the C3H-*Apoe*$^{-/-}$ counterparts (381.7 ± 25.4 vs. 297.4 ± 31.1 mg/dL; $p = 0.06$; $n = 4$ to 7). Compared to the chow diet, the Western diet significantly elevated plasma glucose levels of C3H-*Ldlr*$^{-/-}$ and C3H-*Apoe*$^{-/-}$ mice ($p \leq 0.0055$).

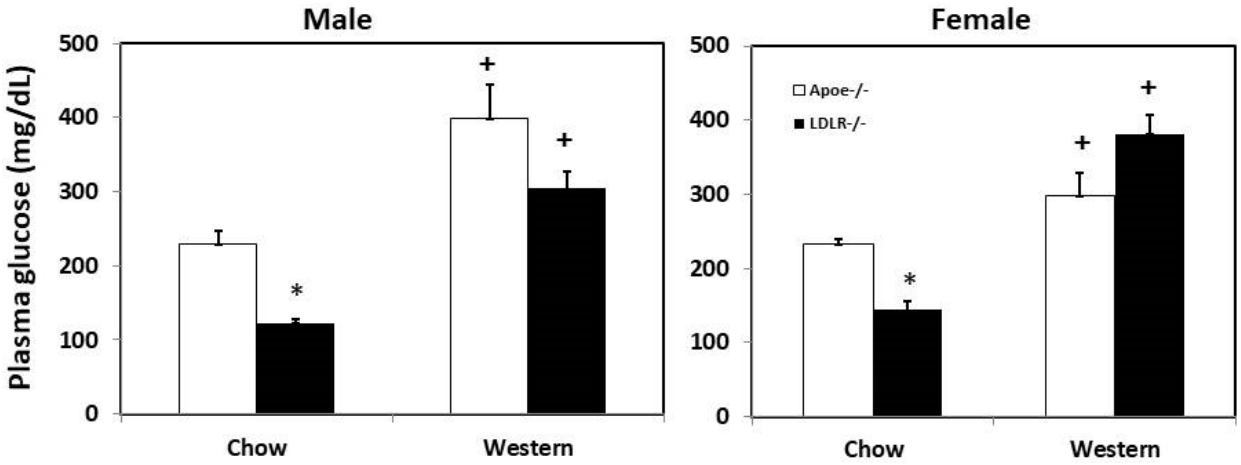

Figure 3. Fasting plasma glucose levels of male and female C3H-*Apoe*$^{-/-}$ and C3H-*Ldlr*$^{-/-}$ mice fed a chow or Western diet. Results are means ± SE of 4 to 29 mice per group. * $p < 0.05$ vs. *Apoe*$^{-/-}$ mice and $^{+}$ $p < 0.05$ vs. chow diet.

3.3. Glucose Tolerance Test (GTT) and Insulin Tolerance Test (ITT)

Intraperitoneal GTT and ITT were performed on both male and female C3H-*Ldlr*$^{-/-}$ and C3H-*Apoe*$^{-/-}$ mice fed the Western diet. In response to injected glucose, blood glucose levels rose quickly to the peak at the 20th min for male C3H-*Ldlr*$^{-/-}$ mice and the 30th min for male *Apoe*$^{-/-}$ mice (Figure 4). Then, glucose levels fell gradually and returned to pre-injection levels by the 120th min. Compared to C3H-*Apoe*$^{-/-}$ counterparts, male C3H-*Ldlr*$^{-/-}$ mice displayed significant glucose tolerance ($p < 0.001$; $n = 4$ to 17), having lower glucose levels at the 10th, 20th, and 30th min. For female mice, blood glucose levels quickly reached the peak at the 10th min and then fell gradually. There was no significant difference in glucose tolerance between female C3H-*Ldlr*$^{-/-}$ and C3H-*Apoe*$^{-/-}$ mice ($p = 0.25$; $n = 4$ to 17).

In response to injected insulin, male C3H-*Ldlr*$^{-/-}$ mice showed a gradual fall in blood glucose levels till the 30th min, which remained low till the 45th min and recovered at the 60th min (Figure 5A). In contrast, male C3H-*Apoe*$^{-/-}$ mice showed an increase in blood glucose levels at the 15th min though glucose levels were comparable to the levels of C3H-*Ldlr*$^{-/-}$ mice from the 30th to 60th min (16% reduction from the basal) (Figure 5C). Female C3H-*Ldlr*$^{-/-}$ mice showed a more obvious fall in blood glucose levels than female C3H-*Apoe*$^{-/-}$ mice (47% vs. 18% decrease from the basal level) (Figure 5B,D). In addition, the basal non-fasting blood glucose level (at 0 min) was significantly higher in female C3H-*Ldlr*$^{-/-}$ mice than in the C3H-*Apoe*$^{-/-}$ counterparts (165.4 ± 13.7 vs. 118.5 ± 5.4 mg/dL; $p = 0.006$; $n = 4$ to 20).

3.4. Plasma insulin Concentration

Fasting plasma insulin levels were measured for female C3H-*Ldlr*$^{-/-}$ and C3H-*Apoe*$^{-/-}$ mice fed the Western diet. C3H-*Ldlr*$^{-/-}$ mice had higher insulin levels than the C3H-*Apoe*$^{-/-}$ mice (0.622 ± 0.121 vs. 0.487 ± 0.074 ng/mL), although the difference was not statistically significant ($p = 0.33$; $n = 7$ to 13) (Figure 6).

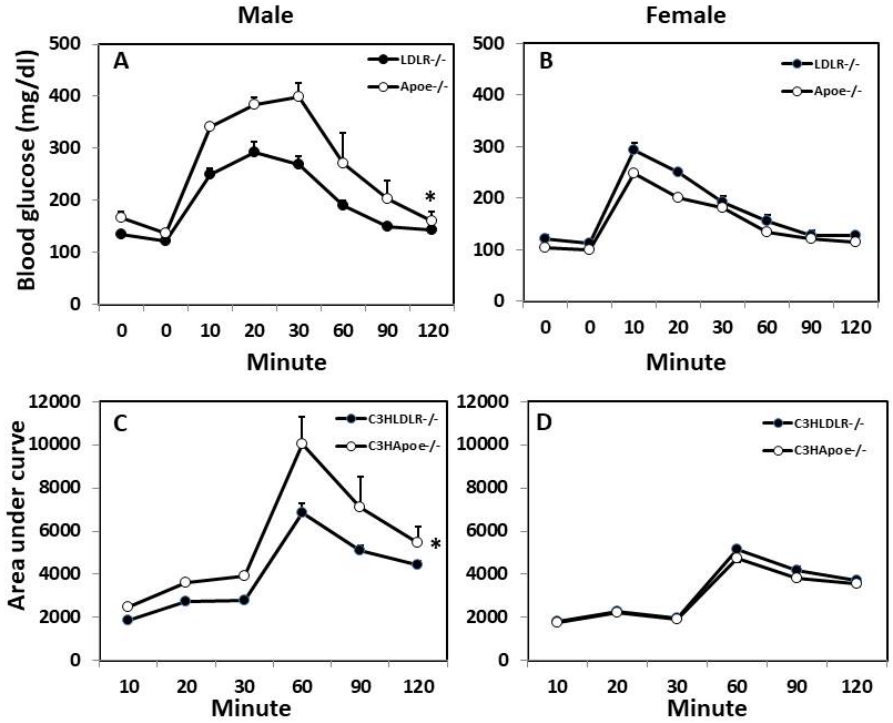

Figure 4. Glucose tolerance test (GTT) (**A**,**B**) and calculated area under the curve (**C**,**D**) for male and female C3H-*Apoe*$^{-/-}$ and C3H-*Ldlr*$^{-/-}$ mice fed a Western diet. Overnight-fasted mice were intraperitoneally injected with 1 g glucose per kg body weight. Blood glucose concentrations were determined with a glucometer using blood taken from cut tail tips at the indicated time points. Values are means ± SE of 4 to 17 mice per group. * $p < 0.05$ vs. *Apoe*$^{-/-}$ mice.

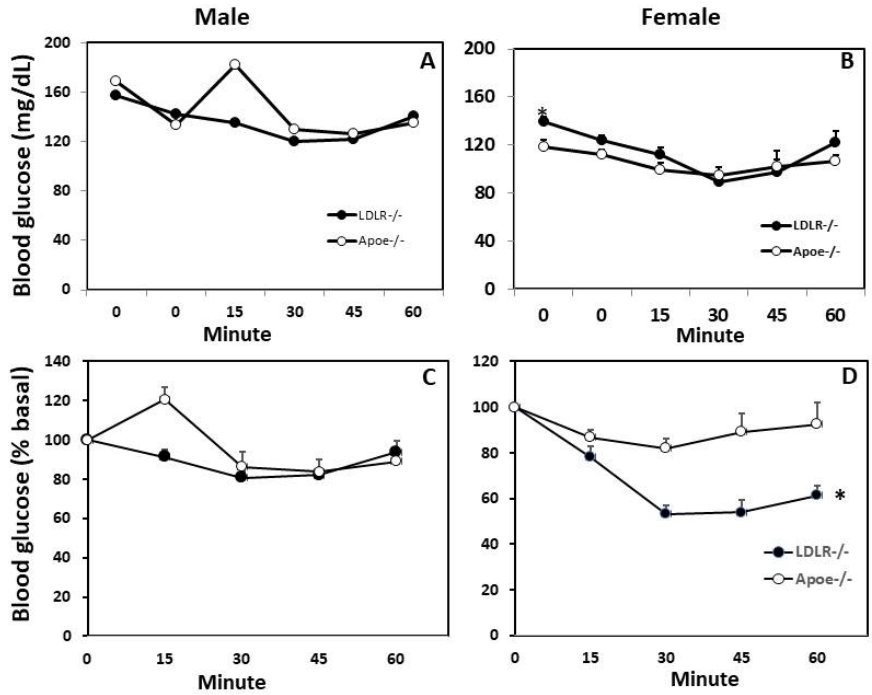

Figure 5. Insulin tolerance test (ITT) for male and female C3H-*Apoe*$^{-/-}$ and C3H-*Ldlr*$^{-/-}$ mice fed a Western diet. Non-fasted mice were intraperitoneally injected with 0.75 U/kg of insulin. Blood glucose concentrations were determined with a glucometer using blood taken from cut tail tips at the indicated time points (**A**,**B**). Values are means ± SE of 4 to 20 mice per group. * $p < 0.05$ vs. *Apoe*$^{-/-}$ mice. (**C**,**D**), Glucose concentrations were expressed as % of the basal.

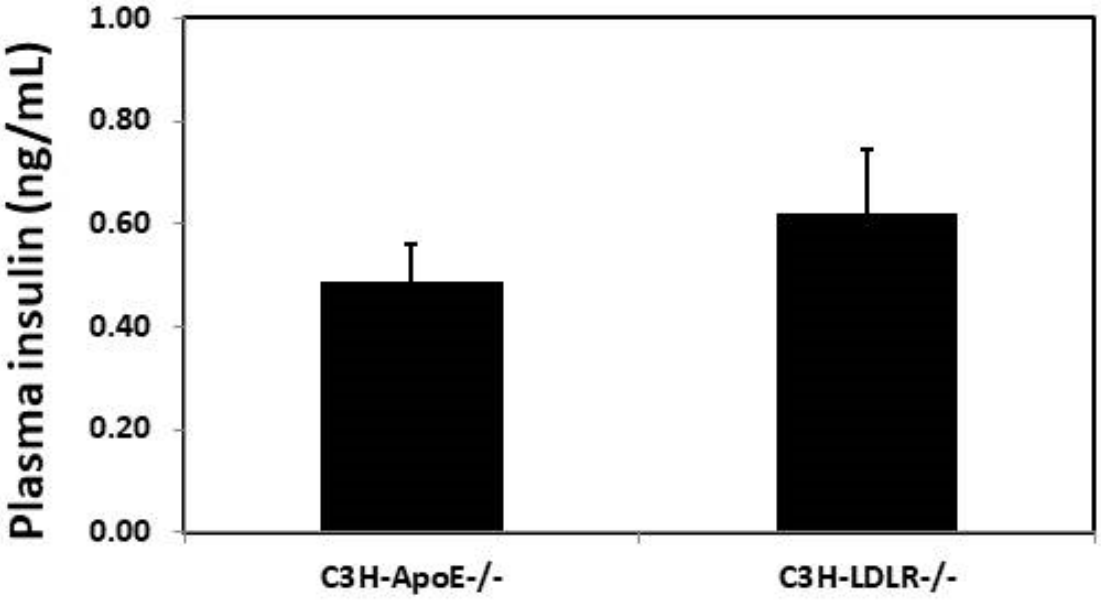

Figure 6. Plasma insulin levels of female C3H-*Apoe*$^{-/-}$ and C3H-*Ldlr*$^{-/-}$ mice fed a Western diet. Blood samples were collected after mice were fasted overnight. Values are means ± SE of 7 or 13 mice per group.

3.5. Body Weight

At 3 months of age on the chow diet, either male or female C3H-*Ldlr*$^{-/-}$ mice had a body weight similar to that of the C3H-*Apoe*$^{-/-}$ mice (male: 23.1 ± 0.9 vs. 23.2 ± 0.7 g; female: 17.2 ± 0.3 vs. 18.1 ± 0.5 g) (Figure 7). After being fed the Western diet for 12 weeks, C3H-*Ldlr*$^{-/-}$ and C3H-*Apoe*$^{-/-}$ mice also had a similar body weight (male: 33.2 ± 0.8 vs. 35.0 ± 0.8 g; female: 23.1 ± 1.2 vs. 23.8 ± 0.8 g). Males had significantly heavier body weight than females for both the C3H-*Ldlr*$^{-/-}$ and C3H-*Apoe*$^{-/-}$ mice fed either chow or a Western diet ($p < 0.05$; $n = 4$ to 26).

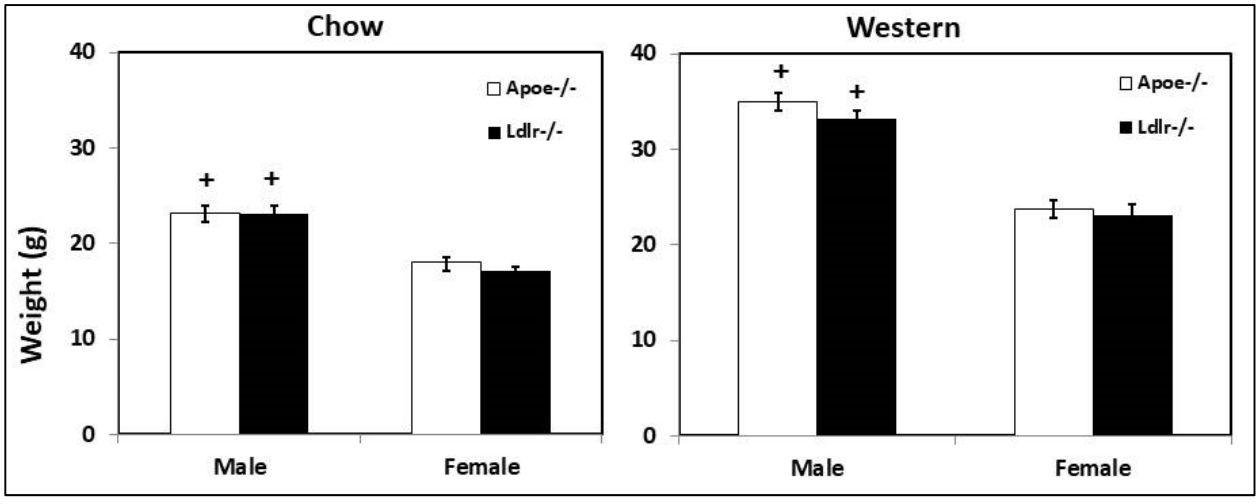

Figure 7. Body weight (g) of male and female C3H-*Apoe*$^{-/-}$ and C3H-*Ldlr*$^{-/-}$ mice fed a chow or a Western diet. Chow-fed mice were weighed at 3 months of age, and Western diet-fed mice were weighed after being euthanized. Results are means ± SE of 4 to 26 mice. $^{+}$ $p < 0.05$ vs. female mice.

4. Discussion

In this study, we characterized type 2 diabetes-associated phenotypes in C3H-*Ldlr*$^{-/-}$ mice through a comparison with C3H-*Apoe*$^{-/-}$ mice, which develop type 2 diabetes on a Western diet [28]. Our results here indicate that Western diet consumption and ensuing

hyperlipidemia lead to the development of type 2 diabetes in hyperlipidemic mice, irrespective of underlying genetic causes. On a chow diet, plasma total and non-HDL cholesterol levels were significantly lower in C3H-*Ldlr*$^{-/-}$ mice than in C3H-*Apoe*$^{-/-}$ mice and so were the fasting glucose levels. When fed a Western diet, C3H-*Ldlr*$^{-/-}$ mice developed just as severe hyperlipidemia as C3H-*Apoe*$^{-/-}$ mice, and the magnitude of hyperglycemia was similar. Male C3H-*Ldlr*$^{-/-}$ mice were more tolerant to glucose loading and more sensitive to insulin than male C3H-*Apoe*$^{-/-}$ mice, while female C3H-*Ldlr*$^{-/-}$ mice were just as tolerant to glucose and sensitive to insulin as female C3H-*Apoe*$^{-/-}$ mice. Moreover, male but not female C3H-*Ldlr*$^{-/-}$ and C3H-*Apoe*$^{-/-}$ mice developed moderate obesity on the Western diet.

A major finding of this study is that C3H-*Ldlr*$^{-/-}$ mice developed type 2 diabetes with fasting plasma glucose levels ranging from 300 to 400 mg/dL after 12 weeks of a Western diet. Diabetes is defined by fasting hyperglycemia. In humans, fasting blood glucose levels of $\geq$126 mg/dL are considered diabetic. For mice, plasma instead of whole blood is often used for glucose measurements. Fasting plasma glucose exceeding 250 mg/dL is considered diabetic for mice [30]. Thus, both male and female C3H-*Ldlr*$^{-/-}$ mice developed diabetes on the Western diet. Compared to the C3H-*Apoe*$^{-/-}$ males, the C3H-*Ldlr*$^{-/-}$ males had lower total and non-HDL cholesterol and higher HDL cholesterol levels, and their plasma glucose levels were also lower. Similarly, C3H-*Ldlr*$^{-/-}$ and C3H-*Apoe*$^{-/-}$ females had comparable total, non-HDL, and HDL cholesterol levels, and their fasting glucose levels were comparable. These results hint at the significance of lipid profiles in determining blood glucose homeostasis.

Schreyer et al. [31] observed a time-dependent increase in fasting glucose levels of B6-*Ldlr*$^{-/-}$ mice but not in B6-*Apoe*$^{-/-}$ mice within 16 weeks on a diabetogenic diet containing 35.5% fat, 36.6% carbohydrates, and no cholesterol, although the increase did not meet the threshold of 250 mg/dL for the diagnosis of diabetes. Phillips et al. [32] found that only the Western diet but not a diabetogenic diet containing 13% fat and 67% carbohydrates raised blood glucose level of B6-*Apoe*$^{-/-}$ mice.

C3H-*Ldlr*$^{-/-}$ mice developed milder hypercholesterolemia on the chow diet than C3H-*Apoe*$^{-/-}$ mice, having lower total and non-HDL cholesterol levels but higher HDL cholesterol levels. These results are in line with what has been found with the two knockouts on the C57BL/6 background [33]. Lipid profiles vary by strains [28], but the distinctions between *Ldlr*$^{-/-}$ and *Apoe*$^{-/-}$ mice in total and HDL and non-HDL cholesterol levels remain on the C3H background. What is more distinct are the fasting glucose levels, which were much lower in the C3H-*Ldlr*$^{-/-}$ mice than in the C3H-*Apoe*$^{-/-}$ mice of both sexes. Differential fasting glucose levels of the two knockouts were in parallel with their differing lipid profiles, with lower non-HDL and higher HDL cholesterol levels being linked with lower fasting glucose levels. Consistently, in multiple F2 cohorts derived from *Apoe*$^{-/-}$ mouse strains, plasma glucose levels are positively correlated with non-HDL cholesterol levels [11–13] and inversely correlated with HDL levels [13].

Although both male and female C3H-*Ldlr*$^{-/-}$ and C3H-*Apoe*$^{-/-}$ mice developed significant hyperglycemia on the Western diet, only C3H-*Apoe*$^{-/-}$ males exhibited noticeable glucose intolerance. Indeed, male C3H-*Apoe*$^{-/-}$ mice showed an increase in blood glucose concentration after intraperitoneal glucose injection. As there was little fall in blood glucose concentration after insulin injection, these mice developed strong insulin resistance on the Western diet. Thus, insulin resistance should be responsible in part for the glucose intolerance and hyperglycemia observed in male *Apoe*$^{-/-}$ mice. Obesity and hyperlipidemia were two obvious factors contributing to the development of insulin resistance. Both C3H-*Ldlr*$^{-/-}$ and C3H-*Apoe*$^{-/-}$ males fed the Western diet developed moderate obesity as evidenced by substantial increases in body weight when compared to age-matched chow-fed mice (33.2 $\pm$ 0.8 vs. 24.1 $\pm$ 1.0 g for C3H-*Ldlr*$^{-/-}$ mice, 35.0 $\pm$ 0.8 vs. 26.2 $\pm$ 1.2 g for C3H-*Apoe*$^{-/-}$ mice). However, the finding that the two knockouts had similar body weight but male *Ldlr*$^{-/-}$ mice did not develop obvious insulin resistance suggests that other factors than obesity also contributed to glucose intolerance and insulin resistance of male C3H-*Apoe*$^{-/-}$ mice. The consumption of a high-fat diet leads to hyperlipidemia, which is

a major driver of oxidative stress and systemic chronic inflammation [34,35]. Besides its role in lipid metabolism, ApoE has antioxidant effects and suppresses inflammation in the body [36]. *Apoe*$^{-/-}$ mice show enhanced responses to oxidative stress and inflammatory stimuli compared to *Ldlr*$^{-/-}$ mice [37,38]. The present finding that female C3H-*Apoe*$^{-/-}$ mice also exhibited an increased insulin resistance relative to the *Ldlr*$^{-/-}$ counterparts supports the speculation on enhanced oxidative stress and inflammatory responses in *Apoe*$^{-/-}$ mice.

Unlike their male counterparts and most other mouse models of type 2 diabetes that develop significant obesity [39], female C3H-*Ldlr*$^{-/-}$ and C3H-*Apoe*$^{-/-}$ mice had no overweight or obesity. Despite the absence of obesity, female C3H-*Ldlr*$^{-/-}$ and C3H-*Apoe*$^{-/-}$ mice developed just as severe hyperglycemia as their male counterparts. In humans, although most type 2 diabetic patients are obese or overweight, a fraction of patients have normal body weight [40]. On the Western diet, the two female knockouts had similar lipid profiles, including total, HDL, non-HDL cholesterol, and triglyceride. Interestingly, they also had comparable fasting plasma glucose and insulin levels. This coincidence supports the significance of lipid profiles in the development of type 2 diabetes. There are quantitative but not qualitative differences in plasma insulin levels between male and female hyperlipidemic mice fed a Western diet [41]. For more than 100 inbred strains examined, male mice have higher plasma insulin levels than female mice. Previous studies showed that a high-fat diet had little or no influence on plasma glucose levels of wild-type B6 mice [42,43], probably due to the moderateness in the increase in plasma lipid levels. This speculation appears applicable to wild-type C3H mice in that they only developed modest hyperlipidemia (plasma cholesterol level: 181 $\pm$ 14 mg/dL) and showed a modest increase in fasting glucose levels on the Western diet (148 $\pm$ 14 vs. 106 $\pm$ 11 mg/dL) (Supplementary Materials).

In humans, *APOE* and *LDLR* polymorphisms have been associated with obesity [44]. We previously observed a deficit in growth and weight gain during postnatal development of *Apoe*$^{-/-}$ mice as compared to wild-type mice [45]. Male *Apoe*$^{-/-}$ mice showed resistance to Western diet-induced obesity [46]. *Ldlr*$^{-/-}$ mice also showed a decreased susceptibility to Western diet-induced obesity due to an increased thermogenesis [47]. Here we also observed that male *Ldlr*$^{-/-}$ mice had a smaller body weight in comparison to male *Apoe*$^{-/-}$ mice on the Western diet.

5. Conclusions

Ldlr deficiency results in increased levels of ApoB-100 containing LDL due to both increased hepatic lipoprotein production and impaired clearance [48,49], while ApoE deficiency leads to the accumulation of ApoB48 containing chylomicron or VLDL remnants due to a delayed clearance into hepatocytes by the LDL receptor, LDL receptor-related protein 1, and cell surface heparan sulphate proteoglycans [50]. Despite different lipoprotein profiles, *Ldlr*$^{-/-}$ mice and *Apoe*$^{-/-}$ mice developed diet-induced type 2 diabetes that is independent of obesity. This finding provides direct evidence for the significance of a Western-type diet and its induced hyperlipidemia in the etiology of type 2 diabetes. The current observations are not specific to C3H mice because *Ldlr*$^{-/-}$ mice with the B6;129 genetic background also developed hyperglycemia on the Western diet, which was alleviated after mice were switched to a low-fat diet [51]. We previously observed that the Western diet-induced increases in plasma glucose and triglyceride levels of *Apoe*$^{-/-}$ mice are time-dependent within the 12-week feeding period [52,53], while the current study only examined one time point on the Western diet. Another limitation is that wild-type C3H mice were not included in this study. In addition, sample sizes in some experiments were small despite the fact that the two knockouts were inbred and tended to have small intragroup variation in the phenotypes tested. Nevertheless, there is no doubt that the two mouse models are useful for investigating type 2 diabetes that is related or unrelated to obesity.

Supplementary Materials: The following supporting information can be downloaded at: https://www.mdpi.com/article/10.3390/biomedicines10061429/s1. All data reported in the article are included in the Supplementary Materials and also accessible via 10.6084/m9.figshare.20032229.

Author Contributions: Conceptualization, W.S. and Z.L.; methodology, W.S., J.L. and M.-H.C.; formal analysis, W.S. and J.L.; investigation, W.S., J.L., K.B., M.-H.C. and Z.L.; resources, W.S.; data curation, W.S., J.L. and K.B.; writing—original draft preparation, W.S. and Z.L.; writing—review and editing, W.S. and Z.L.; supervision, W.S. and Z.L.; project administration, W.S.; funding acquisition, W.S. and Z.L. All authors have read and agreed to the published version of the manuscript.

Funding: The work was supported by NIH grants R01 DK116768 and HL112281 and Commonwealth Health Research Board (CHRB) Virginia.

Institutional Review Board Statement: Not applicable.

Informed Consent Statement: Not applicable.

Data Availability Statement: All data reported in the article are included in the Supplementary Materials and also accessible via 10.6084/m9.figshare.20032229.

Conflicts of Interest: The authors declared they have no conflict of interest.

References

1. Virani, S.S.; Alonso, A.; Aparicio, H.J.; Benjamin, E.J.; Bittencourt, M.S.; Callaway, C.W.; Carson, A.P.; Chamberlain, A.M.; Cheng, S.; Delling, F.N.; et al. Heart Disease and Stroke Statistics—2021 Update. *Circulation* **2021**, *143*, e254–e743.
2. Saeedi, P.; Petersohn, I.; Salpea, P.; Malanda, B.; Karuranga, S.; Unwin, N.; Colagiuri, S.; Guariguata, L.; Motala, A.A.; Ogurtsova, K.; et al. Global and Regional Diabetes Prevalence Estimates for 2019 and Projections for 2030 and 2045: Results from the International Diabetes Federation Diabetes Atlas, 9th Edition. *Diabetes Res. Clin. Pract.* **2019**, *157*, 107843. [CrossRef] [PubMed]
3. Emerging Risk Factors Collaboration; Sarwar, N.; Gao, P.; Seshasai, S.R.K.; Gobin, R.; Kaptoge, S.; Di Angelantonio, E.; Ingelsson, E.; Lawlor, D.A.; Selvin, E.; et al. Diabetes Mellitus, Fasting Blood Glucose Concentration, and Risk of Vascular Disease: A Collaborative Meta-Analysis of 102 Prospective Studies. *Lancet* **2010**, *375*, 2215–2222. [CrossRef]
4. Bloomgarden, Z.T. Cardiovascular Disease in Diabetes. *Diabetes Care* **2008**, *31*, 1260–1266. [CrossRef] [PubMed]
5. Williams, R.; Airey, M.; Baxter, H.; Forrester, J.; Kennedy-Martin, T.; Girach, A. Epidemiology of Diabetic Retinopathy and Macular Oedema: A Systematic Review. *Eye* **2004**, *18*, 963–983. [CrossRef] [PubMed]
6. Alicic, R.Z.; Rooney, M.T.; Tuttle, K.R. Diabetic Kidney Disease: Challenges, Progress, and Possibilities. *Clin. J. Am. Soc. Nephrol.* **2017**, *12*, 2032–2045. [CrossRef] [PubMed]
7. Wilson, P.W.; Meigs, J.B.; Sullivan, L.; Fox, C.S.; Nathan, D.M.; RB, S.D. Prediction of Incident Diabetes Mellitus in Middle-Aged Adults: The Framingham Offspring Study. *Arch. Intern. Med.* **2007**, *167*, 1068–1074. [CrossRef]
8. Mykkanen, L.; Kuusisto, J.; Pyorala, K.; Laakso, M. Cardiovascular Disease Risk Factors as Predictors of Type 2 (Non-Insulin-Dependent) Diabetes Mellitus in Elderly Subjects. *Diabetologia* **1993**, *36*, 553–559. [CrossRef]
9. Austin, M.A.; Mykkanen, L.; Kuusisto, J.; Edwards, K.L.; Nelson, C.; Haffner, S.M.; Pyorala, K.; Laakso, M. Prospective Study of Small LDLs as a Risk Factor for Non-Insulin Dependent Diabetes Mellitus in Elderly Men and Women. *Circulation* **1995**, *92*, 1770–1778. [CrossRef]
10. Brouwers, M.C.G.J.; de Graaf, J.; Simons, N.; Meex, S.; ten Doeschate, S.; van Heertum, S.; Heidemann, B.; Luijten, J.; de Boer, D.; Schaper, N.; et al. Incidence of Type 2 Diabetes in Familial Combined Hyperlipidemia. *BMJ Open Diabetes Res. Care* **2020**, *8*, e001107. [CrossRef]
11. Shi, L.J.; Tang, X.; He, J.; Shi, W. Hyperlipidemia Influences the Accuracy of Glucometer-Measured Blood Glucose Concentrations in Genetically Diverse Mice. *Am. J. Med. Sci.* **2021**, *362*, 297–302. [CrossRef]
12. Shi, W.; Wang, Q.; Choi, W.; Li, J. Mapping and Congenic Dissection of Genetic Loci Contributing to Hyperglycemia and Dyslipidemia in Mice. *PLoS ONE* **2016**, *11*, e0148462. [CrossRef] [PubMed]
13. Wang, Q.; Grainger, A.T.; Manichaikul, A.; Farber, E.; Onengut-Gumuscu, S.; Shi, W. Genetic Linkage of Hyperglycemia and Dyslipidemia in an Intercross between BALB/CJ and SM/J Apoe-Deficient Mouse Strains. *BMC Genet.* **2015**, *16*, 133. [CrossRef] [PubMed]
14. Saleheen, D.; Nazir, A.; Khanum, S.; Haider, S.R.; Frossard, P.M. R1615P: A Novel Mutation in ABCA1 Associated with Low Levels of HDL and Type II Diabetes Mellitus. *Int. J. Cardiol.* **2006**, *110*, 259–260. [CrossRef]
15. Albert, J.S.; Yerges-Armstrong, L.M.; Horenstein, R.B.; Pollin, T.I.; Sreenivasan, U.T.; Chai, S.; Blaner, W.S.; Snitker, S.; O'Connell, J.R.; Gong, D.W.; et al. Null Mutation in Hormone-Sensitive Lipase Gene and Risk of Type 2 Diabetes. *N. Engl. J. Med.* **2014**, *370*, 2307–2315. [CrossRef] [PubMed]
16. Hu, Y.; Ren, Y.; Luo, R.Z.; Mao, X.; Li, X.; Cao, X.; Guan, L.; Chen, X.; Li, J.; Long, Y.; et al. Novel Mutations of the Lipoprotein Lipase Gene Associated with Hypertriglyceridemia in Members of Type 2 Diabetic Pedigrees. *J. Lipid Res.* **2007**, *48*, 1681–1688. [CrossRef]

17. Tan, Y.-X.; Hu, S.-M.; You, Y.-P.; Yang, G.-L.; Wang, W. Replication of Previous Genome-Wide Association Studies of HKDC1, BACE2, SLC16A11 and TMEM163 SNPs in a Gestational Diabetes Mellitus Case-Control Sample from Han Chinese Population. *Diabetes Metab. Syndr. Obes. Targets Ther.* **2019**, *12*, 983–989. [CrossRef]
18. Sattar, N.; Preiss, D.; Murray, H.M.; Welsh, P.; Buckley, B.M.; de Craen, A.J.M.; Seshasai, S.R.K.; McMurray, J.J.; Freeman, D.J.; Jukema, J.W.; et al. Statins and Risk of Incident Diabetes: A Collaborative Meta-Analysis of Randomised Statin Trials. *Lancet* **2010**, *375*, 735–742. [CrossRef]
19. Swerdlow, D.I.; Preiss, D.; Kuchenbaecker, K.B.; Holmes, M.V.; Engmann, J.E.L.; Shah, T.; Sofat, R.; Stender, S.; Johnson, P.C.D.; Scott, R.A.; et al. HMG-Coenzyme A Reductase Inhibition, Type 2 Diabetes, and Bodyweight: Evidence from Genetic Analysis and Randomised Trials. *Lancet* **2015**, *385*, 351–361. [CrossRef]
20. De Lsf, C.; Am, C.; Ac, S. Proprotein Convertase Subtilisin/Kexin Type 9 (PCSK9) Inhibitors and Incident Type 2 Diabetes: A Systematic Review and Meta-Analysis With Over 96,000 Patient-Years. *Diabetes Care* **2017**, *41*, 364–367. [CrossRef]
21. Climent, E.; Pérez-Calahorra, S.; Marco-Benedí, V.; Plana, N.; Sánchez, R.; Ros, E.; Ascaso, J.F.; Puzo, J.; Almagro, F.; Lahoz, C.; et al. Effect of LDL Cholesterol, Statins and Presence of Mutations on the Prevalence of Type 2 Diabetes in Heterozygous Familial Hypercholesterolemia. *Sci. Rep.* **2017**, *7*, 5596. [CrossRef]
22. Besseling, J.; Kastelein, J.J.P.; Defesche, J.C.; Hutten, B.A.; Hovingh, G.K. Association between Familial Hypercholesterolemia and Prevalence of Type 2 Diabetes Mellitus. *JAMA* **2015**, *313*, 1029–1036. [CrossRef] [PubMed]
23. Shi, W.; Wang, N.J.; Shih, D.M.; Sun, V.Z.; Wang, X.; Lusis, A.J. Determinants of Atherosclerosis Susceptibility in the C3H and C57BL/6 Mouse Model: Evidence for Involvement of Endothelial Cells but Not Blood Cells or Cholesterol Metabolism. *Circ. Res.* **2000**, *86*, 1078–1084. [CrossRef] [PubMed]
24. Shi, W.; Wang, X.; Wang, N.J.; McBride, W.H.; Lusis, A.J. Effect of Macrophage-Derived Apolipoprotein E on Established Atherosclerosis in Apolipoprotein E-Deficient Mice. *Arterioscler. Thromb. Vasc. Biol.* **2000**, *20*, 2261–2266. [CrossRef] [PubMed]
25. Shi, W.; Wang, X.; Wong, J.; Hedrick, C.C.; Wong, H.; Castellani, L.W.; Lusis, A.J. Effect of Macrophage-Derived Apolipoprotein E on Hyperlipidemia and Atherosclerosis of LDLR-Deficient Mice. *Biochem. Biophys. Res. Commun.* **2004**, *317*, 223–229. [CrossRef]
26. Tian, J.; Pei, H.; Sanders, J.M.; Angle, J.F.; Sarembock, I.J.; Matsumoto, A.H.; Helm, G.A.; Shi, W. Hyperlipidemia Is a Major Determinant of Neointimal Formation in LDL Receptor-Deficient Mice. *Biochem. Biophys. Res. Commun.* **2006**, *345*, 1004–1009. [CrossRef]
27. Li, J.; Wang, Q.; Chai, W.; Chen, M.H.; Liu, Z.; Shi, W. Hyperglycemia in Apolipoprotein E-Deficient Mouse Strains with Different Atherosclerosis Susceptibility. *Cardiovasc. Diabetol.* **2011**, *10*, 117. [CrossRef]
28. Liu, S.; Li, J.; Chen, M.H.; Liu, Z.; Shi, W. Variation in Type 2 Diabetes-Related Phenotypes among Apolipoprotein E-Deficient Mouse Strains. *PLoS ONE* **2015**, *10*, e0120935. [CrossRef]
29. Yuan, Z.; Pei, H.; Roberts, D.J.; Zhang, Z.; Rowlan, J.S.; Matsumoto, A.H.; Shi, W. Quantitative Trait Locus Analysis of Neointimal Formation in an Intercross between C57BL/6 and C3H/HeJ Apolipoprotein E-Deficient Mice. *Circ. Genet.* **2009**, *2*, 220–228. [CrossRef]
30. Clee, S.M.; Attie, A.D. The Genetic Landscape of Type 2 Diabetes in Mice. *Endocr. Rev.* **2007**, *28*, 48–83. [CrossRef]
31. Schreyer, S.A.; Vick, C.; Lystig, T.C.; Mystkowski, P.; LeBoeuf, R.C. LDL Receptor but Not Apolipoprotein E Deficiency Increases Diet-Induced Obesity and Diabetes in Mice. *Am. J. Physiol. Metab.* **2002**, *282*, E207–E214. [CrossRef]
32. Phillips, J.W.; Barringhaus, K.G.; Sanders, J.M.; Yang, Z.; Chen, M.; Hesselbacher, S.; Czarnik, A.C.; Ley, K.; Nadler, J.; Sarembock, I.J. Rosiglitazone Reduces the Accelerated Neointima Formation after Arterial Injury in a Mouse Injury Model of Type 2 Diabetes. *Circulation* **2003**, *108*, 1994–1999. [CrossRef] [PubMed]
33. Getz, G.S.; Reardon, C.A. Diet and Murine Atherosclerosis. *Arterioscler. Thromb. Vasc. Biol.* **2006**, *26*, 242–249. [CrossRef] [PubMed]
34. Fuller, D.T.; Grainger, A.T.; Manichaikul, A.; Shi, W. Genetic Linkage of Oxidative Stress with Cardiometabolic Traits in an Intercross Derived from Hyperlipidemic Mouse Strains. *Atherosclerosis* **2019**, *293*, 1–10. [CrossRef] [PubMed]
35. Duan, Y.; Zeng, L.; Zheng, C.; Song, B.; Li, F.; Kong, X.; Xu, K. Inflammatory Links Between High Fat Diets and Diseases. *Front. Immunol.* **2018**, *9*, 2649. [CrossRef] [PubMed]
36. Tudorache, I.F.; Trusca, V.G.; Gafencu, A.V. Apolipoprotein E—A Multifunctional Protein with Implications in Various Pathologies as a Result of Its Structural Features. *Comput. Struct. Biotechnol. J.* **2017**, *15*, 359–365. [CrossRef]
37. Tanaka, T.; Oyama, T.; Sugie, S.; Shimizu, M. Different Susceptibilities between Apoe- and Ldlr-Deficient Mice to Inflammation-Associated Colorectal Carcinogenesis. *Int. J. Mol. Sci.* **2016**, *17*, 1806. [CrossRef]
38. Tonini, C.L.; Campagnaro, B.P.; Louro, L.P.S.; Pereira, T.M.C.; Vasquez, E.C.; Meyrelles, S.S. Effects of Aging and Hypercholesterolemia on Oxidative Stress and DNA Damage in Bone Marrow Mononuclear Cells in Apolipoprotein E-Deficient Mice. *Int. J. Mol. Sci.* **2013**, *14*, 3325–3342. [CrossRef]
39. Fang, J.-Y.; Lin, C.-H.; Huang, T.-H.; Chuang, S.-Y. In Vivo Rodent Models of Type 2 Diabetes and Their Usefulness for Evaluating Flavonoid Bioactivity. *Nutrients* **2019**, *11*, 530. [CrossRef]
40. Chobot, A.; Górowska-Kowolik, K.; Sokołowska, M.; Jarosz-Chobot, P. Obesity and Diabetes—Not Only a Simple Link between Two Epidemics. *Diabetes Metab. Res. Rev.* **2018**, *34*, e3042. [CrossRef]
41. Bennett, B.J.; Davis, R.C.; Civelek, M.; Orozco, L.; Wu, J.; Qi, H.; Pan, C.; Packard, R.R.; Eskin, E.; Yan, M.; et al. Genetic Architecture of Atherosclerosis in Mice: A Systems Genetics Analysis of Common Inbred Strains. *PLoS Genet.* **2015**, *11*, e1005711. [CrossRef]

42. De Brito, G.; Lupinacci, F.C.; Beraldo, F.H.; Santos, T.G.; Roffé, M.; Lopes, M.H.; de Lima, V.C.; Martins, V.R.; Hajj, G.N. Loss of Prion Protein Is Associated with the Development of Insulin Resistance and Obesity. *Biochem. J.* **2017**, *474*, 2981–2991. [CrossRef] [PubMed]
43. Vercalsteren, E.; Vranckx, C.; Frederix, L.; Lox, M.; Lijnen, H.R.; Scroyen, I.; Hemmeryckx, B. Advanced-Age C57BL/6JRj Mice Do Not Develop Obesity upon Western-Type Diet Exposure. *Adipocyte* **2019**, *8*, 105–113. [CrossRef] [PubMed]
44. Rankinen, T.; Sarzynski, M.A.; Ghosh, S.; Bouchard, C. Are There Genetic Paths Common to Obesity, Cardiovascular Disease Outcomes, and Cardiovascular Risk Factors? *Circ. Res.* **2015**, *116*, 909–922. [CrossRef] [PubMed]
45. Oriá, R.B.; Vieira, C.M.G.; Pinkerton, R.C.; de Castro Costa, C.M.; Lopes, M.B.; Hussaini, I.; Shi, W.; Brito, G.A.C.; Lima, A.A.M.; Guerrant, R.L. Apolipoprotein E Knockout Mice Have Accentuated Malnutrition with Mucosal Disruption and Blunted Insulin-like Growth Factor I Responses to Refeeding. *Nutr. Res. N. Y. N* **2006**, *26*, 427–435. [CrossRef]
46. Fitzgibbons, T.P.; Kelly, M.; Kim, J.K.; Czech, M.P. Resistance to Diet Induced Obesity in the Apolipoprotein E Deficient Mouse Is Associated with an Attenuated Transcriptional Response in Visceral Fat. *bioRxiv* **2018**. [CrossRef]
47. Ngai, Y.F.; Quong, W.L.; Glier, M.B.; Glavas, M.M.; Babich, S.L.; Innis, S.M.; Kieffer, T.J.; Gibson, W.T. Ldlr−/− Mice Display Decreased Susceptibility to Western-Type Diet-Induced Obesity Due to Increased Thermogenesis. *Endocrinology* **2010**, *151*, 5226–5236. [CrossRef]
48. Ishibashi, S.; Perrey, S.; Chen, Z.; Osuga, J.I.; Shimada, M.; Ohashi, K.; Harada, K.; Yazaki, Y.; Yamada, N. Role of the Low Density Lipoprotein (LDL) Receptor Pathway in the Metabolism of Chylomicron Remnants. A Quantitative Study in Knockout Mice Lacking the LDL Receptor, Apolipoprotein E, or Both. *J. Biol. Chem.* **1996**, *271*, 22422–22427. [CrossRef]
49. Twisk, J.; Gillian-Daniel, D.L.; Tebon, A.; Wang, L.; Barrett, P.H.R.; Attie, A.D. The Role of the LDL Receptor in Apolipoprotein B Secretion. *J. Clin. Investig.* **2000**, *105*, 521–532. [CrossRef]
50. Getz, G.S.; Reardon, C.A. Do the Apoe−/− and Ldlr−/−mice Yield the Same Insight on Atherogenesis? *Arterioscler. Thromb. Vasc. Biol.* **2016**, *36*, 1734–1741. [CrossRef]
51. Lytle, K.A.; Jump, D.B. Is Western Diet-Induced Nonalcoholic Steatohepatitis in Ldlr-/- Mice Reversible? *PLoS ONE* **2016**, *11*, e0146942. [CrossRef]
52. Li, J.; Lu, Z.; Wang, Q.; Su, Z.; Bao, Y.; Shi, W. Characterization of Bglu3, a Mouse Fasting Glucose Locus, and Identification of Apcs as an Underlying Candidate Gene. *Physiol. Genom.* **2012**, *44*, 345–351. [CrossRef] [PubMed]
53. Zhou, W.; Chen, M.H.; Shi, W. Influence of Phthalates on Glucose Homeostasis and Atherosclerosis in Hyperlipidemic Mice. *BMC Endocr. Disord.* **2015**, *15*, 13. [CrossRef] [PubMed]

biomedicines

Article

Orphan GPR26 Counteracts Early Phases of Hyperglycemia-Mediated Monocyte Activation and Is Suppressed in Diabetic Patients

Zahra Abedi Kichi [1,2], Lucia Natarelli [2], Saeed Sadeghian [3], Mohammad ali Boroumand [4], Mehrdad Behmanesh [1,*] and Christian Weber [2,*]

[1] Department of Genetics, Faculty of Biological Sciences, Tarbiat Modares University, Tehran P.O. Box 14115-111, Iran; zahra.abedi@med.uni-muenchen.de
[2] Institute for Cardiovascular Prevention (IPEK), Ludwig-Maximillians University, 80336 Munich, Germany; lucia.natarelli@med.uni-muenchen.de
[3] Department of Electrophysiology, Tehran Heart Center, Cardiovascular Diseases Research Institute, Tehran University of Medical Sciences, Tehran P.O. Box 14155-6559, Iran; ssadeghian@tums.ac.ir
[4] Department of Pathology and Clinical Laboratory, Tehran Heart Center, Tehran University of Medical Sciences, Tehran P.O. Box 14155-6559, Iran; mabroumand@yahoo.com
* Correspondence: behmanesh@modares.ac.ir (M.B.); christian.weber@med.uni-muenchen.de (C.W.); Tel.: +98-2182884451 (M.B.); +49-(0)89-4400-54351 (C.W.)

Abstract: Diabetes is the ninth leading cause of death, with an estimated 1.5 million deaths worldwide. Type 2 diabetes (T2D) results from the body's ineffective use of insulin and is largely the result of excess body weight and physical inactivity. T2D increases the risk of cardiovascular diseases, retinopathy, and kidney failure by two-to three-fold. Hyperglycemia, as a hallmark of diabetes, acts as a potent stimulator of inflammatory condition by activating endothelial cells and by dysregulating monocyte activation. G-protein couple receptors (GPCRs) can both exacerbate and promote inflammatory resolution. Genome-wide association studies (GWAS) indicate that GPCRs are differentially regulated in inflammatory and vessel cells from diabetic patients. However, most of these GPCRs are orphan receptors, for which the mechanism of action in diabetes is unknown. Our data indicated that orphan GPCR26 is downregulated in the PBMC isolated from T2D patients. In contrast, GPR26 was initially upregulated in human monocytes and PBMC treated with high glucose (HG) levels and then decreased upon chronic and prolonged HG exposure. GPR26 levels were decreased in T2D patients treated with insulin compared to non-insulin treated patients. Moreover, GPR26 inversely correlated with the BMI and the HbA1c of diabetic compared to non-diabetic patients. Knockdown of GPR26 enhanced monocyte ROS production, MAPK signaling, pro-inflammatory activation, monocyte adhesion to ECs, and enhanced the activity of Caspase 3, a pro-apoptotic molecule. The same mechanisms were activated by HG and exacerbated when GPR26 was knocked down. Hence, our data indicated that GPR26 is initially activated to protect monocytes from HG and is inhibited under chronic hyperglycemic conditions.

Keywords: diabetes mellitus; GPCRs; GPR26; monocytes; peripheral blood cells; hyperglycemia

Citation: Kichi, Z.A.; Natarelli, L.; Sadeghian, S.; Boroumand, M.a.; Behmanesh, M.; Weber, C. Orphan GPR26 Counteracts Early Phases of Hyperglycemia-Mediated Monocyte Activation and Is Suppressed in Diabetic Patients. *Biomedicines* **2022**, *10*, 1736. https://doi.org/10.3390/biomedicines10071736

Academic Editor: Alfredo Caturano

Received: 9 June 2022
Accepted: 13 July 2022
Published: 19 July 2022

1. Introduction

Diabetes mellitus (DM) is a chronic, metabolic disease characterized by elevated levels of blood glucose (hyperglycaemia). Type 2 diabetes (T2D) is the most common type of diabetes, accounting for approximately 90% of all cases of DM [1]. Hyperglycaemia, a hallmark in T2D, affects the metabolic homeostasis of several organs, like kidney, pancreas, and eyes, and induces vascular cell dysfunction and associated vascular diseases, including cardiovascular diseases (CVD), diabetic nephropathy, and neuropathies [2,3].

Inflammation plays a crucial role in the pathogenesis of T2D and its complications. Vascular cells, especially immune cells, such as lymphocytes and monocytes, are involved

in the development of vascular inflammation, and promote endothelial activation and monocyte adhesion to the endothelium, sustaining diabetic vascular complications [2,4,5]. Despite data on the involvement of neutrophils and blood monocytes in diabetic patients still being contradictory, increased glucose uptake by monocytes from diabetic patients induces monocyte activation and enhances abnormal leukocyte–endothelial interaction [6,7]. Moreover, monocytes from diabetic patients are characterized by a moderate decrease in the activity of enzymes involved in the modulation of monocyte metabolism and inflammatory activation [8]. Mechanistically, high glucose (HG) levels, deriving from diabetes-associated chronic hyperglycaemia, induce inflammation via a variety of mechanisms, including ROS accumulation, pro-inflammatory MAPK cascade signalling, and NF-κB activation [9], which promotes the transcription of pro-inflammatory cytokines and adhesion molecules and related monocyte activation [6,10,11]. Moreover, HG can regulate monocyte apoptosis, although the role of this programmed cell death in diabetic patients is still controversial [12,13].

Cellular receptors are fine-tuned regulators of cell response to environmental changes via translating extracellular signals into intracellular activation cascades. The failure of a physiological process, such as the receptor-derived physiological processes in monocytes, dysregulates their function and mediates monocyte pro-inflammatory activation [3]. G-protein-coupled receptors (GPCRs) are the largest family of cell surface receptors in the human genome that play pivotal roles in a wide variety of physiological processes [14]. GPCRs emerged as novel receptors modulating the response of monocytes and other cells to environmental changes, such as hyperglycaemia [15]. Indeed, GPCRs can regulate the expression of cytokines and adhesion molecules to both exacerbate inflammation or promote its resolution [16,17]. Genome-wide association studies (GWAS) on diabetic patients indicate that GPCRs are differentially regulated in T2D patients and can influence the development and progression of T2D and vascular complications [17–20]. However, most of these GPCRs are orphan receptors, for which the mechanism of action in immune cells in diabetic patients is largely unknown [21]. Only a few studies exist on GPR119, free fatty acid receptor 1 (FFAR1/GPR40) and 4 (FFAR4/GPR120), and the bile acid receptor GPBAR1 (TGR5) as a developer of insulin resistance and β-cell dysfunction [22], receiving particular attention as targets for therapeutic interventions in diabetic patients [22]. Since orphan GPCRs emerged as the most differentially regulated sub-class of GPCRs in diabetic patients, the scientific community started to focus more on this sub-class of receptors [15,16,22]. Three orphan GPCRs have been reported so far to be involved in the development of diabetes and cardiovascular complications: GPR135 [19], GPR55 [23,24], and GPR39 [25]. However, data are still too preliminary and mainly focused on adipocyte-related diabetic complications [19,23–25]. Given the potential role of monocytes and orphan GPCR receptors in diabetes and associated cardiovascular complications, we investigated the role of GPCRs on monocytes from diabetic patients. Among almost 800 GPCRs existing, we focused on orphan GPCRs as the most important target receptor family for therapeutic purposes in biomedicine [21].

2. Materials and Methods

2.1. Bioinformatics Analysis of GWAS Available Databases

GWAS studies on single nucleotides polymorphisms and microarrays data from blood or peripheral blood mononuclear cells (PBMC) samples collected from diabetic patients (T1D and T2D) (GDS3963, GDS3874) were used to identify GPCRs differentially expressed and related to diabetes (Supplement Excel File S1). Among all identified GPCR candidates, we excluded the T1D-related GPCRs and focused on those related to T2D. In the next step, we focused on orphan GPCRs [18,19,21,22]. Finally, GPR26 was selected as a T2D-related orphan GPCR. To predict functional associations between GPR26 and attributes (e.g., genes, proteins, diseases, etc.), we performed a bioinformatics analysis using the Harmonizome (2022 Database, Oxford) [26], JASPAR (9th release, V4.0, 2022) [27], KEGG

(V 103.0, July 2022, Kanehisa Laboratories) [28], and STRING (V11.5, STRING Consortium 2022) databases [29].

2.2. Specimen Collection and Laboratory Investigations

Whole blood samples were obtained from 32 diabetic patients and 32 healthy donors referred to the outpatient clinic of Tehran Heart Center, Iran. The diagnosis of T2D was based on WHO criteria, and diabetic patients were selected based on standard criteria (fasting blood glucose (FBS)), N 125 mg/dL (6.9 mmol/L), and HbA1c N 6.5% (47 mmol/mol) (https://apps.who.int/iris/handle/10665/70523, accessed on 1 June 2022). To exclude any intervening condition due to background diseases, all of participants were examined for T1D, liver and kidney dysfunction, auto-immune diseases, current or prior cancers, acute or chronic inflammatory diseases, and any other unrelated disease. In addition, pregnant, smoking individuals and patients who were receiving immunosuppressive or hormone-containing drugs were excluded from the study. The healthy donors showed normal FBS and HbA1C values and did not report a T2D history, autoimmune disease, obesity, or any other chronic disease. This group was matched to diabetic cases based on gender, age, and ethnicity. Human PBMC were obtained from volunteers following an oral and written informed consent. Institutional approval was obtained from the Ethics Committees of Tarbiat Modares University (IR.MODARES.REC.1397.109). The study was conducted in accordance with the ethical guidelines of the Helsinki declaration.

2.3. Biochemical Analysis of Blood Samples from T2D and Healthy Donors

Whole blood samples were collected from precipitants after an overnight fasting. FBS was determined by glucose hexokinase method (Cobas Integra 400, Roche Diagnostics). HbA1c was quantified using an enzymatic method according to the manufacturer's instructions (Cat no. DZ168A, Diazyme Laboratories, Inc., 12889 Gregg Ct. Poway, CA 92064 USA).

2.4. PBMC Isolation from Iranian Diabetic and Healthy Volunteers

PBMCs were isolated from fresh whole blood samples by density gradient using Ficoll Histopaque (10771, Sigma-Aldrich, St. Loius, MO, USA). In detail, 2 mL of Ficoll Histopaque per 1 mL of blood were placed in a 50 mL conical centrifuge tube. Fifteen mL of anticoagulated blood was diluted with an equal volume of Phosphate-buffered saline (PBS). The diluted blood was layered over the Ficoll Hypaque solution gently. Gradients were centrifuged at 400× *g* for 30 min at room temperature with no brake. Then, the PBMC layer was collected, washed with cold PBS, and centrifuged 10 min at 400× *g* (4 °C). The supernatant was discarded, and a wash step was repeated with PBS. PBMCs were finally collected and used for downstream analyses.

2.5. RNA Extraction and qPCR

Total RNA was extracted from PBMCs using TRIzol Reagent (15596026, Thermofisher Scientific, Waltham, MA, USA) according to the manufacturer's instructions. One μg of RNA was reverse-transcribed with a high-capacity cDNA reverse transcription kit according to the manufacturer's instruction (4368813, Thermofisher Scientific). Gene expression was evaluated by qPCR using the GoTaq qPCR master mix (A6001, Promega, Madison, WI, USA). All samples were tested at least in duplicate (technical replicates). The relative gene expression analysis of GPR26 was according to the Livak method [30]. Expression levels were normalized to B2M as stable internal control gene and expressed as $2^{-\Delta Ct}$. Primer efficiencies for the tested genes were comparable to those for reference genes. Primer sequences are reported in Supplement Table S1.

2.6. Cell Culture and Treatments

PBMCs for cell culture experiments were obtained from additional 12 healthy volunteers after giving oral and written informed consent. Human monocyte cells (THP-1, ATCC,

Rockville, MD, USA) were cultured in a Roswell Park Memorial Institute 1640 medium (RPMI 1640, 11530586, Gibco, Termofisher Scientific) supplemented with 2 mM L-glutamin, 1% penicillin/streptomycin, and 10% fetal bovine serum (Gibco), and incubated at 37 °C in a humidified atmosphere containing 5% CO_2. CTHP-1 were exposed for 24, 48, and 72 h to media containing either 5 mM D-glucose (normal glucose, NG), or 25 mM D-glucose (high glucose, HG) to simulate a condition closed to the diabetic hyperglycemia. PMBCs were treated similarly for 24 and 48 h. Cell viability in each experiment was >90%, as indicated by trypan blue staining. THP-1 and PBMC total RNA was isolated as described above.

2.7. Antisense LNA GapmeRs Cell Transfection

THP-1 were chemically transfected (Lipofectamine RNAiMAX transfection reagent, 13778075, Life Technologies (Waltham, MA, USA), Termofisher Scientific) for 24, 48, and 72 h with LNA single-stranded antisense oligonucleotides (LNA-GapmeRs, 50 nM) designed for highly effective, strand-specific, knockdown of GPR26 mRNA, or with scrambled controls, alone or in combination with NG or HG. RNA isolation and cDNA synthesis were performed as mentioned before. Efficiency of GPR26 Gapmers was validated by qPCR and western blot. All data belong to at least three biological replicates.

2.8. Western Blot Analysis

Whole proteins were extracted from THP-1 using a RIPA lysis buffer (50 mM Tris pH 7.4, 150 mM NaCl, 1% Igepal, 0.5% sodium deoxycholate, 0.1% SDS) containing phosphatase and proteinase inhibitor cocktails (cOmplete Mini Tablets and PhosSTOP, 11836170001, Roche, Basel, Switzerland). The protein content was determined using the Pierce BCA Protein Assay Kit (23227, Thermo Fisher Scientific). Twenty µg of total proteins were loaded on a 4–12% precast polyacrylamide gel (NuPAGE™ 4 bis 12%, Bis-Tris, 1.0–1.5 mm, Mini-Protein-Gel, NP0321PK2, Invitrogen, Waltham, MA, USA) and electrotransferred onto polyvinylidene difluoride (PVDF) 0.45 µm membranes according to the manufacturer's instructions. Proteins were incubated with antibodies indicated in the Supplementary Table S2. The β-actin and α-tubulin proteins were used for protein quantification and internal loading control.

2.9. Reactive Oxygen Species (ROS) Assay

To examine the possible role of GPR26 in generation of ROS, its amount was measured using the OxiSelect Intracellular ROS Assay Kit (STA-342, Cell Biolabs, San Diego, CA, USA) based on the manufacturer's instructions. Briefly, THP-1 cells were transfected with GPR26 GapmeRs and exposed to NG or HG as indicated before. Then, cells were incubated with 2′, 7′-Dichlorodihydrofluorescin diacetate (DCFH-DA) during the last 30 min of treatment. At the end of the incubation, cells were washed three times with PBS to remove any DCFH-DA excess. Fluorescence was analyzed at 485 nm excitation/530 nm emission using a fluorescent plate reader (Infinite® 200 PRO, Tecan, Männedorf, Switzerland). ROS levels were expressed as DCFH-DA relative fluorescence intensity and reported as fold change of the control.

2.10. Caspase-3 Activity Assay

THP-1 cells were cultured and transfected with GPR26 GapmeRs as mentioned above. To determine the activity of caspase-3, cells were incubated at 37 °C with a luminogenic caspase-3 substrate containing the tetrapeptide sequence DEVD (Caspase-Glo® 3/7 Assay Systems, G8091, Promega). Luminescence is proportional to the amount of caspase activity present. Luminescence was measured in a plate luminometer (Infinite® 200 PRO, Tecan). Six technical replicates per condition were performed for each of the 3 biologically independent experiments.

2.11. Monocyte Adhesion Using Calcein-AM

THP-1 were transfected with GPR26 GapmeRs for 24, 48 and 72 h. At the end of the experiment, cells were labeled with 5 μM/L × 10^6 cells calcein-AM (Calcein, AM, Zellfarbstoff, C1430, Invitrogen, Life Technologies) for 45 min as previously described [31], with some modifications. Human Aortic Endothelial cells (HAoECs criopreserved, 500.000 cells, C-12271, PromoCell, Heidelberg, Germany) were cultured on gelatin-coated 96-well black plates. Confluent HAoEC monolayers were co-cultured with fluorescently labeled THP-1 cells for 20 min at 37 °C. Then, the monolayers were washed three times with PBS to remove non-adherent cells. Fluorescence was acquired at 492 nm (excitation) and 535 nm (emission) on a plate reader (Tecan). Relative fluorescence from treated monocytes adherent to HAoECs was normalized on that from the relative monocytes control groups. Comparisons were made between all four groups, as indicated in the Results. Representative images were acquired with a Thunder Imager Live Cell inverted microscope (Leica microsystem, Leica Mikrosysteme Vertrieb GmbH, Wetzlar, Germany) and equipped with a dual fluorescent and brightfield camera. Images were acquired for each of the 4 technical replicates and for all 3 biological replicates.

2.12. 3D Confocal Immunofluorescence for GPR26 Spatial Localization

THP-1 monocytes were plated on 8-well chamber slides (Ibidi) and treated as described before. Cells were fixed using the ViewRNA Cell Plus Assay (Fix & PERM™ Zellpermeabilisierungskit, GAS003, Affymetrix, Thermofisher Scientific), and incubated with antibodies against GPR26 (250 ng/mL dilution, NBP2-57693, R87210, Novusbio) and β-catenin (200 ng/mL, ab16051, Abcam). Proteins were detected using appropriate fluorescently labeled secondary antibodies feasible for 3D confocal microscopy, such as STAR-488-conjugated anti-rabbit IgG antibody (Molecular Probes, #A11034), and Cy™3 AffiniPure Donkey Anti-Rabbit IgG (H+L) (711-165-152, Jackson Immuno Research). Cells were embedded in Vectashield Antifade Mounting Medium with DAPI (H-1200-10, Vector Laboratories, Burlingame, CA, USA) to counterstain nuclei.

For detailed GPR26 localization studies, three-dimensional confocal laser scanning microscopy (CLSM) was performed with a Leica SP8 3X microscope equipped with a 63×/1.40 (Leica) oil immersion objective. Optical zoom was used where applicable. A UV laser (405 nm) was used for excitation of DAPI. A tunable white light laser for selective excitation of Star635P and Cy3 fluorochromes was used for the detection of GPR26 and β-catenin, respectively. Time gating of the detected emission signals (0.8–6.0 ns) was used for all STED channels to enhance image resolution. All data were acquired in three dimensions and voxel size was determined according to Nyquist sampling criterion. Image reconstructions were performed using the LAS X software package v.3.0.2 (Leica) and deconvolution was performed combining the Huygens Professional software package v.19.10 (Scientific Volume, Hilversum, The Netherlands) using the unsupervised CLSM algorithms.

GPR26 quantification and cell localization were performed using the Imaris 8.4.2 software equipped with the imaging processing toolbox MATLAB. Spatial distribution of automatically calculated GPR26 voxels (0.950 μm spot detection value) was defined according to the voxel localization to the cell surface, which corresponded to the membrane surface calculated using the spatial distribution of the β-catenin (0.289 μm smoothing, 3.46 μm threshold). A voxel value of 0.5 μm was used as threshold to discriminate membrane versus cytosolic GPR26. Multiple wells per experimental conditions were performed in independent experiments. The analysis of the staining was performed in a blinded manner.

2.13. Statistical Analysis

Statistical analysis was performed using GraphPad Prism 9.3.1 (GraphPad Software, Inc., San Diego, CA, USA). Data were initially evaluated for normal distribution with the Shapiro-Wilk test. Comparisons between two groups with normally distributed variables were analyzed by Student's unpaired *t* test. Not normally distributed variables were compared by the Mann–Whitney test. Analysis of variance (ANOVA) was used to determine

the significant differences between more than two groups. The correlation between the expression levels of GPR26 and the clinical features of patients were assessed by Spearman or Pearson tests based on the normality test result. In all cases, p values < 0.05 were considered significant.

2.14. Data and Resource Availability

The raw data are available in the Supplementary Files.

3. Results

3.1. GPCRs SNPs and Correlation with Their Expression in Diabetic Patients

Diabetes mellitus is a chronic, metabolic disease characterized by elevated blood glucose levels, which leads to additional chronic complications, such as cardiovascular, inflammatory, and kidney diseases [32]. Diabetes is among the top 10 leading causes of death worldwide, following a significant percentage increase of 70% since 2000 (WHO, https://www.who.int/news-room/fact-sheets/detail/the-top-10-causes-of-death, accessed on 1 June 2022). In Iran, diabetes is the 6th leading cause of death, with a death rate of 27.47 per 100.000 of population (WHO 2018 and World Health Rankings, https://www.worldlifeexpectancy.com/iran-diabetes-mellitus, accessed on 1 June 2022). Genome-wide association studies (GWAS) provided evidence that occurrence of certain single nucleotide polymorphisms (SNPs) in GPCRs are associated with an increased risk for diabetes and cardiovascular complications [33]. Hence, we analysed GWAS available datasets to depict all GPCRs with a reported SNP in diabetic patients. We identified 31 potential GPCRs candidates (Figure 1a). GPCRs are divided into six sub-classes based on their sequence and function. Accordingly, 15 out of 31 GPCRs were members of the Class A-rhodopsin-like receptors, 8 were members of the Class B-secretin family, 5 were members of the Class C-metabotropic of glutamate receptors, and 3 were members of the Frizzled or other GPCR subclasses [34] (Figure 1a).

Next, we analyzed the expression of the selected 31 GPCRs using available GEO datasets from blood samples isolated from T2D patients to define whether the presence of SNPs in the GPCR sequences correlated with a different expression of selected GPCRs in diabetic patients compared to healthy subjects. Twenty-nine out 31 GPCRs were differentially regulated in the blood or PBMC samples (Figure 1b,c). Next, we focused on orphan GPCRs as more attractive candidates for further studies. We end up with three orphan GPCRs, such as GPR35, GPR158, and GPR26. However, since GPR158 expression did not significantly change in the blood nor in the PBMC isolated from diabetic patients, and GPR35 is also known to be modulated in T1D, we end up with the orphan GPR26 as a promising candidate for our subsequent experiments (Figure 1b,c). Indeed, GPR26 was the most promising candidate among other orphan GPCRs, for which expression was decreased in the blood of T2D patients compared to healthy donors [33,35] (Figure 1c). GPR26 expression was slightly decreased in PBMC samples, probably due to the origin of the samples from young patients with an early T2D diagnosed disease.

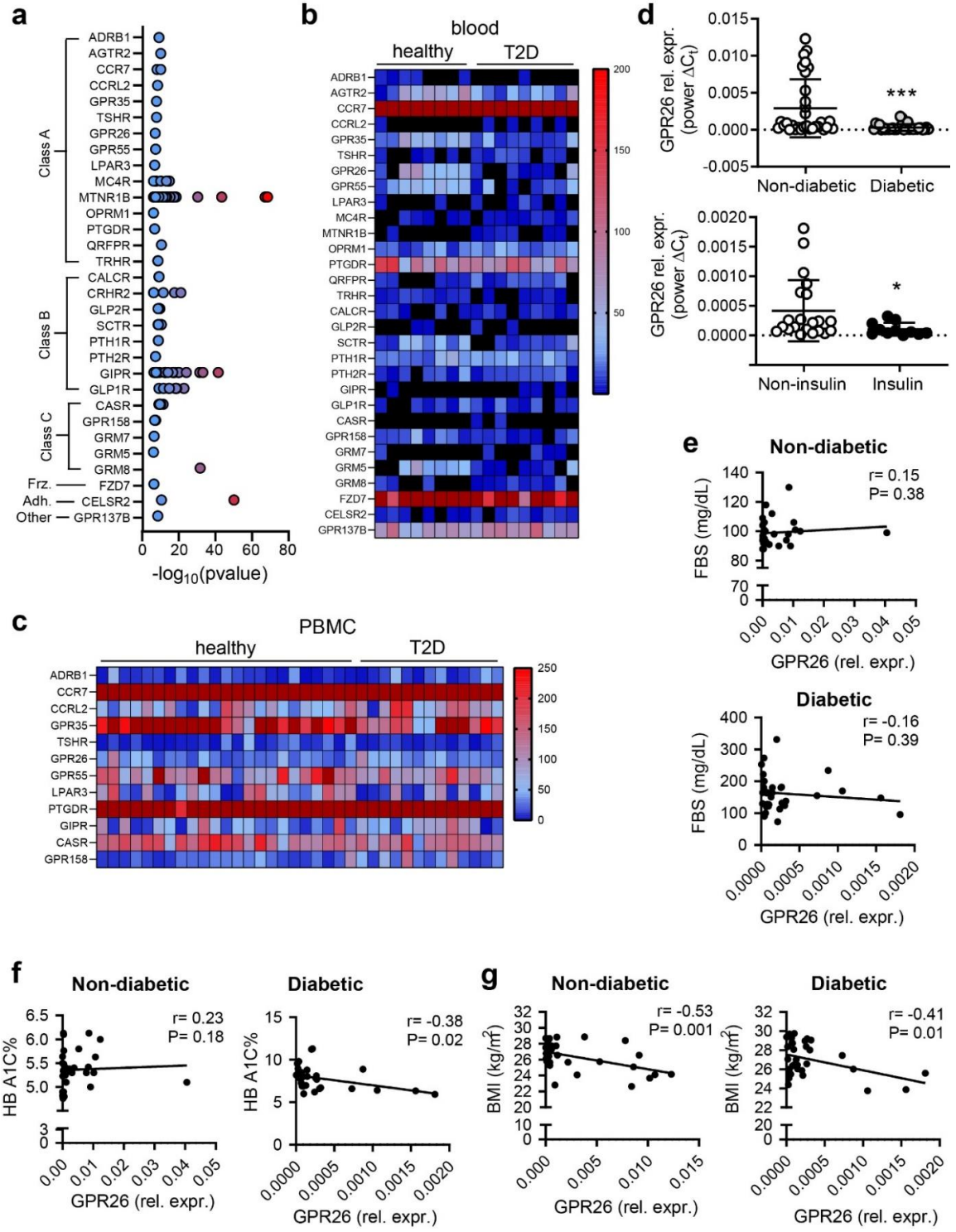

Figure 1. GPCRs candidates from GWAS, GEO datasets, and T2D patients. (**a**) GPCRs showing SNPs associated to diabetes. Analysis of available microarray GEO datasets and relative heatmap of 31 GPCRs differentially expressed (**b**) in the blood and (**c**) in the PBMC isolated from diabetic patients. (**d**) Expression analysis of GPR26 in diabetic patients (n = 32) in comparison to non-diabetic individuals (n = 32) (*** $p < 0.001$). (**e**) *GPR26* expression in patients treated with insulin (n = 11) compared to non-insulin treated patients (n = 21) (* $p < 0.05$). GPR26 mRNA expression was normalized to the corresponding B2M expression and expressed as power ΔCt. (**e**–**g**) Correlation of GPR26 expression with (**e**) FBS, (**f**) HbA1c (%), and (**g**) BMI in non-diabetic and diabetic patients. Pearson correlation and r values are indicated.

To predict functional associations between orphan GPR26 and attributes, like genes and proteins associated with diabetes and related complications, we performed a bioinformatics analysis using the Harmonizome [26], JASPAR [27], KEGG [28], and STRING [29] databases. Harmonizome database results indicated that orphan GPR26 showed 1.763 functional associations with biological entities spanning 8 categories (molecular profile, organism, functional term, phrase or reference, disease, phenotype or trait, chemical, structural feature, cell line, cell type or tissue, gene, protein, or microRNA) extracted from 59 datasets (Supplement Excel File S2). Analysis of functional associations predicted that orphan GPR26 might be involved in the regulation of cAMP catabolic processes (GO:0006198), vesicle formation and transport (GO:0071805), and of ADP-ribosylation factor (ARF) protein signal transduction (GO:0032012), which acts as regulator of phagocytosis and of immunity-related autophagy [36,37]. KEGG pathway analysis indicated that GPR26 might be involved in the cAMP, cGMP-PKG, insulin pancreatic secretion, MAPK, VEGF, oxidative phosphorylation, chemokine, mTOR, autophagy regulation, ABC transporters, T1D, and T2D pathways (Supplement Excel File S3). Similar results were obtained using STRING, where G-protein coupled receptors, cyclic AMP-responsive element-binding proteins, and lysosome-related organelle complexes were predicted as functional partners of GPR26.

3.2. GPR26 Is down Regulated in the PBMC from Diabetic Patients and Negatively Correlates with Their BMI, HbA1c, and Insulin

GPR26 expression was first investigated in the blood collected from T2D and healthy Iranian donors. Demographic and clinical characteristics of control participants and patients are presented in Table 1. In detail, blood samples were collected from 32 patients (19 male, 13 females) with a diagnosed T2D and from 32 healthy donors (13 males, 19 females). None of the healthy donors were smokers or were hypertensive. Eleven diabetic patients got insulin routinely or had a history of using insulin. The diabetic and non-diabetic subjects did not significantly differ in gender, age, and body mass index (BMI) (Table 1). We did not observe sex-related differences within the diabetic or healthy donors in glycated hemoglobin (HbA1c), an index of long-term blood glucose concentrations, fasting blood glucose (FBS), nor on BMI. FBS and HbA1c were high in diabetic patients compared to healthy donors (Table 2). GPR26 expression was downregulated in diabetic patients compared to healthy donors (Figure 1d). We divided the diabetic patients according to their insulin supplementation (Table 2 and Figure 1d). In detail, 11 out of 32 T2D patients got insulin and mainly metformin + glibenclamide, an antidiabetic tablet medication, to lower the hyperglycemic levels and increase the insulin. The other 21 T2D patients did not get insulin but mainly the antidiabetic Glibenclamide medication (Table 2). Analysis of GPR26 expression in insulin versus non-insulin-treated patients indicated that GPR26 expression was decreased in patients taking insulin routinely or showing a history of using insulin compared to antidiabetic medication tablets treated patients, although the glycemic levels (HbA1c) were not different between the two groups (Table 3).

This data suggested that insulin-mediated alleviation of hyperglycemic adverse effects might counteract monocyte activation and GPR26 expression. Accordingly, we evaluated the association of *GPR26* expression with the glycemic profile, the HbA1c, and the BMI. *GPR26* was not correlated with FBS (Figure 1e) but showed a significant correlation with HbA1c ($r = -0.38$ $p = 0.02$) in diabetic patients (Figure 1f, Table 3). The association of *GPR26* with the BMI was also significant in both diabetic ($r = -0.41$ $p = 0.01$) and healthy donors ($r = -0.35$ $p = 0.04$) (Figure 1g, Table 3). Taken together, these data indicated that GPR26 is downregulated in diabetic patients and that insulin treatment might prevent GPR26 putative protective activation.

Table 1. Demographic characteristics of the diabetic patients and healthy control.

Characteristics	Diabetic n = 32 (100%)	Non-Diabetic n = 32 (100%)	p-Value
Sex	19 males,13 females	13 males, 19 females	0.61 [i]
Age (years)	±55.75 ± 7.18	53.56 ± 4.85	0.15 [ii]
BMI (kg/m^2) [a]	25.98 ± 1.4	25.64 ± 1.29	0.32 [i]
Laboratory Plasma glucose [b] (mmol/L)	161.6 (73–331)	99.03 (88–130)	<0.0001
HbA1c [c]	7.83 (5.92–11.29)	5.40 (4.76–6.3)	<0.0001
Glucose-lowering medications	11 (insulin), 21 (other medications)	-	-

[a]: Body mass index; [b]: Low density lipoproteins; [c]: Glycated hemoglobin; Data are presented as mean (SEM) for variables with normal distribution and median (interquartile range) for those without normal distribution. [i] Chi-square or Fisher's exact test is performed to compare variables between diabetic and non-diabetic patients. [ii] Student's *t*-test or Mann–Whitney *U* test is performed to compare variables between diabetic and non-diabetic patients.

Table 2. Glucose-lowering medications used to treat diabetic patients.

		Antidiabetic Medication Tablets	
T2D Patients [32]		Metformin Hydrochloride and Glibenclamide	Glibenclamide
Insulin	11	29	3
Non-insulin	21	3	29

Table 3. Correlation analysis between GPR26 mRNA expression and clinical characteristic of diabetic patients and non-diabetic individuals.

	Diabetic		Non-Diabetic	
Correlation with	r	p-Value	r	p-Value
HbA1c	−0.38	0.02	0.23	0.18
FBS	−0.16	0.39	0.	0.59
BMI	−0.41	0.01	−0.53	0.001

3.3. Hyperglycemia Upregulated GPR26 in PBMC and THP-1 Cultured Cells

We analyzed the expression of GPR26 in human cultured monocytes treated with different doses of glucose to simulate a hyperglycemic condition and to study GPR26 functional role. Accordingly, THP-1 cells were treated with 5 mmol/L (normal glucose, NG) or 25 mmol/L (high glucose, HG) of glucose for 24, 48, and 72 h. Interestingly, treatment of THP-1 with HG increased the expression of GPR26 (Figure 2a). The protein levels of GPR26 decreased over time when THP-1 cells were treated with HG, which increased GPR26 levels only at 24 and slightly at 48, but not at 72 h (Figure 2a). These data suggested that monocytes might response to hyperglycemic conditions by enhancing GPR26 expression, the translation of which into a protein is ineffective when cells are exposed to prolonged and chronic doses of HG.

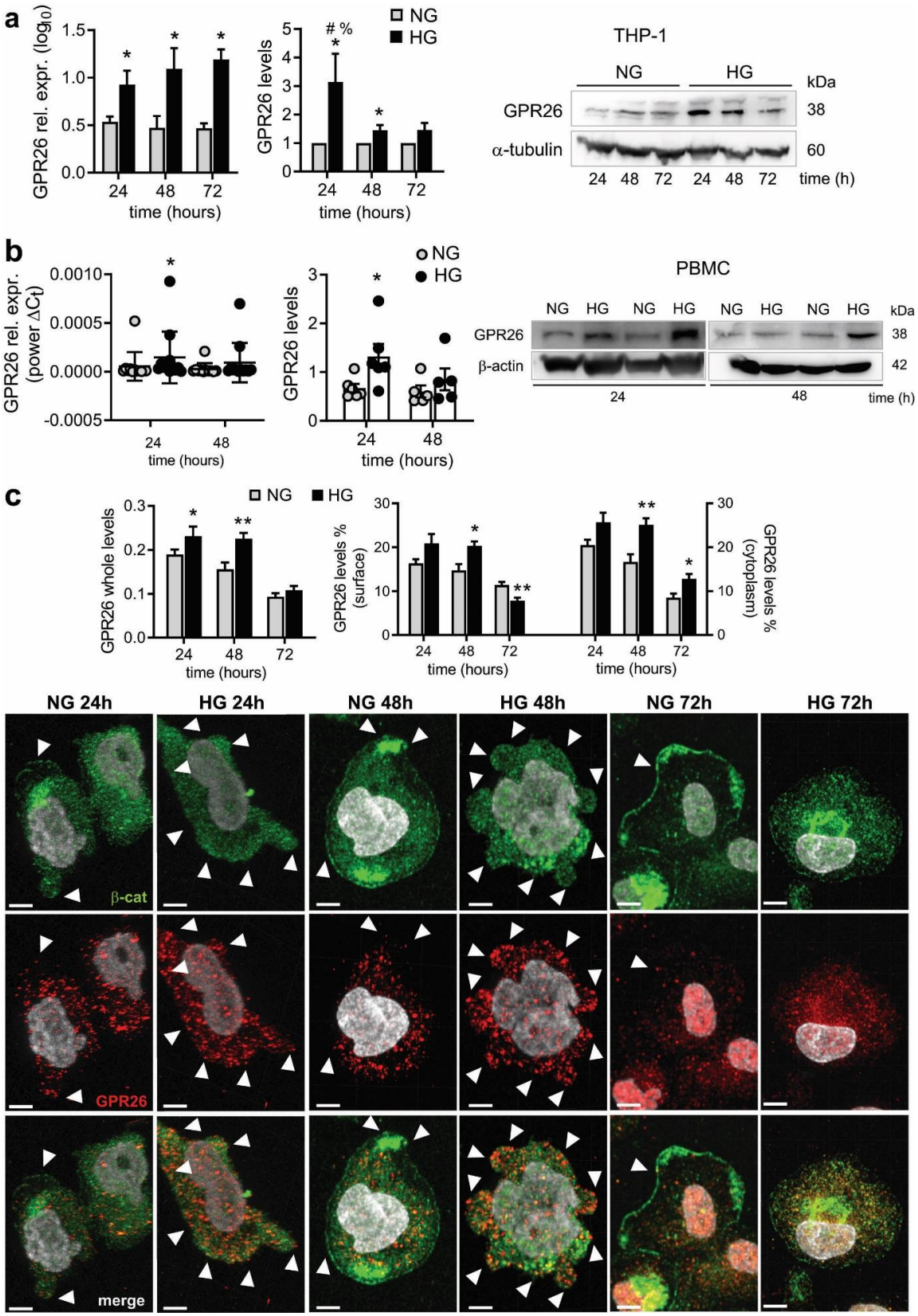

Figure 2. Effect of HG on GPR26 mRNA and protein levels in human monocytes and cellular localization. THP-1 and PBMC were treated with D-glucose 5.5 mM (normal glucose, NG) or 25 mM D-glucose (high glucose, HG) for 24, 48, and 72 h to analyze GPR26 in THP-1 (**a**) at mRNA (left) and protein (right) level. A representative Western blot (left) and relative expression of GPR26 (right).

Densitometry plots report the fold change versus control. GPR26 intensity values were normalized to the corresponding β-tubulin value. GPR26 mRNA expression was normalized to the corresponding B2M expression and expressed as log10 (n = 4 independent experiments) (**b**) GPR26 mRNA (left) and protein (right) levels in PBMCs isolated from healthy donors and treated as indicated for THP-1. Densitometry plots reporting the fold change versus control. GPR26 intensity values were normalized to the corresponding β-actin value. GPR26 mRNA expression was normalized to the corresponding B2M expression and expressed as power ΔCt (n = 4 independent experiments) (**c**) Analysis of GPR26 whole levels and cellular localization in THP-1 cells. Confocal 3D scanning images are representative of 3 independent experiments. White arrowhead indicates GPR26 localizing at the membrane surface. GPR26 levels were normalized to the cell surface, and on total number of cells ($n = 3 \pm$ SEM). Scale bar: 5 μm. * $p < 0.05$ ** $p < 0.01$ versus NG, # $p < 0.05$ 48 h versus 24 h, % $p < 0.05$ 72 h versus 24 h.

To corroborate the data, human PBMC were isolated from healthy donors and treated with NG or HG for 24 and 48 h. Accordingly, we found that GPR26 expression was increased only at 24 but not at 48 h of HG exposure (Figure 2b). Accordingly, HG increased GPR26 protein levels at 24 but not at 48 h (Figure 2b).

Next, we analyzed GPR26 cellular localization and relative levels to test whether HG affected GPR26 exposure on the monocyte membrane surface. THP-1 were treated with NG or HG for 24, 48, and 72 h and stained for GPR26 and β-catenin as membrane marker. Immunofluorescence analysis 3D z-scan confocal images confirmed that HG increased whole GPR26 levels at 24, 48 but not at 72 h (Figure 2c). The number of voxels relative to GPR26 close to the β-catenin surface were reduced compared to that far from the surface, a value relative to the cytoplasmic GPR26 (Figure 2c). HG increased both cytoplasmic- and membrane-associated GPR26 levels at 24 and 48 h (Figure 2c). However, analysis of GPR26 localization at 72 h, a time point at which the GPR26 protein levels are no longer increased by HG, indicated that HG impaired GPR26 localization on the membrane surface of THP-1 and increased GPR26 cytoplasmic levels (Figure 2c).

Taken together, these data suggested that GPR26 might be activated to counteract the deleterious effects promoted by HG, which in turn impaired GPR26-related protective effect by inhibiting its membrane localization on the monocytes from T2D patients.

3.4. Knockdown of GPR26 Induced ROS Generation in THP1

To study the functional role of GPR26, THP-1 cells cultured in NG or HG were transfected for 24, 48, and 72 h with 50 nM of LNA single-stranded antisense oligonucleotides to knockdown GPR26, or with scrambled controls. GPR26 knockdown was confirmed by the analysis of GPR26 at mRNA and protein levels at all time points (Figure 3a). Transfection of THP-1 with LNA GapmeRs suppressed HG-mediated increase of GPR26 expression at levels lower than cells cultured with NG and transfected with scrambled controls (Figure 3a). Knockdown of GPR26 was confirmed at protein levels, in NG and HG treated THP-1 cells at 24 and 48 h (Figure 3a). No differences were visible at 72 h on GPR26 protein levels (Figure 3a). Immunofluorescence analysis confirmed that the main effect exerted by knockdown of GPR26 was in its cellular localization. Indeed, HG increased whole GPR26 levels at 24 and 48 h and decreased GPR26 at 72 h (Figure 3b). Knockdown of GPR26 inhibited the HG-mediated membrane localization and enhanced GPR26 cytoplasmic levels (Figure 3b). Taken together, these data suggested that GPR26 might be exposed on monocyte membrane to promote a mechanism of defense in monocytes, which is then inhibited by prolonged and chronic exposure to HG.

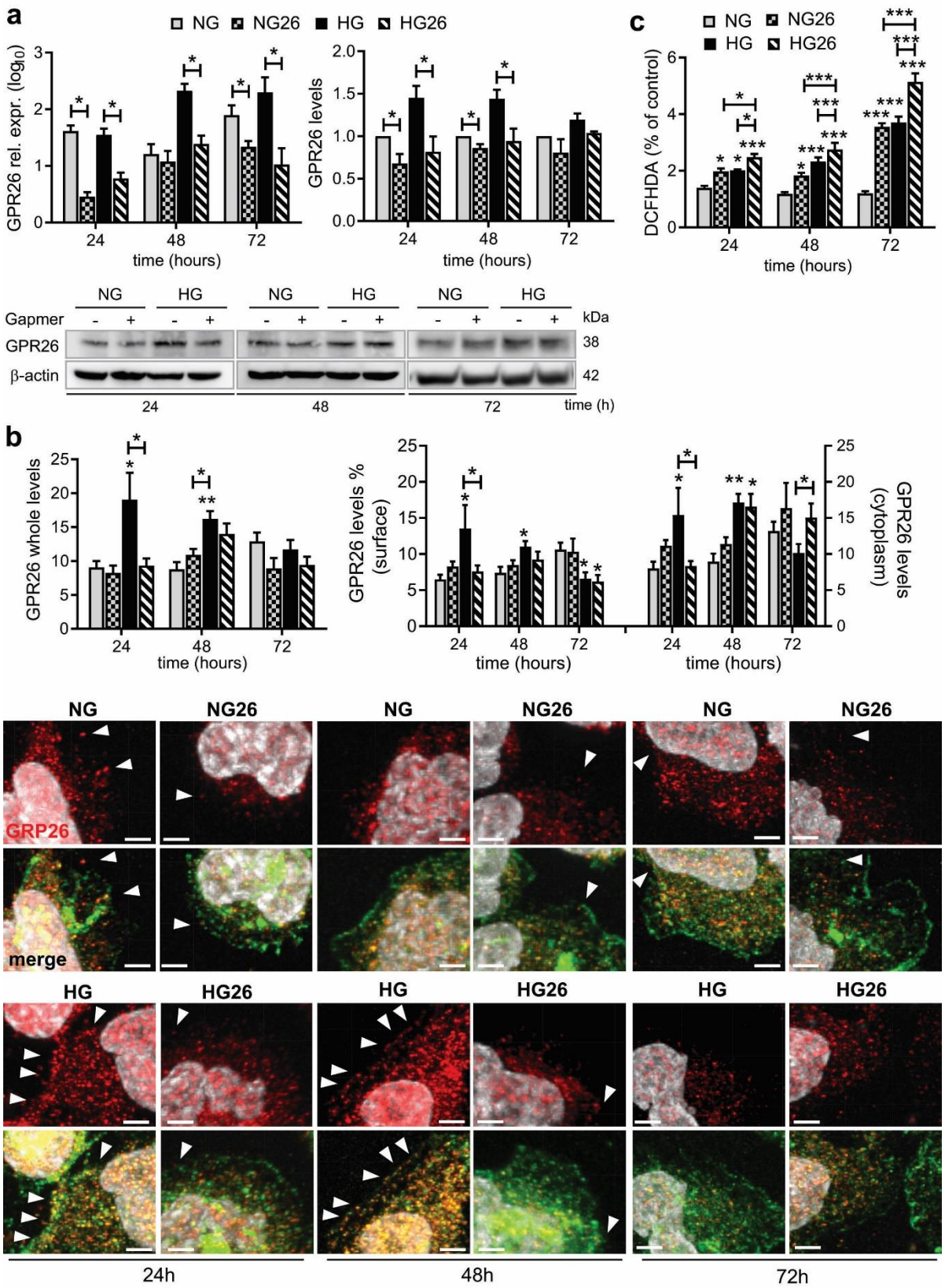

Figure 3. GPR26 levels and localization in HG-treated THP-1 transfected with GPR26 Gapmers. THP-1 were treated with NG or HG for 24, 48, and 72 h and transfected with GPR26 (+) or scrambled GapmeRs (−). (**a**) GPR26 mRNA expression was normalized to the corresponding B2M expression and expressed as relative expression (log_{10}) (**left**). Densitometry plots reporting the fold change versus control. GPR26 intensity values were normalized to the corresponding β-actin value (**right**).

(**b**) Confocal laser scanning microscopy images of THP-1 stained for GPR26 to analyze GPR26 whole levels, cytoplasmic, and membrane localization levels. White arrowhead indicates GPR26 localizing at the membrane surface. GPR26 levels were normalized to the cell surface, and then on total number of the cells. All values are represented as mean of at least 3 independent experiments ($n = 3 \pm$ SEM). (**c**) Intracellular ROS production. Data are expressed as percentage (%) of DCFH-DA fluorescence intensity relative to control. All values are represented as mean of at least 3 independent experiments. Scale bar: 5 μm. * $p < 0.05$; ** $p < 0.01$; *** $p < 0.001$ versus NG.

Accumulating evidence indicates that high levels of glucose promote dysfunctional monocyte activation, characterized by an increased inflammatory and apoptotic activity, partly by enhancing the production and accumulation of reactive oxygen species (ROS). To study the role of GPR26 on HG-mediated production of ROS, GPR26 was knocked down in THP-1 cells treated with NG or HG for 24, 48, and 72 h. Accordingly, we confirmed that HG increased ROS levels in HG-induced THP-1 cells compared to NG throughout the entire 72 h (Figure 3c). Knockdown of GPR26 exacerbated ROS production in a time dependent manner (Figure 3c), and enhanced HG-mediated ROS production (Figure 3c). Taken together, these data indicated that GPR26 played a protective role against the formation of free radical oxygen species, the production of which is enhanced by HG through the inhibition of GPR26 exposure on monocyte membrane and through GPR26 cytoplasmic localization.

3.5. Knockdown of GPR26 Increased ERK1/2 and p38 MAPK Activation in THP1 Cells

High levels of glucose can promote the activation of the MAPK signaling pathway, including p38 and ERK1/2, to promote monocytes-endothelial cell adhesion [38,39]. Moreover, recent findings indicate that ERK1/2 is regulated in response to the activation of various types of GPCRs [40,41], and that GPCRs mediate p38 MAPK activation to control monocyte inflammatory gene expression [42,43]. To explore whether GPR26 affected p38 and ERK1/2 activation, we assessed the levels of phosphorylated ERK1/2 and p38 by western blot, in THP-1 transfected with GPR26 GapmeRs, alone or in combination with NG or HG. Our results indicated that knockdown of GPR26 enhanced ERK1/2 and p38 MAPK activation in NG-cultured THP-1 at all time points (Figure 4a,b). ERK1/2 activation was increased in HG-treated THP-1 cells at 24 and 48 h. However, ERK1/2 activation persisted at 72 h only in HG-induced THP-1 cells where GPR26 was knocked down (Figure 4a).

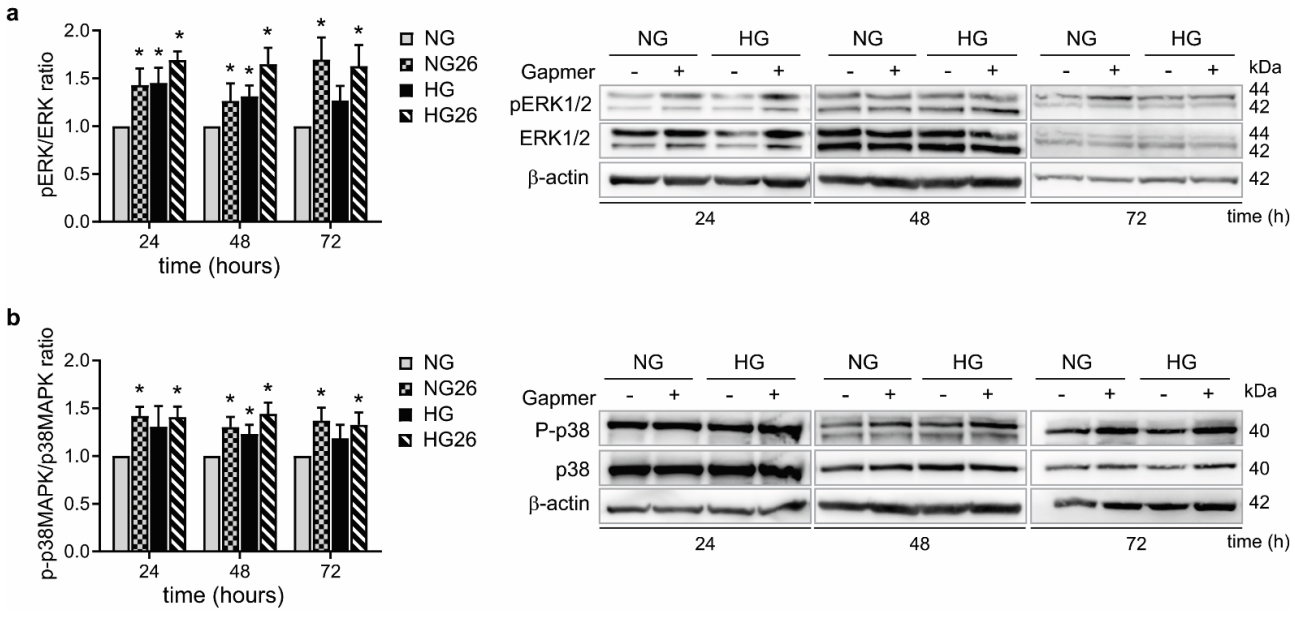

Figure 4. The effect of GPR26 knockdown alone or in combination with HG on ERK1/2 and p38 MAPK activation. THP-1 were treated and transfected for 24, 48, and 72 h with GPR26 (+) or scrambled

GapmeRs (−), as indicated in the figures. (**a**) A representative Western blot of ERK1/2 and p-ERK1/2. Densitometry plot reporting the fold change versus control. ERK1/2 and p-ERK1/2 intensity values were normalized to the corresponding β-actin value and the ratio of p-ERK1/2 to ERK1/2 are presented as ERK1/2 activation. (**b**) A representative Western blot of p38 MAPK and p-p38 MAPK. Densitometry plot reporting the fold change versus control. p38 MAPK and p-p38 MAPK intensity values were normalized to the corresponding β-actin value and the ratio of p-p38 MAPK to p38 MAPK are presented as P38 MAPK activation. Images report one representative experiment out of at least 3 independent experiments. All values are represented as mean of at least 3 independent experiments ($n = 3 \pm$ SEM). * $p < 0.05$ versus NG).

Knockdown of GPR26 increased p38 MAPK activation at all time points (Figure 4b). P38 phosphorylation was promoted by HG only at 48 h, but remarkably induced at all time points when GPR26 was knocked down (Figure 4b). Taken together, these data indicate that GPR26 inhibits MAPK signaling pathways piloted by p38 and ERK1/2, independently from HG.

3.6. Knockdown of GPR26 Induced NF-κB p65 Activation and Monocyte Adhesion

Treatment of human monocytes with HG promotes the phosphorylation of p38 MAPK and ERK1/2, leading to NF-κB transactivation and related monocyte inflammatory activation [44]. GPRCs can regulate leukocyte activation and binding to the vessel wall through the endothelial-mediated expression of chemokines [45]. Despite controversy existing on the role of GPCRs as pro- or anti-inflammatory molecules, especially in diabetic patients, emerging evidence suggests that GPCRs and NF-κB might be connected in the regulation of inflammatory diseases [46].

To explore whether GPR26 affected NF-κB (p65) activation, THP-1 were transfected with GPR26 GapmeRs alone or in combination with NG or HG incubation [47]. Our results indicated that knockdown of GPR26 increased p65 expression at 24 and 48 h of NG (Figure 5a). HG and GPR26 knockdown showed similar effects on p65 activation (Figure 5a). However, p65 was enhanced at 72 h only when GPR26 was knocked down in HG-treated cells (Figure 5a). Hence, inhibition of GPR26 in diabetic patients might sustain hyperglycemia-mediated NF-κB activation.

Next, we examined the role of GPR26 on hyperglycemia-mediated monocyte inflammatory activation and adhesion to HAoECs. Accordingly, knockdown of GPR26 increased the adhesion of THP-1 to HAoECs at 48 and 72 h of NG (Figure 5b). HG-induced THP-1 adhesion to HAoECs was increased at all time points (Figure 5b). Knockdown of GPR26 enhanced the adhesion of THP-1 treated with HG compared to their respective HG-treated cells (Figure 5b). Moreover, knockdown of GPR26 enhanced the number of THP-1 cells adhering to HAoECs at all time points, especially of those co-treated with HG compared to NG (Figure 5b). Taken together, these data indicated that hyperglycemia promotes monocyte adhesion to ECs by suppressing GPR26′s anti-inflammatory role.

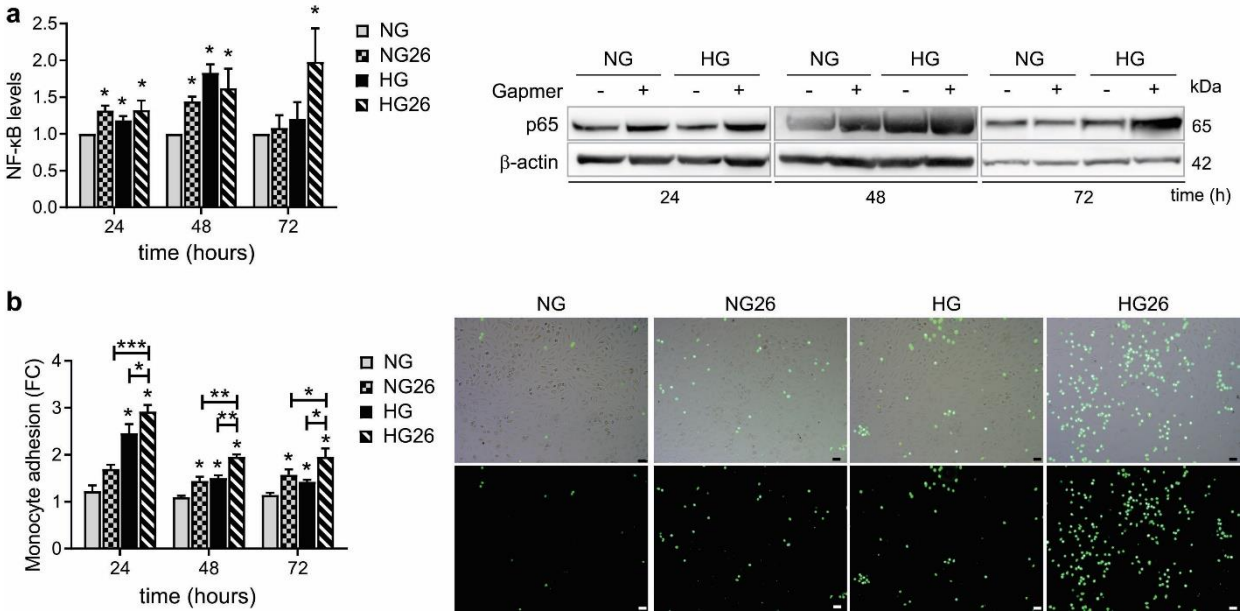

Figure 5. The effect of GPR26 knockdown and HG on NF-kB and monocyte adhesion. THP-1 were transfected with GPR26 gapmers (+) or scrambled GapmeRs (−) and treated with NG or HG to analyze NF-κβ (p65) activation and monocyte adhesion at 24, 48, and 72 h indicated in the figures. Panels show (**a**) a representative Western blot of NF-κβ. Densitometry plots reporting the fold change versus control. NF-κβ intensity values were normalized to the corresponding β-actin value. (**b**) Monocyte adhesion is reported as fold of change versus the basal adhesion of monocyte to HAoECs control (cells cultured in NG) that was set to 1. Right panels are fluorescence images of the monocytes, confirming that the small and bright spherical cells visible under microscope are indeed monocytes that were pre-labeled with Calcein AM. Images were taken using a 10X objective. All values are represented as mean of at least 3 independent experiments ($n = 3 \pm$ SEM). Scale bar: 50 μm. * $p < 0.05$; ** $p < 0.01$; *** $p < 0.001$ versus NG.

3.7. Knockdown of GPR26 Increased Caspase-3 Activity Promoted by HG

Several in vitro studies indicate that HG induces cell apoptosis in monocytes [48,49]. Caspase 3 plays a pivotal role in the apoptotic cell death process and therefore is widely used as a pro-apoptotic marker. Therefore, we investigated the effect of GPR26 knockdown, alone or in combination with HG, on THP-1 apoptosis by evaluating caspase 3 activation (cleavage of caspase 3 and its activity). Our data indicated that knockdown of GPR26 slightly affected Caspase 3 cleavage at 48 h (Figure 6a). Caspase 3 cleavage was increased when GPR26 was knocked down in THP-1 cells incubated with HG for 24 and 48 h, and the effect persisted even at 72 h (Figure 6a). HG alone significantly enhanced the ratio of cleaved caspase3 on total caspase 3 compared to NG at 24 and 48 h (Figure 6a). To confirm the functional activation of cleaved Caspase 3, we measured caspase-3 and -7 activity using an enzymatic assay. Our data indicated that knockdown of GPR26 increased Caspase 3/7 activity at levels comparable to that of HG at all time points (Figure 6b). Caspase 3/7 activity was significantly enhanced when GPR26 was knocked down in HG-treated cells at all time points (Figure 6b). These results confirmed that GPR26 plays an anti-apoptotic role and that GPR26 in monocytes might counteract HG-mediated increase of THP1 apoptosis. Indeed, inhibition of GPR26 increased the pro-apoptotic activity of caspase 3/7 mediated by HG after 72 h.

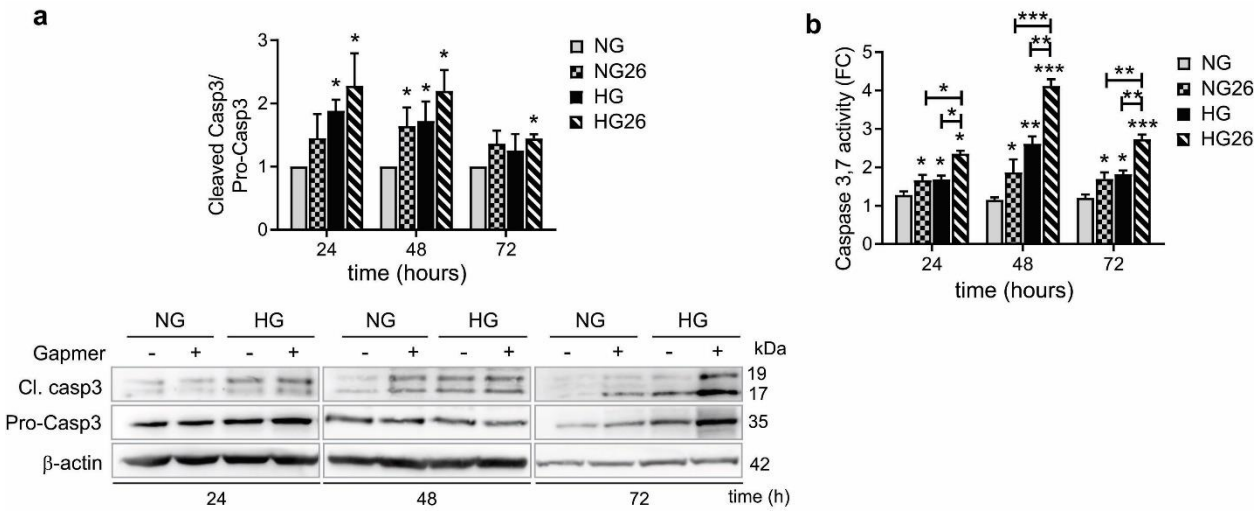

Figure 6. The effect of GPR26 knockdown and HG on Caspase 3 activity. The effect of GPR26 knockdown alone or in combination with HG on caspase activation at 24, 48, and 72 h with GPR26 (+) or scrambled GapmeRs (−), as indicated in the figures. (**a**) A representative Western blot of cleaved caspase-3 and total caspase-3. Densitometry plot reporting the fold change versus control. Cleaved caspase-3 and total caspase-3 intensity values were normalized to the corresponding β-actin value and the ratio of cleaved caspase-3 to total caspase-3 were presented as caspase activity. (**b**) Caspase 3,7 activity was measured using an enzymatic assay. Data are expressed as fold of change versus control (cells cultured in NG) that was set to 1. All values are represented as mean of at least 3 independent experiments ($n = 3 \pm$ SEM). (* $p < 0.05$ ** $p < 0.01$, *** $p < 0.001$ versus NG).

3.8. GPR26 down Regulation Significantly Inhibited Autophagy

Autophagy is an important physiological process activated to maintain cellular homeostasis and to adapt to extracellular cues. Autophagy is closely associated with ROS generation and inflammation [50]. Indeed, HG inhibits autophagy to promote ROS-mediated inflammasome activation and cytokine secretion in immune cells [50]. Microtubule-associated protein 1A/1B-light chain 3 (LC3) is a soluble protein that exists in the two forms of LC3-I and LC3-II, the second converted from LC3-I to initiate the formation and lengthening of the autophagosome. Measurement of LC3-II/LC3-I ratio consents the quantification of autophagy activation levels [51]. In addition, measurement of p62, a selective substrate of autophagy, is an additional method to measure autophagy, since it inversely correlates with the autophagy activation [52]. Thus, to explore the role of GPR26 in regulating autophagy in monocytes, we examined LC3-II/LC3-I ratio and p62 levels in THP-1 cells treated with NG or HG and transfected for 24, 48, and 72 h with GPR26 Gapmers. Our results indicated that knockdown of GPR26 decreased LC3-II/LC3-I ratio at 24 and 48 h (Figure 7a). HG decreased LC3-II at all time points compared to NG treated cells (Figure 7a). A significant decrease in LC3-II/LC3-I ratio was detected in THP-1, knocked down for GPR26, and treated with HG at 24, 48, and 72 h, a time point at which only the knockdown of GPR26 in combination with HG showed a significant effect on LC3-II decrease (Figure 7a). Next, we analyzed the levels of p62, the levels of which should inversely correlate with that of LC3-II. Accordingly, knockdown of GPR26 increased p62 levels in THP-1 cultured in NG at 24 h and 48 h (Figure 7b). HG increased p62 levels only at 48 h (Figure 7b). Knockdown of GPR26 enhanced p62 levels in HG-treated THP-1 at 24, 48, and 72 h, a time point at which neither GPR26 knockdown nor HG increased p62 levels (Figure 7b). Taken together, these data indicated that GPR26 promotes autophagy and might counteract HG-mediated autophagy inhibition. Hence, hyperglycemia might impair GPR26 to inhibit autophagy in monocytes.

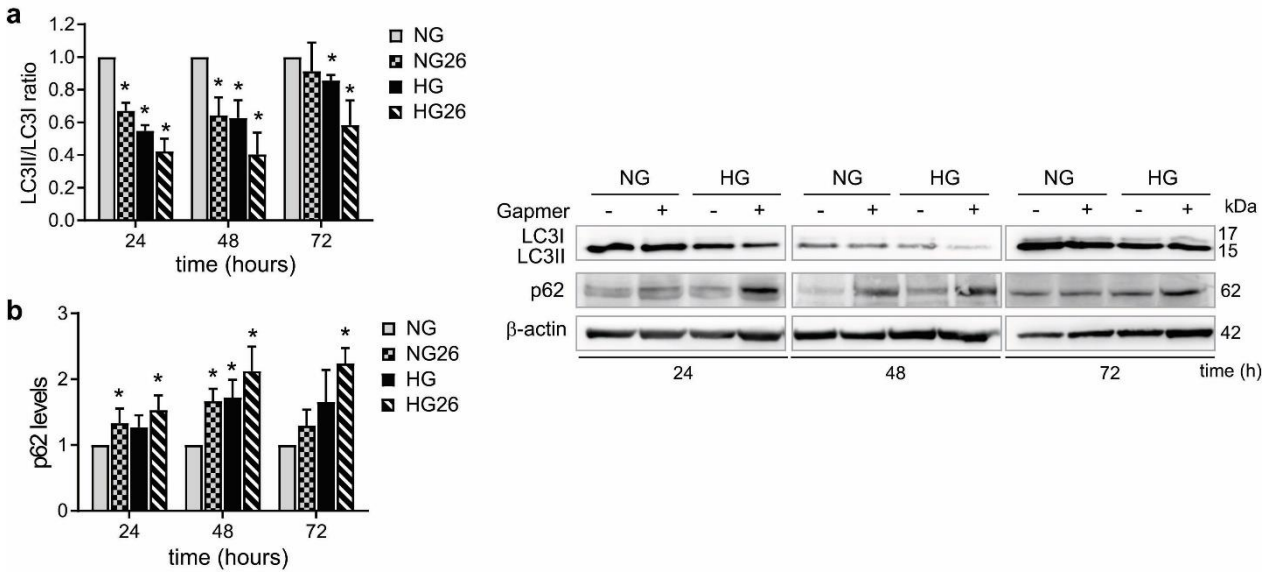

Figure 7. The effect of GPR26 knockdown and HG on autophagy. The effect of GPR26 knockdown alone or in combination with HG on autophagy at 24, 48, and 72 h with GPR26 (+) or scrambled GapmeRs (−), indicated in the figures. Panels show (**a**,**b**) a representative Western blot of LC3II, LC3I, and p62. Densitometry plot reporting the fold change versus control. LC3II, LC3I, and p62 intensity values were normalized to the corresponding β-actin value. The ratio of LC3II, LC3I were presented as the levels of activated autophagy. Images report one representative experiment out of at least 3 independent experiments. All values are represented as mean of at least 3 independent experiments ($n = 3 \pm$ SEM). * $p < 0.05$; versus NG.

4. Discussion

Diabetes is among the top 10 leading causes of death worldwide (WHO, https://www.who.int/news-room/fact-sheets/detail/the-top-10-causes-of-death, last accessed on 1 June 2022). T2D is one of the major public health diseases diffused in Iran, the Middle East's second-largest country, due to its high prevalence rate [53]. Inflammation plays a crucial role in the pathogenesis of T2D and related complications [2,5]. The dysregulation of immune cells is strongly linked to T2D and vascular complications. Vascular inflammation is thought to be regulated by changes in monocyte and macrophage numbers, function, and related imbalance of pro-inflammatory signaling cascade [5]. Hyperglycemia acts as a strong activator of inflammatory response by activating endothelial cells and by dysregulating monocyte activation, leading to a chronic pro-inflammatory phenotype in monocytes and immune cells [2,5].

GPCRs play pivotal roles in a wide variety of immunological processes and are the target of nearly a third of all clinically utilized drugs [17]. Recently, several GPCRs involved in the development of insulin resistance and pancreatic β-cell dysfunction, such as GPR119, GPR146, GPR40, GPR120, and TGR5, have received attention as targets for therapeutic interventions in diabetic patients [54–56]. Although the mechanisms by which GPCRs regulate insulin sensitivity and immunological processes are unknown, the existence of GPCRs receptors as a very large and conserved family suggests that they might potentially modulate the response of immune cells in pathologies such as diabetes, atherosclerosis, and chronic inflammatory disease [17].

Accordingly, emerging studies on GPCRs, especially on orphan GPCRs, indicates their involvement in the regulation of immune cells biology and function [57]. For example, GPCR MRGPRX2 is expressed by monocytes to activate the intracellular pathways for an immunomodulatory action, leading to monocyte interaction with endothelial cells [58–60]. Our data indicated that orphan GPR26 is downregulated in diabetic patients and might be initially activated in monocytes and PBMCs to counteract the pro-inflammatory and apop-

totic activation mediated by hyperglycemia. Chronic and prolonged exposure of monocytes to hyperglycemia impaired GPR26 protective effects and lead to its internalization and ineffective activation. Despite GPR26 ligand and mechanism of action needing to be further investigated, it emerged as a promising target to develop therapeutic strategies against inflammatory and diabetic diseases.

Analysis of GWAS studies from diabetic patients indicated that occurrence of certain SNPs in GPCRs are associated with an increased risk for diabetes and cardiovascular complications [33]. In addition, recent studies indicated that certain GPCRs are differentially regulated in diabetic patients [17–20]. However, the majority of these GPCRs are orphan receptors, for which the mechanism of action in diabetes and related complications is still unknown. In this study, we used GWAS studies to identify potential GPCR candidates with diabetes-associated SNPs and differentially expressed in diabetic samples. We selected orphan GPR26 as a promising candidate, presenting certain SNPs and downregulated in the blood samples from T2D patients. GPR26 is a central orphan GPCR that is most closely related to the serotonin receptor 5-HT5A and gastrin releasing hormone BB2 receptor, suggesting a possible role in the regulation of energy homeostasis and cell metabolism [61,62]. So far, the knowledge we have on GPR26 role belong to studies from *Caenorabditis elegans*, where depletion of GPR26 increases fat storage, and from rodents, where GPR26 deficiency in the hypothalamus increases genetic susceptibility to the onset of obesity, including glucose intolerance, hyperinsulinemia, and dyslipidemia (61). However, data regarding the role of GPR26 in diabetes and inflammatory associated complications are missing. We analyzed the expression of orphan GPR26 in the PBMC isolated from T2D patients and confirmed that GPR26 was downregulated. However, GPR26 expression was initially enhanced in human monocytes (THP-1) and human PBMCs treated with HG, a surrogate of hyperglycemia, whereas it was decreased when cells were exposed to prolonged and chronic HG levels. Two hypotheses were generated to explain these results. First, the group of diabetic patients was composed of insulin and non-insulin treated patients, which might have influenced the expression of GPR26. Second, GPR26 might be initially activated to protect monocytes against HG, whereas prolonged and chronic monocyte exposure to HG might impair GPR26 protective role. Our data indicated that both hypotheses might be reliable. Indeed, when diabetic patients were divided according to their insulin treatment, we found that GPR26 expression was further downregulated in insulin patients compared to non-insulin treated patients. This data might be due to insulin-mediated alleviation of hyperglycemic adverse effects on monocyte activation. In line with this, we noticed that the expression of GPR26 negatively correlated with the BMI and HbA1c percentage in diabetic and non-diabetic subjects. In addition, GPR26 exposure on monocyte membranes was decreased by chronic levels of HG, whereas GPR26 accumulated in the cytoplasm. Hence, these data supported the hypothesis that GPR26 might be activated to protect monocytes against hyperglycemia-mediated detrimental effects.

In the diabetic state, chronic or intermittent hyperglycemia promotes a phenotype named "glucose toxicity", which is often associated with an imbalance of the cellular redox state, inflammation, and related apoptosis [63]. Indeed, several signaling pathways are altered and promote the formation of ROS, as well as the secretion of pro-inflammatory cytokines and cellular death (pathological autophagy and/or apoptosis). ROS plays a pivotal roles in triggering all these diabetic complications [63]. Accordingly, we investigated the role of GPR26 against all these HG-related complications. Our data indicated that orphan GPR26 knockdown promoted ROS production, MAPK-related inflammatory activation, monocyte adhesion, and apoptosis. Autophagy, commonly activated in immune cells to regulate inflammation following oxidative injury in diabetes [64], was impaired by GPR26 knockdown. Hence, our data revealed that GPR26 tightly regulates all crucial pathways related to monocyte cell biology and metabolism. Our data indicated that GPR26 protected monocytes from HG-mediated increase of inflammation and ROS production.

Previous studies showed that elevated ROS production leads to p38 MAPK andERK1/2 activation, which in turn promotes NF-κB-mediated transcription of pro-inflammatory genes

and monocyte activation [38,44]. Our data indicated that lack of GPR26 protection under chronic hyperglycemic conditions enhanced MAPK and NF-κB activation. Hence, these data supported our hypothesis about GPR26′s protective role against T2D.

ROS induced -p38 MAPK and ERK1/2 activation results in caspase 3 activation and apoptotic cell death [65], despite several in vitro studies indicating that HG induces cell apoptosis in monocytes [48,49], Contradictory data exist regarding the role of apoptosis in monocytes from diabetic patients [12,13]. Indeed, inhibition of monocyte apoptosis impedes wound healing in diabetic mice, but it also promotes the development of diabetic complications in T1D patients [12,13]. Our data indicated that knockdown of GPR26 increased apoptosis and enhanced HG-mediated Caspase 3 activation, suggesting that GPR26 plays an anti-apoptotic role against HG.

Autophagy is fundamental to maintain cell homeostasis, removal of ROS, and inflammation [50]. Our results provided evidence that orphan GPR26 might play a protective role against HG by activating autophagy. Moreover, we identified a new role for GPR26 in promoting autophagy that is independent from HG. Although we did not investigate the mechanism in detail, HG and GPR26 might influence autophagic flux partly through p38 MAPK.

To the best of our knowledge, this is the first work demonstrating the expression and role of orphan GPR26 in monocytes from diabetic patients. Although additional data are needed to prove the protective role of GPR26 against T2D in vivo, we started to depict possible signaling pathways differentially regulated by GPR26 in THP1, independently or not from HG.

Indeed, our study has some limitations. Expression assay of GPR26 in PBMCs of diabetic patients was performed in limited samples, and future studies with a large number of samples are needed to confirm our results. Moreover, analysis of GPR26 expression and function in other cell types related to diabetes and cardiovascular complications, such as endothelial cells that are closely related to immune cell activation in diabetic patients, could provide more information and better clarify the role of GPR26 in T2D. Since the ligands of GPR26 are still unknown, future studies devoted to their identification might offer the basis for modulating the expression and activation of GPR26 in T2D patients.

5. Conclusions

The results obtained in the present study defined a new role for GPR26 in human monocytes and PBMCs in T2D patients. Our data suggested that THP1 might initially activate a mechanism of defense in response to hyperglycemia, which is partly mediated by a positive feedback loop that involves GPR26 activation. The protective effect might be impaired by chronic and intermittent hyperglycemic conditions. Treatment of T2D patients with insulin might counteract HG-mediated pathological activation of monocytes, a phenomenon partly reflected from a reduction in GPR26 expression. Moreover, our data suggested that GPR26 exerts a protective role independently from HG by inhibiting pro-inflammatory monocyte activation, ROS production, and apoptosis.

Supplementary Materials: The following are available online at https://www.mdpi.com/article/10.3390/biomedicines10071736/s1, Table S1: Sequence of primers against the human genes analyzed by qPCR; Table S2: List of antibodies for western blot (WB); File S1: GPR26 assotiations-Microarray values blood GPCRs from GWAS SNP; File S2: GPR26 assotiations; File S3: KEGG predicted pathways.

Author Contributions: Z.A.K. researched data and wrote the manuscript. L.N. contributed to discussion and edited the manuscript. S.S. contributed to sample collections. M.a.B. contributed to sample collections and reviewed the manuscript. C.W. contributed to reviewed/edited the manuscript. M.B. contributed to reviewed/edited the manuscript. All authors have read and agreed to the published version of the manuscript.

Funding: Funding for the present work was provided by Zahra Abedi Kichi, from the Deutsche Forschungsgemeinschaft (DFG), TRR267, and SFB1123 to C.W. and L.N.

Institutional Review Board Statement: The study was conducted in accordance with the Declaration of Helsinki, and approved by the Institutional Review Board (or Ethics Committee) of Tarbiat Modares University (protocol code REC.1397.109, date of approval: 17 October 2018).

Informed Consent Statement: Informed consent was obtained from all subjects involved in the study.

Data Availability Statement: C.W. and M.B. had full access to all data in the study and take responsibility for the integrity of data and accuracy of the data analysis.

Conflicts of Interest: The authors declare no conflict of interest.

References

1. American Diabetes, A. Diagnosis and classification of diabetes mellitus. *Diabetes Care* **2014**, *37* (Suppl. S1), S81–S90. [CrossRef] [PubMed]
2. Altabas, V. Diabetes, Endothelial Dysfunction, and Vascular Repair: What Should a Diabetologist Keep His Eye on? *Int. J. Endocrinol.* **2015**, *2015*, 848272. [CrossRef] [PubMed]
3. Pi, X.; Xie, L.; Patterson, C. Emerging Roles of Vascular Endothelium in Metabolic Homeostasis. *Circ. Res.* **2018**, *123*, 477–494. [CrossRef] [PubMed]
4. Natarelli, L.; Ranaldi, G.; Leoni, G.; Roselli, M.; Guantario, B.; Comitato, R.; Ambra, R.; Cimino, F.; Speciale, A.; Virgili, F.; et al. Nanomolar Caffeic Acid Decreases Glucose Uptake and the Effects of High Glucose in Endothelial Cells. *PLoS ONE* **2015**, *10*, e0142421. [CrossRef]
5. Kanter, J.E.; Hsu, C.C.; Bornfeldt, K.E. Monocytes and Macrophages as Protagonists in Vascular Complications of Diabetes. *Front. Cardiovasc. Med.* **2020**, *7*, 10. [CrossRef]
6. Dorenkamp, M.; Muller, J.P.; Shanmuganathan, K.S.; Schulten, H.; Muller, N.; Loffler, I.; Muller, U.A.; Wolf, G.; Bohmer, F.D.; Godfrey, R.; et al. Hyperglycaemia-induced methylglyoxal accumulation potentiates VEGF resistance of diabetic monocytes through the aberrant activation of tyrosine phosphatase SHP-2/SRC kinase signalling axis. *Sci. Rep.* **2018**, *8*, 14684. [CrossRef]
7. Pavlou, S.; Lindsay, J.; Ingram, R.; Xu, H.; Chen, M. Sustained high glucose exposure sensitizes macrophage responses to cytokine stimuli but reduces their phagocytic activity. *BMC Immunol.* **2018**, *19*, 24. [CrossRef]
8. Galicia-Garcia, U.; Benito-Vicente, A.; Jebari, S.; Larrea-Sebal, A.; Siddiqi, H.; Uribe, K.B.; Ostolaza, H.; Martín, C. Pathophysiology of Type 2 Diabetes Mellitus. *Int. J. Mol. Sci.* **2020**, *21*, 6275. [CrossRef]
9. Fratantonio, D.; Speciale, A.; Canali, R.; Natarelli, L.; Ferrari, D.; Saija, A.; Virgili, F.; Cimino, F. Low nanomolar caffeic acid attenuates high glucose-induced endothelial dysfunction in primary human umbilical-vein endothelial cells by affecting NF-kappaB and Nrf2 pathways. *BioFactors* **2017**, *43*, 54–62. [CrossRef]
10. Nandy, D.; Janardhanan, R.; Mukhopadhyay, D.; Basu, A. Effect of hyperglycemia on human monocyte activation. *J. Investig. Med. Off. Publ. Am. Fed. Clin. Res.* **2011**, *59*, 661–667. [CrossRef]
11. Pezhman, L.; Tahrani, A.; Chimen, M. Dysregulation of Leukocyte Trafficking in Type 2 Diabetes: Mechanisms and Potential Therapeutic Avenues. *Front. Cell Dev. Biol.* **2021**, *9*, 624184. [CrossRef] [PubMed]
12. Myśliwska, J.; Ryba-Stanisławowska, M.; Smardzewski, M.; Słomiński, B.; Myśliwiec, M.; Siebert, J. Enhanced Apoptosis of Monocytes from Complication-Free Juvenile-Onset Diabetes Mellitus Type 1 May Be Ameliorated by TNF-α Inhibitors. *Mediat. Inflamm.* **2014**, *2014*, 946209. [CrossRef] [PubMed]
13. Pang, J.; Maienschein-Cline, M.; Koh, T.J. Reduced apoptosis of monocytes and macrophages is associated with their persistence in wounds of diabetic mice. *Cytokine* **2021**, *142*, 155516. [CrossRef] [PubMed]
14. Oh, D.Y.; Lagakos, W.S. The role of G-protein-coupled receptors in mediating the effect of fatty acids on inflammation and insulin sensitivity. *Curr. Opin. Clin. Nutr. Metab. Care* **2011**, *14*, 322–327. [CrossRef]
15. Lattin, J.E.; Schroder, K.; Su, A.I.; Walker, J.R.; Zhang, J.; Wiltshire, T.; Saijo, K.; Glass, C.K.; Hume, D.A.; Kellie, S.; et al. Expression analysis of G Protein-Coupled Receptors in mouse macrophages. *Immunome Res.* **2008**, *4*, 5. [CrossRef]
16. Lattin, J.; Zidar, D.A.; Schroder, K.; Kellie, S.; Hume, D.A.; Sweet, M.J. G-protein-coupled receptor expression, function, and signaling in macrophages. *J. Leukoc. Biol.* **2007**, *82*, 16–32. [CrossRef]
17. Wang, X.; Iyer, A.; Lyons, A.B.; Korner, H.; Wei, W. Emerging Roles for G-protein Coupled Receptors in Development and Activation of Macrophages. *Front. Immunol.* **2019**, *10*, 2031. [CrossRef]
18. Ruiz-Hernandez, A.; Sanchez-Munoz, F.; Rodriguez, J.; Calderon-Zamora, L.; Romero-Nava, R.; Huang, F.; Hong, E.; Villafana, S. Expression of orphan receptors GPR22 and GPR162 in streptozotocin-induced diabetic rats. *J. Recept. Signal Transduct. Res.* **2015**, *35*, 46–53. [CrossRef]
19. Ruiz-Hernandez, A.; Romero-Nava, R.; Huang, F.; Hong, E.; Villafana, S. Altered function and expression of the orphan GPR135 at the cardiovascular level in diabetic Wistar rats. *J. Recept. Signal Transduct. Res.* **2018**, *38*, 484–491. [CrossRef]
20. Calderon-Zamora, L.; Ruiz-Hernandez, A.; Romero-Nava, R.; Leon-Sicairos, N.; Canizalez-Roman, A.; Hong, E.; Huang, F.; Villafana, S. Possible involvement of orphan receptors GPR88 and GPR124 in the development of hypertension in spontaneously hypertensive rat. *Clin. Exp. Hypertens.* **2017**, *39*, 513–519. [CrossRef]
21. Tang, X.-l.; Wang, Y.; Li, D.-l.; Luo, J.; Liu, M.-y. Orphan G protein-coupled receptors (GPCRs): Biological functions and potential drug targets. *Acta Pharmacol. Sin.* **2012**, *33*, 363–371. [CrossRef]

22. Ghislain, J.; Poitout, V. Targeting lipid GPCRs to treat type 2 diabetes mellitus—Progress and challenges. *Nat. Rev. Endocrinol.* **2021**, *17*, 162–175. [CrossRef] [PubMed]
23. Moreno-Navarrete, J.M.; Catalan, V.; Whyte, L.; Diaz-Arteaga, A.; Vazquez-Martinez, R.; Rotellar, F.; Guzman, R.; Gomez-Ambrosi, J.; Pulido, M.R.; Russell, W.R.; et al. The L-alpha-lysophosphatidylinositol/GPR55 system and its potential role in human obesity. *Diabetes* **2012**, *61*, 281–291. [CrossRef] [PubMed]
24. Lipina, C.; Walsh, S.K.; Mitchell, S.E.; Speakman, J.R.; Wainwright, C.L.; Hundal, H.S. GPR55 deficiency is associated with increased adiposity and impaired insulin signaling in peripheral metabolic tissues. *FASEB J. Off. Publ. Fed. Am. Soc. Experimental Biol.* **2019**, *33*, 1299–1312. [CrossRef] [PubMed]
25. Verhulst, P.J.; Lintermans, A.; Janssen, S.; Loeckx, D.; Himmelreich, U.; Buyse, J.; Tack, J.; Depoortere, I. GPR39, a receptor of the ghrelin receptor family, plays a role in the regulation of glucose homeostasis in a mouse model of early onset diet-induced obesity. *J. Neuroendocrinol.* **2011**, *23*, 490–500. [CrossRef] [PubMed]
26. Rouillard, A.D.; Gundersen, G.W.; Fernandez, N.F.; Wang, Z.; Monteiro, C.D.; McDermott, M.G.; Ma'ayan, A. The harmonizome: A collection of processed datasets gathered to serve and mine knowledge about genes and proteins. *Database* **2016**, *2016*, 100. [CrossRef] [PubMed]
27. Castro-Mondragon, J.A.; Riudavets-Puig, R.; Rauluseviciute, I.; Lemma, R.B.; Turchi, L.; Blanc-Mathieu, R.; Lucas, J.; Boddie, P.; Khan, A.; Manosalva Pérez, N.; et al. JASPAR 2022: The 9th release of the open-access database of transcription factor binding profiles. *Nucleic Acids Res.* **2022**, *50*, D165–D173. [CrossRef]
28. Kanehisa, M.; Furumichi, M.; Sato, Y.; Ishiguro-Watanabe, M.; Tanabe, M. KEGG: Integrating viruses and cellular organisms. *Nucleic Acids Res.* **2021**, *49*, D545–D551. [CrossRef]
29. Jensen, L.J.; Kuhn, M.; Stark, M.; Chaffron, S.; Creevey, C.; Muller, J.; Doerks, T.; Julien, P.; Roth, A.; Simonovic, M.; et al. STRING 8—A global view on proteins and their functional interactions in 630 organisms. *Nucleic Acids Res.* **2009**, *37*, D412–D416. [CrossRef]
30. Livak, K.J.; Schmittgen, T.D. Analysis of relative gene expression data using real-time quantitative PCR and the $2^{-\Delta\Delta CT}$ Method. *Methods* **2001**, *25*, 402–408. [CrossRef]
31. Ramirez, S.H.; Heilman, D.; Morsey, B.; Potula, R.; Haorah, J.; Persidsky, Y. Activation of peroxisome proliferator-activated receptor gamma (PPARgamma) suppresses Rho GTPases in human brain microvascular endothelial cells and inhibits adhesion and transendothelial migration of HIV-1 infected monocytes. *J. Immunol.* **2008**, *180*, 1854–1865. [CrossRef] [PubMed]
32. Zheng, Y.; Ley, S.H.; Hu, F.B. Global aetiology and epidemiology of type 2 diabetes mellitus and its complications. *Nat. Rev. Endocrinol.* **2018**, *14*, 88–98. [CrossRef] [PubMed]
33. Divers, J.; Palmer, N.D.; Langefeld, C.D.; Brown, W.M.; Lu, L.; Hicks, P.J.; Smith, S.C.; Xu, J.; Terry, J.G.; Register, T.C.; et al. Genome-wide association study of coronary artery calcified atherosclerotic plaque in African Americans with type 2 diabetes. *BMC Genet.* **2017**, *18*, 105. [CrossRef] [PubMed]
34. Basith, S.; Cui, M.; Macalino, S.J.Y.; Park, J.; Clavio, N.A.B.; Kang, S.; Choi, S. Exploring G Protein-Coupled Receptors (GPCRs) Ligand Space via Cheminformatics Approaches: Impact on Rational Drug Design. *Front. Pharmacol.* **2018**, *9*, 128. [CrossRef] [PubMed]
35. Karolina, D.S.; Armugam, A.; Tavintharan, S.; Wong, M.T.; Lim, S.C.; Sum, C.F.; Jeyaseelan, K. MicroRNA 144 impairs insulin signaling by inhibiting the expression of insulin receptor substrate 1 in type 2 diabetes mellitus. *PLoS ONE* **2011**, *6*, e22839. [CrossRef]
36. Hansen, M.D.; Johnsen, I.B.; Stiberg, K.A.; Sherstova, T.; Wakita, T.; Richard, G.M.; Kandasamy, R.K.; Meurs, E.F.; Anthonsen, M.W. Hepatitis C virus triggers Golgi fragmentation and autophagy through the immunity-related GTPase M. *Proc. Natl. Acad. Sci. USA* **2017**, *114*, E3462–E3471. [CrossRef]
37. Someya, A.; Moss, J.; Nagaoka, I. The guanine nucleotide exchange protein for ADP-ribosylation factor 6, ARF-GEP100/BRAG2, regulates phagocytosis of monocytic phagocytes in an ARF6-dependent process. *J. Biol. Chem.* **2010**, *285*, 30698–30707. [CrossRef]
38. Li, M.; Zhang, X.; Yu, J.; Wu, X.; Sun, L. Monocyte-Derived Procoagulant Microvesicles Induced by High Glucose Can Be Attenuated by the Antioxidant N-Acetyl-L-Cysteine, Partly Through the P38/MAPK Pathway. *Metab. Syndr. Relat. Disord.* **2017**, *15*, 521–526. [CrossRef]
39. Shanmugam, N.; Reddy, M.A.; Guha, M.; Natarajan, R. High glucose-induced expression of proinflammatory cytokine and chemokine genes in monocytic cells. *Diabetes* **2003**, *52*, 1256–1264. [CrossRef]
40. Leroy, D.; Missotten, M.; Waltzinger, C.; Martin, T.; Scheer, A. G protein-coupled receptor-mediated ERK1/2 phosphorylation: Towards a generic sensor of GPCR activation. *J. Recept. Signal Transduct. Res.* **2007**, *27*, 83–97. [CrossRef]
41. Liu, P.; Yin, Y.L.; Wang, T.; Hou, L.; Wang, X.X.; Wang, M.; Zhao, G.G.; Shi, Y.; Xu, H.E.; Jiang, Y. Ligand-induced activation of ERK1/2 signaling by constitutively active Gs-coupled 5-HT receptors. *Acta Pharmacol. Sin.* **2019**, *40*, 1157–1167. [CrossRef] [PubMed]
42. Devaraj, S.; Venugopal, S.K.; Singh, U.; Jialal, I. Hyperglycemia induces monocytic release of interleukin-6 via induction of protein kinase c-α and-β. *Diabetes* **2005**, *54*, 85–91. [CrossRef] [PubMed]
43. Sharmin, O.; Abir, A.H.; Potol, A.; Alam, M.; Banik, J.; Rahman, A.; Tarannum, N.; Wadud, R.; Habib, Z.F.; Rahman, M. Activation of GPR35 protects against cerebral ischemia by recruiting monocyte-derived macrophages. *Sci. Rep.* **2020**, *10*, 9400. [CrossRef] [PubMed]

44. Dasu, M.R.; Devaraj, S.; Jialal, I. High glucose induces IL-1beta expression in human monocytes: Mechanistic insights. *Am. J. Physiol. Endocrinol. Metab.* **2007**, *293*, E337–E346. [CrossRef]
45. Mauersberger, C.; Hinterdobler, J.; Schunkert, H.; Kessler, T.; Sager, H.B. Where the Action Is—Leukocyte Recruitment in Atherosclerosis. *Front. Cardiovasc. Med.* **2022**, *8*, 2091. [CrossRef]
46. Fraser, C.C. G protein-coupled receptor connectivity to NF-kappaB in inflammation and cancer. *Int. Rev. Immunol.* **2008**, *27*, 320–350. [CrossRef]
47. Dai, J.; Jiang, C.; Chen, H.; Chai, Y. Rapamycin Attenuates High Glucose-Induced Inflammation Through Modulation of mTOR/NF-kappaB Pathways in Macrophages. *Front. Pharmacol.* **2019**, *10*, 1292. [CrossRef]
48. Anandan, V.; Thankayyan Retnabai, S.K.; Jaleel, A.; Thulaseedharan, T.; Mullasari, A.; Pillai, M.R.; Kartha, C.C.; Ramachandran, S. Cyclophilin A induces macrophage apoptosis and enhances atherosclerotic lesions in high-fat diet-fed hyperglycemic rabbits. *FASEB Bioadv.* **2021**, *3*, 305–322. [CrossRef]
49. Tseng, H.H.; Vong, C.T.; Kwan, Y.W.; Lee, S.M.; Hoi, M.P. TRPM2 regulates TXNIP-mediated NLRP3 inflammasome activation via interaction with p47 phox under high glucose in human monocytic cells. *Sci. Rep.* **2016**, *6*, 35016. [CrossRef]
50. Dai, J.; Zhang, X.; Li, L.; Chen, H.; Chai, Y. Autophagy Inhibition Contributes to ROS-Producing NLRP3-Dependent Inflammasome Activation and Cytokine Secretion in High Glucose-Induced Macrophages. *Cell. Physiol. Biochem. Int. J. Exp. Cell. Physiol. Biochem. Pharmacol.* **2017**, *43*, 247–256. [CrossRef]
51. Lee, J.H.; Parveen, A.; Do, M.H.; Kang, M.C.; Yumnam, S.; Kim, S.Y. Molecular mechanisms of methylglyoxal-induced aortic endothelial dysfunction in human vascular endothelial cells. *Cell Death Dis.* **2020**, *11*, 403. [CrossRef] [PubMed]
52. Chen, F.; Chen, B.; Xiao, F.Q.; Wu, Y.T.; Wang, R.H.; Sun, Z.W.; Fu, G.S.; Mou, Y.; Tao, W.; Hu, X.S.; et al. Autophagy protects against senescence and apoptosis via the RAS-mitochondria in high-glucose-induced endothelial cells. *Cell. Physiol. Biochem. Int. J. Exp. Cell. Physiol. Biochem. Pharmacol.* **2014**, *33*, 1058–1074. [CrossRef] [PubMed]
53. Mohseni, M.; Shams Ghoreishi, T.; Houshmandi, S.; Moosavi, A.; Azami-Aghdash, S.; Asgarlou, Z. Challenges of managing diabetes in Iran: Meta-synthesis of qualitative studies. *BMC Health Serv. Res.* **2020**, *20*, 534. [CrossRef]
54. Kolar, G.R.; Grote, S.M.; Yosten, G.L. Targeting orphan G protein-coupled receptors for the treatment of diabetes and its complications: C-peptide and GPR146. *J. Intern. Med.* **2017**, *281*, 25–40. [CrossRef]
55. Hara, T.; Hirasawa, A.; Ichimura, A.; Kimura, I.; Tsujimoto, G. Free fatty acid receptors FFAR1 and GPR120 as novel therapeutic targets for metabolic disorders. *J. Pharm. Sci.* **2011**, *100*, 3594–3601. [CrossRef]
56. Sloop, K.W.; Emmerson, P.J.; Statnick, M.A.; Willard, F.S. The current state of GPCR-based drug discovery to treat metabolic disease. *Br. J. Pharmacol.* **2018**, *175*, 4060–4071. [CrossRef]
57. Sun, L.; Ye, R.D. Role of G protein-coupled receptors in inflammation. *Acta Pharmacol. Sin.* **2012**, *33*, 342–350. [CrossRef] [PubMed]
58. Shurtz-Swirski, R.; Sela, S.; Herskovits, A.T.; Shasha, S.M.; Shapiro, G.; Nasser, L.; Kristal, B. Involvement of peripheral polymorphonuclear leukocytes in oxidative stress and inflammation in type 2 diabetic patients. *Diabetes Care* **2001**, *24*, 104–110. [CrossRef]
59. Thomas-Ecker, S.; Lindecke, A.; Hatzmann, W.; Kaltschmidt, C.; Zanker, K.S.; Dittmar, T. Alteration in the gene expression pattern of primary monocytes after adhesion to endothelial cells. *Proc. Natl. Acad. Sci. USA* **2007**, *104*, 5539–5544. [CrossRef]
60. Duraisamy, K.; Singh, K.; Kumar, M.; Lefranc, B.; Bonnafé, E.; Treilhou, M.; Leprince, J.; Chow, B.K. P17 induces chemotaxis and differentiation of monocytes via MRGPRX2-mediated mast cell–line activation. *J. Allergy Clin. Immunol.* **2021**, *149*, 275–291. [CrossRef]
61. Chen, D.; Liu, X.; Zhang, W.; Shi, Y. Targeted inactivation of GPR26 leads to hyperphagia and adiposity by activating AMPK in the hypothalamus. *PloS ONE* **2012**, *7*, e40764.
62. Romero-Nava, R.; Zhou, D.S.; Garcia, N.; Ruiz-Hernandez, A.; Si, Y.C.; Sanchez-Munoz, F.; Huang, F.; Hong, E.; Villafana, S. Evidence of alterations in the expression of orphan receptors GPR26 and GPR39 due to the etiology of the metabolic syndrome. *J. Recept. Signal Transduct. Res.* **2017**, *37*, 422–429. [CrossRef] [PubMed]
63. Volpe, C.M.O.; Villar-Delfino, P.H.; Dos Anjos, P.M.F.; Nogueira-Machado, J.A. Cellular death, reactive oxygen species (ROS) and diabetic complications. *Cell Death Dis.* **2018**, *9*, 119. [CrossRef] [PubMed]
64. Wang, Y.; Li, Y.B.; Yin, J.J.; Wang, Y.; Zhu, L.B.; Xie, G.Y.; Pan, S.H. Autophagy regulates inflammation following oxidative injury in diabetes. *Autophagy* **2013**, *9*, 272–277. [CrossRef] [PubMed]
65. Schleicher, E.; Friess, U. Oxidative stress, AGE, and atherosclerosis. *Kidney Int.* **2007**, *72* (Suppl. S106), S17–S26. [CrossRef]

biomedicines

MDPI

Article

Tetrahydrobiopterin (BH_4) Supplementation Prevents the Cardiorenal Effects of Diabetes in Mice by Reducing Oxidative Stress, Inflammation and Fibrosis

Ulises Novoa [1], Karen Soto [1], Cristian Valdés [2], Jorge Villaseñor [3], Adriana V. Treuer [4] and Daniel R. González [1,*]

[1] Departamento de Ciencias Básicas Biomédicas, Facultad de Ciencias de la Salud, Universidad de Talca, Avenida Lircay s/n, Talca 3460000, Chile
[2] Centro de Investigación de Estudios Avanzados del Maule (CIEAM), Vicerrectoría de Investigación y Postgrado, Universidad Católica del Maule, Talca 3466706, Chile
[3] Instituto de Química de Recursos Naturales, Universidad de Talca, Talca 3460000, Chile
[4] Departamento de Biología y Química, Facultad de Ciencias Básicas, Universidad Catolica del Maule, Talca 3466706, Chile
* Correspondence: dagonzalez@utalca.cl; Tel.: +56-71-2-418856

Abstract: Background: The effects of diabetes on the cardiovascular system as well as in the kidney are profound, which include hypertrophy and fibrosis. Diabetes also induces oxidative stress, at least in part due to the uncoupling of nitric oxide synthase (NOS); this is a shift in NO production toward superoxide production due to reduced levels of the NOS cofactor tetrahydrobiopterin (BH_4). With this in mind, we tested the hypothesis that BH_4 supplementation may prevent the development of diabetic cardiomyopathy and nephropathy. Methods: Diabetes was induced in Balb/c mice with streptozotocin. Then, diabetic mice were divided into two groups: one group provided with BH_4 (sapropterin) in drinking water (daily doses of 15 mg/kg/day, during eight weeks) and the other that received only water. A third group of normoglycemic mice that received only water were used as the control. Results: Cardiac levels of BH_4 were increased in mice treated with BH_4 ($p = 0.0019$). Diabetes induced cardiac hypertrophy, which was prevented in the group that received BH_4 ($p < 0.05$). In addition, hypertrophy was evaluated as cardiomyocyte cross-sectional area. This was reduced in diabetic mice that received BH_4 ($p = 0.0012$). Diabetes induced cardiac interstitial fibrosis that was reduced in mice that received BH_4 treatment ($p < 0.05$). We also evaluated in the kidney the impact of BH_4 treatment on glomerular morphology. Diabetes induced glomerular hypertrophy compared with normoglycemic mice and was prevented by BH_4 treatment. In addition, diabetic mice presented glomerular fibrosis, which was prevented in mice that received BH_4. Conclusions: These results suggest that chronic treatment with BH_4 in mice ameliorates the cardiorenal effects of diabetes,, probably by restoring the nitroso–redox balance. This offers a possible new alternative to explore a BH_4-based treatment for the organ damage caused by diabetes.

Keywords: nitric oxide synthase uncoupling; sapropterin; diabetic nephropathy

Citation: Novoa, U.; Soto, K.; Valdés, C.; Villaseñor, J.; Treuer, A.V.; González, D.R. Tetrahydrobiopterin (BH_4) Supplementation Prevents the Cardiorenal Effects of Diabetes in Mice by Reducing Oxidative Stress, Inflammation and Fibrosis. *Biomedicines* **2022**, *10*, 2479. https://doi.org/10.3390/biomedicines10102479

Academic Editors: Alfredo Caturano and Raffaele Galiero

Received: 27 June 2022
Accepted: 5 September 2022
Published: 4 October 2022

1. Introduction

Diabetes mellitus is one of the most common chronic diseases worldwide, and continues to increase in numbers and significance, with characteristics of an epidemic, as modern lifestyles lead to reduced physical activity and increased obesity [1]. Diabetic cardiomyopathy is the manifestation in the myocardium of the alterations produced by the altered homeostasis of glucose metabolism, independent of coronary artery disease [2]. This cardiomyopathy is initially characterized by diastolic dysfunction and cardiac hypertrophy, with preserved ejection fraction. As diabetes progresses, systolic dysfunction and reduced ejection fraction develop. This process of cardiac deterioration in diabetes

includes altered metabolism, inflammation, and oxidative stress, which result in apoptosis and fibrosis that further deteriorate the myocardium [3–6]. In addition, altered calcium handling was characterized in the diabetic cardiac myocytes. The reduced capacity of the sarcoplasmic reticulum Ca^{2+} pump SERCA2 results in a diminished storage capacity of Ca^{2+}, which impairs cardiac contractility. Importantly, it also alters cardiac relaxation, which is evidenced in the diastolic dysfunction [7].

Diabetic nephropathy is another of the main complications of diabetes. In advanced stages, it is characterized by urinary albumin excretion [8]. It begins with a series of cellular and molecular changes that lead to morphological alterations, first in the glomerulus, then, in more advanced stages, in the tubules and interstitial space [8]. Glomeruli undergo hypertrophy, with a thickening of the basal membrane and basal tubular membrane, with a progressive accumulation of extracellular matrix components [9]. These ultrastructure changes are responsible for the functional alterations observed in diabetic nephropathy, such as proteinuria, hypertension, and, finally, renal failure. After hyperglycemia is chronically established, oxidative stress is one the main biochemical alterations that occur in the kidney [10,11], leading to a proinflammatory state [11].

Current treatments for the cardiorenal complications of diabetes are based on the control of blood glucose levels, mainly with metformin and sulfonylureas in type 2 diabetes mellitus and insulin mainly in type 1 diabetes [12]. More recently, clinical trials evaluating the organ target damage such as cardiac and renal complications with the use of di-peptidyl peptidase-4 (DPP4) inhibitors, glucagon-like peptide (GLP1) receptor agonists, and sodium-glucose co-transporter 2 (SGLT2) inhibitors have shown promising results [13–16]. At the preclinical level, pharmacological strategies are now directly focusing on end-organ damage processes such as fibrosis, inflammation, and oxidative stress [3].

In diabetes, several sources may contribute to the observed oxidative stress, such as xanthine oxidoreductase, nicotinamide adenine dinucleotide phosphate (NADPH) oxidases, mitochondria, and uncoupled nitric oxide synthases (NOS) [17]. A direct consequence of the increased production of reactive oxygen species (ROS) is the uncoupling of nitric oxide synthase [18]. This is due to the oxidation of tetrahydrobiopterin (BH_4), an essential cofactor for NOS activity. When NOS is uncoupled, its activity is redirected toward the production of superoxide, instead of NO, further contributing to the oxidative process [19]. Because BH_4 oxidation may also occur in oxidative states in the kidney, this leads to endothelial NOS uncoupling, which generates endothelial dysfunction in the kidney vasculature, including the glomerular capillaries, and afferent and efferent arterioles [20].

We tested the hypothesis that in diabetes, tetrahydrobiopterin supplementation leads to the recoupling of nitric oxide synthase 1 (NOS1), preventing cardiac remodeling and the advance of diabetic nephropathy, two of the main complications of chronic diabetes.

These findings in the diabetic heart and kidney represent a potential translational tool with therapeutic value. The proposed investigation may have a translational impact and contribute to the basic knowledge of NOS uncoupling in the setting of diabetic cardiomyopathy.

2. Methods

2.1. Experimental Model and Protocol

Diabetes was induced in Balb/c mice (n = 30, male, 30–40 g) with the intraperitoneal injection of three doses (100, 100, and 200 mg/kg) of streptozotocin (Sigma, St. Louis, MO, USA) in 10 mM citrate buffer, pH 4.5. The control group received an injection of citrate. Then, diabetic mice were divided into two groups: one group provided with BH_4 (sapropterin, Inpheno, InnoPharmax, Inc., Taipei City, Taiwan, Lot # 6P001) in drinking water (daily doses of 15 mg/kg/day, during eight weeks), and the other received only water. A third group of normoglycemic mice that received only water were used as the control. The protocol was approved by the Bioethics Committee of Universidad de Talca (# 2015-087-DG). Mice were kept in the animal facility of the institution, at room temperature (22 °C), under a 12 h light/dark cycle.

2.2. Sample Collection and Storage

At the end of the eight weeks, animals were induced anesthesia with ketamine 90 mg/kg and 10 mg/kg xylazine. Then, a midline incision was made and blood was obtained from the cava vein. After blood withdrawing, the heart and kidney were extracted.

2.3. Plasma Biochemical Measurements

For plasma biochemical measurements, we used a brain natriuretic peptide (BNP) Kit ELISA mouse (Elabscience Biotech Co., Ltd., Wuhan, China). Plasma glucose was determined using a kit from Valtek (Santiago, Chile). Insulin was determined using an ELISA from EMD Millipore, Billerica, MA, U.S.A.

2.4. Histological Analyses

Cardiac and renal sections were obtained for pathology analysis. For this, hearts and kidneys were fixed in Bouin solution. Then, pieces of the organs were dissected, dehydrated in alcohol-xylol solutions and included in Paraplast. In a microtome, 5 μm sections were obtained and mounted in 0.1% polylysine-treated slides. After this, sections were rehydrated and prepared for hematoxylin–eosin, Masson's trichrome, and periodic acid Schiff's staining.

Glomerular pathological analysis was performed by a blinded investigator, scoring the degree of fibrosis, glomerular hypertrophy, and mesangial expansion according to previous reports [21–24].

2.5. TUNEL Assay

Cardiac sections were probed with a Click-iT™ TUNEL Colorimetric IHC Detection Kit (Catalogue N° C10625, Thermo Fisher Scientific Inc., Carlsbad, CA, USA), for detection of apoptotic cells, as previously described [25,26].

2.6. Confocal Microscopy

Cardiac and renal sections were prepared for confocal microscopy, as previously described [27]. Renal sections were stained with anti-α-smooth muscle actin or F4/80 (Santa Cruz Biotechnology, Dallas, Texas, USA), followed by fluorescein isothiocyanate conjugated (FITC) antimouse (Jackson Inmunoresearch, West Grove, PA, USA). Nuclei were counterstained with propidium iodine (100 μM). Cardiac sections were probed for F4/80 to detect macrophages. Images were obtained with an LSM700 confocal microscope (Carl Zeiss, Jena, Germany).

2.7. Tetrahydrobiopterin (BH_4) Quantification

Plasma and cardiac BH_4 were determined as previously described [25,28] using a differential oxidation of biopterins protocol. Briefly, samples were submitted either to acidic or basic conditions (pH 3 or 9). Then, samples were oxidized with iodine. BH_2 and BH_4 contents were quantified by HPLC using HPLC (Perkin Elmer series 200, Waltham, MA) with fluorescence detection with excitation at 350 nm and emission at 450 nm.

2.8. Western Blot

Cardiac proteins were prepared as previously described for Western blot analysis [29]. Cardiac homogenates (30 μg) were mixed with loading buffer and summited to SDS-PAGE in 7.5% gels. Then, proteins were electro-transferred to nitrocellulose membranes. After blocking with Tween-buffered saline solution supplemented with 5% nonfat milk, membranes were incubated overnight at 4 °C with specific antibodies antinitrotyrosine (Badrilla, Leeds, U.K.). For NOS, SDS-PAGE was performed in nonreducing conditions of the loading buffer, and electrophoresis was run with the chamber immersed in ice. After electro-blotting, nitrocellulose membranes were incubated with anti-NOS1 antibody (Cell Signaling, Danvers, MA, USA) or NOS3 (BD Biosciences, Franklin Lakes, NJ, USA).

2.9. Statistical Analysis

Data are presented as means ± SEM, compared using ANOVA (normally distributed data) or Kruskal–Wallis test (nonparametric data) with Tukey's or Dunn's post hoc tests for comparisons between groups. A value of $p < 0.05$ was considered statistically significant.

3. Results

Three groups of mice were used: a group of normoglycemic mice, a group of streptozot ocin-induced diabetic mice, and a third group of diabetic mice that received sapropterin (BH_4) in drinking water, for eight weeks. At the end of the experimental period, mice were euthanized, and blood and organs were collected. Morphometric and blood parameters are presented in Table 1. These data confirmed the presence of hyperglycemia and reduced insulin levels in streptozotocin-treated mice. Additionally, cardiac hypertrophy was appreciated. Of these parameters, only cardiac hypertrophy was prevented by sapropterin treatment.

Table 1. Morphometric and plasmatic parameters of control, diabetic and diabetic mice treated with tetrahydrobiopterin (BH_4). BNP; brain natriuretic peptide. ANOVA followed by Tukey as *post-hoc* test. * $p < 0.05$ vs. control, ** $p < 0.005$ vs. control.

	Control	**Diabetics**	**Diabetics + BH4**	***p* Value**
n	9	9	10	
Body weight (g)	40.7 ± 1.3	36.8 ± 1.0	34.0 ± 1.3 *	0.0026
Heart weight (g)	0.157 ± 0.010	0.161 ± 0.007	0.139 ± 0.003	0.0616
Heart weight/tibia length (g/mm)	7.57 ± 0.39	8.59 ± 0.34 *	7.39 ± 0.16	0.0495
Insulin (ng/mL)	1.09 ± 0.30 *	0.29 ± 0.12	0.21 ± 0.08	0.0037
BNP (pg/mL)	227.9 ± 25.3 **	96.1 ±13.5	66.6 ± 12.6	0.0495
Glucose (mg/dL)	137 ± 7.7 *	316 ± 69.7	247.3 ± 29.7	0.0132

Next, we evaluated plasma levels of BH_4 (Figure 1). These were reduced in diabetic mice compared with those in normoglycemic controls, and increased toward normal in mice treated with sapropterin (39.1 ± 5.7 control, 12.5 ± 5 diabetic mice, and 22.9 ± 8.4 pmol/L in diabetic mice treated with BH_4, $p < 0.05$), as well as the ratio between BH_4 and its oxidized form BH_2: 3.6 ± 1 control, 1.1 ± 0.6 diabetic mice, and 12.7 ± 4.1 in diabetic mice treated with BH_4, $p < 0.05$ diabetic mice vs. diabetic mice + BH_4. Intracardiac (intra-atrial) levels of BH_4 were significantly increased in sapropterin-treated mice (8.8 ± 2.2 control, 9.6 ± 4.7 diabetic mice, and 209.7 ± 99.9 pmol BH_4 mg/protein in diabetic mice + BH_4, $p = 0.0019$).

Next, we evaluated the impact of sapropterin treatment on cardiac oxidative stress (Figure 2). For this, we evaluated the levels of nitrotyrosine on intracardiac proteins by Western blot. This assay showed a significant increase in the content of nitrated proteins in diabetic mice compared with that of normoglycemic controls ($p < 0.001$), and this content was reduced in sapropterin-treated mice. In addition, we evaluated the levels of NOS1 presented as the dimer or monomer. Under reduced levels of BH_4, NOS was unable to stabilize as a dimer and, as a consequence, was found in its monomeric form. Using SDS-PAGE under nonreducing conditions, the forms could be appreciated by Western blotting. This analysis showed that in our conditions, both the monomer and dimer of NOS1 were present. The NOS1 dimer and monomer levels were similar in the control and diabetic hearts. Nevertheless, the treatment with sapropterin increased the levels of dimer to monomer in diabetic hearts ($p < 0.05$). In the case of NOS3, the presence of the monomer was almost indistinguishable from that of the dimer. Neither of these constitutively expressed NOS showed changes in their expression levels ($p > 0.05$). These data suggested that sapropterin treatment was able to reduce intracardiac oxidative stress, probably independent of changes in NOS1 activity.

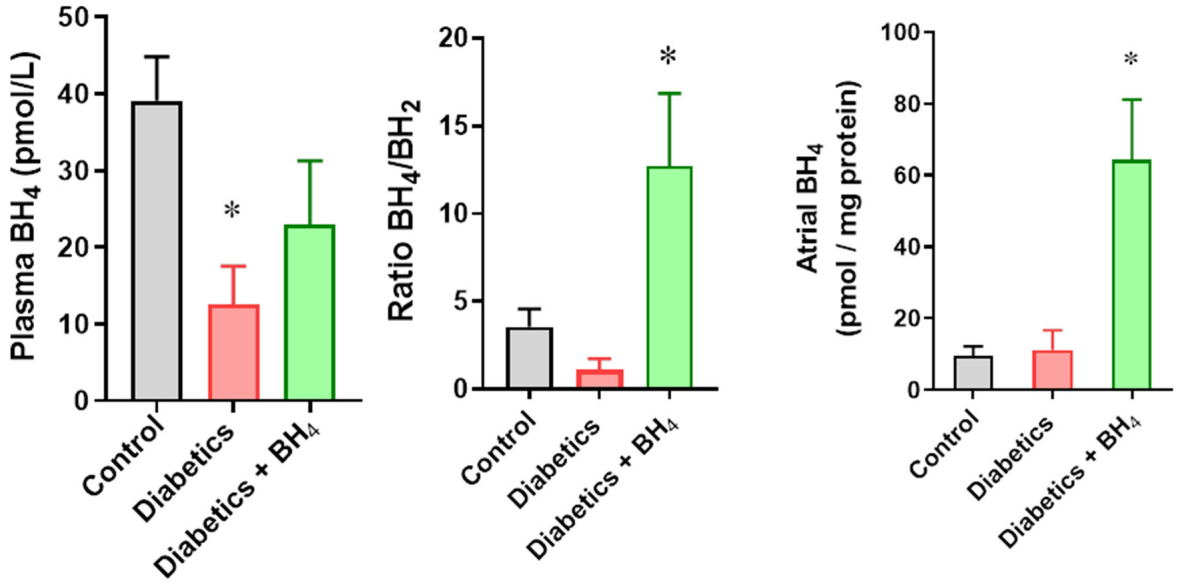

Figure 1. Oral administration of sapropterin restores levels of tetrahydrobiopterin (BH_4). Left, plasma levels of BH_4 in control, diabetics, and diabetic mice that received sapropterin (BH_4) in drinking water. Right, intracardiac BH_4 levels in control (black), diabetic mice (red), and diabetic mice that received BH_4 (green). $n = 6$ in each group. * $p < 0.05$ vs. control and diabetics.

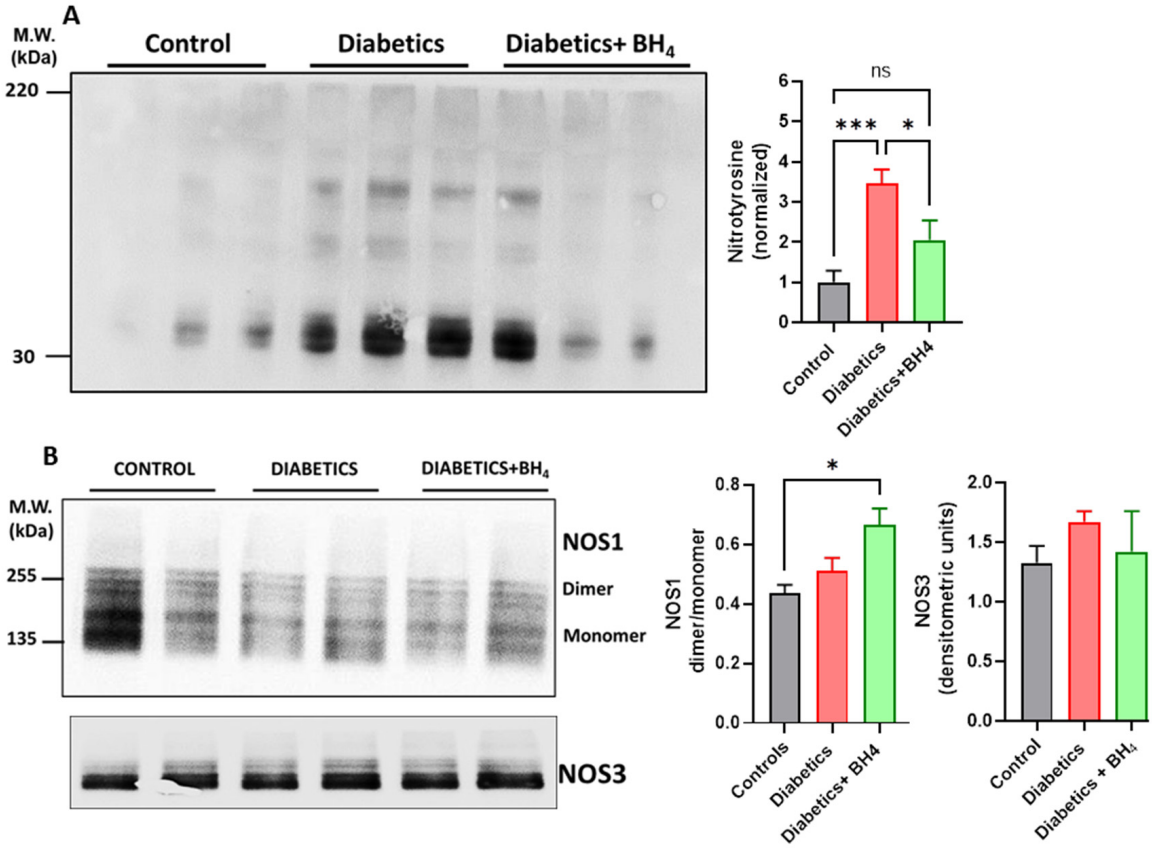

Figure 2. Oral administration of sapropterin reduces the intracardiac levels of oxidative stress. (**A**) Western blot analysis of nitrotyrosine in cardiac protein extracts from control, diabetic mice, and diabetic mice that received sapropterin (BH_4) in drinking water. (**B**) Western blot for the levels of NOS1 and NOS3 in homogenates from control, diabetics and diabetics mice that received sapropterin (BH4) in drinking water. * $p < 0.05$, ***, $p < 0.001$. ns = not significant.

3.1. Cardiac Remodeling

Diabetes induced cardiac hypertrophy, evaluated as the ratio of heart weight/tibia length, which was prevented in the group that received BH_4: (7.6 ± 1.03 g/mm control, 8.6 ± 0.63 g/mm diabetic mice, and 7.38 ± 0.5 g/mm diabetic mice + BH_4, $p < 0.05$, Table 1). In addition, hypertrophy was evaluated as cardiomyocyte cross-sectional area (Figure 3). This area was reduced in diabetic mice that received BH_4 (1190 ± 460 μm^2 control, 1194 ± 389 μm^2 diabetic mice, and 1106 ± 375 μm^2 diabetic mice + BH_4, $p = 0.0012$). In addition, we evaluated cardiac fibrosis, which is also a hallmark of diabetic cardiomyopathy, by Masson's trichrome staining. Diabetes induced cardiac interstitial fibrosis, which was reduced in mice that received BH_4 treatment (2.2 ± 1.1% control, 4.12 ± 1.6% in diabetic mice, and 2.16 ± 1.2% in diabetic mice + BH_4, $p < 0.05$).

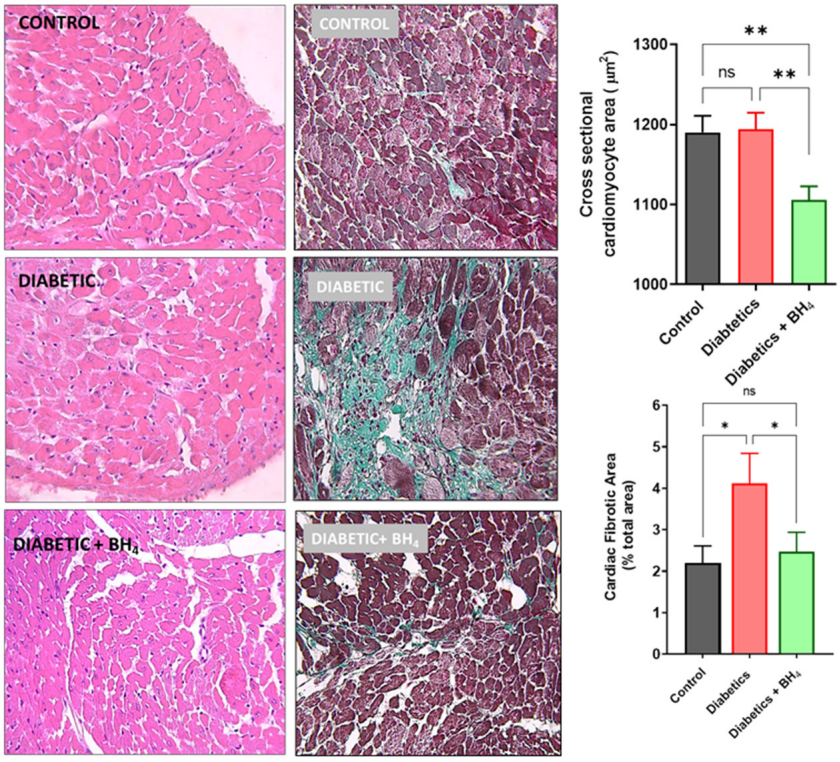

Figure 3. Cardiac remodeling in diabetes is ameliorated by oral administration of BH_4. Left panel, representative hematoxylin and eosin stained cross-sections of hearts from control, diabetic, and diabetic mice that received BH_4. Middle panel, representative Masson´s trichrome staining for collagen. Right panel, bar graphs depicting cardiac hypertrophy and fibrosis in control (black), diabetic mice (red), and diabetic mice treated with BH_4 (green). * $p < 0.05$; ** $p < 0.005$ vs. the other groups. ns = not significant.

3.2. Apoptosis and Inflammatory Cells

Because there is significant cardiac damage in chronic diabetes, both apoptosis and the presence of inflammatory cells has been described in the diabetic myocardium. Apoptosis was evaluated as the presence of TUNEL-positive cells in cardiac sections (Figure 4A). Diabetes induced an increase in the percentage of $TUNEL^+$ cardiomyocytes compared with normoglycemic hearts, but this increase was not modified in the hearts from sapropterin-treated mice. We also evaluated the presence of infiltrative inflammatory cells by immunofluorescence of F4/80, a cell surface marker that is present in macrophages (Figure 4B). Diabetic hearts showed an increase in the number of macrophages present in the myocardium compared with normoglycemic controls. This number was significantly decreased in the hearts of sapropterin-treated mice.

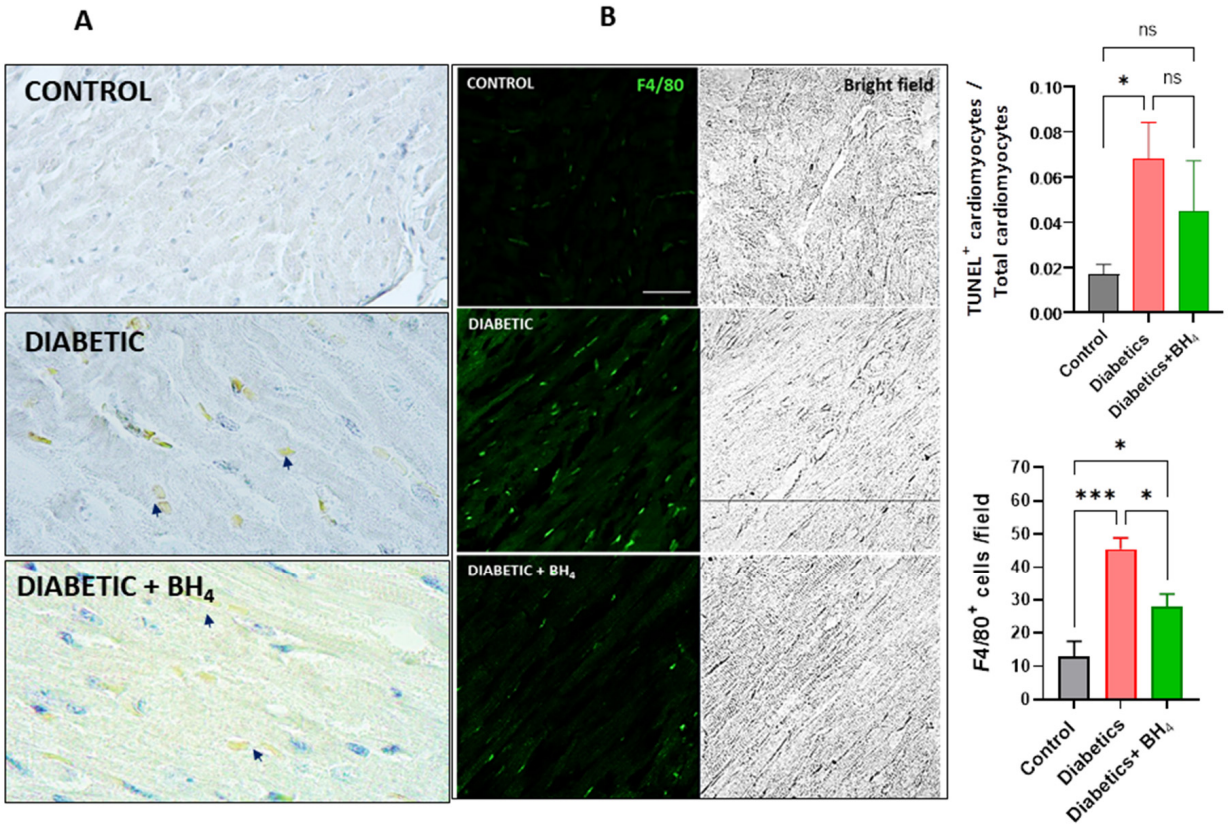

Figure 4. Impact of sapropterin in macrophage infiltration and cardiac apoptosis in diabetic mice. (**A**), representative images of TUNEL positive cells in cardiac sections obtained from control, diabetic and diabetic mice that received BH_4. Arrows indicate TUNEL positive nuclei. (**B**), representative confocal microscopy immunofluorescence images of F4/80 (green) in cardiac sections from control, diabetic and diabetic mice treated with sapropterin (BH_4). Asterisk * $p < 0.05$, *** $p < 0.001$ compared to the group indicated by brackets. ANOVA followed by Tukey *post hoc* test. Scale bar indicates 30 μm. ns = not significant.

3.3. Renal Changes

Next, we evaluated the impact of sapropterin treatment on diabetic nephropathy, evaluating glomerular morphology (Figure 5).

Diabetes induced glomerular hypertrophy compared to normoglycemic mice and was prevented by BH_4 treatment (0.79 ± 0.08 mm^2 in control, 1.12 ± 0.1 in diabetic and 0.98 ± 0.15 mm^2 glomerular tuft size in diabetics + BH_4, $p = 0.0004$).

In addition, diabetic mice presented glomerular fibrosis, evaluated by Masson's trichrome staining, which was prevented in mice that received BH_4: 1.01 ± 0.25 in control, 2.25 ± 0.29 in diabetics and 1.46 ± 0.33 score units in diabetics + BH_4 ($p < 0.0001$). Next, we evaluated mesangial expansion, which was increased in diabetic mice compared to controls, but was not reduced by sapropterin treatment (96.1 ± 10.7% control, 145.7 ± 10.4% diabetics, 143.5 ± 17.6% diabetics treated with sapropterin, $p < 0.05$ diabetics vs. control).

Next, we evaluated the degree of macrophage infiltration and the expression of α-smooth muscle actin. Macrophage infiltration was evaluated by immunofluorescence staining of the cell surface marker F4/80 (Figure 6). Renal sections of control normoglycemic mice did not show the presence of infiltrating inflammatory cells, neither in the glomeruli nor in the peritubular interstitium. On the contrary, F4/80-positive cells were extensively found in the peritubular space of diabetic mice. This infiltration was dramatically reduced in the diabetic kidneys from mice treated with sapropterin.

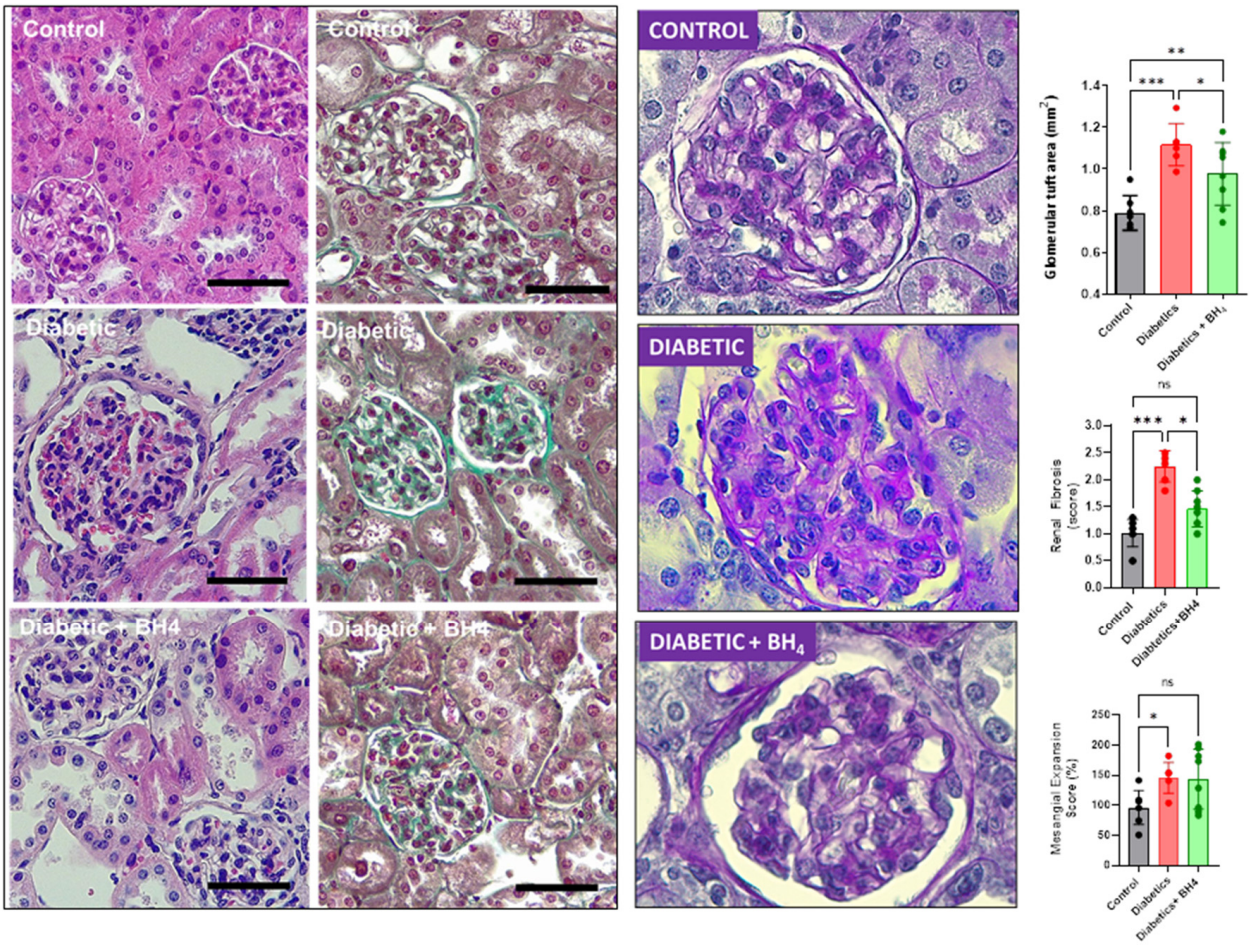

Figure 5. Renal morphological changes of diabetes are ameliorated by oral administration of BH_4. Left panel, representative images of hematoxylin–eosin staining in renal sections from kidneys of control, diabetic, and diabetic mice that received BH_4. Middle panel, representative Masson's trichrome staining for collagen IV. Right panel, periodic acid-Schiff (PAS)-stained renal sections from kidneys of control, diabetic, and diabetic mice that received BH4. * $p < 0.05$; ** $p < 0.01$; *** $p < 0.001$ vs. the groups indicated by brackets. Bar indicates 50 μm. ns = not significant.

In addition, we evaluated the presence of myofibroblasts as a marker of initial fibrosis (Figure 7). For this, renal sections were analyzed for α-smooth muscle actin (α-SMA). As expected, in the kidneys from normoglycemic control mice, there was no evidence of the presence of myofibroblasts in the peritubular space. On the contrary, the renal sections of diabetic mice showed the presence of these cells in the peritubular space mainly. Kidneys from sapropterin-treated mice showed almost no signal for α-SMA.

These results suggested that sapropterin treatment reduced macrophage infiltration and peritubular fibrosis in the diabetic kidneys. Overall, these results suggested that chronic treatment with BH_4 in mice ameliorates the cardiorenal effects of diabetes, probably by restoring the nitric oxide production. This offers a possible new alternative to explore a BH_4-based treatment for the organ damage of diabetes.

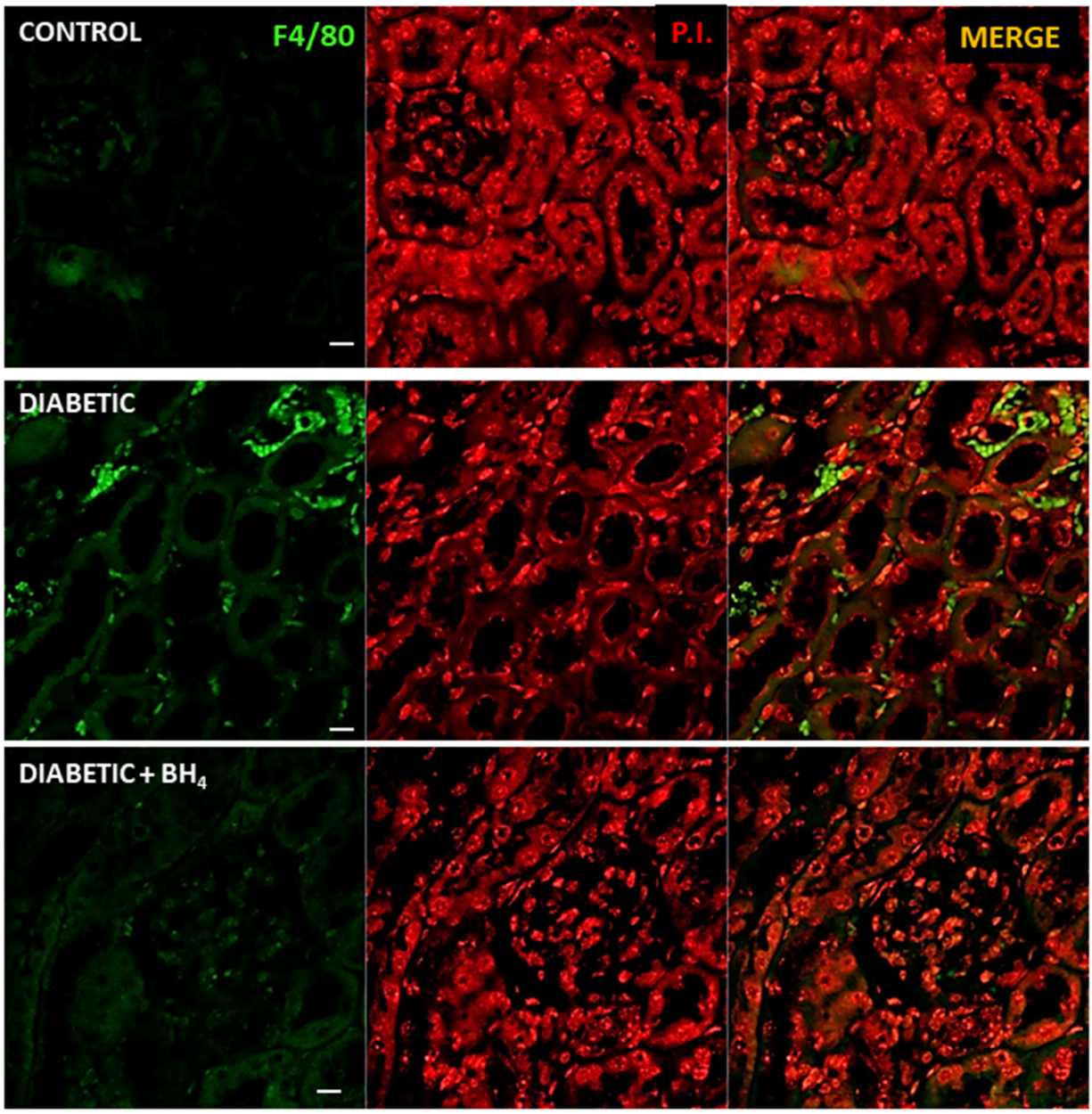

Figure 6. Renal tubular macrophage infiltration is prevented by oral administration of BH_4 to diabetic mice. Representative confocal images of renal sections probed for F4/80 (green), a marker of macrophages, in normoglycemic control, diabetic, and diabetic mice treated with sapropterin (BH_4). Middle panel, corresponding section counterstained with propidium iodide (P.I., red) for nuclei. Right panel, merge of both F4/80 and P.I: signals. Images were obtained at 40× magnification. Scale bar indicates 10 μm.

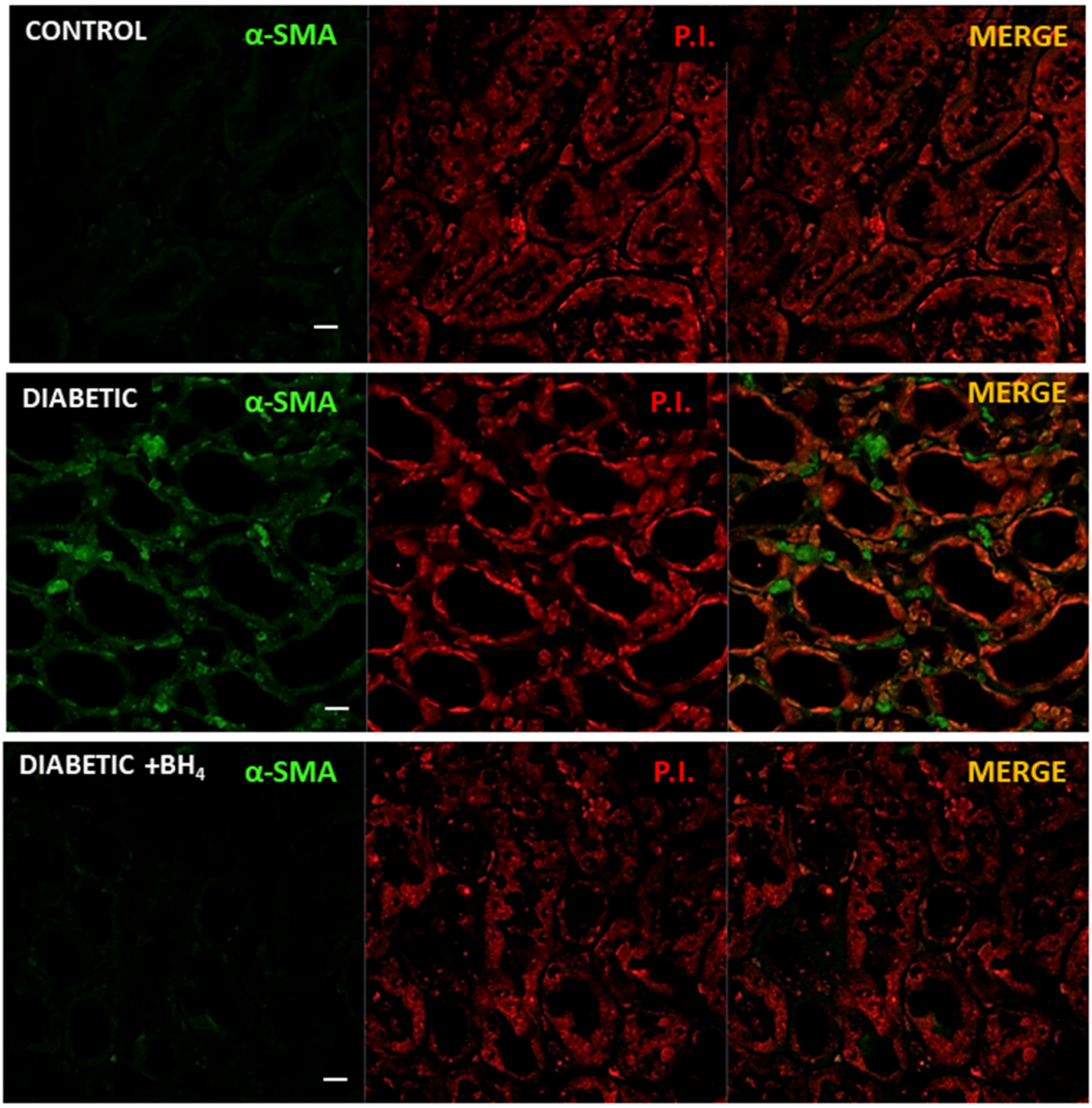

Figure 7. Renal tubular fibrosis was prevented by oral administration of BH_4 to diabetic mice. Representative confocal images of renal sections (medulla) enriched in tubules probed for alpha smooth muscle actin (α-SMA, green), a marker of myofibroblast, in normoglycemic control, diabetic, and diabetic mice treated with sapropterin (BH_4). Middle panel, corresponding section counterstained with propidium iodide (P.I., red) for nuclei. Right panel, merge of both α-SMA and P.I: signals. Images were obtained at 40× magnification. Scale bar indicates 10 μm.

4. Discussion

Our present results showed that oral administration of sapropterin (BH_4) for one month to diabetic mice was able to ameliorate some pathological changes in both the heart and kidneys, two of the main organ targets of diabetes. Notably, BH_4 administration reduced cardiac hypertrophy and fibrosis, while preventing glomerular hypertrophy in the kidney. These effects were associated with the reduction in oxidative stress, but apparently independent of NOS1 recoupling. Previous reports have shown that eNOS uncoupling is an important source of ROS in the diabetic kidney [30–34].

Reduced levels of tetrahydrobiopterin were attributed to the reduced expression of guanosine5′-triphosphate cyclohydrolase I (GTPCH), a rate-limiting enzyme in the synthesis of BH_4 [35]. Experiments where GTPCH was overexpressed then reverted the phenotypes associated with diabetic nephropathy [32] and cardiomyopathy [36,37].

In the diabetic heart, NOS uncoupling has emerged as an important source of ROS [36–39], in a way that appears as an important therapeutic target to prevent the development of diabetic cardiomyopathy. Our results agree with those obtained by recent studies regarding the role of NOS1 uncoupling in the heart, which indicate that BH_4 supplementation or genetic modifications that lead to the increased intracellular production of BH_4 has a beneficial impact on the left ventricular function of diabetic mice. This effect is achieved by improving intracellular calcium handling, hence left ventricular systolic and diastolic mechanics. Interestingly, some of the positive effects of BH_4 supplementation in the diabetic heart appear to be independent of NOS recoupling [39]. Our results are consistent with those findings because we did not observe significant recoupling of NOS1 in the diabetic heart after BH_4 treatment, although we observed reduction in cardiac oxidative stress. It was suggested that this protective effect may be exerted by a metabolic action of NOS1, increasing the expression of insulin-independent glucose transporters (GLUT-1), which improved myocardial energetics [39]. In addition, it was also shown that BH_4 exerts its beneficial effects in diabetic cardiomyopathy by activating peroxisome proliferator-activated receptor-γ coactivator 1-α (PGC-1α) signaling by interacting with calcium/calmodulin-dependent protein kinase kinase 2 (CaMKK2). These effects are also independent of NOS1 activity [40].

It was described in a model of cardiac hypertrophy by transverse aortic constriction that BH_4 supplementation inhibits macrophage infiltration in the myocardium, probably by reducing the inflammatory signaling [41]. Interestingly, this protection is also independent of NOS uncoupling, which is consistent with a role of BH_4 in macrophages biology. The exact mechanism through which BH_4 mediates these anti-inflammatory effects remains to be determined, but it has been reported that BH_4 is important for the macrophage functions, dependent and independent of iNOS [42,43].

We also observed a reduction in the number of macrophages present in the diabetic myocardium after treatment with BH_4. Nevertheless, we did not evaluate the origin of these macrophages. The recent literature indicates the presence of at least four types of macrophages in the heart, with one being the infiltrating-monocytes-derived macrophages [44–46]. Particularly, a study using streptozotocin-induced diabetes in mice showed that cardiac macrophages producing interleukin 1β play an important role in the generation of arrhythmias in the diabetic heart [47]. A recent study documented that BH_4 deficiency in macrophages increased the production of interleukin 1β and the inflammatory profile of these cells [48].

In the context of the diabetic patient, it is relevant to consider both the development of cardiomyopathy and nephropathy. Here, we showed that BH_4 treatment was able to prevent the cardiac damage associated with the initial stages of diabetic cardiomyopathy, reducing macrophage infiltration, fibrosis, and hypertrophy, and similar effects were observed in the kidney at the glomerular and tubular levels. Interestingly, even though we observed a general beneficial effect of BH_4 supplementation on renal morphology in diabetic mice, BH_4 mesangial expansion was not modified. This is consistent with a previous report that suggested that BH_4 may induce mesangial proliferation [49]. Plasma BH_4 concentration was postulated as a predictor of renal function in diabetic patients [50].

Fibrosis has been identified as a common factor in cardiorenal syndrome [51,52], which is a reciprocal interaction between cardiac and renal dysfunction in several pathological states, including diabetes [53,54]. Here we verified that fibrosis affected both organs and was prevented by BH_4 administration.

Importantly, sapropterin, a form of BH_4, is available and approved for use in humans in phenylketonuric patients [55]. This opens the possibility that this drug may be considered for use in diabetes clinical trials.

5. Conclusions

The results of the present study indicated that chronic oral administration of sapropterin (BH_4) in mice ameliorates the morphological changes produced by diabetes in the heart and the kidney, probably by reducing oxidative stress, reducing inflammation, and the fibrotic processes that occur in the myocardium and at the glomerular and peritubular space in the kidney. This offers a possible new alternative to explore a BH_4-based treatment for the organ damage caused by diabetes.

Author Contributions: Conceptualization, D.R.G. and K.S.; methodology, K.S.; validation, D.R.G., J.V. and U.N.; formal analysis, D.R.G.; investigation, C.V.; data curation, D.R.G.; writing—original draft preparation, D.R.G.; writing—review and editing, D.R.G.; visualization, A.V.T.X; supervision, J.V.; project administration, D.R.G.; funding acquisition, D.R.G. All authors have read and agreed to the published version of the manuscript.

Funding: This work was supported by FONDECYT grant 1150662.

Institutional Review Board Statement: The protocol involving animal experimentation was approved by the Animal Care Committee of Universidad de Talca (# 2015-087-DG).

Informed Consent Statement: Not applicable.

Data Availability Statement: Data is available upon request.

Conflicts of Interest: The authors declare no conflict of interest.

References

1. Laditka, S.B.; Laditka, J.N. Active life expectancy of Americans with diabetes: risks of heart disease, obesity, and inactivity. *Diabetes Res. Clin. Pract.* **2015**, *107*, 37–45. [CrossRef] [PubMed]
2. Miki, T.; Yuda, S.; Kouzu, H.; Miura, T. Diabetic cardiomyopathy: Pathophysiology and clinical features. *Heart Fail. Rev.* **2013**, *18*, 149–166. [CrossRef]
3. Tan, Y.; Zhang, Z.; Zheng, C.; Wintergerst, K.A.; Keller, B.B.; Cai, L. Mechanisms of diabetic cardiomyopathy and potential therapeutic strategies: preclinical and clinical evidence. *Nat. Rev. Cardiol.* **2020**, *17*, 585–607. [CrossRef] [PubMed]
4. Jia, G.; Hill, M.A.; Sowers, J.R. Diabetic Cardiomyopathy: An Update of Mechanisms Contributing to This Clinical Entity. *Circ. Res.* **2018**, *122*, 624–638. [CrossRef] [PubMed]
5. Salvatore, T.; Pafundi, P.C.; Galiero, R.; Albanese, G.; Di Martino, A.; Caturano, A.; Vetrano, E.; Rinaldi, L.; Sasso, F.C. The Diabetic Cardiomyopathy: The Contributing Pathophysiological Mechanisms. *Front. Med. (Lausanne)* **2021**, *8*, 695792. [CrossRef] [PubMed]
6. Kaur, N.; Guan, Y.; Raja, R.; Ruiz-Velasco, A.; Liu, W. Mechanisms and Therapeutic Prospects of Diabetic Cardiomyopathy Through the Inflammatory Response. *Front. Physiol.* **2021**, *12*, 694864. [CrossRef]
7. Shah, M.S.; Brownlee, M. Molecular and Cellular Mechanisms of Cardiovascular Disorders in Diabetes. *Circ. Res.* **2016**, *118*, 1808–1829. [CrossRef]
8. Fu, J.; Lee, K.; Chuang, P.Y.; Liu, Z.; He, J.C. Glomerular endothelial cell injury and cross talk in diabetic kidney disease. *Am. J. Physiol. Renal. Physiol.* **2015**, *308*, F287–F297. [CrossRef]
9. Hung, P.H.; Hsu, Y.C.; Chen, T.H.; Lin, C.L. Recent Advances in Diabetic Kidney Diseases: From Kidney Injury to Kidney Fibrosis. *Int. J. Mol. Sci.* **2021**, *22*, 11857. [CrossRef]
10. Fakhruddin, S.; Alanazi, W.; Jackson, K.E. Diabetes-Induced Reactive Oxygen Species: Mechanism of Their Generation and Role in Renal Injury. *J. Diabetes Res.* **2017**, *2017*, 8379327. [CrossRef]
11. Sifuentes-Franco, S.; Padilla-Tejeda, D.E.; Carrillo-Ibarra, S.; Miranda-Diaz, A.G. Oxidative Stress, Apoptosis, and Mitochondrial Function in Diabetic Nephropathy. *Int. J. Endocrinol.* **2018**, *2018*, 1875870. [CrossRef] [PubMed]
12. Chen, C.; Yuan, S.; Zhao, X.; Qiao, M.; Li, S.; He, N.; Huang, L.; Lyu, J. Metformin Protects Cardiovascular Health in People with Diabetes. *Front. Cardiovasc. Med.* **2022**, *9*, 949113. [CrossRef]
13. Wu, L.; Gunton, J.E. The Changing Landscape of Pharmacotherapy for Diabetes Mellitus: A Review of Cardiovascular Outcomes. *Int. J. Mol. Sci.* **2019**, *20*, 5853. [CrossRef] [PubMed]
14. Van Ruiten, C.C.; Hesp, A.C.; van Raalte, D.H. Sodium glucose cotransporter-2 inhibitors protect the cardiorenal axis: Update on recent mechanistic insights related to kidney physiology. *Eur. J. Intern. Med.* **2022**, *100*, 13–20. [CrossRef]
15. Wiviott, S.D.; Raz, I.; Bonaca, M.P.; Mosenzon, O.; Kato, E.T.; Cahn, A.; Silverman, M.G.; Zelniker, T.A.; Kuder, J.F.; Murphy, S.A.; et al. Dapagliflozin and Cardiovascular Outcomes in Type 2 Diabetes. *N. Engl. J. Med.* **2019**, *380*, 347–357. [CrossRef] [PubMed]
16. Kluger, A.Y.; Tecson, K.M.; Lee, A.Y.; Lerma, E.V.; Rangaswami, J.; Lepor, N.E.; Cobble, M.E.; McCullough, P.A. Class effects of SGLT2 inhibitors on cardiorenal outcomes. *Cardiovasc. Diabetol.* **2019**, *18*, 99. [CrossRef] [PubMed]

17. Faria, A.; Persaud, S.J. Cardiac oxidative stress in diabetes: Mechanisms and therapeutic potential. *Pharmacol. Ther.* **2017**, *172*, 50–62. [CrossRef]
18. Schmidt, T.S.; Alp, N.J. Mechanisms for the role of tetrahydrobiopterin in endothelial function and vascular disease. *Clin. Sci.* **2007**, *113*, 47–63. [CrossRef]
19. Kim, H.L.; Park, Y.S. Maintenance of cellular tetrahydrobiopterin homeostasis. *BMB Rep.* **2010**, *43*, 584–592. [CrossRef]
20. Okumura, M.; Masada, M.; Yoshida, Y.; Shintaku, H.; Hosoi, M.; Okada, N.; Konishi, Y.; Morikawa, T.; Miura, K.; Imanishi, M. Decrease in tetrahydrobiopterin as a possible cause of nephropathy in type II diabetic rats. *Kidney Int.* **2006**, *70*, 471–476. [CrossRef]
21. Raij, L.; Azar, S.; Keane, W. Mesangial immune injury, hypertension, and progressive glomerular damage in Dahl rats. *Kidney Int.* **1984**, *26*, 137–143. [CrossRef] [PubMed]
22. Xu, S.; Jiang, B.; Maitland, K.A.; Bayat, H.; Gu, J.; Nadler, J.L.; Corda, S.; Lavielle, G.; Verbeuren, T.J.; Zuccollo, A.; et al. The thromboxane receptor antagonist S18886 attenuates renal oxidant stress and proteinuria in diabetic apolipoprotein E-deficient mice. *Diabetes* **2006**, *55*, 110–119. [CrossRef] [PubMed]
23. Guimaraes-Souza, N.K.; Yamaleyeva, L.M.; Lu, B.; Ramos, A.C.; Bishop, C.E.; Andersson, K.E. Superoxide overproduction and kidney fibrosis: A new animal model. *Einstein*, 2015; 13, 79–88.
24. Zhao, X.F.; Liu, Y.H.; Han, Z.M.; Xu, Y.U. Effect of erythropoietin on the expression of dynamin-related protein-1 in rat renal interstitial fibrosis. *Exp. Ther. Med.* **2015**, *9*, 2065–2071. [CrossRef]
25. Novoa, U.; Arauna, D.; Moran, M.; Nunez, M.; Zagmutt, S.; Saldivia, S.; Valdes, C.; Villasenor, J.; Zambrano, C.G.; Gonzalez, D.R. High-Intensity Exercise Reduces Cardiac Fibrosis and Hypertrophy but Does Not Restore the Nitroso-Redox Imbalance in Diabetic Cardiomyopathy. *Oxid. Med. Cell Longev.* **2017**, *2017*, 7921363. [CrossRef] [PubMed]
26. Vielma, A.Z.; Leon, L.; Fernandez, I.C.; Gonzalez, D.R.; Boric, M.P. Nitric Oxide Synthase 1 Modulates Basal and beta-Adrenergic-Stimulated Contractility by Rapid and Reversible Redox-Dependent S-Nitrosylation of the Heart. *PLoS One* **2016**, *11*, e0160813. [CrossRef]
27. Soto, G.; Rodriguez, M.J.; Fuentealba, R.; Treuer, A.V.; Castillo, I.; Gonzalez, D.R.; Zuniga-Hernandez, J. Maresin 1, a Proresolving Lipid Mediator, Ameliorates Liver Ischemia-Reperfusion Injury and Stimulates Hepatocyte Proliferation in Sprague-Dawley Rats. *Int. J. Mol. Sci.* **2020**, *22*, 540. [CrossRef]
28. Valdes, C.; Arauna, D.; Gonzalez, D.; Villasenor, J. Simplified HPLC methodology for quantifying biological pterins by selective oxidation. *J. Chromatogr. B Analyt. Technol. Biomed. Life Sci.* **2017**, *1055–1056*, 113–118. [CrossRef]
29. Vielma, A.Z.; Boric, M.P.; Gonzalez, D.R. Apocynin Treatment Prevents Cardiac Connexin 43 Hemichannels Hyperactivity by Reducing Nitroso-Redox Stress in Mdx Mice. *Int. J. Mol. Sci.* **2020**, *21*, 5415. [CrossRef]
30. Satoh, M.; Fujimoto, S.; Arakawa, S.; Yada, T.; Namikoshi, T.; Haruna, Y.; Horike, H.; Sasaki, T.; Kashihara, N. Angiotensin II type 1 receptor blocker ameliorates uncoupled endothelial nitric oxide synthase in rats with experimental diabetic nephropathy. *Nephrol. Dial. Transplant* **2008**, *23*, 3806–3813. [CrossRef]
31. Cheng, H.; Wang, H.; Fan, X.; Paueksakon, P.; Harris, R.C. Improvement of endothelial nitric oxide synthase activity retards the progression of diabetic nephropathy in db/db mice. *Kidney Int.* **2012**, *82*, 1176–1183. [CrossRef]
32. Kidokoro, K.; Satoh, M.; Channon, K.M.; Yada, T.; Sasaki, T.; Kashihara, N. Maintenance of endothelial guanosine triphosphate cyclohydrolase I ameliorates diabetic nephropathy. *J. Am. Soc. Nephrol.* **2013**, *24*, 1139–1150. [CrossRef] [PubMed]
33. Satoh, M.; Fujimoto, S.; Haruna, Y.; Arakawa, S.; Horike, H.; Komai, N.; Sasaki, T.; Tsujioka, K.; Makino, H.; Kashihara, N. NAD(P)H oxidase and uncoupled nitric oxide synthase are major sources of glomerular superoxide in rats with experimental diabetic nephropathy. *Am. J. Physiol. Renal. Physiol.* **2005**, *288*, F1144–F1152. [CrossRef] [PubMed]
34. Faria, A.M.; Papadimitriou, A.; Silva, K.C.; Lopes de Faria, J.M.; Lopes de Faria, J.B. Uncoupling endothelial nitric oxide synthase is ameliorated by green tea in experimental diabetes by re-establishing tetrahydrobiopterin levels. *Diabetes* **2012**, *61*, 1838–1847. [CrossRef] [PubMed]
35. Xu, J.; Wu, Y.; Song, P.; Zhang, M.; Wang, S.; Zou, M.H. Proteasome-dependent degradation of guanosine 5′-triphosphate cyclohydrolase I causes tetrahydrobiopterin deficiency in diabetes mellitus. *Circulation* **2007**, *116*, 944–953. [CrossRef] [PubMed]
36. Wu, H.E.; Baumgardt, S.L.; Fang, J.; Paterson, M.; Liu, Y.; Du, J.; Shi, Y.; Qiao, S.; Bosnjak, Z.J.; Warltier, D.C.; et al. Cardiomyocyte GTP Cyclohydrolase 1 Protects the Heart Against Diabetic Cardiomyopathy. *Sci. Rep.* **2016**, *6*, 27925. [CrossRef]
37. Carnicer, R.; Hale, A.B.; Suffredini, S.; Liu, X.; Reilly, S.; Zhang, M.H.; Surdo, N.C.; Bendall, J.K.; Crabtree, M.J.; Lim, G.B.; et al. Cardiomyocyte GTP cyclohydrolase 1 and tetrahydrobiopterin increase NOS1 activity and accelerate myocardial relaxation. *Circ. Res.* **2012**, *111*, 718–727. [CrossRef]
38. Jo, H.; Otani, H.; Jo, F.; Shimazu, T.; Okazaki, T.; Yoshioka, K.; Fujita, M.; Kosaki, A.; Iwasaka, T. Inhibition of nitric oxide synthase uncoupling by sepiapterin improves left ventricular function in streptozotocin-induced diabetic mice. *Clin. Exp. Pharmacol. Physiol.* **2011**, *38*, 485–493. [CrossRef]
39. Carnicer, R.; Duglan, D.; Ziberna, K.; Recalde, A.; Reilly, S.; Simon, J.N.; Mafrici, S.; Arya, R.; Rosello-Lleti, E.; Chuaiphichai, S.; et al. BH4 Increases nNOS Activity and Preserves Left Ventricular Function in Diabetes. *Circ. Res.* **2021**, *128*, 585–601. [CrossRef]
40. Kim, H.K.; Ko, T.H.; Song, I.S.; Jeong, Y.J.; Heo, H.J.; Jeong, S.H.; Kim, M.; Park, N.M.; Seo, D.Y.; Kha, P.T.; et al. BH4 activates CaMKK2 and rescues the cardiomyopathic phenotype in rodent models of diabetes. *Life Sci. Alliance* **2020**, 3. [CrossRef]

41. Hashimoto, T.; Sivakumaran, V.; Carnicer, R.; Zhu, G.; Hahn, V.S.; Bedja, D.; Recalde, A.; Duglan, D.; Channon, K.M.; Casadei, B.; et al. Tetrahydrobiopterin Protects Against Hypertrophic Heart Disease Independent of Myocardial Nitric Oxide Synthase Coupling. *J. Am. Heart Assoc.* **2016**, *5*, e003208. [CrossRef]
42. McNeill, E.; Crabtree, M.J.; Sahgal, N.; Patel, J.; Chuaiphichai, S.; Iqbal, A.J.; Hale, A.B.; Greaves, D.R.; Channon, K.M. Regulation of iNOS function and cellular redox state by macrophage Gch1 reveals specific requirements for tetrahydrobiopterin in NRF2 activation. *Free Radic. Biol. Med.* **2015**, *79*, 206–216. [CrossRef]
43. McNeill, E.; Stylianou, E.; Crabtree, M.J.; Harrington-Kandt, R.; Kolb, A.L.; Diotallevi, M.; Hale, A.B.; Bettencourt, P.; Tanner, R.; O'Shea, M.K.; et al. Regulation of mycobacterial infection by macrophage Gch1 and tetrahydrobiopterin. *Nat. Commun.* **2018**, *9*, 5409. [CrossRef] [PubMed]
44. Lavine, K.J.; Epelman, S.; Uchida, K.; Weber, K.J.; Nichols, C.G.; Schilling, J.D.; Ornitz, D.M.; Randolph, G.J.; Mann, D.L. Distinct macrophage lineages contribute to disparate patterns of cardiac recovery and remodeling in the neonatal and adult heart. *Proc. Natl. Acad. Sci. USA* **2014**, *111*, 16029–16034. [CrossRef] [PubMed]
45. Heidt, T.; Courties, G.; Dutta, P.; Sager, H.B.; Sebas, M.; Iwamoto, Y.; Sun, Y.; Da Silva, N.; Panizzi, P.; van der Laan, A.M.; et al. Differential contribution of monocytes to heart macrophages in steady-state and after myocardial infarction. *Circ. Res.* **2014**, *115*, 284–295. [CrossRef] [PubMed]
46. Bajpai, G.; Bredemeyer, A.; Li, W.; Zaitsev, K.; Koenig, A.L.; Lokshina, I.; Mohan, J.; Ivey, B.; Hsiao, H.M.; Weinheimer, C.; et al. Tissue Resident CCR2- and CCR2+ Cardiac Macrophages Differentially Orchestrate Monocyte Recruitment and Fate Specification Following Myocardial Injury. *Circ. Res.* **2019**, *124*, 263–278. [CrossRef]
47. Monnerat, G.; Alarcon, M.L.; Vasconcellos, L.R.; Hochman-Mendez, C.; Brasil, G.; Bassani, R.A.; Casis, O.; Malan, D.; Travassos, L.H.; Sepulveda, M.; et al. Macrophage-dependent IL-1beta production induces cardiac arrhythmias in diabetic mice. *Nat. Commun.* **2016**, *7*, 13344. [CrossRef]
48. Bailey, J.D.; Diotallevi, M.; Nicol, T.; McNeill, E.; Shaw, A.; Chuaiphichai, S.; Hale, A.; Starr, A.; Nandi, M.; Stylianou, E.; et al. Nitric Oxide Modulates Metabolic Remodeling in Inflammatory Macrophages through TCA Cycle Regulation and Itaconate Accumulation. *Cell Rep.* **2019**, *28*, 218–230.e7. [CrossRef]
49. Wang, J.; Yang, Q.; Nie, Y.; Guo, H.; Zhang, F.; Zhou, X.; Yin, X. Tetrahydrobiopterin contributes to the proliferation of mesangial cells and accumulation of extracellular matrix in early-stage diabetic nephropathy. *J. Pharm. Pharmacol.* **2017**, *69*, 182–190. [CrossRef]
50. Deng, C.; Wang, S.; Niu, Z.; Ye, Y.; Gao, L. Newly established LC-MS/MS method for measurement of plasma BH4 as a predictive biomarker for kidney injury in diabetes. *Free Radic. Biol. Med.* **2022**, *178*, 1–6. [CrossRef]
51. Zannad, F.; Rossignol, P. Cardiorenal Syndrome Revisited. *Circulation* **2018**, *138*, 929–944. [CrossRef]
52. Delgado-Valero, B.; Cachofeiro, V.; Martinez-Martinez, E. Fibrosis, the Bad Actor in Cardiorenal Syndromes: Mechanisms Involved. *Cells* **2021**, *10*, 1824. [CrossRef] [PubMed]
53. Zhang, J.; Bottiglieri, T.; McCullough, P.A. The Central Role of Endothelial Dysfunction in Cardiorenal Syndrome. *Cardiorenal. Med.* **2017**, *7*, 104–117. [CrossRef] [PubMed]
54. Boudoulas, K.D.; Triposkiadis, F.; Parissis, J.; Butler, J.; Boudoulas, H. The Cardio-Renal Interrelationship. *Prog. Cardiovasc. Dis.* **2017**, *59*, 636–648. [CrossRef] [PubMed]
55. Sanford, M.; Keating, G.M. Sapropterin: A review of its use in the treatment of primary hyperphenylalaninaemia. *Drugs* **2009**, *69*, 461–476. [CrossRef] [PubMed]

biomedicines

MDPI

Article

Effects of a Combination of Empagliflozin Plus Metformin vs. Metformin Monotherapy on NAFLD Progression in Type 2 Diabetes: The IMAGIN Pilot Study

Alfredo Caturano [1,2,†], Raffaele Galiero [1,†], Giuseppe Loffredo [1], Erica Vetrano [1], Giulia Medicamento [1], Carlo Acierno [1], Luca Rinaldi [1], Aldo Marrone [1], Teresa Salvatore [2], Marcellino Monda [2], Celestino Sardu [1], Raffaele Marfella [1] and Ferdinando Carlo Sasso [1,*]

[1] Department of Advanced Medical and Surgical Sciences, University of Campania Luigi Vanvitelli, I-80138 Naples, Italy
[2] Department of Precision Medicine, University of Campania Luigi Vanvitelli, I-80138 Naples, Italy
* Correspondence: ferdinando.sasso@unicampania.it; Tel.: +39-(08)-15665010
† These authors contributed equally to this work.

Abstract: Non-alcoholic fatty liver disease (NAFLD) comprises a heterogeneous group of metabolic liver diseases and is characterized by the presence of steatosis in at least 5% of hepatocytes. The aim of our study was to assess the effect of the combination therapy of empagliflozin + metformin vs. metformin monotherapy on NAFLD progression in type 2 diabetic (T2DM) patients. Sixty-three metformin-treated T2DM patients who were SGLT2i-naïve and had an ultrasound diagnosis of NAFLD (aged 60.95 ± 11.14 years; males, 57.1%) were included in the present analysis. Thirty-three started the combination therapy. All patients were observed for 6 months and routinely monitored with anthropometry, blood biochemistry, and FibroScan®/CAP. At the 6-month follow-up, the combination therapy group presented a significant reduction in BMI (30.83 ± 3.5 vs. 28.48 ± 3.25), glycated hemoglobin (8.2 (7.4–8.8)) vs. 7.2 (6.8–7.9), ALT (68.5 (41.5–88.0) vs. 45.00 (38.00, 48.00)), CAP parameter (293.5 (270.0–319.25) vs. 267.00 (259.50, 283.75)) and steatosis degree ($p = 0.001$) in comparison with the control group, whose parameters remained almost stable over time. In patients affected by T2DM, the combination of empagliflozin + metformin vs. metformin monotherapy ameliorated liver steatosis, ALT levels, body weight, and glycated hemoglobin after a 6-month follow-up.

Keywords: type 2 diabetes; non-alcoholic fatty liver disease; sodium-glucose cotransporter inhibitors; metformin; FibroScan®; controlled attenuation parameter

Citation: Caturano, A.; Galiero, R.; Loffredo, G.; Vetrano, E.; Medicamento, G.; Acierno, C.; Rinaldi, L.; Marrone, A.; Salvatore, T.; Monda, M.; et al. Effects of a Combination of Empagliflozin Plus Metformin vs. Metformin Monotherapy on NAFLD Progression in Type 2 Diabetes: The IMAGIN Pilot Study. *Biomedicines* **2023**, *11*, 322. https://doi.org/10.3390/biomedicines11020322

Academic Editor: Albrecht Piiper

Received: 31 December 2022
Revised: 18 January 2023
Accepted: 20 January 2023
Published: 23 January 2023

1. Introduction

Non-alcoholic fatty liver disease (NAFLD) comprises a heterogeneous group of metabolic liver diseases, ranging from simple non-alcoholic fatty liver to non-alcoholic steatohepatitis, and is characterized by the presence of steatosis in at least 5% of hepatocytes (demonstrated by imaging or histology) not associated with excessive alcohol consumption or other causes (medications or congenital disorders) [1]. NAFLD has currently reached a prevalence of epidemic proportions, ranging from 20–30% in the general adult population to peaks of over 70% among diabetics [2]. The pathophysiological mechanisms underlying the close relationship between NAFLD and T2DM are multiple (mainly insulin resistance), complex, and only partially known [3] Liver biopsy is the gold standard for NAFLD diagnosis, though it is highly invasive and expensive. Proton density fat fraction calculated by magnetic resonance imaging is the most sensitive and specific non-invasive method for detecting even the slightest degree of hepatic steatosis involving 5–10% of the parenchyma. However, given its scarce availability and high cost, it cannot be used as a screening method. Thus, more economic and less invasive technics have spread and are routinely used in daily practice, such as abdomen ultrasound and the fatty liver index, which makes use of four

clinical laboratory parameters (body mass index, waist circumference, serum triglycerides, and serum gamma-glutamyl-transferase). FibroScan®, implemented with CAP (controlled attenuation parameter), is another non-invasive and less expensive diagnostic tool that is able to evaluate liver fibrosis by testing its stiffness (rigidity), expressed in kiloPascals (kPa), and quantify the hepatic steatosis with good accuracy [1,4].

The increasing concern about this disease is strictly linked to the rise in liver complications (non-alcoholic steatohepatitis, liver cirrhosis, and hepatocellular carcinoma), increased cardiovascular complications, and overall mortality [5–7]. Moreover, there is still uncertainty about the safety of antihyperglycemic treatments in diabetic patients with NAFLD [1,8].

According to most recent guidelines, NAFLD's only therapeutic option is represented by lifestyle change to promote weight loss through diet and/or physical activity [1]. No pharmacological therapy has been approved for NAFLD treatment. Metformin is not only the first pharmacological line in the treatment of T2DM according to all international scientific guidelines, but it also exerts numerous extra anti-hyperglycaemic ancillary effects, which could soon broaden its therapeutic indications [9,10]. Metformin's benefits, including inhibiting hepatic gluconeogenesis, modifying hepatic fatty acid metabolism, increasing fatty acid oxidation, reducing lipogenesis, enhancing insulin sensitivity, and increasing antioxidant properties, are well-established [11–13]. Several studies have reported that these favorable effects might induce amelioration of liver histology in patients with NAFLD/NASH [11]. In subjects with high CV risk or heart failure and renal damage, the association with sodium–glucose cotransporter-2 inhibitors (SGLT2i) is strongly suggested [14]. Although several hypotheses currently exist, the effects of SGLT2i inhibitors on NAFLD development and/or regression are not fully understood, and further investigations are required [15]. Up to now, only a few observational studies and one randomized control trial on a limited number of patients have suggested SGLT2i's efficacy in ameliorating liver steatosis with FibroScan®/CAP evaluation [16].

The aim of the present pilot study was to compare the effects of a combination of empagliflozin plus metformin vs. metformin monotherapy on liver steatosis using FibroScan®/CAP in a cohort of diabetic patients.

2. Methods and Materials

2.1. Study Population

"Impact of anti-hyperglyceMic Agents on NAFLD proGressIoN in type 2 Diabetes" (IMAGIN) is a single-center prospective observational pilot study. SGLT2i-naïve patients aged $\geq$18 years with metformin-treated T2DM, an estimated glomerular filtration rate of $\geq$45 mL/min/m^2 calculated according to CKD-EPI, and the presence of NAFLD documented by B-mode ultrasound (mild, moderate, or severe bright liver in a patient with no history of hemochromatosis, cystinosis, and/or glycosphingolipidosis of Gaucher type 1) were included in the study. The exclusion criteria were any other form of diabetes; severe cardiac, liver and/or renal insufficiency; an acute cardiovascular event that occurred in the previous 3 months, pregnancy; neoplasm without 6 months of remission; other forms of hepatitis; any inflammatory disease; prolonged use of steroids; and daily alcohol consumption of >20 g (for males) or >10 g (for females). A total of 127 patients with metformin-treated T2DM who were followed at the internal medicine clinic of the University of Campania "Luigi Vanvitelli" were consecutively screened between March 2021 and May 2022. Patients who were not SGLT2i-naïve (n = 7), were already undergoing combination therapy (n = 30) or insulin therapy (n = 7), had severe kidney impairment (n = 12), and did not provide written consent (n = 8) were excluded. Thus, 63 patients were enrolled in the present study, and follow-up was censored in October 2022. Patients were assigned to a metformin monotherapy group or started the combination therapy of metformin + SGLT2i according to the standards of care of the American Diabetes Association [17].

All patients provided written informed consent for data storage and analysis. The study was conducted in accordance with the Declaration of Helsinki and was approved by

the ethics committee of the Azienda Ospedialiera Universitaria of Università degli Studi della Campania "Luigi Vanvitelli" (Ethics Committee Review (2021) No. 0005501).

2.2. Procedures

Anthropometric clinical data and blood samples were collected on the same date of the FibroScan® examinations at visit 0 and follow-up (6 months). Blood samples were collected after an 8-h overnight fast and included hemochrome, albumin, transaminases, and glycated hemoglobin.

2.3. FibroScan®/CAP Measurements

FibroScan® Mini + 430 powered with CAP (Echosens SA, France) was used for the present analysis. CAP and liver stiffness were measured by the same trained operator with an M probe (3.5 MHz), which was placed on the skin in the intercostal space over the right lobe of the liver. Liver stiffness was calculated over at least 10 valid measurements, with a ratio of the interquartile range (IQR) to the median of the liver stiffness (IQR/Median) of $\leq$30%. Notably, CAP, through the SmartExam program, was continuously computed during the entire examination until the CAP gauge reached 100%. The hepatic steatosis grade was defined by the cut-off values of CAP according to previous reports (sensitivity 82.3%, specificity 55.7% for the 238 dB/m cut-off). CAP < 238 dB/m denoted the absence of steatosis (S0), 238 $\leq$ CAP $\leq$ 259 dB/m denoted mild steatosis (grade S1), 260 $\leq$ CAP $\leq$ 291 dB/m denoted moderate steatosis (grade S2), and CAP > 291 dB/m denoted severe steatosis (grade S3). ΔCAP was measured by the following formula: (initial CAP—follow-up CAP)/initial CAP. The hepatic fibrosis cut-off value was liver stiffness $\geq$ 7.0 kPa [18].

2.4. Study Endpoint

The primary study endpoint was to assess the effects of a combination of gliflozin plus metformin vs. metformin monotherapy on NAFLD in our cohort of T2DM patients.

2.5. Statistical Analysis

Categorical data were expressed as numbers and percentages, whereas continuous variables were expressed as either the median (interquartile range (IQR)) or mean ± SD, depending on their distribution as assessed by the Shapiro–Wilk test. Population data were divided into different groups according to the antidiabetic treatment (metformin of metformin + SGLT2i). Between-group differences for categorical variables were assessed by the chi-square test with the application of Yates correction where appropriate. Either the parametric Student's t-test or the nonparametric Mann–Whitney U test was used to compare continuous variables, depending on their distribution. All statistical tests for the two subgroups were two-sided and evaluated at the 0.05 level of significance. Finally, we performed a box plot analysis to evaluate the CAP variation between the two subgroups. All statistical analyses were performed through the RStudio® software (RStudio, Boston, MA, USA).

3. Results

Sixty-three metformin-treated T2DM patients with an echographic diagnosis of NAFLD (aged 60.95 ± 11.14 years; males, 57.1%) were included in the present analysis. Among them, 33 patients continued metformin monotherapy (control group), whilst 30 patients (47.6%) received a combination of metformin + empagliflozin (experimental group). The case group showed a higher level of glycated hemoglobin and AST, and fewer patients were treated with angiotensin-converting enzyme inhibitors (ACEi) and diuretics. All baseline characteristics are reported in Tables 1 and 2. At the 6-month follow-up, the experimental group presented a significant reduction in BMI, glycated hemoglobin, ALT, CAP parameter, and steatosis degree in comparison with the control group (Table 2). The box plot analysis showed that the median ΔCAP was significantly lower in patients in the experimental group compared with those in the control group (Figure 1).

Table 1. Baseline clinical characteristics of the study sample.

BASELINE				
Parameter	**Overall (*n* = 63)**	**Control Group (*n* = 33)**	**Combination Group (*n* = 30)**	***p*-Value**
Age, mean (SD)	60.95 (11.14)	60.09 (11.47)	61.90 (10.88)	0.524
Sex, *n* (%)				
Male	36 (57.1)	19 (57.6)	17 (56.7)	1.000
Female	27 (42.9)	14 (42.4)	13 (43.3)	
Hypertension, *n* (%)	43 (68.3)	21 (63.6)	22 (73.3)	0.579
Smoking habit, *n* (%)	26 (41.3)	13 (39.4)	13 (43.3)	0.951
ACEi, *n* (%)	12 (19.0)	10 (30.3)	2 (6.7)	**0.039**
ARB, *n* (%)	12 (19.0)	9 (27.3)	3 (10.0)	0.155
Diuretic, *n* (%)	6 (9.5)	6 (18.2)	-	**0.043**
Beta-blockers, *n* (%)	8 (12.7)	6 (18.2)	2 (6.7)	0.321
Alfa blockers, *n* (%)	1 (1.6)	-	1 (3.3)	0.962
Ca antagonist, *n* (%)	4 (6.3)	2 (6.1)	2 (6.7)	1.000
Statin, *n* (%)	31 (49.2)	15 (45.5)	16 (53.3)	0.710

SD, standard deviation; ACEi, angiotensin-converting enzyme inhibitor; ARB, angiotensin receptor blocker; Ca, calcium.

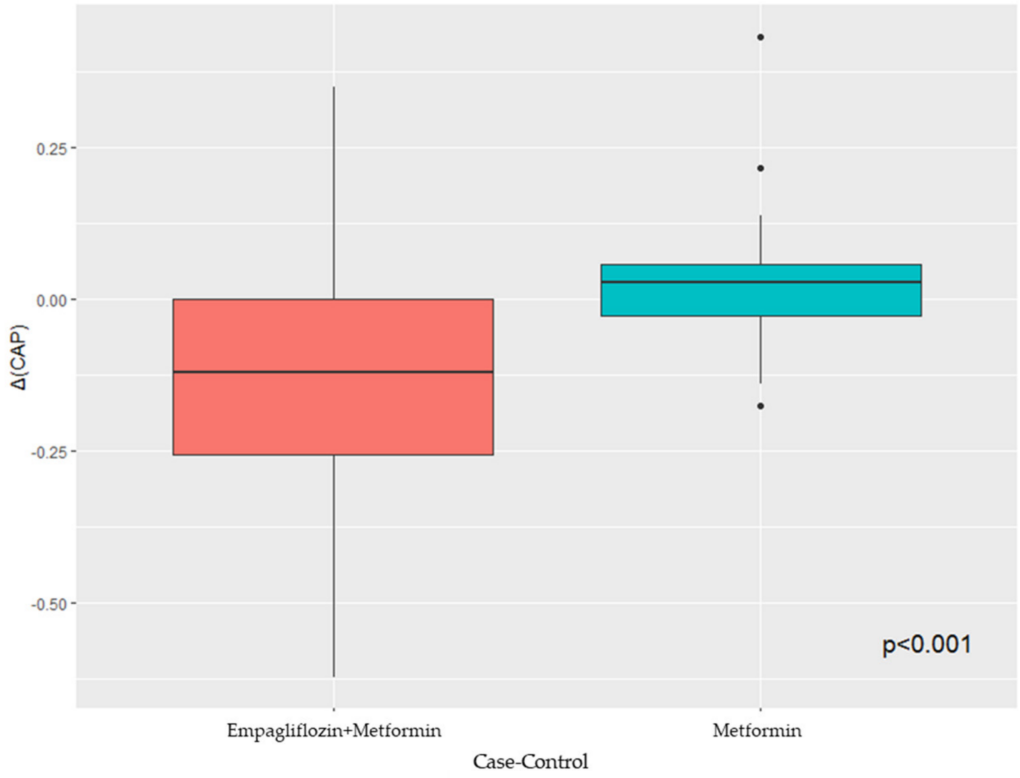

Figure 1. Box plot analysis of CAP variation in case and control groups.

Of note, no adverse events were reported by our patients during the observation phase.

Table 2. Comparison of baseline and follow-up clinical, anthropometric, and laboratory data of the study sample.

	PROGRESSION TIME					
	Time 0 (Baseline)			Time 1 (=6 months)		
Parameter	**Control Group (*n* = 33)**	**Combination Group (*n* = 30)**	***p*-Value**	**Control Group (*n* = 33)**	**Combination Group (*n* = 30)**	***p*-Value**
Bmi, mean (SD)	31.89 (4.65)	30.83 (3.52)	0.314	31.91 (4.66)	28.48 (3.25)	**0.023**
HbA1$_c$, median [IQR]	7.10 [6.50, 7.50]	8.20 [7.40, 8.80]	**0.002**	7.20 [6.50, 7.50]	7.20 [6.80, 7.90]	0.552
Ast, median [IQR]	38.00 [26.00, 42.00]	44.00 [28.50, 47.75]	0.139	38.00 [27.00, 44.00]	41.00 [25.00, 46.00]	0.789
Alt, median [IQR]	49.00 [32.00, 67.00]	68.5 [41.50, 88.00]	**0.050**	56.00 [43.00, 72.00]	45.00 [38.00, 48.00]	**0.006**
Platelet, median [IQR]	210000 [143000, 243000]	236500 [193250, 287500]	0.054	221000 [145000, 242000]	234000 [199000, 250000]	0.253
Albumin, median [IQR]	4.10 [3.80, 4.32]	4.00 [3.80, 4.40]	0.873	4.20 [4.00, 4.30]	4.16 [3.98, 4.40]	0.911
Stiffness kPa, median [IQR]	7.20 [5.70, 10.40]	8.30 [6.42, 10.15]	0.248	7.40 [6.00, 10.62]	6.80 [5.55, 8.10]	0.237
Degree Fibrosis, *n* (%)						
0–1	14 (42.4)	9 (30.0)	0.566	11 (33.3)	17 (56.7)	0.151
2	10 (30.3)	12 (40.0)		12 (36.4)	9 (30.0)	
3	6 (18.2)	4 (13.3)		6 (18.2)	1 (3.3)	
4	3 (9.1)	5 (16.7)		4 (12.1)	3 (10.0)	
CAP, median [IQR]	280.00 [258.00, 310.00]	293.50 [270.00, 319.25]	0.401	289.00 [259.00, 324.00]	267.00 [259.50, 283.75]	**0.036**
Degree Steatosis, *n* (%)						
0	4 (12.1)	2 (6.7)		6 (18.2)	3 (10.0)	
1	6 (18.2)	2 (6.7)	0.382	3 (9.1)	5 (16.7)	**0.001**
2	7 (21.2)	10 (33.3)		9 (27.3)	20 (66.7)	
3	16 (48.5)	16 (53.3)		15 (45.5)	2 (6.7)	
FIB-4, median [IQR]	1.33 [0.94, 1.84]	1.39 [1.08, 1.68]	0.934	1.42 [1.13, 1.55]	1.58 [1.35, 1.87]	0.174

SD, standard deviation; BMI, body mass index; HbA1$_c$, glycated hemoglobin; IQR, interquartile range; AST, aspartate aminotransferase; ALT, alanine aminotransferase; CAP, controlled attenuated parameter; FIB-4, fibrosis-4.

4. Discussion

Among our cohort of metformin-treated T2DM patients, the addition of an SGLT2i proved to reduce ALT levels, body weight, CAP parameter and variation, steatosis degree, and glycaemic control improvement.

SGLT2i exerts its action by selectively inhibiting SGLT2 in the kidneys, leading to an insulin-independent lowering of blood glucose levels (0.6–0.8% glycated hemoglobin reduction) through a boosted daily urinary loss of up to 100 g of glucose (200–300 kcal) and an increased natriuretic effect due to sodium reabsorption inhibition [14,19,20].

Adipose tissue is considered a real endocrine organ capable of producing various biochemical compounds called adipokines, which exert autocrine, paracrine, and endocrine functions by acting on the body's energetic metabolism [21]. One of the hormones produced by adipose tissue is leptin, which communicates within the liver by activating the JAK-2, STAT-3, MAPK/ERK, and PI3K/AKT/mTOR pathways [22]. At low levels, it exerts a protective effect on hepatic steatosis due to its insulin-sensitizing effects, suppression of gluconeogenesis, and de novo lipogenesis, as well as its stimulation of FFA beta-oxidation [23]. However, leptin overproduction, due to increased adipose tissue, acts as a pro-inflammatory and fibrogenic factor acting on metalloproteinases (TIMP metallopeptidase inhibitor 1 and matrix metalloproteinase-1), stimulating TGF-β, and upregulating CD14 on liver Kupffer cells, thus worsening liver steatosis [24–27]. SGLT2i clinical trials have reported moderate weight loss caused by a reduction in the volume of both the abdominal visceral adipose tissue and subcutaneous adipose tissue, thus also ameliorating metabolic syndrome. These mechanisms lead to a reduction in insulin resistance, which has been shown to play a central role in the reduction of other important clinical outcomes closely related to metabolic syndrome [28–31]. In particular, endothelial dysfunction amelioration, together with the reduction in inflammation and reactive oxygen species production as well as metabolic changes, are involved in cardiorenal and hepatic risk reduction [28–31]. In fact, insulin resistance is involved in both glucose and lipid metabolism and is responsible for increased gluconeogenesis and decreased glucose consumption and re-uptake, as well as increased lipogenesis and decreased lipolysis with an increase in the level of triglyceride accumulation in the liver, due to the FOXO1-mediated pathway [32,33]. Indeed, FOXO1 intensifies the transcription of the sterol regulatory element-binding transcription factor 1c involved in lipogenesis. At the same time, once FOXO1 is translocated out of the nucleus, it hinders the transcription of G6P, triggering an increase in lipogenesis against glycogen production [34].

Since SGLT2i commercialization, increasing evidence has reported the efficacy of this class of drug in several clinical scenarios, with particular emphasis on cardiovascular risk reduction, which is enhanced in T2DM and NAFLD patients regardless of other major risk factors. In animal models, SGLT2i proved to have efficacy in reducing liver steatosis, fibrosis, and inflammation [15]. It has been suggested that these changes might be due to a negative energy balance, which in turn is a result of enhanced glycosuria and a substrate shift toward lipids that might be promoted by an increased glucagon/insulin ratio [35]. These same effects are also responsible for both improved glycaemic control and weight loss, as reported by several studies [35,36]. Due to this, the use of SGLT2i has been considered for the treatment of NAFLD patients. In our study, the addition of the SGLT2i empagliflozin to metformin induced a statistically significant reduction in the median CAP parameter of 9% (3.9–11.1%). Similar findings were reported by a Japanese open-label trial on 57 patients with T2DM and NAFLD randomized to 5 mg dapagliflozin per day for 24 weeks (n = 33) or to a control group (n = 24). They reported a CAP parameter reduction from a baseline of 315 ± 61 dB/m to 290 ± 73 dB/m at follow-up [37]. By contrast, the only randomized control trial published, which enrolled 44 patients with T2DM and NAFLD who were randomized to receive 50 mg/day of ipragliflozin as an add-on treatment (n = 29) or continued metformin and pioglitazone (n = 15) for 24 weeks, exhibited a non-significant CAP decline in the intervention group [16]. However, the authors reported improvement in NAFLD parameters and serum ALT levels, similar to our results, and this has been suggested to be associated with reductions in body weight

and HbA1c levels [16,38]. Moreover, in a prospective randomized, double-blind, placebo-controlled trial enrolling 106 patients with both NAFLD and T2DM who were assigned to receive empagliflozin 10 mg (n = 35), pioglitazone 30 mg (n = 34), or placebo (n = 37) for 24 weeks, only a borderline significant decrease in CAP score was observed with empagliflozin compared with placebo (−29.6 dB/m (−39.5 to −19.6) vs. −16.4 dB/m (−25.0 to −7.8), respectively; p = 0.05) [39].

Liver fat content amelioration associated with SGLT2is treatment has also been assessed through magnetic resonance imaging. A potentially consistent reduction in liver fat, especially when ALT levels are high, was suggested by the analysis of several datasets collected in individuals with T2DM, including the EMPA-REG OUTCOME® trial. However, liver fat was not directly measured in any of the studies included in these analyses, and only one study using magnetic resonance spectroscopy showed that ALT levels reasonably correlated with liver fat in individuals with T2DM (r = 0.66) [40]. In a recent meta-analysis of 12 randomized controlled trials estimating the efficacy of different SGLT2is on NAFLD and enrolling 850 overweight or obese individuals followed for 24 weeks, a decrease in ALT levels as well as fatty liver content was reported [28]. These conclusions were also confirmed by another larger meta-analysis, enrolling 1950 patients with T2DM with and without NAFLD who were treated with SGLT2i for at least 8 weeks and 1900 control patients [41]. In the E-LIFT trial, 50 patients with type 2 diabetes and NAFLD were enrolled and randomized to an empagliflozin group (standard treatment plus empagliflozin 10 mg daily) or a control group (standard treatment without empagliflozin). After 20 weeks, they reported a significant reduction in liver fat content according to magnetic resonance imaging (about 4.9%) and reduced ALT levels [42].

Eight patients enrolled in our study had liver stiffness of severe grade of fibrosis according to the FibroScan® evaluations. At follow-up, we assisted in a reduction in patients' median stiffness value, though this was not statistically significant. It seems possible that this may be due to the reduced glucotoxicity secondary to better glycaemic control and the reduced liver fat accumulation and inflammation. Moreover, it is also possible that several patients could have been affected by undiagnosed NASH. Cumulative evidence in both preclinical and clinical scenarios has proven SGLT2i's efficacy in NASH resolution. It is possible that, beyond the aforementioned mechanisms, SGLT2i could have played a role in reducing stiffness parameters, though more studies are needed [15,43]. FIB-4 evaluation, instead, showed a numerical increase, though it was not significant. This may be due to the mathematical formula used to calculate FIB-4. In fact, the ALT levels, which were reduced during treatment, are reported in the denominator, thus increasing their value. In any case, the mean value reported was not significant for fibrosis [44].

5. Limitations

Our study presents some limitations. First of all, this is a single-center pilot study with a small sample size, thus limiting the generalization of our results. Moreover, dietary habits, which are potential confounders, were not documented systematically during the study. However, none of our patients reported changes in their lifestyles regarding dietary habits or physical exercise. Finally, this prospective observational study does not allow us to define a cause–effect relationship but only an association between metformin plus empagliflozin combination therapy and an improvement in the assessed endpoints.

6. Conclusions

In T2DM patients, the combination of empagliflozin + metformin vs. metformin monotherapy ameliorated liver steatosis (with amelioration of 9% of the CAP value), ALT levels, body weight, and glycated haehemoglobinter only a 6-month follow-up. The promising preliminary results of this pilot study need to be confirmed in a larger population and above all by ad hoc-designed RCTs.

Author Contributions: Conceptualization, A.C., C.A., R.G. and F.C.S.; investigation, A.C., R.G., C.A., E.V., G.M. and A.M.; formal analysis, G.L.; writing—original draft preparation, A.C., R.G. and F.C.S.; writing—review and editing, A.C., R.G., T.S., L.R. and F.C.S.; supervision, R.M., L.R., T.S., C.S., M.M. and F.C.S. All authors have read and agreed to the published version of the manuscript.

Funding: The project was supported by the Programma VALERE, University of Campania "Luigi Vanvitelli".

Institutional Review Board Statement: Azienda Ospedialiera Universitaria of Università degli Studi della Campania "Luigi Vanvitelli" (Ethics Committee Review (2021) No. 0005501).

Informed Consent Statement: Informed consent was obtained from all subjects involved in the study.

Data Availability Statement: The data that support the findings of this study are available upon reasonable request from the corresponding author.

Conflicts of Interest: The authors declare no conflict of interest.

References

1. European Association for the Study of the Liver (EASL); European Association for the Study of Diabetes (EASD); European Association for the Study of Obesity (EASO). EASL-EASD-EASO Clinical Practice Guidelines for the management of non-alcoholic fatty liver disease. *J. Hepatol.* **2016**, *64*, 1388–1402. [CrossRef] [PubMed]
2. Rinaldi, L.; Pafundi, P.C.; Galiero, R.; Caturano, A.; Morone, M.V.; Silvestri, C.; Giordano, M.; Salvatore, T.; Sasso, F.C. Mechanisms of Non-Alcoholic Fatty Liver Disease in the Metabolic Syndrome. A Narrative Review. *Antioxidants* **2021**, *10*, 270. [CrossRef]
3. Acierno, C.; Caturano, A.; Pafundi, P.C.; Nevola, R.; Adinolfi, L.E.; Sasso, F.C. Nonalcoholic fatty liver disease and type 2 diabetes: Pathophysiological mechanisms shared between the two faces of the same coin. *Explor. Med.* **2020**, *1*, 287–306. [CrossRef]
4. Sasso, M.; Tengher-Barna, I.; Ziol, M.; Miette, V.; Fournier, C.; Sandrin, L.; Poupon, R.; Cardoso, A.C.; Marcellin, P.; Douvin, C.; et al. Novel controlled attenuation parameter for noninvasive assessment of steatosis using Fibroscan(®): Validation in chronic hepatitis C. *J. Viral Hepat.* **2012**, *19*, 244–253. [CrossRef] [PubMed]
5. Galiero, R.; Caturano, A.; Vetrano, E.; Cesaro, A.; Rinaldi, L.; Salvatore, T.; Marfella, R.; Sardu, C.; Moscarella, E.; Gragnano, F.; et al. Pathophysiological mechanisms and clinical evidence of relationship between Nonalcoholic fatty liver disease (NAFLD) and cardiovascular disease. *Rev. Cardiovasc. Med.* **2021**, *22*, 755–768. [CrossRef] [PubMed]
6. Caturano, A.; Acierno, C.; Nevola, R.; Pafundi, P.C.; Galiero, R.; Rinaldi, L.; Salvatore, T.; Adinolfi, L.E.; Sasso, F.C. Non-Alcoholic Fatty Liver Disease: From Pathogenesis to Clinical Impact. *Processes* **2021**, *9*, 135. [CrossRef]
7. Sasso, F.C.; Carbonara, O.; Cozzolino, D.; Rambaldi, P.; Mansi, L.; Torella, D.; Gentile, S.; Turco, S.; Torella, R.; Salvatore, T. Effects of insulin-glucose infusion on left ventricular function at rest and during dynamic exercise in healthy subjects and noninsulin dependent diabetic patients: A radionuclide ventriculographic study. *J. Am. Coll. Cardiol.* **2000**, *36*, 219–226. [CrossRef]
8. Gentile, S.; Turco, S.; Guarino, G.; Oliviero, B.; Annunziata, S.; Cozzolino, D.; Sasso, F.C.; Turco, A.; Salvatore, T.; Torella, R. Effect of treatment with acarbose and insulin in patients with non-insulin-dependent diabetes mellitus associated with non-alcoholic liver cirrhosis. *Diabetes Obes. Metab.* **2001**, *3*, 33–40. [CrossRef]
9. Salvatore, T.; Pafundi, P.C.; Morgillo, F.; Di Liello, R.; Galiero, R.; Nevola, R.; Marfella, R.; Monaco, L.; Rinaldi, L.; Adinolfi, L.E.; et al. Metformin: An old drug against old age and associated morbidities. *Diabetes Res. Clin. Pract.* **2020**, *160*, 108025. [CrossRef]
10. Salvatore, T.; Pafundi, P.C.; Galiero, R.; Rinaldi, L.; Caturano, A.; Vetrano, E.; Aprea, C.; Albanese, G.; Di Martino, A.; Ricozzi, C.; et al. Can Metformin Exert as an Active Drug on Endothelial Dysfunction in Diabetic Subjects? *Biomedicines* **2020**, *9*, 3. [CrossRef]
11. Zhou, J.; Massey, S.; Story, D.; Li, L. Metformin: An Old Drug with New Applications. *Int. J. Mol. Sci.* **2018**, *19*, 2863. [CrossRef] [PubMed]
12. Di Francia, R.; Rinaldi, L.; Troisi, A.; Di Benedetto, F.; Berretta, M. Effect of anti-oxidant agents in patients with hepatocellular diseases. *Eur. Rev. Med. Pharmacol. Sci.* **2015**, *19*, 3993–3995. [PubMed]
13. Di Francia, R.; Rinaldi, L.; Cillo, M.; Varriale, E.; Facchini, G.; D'Aniello, C.; Marotta, G.; Berretta, M. Antioxidant diet and genotyping as tools for the prevention of liver disease. *Eur. Rev. Med. Pharmacol. Sci.* **2016**, *20*, 5155–5163. [PubMed]
14. American Diabetes Association Professional Practice Committee; Draznin, B.; Aroda, V.R.; Bakris, G.; Benson, G.; Brown, F.M.; Freeman, R.; Green, J.; Huang, E.; Isaacs, D.; et al. 9. Pharmacologic Approaches to Glycemic Treatment: Standards of Medical Care in Diabetes-2022. *Diabetes Care* **2022**, *45* (Suppl. 1), S125–S143. [CrossRef]
15. Katsiki, N.; Perakakis, N.; Mantzoros, C. Effects of sodium-glucose co-transporter-2 (SGLT2) inhibitors on non-alcoholic fatty liver disease/non-alcoholic steatohepatitis: Ex quo et quo vadimus? *Metabolism* **2019**, *98*, iii–ix. [CrossRef]
16. Han, E.; Lee, Y.H.; Lee, B.W.; Kang, E.S.; Cha, B.S. Ipragliflozin Additively Ameliorates Non-Alcoholic Fatty Liver Disease in Patients with Type 2 Diabetes Controlled with Metformin and Pioglitazone: A 24-Week Randomized Controlled Trial. *J. Clin. Med.* **2020**, *9*, 259. [CrossRef]

17. American Diabetes Association. 9. Pharmacologic Approaches to Glycemic Treatment: Standards of Medical Care in Diabetes-2021. *Diabetes Care* **2021**, *44* (Suppl. 1), S111–S124. [CrossRef]
18. Huang, Z.; Ng, K.; Chen, H.; Deng, W.; Li, Y. Validation of Controlled Attenuation Parameter Measured by FibroScan as a Novel Surrogate Marker for the Evaluation of Metabolic Derangement. *Front. Endocrinol.* **2022**, *12*, 739875. [CrossRef]
19. Saisho, Y. SGLT2 Inhibitors: The Star in the Treatment of Type 2 Diabetes? *Diseases* **2020**, *8*, 14. [CrossRef]
20. Salvatore, T.; Pafundi, P.C.; Galiero, R.; Albanese, G.; Di Martino, A.; Caturano, A.; Vetrano, E.; Rinaldi, L.; Sasso, F.C. The Diabetic Cardiomyopathy: The Contributing Pathophysiological Mechanisms. *Front. Med.* **2021**, *30*, 695792. [CrossRef]
21. Polyzos, S.A.; Mantzoros, C.S. Leptin in health and disease: Facts and expectations at its twentieth anniversary. *Metabolism* **2015**, *64*, 5–12. [CrossRef] [PubMed]
22. Robertson, S.A.; Leinninger, G.M.; Myers, M.G., Jr. Molecular and neural mediators of leptin action. *Physiol. Behav.* **2008**, *94*, 637–642. [CrossRef] [PubMed]
23. Polyzos, S.A.; Kountouras, J.; Mantzoros, C.S. Leptin in nonalcoholic fatty liver disease: A narrative review. *Metabolism* **2015**, *64*, 60–78. [CrossRef] [PubMed]
24. Aleffi, S.; Petrai, I.; Bertolani, C.; Parola, M.; Colombatto, S.; Novo, E.; Vizzutti, F.; Anania, F.A.; Milani, S.; Rombouts, K.; et al. Upregulation of proinflammatory and proangiogenic cytokines by leptin in human hepatic stellate cells. *Hepatology* **2005**, *42*, 1339–1348. [CrossRef]
25. Yan, K.; Deng, X.; Zhai, X.; Zhou, M.; Jia, X.; Luo, L.; Niu, M.; Zhu, H.; Qiang, H.; Zhou, Y. p38 mitogen-activated protein kinase and liver X receptor-α mediate the leptin effect on sterol regulatory element binding protein-1c expression in hepatic stellate cells. *Mol. Med.* **2012**, *18*, 10–18. [CrossRef]
26. Cao, Q.; Mak, K.M.; Ren, C.; Lieber, C.S. Leptin stimulates tissue inhibitor of metalloproteinase-1 in human hepatic stellate cells: Respective roles of the JAK/STAT and JAK-mediated H2O2-dependant MAPK pathways. *J. Biol. Chem.* **2004**, *279*, 4292–4304. [CrossRef] [PubMed]
27. Ikejima, K.; Takei, Y.; Honda, H.; Hirose, M.; Yoshikawa, M.; Zhang, Y.J.; Lang, T.; Fukuda, T.; Yamashina, S.; Kitamura, T.; et al. Leptin receptor-mediated signaling regulates hepatic fibrogenesis and remodeling of extracellular matrix in the rat. *Gastroenterology* **2002**, *122*, 1399–1410. [CrossRef]
28. Mantovani, A.; Petracca, G.; Csermely, A.; Beatrice, G.; Targher, G. Sodium-Glucose Cotransporter-2 Inhibitors for Treatment of Nonalcoholic Fatty Liver Disease: A Meta-Analysis of Randomized Controlled Trials. *Metabolism* **2020**, *11*, 22. [CrossRef]
29. Salvatore, T.; Caturano, A.; Galiero, R.; Di Martino, A.; Albanese, G.; Vetrano, E.; Sardu, C.; Marfella, R.; Rinaldi, L.; Sasso, F.C. Cardiovascular Benefits from Gliflozins: Effects on Endothelial Function. *Biomedicines* **2021**, *9*, 1356. [CrossRef]
30. Sasso, F.C.; Pafundi, P.C.; Caturano, A.; Galiero, R.; Vetrano, E.; Nevola, R.; Petta, S.; Fracanzani, A.L.; Coppola, C.; Di Marco, V.; et al. Impact of direct acting antivirals (DAAs) on cardiovascular events in HCV cohort with pre-diabetes. *Nutr. Metab. Cardiovasc. Dis.* **2021**, *31*, 2345–2353. [CrossRef]
31. Adinolfi, L.E.; Petta, S.; Fracanzani, A.L.; Nevola, R.; Coppola, C.; Narciso, V.; Rinaldi, L.; Calvaruso, V.; Pafundi, P.C.; Lombardi, R.; et al. Reduced incidence of type 2 diabetes in patients with chronic hepatitis C virus infection cleared by direct-acting antiviral therapy: A prospective study. *Diabetes Obes. Metab.* **2020**, *22*, 2408–2416. [CrossRef] [PubMed]
32. Haeusler, R.A.; Hartil, K.; Vaitheesvaran, B.; Arrieta-Cruz, I.; Knight, C.M.; Cook, J.R.; Kammoun, H.L.; Febbraio, M.A.; Gutierrez-Juarez, R.; Kurland, I.J.; et al. Integrated control of hepatic lipogenesis versus glucose production requires FoxO transcription factors. *Nat. Commun.* **2014**, *5*, 5190. [CrossRef]
33. Chen, L.; Chen, X.W.; Huang, X.; Song, B.L.; Wang, Y.; Wang, Y. Regulation of glucose and lipid metabolism in health and disease. *Sci. China Life Sci.* **2019**, *62*, 1420–1458. [CrossRef]
34. Choi, D.H.; Jung, C.H.; Mok, J.O.; Kim, C.H.; Kang, S.K.; Kim, B.Y. Effect of dapagliflozin on alanine aminotransferase improvement in type 2 diabetes mellitus with non-alcoholic fatty liver disease. *Endocr. Metab.* **2018**, *33*, 387–394. [CrossRef] [PubMed]
35. Gunhan, H.G.; Imre, E.; Erel, P.; Ustay, O. Empagliflozin is more effective in reducing microalbuminuria and alt levels compared with dapagliflozin: Real life experience. *Acta Endocrinol.* **2020**, *16*, 59–67. [CrossRef]
36. Salvatore, T.; Galiero, R.; Caturano, A.; Rinaldi, L.; Di Martino, A.; Albanese, G.; Di Salvo, J.; Epifani, R.; Marfella, R.; Docimo, G.; et al. An Overview of the Cardiorenal Protective Mechanisms of SGLT2 Inhibitors. *Int. J. Mol. Sci.* **2022**, *23*, 3651. [CrossRef] [PubMed]
37. Shimizu, M.; Suzuki, K.; Kato, K.; Jojima, T.; Iijima, T.; Murohisa, T.; Iijima, M.; Takekawa, H.; Usui, I.; Hiraishi, H.; et al. Evaluation of the effects of dapagliflozin, a sodium-glucose co-transporter-2 inhibitor, on hepatic steatosis and fibrosis using transient elastography in patients with type 2 diabetes and non-alcoholic fatty liver disease. *Diabetes Obes. Metab.* **2019**, *21*, 285–292. [CrossRef]
38. Leiter, L.A.; Forst, T.; Polidori, D.; Balis, D.A.; Xie, J.; Sha, S. Effect of canagliflozin on liver function tests in patients with type 2 diabetes. *Diabetes Metab.* **2016**, *42*, 25–32. [CrossRef]
39. Chehrehgosha, H.; Sohrabi, M.R.; Ismail-Beigi, F.; Malek, M.; Reza Babaei, M.; Zamani, F.; Ajdarkosh, H.; Khoonsari, M.; Fallah, A.E.; Khamseh, M.E. Empagliflozin Improves Liver Steatosis and Fibrosis in Patients with Non-Alcoholic Fatty Liver Disease and Type 2 Diabetes: A Randomized, Double-Blind, Placebo-Controlled Clinical Trial. *Diabetes Ther.* **2021**, *12*, 843–861. [CrossRef]

40. Sattar, N.; Fitchett, D.; Hantel, S.; George, J.T.; Zinman, B. Empagliflozin is associated with improvements in liver enzymes potentially consistent with reductions in liver fat: Results from randomised trials including the EMPA-REG OUTCOME® trial. *Diabetologia* **2018**, *61*, 2155–2163. [CrossRef]
41. Coelho, F.D.S.; Borges-Canha, M.; von Hafe, M.; Neves, J.S.; Vale, C.; Leite, A.R.; Carvalho, D.; Leite-Moreira, A. Effects of sodium-glucose co-transporter 2 inhibitors on liver parameters and steatosis: A meta-analysis of randomized clinical trials. *Diabetes Metab. Res Rev.* **2021**, *37*, e3413. [CrossRef] [PubMed]
42. Kuchay, M.S.; Krishan, S.; Mishra, S.K.; Farooqui, K.J.; Singh, M.K.; Wasir, J.S.; Bansal, B.; Kaur, P.; Jevalikar, G.; Gill, H.K.; et al. Effect of Empagliflozin on Liver Fat in Patients With Type 2 Diabetes and Nonalcoholic Fatty Liver Disease: A Randomized Controlled Trial (E-LIFT Trial). *Diabetes Care* **2018**, *41*, 1801–1808. [CrossRef] [PubMed]
43. Eriksson, J.W.; Lundkvist, P.; Jansson, P.A.; Johansson, L.; Kvarnström, M.; Moris, L.; Miliotis, T.; Forsberg, G.B.; Risérus, U.; Lind, L.; et al. Effects of dapagliflozin and n-3 carboxylic acids on non-alcoholic fatty liver disease in people with type 2 diabetes: A double-blind randomised placebo-controlled study. *Diabetologia* **2018**, *61*, 1923–1934. [CrossRef] [PubMed]
44. Sterling, R.K.; Lissen, E.; Clumeck, N.; Sola, R.; Correa, M.C.; Montaner, J.; Sulkowski, M.; Torriani, F.J.; Dieterich, D.T.; APRICOT Clinical Investigators; et al. Development of a simple noninvasive index to predict significant fibrosis in patients with HIV/HCV coinfection. *Hepatology* **2006**, *43*, 1317–1325. [CrossRef]

biomedicines

MDPI

Article

The Impact of SGLT2 Inhibitor Dapagliflozin on Adropin Serum Levels in Men and Women with Type 2 Diabetes Mellitus and Chronic Heart Failure

Alexander A. Berezin [1,2], Zeljko Obradovic [2], Ivan M. Fushtey [1], Tetiana A. Berezina [3], Evgen V. Novikov [4], Lukas Schmidbauer [5], Michael Lichtenauer [5] and Alexander E. Berezin [5,6,*]

1 Internal Medicine Department, Zaporozhye Medical Academy of Postgraduate Education, 69000 Zaporozhye, Ukraine
2 Department of Psychosomatic Medicine and Psychotherapy, Klinik Barmelweid, 5017 Barmelweid, Switzerland
3 Department of Internal Medicine and Nephrology, VitaCenter, 69000 Zaporozhye, Ukraine
4 Educational and Research Center—Ukrainian Family Medicine Training Center, Bogomolets National Medical University, 01601 Kyiv, Ukraine
5 Department of Internal Medicine II, Division of Cardiology, Paracelsus Medical University Salzburg, 5020 Salzburg, Austria
6 Internal Medicine Department, Zaporozhye State Medical University, 69035 Zaporozhye, Ukraine
* Correspondence: aeberezin@gmail.com; Tel.: +380-612-894-585

Abstract: Background: adropin plays a protective role in cardiac remodeling through supporting energy metabolism and water homeostasis and suppressing inflammation. Low circulating levels of adropin were positively associated with the risk of cardiovascular diseases and type 2 diabetes mellitus (T2DM). We hypothesized that sodium–glucose linked transporter 2 (SGLT2) inhibitor dapagliflosin might represent cardiac protective effects in T2DM patients with known chronic HF through the modulation of adropin levels. Methods: we prospectively enrolled 417 patients with T2DM and HF from an entire cohort of 612 T2DM patients. All eligible patients were treated with the recommended guided HF therapy according to their HF phenotypes, including SGLT2 inhibitor dapagliflozin 10 mg, daily, orally. Anthropometry, clinical data, echocardiography/Doppler examinations, and measurements of biomarkers were performed at the baseline and over a 6-month interval of SGLT2 inhibitor administration. Results: in the entire group, dapagliflozin led to an increase in adropin levels by up to 26.6% over 6 months. In the female subgroup, the relative growth (Δ%) of adropin concentrations was sufficiently higher (Δ% = 35.6%) than that in the male subgroup (Δ% = 22.7%). A multivariate linear regression analysis of the entire group showed that the relative changes (Δ) in the left ventricular (LV) ejection fraction (LVEF), left atrial volume index (LAVI), and E/e' were significantly associated with increased adropin levels. In the female subgroup, but not in the male subgroup, ΔLVEF ($p = 0.046$), ΔLAVI ($p = 0.001$), and ΔE/e' ($p = 0.001$) were independent predictive values for adropin changes. Conclusion: the levels of adropin seem to be a predictor for the favorable modification of hemodynamic performances during SGLT2 inhibition, independent ofN-terminal brain natriuretic pro-peptide levels.

Keywords: type 2 diabetes mellitus; heart failure; hemodynamics; dapagliflosin; adropin; natriuretic peptide

Citation: Berezin, A.A.; Obradovic, Z.; Fushtey, I.M.; Berezina, T.A.; Novikov, E.V.; Schmidbauer, L.; Lichtenauer, M.; Berezin, A.E. The Impact of SGLT2 Inhibitor Dapagliflozin on Adropin Serum Levels in Men and Women with Type 2 Diabetes Mellitus and Chronic Heart Failure. *Biomedicines* **2023**, *11*, 457. https://doi.org/10.3390/biomedicines11020457

Academic Editors: Alfredo Caturano and Raffaele Galiero

Received: 4 January 2023
Revised: 31 January 2023
Accepted: 1 February 2023
Published: 4 February 2023

1. Introduction

During the last decades, the prevalence of type 2 diabetes mellitus (T2DM) has continued to increase [1]. According to an evaluation by WHO statistics experts, more than 422 million adults globally had DM in 2014, and this number is expected to rise 3-fold by 2035, which makes the global burden of this disease extremely challenging [1,2]. In

light of this fact, several complications of T2DM, such as heart failure (HF) and cardiovascular diseases (CVD), have steadily arisen in the general population [3,4]. In fact, T2DM is a powerful risk factor in any phenotype of HF for all-cause and cardiovascular (CV) mortality [5,6]. Moreover, the increase in HF with a preserved ejection fraction (HFpEF) worldwide mainly relates to the increase in the prevalence of T2DM and other metabolic conditions, including abdominal obesity and CVD [7]. Despite a tendency of new cases of HF with reduced ejection fractions (HFrEF) to decline in the majority of developed countries due to the wide implementation of novel diagnostics and treatment standards, the global prevalence of HF seems to have increased as result of the impact of conventional CV factors, such as T2DM as well as gender- and age-related causes [8].

It has been considered that the main underlying pathogenetic mechanisms of the development of diabetes-related vascular complications and adverse cardiac remodeling leading to HF exhibit strict resemblance [9]. Impaired myokine production, along with microvascular and inflammatory activation due to myocardium and skeletal muscle-adipose tissue axis dysfunction, mediates the accumulation of collagen in the extracellular matrix of the myocardium, accelerating atherosclerosis and worsening endothelial function, oxidative stress, and mitochondrial dysfunction, leading to adverse cardiac remodeling, reduced angiogenesis, altered coronary reserve, skeletal muscle weakness, and myopathy [10,11]. All these play a pivotal role in the development of HF in T2DM and the response to conventional therapies [10,11]. Previous studies have shown that, being produced by skeletal muscles as well as the myocardium and adipose tissue, myokines can provide potentially far-reaching effects on non-muscle tissues, including vascular and kidney tissue [12]. Indeed, the autocrine, paracrine, and endocrine actions of myokines include the regulation of energy expenditure, insulin sensitivity, the oxidation of free fatty acid, adipocyte browning, glycogenolysis, glycogenesis, water and electrolyte homeostasis, and bone metabolism [13]. Many myokines (adropin, apelin, isirin) are organ-protective molecules that stimulate autophagy, reduce inflammation, inhibit endoplasmic reticulum stress, and improve reparation, whereas others (myostatin) induce maladaptive mechanisms in the myocardium and skeletal muscles [14,15]. Recently, several clinical studies confirmed the predictive values of irisin and apelin in HF patients with T2DM [16–18]. Less known, the role of dynamic changes in adropin in HF patients with T2DM in connection to cardiac function depends on gender, because the accumulation of adipose tissue and skeletal muscle mass differs between male and female populations.

Adropin is a unique multi-functional circulating protein that is encoded by the energy-homeostasis-associated gene (*Enho*) and produced by the myocardium, skeletal muscles, liver, adipocites, as well as the brain, lung, kidney medulla, and circulating peripheral blood mononuclear cells [19]. Adropin acts through the G protein-coupled (GPR19) receptor, regulates energy homeostasis and lipid metabolism, suppresses inflammation and water consumption, stimulates diuresis, prevents insulin resistance, and impairs glucose tolerance [20,21]. Low circulating levels of adropin were found in patients with abdominal obesity, T2DM, atherosclerosis, myocardial infarction, and HF [22–25]. Furthermore, adropin concentrations are correlated with age, gender, and the number of CV and metabolic risk factors, and increase in humans after gastric bypass surgery and after reaching good glycemic control [26]. Several previous meta-analyses showed that decreased adropin levels might play a crucial role in the development of CVD and HF [27,28].

Currently, sodium–glucose linked transporter 2 (SGLT2) inhibitors are included in the contemporary therapy of different phenotypes of HF regardless of T2DM presentation, while until now, the underlying mechanisms by which these agents are exerted, and their ability to improve clinical outcomes and hemodynamics, are not deeply understood. Perhaps the cardiac protective effects of SGLT2 inhibitors relate to their ability to enhance gluconeogenesis and ketogenesis through the activation of sirtuin-1 and its two downstream mediators–such as the proliferator-activated receptors gamma coactivator 1-alpha and fibroblast growth factor-21–as well as via supporting vasodilation and nitric oxide bioavailability [29]. Adropin intervenes in oxidative stress and modulates autophagy

through the lysosome-dependent degradative pathway, which contains molecular targets for SGLT2 inhibitors. It remains uncertain whether SGLT2 inhibitors can modulate the level of adropin in peripheral circulation and thereby exert several favorable effects in HF patients with T2DM. The aim of this study was to investigate the effect of SGLT2 inhibitor dapagliflosin on the levels of adropin in males and females with T2DM with chronic HF.

2. Materials and Methods

2.1. Study Population and Design

The study was an open-label, multicenter (VitaCenter Zaporozhye, Ukraine, EliteMed-Service, Zaporozhye, Ukraine and City Hospital #7, Zaporozhye, Ukraine) non-randomized cohort investigation. Patients of both sexes were included from October 2020 to July 2022 who were aged $\geq$ 18 years and had established T2DM with HbAc1 < 6.9%, hemodynamically stable HF (II-III NYNA functional classes), and written consent to participate in the study. The main inclusion and exclusion criteria were reported in detail in a previously published article [30]. According to these criteria, we prospectively enrolled 417 patients with T2DM and HF from the entire cohort of 612 T2DM patients. Figure 1 reports the study design and the list of procedures in detail.

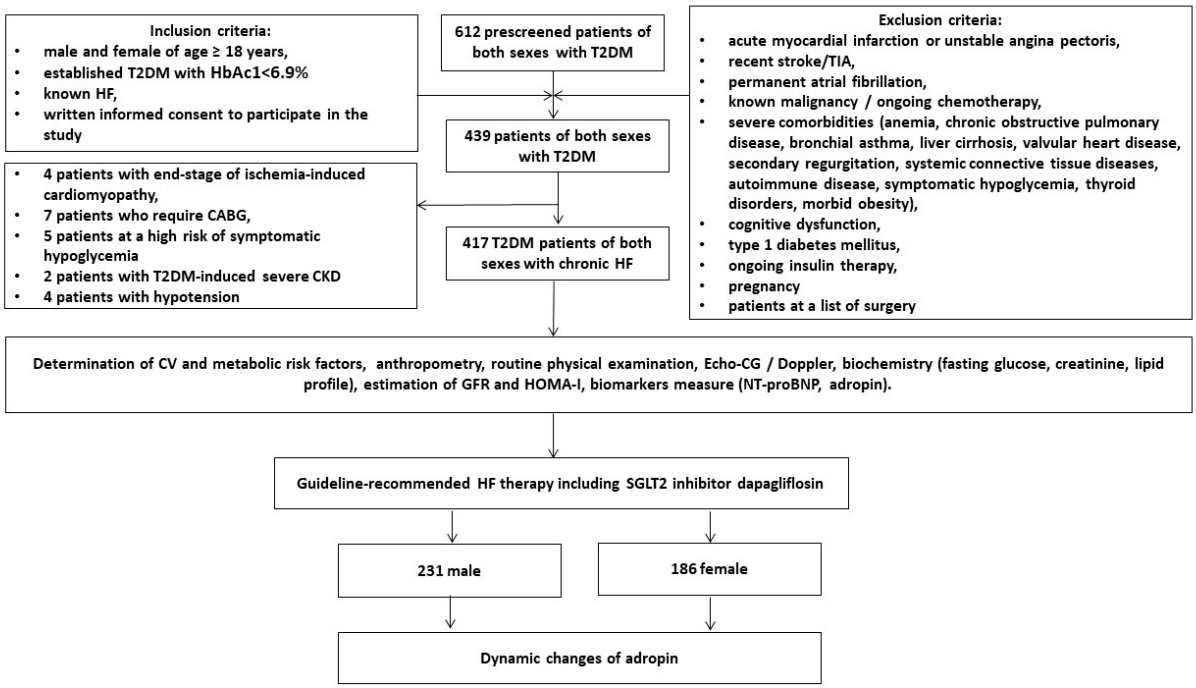

Figure 1. Flow chart of the study design. Abbreviations: T2DM, type 2 diabetes mellitus; CABG, coronary artery bypass grafting; CKD, chronic kidney disease; TIA, transient ischemic attack; HF, heart failure.

The eligible patients were treated with the recommended guided HF therapy according to their HF phenotypes, including the consumption of SGLT2 inhibitor dapagliflozin at a dose of 10 mg OD orally, along with that of an angiotensin receptor-neprilysin inhibitor (ARNI)/ACE inhibitors/angiotensin-II receptor blockers (ARBs), a mineralocorticoid receptor antagonist (MRA), and beta-blockers. As a basic antidiabetic medication, metformin was administered, the dose of which was personally adjusted to the patients at the beginning of the study so that the patients had a criterion of HbAc1 < 6.9%. The lifestyle modification program was adjusted to the patients with T2DM before their enrollment and entry in the study. Blood-pressure-lowering agents were administered to maintain office BP < 140/90 mmHg and/or average daily BP < 130/80 mm Hg. Diuretic management was performed with loop diuretics, which were given in individually adjusted daily doses

according to the current clinical situation, the dynamics of body mass and edema, daily diuresis, and when clinical signs of fluid retention were found.

Lipid-lowering agents were administered in the patients with dyslipidemia, established coronary artery disease, or chronic kidney disease who did not show conventional contraindications. Antiplatelet drugs and oral anticoagulants were used when needed to prevent CV complications and/or systemic/local thromboembolic events. The observation period was 6 months.

2.2. Methods

2.2.1. Anthropometric Assessment

The standard anthropometric examinations included height, weight, waist circumference, hip-to-waist ratio (WHR), and body mass index (BMI), which was calculated as weight (kg)/height $(m)^2$ for each person.

2.2.2. Determination of HF, CV Disease, CV Risk Factors, and Clinically Significant Co-Morbidities

A routine clinical assessment included interviews, reviews of medical records, standard physical examinations to poll clinically significant data on a background profile, CV risk factors, previous and current medication use, symptoms of HF and T2DM, and HF functional status, according to the New York Heart Association (NYHA). Conventional factors of CV risk including hypertension, dyslipidemia, and a smoking habit were evaluated in compliance with the current guidelines of the European Society of Cardiology (ESC) [31]. T2DM, stable coronary artery disease, chronic kidney disease, and HF were diagnosed according to the current recommendations [32–36].

2.2.3. Echocardiography Examination

A standard transthoracic B-mode echocardiography/Doppler examination was carried out with commercially available ultrasound systems, comprising "GE Medical Systems" (General Electric, Freiburg, Germany), "Aplio 400" (Canon Medical Systems, Tochigi, Japan), and "Vivid E9" (General Electric Vingmed Ultrasound AS, Horten, Norway), in accordance with the current guidelines of the American Society of Echocardiography/European Association of Cardiovascular Imaging [37]. The echocardiographic Doppler assessments were focused on LV systolic and diastolic functions and LV hypertrophy (LVH) [38]. Cardiac volumes, left ventricular (LV) ejection fractions (LVEF), and left atrial volume indices (LAVI) were measured using the Simpson method. The LV end-diastolic volume (LVEDV) and LV end-systolic volume (LVESV) were normalized to the body surface area (BSA) and given as the LVEDV index (LVEDVi) and LVESV index (LVESVi). LVH was determined by the conventional echo criteria (LV mass/body surface area $\geq$125 g/m^2 in males or $\geq$110 g/m^2 in females). The early diastolic wave velocity (E) and mitral annular early diastolic velocity, given as averaged septal and lateral e' (e') and E/e' ratios, were determined by a pulsed-wave Doppler and a spectral tissue Doppler obtained from the apical 4-chamber view.

2.2.4. Estimating Glomerular Filtration Rate and Insulin Resistance Evaluation

The glomerular filtration rate (GFR) was calculated using the CKD-EPI formula [39]. Insulin resistance was evaluated with the Homeostatic Assessment Model of Insulin Resistance (HOMA-IR) using the conventional equation [40].

2.2.5. Blood Sampling and Biomarkers' Measurement

Fasting blood samples were collected from an antecubital vein and then they were placed in silicon tubes. Within 30 min of blood sampling collection, each sample was transferred to the laboratory. The plasma was received after centrifugation for 15 min at 1600$\times$ *g* at 4 °C. Then, the polled serum aliquots were immediately stored in a refrigerator at ≤ -70 °C until further analysis. We routinely used Roche P800 analyzer (Roche,

Basel, Switzerland) to measure the fasting levels of fasting glucose, insulin, glycosylated hemoglobin (HbA1c), total cholesterol (TC), low-density lipoprotein (LDL-C) cholesterol, high-density lipoprotein (HDL-C) cholesterol, and triglycerides (TG). The serum levels of adropin and NT-proBNP were detected using commercially available ELISA kits (Elabscience, Houston, TX, USA) according to the manufacturer's instructions.

2.2.6. Definitions of End-Point

The primary end-point was defined as a 6-month change in serum levels of adropin after the beginning of dapagliflozin administration.

2.2.7. Statistical Analysis

v. 23 Statistical Packages for Social Sciences (SPSS; IBM, Armonk, NY, USA) software and v. 9 GraphPad Prism (GraphPad Software, San Diego, CA, USA) software were used for statistical analysis. The Kolmogorov–Smirnov test was performed to determine the normality of the data distribution. Continuous variables with normal distribution were characterized by the mean (M) ± the standard deviation (SD), whereas continuous, non-normally distributed variables were specified by the median (Me) and interquartile range (IQR). Categorical variables were reported as frequencies and percentages. To compare the categorical variables between the female and male subgroups, we performed a Chi-square family test. We used Student's *t*-test for comparisons of continuous data, which are normally distributed. Differences in the parameters at the baseline and over a 6-month treatment period were compared by paired Student *t*-tests or the Wilcoxon signed-rank test. Links between changes in adropin levels with clinical status, cardiac performances, and circulating biomarkers were evaluated by univariate linear regressions. The variables of $p < 0.1$ in the univariate analysis were included in the automatic forward stepwise variable selection procedure for multivariate regression tests. Tukey's honestly significant difference test for post hoc multiple testing was applied. Thye determination of the inter- and intra-observer reproducibility of adropin concentrations in the peripheral blood of 60 randomly selected patients was performed by estimating the intra-class correlation coefficient. Differences were considered significant at the level of statistical significance $p < 0.05$.

3. Results

3.1. Patients' Characteristics

Table 1 reports the baseline clinical characteristics, echocardiographic features, and biomarkers of T2DM patients with known HF. The patients' mean age was 53 (41–64) years, the mean body mass index (BMI) was 25.8 kg/m^2, the mean waist circumference was 85.1 cm, and the mean waist-to-hip ratio (WHR) was 0.85 units. The coexisting conditions and risk factors were composed of dyslipidemia (83%), arterial hypertension (84.4%), stable coronary artery disease (33.8%), smoking (40.3%), abdominal obesity (42.9%), microalbuminuria (32.4%), left ventricular hypertrophy (80.1%), chronic kidney disease (26.9%), and atrial fibrillation (13.7%). Eligible patients were in the II (67.6%) and III (32.4%) HF NYHA classes and were qualified as having HFpEF (31.7%), HFmrEF (33.6%), and HFrEF (34.8%). All patients were hemodynamically stable. The average of the LV ejection fraction (LVEF) was 46% (39–54%), the LAVI was 43 mL/m^2, and the E/e' ratio was 13.5 units. The mean levels of HbA1c, creatinine, NTproBNP, and adropin were 6.59 ± 0.02 %, 108.6 ± 8.5 µmol/L, 2615 (1380–3750) pmol/mL, and 237.40 (190.50–275.30) pg/mL, respectively. We did not notice significant differences between subgroups in age, BMI, waist circumference, WHR, presentations of dyslipidemia, hypertension, stable CAD, CKD 1–3 grades, atrial fibrillation (AF), blood pressure (BP), eGFR, HOMA-IR, HbA1c, creatinine, lipid profiles, or concomitant medications.

On the contrary, abdominal obesity ($p = 0.046$) was detected more frequently in the female subgroup than in the male subgroup. Additionally, the HFpEF and HF NYHA class II were detected more frequently in the female subgroup ($p = 0.044$ and $p = 0.040$,

respectively), whereas the HFrEF and HF NYHA class III were found less often in the male subgroup (p = 0.042 and p = 0.040, respectively). Aligned with this, the male subgroup demonstrated significantly higher values for LV volume, LVEDVi, LVESVi, LVMMI, and LAVI, and marginally lower LVEFs than the female subgroup. Furthermore, patients from the male subgroup had higher levels of NT-proBNP (p = 0.020) and lower levels of adropin (p = 0.010) than the female subgroup did. Liver enzymes were detected in the circulating blood before and after SGLT2 inhibitor administration, but we did not find clinically significant changes in their concentrations in both groups. Evidence of ketosis was not found in urine samples in any patients in the study at the baseline and at the beginning of the study.

Table 1. Baseline general characteristics of eligible T2DM patients.

Variables	Entire Patient Population (n = 417)	Male Population (n = 231)	Female Population (n = 186)	p Value
Demographics and anthropomorphic parameters				
Age, year	53 (41–64)	52 (40–63)	54 (42–66)	0.262
BMI, kg/m^2	25.8 ± 2.8	26.4 ± 2.5	25.4 ± 2.2	0.722
Waist circumference, cm	85.1 ± 3.2	86.9 ± 3.0	83.5 ± 2.6	0.180
WHR, units	0.85 ± 0.05	0.87 ± 0.06	0.84 ± 0.04	0.321
Concomitant diseases, comorbidities and CV risk factors				
Dyslipidemia, n (%)	346 (83.0)	198 (85.7)	150 (80.6)	0.822
Hypertension, n (%)	352 (84.4)	192 (83.1)	160 (86.0)	0.781
Stable CAD, n (%)	141 (33.8)	75 (32.5)	66 (35.5)	0.800
Smoking, n (%)	168 (40.3)	98 (42.4)	70 (37.6)	0.052
Abdominal obesity, n (%)	179 (42.9)	106 (45.9)	73 (39.2)	0.046
Microalbuminuria, n (%)	135 (32.4)	79 (34.2)	56 (30.1)	0.120
LV hypertrophy, n (%)	334 (80.1)	191 (82.7)	143 (76.9)	0.051
CKD 1–3 grades, n (%)	112 (26.9)	62 (26.8)	50 (28.9)	0.822
Paroxysmal/persistence form of atrial fibrillation, n (%)	57 (13.7)	34 (14.7)	23 (12.4)	0.120
HF phenotypes and functional classification				
HFpEF, n (%)	132 (31.7)	64 (27.7)	68 (36.6)	0.044
HFmrEF, n (%)	140 (33.6)	74 (32.0)	66 (35.5)	0.661
HFrEF, n (%)	145 (34.8)	93 (40.3)	52 (27.9)	0.042
II/III HF NYHA class, n (%)	282 (67.6)/135 (32.4)	143 (61.9)/88 (38.1)	139 (74.7)/47 (25.3)	0.040
Hemodynamics parameters				
SBP, mm Hg	129 ± 6	131 ± 7	129 ± 5	0.864
DBP, mm Hg	78 ± 5	79 ± 6	77 ± 4	0.803
LVEDV, mL	162 (154–170)	166 (159–178)	161 (153–168)	0.040
LVEDVi, mL/m^2	79 (75–83)	81 (77–87)	78 (75–81)	0.048
LVESV, mL	86 (80–93)	92 (85–98)	83 (80–93)	0.030
LVESVi, mL/m^2	42 (39–45)	44 (41–48)	40 (38–42)	0.042
LVEF, %	46 (39–54)	44 (37–50)	48 (41–56)	0.050
LVMMI, g/m^2	154 ± 5	169 ± 6	152 ± 4	0.040
LAVI, mL/m^2	43 (37–52)	47 (41–56)	39 (36–45)	0.010
E/e', unit	13.5 ± 0.3	14.9 ± 0.3	12.8 ± 0.2	0.010
Biomarkers				
eGFR, mL/min/1.73 m^2	75 ± 4.0	73 ± 3.0	76 ± 5.0	0.703
HOMA-IR	7.95 ± 2.3	8.12 ± 2.2	7.81 ± 2.5	0.682
Fasting glucose, mmol/L	5.62 ± 1.3	5.70 ± 1.2	5.60 ± 1.3	0.804
HbA1c, %	6.59 ± 0.02	6.59 ± 0.02	6.58 ± 0.03	0.820
Creatinine, μmol/L	108.6 ± 8.5	112.3 ± 9.3	106.5 ± 7.8	0.240
TC, mmol/L	6.43 ± 0.60	6.60 ± 0.70	6.32 ± 0.55	0.682
HDL-C, mmol/L	0.97 ± 0.17	0.95 ± 0.19	0.99 ± 0.13	0.881
LDL-C, mmol/L	4.38 ± 0.10	4.50 ± 0.12	4.31 ± 0.12	0.860
TG, mmol/L	2.21 ± 0.17	2.27 ± 0.12	2.18 ± 0.15	0.780
NT-proBNP, pmol/mL	2615 (1380–3750)	3218 (1450–4120)	2344 (1296–3901)	0.020
Adropin, ng/mL	2.37 (1.91–2.75)	2.11 (1.82–2.68)	2.69 (2.32–3.04)	0.010

Table 1. *Cont.*

Variables	Entire Patient Population (*n* = 417)	Male Population (*n* = 231)	Female Population (*n* = 186)	*p* Value
Concomitant medications				
ACEI, *n* (%)	198 (47.5)	106 (45.9)	92 (49.4)	0.880
ARB, *n* (%)	67 (16.1)	34 (14.7)	33 (17.7)	0.760
ARNI, *n* (%)	165 (39.6)	92 (39.8)	73 (39.2)	0.880
Beta-blocker, *n* (%)	372 (89.2)	201 (87.0)	171 (91.9)	0.223
Ivabradine, *n* (%)	59 (14.1)	32 (13.9)	27 (14.5)	0.864
Calcium channel blocker, *n* (%)	75 (18.0)	38 (16.5)	37 (19.9)	0.481
MRA, *n* (%)	283 (67.8)	150 (64.9)	133 (71.5)	0.053
Loop diuretic, *n* (%)	358 (85.9)	196 (84.8)	162 (87.1)	0.871
Antiplatelet, *n* (%)	367 (88.0)	201 (87.0)	166 (89.2)	0.882
Anticoagulant, *n* (%)	51 (12.2)	34 (14.7)	17 (9.1)	0.040
Metformin, *n* (%)	387 (92.8)	210 (90.9)	177 (95.2)	0.623
Statins, *n* (%)	408 (97.8)	226 (97.9)	182 (97.8)	0.990

Abbreviations: ACEI, angiotensin-converting enzyme inhibitor; ARNI angiotensin receptor neprilysin inhibitor; CAD, coronary artery disease; CKD, chronic kidney disease; BMI, body mass index; DBP, diastolic blood pressure; E/e', early diastolic blood filling to longitudinal strain ratio; GFR, glomerular filtration rate; HDL-C, high-density lipoprotein cholesterol; HFpEF, heart failure with preserved ejection fraction; HFmrEF, heart failure with mildly reduced ejection fraction; HFrEF, heart failure with reduced ejection fraction; LVEDV, left ventricular end-diastolic volume; LVEDVi, left ventricular end-diastolic volume index; LVESV, left ventricular end-systolic volume index; LVEF, left ventricular ejection fraction; LVMMI, left ventricle myocardial mass index; LAVI, left atrial volume index; LDL-C, low-density lipoprotein cholesterol; MRA, mineralocorticoid receptor antagonist; SBP, systolic blood pressure; TG, triglycerides; TC, total cholesterol; WHR, waist-to-hip ratio. Notes: data of variables are given as mean ± SD and median (25%−75% interquartile range).

3.2. Spearman's Correlation between Circulating Levels of Adropin and Other Parameters

In the entire group of patients, we found positive correlations of adropin levels with LAVI (r = 0.32; $p = 0.001$), NYHA HF class II (r = 0.30, $p = 0.012$), BMI (r = 0.29, $p = 0.010$), and eGFR (r = 0.31; $p = 0.001$), and negative correlations of adropin levels with LVEF (r = −0.34; $p = 0.001$) and NT-proBNP (r = −0.36; $p = 0.001$), but these were not associated with the HOMA index. There were no significant correlations between the baseline levels of NT-proBNP and adropin and concomitant medications. In the female subgroup, the negative correlation between adropin and NT-proBNP was more profound (r = −0.40; $p = 0.001$) than that in male subgroup (r = −0.36; $p = 0.001$). Therefore, in the female subgroup, we found a significant correlation of adropin with LVMMI (r = −0.38; $p = 0.001$) and microalbuminuria (r = 0.32; $p = 0.001$), whereas in the male subgroup, there were no significant associations along these parameters (r = −0.11; $p = 0.216$ and r = 0.142; $p = 0.223$, respectively).

3.3. Changes in Serum Levels of Adropin in Comparisson with NT-proBNP during Dapagliflozin Administration in Males and Females

Over a 6-month period after the initial prescription of SGLT2 inhibitor dapagliflozin, the levels of adropin in the entire group demonstrated a significant increase of up to 26.6% (from 2.37 [25–75% IQR = 1.91–2.75] ng/mL to 3.00 [25−75% IQR = 2.68–3.36] ng/mL, $p = 0.042$) (Figure 2a). In the female subgroup, the increase in the circulating levels of adropin was sufficiently higher (Δ% = 35.6%, from 2.69 [25–75% IQR = 2.31–2.99] ng/mL to 3.65 [25–75% IQR = 3.40–3.89] ng/mL, $p = 0.010$)when compared with those of the male subgroup (Δ% = 22.7%, from 2.11 [25–75% IQR = 1.90–2.37] ng/mL to 2.60 [25–75% IQR = 2.07–3.21] ng/mL, $p = 0.161$).

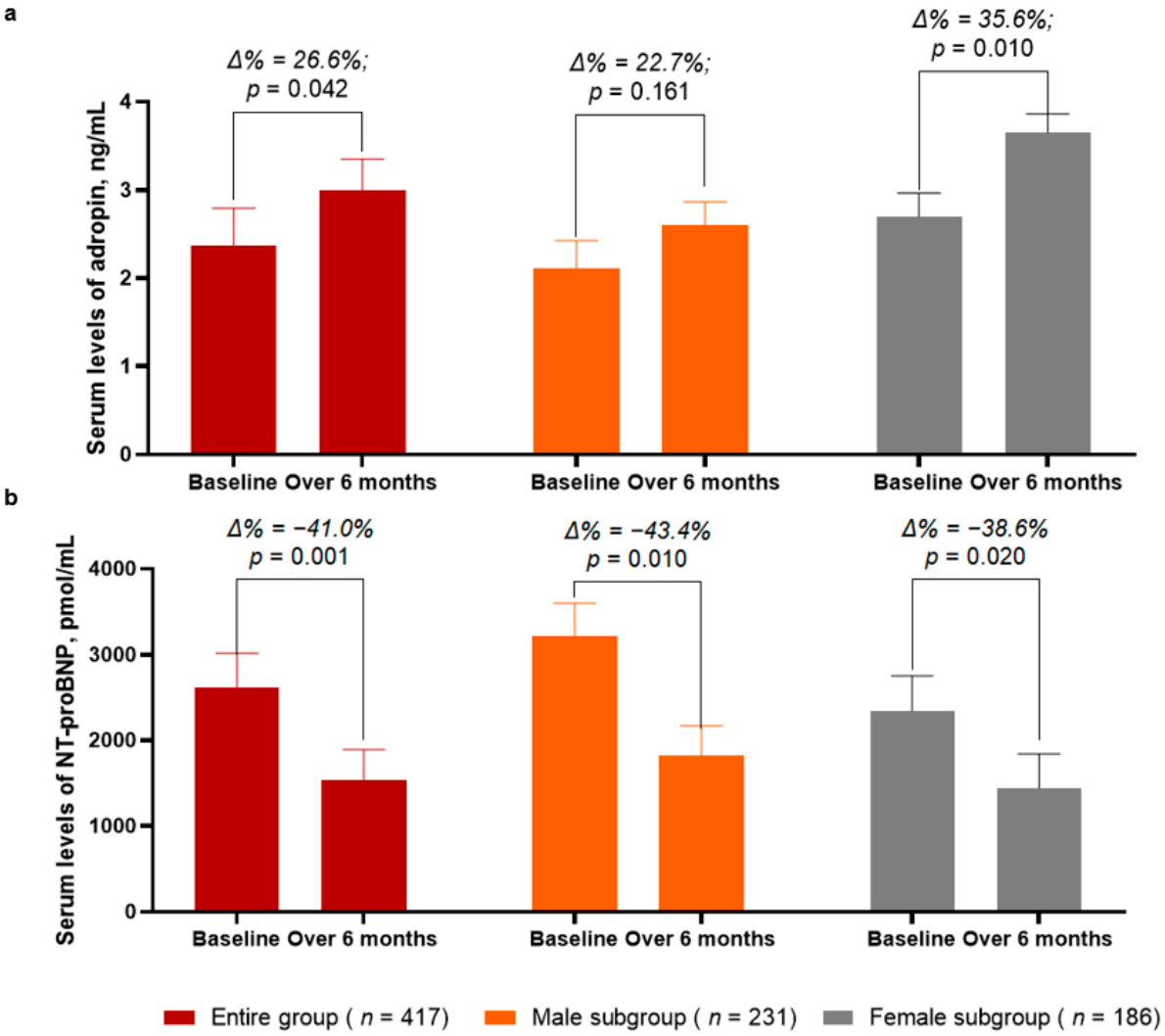

Figure 2. Bar graphs at baseline and 6 months after administration of SGLT2 inhibitor dapagliflozin, showing dynamics of serum levels of adropin (**a**) and NT-proBNP (**b**). Abbreviations: Δ%, respective percentage of changes of parameters.

In the entire group, the circulating levels of NT-proBNP significantly decreased from 2615 (1380–3750) pmol/mL to 1542 (25–75% IQR = 970–2075) pmol/mL (Δ% = −41.0%, p = 0.001) between the baseline and 6 months after dapagliflozin administration (Figure 2b). Although in both subgroups the levels of NT-proBNP were found to be significantly decreased, in the male subgroup, the decrease of NT-proBNP was a little bit better (Δ% = −43.4%, from 3218 [25–75% IQR = 2870–3689] pmol/mL to 1820 [25−75% IQR = 1440–2310] pmol/mL, p = 0.010) when compared with that of the female subgroup (Δ% = −38.6%, from 2344 [25–75% IQR = 1930–2750] pmol/mL to 1440 [25–75% IQR = 1015–1870] pmol/mL, p = 0.020).

3.4. Changes in Clinical Performances and Hemodynamics Parameters during Dapagliflozin Administration

Table 2 reports the dynamics of the clinical data, hemodynamics characteristics, and biomarkers in the patients during SGLT2 inhibitor dapagliflozin administration.

Table 2. Comparisons between baseline and 6-month variables after the administration of SGLT2 inhibitor dapagliflozin in males and females.

Variables	Baseline	Over 6 Months	Δ%	*p* Value
Clinical characteristics				
BMI, kg/m^2	25.8 ± 2.8	24.1 ± 1.9	−4.30	0.113
Male	26.4 ± 2.5	25.3 ± 1.7	−4.10	0.142
female	25.4 ± 2.2	23.9 ± 1.8	−5.90	0.104
II HF NYHA class, *n* (%)	282 (67.6)	329 (78.9)	+14.3	0.040
Male	143 (50.7)	154 (46.8)	+11.0	0.040
female	139 (49.3)	175 (53.2)	+36.0	0.010
III HF NYHA class, *n* (%)	135 (32.4)	88 (21.1)	−34.8	0.040
Male	88 (65.2)	77 (87.5)	−12.5	0.040
female	47 (34.8)	11 (12.5)	−76.5	0.001
Hemodynamics performances				
LVEDV, mL	162 (154–170)	158 (150–167)	−1.90	0.460
Male	166 (159–178)	165 (156–173)	−0.60	0.904
female	161 (153–168)	156 (151–162)	−3.10	0.061
LVESV, mL	86 (80–93)	80 (76–85)	−7.00	0.040
Male	92 (85–98)	87 (83–93)	−5.40	0.052
female	83 (80–93)	75 (71–79)	−9.60	0.020
LVEF, %	46 (39–54)	50 (44–57)	+8.60	0.054
Male	44 (37–50)	47 (39–54)	+6.80	0.160
female	48 (41–56)	52 (48–59)	+8.70	0.050
LVMMI, g/m^2	154 ± 5	141 ± 5	−8.40	0.020
Male	169 ± 6	155 ± 7	−8.20	0.050
female	152 ± 4	138 ± 4	−9.20	0.010
LAVI, mL/m^2	39 (34–45)	35 (31–39)	−10.3	0.040
Male	47 (41–56)	43 (37–49)	−8.5	0.050
female	39 (36–45)	34 (32–37)	−12.8	0.010
E/e', unit	13.5 ± 0.3	10.7 ± 0.5	−20.7	0.020
Male	14.9 ± 0.3	12.6 ± 0.4	−15.4	0.040
female	12.8 ± 0.2	9.88 ± 0.3	−22.8	0.020
Biomarkers				
eGFR, mL/min/1.73 m^2	75 ± 4.0	78 ± 3.0	+4.0	0.820
male	73 ± 3.0	76± 4.0	+3.9	0.842
female	76 ± 5.0	80± 5.0	+5.2	0.813
Fasting glucose, mmol/L	5.62 ± 1.3	4.90 ± 1.0	−12.8	0.240
male	5.70 ± 1.2	4.95 ± 1.1	−13.1	0.240
female	5.60 ± 1.3	4.94 ± 1.2	−11.7	0.260
HbA1c, %	6.59 ± 0.02	6.47 ± 0.03	−1.74	0.312
male	6.59 ± 0.02	6.49 ± 0.03	−1.50	0.263
female	6.58 ± 0.03	6.46 ± 0.03	−1.80	0.204
Creatinine, μmol/L	108.6 ± 8.5	112.5 ± 7.0	+3.50	0.282
male	112.3 ± 9.3	116.8 ± 8.5	+3.80	0.404
female	106.5 ± 7.8	109.8 ± 8.0	+3.10	0.361

Notes: data of variables are given as mean ± SD and median (25−75% interquartile range). Abbreviations: E/e', early diastolic blood filling to longitudinal strain ratio; HF, heart failure; HbA1c, glycosylated hemoglobin; GFR, glomerular filtration rate; LVESV, left ventricular end-systolic volume; LVEF, left ventricular ejection fraction; LVMMI, left ventricle myocardial mass index; LAVI, left atrial volume index; Δ%, respective percentage of changes of parameters.

There were no significant changes in BMI in the entire group as well as in the male and female subgroups. However, the proportion of HF patients in the II and III NYHA classes demonstrated sufficient changes over the treatment period. In the entire population,

there was a significant increase in the amount of HF patients with class II HF NYHA and a decrease in those who had class III HF NYHA. Along with this, the number of females whose HF functional class improved was significantly higher compared to that of males, while the total number of patients of both genders with HF functional class III was sufficiently reduced. In addition, we found that in the entire group, the left ventricular end-systolic volume (LVESV), left ventricular myocardial mass index (LVMMI), left atrial volume index (LAVI), and early diastolic blood filling to longitudinal strain ratio (E/e') significantly decreased, whereas there were no significant changes in the left ventricular end-diastolic volume (LVEDV) and left ventricular ejection fraction (LVEF). We noticed that the LVESV, LVMMI and LAVI decreased only in the female subgroup, whereas E/e' significantly decreased in all sexes. Along with this, there were no changes in the profile of conventional biomarkers (eGFR, fasting glucose, creatinine and HbAc1) in eligible patients regardless of gender.

3.5. Association of Adropin Changes with Clinical Parameters, Hemodynamics Performances and Circulating Biomarkers during Administration of SGLT2 Inhibitor Dapagliflozin

To evaluate the plausible associations of adropin dynamics with other variables after the administration of dapagliflozin in gender-related aspects, we performed univariate and multivariate linear regression analyses in the entire patient group and then in the subgroups of males and females (Table 3).

Table 3. Univariate and multivariate linear regression analyses of the association of adropin levels with age, abdominal obesity, BMI, NYHA class, and relative changes in hemodynamics and NT-proBNP.

Variables	Univariate Linear Regression			Multivariate Linear Regression		
	B Coefficient	**SD**	***p* Value**	**B Coefficient**	**SD**	***p* Value**
Entire patient cohort						
Age	0.73	0.30	0.290		-	
Obesity	0.90	0.25	0.05	0.71	0.20	0.060
BMI at baseline	1.10	0.38	0.046	0.66	0.25	0.104
ΔBMI	−1.64	0.29	0.055	−1.65	0.22	0.052
NYHA class	−1.92	0.35	0.042	−1.36	0.24	0.052
ΔLVESV	−2.10	0.72	0.053	−1.99	0.52	0.120
ΔLVEF	3.26	0.42	0.040	2.73	0.50	0.046
ΔLVMMI	−2.61	1.20	0.012	−2.40	1.14	0.052
ΔLAVI	−6.15	1.60	0.001	−6.10	1.54	0.001
ΔE/e'	−7.90	1.26	0.001	−7.83	1.22	0.001
ΔNT-proBNP	−3.22	1.92	0.012	−2.06	0.66	0.050
Male subgroup						
Age	0.75	0.33	0.266		-	
Obesity	0.90	0.27	0.05	0.66	0.25	0.104
BMI at baseline	1.10	0.38	0.046	1.02	0.29	0.216
ΔBMI	−1.29	0.22	0.162		-	
NYHA class	−0.68	0.20	0.640		-	
ΔLVESV	−1.23	0.55	0.600		-	
ΔLVEF	2.01	0.17	0.120		-	
ΔLVMMI	−2.42	0.98	0.050	−2.40	1.14	0.054

Table 3. *Cont.*

Variables	Univariate Linear Regression			Multivariate Linear Regression		
	B Coefficient	**SD**	***p* Value**	**B Coefficient**	**SD**	***p* Value**
ΔLAVI	−5.80	1.20	0.042	−2.30	1.17	0.050
ΔE/e′	−7.30	1.50	0.012	−5.90	1.70	0.014
ΔNT-proBNP	−3.10	1.68	0.014	−2.10	1.52	0.060
Female subgroup						
Age	0.71	0.26	0.293		-	
Obesity	0.90	0.27	0.048	0.78	0.22	0.062
BMI at baseline	1.12	0.31	0.041	1.06	0.31	0.055
ΔBMI	−1.76	0.27	0.042	−1.70	0.23	0.044
NYHA class	−1.92	0.35	0.042	−1.36	0.24	0.050
ΔLVESV	−2.10	0.72	0.053	−1.99	0.52	0.121
ΔLVEF	3.26	0.42	0.040	2.73	0.50	0.046
ΔLVMMI	−2.61	1.20	0.001	−2.40	1.14	0.050
ΔLAVI	−6.15	1.60	0.001	−6.10	1.54	0.001
ΔE/e′	−7.90	1.26	0.001	−7.83	1.22	0.001
ΔNT-proBNP	−1.22	0.92	0.012	−1.06	0.66	0.050

Abbreviations: BMI, body mass index; SD, standard deviation; NYHA, New York Heart Association; Δ, a relative change in variables after 6-month administration of dapagliflozin.

An unadjusted univariate linear regression analysis showed that the BMI at the baseline (p = 0.046) and relative changes (Δ) of LVEF (p = 0.040), LAVI (p = 0.001), LVMMI (p = 0.012), E/e′ (p = 0.001), NYHA class (p = 0.042), and NT-proBNP (p = 0.012) were significantly associated with the adropin levels during SGLT2 inhibitor dapagliflozin administration, whereas age, abdominal obesity, and ΔBMI were not. Multivariate linear regression indicated that only ΔLVEF (p = 0.046), ΔLAVI (p = 0.001), and ΔE/e′ (p = 0.001) remained strongly associated with the changes in adropin levels, whereas ΔBMI (p = 0.052), ΔLVMMI (p = 0.052), and ΔNT-proBNP (p = 0.050) exhibited borderline significance in this matter.

In the male subgroup, the BMI at the baseline (p = 0.046), ΔLAVI (p = 0.042), ΔE/e′ (p = 0.012), and ΔNT-proBNP (p = 0.014) were found to be predictors for changes in adropin levels in the peripheral circulation in the unadjusted univariate linear regression analysis, whereas multivariate linear regression indicated that the only ΔE/e′ retained its independent predictive potency (p = 0.014).

In the female subgroup, abdominal obesity (p = 0.048), BMI at the baseline (p = 0.041), ΔBMI (p = 0.042), ΔNYHA class (p = 0.042), ΔLVEF (p = 0.040), ΔLVMMI (p = 0.001), ΔLAVI (p = 0.001), ΔE/e′ (p = 0.001), and ΔNT-proBNP (p = 0.012) were found to be predictors for adropin level changes in the unadjusted univariate linear regression. However, ΔLVEF (p = 0.046), ΔLAVI (p = 0.001), and ΔE/e′ (p = 0.001) exhibited their independent predictive values in multivariate linear regression.

3.6. Reproducibility of Adropin

We evaluated the reproducibility of adropin in comparison with NT-proBNP in the patients of both genders. The intra-class correlation coefficient for the inter-observer reproducibility of NT-proBNP was 0.88 (95% confidence interval [CI] = 0.83–0.92). The intra-class correlation coefficient for the intra-observer reproducibility of adropin was 0.91 (95% CI = 0.85–0.97). We did not find significant changes in the intra-observer reproducibility of adropin depending on the gender of eligible patients (p = 0.382).

4. Discussion

The results of the study revealed a convincing difference among the adropin levels over time for male versus female patients. Additionally, we noticed that the 6-month administration of SGLT2 inhibitor dapagliflosin was associated with NYHA HF class improvement and favorable changes in LVESV, LVEF, LVMMI, and diastolic function parameters, which corresponded to a trend of decrease in NT-proBNP and the opposite dynamic in serum levels of adropin. We noticed that the elevation of adropin concentrations in peripheral blood predicted favorable changes in cardiac remodeling performances (LVEF, LAVI and $\Delta E/e'$) mainly in the female population of eligible patients and not in male population. We are the first to report these findings, so we believe that this particularity of SGLT2 inhibitor dapagliflosin seems to explain the innate capability of the agent to work actively in the female population, although it requires further investigation in the future.

The difference in the circulating levels of adropin in males and females may relate to adipose tissue accumulation, the mass of skeletal muscles, and dietary macronutrient intake, which seem to be different between these populations [19]. Moreover, estrogen impact on the expression of the adropin gene in the liver, adipose tissues, and skeletal myocytes is crucial for glucose and lipid homeostasis supported by adropin [10,12,13]. Perhaps, gender-related differences in adropin levels deserve to be investigated in the future in the context of the adaptive role of this protein in the regulation of energy homeostasis and cardiac remodeling in HF individuals.

We speculate that the relative changes in hemodynamics are crucially important because the use of SGLT2 inhibitors did not affect the clinical conditions and conventional parameters of cardiac remodeling, while the dynamics of LVEF and cardiac volumes might be considered a predictor for the benefits of SGLT2 inhibitors. On the other hand, changes of hemodynamics may be predictable by biomarkers, such as NT-proBNP and adropin. Previous studies showed that SLGT2i were effective in improving the prognosis of HF patients regardless of NT-proBNP, so there is a need for a new surrogate marker by which the dynamic changes of hemodynamics are considered and predicted. In addition, SGLT2 inhibitors have been shown to have a protective endothelial function and to protect the myocardial microvascular compartment in T2DM [41,42].

In fact, there is still no strong evidence of the theory that, in several populations with HF, including HFpEF, SGLT2 inhibitors exert a more profound impact on the clinical outcomes, surrogate image, and circulating biomarkers of adverse cardiac remodeling in female than in male patients [43]. Moreover, these agents demonstrated strict similarity in benefits among patients with and without atherosclerotic CV disease, a history or presentation of HF, T2DM, and chronic kidney disease [44–46]. There are numerous explanations for this, which partially include the difference in pre-existing comorbidity profiles, anthropomorphic characteristics, the etiology of HF, and responses to the treatment [47–50]. Another possible explanation may be the plausible role of sex-hormone-related regulation of the activity of the sodium–hydrogen exchanger (NHE)−1 co-transporter by which SGLT2 inhibitors are enabled to restore an expression of the X-linked inhibitor of apoptosis and the baculoviral IAP repeat-containing protein 5 (BIRC5), and thereby, to ameliorate cardiomyocyte cell death, prevent extracellular matrix accumulation, and suppress oxidative stress and mitochondrial dysfunction [51–53]. Additionally, there is an assumption that the expression of the target signaling molecules of SGLT2 inhibitors on cell surfaces may directly relate to gender and indirectly relate to an accumulation of adipose tissue, so the final effect of SGLT2 inhibitors is considered to be attributed to sex-hormone impacts [54]. Indeed, SGLT2 inhibitors, through promoting a nutrient deprivation signaling system–which is composed of Sirtuin-1, fibroblast growth factor-21, and peroxisome proliferator-activated receptor-gamma coactivator-1 alpha–are able to stimulate ketogenesis and gluconeogenesis in target cells, ultimately attenuating maladaptive cardiac remodeling, reducing microvascular inflammation and oxidative stress, and improving endothelial function [55]. There was a strong difference in the tissue expression of the main components of this system between both sexes [56]. Thus, SGLT-2 inhibitors have numerous remarkable effects on

suppressing the progression of HF and preventing adverse cardiac remodeling in T2DM through multiple molecular mechanisms, part of them exhibiting gender-based activity and being under the control of autocrine signaling pathways.

In the study, we concentrated on our hypothesis, which is based on the speculation that adropin may be a promising biomarker, allowing us to identify patients with HF who show a tendency of declining levels of NT-proBNP in their peripheral blood. Although the recent trials and meta-analyses revealed that the effects of SGLT2 inhibitors in HF patients on all-cause and CV mortality did not vary by sex, T2DM duration, or the presence of CV disease [57–60], this does not mean that all HF patients will receive benefits from SGLT2 inhibitors. In fact, patients with HF with improved levels of NT-proBNP, as a result, t, may be overvalued at the risk of poor response in cardiac performances and outcomes in conventional treatment. In this connection, the surrogate and validated circulating biomarker, which illustrates well the overlapping pathogenetic mechanisms of both HF and T2DM, seems to be promising for further investigations in large clinical studies.

Although adropin was found to be a potential regulator of CV functions, playing a key protective role in the pathogenesis of HF and T2DM [60], there is a limiting number of preclinical data and clinical evidence corresponding to our hypothesis. In a cohort of patients with end-stage kidney disease, there was no evidence of a significant correlation between serum levels of adropin and LV septal thickness [61], whereas adropin negatively regulated cell proliferation through the AMP-activated protein kinase/acetyl-CoA carboxylase signaling pathway and thereby prevented hypertrophy [62]. In some studies, increased levels of adropin related to the severity of acute HF and cardiac cachexia [28,63], but in patients with chronic HF, adropin levels in the peripheral blood were sustainably low [27]. In our study, in patients with T2DM of both sexes, there was a trend of increase in the circulating levels of adropin in response to the administration of SGLT2 inhibitor dapagliflosin, accompanied by an improvement of cardiac hemodynamics performances. We did not notice the impact of comorbidities–including atrial fibrillation, abdominal obesity, and BMI at the baseline–on adropin changes in circulation, while there was a relation between ΔBMI and an increase in adropin levels in the female population. Therefore, adropin demonstrated its predictive ability for the improvement of hemodynamics beyond NT-proBNP dynamics. It is a surprise that the tendency of BMI to decline was associated with an increase in adropin, although there are several plausible explanations of this finding. First, ΔBMI might be a surrogate marker of a euvolemic condition, which illustrates the relation of improving hemodynamic performances to decreasing neurohumoral activation [64]. Second, SGLT2 inhibitors may stimulate weight loss through improving glucose and lipid metabolism. Third, a difference in adipose tissue accumulation in females and males may be the indirect gender-related effect of SGLT2 inhibitors on clinical outcomes [29]. Another explanation may relate to the role of enlarged epicardial adipose tissue (EAT) in the regulation of cardiac function. In fact, EAT is not only a conventional cause of the mechanical constriction of the diastolic filling, but it is also a source of pro-inflammatory mediators capable of causing inflammation, microcirculatory dysfunction, and fibrosis of the underlying myocardium, thus impairing the relatability of the LV. Indeed, a recent clinical study revealed that SGLT2 inhibitors have been associated with the attenuation of EAT enlargement [65]. Fifth, SGLT2 inhibitors with anti-inflammatory potency may regulate the synthesis and secretion of adropin by hepatocytes [66]. Finally, SGLT2 inhibitors may increase the circulating levels of adropin indirectly through ketogenesis, and decrease body mass [29,67]. However, the impact of ΔBMI on dynamic changes in adropin in T2DM patients with HF deserves thorough investigation in the future.

Nonetheless, adropin appears to be valuable biomarker that seems to have an additive effect on risk stratification among T2DM patients with HF treated with SGLT2 inhibitors. However, this effect seems to be gender-relative. Indeed, the changes in the adropin levels are regarded to be a predictor, independent of NT-proBNP, for the favorable modification of hemodynamic performances mainly in the female population with T2DM and HF. Perhaps continuous serial measures of adropin may be practically useful for predicting the ability of

current HF strategies to reverse cardiac remodeling in both genders, especially taking into consideration of the affordability of the single measure of this biomarker. More studies are required to clearly elucidate the origin of specific mechanisms underlying the association between adropin and the suppression of adverse cardiac remodeling mainly in the female population. Therefore, it would be interesting to use IL-10, adiponectin, or leptin to explain the change in adipose tissue during therapy with SGLT2 inhibitors in connection with the dynamics of adropin.

This study has several limitations, one of which is the open-label design and the lack of a placebo comparison and control group. We understand that a control group is essential for clinical studies, but SGLT2 inhibitors are now generally recommended in HF patients regardless of T2DM presence, so there was no possibility of creating a control group beyond SGLT2 inhibitor administration. However, this is the first study in which the effect of SGLT2 inhibitor dapagliflosin on adropin levels in connection with gender and cardiac remodeling parameters was successfully detected. The next limitation is the lack of measurement of adipose tissue accumulation, which was due to the plausibility of the gender-dependent mechanisms of adropin co-regulation corresponding to body fat composition. This hypothesis deserves to be evaluated in clinical studies in the future. Moreover, we included in the study the patients with HbAc1 < 6.9% who were not treated with insulin to exclude the direct effect of hyperglycemia and insulin therapy on adropin levels. The age of the population studied was relatively young; however, it cannot be ignored that a larger sample could have nullified the differences that emerged between the two genders, particularly with cohorts of older and senior people. All of these factors require further investigation in the future. However, we think these limitations will not intervene in interpreting the results of the study.

5. Conclusions

In the population of T2DM patients with HF, mainly in females, the increased circulating levels of adropin seemed to be independent from the NT-proBNP predictor for the favorable modification of hemodynamic performances during the long-term administration of SGLT2 inhibitor dapagliflosin.

Author Contributions: Conceptualization, I.M.F., M.L. and A.E.B.; methodology, A.E.B. and I.M.F.; validation, I.M.F., M.L. and A.E.B.; formal analysis, A.A.B. and L.S.; investigation, A.A.B., T.A.B. and E.V.N.; data curation, A.A.B.; writing—original draft preparation, A.A.B., Z.O., T.A.B., E.V.N., L.S., M.L. and A.E.B.; writing—review and editing, I.M.F., M.L., Z.O. and A.A.B.; visualization, A.A.B. and E.V.N.; supervision, I.M.F.; project administration, T.A.B. and A.A.B. All authors have read and agreed to the published version of the manuscript.

Funding: This research received no external funding.

Institutional Review Board Statement: The study was conducted according to the guidelines of the Declaration of Helsinki, and approved by the Institutional Ethics Committee of Zaporozhye Medical Academy of Post-graduate Education (protocol number: 8; date of approval: 10 October 2020).

Informed Consent Statement: Informed consent was obtained from all subjects involved in the study.

Data Availability Statement: Not applicable.

Acknowledgments: Authors thanks all the patients who gave their consent to participate in the study and also the administrative staff of Private Hospital "VitaCenter" (Zaporozhye, Ukraine), Medical Center "EliteMedService" (Zaporozhye, Ukraine) and City Hospital #7 (Zaporozhye, Ukraine), for assistance in the study.

Conflicts of Interest: The authors declare no conflict of interest.

References

1. Lovic, D.; Piperidou, A.; Zografou, I.; Grassos, H.; Pittaras, A.; Manolis, A. The Growing Epidemic of Diabetes Mellitus. *Curr. Vasc. Pharmacol.* **2020**, *18*, 104–109. [CrossRef] [PubMed]
2. Glovaci, D.; Fan, W.; Wong, N.D. Epidemiology of Diabetes Mellitus and Cardiovascular Disease. *Curr. Cardiol. Rep.* **2019**, *21*, 21. [CrossRef]
3. Avilés-Santa, M.L.; Monroig-Rivera, A.; Soto-Soto, A.; Lindberg, N.M. Current State of Diabetes Mellitus Prevalence, Awareness, Treatment, and Control in Latin America: Challenges and Innovative Solutions to Improve Health Outcomes Across the Continent. *Curr. Diabetes Rep.* **2020**, *20*, 62. [CrossRef] [PubMed]
4. Lehrke, M.; Marx, N. Diabetes Mellitus and Heart Failure. *Am. J. Med.* **2017**, *130*, S40–S50. [CrossRef]
5. Aune, D.; Schlesinger, S.; Neuenschwander, M.; Feng, T.; Janszky, I.; Norat, T.; Riboli, E. Diabetes mellitus, blood glucose and the risk of heart failure: A systematic review and meta-analysis of prospective studies. *Nutr. Metab. Cardiovasc. Dis.* **2018**, *28*, 1081–1091. [CrossRef] [PubMed]
6. Berezin, A.E.; Lichtenauer, M.; Berezin, A.A. Heart failure among patients with prediabetes and type 2 diabetes mellitus: Diagnostic and predictive biomarkers: A narrative review. *J. Lab. Precis Med. Med.* **2022**, *7*, 5. [CrossRef]
7. Kristensen, S.L.; Jhund, P.; Lee, M.; Køber, L.; Solomon, S.D.; Granger, C.B.; Yusuf, S.; Pfeffer, M.A.; Swedberg, K.; McMurra, J.J.V.; et al. Prevalence of Prediabetes and Undiagnosed Diabetes in Patients with HFpEF and HFrEF and Associated Clinical Outcomes. *Cardiovasc. Drugs Ther.* **2017**, *31*, 545–549. [CrossRef]
8. McHugh, K.; DeVore, A.D.; Wu, J.; Matsouaka, R.A.; Fonarow, G.C.; Heidenreich, P.A.; Yancy, C.W.; Green, J.B.; Altman, N.; Hernandez, A.F. Heart Failure With Preserved Ejection Fraction and Diabetes: JACC State-of-the-Art Review. *J. Am. Coll. Cardiol.* **2019**, *73*, 602–611. [CrossRef]
9. Jankauskas, S.S.; Kansakar, U.; Varzideh, F.; Wilson, S.; Mone, P.; Lombardi, A.; Gambardella, J.; Santulli, G. Heart failure in diabetes. *Metabolism* **2021**, *125*, 154910. [CrossRef]
10. Berezin, A.E.; Berezin, A.A.; Lichtenauer, M. Myokines and Heart Failure: Challenging Role in Adverse Cardiac Remodeling, Myopathy, and Clinical Outcomes. *Dis. Mark.* **2021**, *2021*, 6644631. [CrossRef]
11. Yap, E.P.; Kp, M.M.J.; Ramachandra, C.J. Targeting the Metabolic-Inflammatory Circuit in Heart Failure With Preserved Ejection Fraction. *Curr. Hear. Fail. Rep.* **2022**, *19*, 63–74. [CrossRef]
12. Kirk, B.; Feehan, J.; Lombardi, G.; Duque, G. Muscle, Bone, and Fat Crosstalk: The Biological Role of Myokines, Osteokines, and Adipokines. *Curr. Osteoporos. Rep.* **2020**, *18*, 388–400. [CrossRef] [PubMed]
13. Takada, S.; Sabe, H.; Kinugawa, S. Abnormalities of Skeletal Muscle, Adipocyte Tissue, and Lipid Metabolism in Heart Failure: Practical Therapeutic Targets. *Front. Cardiovasc. Med.* **2020**, *7*, 79. [CrossRef] [PubMed]
14. Li, R.-L.; Wu, S.-S.; Wu, Y.; Wang, X.-X.; Chen, H.-Y.; Xin, J.-J.; Li, H.; Lan, J.; Xue, K.-Y.; Li, X.; et al. Irisin alleviates pressure overload-induced cardiac hypertrophy by inducing protective autophagy via mTOR-independent activation of the AMPK-ULK1 pathway. *J. Mol. Cell. Cardiol.* **2018**, *121*, 242–255. [CrossRef] [PubMed]
15. Li, Y.; Lu, H.; Xu, W.; Shang, Y.; Zhao, C.; Wang, Y.; Yang, R.; Jin, S.; Wu, Y.; Wang, X.; et al. Apelin ameliorated acute heart failure via inhibiting endoplasmic reticulum stress in rabbits. *Amino Acids* **2021**, *53*, 417–427. [CrossRef] [PubMed]
16. Berezin, A.A.; Fushtey, I.M.; Berezin, A.E. The Effect of SGLT2 Inhibitor Dapagliflozin on Serum Levels of Apelin in T2DM Patients with Heart Failure. *Biomedicines* **2022**, *10*, 1751. [CrossRef] [PubMed]
17. Shen, S.; Gao, R.; Bei, Y.; Li, J.; Zhang, H.; Zhou, Y.; Yao, W.; Xu, D.; Zhou, F.; Jin, M.; et al. Serum Irisin Predicts Mortality Risk in Acute Heart Failure Patients. *Cell. Physiol. Biochem.* **2017**, *42*, 615–622. [CrossRef]
18. Berezin, A.A.; Fushtey, I.M.; Pavlov, S.V.; Berezin, A.E. Predictive value of serum irisin for chronic heart failure in patients with type 2 diabetes mellitus. *Mol. Biomed.* **2022**, *3*, 34. [CrossRef]
19. Kumar, K.G.; Trevaskis, J.L.; Lam, D.D.; Sutton, G.M.; Koza, R.A.; Chouljenko, V.N.; Kousoulas, K.G.; Rogers, P.M.; Kesterson, R.A.; Thearle, M.; et al. Identification of Adropin as a Secreted Factor Linking Dietary Macronutrient Intake with Energy Homeostasis and Lipid Metabolism. *Cell Metab.* **2008**, *8*, 468–481. [CrossRef] [PubMed]
20. Yolbas, S.; Kara, M.; Kalayci, M.; Yildirim, A.; Gundogdu, B.; Aydin, S.; Koca, S.S. ENHO gene expression and serum adropin level in rheumatoid arthritis and systemic lupus erythematosus. *Adv. Clin. Exp. Med.* **2018**, *27*, 1637–1641. [CrossRef]
21. Stein, L.M.; Yosten, G.L.C.; Samson, W.K. Adropin acts in brain to inhibit water drinking: Potential interaction with the orphan G protein-coupled receptor, GPR19. *Am. J. Physiol. Integr. Comp. Physiol.* **2016**, *310*, R476–R480. [CrossRef] [PubMed]
22. Ganesh-Kumar, K.; Zhang, J.; Gao, S.; Rossi, J.; McGuinness, O.P.; Halem, H.H.; Culler, M.D.; Mynatt, R.L.; Butler, A.A. Adropin Deficiency Is Associated With Increased Adiposity and Insulin Resistance. *Obesity* **2012**, *20*, 1394–1402. [CrossRef] [PubMed]
23. Yu, H.-Y.; Zhao, P.; Wu, M.-C.; Liu, J.; Yin, W. Serum adropin levels are decreased in patients with acute myocardial infarction. *Regul. Pept.* **2014**, *190–191*, 46–49. [CrossRef] [PubMed]
24. Jurrissen, T.J.; Ramirez-Perez, F.I.; Cabral-Amador, F.J.; Soares, R.N.; Pettit-Mee, R.J.; Betancourt-Cortes, E.E.; McMillan, N.J.; Sharma, N.; Rocha, H.N.M.; Fujie, S.; et al. Role of adropin in arterial stiffening associated with obesity and type 2 diabetes. *Am. J. Physiol. Circ. Physiol.* **2022**, *323*, H879–H891. [CrossRef] [PubMed]

25. Wu, L.; Fang, J.; Chen, L.; Zhao, Z.; Luo, Y.; Lin, C.; Fan, L. Low serum adropin is associated with coronary atherosclerosis in type 2 diabetic and non-diabetic patients. *Clin. Chem. Lab. Med.* **2014**, *52*, 751–758. [CrossRef]
26. Butler, A.A.; Tam, C.S.; Stanhope, K.L.; Wolfe, B.M.; Ali, M.R.; O'Keeffe, M.; St-Onge, M.-P.; Ravussin, E.; Havel, P.J. Low Circulating Adropin Concentrations with Obesity and Aging Correlate with Risk Factors for Metabolic Disease and Increase after Gastric Bypass Surgery in Humans. *J. Clin. Endocrinol. Metab.* **2012**, *97*, 3783–3791. [CrossRef] [PubMed]
27. Zheng, J.; Liu, M.; Chen, L.; Yin, F.; Zhu, X.; Gou, J.; Zeng, W.; Lv, Z. Association between serum adropin level and coronary artery disease: A systematic review and meta-analysis. *Cardiovasc. Diagn. Ther.* **2019**, *9*, 1–7. [CrossRef]
28. Yosaee, S.; Soltani, S.; Sekhavati, E.; Jazayeri, S. Adropin- A Novel Biomarker of Heart Disease: A Systematic Review Article. *Iran. J. Public Health* **2016**, *45*, 1568–1576.
29. Packer, M. Cardioprotective effects of sirtuin-1 and its downstream effectors: Potential role in mediating the heart failure benefits of SGLT2 (sodium glucose linked transporter 2) inhibitors. *Circ. Heart Fail.* **2020**, *13*, e007197. [CrossRef] [PubMed]
30. Berezin, A.A.; Lichtenauer, M.; Boxhammer, E.; Stöhr, E.; Berezin, A.E. Discriminative Value of Serum Irisin in Prediction of Heart Failure with Different Phenotypes among Patients with Type 2 Diabetes Mellitus. *Cells* **2022**, *11*, 2794. [CrossRef]
31. Piepoli, M.F.; Hoes, A.W.; Agewall, S.; Albus, C.; Brotons, C.; Catapano, A.L.; Cooney, M.-T.; Corrà, U.; Cosyns, B.; Deaton, C.; et al. ESC Scientific Document Group. 2016 European Guidelines on cardiovascular disease prevention in clinical practice: The Sixth Joint Task Force of the European Society of Cardiology and Other Societies on Cardiovascular Disease Prevention in Clinical Practice (constituted by representatives of 10 societies and by invited experts) Developed with the special contribution of the European Association for Cardiovascular Prevention & Rehabilitation (EACPR). *Eur. Heart J.* **2016**, *37*, 2315–2381. [CrossRef]
32. American Diabetes Association. 2. Classification and Diagnosis of Diabetes: Standards of Medical Care in Diabetes-2021. *Diabetes Care* **2021**, *44* (Suppl. S1), S15–S33, Erratum in: *Diabetes Care* **2021**, *44*, 2182. [CrossRef]
33. Knuuti, J.; Wijns, W.; Saraste, A.; Capodanno, D.; Barbato, E.; Funck-Brentano, C.; Prescott, E.; Storey, R.F.; Deaton, C.; Cuisset, T.; et al. 2019 ESC Guidelines for the diagnosis and management of chronic coronary syndromes. *Eur. Heart J.* **2020**, *41*, 407–477. [CrossRef]
34. de Boer, I.H.; Khunti, K.; Sadusky, T.; Tuttle, K.R.; Neumiller, J.J.; Rhee, C.M.; Rosas, S.E.; Rossing, P.; Bakris, G. Diabetes Management in Chronic Kidney Disease: A Consensus Report by the American Diabetes Association (ADA) and Kidney Disease: Improving Global Outcomes (KDIGO). *Diabetes Care* **2022**, *45*, dci220027. [CrossRef]
35. Levey, A.S.; Eckardt, K.-U.; Tsukamoto, Y.; Levin, A.; Coresh, J.; Rossert, J.; Zeeuw, D.D.; Hostetter, T.H.; Lameire, N.; Eknoyan, G. Definition and classification of chronic kidney disease: A position statement from Kidney Disease: Improving Global Outcomes (KDIGO). *Kidney Int.* **2005**, *67*, 2089–2100. [CrossRef] [PubMed]
36. McDonagh, T.A.; Metra, M.; Adamo, M.; Gardner, R.S.; Baumbach, A.; Böhm, M.; Burri, H.; Butler, J.; Čelutkienė, J.; Chioncel, O.; et al. 2021 ESC Guidelines for the diagnosis and treatment of acute and chronic heart failure. *Eur. Heart J.* **2021**, *42*, 3599–3726. [CrossRef] [PubMed]
37. Nagueh, S.F.; Smiseth, O.A.; Appleton, C.P.; Byrd, B.F., 3rd; Dokainish, H.; Edvardsen, T.; Flachskampf, F.A.; Gillebert, T.C.; Klein, A.L.; Lancellotti, P.; et al. Recommendations for the Evaluation of Left Ventricular Diastolic Function by Echocardiography: An Update from the American Society of Echocardiography and the European Association of Cardiovascular Imaging. *J. Am. Soc. Echocardiogr.* **2016**, *29*, 277–314. [CrossRef] [PubMed]
38. Yamamoto, J.; Wakami, K.; Muto, K.; Kikuchi, S.; Goto, T.; Fukuta, H.; Seo, Y.; Ohte, N. Verification of Echocardiographic Assessment of Left Ventricular Diastolic Dysfunction in Patients With Preserved Left Ventricular Ejection Fraction Using the American Society of Echocardiography and European Association of Cardiovascular Imaging 2016 Recommendations. *Circ. Rep.* **2019**, *1*, 525–530, PMCID:PMC7897561. [CrossRef] [PubMed]
39. Levey, A.S.; Stevens, L.A.; Schmid, C.H.; Zhang, Y.L.; Castro, A.F., 3rd; Feldman, H.I.; Kusek, J.W.; Eggers, P.; Van Lente, F.; Greene, T.; et al. A New Equation to Estimate Glomerular Filtration Rate. *Ann. Intern. Med.* **2009**, *150*, 604–612. [CrossRef] [PubMed]
40. Matthews, D.R.; Hosker, J.P.; Rudenski, A.S.; Naylor, B.A.; Treacher, D.F.; Turner, R.C. Homeostasis model assessment: Insulin resistance and β-cell function from fasting plasma glucose and insulin concentrations in man. *Diabetologia* **1985**, *28*, 412–419. [CrossRef] [PubMed]
41. Salvatore, T.; Caturano, A.; Galiero, R.; Di Martino, A.; Albanese, G.; Vetrano, E.; Sardu, C.; Marfella, R.; Rinaldi, L.; Sasso, F.C. Cardiovascular Benefits from Gliflozins: Effects on Endothelial Function. *Biomedicines* **2021**, *9*, 1356. [CrossRef] [PubMed]
42. Salvatore, T.; Galiero, R.; Caturano, A.; Vetrano, E.; Loffredo, G.; Rinaldi, L.; Catalini, C.; Gjeloshi, K.; Albanese, G.; Di Martino, A.; et al. Coronary Microvascular Dysfunction in Diabetes Mellitus: Pathogenetic Mechanisms and Potential Therapeutic Options. *Biomedicines* **2022**, *10*, 2274. [CrossRef] [PubMed]
43. Dunlay, S.M.; Givertz, M.M.; Aguilar, D.; Allen, L.A.; Chan, M.; Desai, A.S.; Deswal, A.; Dickson, V.V.; Kosiborod, M.N.; Lekavich, C.L.; et al. Type 2 Diabetes Mellitus and Heart Failure: A Scientific Statement From the American Heart Association and the Heart Failure Society of America: This statement does not represent an update of the 2017 ACC/AHA/HFSA heart failure guideline update. *Circulation* **2019**, *140*, e294–e324. [CrossRef] [PubMed]

44. Zannad, F.; Ferreira, J.P.; Pocock, S.J.; Anker, S.D.; Butler, J.; Filippatos, G.; Brueckmann, M.; Ofstad, A.P.; Pfarr, E.; Jamal, W.; et al. SGLT2 inhibitors in patients with heart failure with reduced ejection fraction: A meta-analysis of the EMPEROR-Reduced and DAPA-HF trials. *Lancet* **2020**, *396*, 819–829. [CrossRef] [PubMed]
45. Alba, A.C.; Agoritsas, T.; Jankowski, M.; Courvoisier, D.; Walter, S.D.; Guyatt, G.H.; Ross, H.J. Risk Prediction Models for Mortality in Ambulatory Patients With Heart Failure: A systematic review. *Circ. Heart Fail.* **2013**, *6*, 881–889. [CrossRef]
46. Chilton, R.J. Effects of sodium-glucose cotransporter-2 inhibitors on the cardiovascular and renal complications of type 2 diabetes. *Diabetes Obes. Metab.* **2019**, *22*, 16–29. [CrossRef]
47. Zhang, N.; Wang, Y.; Tse, G.; Korantzopoulos, P.; Letsas, K.P.; Zhang, Q.; Li, G.; Lip, G.Y.H.; Liu, T. Effect of sodium-glucose cotransporter-2 inhibitors on cardiac remodelling: A systematic review and meta-analysis. *Eur. J. Prev. Cardiol.* **2021**, *28*, 1961–1973. [CrossRef]
48. Jiang, Y.; Yang, P.; Fu, L.; Sun, L.; Shen, W.; Wu, Q. Comparative Cardiovascular Outcomes of SGLT2 Inhibitors in Type 2 Diabetes Mellitus: A Network Meta-Analysis of Randomized Controlled Trials. *Front. Endocrinol.* **2022**, *13*, 802992. [CrossRef]
49. Zhang, J.; Huan, Y.; Leibensperger, M.; Seo, B.; Song, Y. Comparative Effects of Sodium-Glucose Cotransporter 2 Inhibitors on Serum Electrolyte Levels in Patients with Type 2 Diabetes: A Pairwise and Network Meta-Analysis of Randomized Controlled Trials. *Kidney360* **2022**, *3*, 477–487. [CrossRef]
50. Rao, S. Use of Sodium-Glucose Cotransporter-2 Inhibitors in Clinical Practice for Heart Failure Prevention and Treatment: Beyond Type 2 Diabetes. A Narrative Review. *Adv. Ther.* **2022**, *39*, 845–861. [CrossRef]
51. Berezin, A.E. Plausible effects of sodium-glucose cotransporter-2 inhibitors on adverse cardiac remodelling. *Eur. J. Prev. Cardiol.* **2021**, *29*, zwab203. [CrossRef] [PubMed]
52. Segers, V.F.M.; De Keulenaer, G.W. Autocrine Signaling in Cardiac Remodeling: A Rich Source of Therapeutic Targets. *J. Am. Heart Assoc.* **2021**, *10*, e019169. [CrossRef] [PubMed]
53. Iborra-Egea, O.; Santiago-Vacas, E.; Yurista, S.R.; Lupón, J.; Packer, M.; Heymans, S.; Zannad, F.; Butler, J.; Pascual-Figal, D.; Lax, A.; et al. Unraveling the Molecular Mechanism of Action of Empagliflozin in Heart Failure With Reduced Ejection Fraction With or Without Diabetes. *JACC Basic Transl. Sci.* **2019**, *4*, 831–840. [CrossRef]
54. Pruett, J.E.; Everman, S.J.; Hoang, N.H.; Salau, F.; Taylor, L.C.; Edwards, K.S.; Hosler, J.P.; Huffman, A.M.; Romero, D.G.; Cardozo, L.L.Y. Mitochondrial function and oxidative stress in white adipose tissue in a rat model of PCOS: Effect of SGLT2 inhibition. *Biol. Sex Differ.* **2022**, *13*, 45. [CrossRef] [PubMed]
55. Sullivan, R.D.; McCune, M.E.; Hernandez, M.; Reed, G.L.; Gladysheva, I.P. Suppression of Cardiogenic Edema with Sodium-Glucose Cotransporter-2 Inhibitors in Heart Failure with Reduced Ejection Fraction: Mechanisms and Insights from Pre-Clinical Studies. *Biomedicines* **2022**, *10*, 2016. [CrossRef]
56. Shimabukuro, M. SIRT1 and Gender Differences in Atherosclerotic Cardiovascular Disease. *J. Atheroscler. Thromb.* **2020**, *27*, 8–10. [CrossRef]
57. Mordi, N.A.; Mordi, I.R.; Singh, J.S.; McCrimmon, R.J.; Struthers, A.D.; Lang, C.C. Renal and Cardiovascular Effects of SGLT2 Inhibition in Combination With Loop Diuretics in Patients With Type 2 Diabetes and Chronic Heart Failure: The RECEDE-CHF Trial. *Circulation* **2020**, *142*, 1713–1724. [CrossRef]
58. Koufakis, T.; Mustafa, O.G.; Ajjan, R.A.; Garcia-Moll, X.; Zebekakis, P.; Dimitriadis, G.; Kotsa, K. From Skepticism to Hope: The Evolving Concept of the Initiation and Use of Sodium-Glucose Cotransporter 2 Inhibitors in Hospitalized Patients. *Drugs* **2022**, *82*, 949–955. [CrossRef]
59. Eroglu, E.T.; Coronel, R.; Zuurbier, C.J.; Blom, M.; de Boer, A.; Souverein, P.C. Use of sodium-glucose cotransporter-2 inhibitors and the risk for sudden cardiac arrest and for all-cause death in patients with type 2 diabetes mellitus. *Eur. Heart J.–Cardiovasc. Pharmacother.* **2022**, *9*, pvac043. [CrossRef]
60. Li, L.; Xie, W.; Zheng, X.-L.; Yin, W.-D.; Tang, C.-K. A novel peptide adropin in cardiovascular diseases. *Clin. Chim. Acta* **2016**, *453*, 107–113. [CrossRef]
61. Liu, F.; Cui, B.; Zhao, X.; Wu, Y.; Qin, H.; Guo, Y.; Wang, H.; Lu, M.; Zhang, S.; Shen, J.; et al. Correlation of Serum Adropin Levels with Risk Factors of Cardiovascular Disease in Hemodialysis Patients. *Metab. Syndr. Relat. Disord.* **2021**, *19*, 401–408. [CrossRef] [PubMed]
62. Wang, L.; Zhao, L.-P.; Chen, Y.-Q.; Chang, X.-S.; Xiong, H.; Zhang, D.-M.; Xu, W.-T.; Chen, J.-C. Adropin inhibits the phenotypic modulation and proliferation of vascular smooth muscle cells during neointimal hyperplasia by activating the AMPK/ACC signaling pathway. *Exp. Ther. Med.* **2021**, *21*, 560. [CrossRef] [PubMed]
63. Lian, W.; Gu, X.; Qin, Y.; Zheng, X. Elevated Plasma Levels of Adropin in Heart Failure Patients. *Intern. Med.* **2011**, *50*, 1523–1527. [CrossRef] [PubMed]
64. Mushala, B.A.S.; Scott, I. Adropin: A hepatokine modulator of vascular function and cardiac fuel metabolism. *Am. J. Physiol. Circ. Physiol.* **2021**, *320*, H238–H244. [CrossRef] [PubMed]
65. Salvatore, T.; Galiero, R.; Caturano, A.; Vetrano, E.; Rinaldi, L.; Coviello, F.; Di Martino, A.; Albanese, G.; Colantuoni, S.; Medicamento, G.; et al. Dysregulated Epicardial Adipose Tissue as a Risk Factor and Potential Therapeutic Target of Heart Failure with Preserved Ejection Fraction in Diabetes. *Biomolecules* **2022**, *12*, 176. [CrossRef] [PubMed]

66. Li, N.; Xie, G.; Zhou, B.; Qu, A.; Meng, H.; Liu, J.; Wang, G. Serum Adropin as a Potential Biomarker for Predicting the Development of Type 2 Diabetes Mellitus in Individuals With Metabolic Dysfunction-Associated Fatty Liver Disease. *Front. Physiol.* **2021**, *12*, 696163. [CrossRef] [PubMed]
67. Bozic, J.; Kumric, M.; Kurir, T.T.; Males, I.; Borovac, J.A.; Martinovic, D.; Vilovic, M. Role of Adropin in Cardiometabolic Disorders: From Pathophysiological Mechanisms to Therapeutic Target. *Biomedicines* **2021**, *9*, 1407. [CrossRef]

biomedicines

MDPI

Review

Diabetes-Induced Cardiac Autonomic Neuropathy: Impact on Heart Function and Prognosis

Susumu Z. Sudo [1], Tadeu L. Montagnoli [2], Bruna de S. Rocha [2,3], Aimeé D. Santos [4,5], Mauro P. L. de Sá [5] and Gisele Zapata-Sudo [1,2,3,5,*]

[1] Programa de Pós-Graduação em Medicina (Cirurgia Geral), Faculdade de Medicina, Universidade Federal do Rio de Janeiro, Rio de Janeiro 21941-902, Brazil
[2] Programa de Pesquisa em Desenvolvimento de Fármacos, Instituto de Ciências Biomédicas, Universidade Federal do Rio de Janeiro, Rio de Janeiro 21941-902, Brazil
[3] Programa de Pós-Graduação em Cardiologia, Instituto do Coração Edson Saad, Universidade Federal do Rio de Janeiro, Rio de Janeiro 21941-913, Brazil
[4] Faculdade de Enfermagem, Universidade Federal do Estado do Rio de Janeiro, Rio de Janeiro 22290-180, Brazil
[5] Instituto do Coração Edson Saad, Faculdade de Medicina, Universidade Federal do Rio de Janeiro, Rio de Janeiro 21941-913, Brazil
* Correspondence: gsudo@icb.ufrj.br or gzsudo@gmail.com; Tel./Fax: +55-21-39386505

Abstract: Cardiovascular autonomic neuropathy (CAN) is a severe complication of the advance stage of diabetes. More than 50% of diabetic patients diagnosed with peripheral neuropathy will have CAN, with clinical manifestations including tachycardia, severe orthostatic hypotension, syncope, and physical exercise intolerance. Since the prevalence of diabetes is increasing, a concomitant increase in CAN is expected and will reduce quality of life and increase mortality. Autonomic dysfunction is associated with reduced baroreflex sensitivity and impairment of sympathetic and parasympathetic modulation. Various autonomic function tests are used to diagnose CAN, a condition without adequate treatment. It is important to consider the control of glucose level and blood pressure as key factors for preventing CAN progression. However, altered biomarkers of inflammatory and endothelial function, increased purinergic receptor expression, and exacerbated oxidative stress lead to possible targets for the treatment of CAN. The present review describes the molecular alterations seen in CAN, diagnosis, and possible alternative treatments.

Keywords: cardiac autonomic neuropathy; diabetes; oxidative stress; inflammation; endothelium dysfunction

Citation: Sudo, S.Z.; Montagnoli, T.L.; Rocha, B.d.S.; Santos, A.D.; de Sá, M.P.L.; Zapata-Sudo, G. Diabetes-Induced Cardiac Autonomic Neuropathy: Impact on Heart Function and Prognosis. *Biomedicines* **2022**, *10*, 3258. https://doi.org/10.3390/biomedicines10123258

Academic Editors: Alfredo Caturano and Raffaele Galiero

Received: 17 November 2022
Accepted: 8 December 2022
Published: 15 December 2022

Publisher's Note: MDPI stays neutral with regard to jurisdictional claims in published maps and institutional affiliations.

1. Introduction

Diabetes mellitus (DM) has become one of the leading causes of premature death in most countries, mainly through increased risk of cardiovascular diseases, which are responsible for 50 to 80% of deaths in diabetic patients [1]. The number of diabetic patients is increasing due to population growth and aging, the progressive prevalence of obesity, and sedentary lifestyle. In the period 1980–2014, there was an increase from 108 to 422 million DM diagnoses, and the prevalence has increased more rapidly in low- and middle-income countries [2]. In 2017, DM overall incidence, prevalence, disability-adjusted death, and years of quality life were 22.9; 476.0; 1.37, and 67.9 million, respectively. Additionally, it is estimated that in 2025, DM will affect 26.6; 570.9; 1.59, and 79.3 million, respectively [3]. Progression of DM is associated with chronic complications including cardiomyopathy, retinopathy, nephropathy, and neuropathy. Diabetic neuropathy provokes an autonomic nervous system dysfunction with nervous fibers damaged, which causes cardiovascular autonomic neuropathy (CAN). This review includes an overview of the DM-induced CAN regarding its definition, epidemiology, molecular mechanisms, and therapeutics.

2. Pathogenesis

Changes in insulin concentration and activity observed in DM promote abnormalities in lipid metabolism, favoring microvascular and macrovascular complications [4]. Lipid accumulation, oxidative stress, and inflammation cause activation of stress-sensitive kinases with consequent inhibition of insulin signaling [5]. These changes in organs sensitive to the action of insulin develop renal, neuronal, and cardiac comorbidities. DM cause mitochondrial and endoplasmic reticulum dysfunctions in cardiomyocytes, which lead respectively to oxidative stress and abnormal Ca^{2+} handling, which are responsible for death and rigidity of myocytes and inducing diabetic cardiomyopathy, respectively [6]. Impairment of cytosolic Ca^{2+} flux in DM cardiomyocytes can decrease diastolic and systolic cardiac function, promoting ventricular dysfunction in the absence of coronary artery disease or hypertension. High levels of blood glucose cause vascular and neural damage because glucose in the cytosol is directed into the polyol pathway, in which it is converted to sorbitol by the enzyme aldose reductase, using the nitric acid adenine dinucleotide phosphate (NADPH) as a cofactor. The excessive consumption of NADPH culminates in its depletion, resulting in the generation of reactive oxygen species (ROS) [7]. ROS stimulates the oxidation of low-density lipoprotein (LDL) and ox-LDL, which are not recognized by the LDL receptor and are captured by macrophages, causing the formation of foam cells and atherosclerotic plaques, which leads to vascular disorders associated with DM [8]. Excessive ROS production results in increased oxidative stress and provokes hyperglycemia-induced damage through an increase in advanced glycation end product (AGE) formation, which results from the glycosylation of lipids, lipoproteins, and amino acids, promoting their deposition in the sub-endothelial layer and inducing endothelial dysfunction [9]. In fact, AGEs can directly inactivate the endothelium nitric oxide (eNO), which determines the lack of endothelium-dependent vasodilation [10]. The activation of the gene-binding receptor (RAGE) induces the production of ROS, which activates NF-kB, causing multiple pathological changes in gene expression [11]. Several factors could explain the pathogenesis of diabetic cardiomyopathy, including cardiac metabolic disorders, subcellular signaling abnormalities, autonomic dysfunction, activated renin-angiotensin-aldosterone system, inflammation, oxidative stress, and maladaptive immune response [7]. The inflammatory response involves a complex cascade of events involving many types of cells. Inflammatory signaling in cardiomyocytes usually occurs in an early phase of response to myocardial injury and implies overproduction of mitochondrial ROS [12]. The activation of several signaling pathways, such as NF-κB, c-jun NH_2-terminal kinase, or p38-MAPK, can mediate the state of inflammation, which is linked to insulin resistance, playing an important role in diabetic complications. NF-kB represents one of the most important mediators of the inflammatory process because its activation is associated with increased release of cytokines, such as tumor necrosis factor alpha (TNF-α)—which is often involved in cardiac damage contributing to cardiac hypertrophy and fibrosis—as well as ventricular dysfunction in the diabetic heart [13].

CAN characterized by an imbalance between sympathetic and parasympathetic activity is a major complication of DM [14]. The predominance of sympathetic activity can exacerbate cardiomyopathy in diabetic patients because of the increase of release of myocardial catecholamines, activation of adrenergic receptors, and activation of the renin–angiotensin–aldosterone system (RAAS) [15] (Figure 1).

CAN is classified according to its progress: 1. subclinical stage—characterized by lack of symptoms but with abnormal simpatovagal balance, decreased baroreflex sensitivity; [16,17] 2. early stage—tachycardia at rest; 3. advanced stage—exercise intolerance, cardiomyopathy with left ventricular dysfunction, orthostatic hypotension, and silent myocardial ischemia [18,19].

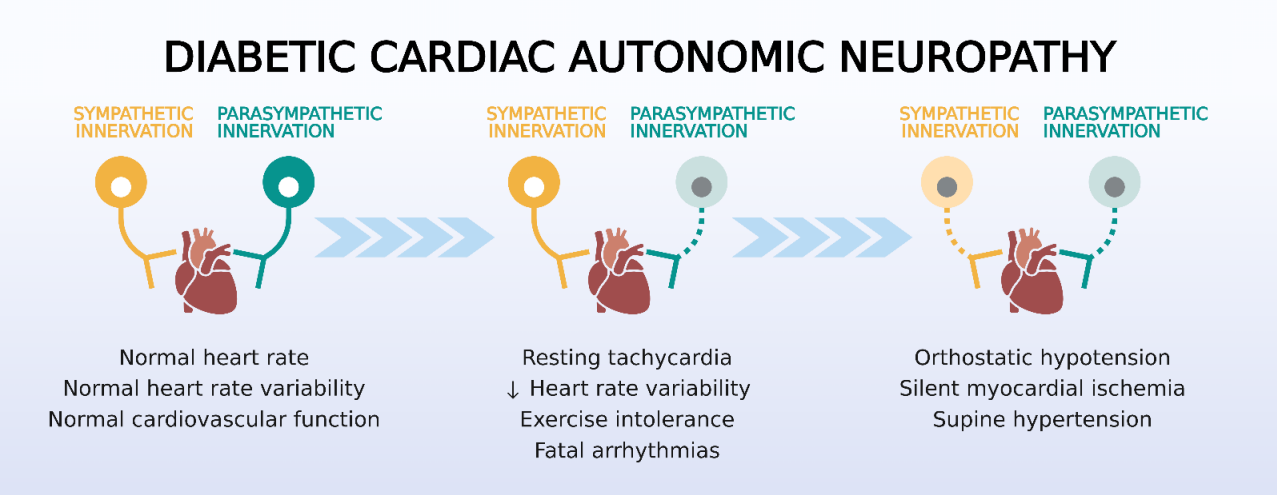

Figure 1. Evolution of symptoms of cardiac autonomic neuropathy (CAN) in diabetes. Patients display reduced variability in heart rate and resting tachycardia in the early phase of parasympathetic dysfunction, which underlie the reduced exercise tolerance and the increased arrhythmogenesis. Later stages of CAN involve sympathetic denervation and cause hemodynamic dysregulation and silent myocardial ischemia. Source: Own authorship.

3. Diagnosis of DM-Induced Cardiac Autonomic Neuropathy

As the prevalence of DM increases, a concomitant increase in CAN occurs, which cannot be diagnosed in the early stage, also occurs [18,20]. DM can induce neuron injury to the autonomic nervous system, which causes autonomic dysfunction involving initially the parasympathetic and later the sympathetic system. Although the mechanism of neuronal dysfunction is not completely clear, hyperglycemia, which is responsible for the increase of ROS and AGE, leads to the damage of peripheral nerves affecting initially the vagus nerve [21]. Long-term progression of DM is associated with lack of blood pressure response to sleep or exercise, indicating damage to the sympathetic system, which is correlated with high mortality. The severity of CAN depends on glucose level, time of DM, blood pressure, and aging-induced neuronal death [22]. Initially, altered HRV occurs, and it is followed by resting tachycardia. The next step of the sympathetic predominance consists of decrease in coronary flow and consequent cardiac dysfunction. The progression of CAN reveals a denervation of sympathetic vasomotor producing an inadequate vascular and HR response combined with orthostatic hypotension.

Diagnosis involves the use of cardiac autonomic reflex tests (CARTs), including the evaluation of blood pressure and heart rate variability (HRV) during different maneuvers. HRV consists of spontaneous and induced fluctuations in heart rate (HR—very low, low, and high frequency) [23]. The spectral analysis of the balance between sympathetic and vagal activities is most sensitive in early stages of CAN. It is essential to perform HRV and the gold standard tests (deep breathing, Valsalva, and orthostatic) to achieve early diagnosis of this complication of DM [24].

3.1. Diagnostic Tests for CAN

3.1.1. Autonomic Testing

The gold standard tests of CARTs involve the measurement of changes in HR and BP to physiological maneuvers [25]. The standard CARTs recommended for diagnosis of CAN include: the deep breathing (DB) test, the Valsalva maneuver (VM) test, the lying-to-standing (LS) test at 30:15, and the BP response to orthostasis [25,26].

- Deep breathing (DB) test

The DB test is performed by measuring beat-to-beat HRV in a supine position. Patient respiration is paced at six breaths per minute by a metronome or similar device during

electrocardiogram (EKG) recording. The expiration-to-inspiration (E/I) index is calculated as the ratio between the three maximum and the three minimum RR intervals in a respiration cycle [25]. Minimal threshold for normal E/I ratios depend on patient age and decline from 1.17 at 20–24 years to 1.02 at 70–75 years [26]. Differences in HR under 10 bpm and E/I ratios lower than the threshold are considered abnormal [26].

- HR response to Valsalva maneuver

The patient is asked to perform forced exhalation (to 40 mmHg in a manometer) for 15 s with simultaneous EKG recording. Healthy subjects develop tachycardia during exhalation and bradycardia after release. The ratio of the longest RR interval after exhalation and the shortest RR interval during exhalation is calculated, and normal values should be 1.2 or higher [25,26].

- Lying-to-standing (LS) test

During continuous EKG monitoring, the patient changes from a supine position to standing up. The longest RR interval between the 25th and 35th beat and the shortest RR interval between the 10th and 20th beat after change of posture are measured [25]. Values under 1.03 and ratios of 30:15 are considered abnormal [26].

- Blood pressure (BP) response to orthostasis

BP is measured initially in the supine position and 2 min after standing up. A reduction in BP of between 10–29 mmHg or over 30 mmHg is indicative of borderline or abnormal BP response [25,26]. Moreover, a decrease of over 20 mmHg in systolic or over 10 mmHg in diastolic BP is also used as being indicative of orthostatic incompetence [25].

3.1.2. HR Variability (HRV) Measures Used for Diagnosis

HRV is determined as the variations in consecutive RR intervals and may be analyzed using long (usually 24 h) or short (<10 min) EKG measurements, although the latter may be preferred for investigation purposes. Direct analysis provides HRV parameters in the time domain, mainly standard deviations (SDNN) or root mean squared deviations (RMSSD) of successive RR intervals [25]. Frequency–domain analysis is performed after data transform (e.g., fast Fourier transform) to obtain HRV spectra. These histograms are divided in low (LF) and high frequency (HF) regions, which provide information on the influences of both autonomic branches on HR. The ratio LF/HF is mainly used as an index of autonomic balance, generally referred as the sympathetic-to-parasympathetic ratio. Although a reduction in the HF band may reflect a vagal dysfunction in early CAN, it may be accompanied by reduction in LF, indicating concomitant dysregulation of sympathetic tone [25,26].

A confirmed diagnosis of CAN consists in the presence of three altered tests and the presence of associated orthostatic hypotension reflects greater severity and poor prognosis. DM causes autonomic neuropathy, which is the disability of the compensatory autonomic mechanism to regulate blood pressure. The increase in vascular resistance in response to the activation of baroreceptors induced by hypotension does not occur because of failure of the sympathetic reflex in diabetic patients. For that reason, patients have orthostatic hypotension as a result of damage to the efferent sympathetic vasomotor fibers. More than 50% of diabetic patients diagnosed with peripheral neuropathy will have CAN. When in an advanced condition, ischemia and asymptomatic myocardial infarction can occur, as can left ventricular dysfunction, which is linked to increased risk of renal failure and sudden death [27]. Sudden cardiac death can also be a consequence of the arrhythmogenic effect, which promotes atrial and ventricular arrhythmias [14]. Therefore, arrhythmias can manifest in early stages of CAN during the decreased parasympathetic activity phase. Among diabetic patients, 38–44% may suffer from cardiac dysautonomia with prognostic implications and higher cardiovascular mortality. There are slight differences in relation to risk factors between DM type-1- or type-2-induced CAN, leading to a multifactorial approach in its prevention [28]. Thus, an intensive treatment of hyperglycemia added to a

multifactorial approach is beneficial in patients with DM and can result in the delay and prevention of CAN.

4. Molecular Mechanisms of DM-Induced Cardiac Autonomic Neuropathy

DM-induced macrovascular changes can lead to coronary artery disease, atherosclerosis, and heart failure, but microvascular changes cause peripheral vascular dysfunction, stroke, nephropathy, polyperipheral neuropathy, and retinopathy [19]. Inflammation plays an important role in the development of those complications resulting from DM. The pro-inflammatory environment resulting from hyperglycemia and/or insulin resistance is the result of the higher expression of inflammatory mediators, such as IL-1β, IL-6, TNF-α, TGF-β, IKKβ, and JNK, that may have local or systemic action. Inflammatory mediators act on the endothelium so that these cells alter their transcription profile, promoting a greater expression of cell recognition markers (ICAM-1 and VCAM-1) and facilitating the diapedesis of hematopoietic cells (lymphocytes and monocytes). Released cytokines and chemokines can activate other cells in addition to macrophages, antigen presenting cells (APC), effector cells (Th1, Th2), or memory cells (lymphocyte B). This can occur in the heart, promoting an immune response that perpetuates inflammation, leading to an oxidative and hypoxic environment. These events promote autophagy, apoptosis, necrosis, non-effective neovascularization, hypertrophy, collagen deposition, and fibrosis, which—in the long term—cause cardiac dysfunction and failure. Briefly, the mitochondrial overproduction of ROS, which leads to usually irreversible tissue damage, such as apoptosis, hyperplasia, hypertrophy, remodeling, or fibrosis, alters the glycolytic metabolism, increasing the use of glucose by routes other than ATP production [29].

Additionally, diabetic peripheral neuropathy is caused by the effects of chronic exposure to hyperglycemia, which promote glycotoxic stress, inducing increased oxidative stress with increased ROS; dysfunction of the antioxidant system; activation of the JNK, AP-1, PKC, NFκB, and MAPK; the additional formation of polyols and glycosamines; AGE favoring the transcription of genes encoding TGF-β, IL-1, IL-6, and TNF-α; and induced nitric oxide (iNOS). ROS induces depression of autonomic ganglion synaptic transmission, contributing to increased risk of fatal cardiac arrhythmias as well as to sudden death after myocardial infarction [29]. Mitochondrial dysfunction is associated to all these processes that lead to apoptosis and autophagy, bioenergetic dysregulation, neurovascular dysfunction, and inflammation and demyelination of nerves [30].

CAN is considered a diffuse neuropathy characterized as chronic and progressive with altered signaling pathways (polyol, poly (ADP ribose) polymerase (PARP), PKC, AGE) in neuronal cells (Figure 2).

It also has increased concentration of pro-inflammatory cytokines (IL-1β, IL-6, TNF-α), and exacerbation of oxidative stress. High glucose levels cause the following changes: 1. conversion into sorbitol, whose intracellular increase promotes osmotic stress and greater electrolyte output from the cell, which causes impairment of Schwann cells from peripheral neurons; 2. positive regulation of the hexosamine pathway, resulting in increased N-acetyl glucosamine (GlcNAc) and, consequently, the induction of oxidative stress; 3. exacerbation of oxidative stress due to lipid peroxidation and reduction of glutathione (GSH) levels and enzymes involved in antioxidant defense, such as catalase and superoxide dismutase (SOD); 4. increase inTNF-α levels, which provides, indirectly, the occurrence of neuronal apoptosis; 5. increase in AGE receptors (RAGE) in endothelial and Schwann cells of peripheral nerves; 6. activation of PKC in nerve tissue. Considering the oxidative stress in the vagus nerve (first nerve affected), an increase in malondialdehyde (MDA) levels and reduced levels of GSH, SOD are detected in diabetic animals [31].

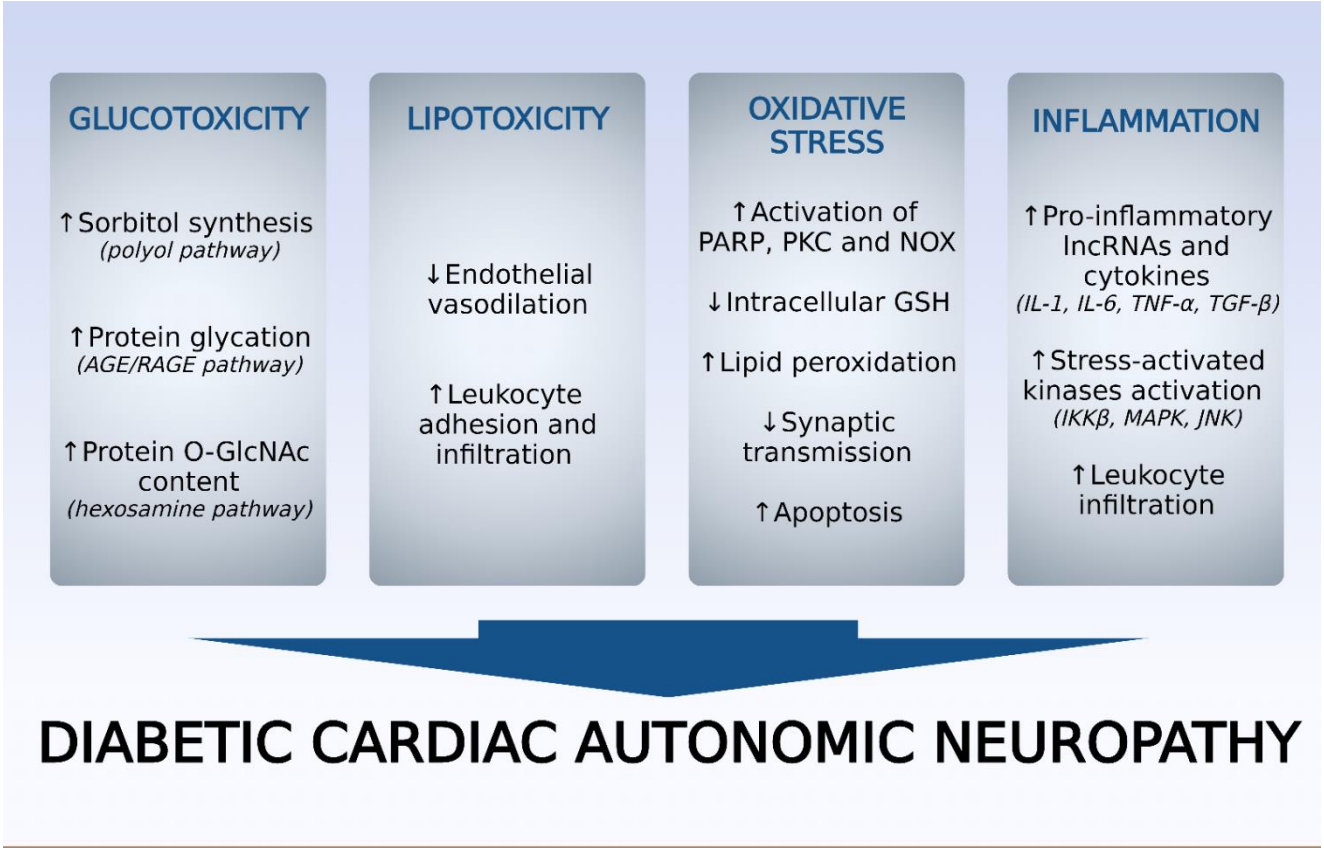

Figure 2. Pathophysiological factors underlying the development and aggravation of diabetic cardiac autonomic neuropathy (DCAN). AGE, advanced glycation end-products; RAGE, receptor for advanced glycation end-products; GlcNAc, *N*-acetyl glucosamine; PARP, poly(ADP-ribose) polymerase; PKC, protein kinase C; NOX, reduced nicotinamide adenine dinucleotide phosphate oxidase; GSH, reduced glutathione; IL, interleukin; TNF-α, tumor necrosis factor-α; TGF-β, transforming growth factor-β; IKKβ, inhibitor of nuclear factor kappa B kinase; MAPK, mitogen-activated protein kinase; JNK, c-Jun N-terminal kinase. Source: Own authorship.

DM induces autonomic dysfunction since baroreflex sensitivity is decreased and sympathetic and parasympathetic modulation is impaired. Reduced HRV and vagal modulation index are probably consequent to high glycemic levels [15]. Parasympathetic denervation and sympathetic predominance reduce blood pressure and HR, causing exercise intolerance. Increased sympathetic activity is also attributed to upregulated chemoreflex associated with sleep apnea syndrome (intermittent hypoxia) in diabetic patients [32].

A correlation between cardiac autonomic control parameters and biomarkers of inflammatory and endothelial function is detected in patients with DM type 2 [33]. Thus, the levels of subclinical inflammation biomarkers, such as IL-6, IL-1beta, and high-sensitivity C-reactive protein, were inversely associated with cardiac vagal control parameters. In contrast, biomarkers of endothelial function, nitric oxide, and nitric oxide endothelial synthase were positively related to cardiac vagal control parameters, suggesting that there is a relationship between inflammation, endothelial dysfunction, and cardiac autonomic dysfunction in DM type 2 [33]. Early investigation of these reported biomarkers is important in interfering with the prognosis of CAN.

The profiles of non-coding long RNAs (lncRNAs) related to inflammation were demonstrated to be co-expressed with messenger RNA (mRNA) in cervical ganglia after lesion due to DM [34]. The functional target genes of lncRNAs were identified, revealing that the genes interacted with lncRNAs and participate in various functions related to cervical sympathetic ganglia, such as immune response, cell migration, and chemotaxis, indicating

that lncRNAs could be potential target for treatment of diabetic patients with CAN or for diagnostic molecular markers.

Increased P2Y14 purinergic receptor expression is observed in DM, with consequent activation of satellite glial cells [35]. Treatment with short hairpin RNA (shRNA) P2Y14 or naringin reduced the overexpression, indicating that naringin may negatively regulate the expression of the P2Y14 receptor of glial cells in the upper cervical ganglia and can attenuate CAN. In addition, naringin shRNA also decreased changes in HR and blood pressure induced by DM and partially restored the low frequency/high frequency ratio that was increased. Partial recovery of the abnormal sympathetic nerve discharge was promoted via naringin shRNA treatment, which also normalized the levels of ROS and antioxidant factors in DM. In addition to this, the enzyme glucokinase (GCK) is overexpressed in ganglia and may be involved in diabetic cardiac sympathetic neuropathy mediated by the activation of P2X3 receptor. This role was confirmed through electrophysiological study in which the currents activated by the P2X3 agonist increased in ganglia neurons isolated and transfected with GCK plasmid [36]. To investigate the role of the P2X3 receptor in sympathetic nerve activity in diabetic cardiac autonomic neuropathy, shRNA was used, which led to attenuation of increased blood pressure and heart rate as well as normalized heart rate variability [37]. Furthermore, the administration of shRNA P2X3 reduced IL-1β and TNF-α levels in the ganglia and serum level of epinephrine and decreased the phosphorylation level of extracellular regulated proteins 1/2 (ERK1/2), suggesting that the P2X3 receptor could be a therapeutic target of diabetic cardiac autonomic neuropathy.

The increase in angiotensin II (Ang II) levels due to the high genic expression of the angiotensin-converting enzyme (ACE) associated with DM impairs autonomic function, intensifying sympathetic modulation of the heart and reducing its vagal modulation. DM induced in rats could promote significant reduction in HRV, sympathetic dominance, and increased HR and BP with increased cardiac hydroxylase tyrosine activity [38]. Apolipoprotein B, oxidative stress, and inflammatory markers were significantly reduced after treatment with vitamin C. In addition, administration of vitamin C in diabetic rats can restore HRV, suggesting that vitamin C can have effects on the improvement of diabetic CAN [38].

Lipid metabolites of the phosphatidylcholine and sphingomyelin classes were found at elevated plasma levels and linked to cardiac autonomic dysfunction in patients with recently diagnosed type 2 DM but not type 1 DM. This fact indicates that alteration of lipid metabolism occurs in the initial phase of diabetic CAN [39].

5. Alternative Treatment of DM-Cardiac Autonomic Neuropathy

Prevention of CAN includes the maintenance of controlled plasmatic glucose levels, treatment of risk factors regulating dyslipidemia and hypertension, and lifestyle intervention. The treatment of CAN relies on the relief of symptoms, but the high mortality can be explained by the imbalance in sympatovagal activity, damage of cardiac sympathetic innervation, impaired vasodilation of coronary arteries mediated by reduced sympathetic activity, deregulation of calcium mobilization, and inflammation [20] (Figure 3). Cardiovascular autonomic reflex tests, including the evaluation of autonomic response using alterations of HR and blood pressure, determine the progression of CAN [20].

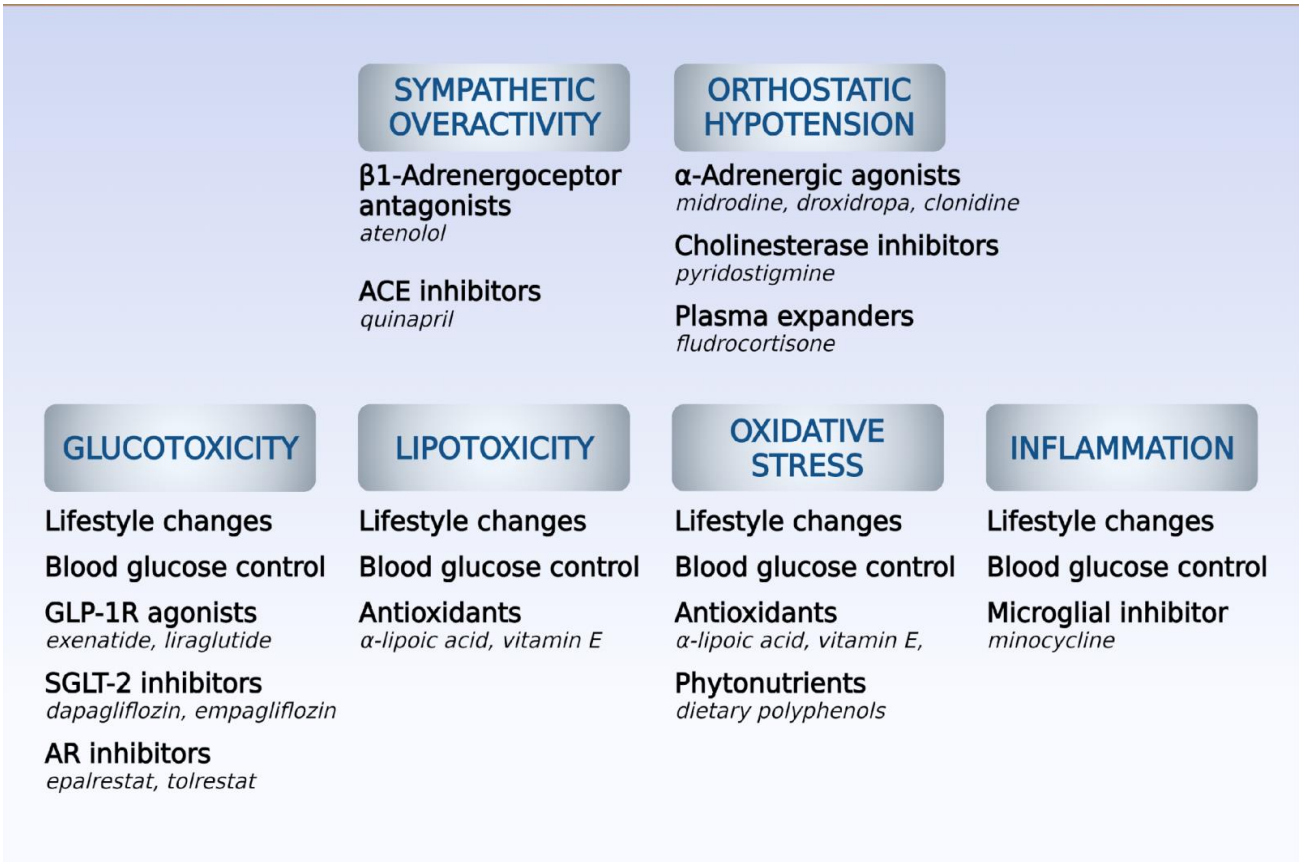

Figure 3. Pharmacological strategies for management of main causes and symptoms of diabetic cardiac autonomic neuropathy (DCAN). ACE, angiotensin-converting enzyme; GLP-1R, receptor for glucagon-like peptide-1; SGLT-2, sodium/glucose cotransporter 2; AR, aldose reductase. Source: Own authorship.

5.1. Symptomatic Treatment

The main non-pharmacological approach to treating DM consists of aerobic exercise and reductions in fat and carbohydrate intake. The Diabetes Prevention Program (DPP) study demonstrated beneficial effects of lifestyle intervention because of reductions in HR, HRV, and QT interval in diabetic patients [40], which could delay the appearance of cardiac complications. However, a study involving 25 non-diabetic patients with metabolic syndrome undergoing a 24-week lifestyle intervention showed a reduction in oxidative stress markers but no alteration in CAN indices [28]. Lifestyle change and exercise are generally indicated and contribute to the improvement of orthostatic hypotension associated with autonomic dysfunction [19,28]. Avoid use of tricyclic antidepressants, diuretics, and α-adrenoreceptor antagonists to reduce possible worsening of orthostatic hypotension. It is important to increase water consumption and the number of small meals and avoid abrupt changes in body posture. The resting tachycardia characteristic of the worsened stage of vagal dysfunction in CAN may be treated with cardioselective (i.e., beta-1) beta-adrenergic antagonists to improve vagal function [19,29,30,41]. As CAN progresses, reduced sympathetic response occurs and provokes orthostatic hypotension [20], which is treated with approved drugs targeted at primary or neurogenic orthostatic hypotension, such as droxidopa, midodrine, clonidine, pyridostigmine, and fludrocortisone. Midrodine, an alpha-1 adrenergic agonist is a vasopressor and fludrocortisone is a mineralocorticoid promoting increase of plasma volume, and both increase blood pressure in non-responsive patients to other therapy [15,30,31]. In advanced CAN, there is a denervated heart because of the abolished parasympathetic and sympathetic activities, with lack of HR change in response to exercise, stress, or sleep [31,42].

5.2. Disease Modifying Therapies

Moderate weight reduction associated with caloric restriction could improve autonomic cardiovascular modulation, sympathetic–vagal balance, and reduction of sympathetic tone in patients with metabolic syndrome or obesity [32,43]. The effects of 10% reduction in body mass in overweight or obese patients [33–37] improved autonomic status, HRV, and sympathetic–vagal balance.

Glycemia and blood pressure control are key factors in preventing CAN progression and should be addressed as main outcomes for therapy [15,31,38]. However, long-term therapy with metformin, an insulin sensitizer, was recently associated with CAN aggravation due to its interference in vitamin B12 absorption in diabetic patients. Vitamin supplementation is recommended for diabetic patients in biguanide therapy for over 5 years or with additional risk factors (advanced age, bariatric surgery, or anti-ulcer therapy) and may be combined with calcium supplementation [41].

Since DM promotes chronic inflammation with high levels of interleukin-6, which has been associated with reduced HRV; treatment with agonist of glucagon-like peptide-1 (GLP-1) has shown anti-inflammatory and neuroprotective effects and could result in the prevention of CAN. Treatment with metformin reduces vascular and systemic inflammation detected by the reduction of TNF-alpha level. Metformin not only reduces adipose tissue inflammation but also oxidative stress in myocardium through the activation of adenosine monophosphate-activated protein kinase. In addition to this, metformin reduces sympathetic predominance of CAN early stage [44,45].

GLP-1 receptor agonists cause weight-lowering and glycemic control effects, leading to a reduction in cardiovascular mortality [46]. However, despite preclinical evidence and reduced cardiovascular risk, short-term (3–18 months) therapy with GLP-1 agonists (exenatide 0.15–2.0 mg weekly or liraglutide 1.2–1.8 mg daily) does not improve cardiac autonomic function in diabetic patients but significantly increases HR [25,47].

Both sodium–glucose transporter-2 (SGLT-2) and angiotensin-converting enzyme (ACE) inhibitors promote preventive and therapeutic effects in attenuating diabetic cardiac dysautonomia [25,46–51]. Despite the lack of SGLT-2 in the heart, studies with gliflozins demonstrated a significant reduction in cardiovascular risk and deaths consequent of DM, which could result in part from the regulation of the autonomic nervous system through the inhibition of renal reabsorption of glucose [47,50,52]. Recently, the EMBODY trial indicated that medium-term (6 months) use of empagliflozin (10 mg p.o. daily) improved most heart rate variability indexes in type 2 diabetic patients taking beta blockers when compared to baseline measurements [47]. Although there is some remaining controversy, the effect of SGLT-2 inhibitors on cardiac autonomic tone is still the object of current research. Another SGLT-2 inhibitor, dapagliflozin, interferes with the cardiac autonomic function measurements (improved HRV) in patients with type 2 DM and cardiac autonomic neuropathy [53].

ACE inhibitor controls the systemic inflammation and oxidative stress because its effect of normalizing sympathetic activity. Carvedilol, a non-selective beta antagonist and alpha antagonist, promotes antioxidant activity and when in combination with ACE inhibitor produces vascular relaxation [19].

In a series of small trials in diabetic patients with CAN free of other cardiovascular disease, chronic oral treatment (3–12 months) with quinapril (20 mg daily) increased parasympathetic tone as measured via CARTs, spectral analysis of HR, and LF/HF ratio. Combination with losartan (100 mg daily) showed little further improvement, which suggested that an additional beta blockade by quinapril not seen in other ACE inhibitors could underlie the effect seen in autonomic control of HR [50]. Beta blockers also show some beneficial effects on cardiac autonomic function in diabetic patients with high cardiovascular risk, but the lack of solid evidence restricts their widespread use [47–49].

Antioxidants, which are scavengers of free radicals, can reduce the formation of ROS and consequently decrease orthostatic hypotension. Antioxidant therapy (alpha-lipoic acid, vitamin E) or C peptide is responsible for better prognosis for CAN. Alpha-lipoic

acid inhibits hexosamine and AGE pathways, while vitamins are immune stimulators and inhibitors of ROS-metabolite-induced DNA damage [19,47,48]. Attenuation of CAN progression through vitamin D supplementation shows a U-shaped dose–response relationship, and studies suggest that clinical benefit is achieved only for diabetic patients with insufficient serum levels (<50 nmol/L) [54]. Administration of minocycline—an inhibitor of microglial activation—was also investigated, and its use for 6 weeks demonstrated improvement of CAN in diabetic patients with good tolerability [48].

A systematic review [55] evidenced the beneficial effects of aldose reductase inhibitors in initial stages of CAN because they reduce the glucose used in polyol pathway and prevent the deleterious effects of reduced accumulated sorbitol and fructose in neuronal tissue. Oral treatment with epalrestat (50 mg tid) or tolrestat (200 mg qd) in diabetic patients with clinical CAN improved the HRV and postural BP and was devoid of interferences in glycemic control or adverse effects.

Administration of catechin, a phytonutrient of the polyphenol family, controlled body weight loss and reduced plasma glucose levels and cardiac hypertrophy in diabetic animals [31]. In addition, catechin reversed the increased level of MDA and the reduced levels of GSH, catalase, and SOD in the vagus nerve, indicating the contribution of this compound to the reduction of oxidative stress in the DM model. The reduction in Schwann cell proliferation, lymphocytic infiltration, axonal edema, and demyelization of the vagus nerve after catechin administration suggests that this polyphenol attenuated neural damage. Since catechin also improved hemodynamic parameters, it is a promising candidate in the treatment of cardiac diabetic autonomic neuropathy with focus on neural damage reduction.

It is crucial to diagnose and treat CAN early to reduce the morbidity and mortality associated with this chronic disease. For that reason, interventions to reduce adipose tissue inflammation are essential in retarding the progress of CAN.

6. Conclusions

CAN etiology is multifactorial and, despite being a common complication of DM, is still under-diagnosed, having a great impact on morbidity and prognosis. CAN is a microvascular complication, the development of which is associated with obesity, smoking, hypertension, and dyslipidemia. Chronic high glucose levels promote oxidative stress and inflammation, which are responsible for the vascular endothelial, cardiac, and neuronal damage. It is essential the prevention of CAN or early and adequate treatment because its progression is associated with the appearance of diabetic nephropathy. In addition to glucose and hyperlipidemia control combined with lifestyle modification, it is essential to interfere with vascular endothelial dysfunction and thrombosis and use specific treatment of orthostatic hypotension induced by oxidative and nitrosative stress. The complexity of CAN's pathophysiological mechanism contributes to the need to identify new treatment strategies.

Author Contributions: Conceptualization, S.Z.S., T.L.M., and G.Z.-S. Research, data curation, original draft preparation: S.Z.S., T.L.M., B.d.S.R., A.D.S., M.P.L.d.S., and G.Z.-S. Manuscript review, editing, supervision: M.P.L.d.S. and G.Z.-S. All authors have read and agreed to the published version of the manuscript.

Funding: This research was funded by Coordenação de Aperfeiçoamento de Pessoal de Nível Superior (CAPES), Conselho Nacional de Desenvolvimento Científico e Tecnológico (CNPq, #309498/2020-1), and Fundação de Amparo à Pesquisa do Estado do Rio de Janeiro (FAPERJ, #E-26/200.881/2021), and APC was funded by Fundação de Amparo à Pesquisa do Estado do Rio de Janeiro (FAPERJ, #E-26/211.114/2021).

Institutional Review Board Statement: Not applicable.

Informed Consent Statement: Not applicable.

Data Availability Statement: Not applicable.

Conflicts of Interest: The authors declare no conflict of interest.

References

1. Saely, C.H.; Drexel, H. Is Type 2 Diabetes Really a Coronary Heart Disease Risk Equivalent? *Vascul. Pharmacol.* **2013**, *59*, 11–18. [CrossRef] [PubMed]
2. World Health Organization. Diabetes. Available online: https://www.who.int/news-room/fact-sheets/detail/diabetes#:~{}:text=Key%20facts,stroke%20and%20lower%20limb%20amputation (accessed on 30 November 2022).
3. Lin, X.; Xu, Y.; Pan, X.; Xu, J.; Ding, Y.; Sun, X.; Song, X.; Ren, Y.; Shan, P.-F. Global, regional, and national burden and trend of diabetes in 195 countries and territories: An analysis from 1990 to 2025. *Sci. Rep.* **2020**, *10*, 14790. [CrossRef] [PubMed]
4. Pitocco, D.; Tesauro, M.; Alessandro, R.; Ghirlanda, G.; Cardillo, C. Oxidative Stress in Diabetes: Implications for Vascular and Other Complications. *Int. J. Mol. Sci.* **2013**, *14*, 21525–21550. [CrossRef] [PubMed]
5. Jia, G.; Whaley-Connell, A.; Sowers, J.R. Diabetic Cardiomyopathy: A Hyperglycaemia- and Insulin-Resistance-Induced Heart Disease. *Diabetologia* **2018**, *61*, 21–28. [CrossRef]
6. Dillmann, W.H. Diabetic Cardiomyopathy: What Is It and Can It Be Fixed? *Circ. Res.* **2019**, *124*, 1160–1162. [CrossRef]
7. Jia, G.; DeMarco, V.G.; Sowers, J.R. Insulin Resistance and Hyperinsulinaemia in Diabetic Cardiomyopathy. *Nat. Rev. Endocrinol.* **2016**, *12*, 144–153. [CrossRef]
8. Matsuda, M.; Shimomura, I. Roles of Adiponectin and Oxidative Stress in Obesity-Associated Metabolic and Cardiovascular Diseases. *Rev. Endocr. Metab. Disord.* **2014**, *15*, 1–10. [CrossRef]
9. Volpe, C.M.; Villar-Delfino, P.H.; Anjos, P.M.; Nogueira-Machado, J.A. Cellular Death, Reactive Oxygen Species (ROS) and Diabetic Complications. *Cell. Death Dis.* **2018**, *9*, 119. [CrossRef]
10. Wautier, J.; Schmidt, A. Protein Glycation a Firm Link to Endothelial Cell Dysfunction. *Circ. Res.* **2004**, *95*, 233–238. [CrossRef]
11. Yan, L.-J. Pathogenesis of Chronic Hyperglycemia: From Reductive Stress to Oxidative Stress. *J. Diabetes Res.* **2014**, *2014*, 137919. [CrossRef]
12. Nishida, K.; Otsu, K. Inflammation and Metabolic Cardiomyopathy. *Cardiovasc. Res.* **2017**, *113*, 389–398. [CrossRef] [PubMed]
13. Nunes, S.; Soares, E.; Pereira, F.; Reis, F. The Role of Inflammation in Diabetic Cardiomyopathy. *Int. J. Interf. Cytokine Mediat. Res.* **2012**, *4*, 59–73. [CrossRef]
14. Williams, S.M.; Eleftheriadou, A.; Alam, U.; Cuthbertson, D.J.; Wilding, J.P.H. Cardiac Autonomic Neuropathy in Obesity, the Metabolic Syndrome and Prediabetes: A Narrative Review. *Diabetes Ther.* **2019**, *10*, 1995–2021. [CrossRef] [PubMed]
15. Murtaza, G.; Virk, H.U.H.; Khalid, M.; Lavie, C.J.; Ventura, H.; Mukherjee, D.; Ramu, V.; Bhogal, S.; Kumar, G.; Shanmugasundaram, M.; et al. Diabetic Cardiomyopathy—A Comprehensive Updated Review. *Prog. Cardiovasc. Dis.* **2019**, *62*, 315–326. [CrossRef]
16. Liu, L.; Wu, Q.; Yan, H.; Chen, B.; Zheng, X.; Zhou, Q. Association between Cardiac Autonomic Neuropathy and Coronary Artery Lesions in Patients with Type 2. *Diabetes Dis. Markers* **2020**, *2020*, 6659166. [CrossRef]
17. Nattero-Chávez, L.; López, S.R.; Díaz, S.A.; Ureña, M.G.; Fernández-Durán, E.; Escobar-Morreale, H.F.; Luque-Ramirez, M. Association of Cardiovascular Autonomic Dysfunction with Peripheral Arterial Stiffness in Patients with Type 1 Diabetes. *J. Clin. Endocrinol. Metab.* **2019**, *104*, 2675–2684. [CrossRef]
18. Spallone, V.; Ziegler, D.; Freeman, R.; Bernardi, L.; Frontoni, S.; Pop-Busui, R.; Stevens, M.; Kempler, P.; Hilsted, J.; Tesfaye, S.; et al. Cardiovascular Autonomic Neuropathy in Diabetes: Clinical Impact, Assessment, Diagnosis, and Management. *Diabetes Metab. Res. Rev.* **2011**, *27*, 639–653. [CrossRef]
19. Serhiyenko, V.A.; Serhiyenko, A.A. Cardiac Autonomic Neuropathy: Risk Factors, Diagnosis and Treatment. *World J. Diabetes* **2018**, *9*, 1–24. [CrossRef]
20. Spallone, V. Update on the Impact, Diagnosis and Management of Cardiovascular Autonomic Neuropathy in Diabetes: What Is Defined, What Is New, and What Is Unmet. *Diabetes Metab. J.* **2019**, *43*, 3–30. [CrossRef]
21. Agashe, S.; Petak, S. Cardiac Autonomic Neuropathy in Diabetes Mellitus. *Method. Debakey Cardiovasc. J.* **2018**, *14*, 251–256. [CrossRef]
22. Pop-Busui, R. Cardiac Autonomic Neuropathy in Diabetes: A Clinical Perspective. *Diabetes Care* **2010**, *33*, 434–441. [CrossRef] [PubMed]
23. Dutra-Marques, A.C.; Rodrigues, S.; Cepeda, F.X.; Toschi-Dias, E.; Rondon, E.; Carvalho, J.C.; Alves, M.J.N.N.; Braga, A.M.F.W.; Rondon, M.U.P.B.; Trombetta, I.C. Exaggerated Exercise Blood Pressure as a Marker of Baroreflex Dysfunction in Normotensive Metabolic Syndrome Patients. *Front. Neurosci.* **2021**, *15*, 680195. [CrossRef] [PubMed]
24. Solanki, J.D.; Basida, S.D.; Mehta, H.B.; Panjwani, S.J.; Gadhavi, B.P. Comparative Study of Cardiac Autonomic Status by Heart Rate Variability Between Under-Treatment Normotensive and Hypertensive Known Type 2 Diabetics. *Indian Heart J.* **2017**, *69*, 52–56. [CrossRef]
25. Greco, C.; Santi, D.; Brigante, G.; Pacchioni, C.; Simoni, M. Effect of the Glucagon-Like Peptide-1 Receptor Agonists on Autonomic Function in Subjects with Diabetes: A Systematic Review and Meta-Analysis. *Diabetes Metab. J.* **2022**, *46*, 901–911. [CrossRef]
26. Vinik, A.; Erbas, T.; Pfeifer, M.; Feldman, E.; Stevens, M.; Russell, J. Diabetic Autonomic Neuropathy. In *The Diabetes Mellitus Manual: A Primary Care Companion to Ellenberg and Rifkin's*, 6th ed.; Inzucchi, S.E., Ed.; McGraw Hill: New York, NY, USA, 2004.
27. Neki, N.S.; Ankur, J.; Rohit, B.; Mohit, M.; Vishvanath, C.; Harsh, K. Cardiovascular Autonomic Disturbances in Patients with Diabetes Mellitus. *World Heart J.* **2015**, *7*, 177–186.

28. Shrestha, B.; Nepal, B.; Shakya, Y.L.; Regmi, B. Life Style Factors Associated with the Risk of Type 2 Diabetes Mellitus. *Gd. Med. J.* **2019**, *1*, 77–83. [CrossRef]
29. Shah, M.S.; Brownlee, M. Molecular and Cellular Mechanisms of Cardiovascular Disorders in Diabetes. *Circ. Res.* **2016**, *118*, 1808–1829. [CrossRef]
30. Areti, A.; Yerra, V.G.; Komirishetty, P.; Kumar, A. Potential Therapeutic Benefits of Maintaining Mitochondrial Health in Peripheral Neuropathies. *Curr. Neuropharmacol.* **2016**, *14*, 593–609. [CrossRef] [PubMed]
31. Addepalli, V.; Suryavanshi, S.V. Catechin Attenuates Diabetic Autonomic Neuropathy in Streptozotocin Induced Diabetic Rats. *Biomed. Pharmacother.* **2018**, *108*, 1517–1523. [CrossRef]
32. Vinik, A.I.; Casellini, C.; Parson, H.K.; Colberg, S.R.; Nevoret, M.-L. Cardiac Autonomic Neuropathy in Diabetes: A Predictor of Cardiometabolic Events. *Front. Neurosci.* **2018**, *12*, 591. [CrossRef]
33. Bhati, P.; Shenoy, S.; Hussain, M.E. Exercise Training and Cardiac Autonomic Function in Type 2 Diabetes Mellitus: A Systematic Review. *Diabetes Metab. Syndr.* **2018**, *12*, 69–78. [CrossRef] [PubMed]
34. Li, G.; Sheng, X.; Xu, Y.; Jiang, H.; Zheng, C.; Guo, J.; Sun, S.; Yi, Z.; Qin, S.; Liu, S.; et al. Co-Expression Changes of LncRNAs and MRNAs in the Cervical Sympathetic Ganglia in Di-abetic Cardiac Autonomic Neuropathic Rats. *J. Neurosci. Res.* **2017**, *95*, 1690–1699. [CrossRef] [PubMed]
35. Tang, G.; Pi, L.; Guo, H.; Hu, Z.; Zhou, C.; Hu, Q.; Peng, H.; Xiao, Z.; Zhang, Z.; Wang, M.; et al. Naringin Relieves Diabetic Cardiac Autonomic Neuropathy Mediated by P2Y(14) Receptor in Superior Cervical Ganglion. *Front. Pharmacol.* **2022**, *13*, 873090. [CrossRef] [PubMed]
36. Xu, X.; Liu, B.; Yang, J.; Zou, Y.; Sun, M.; Li, Z.; Lin, L.; Yang, R.; Zou, L.; Li, G.; et al. Glucokinase in Stellate Ganglia Cooperates with P2X3 Receptor to Develop Cardiac Sympathetic Neuropathy in Type 2 Diabetes Rats. *Brain Res. Bull.* **2020**, *165*, 290–297. [CrossRef] [PubMed]
37. Sheng, X.; Dan, Y.; Dai, B.; Guo, J.; Ji, H.; Zhang, X.; Xie, Z.; Song, S.; Pan, Q.; Wang, J. Knockdown the P2X3 Receptor in the Stellate Ganglia of Rats Relieved the Diabetic Cardiac Autonomic Neuropathy. *Neurochem. Int.* **2018**, *120*, 206–212. [CrossRef]
38. Fabiyi-Edebor, T.D. Vitamin C Ameliorated Cardiac Autonomic Neuropathy in Type 2 Diabetic Rats. *World J. Diabetes* **2020**, *11*, 52–65. [CrossRef]
39. Ziegler, D.; Strom, A.; Straßburger, K.; Knebel, B.; Bönhof, G.J.; Kotzka, J.; Szendroedi, J.; Roden, M. Association of Car-diac Autonomic Dysfunction with Higher Levels of Plasma Lipid Metabolites in Recent-Onset Type 2 Diabetes. *Diabetologia* **2021**, *64*, 458–468. [CrossRef]
40. Carnethon, M.R.; Prineas, R.J.; Temprosa, M.; Zhang, Z.-M.; Uwaifo, G.; Molitch, M.E. The Association among Autonomic Nervous System Function, Incident Diabetes, and Intervention Arm in the Diabetes Prevention Program. *Diabetes Care* **2006**, *29*, 914–919. [CrossRef]
41. Bell, D.S.H. Metformin Induced Vitamin B12 Deficiency Can Cause or Worsen Distal Symmetrical, Autonomic and Cardiac Neuropathy in the Patient with Diabetes. *Diabetes Obes. Metab.* **2022**, *24*, 1423–1428. [CrossRef]
42. Fisher, V.L.; Tahrani, A.A. Cardiac Autonomic Neuropathy in Patients with Diabetes Mellitus: Current Perspectives. *Diabetes Metab. Syndr. Obes.* **2017**, *10*, 419–434. [CrossRef]
43. Achmad, C.; Lim, N.S.; Pramudyo, M.; Iqbal, M.; Karwiky, G.; Febrianora, M.; Natalia, N. Relation Between Glycemic Control and Cardiac Autonomic Neuropathy in Patients with Diabetes Mellitus Type 2. *Curr. Probl. Cardiol.* **2022**, 101135. [CrossRef] [PubMed]
44. Guarino, D.; Nannipieri, M.; Iervasi, G.; Taddei, S.; Bruno, R.M. The Role of the Autonomic Nervous System in the Pathophysiology of Obesity. *Front. Physiol.* **2017**, *8*, 665. [CrossRef] [PubMed]
45. Oliveira, P.W.C.; de Sousa, G.J.; Birocale, A.M.; Gouvêa, S.A.; de Figueiredo, S.G.; de Abreu, G.R.; Bissoli, N.S. Chronic Metformin Reduces Systemic and Local Inflammatory Proteins and Improves Hypertension-Related Cardiac Autonomic Dysfunction. *Nutr. Metab. Cardiovasc. Dis.* **2020**, *30*, 274–281. [CrossRef] [PubMed]
46. Brown, E.; Wilding, J.P.H.; Barber, T.M.; Alam, U.; Cuthbertson, D.J. Weight Loss Variability with SGLT2 Inhibitors and GLP-1 Receptor Agonists in Type 2 Diabetes Mellitus and Obesity: Mechanistic Possibilities. *Obes. Rev.* **2019**, *20*, 816–828. [CrossRef]
47. Spallone, V.; Valensi, P. SGLT2 Inhibitors and the Autonomic Nervous System in Diabetes: A Promising Challenge to Better Understand Multiple Target Improvement. *Diabetes Metab.* **2021**, *47*, 101224. [CrossRef]
48. Burakgazi, A.Z.; Almahameed, S. Cardiac Involvement in Peripheral Neuropathies. *J. Clin. Neuromuscul. Dis.* **2016**, *17*, 120–128. [CrossRef]
49. Ang, L.; Dillon, B.; Mizokami-Stout, K.; Pop-Busui, R. Cardiovascular Autonomic Neuropathy: A Silent Killer with Long Reach. *Auton. Neurosci.* **2020**, *225*, 102646. [CrossRef]
50. Didangelos, T.; Veves, A. Treatment of Diabetic Cardiovascular Autonomic, Peripheral and Painful Neuropathy. Focus on the Treatment of Cardiovascular Autonomic Neuropathy with ACE Inhibitors. *Curr. Vasc. Pharmacol.* **2020**, *18*, 158–171. [CrossRef]
51. Lopaschuk, G.D.; Verma, S. Mechanisms of Cardiovascular Benefits of Sodium Glucose Co-Transporter 2 (SGLT2) Inhibitors: A State-of-the-Art Review. *JACC Basic Transl. Sci.* **2020**, *5*, 632–644. [CrossRef]
52. Lim, V.G.; He, H.; Lachlan, T.; Ng, G.A.; Kyrou, I.; Randeva, H.S.; Osman, F. Impact of Sodium-Glucose Co-Transporter Inhibitors on Cardiac Autonomic Function and Mortality: No Time to Die. *Europace* **2022**, *24*, 1052–1057. [CrossRef]

53. Balcioglu, A.S.; Celik, E.; Sahin, M.; Gocer, K.; Aksu, E.; Aykan, A.C. Dapagliflozin Improves Cardiac Autonomic Func-tion Measures in Type 2 Diabetic Patients with Cardiac Autonomic Neuropathy. *Anatol. J. Cardiol.* **2022**, *26*, 832–840. [CrossRef] [PubMed]
54. Putz, Z.; Tordai, D.; Hajdú, N.; Vági, O.E.; Kempler, M.; Békeffy, M.; Körei, A.E.; Istenes, I.; Horváth, V.; Stoian, A.P.; et al. Vitamin D in the Prevention and Treatment of Diabetic Neuropathy. *Clin. Ther.* **2022**, *44*, 813–823. [CrossRef] [PubMed]
55. Hu, X.; Li, S.; Yang, G.; Liu, H.; Boden, G.; Li, L. Efficacy and Safety of Aldose Reductase Inhibitor for the Treatment of Diabetic Cardiovascular Autonomic Neuropathy: Systematic Review and Meta-Analysis. *PLoS ONE* **2014**, *9*, e87096. [CrossRef] [PubMed]

biomedicines

MDPI

Article

Incidence, Risk Factors and Clinical Implications of Glucose Metabolic Changes after Heart Transplant

Emanuele Durante-Mangoni [1,2,*], Domenico Iossa [1], Valeria Iorio [1], Irene Mattucci [1,3], Umberto Malgeri [1], Daniela Pinto [1], Roberto Andini [1], Ciro Maiello [3] and Rosa Zampino [1,4]

[1] Unit of Infectious and Transplant Medicine, AORN Ospedali dei Colli-Monaldi Hospital, Piazzale Ettore Ruggieri Snc, 80131 Naples, Italy
[2] Department of Precision Medicine, University of Campania 'Luigi Vanvitelli', 80138 Naples, Italy
[3] Unit of Heart Transplant, AORN Ospedali dei Colli-Monaldi Hospital, 80131 Naples, Italy
[4] Department of Advanced Medical and Surgical Sciences, University of Campania 'Luigi Vanvitelli', 80138 Naples, Italy
* Correspondence: emanuele.durante@unicampania.it; Tel.: +39-081-706-2475 or +39-081-706-4153

Abstract: Diabetes mellitus (DM) arising *de novo* after transplant is a common complication, sharing many features with type 2 DM but also specific causes, such as administration of steroids and immunosuppressive drugs. Although post-transplant DM (PTDM) is generally assumed to worsen recipients' outcomes, its impact on renal function, cardiac allograft vasculopathy and mortality remains understudied in heart transplant (HT). We evaluated incidence and risk factors of PTDM and studied glucose metabolic alterations in relation to major HT outcomes. 119 subjects were included in this retrospective, single centre, observational study. A comprehensive assessment of glucose metabolic state was done pre-transplant and a median of 60 months [IQR 30–72] after transplant. Most patients were males (75.6%), with prior non-ischemic cardiomyopathy (64.7%) and median age of 58 years [IQR 48–63]. 14 patients developed PTDM, an incidence of 3.2 cases/100 patient-years. Patients with worsening glucose metabolic pattern were the only who showed a significant increase of BMI and metabolic syndrome prevalence after transplant. 23 (19.3%) patients died during follow up. Early mortality was lower in those with stably normal glucose metabolism, whereas improvement of glucose metabolic state favorably affected mid-term mortality (log-rank $p = 0.028$). No differences were observed regarding risk of infections and cancer. PTDM is common, but glucose metabolism may also improve after HT. PTDM is strictly related with BMI increase and metabolic syndrome development and may impact recipient survival.

Keywords: diabetes mellitus; transplant; complications; mortality; outcome; glucose metabolism; body mass index; metabolic syndrome

Citation: Durante-Mangoni, E.; Iossa, D.; Iorio, V.; Mattucci, I.; Malgeri, U.; Pinto, D.; Andini, R.; Maiello, C.; Zampino, R. Incidence, Risk Factors and Clinical Implications of Glucose Metabolic Changes after Heart Transplant. *Biomedicines* **2022**, *10*, 2704. https://doi.org/10.3390/biomedicines10112704

Academic Editors: Alfredo Caturano and Raffaele Galiero

Received: 29 August 2022
Accepted: 24 October 2022
Published: 26 October 2022

1. Introduction

Metabolic disorders, particularly diabetes mellitus (DM), are among the most common and serious complications observed in heart transplant (HT) recipients [1–3]. Often a pre-transplant comorbidity, DM arising *de novo* after transplant, previously referred to as *new onset diabetes after transplantation* [4], is now defined as *post-transplant diabetes mellitus* (PTDM). Specific criteria are in place to identify and classify the emergence of PTDM [2,5]. Absence of DM before transplant and HbA1c values defining DM have been added to the ADA criteria [6,7] for the diagnosis of PTDM.

PTDM prevalence ranged between 17% and 30% in recent studies [2,8–10]. PTDM shares with type 2 DM many common causes (age, body mass index [BMI], family history, metabolic syndrome, ethnicity) [2,11,12] but also presents specific, transplant-related causes, such as administration of steroids and different immunosuppressive drugs, including calcineurin inhibitors and m-TOR inhibitors [13–17].

Although PTDM can worsen the outcome of recipients over time, increasing their cardiovascular risk [1], available data did not show a clear association with Cardiac Allograft Vasculopathy (CAV) or other signs of graft dysfunction [18,19]. Also, most of the knowledge on PTDM comes from kidney transplant [20] and might not be entirely applicable to different organ transplant settings. Indeed, the incidence of PTDM appears to be highest in patients receiving lung and liver transplants, intermediate in recipients of heart transplants and lowest in recipients of kidney transplants, the latter being the most studied subgroup [20]. However, PTDM is associated to higher mortality regardless of the organ being transplanted (kidney, liver, lung or heart) [21–24]. In contrast with what was observed in other transplant recipients, no specific cardiac disease has been considered as a risk factor for the development of PTDM [25]. The evaluation of glucose metabolic changes not fulfilling a formal PTDM diagnosis could also provide interesting clinical insights on cardiovascular risk and metabolic derangement after HT.

Accordingly, aims of the present study were: (i) to describe changes in glucose metabolism after HT in a large cohort of HT recipients; (ii) to evaluate the incidence and risk factors of pre-diabetes and/or PTDM in the study group; (iii) to relate glucose metabolic alterations to HT outcomes.

2. Patients and Methods

2.1. Study Design

This is a retrospective observational study aimed to detect incidence of and risk factors for PTDM in a single center cohort of HT recipients. PTDM diagnosis was made according to the current International Guidelines [ADA, Chowdry] where PTDM diagnosis is based on the same criteria of DM diagnosis in the general population.

Patients who had received HT between January 2008 and December 2017 at the Monaldi Hospital, Naples, were included in the study. Recipients of emergency transplants, for whom a specific pre-transplant evaluation was not available, were excluded.

Retrospective data collection from heart transplant recipients' electronic records was approved by the University of Campania and AORN OspedalideiColli Ethics Committee (protocol n. 28/2019). Patient informed consent was waived.

2.2. Pre-Transplant Assessment

A comprehensive pre-transplant screening was performed, according to a predefined clinical protocol in use in our centre. It included collection of clinical history data, a general physical examination, and hematochemical and imaging studies.

For each patient, we collected and stored in an electronic database age, sex, current drug therapy, arterial blood pressure, heart rate, body weight, height and waist circumference. At history taking, we assessed the etiology of dilative cardiomyopathy, the presence of a positive family history of DM, the presence of atherosclerotic cardiovascular disorders/events, arterial hypertension and DM.

Systolic blood pressure was classified according to the ESC guidelines [26]. BMI, computed as the ratio between the body weight (in kilograms) and the square of the height (in meters), allowed patients' classification as underweight (<18.5 kg/m^2), normal (M: 18.5–24.9 kg/m^2; F: 18.5–23.9 kg/m^2), overweight (M: 25–29.9 kg/m^2; F: 24–29.9 kg/m^2), and obese: 1st degree (30–34.9 kg/m^2), 2nd degree (35–39.9 kg/m^2), 3rd degree obesity ($\geq$40 kg/m^2). Waist circumference (WC) was measured and used as an indicator of central/visceral adiposity. In particular, as all patients studied were of European descent, a WC >88 cm and >102 cm among women and men, respectively, were considered as visceral obesity diagnostic cut-offs. Furthermore, presence of Metabolic Syndrome (MetS) was defined for each patient, according to ATP III criteria [27].

Among hematochemical parameters, all measured by our hospital central laboratory with standard techniques, we considered: fasting glycemia, glycated hemoglobin (HbA1c), LDL, HDL and total cholesterol, and triglycerides. Creatinine was measured and used to assess the estimated glomerular filtration rate (eGFR) according to the CDK-EPI formula.

Fasting glycemia values allowed an initial stratification of each subject in terms of possible presence of DM, impaired fasting glycemia, or normal glycemia. For fasting glycemia levels < 126 mg/dL and HbA1c <48 mmol/mol (<6.5%) with a negative DM clinical history and no anti-diabetic therapy, a standard oral glucose tolerance test (OGTT) was performed. A 2 h post-OGTT serum glucose range of 140–200 mg/dL identified impaired glucose tolerance, whilst glucose levels > 200 mg/dL were diagnostic of DM. Normal glucose tolerance was defined as a post-load glycemia value < 140 mg/dL.

2.3. Post-Transplant Evaluation

Patients who died during the same hospital admission when the transplantation procedure was performed were excluded from this study. Therefore, the study group involved only subjects who survived the initial hospitalization and returned as outpatients with a follow-up of at least 6 months. The maintenance immune suppressive protocol comprised a calcineurin inhibitor (either cyclosporine A or tacrolimus), an antiproliferative agent (either mycophenolate or everolimus) and prednisone, at a starting dose of 10 mg every 12 h, progressively tapered off by 2.5 mg every 4 weeks down to a flat dose of 5 mg/day life-long in the absence of specific complications. The dosage of immunosuppressive drugs was generally adapted on the bases of Therapeutic Drug Monitoring (TDM) and assessment of white blood cell counts.

Glycemic evaluation was performed every 1 to 3 months after transplant during routine outpatient assessments and irrespective of each subject clinical history. Prospective clinical and laboratory evaluations, aimed to completely reassess glucose metabolism, body composition and metabolic syndrome components, were repeated once in each transplant recipient after a median of 60 months after transplant. Measured parameters were: BMI, WC, hematochemical parameters (i.e., fasting glycemia, total cholesterol, LDL-cholesterol, HDL-cholesterol, triglycerides, and glycatedhaemoglobin). Furthermore, non-diabetic patients (fasting glycemia $\leq$ 126 mg/dL and HbA1c values $\leq$ 48 mmol/mol) underwent an OGTT to unmask possible, undiagnosed DM.

After the post-tx OGTT and by considering fasting glycemia values, patients were classified as normal, with impaired fasting glycemia, glucose intolerant or diabetics.

2.4. Study Outcomes

In order to study the effects of glucose metabolism alteration on HT outcomes we collected data about graft rejection (type, number of episodes), including development of graft coronary artery disease, i.e., chronic rejection. Being DM a major risk factor for kidney disease, we assessed the effect of PTDM on recipients' renal function. In light of the known effect of DM on immune function and cell proliferation, we assessed other important post-transplant outcomes, such as occurrence of infections (>6 months post-transplant) or CMV reactivation and development of malignancies. We finally assessed the relationship between PTDM and post-transplant mortality.

2.5. Statistical Analysis

Statistical analyses were performed by using SPSS software 23.0. A p-value ≤ 0.05 was considered to denote statistical significance of the differences. Numerical data are shown as median and interquartile range (IQR) or as mean $\pm$ standard deviation (DS), whilst categorical data as number and percent. The Fisher's exact test was used to evaluate differences in nominal variables between 2 or more groups; the Mann-Whitney U test to compare numerical variables between 2 distinct groups and the Kruskal Wallis test to evaluate more than two groups. Kaplan-Meir curves were constructed to compare survival between subgroups, and differences were assessed with the log-rank test. Logistic regression was used to analyse independent predictors of mortality.

3. Results

3.1. Clinical Characteristics of the Study Cohort

Table 1 shows the general characteristics of the 119 patients included in the study. Most were males (75.6%), with a median age equal to 58 years [IQR 48–63] at the post-transplant assessment. Evaluations were performed after a median interval of time after HT equal to 60 months [IQR 30–72], and always in the context of a phase of clinical stability in the outpatient setting. A family history of DM and cardiovascular disease was overall common.

Table 1. Clinical features of the study cohort (N = 119).

Parameter	
Age, yrs	58 [50–65]
Sex	
M	90 (75.6)
F	29 (24.4)
Donor age, yrs	36 [23–48]
Family history of DM	38 (31.9)
Family history of CV disease	69 (58)
Family history of arterial hypertension	26 (21.8)
Smoking	61 (51.3)
History of DM pre-transplant	17 (14.3)
History of arterial hypertension pre-transplant	35 (29.4)
Years from transplant	5 [2.5–6]
Creatinine, mg/dL	
pre-tx	1.1 [0.9–1.4]
post-tx	1.1 [0.9–1.5]
eGFR CDK-EPI, mL/min	
pre-tx	72.6 [57–90.3]
post-tx	68.6 [50.2–96.4]
Immune suppressing agents	
Cyclosporine A	88 (73.9)
Tacrolimus	30 (25.2)
Everolimus	43 (36.1)
Mycophenolate	73 (61.3)
Prednisone	99 (83.2)
Diuretics	
Furosemide	61 (51.3)
Mineralocorticoid receptor antagonists	38 (31.9)
Beta-blockers	88 (73.9)
Anti-platelet agents	100 (84)
Oral anticoagulants	12 (10.2)
Mortality	23 (19.3)
Pre-transplant cardiac parameters	
Ischemic heart disease pre-transplant	42 (35.3)
Serum NT-pro BNP, pg/mL	3198 [1453–5271]
Left ventricle ejection fraction, %	25 [20–30]
Left ventricle diameter in diastole, cm	6.7 [5.9–7.5]
Cardiac Index, L/min/m^2	2.1 [1.8–2.7]
Cardiac Output, L/min	3.9 [3.2–4.86]
Wedge pressure, mmHg	26 [18.75–31]
NYHA class	
I	0 (-)
II	20 (16.8)
III	78 (65.5)
IV	21 (17.6)

Data are expressed as number (percent) or median [interquartile range-IQR].

On past clinical history, non-ischemic dilative cardiomyopathy (64.7%) was the prevalent indication for transplant, with 35.3% of patients showing a prior ischemic heart disease.

Twenty-three (19.3%) patients died during the post-transplant follow up, with a median survival time equal to 24 months [IQR 9–72] in this subgroup.

Immunosuppression maintenance hinged on cyclosporine A in more than 75% of patients, alone (3 patients) or combined with mycophenolate mophetil (MMF) or everolimus. The other patients were treated with tacrolimus combined with MMF (Table 1). Cardiovascular drugs taken during the post-transplant follow-up are also presented in Table 1.

Table 2 summarizes the most important post-transplant outcomes. There was a high rate of infectious and neoplastic complications, and most patients were hypertensive after transplant.

Table 2. Post-transplant cardiovascular and non-cardiovascular outcomes.

Parameter	
Cardiac Allograft Vasculopathy	8 (6.8)
Number di cellular rejection episodes	
0	95 (80.5)
1	19 (16.1)
2	4 (3.4)
Neoplasia	20 (16.8)
Infections	64 (53.8)
Post-tx arterial hypertension	61 (51.3)
CMV infection	
No infection/low level replication	81 (68.1)
Clinically significant reactivation	37 (31.1)

Data are expressed as number (percent).

3.2. Anthropometric and Metabolic Changes after Heart Transplant

A comparison between metabolic parameters before and after HT is shown in Table 3. Despite of worsening anthropometric parameters, glucose metabolism overall improved. Specifically, after transplant, a significant reduction of IFG/IGF prevalence was observed and the number of patients showing a normal glucose profile increased (Table 3). In contrast, the prevalence of lipid metabolic changes significantly increased. MetS prevalence also rose, although not significantly (42.4% pre-transplant vs. 57.6% post-transplant; $p = 0.062$).

Table 3. Metabolic parameters before and after transplant.

Variables	Pre-Transplant		Post-Transplant		
	N, (%)	Median (IQR)	N, (%)	Median (IQR)	*p*
Body mass index, kg/m^2		24.9 [22–28]		25.2 [22.8–28.4]	0.022
Waist circumference, cm		98 [89–102]		102 [94–110]	0.001
Fasting glycemia, mg/dL		101 [88–122.5]	94	94 [88–108]	0.010
Glucose metabolic profile					
Normal	47 (39.5)		66 (55.5)		0.000
IFG/IGT	41 (34.5)		16 (13.4)		
Diabetes mellitus	31 (26.1)		37 (31.1)		
Cholesterol, mg/dL					
Total		153 [126–186]		184 [148–217]	0.000
HDL		43 [34.75–51]		54.5 [44–68]	0.000
LDL		93 [70.75–118]		100.5 [74.7–123.8]	0.737
Hypercholesterolemia	50 (43.5)		68 (57.1)		0.002
Triglycerides, mg/dL		95 [71–135]		151 [113–190]	0.000
Hypertriglyceridemia	26 (21.8)		62 (52.1)		0.000
Metabolic syndrome	39 (42.4)		53 (57.6)		0.062
eGFR (CKD-EPI), mL/min		72.6 [57–90.3]		68.6 [50.2–96.4]	0.276

Data are expressed as number (percent) or median [interquartile range-IQR].

Comparing glucose metabolic status case-by-case before and after HT, we detected 14 patients who developed *de novo* PTDM. Indeed, based on our observations, patients

with a pre-transplant normal glucose metabolism showed an incidence of PTDM equal to 3.2 cases/100 patient-years.

3.3. Relation of Glucose Metabolic Changes with Anthropometric and Metabolic Dysfunction

The comparison of pre- and post-transplant changes in glucose metabolism allowed us to divide patients into four subgroups. Group A: worsened, including PTDM development (N = 23); group B: improved (N = 31); group C: persistently normal glucose metabolism (N = 36); and group D: unchanged pre-diabetes/DM (N = 29). Table 4 shows the variations of metabolic parameters in these four groups. PTDM was treated with diet in all patients. In addition, oral antidiabetics (metformin, gliclazide or repaglinide) were prescribed to 21 patients, whereas insulin was administered to 15 patients, as clinically indicated.

No significant differences between the 4 groups were observed in terms of age ($p = 0.068$), heart disease etiology ($p = 0.172$) and median duration of follow-up ($p = 0.793$) (data not shown). Also, immune suppressive treatment as well as use of prednisone did not differ. Immune suppressive drug regimens in use in the 4 subgroups of patients are detailed in Supplementary Table S1. As shown, there were no significant differences across subgroups.

HDL cholesterol and triglyceride levels increased significantly in all patients. Patients with worsening glucose metabolic pattern were the only who showed a significant increase of BMI and of MetS prevalence after HT (Figure 1). LDL cholesterol did not show significant changes. Median BMI was also significantly higher in patients with worsening or stably abnormal glucose metabolism (groups A and D) compared with counterparts (groups B and C) at both pre- and post-transplant time points (data not shown).

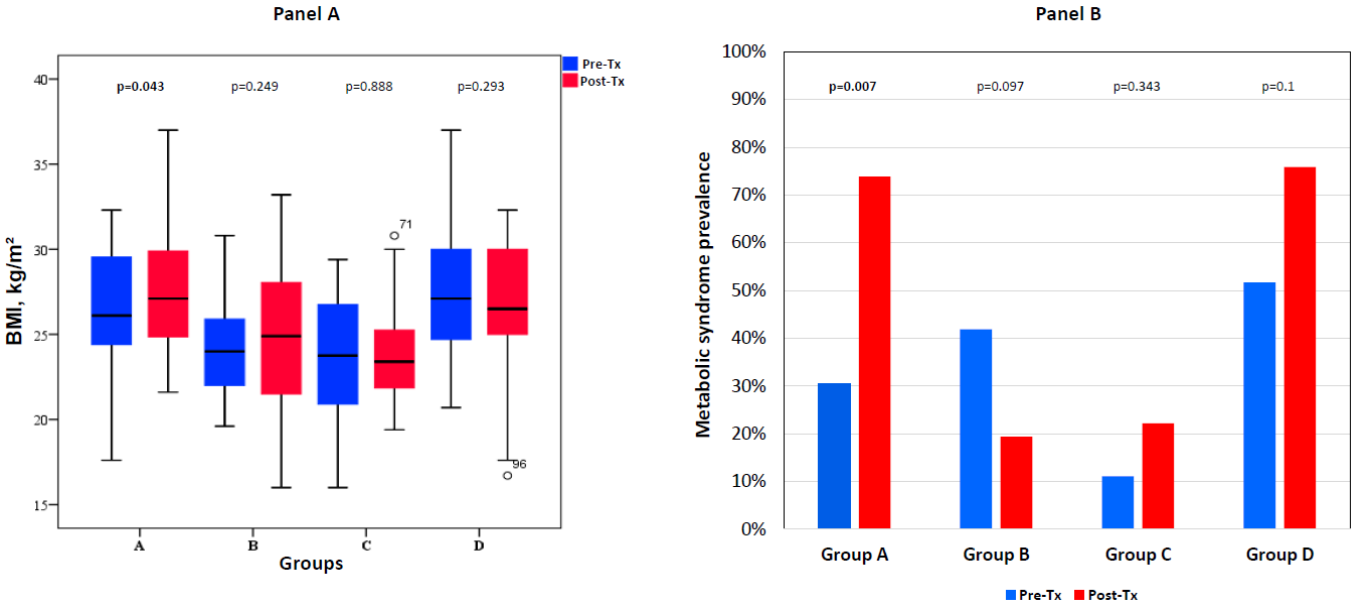

Figure 1. Changes in body mass index (BMI) [Panel A] and in metabolic syndrome prevalence [Panel B] from pre-transplant to post-transplant assessment in patients grouped according to changes in glucose metabolic state. Group A: worsened, including PTDM (N = 23); group B: improved (N = 31); group C: persistently normal glucose metabolism (N = 36); group D: unchanged pre-diabetes/DM (N = 29).

Changes in glucose metabolic state also appeared to associate with the post-transplant dynamics of renal function. Indeed, as graphically shown in Figure 2, the eGFR showed a trend for a decrease in group A (worsening glucose metabolism) and group D (persistently altered glucose metabolism), while eGFR remained stable in groups B (improving) and C (stably normal).

Table 4. Metabolic data before and after heart transplant in patients grouped according to changes in glucose metabolism.

	Group A, Worsened (N = 23)			**Group B, Improved (N = 31)**			**Group C, Stably Normal (N = 36)**			**Group D, Stably Abnormal (N = 29)**		
Variables	**Pre-tx**	**Post-tx**		**Pre-tx**	**Post-tx**		**Pre-tx**	**Post-tx**		**Pre-tx**	**Post-tx**	
			p			*p*			*p*			*p*
Glycemia, mg/dL	112.5 [92–121]	111 [105–124]	0.107	105 [100–123]	91 [85–95]	**0.000**	87 [83.5–92]	88.5 [82.2–94]	0.604	129 [104–157]	108 [95.5–145.5]	0.104
Cholesterol, mg/dL	176 [154–212]	210 [167.2–256.2]	0.692	153 [124–187]	180 [157–214]	**0.015**	144.5 [122.5–167.2]	173.5 [141.5–224]	**0.005**	147 [120.5–182]	177 [150–224]	0.107
Total	111.5 [90–147.3]	105.3 [76–124.7]	0.093	97 [71.5–116]	103.6 [68.4–125.2]	0.290	87 [66–114]	97.6 [71.9–122.9]	0.523	96.1 [56.7–118]	92.6 [77.2–129]	0.881
LDL	44 [37–54.7]	52.5 [44–65.7]	**0.035**	44 [35.5–50.5]	53 [42.5–67.5]	**0.004**	44 [35–56]	57 [46.2–67.7]	**0.002**	38 [30.5–48]	53 [42–74]	**0.003**
HDL												
Hypercholesterolemia	9 (42.9)	17 (81)	0.422	17 (54.8)	19 (61.3)	**0.012**	7 (20.6)	13 (38.2)	0.387	17 (58.6)	17 (58.6)	0.471
Triglycerides, mg/dL	103.5 [73.2–168.7]	172 [123–255]	**0.023**	97 [61–151]	152 [104–190]	**0.002**	82.5 [68.2–125]	124.5 [90.2–190.2]	**0.003**	101 [82.5–143.5]	156 [123.5–187]	**0.001**
Hypertriglyceridemia	7 (30.4)	12 (52.2)	0.752	8 (25.8)	17 (54.8)	0.698	5 (13.9)	16 (44.4)	0.085	6 (20.7)	17 (58.6)	0.669
BMI, kg/m^2	26.1 [24.3–30]	26.5 [24.9–30]	**0.043**	24 [22–26.3]	24.1 [22–27]	0.249	23.7 [20.8–26.8]	23.6 [21–26.8]	0.888	27.1 [24.5–30]	27.3 [24.7–30]	0.293
Metabolic syndrome	7 (30.4)	17 (73.9)	**0.007**	13 (41.9)	6 (19.4)	0.097	4 (11.1)	8 (22.2)	0.343	15 (51.7)	22 (75.9)	0.100
eGFR(CKD-EPI), mL/min	80.1 [69.2–94.5]	68.6 [58.2–91.9]	0.128	67.2 [50.2–87.4]	75.9 [52–99.2]	0.624	73.7 [61–90.6]	80.2 [44.2–98.9]	0.857	69 [50.3–87.9]	54.6 [44.4–77.6]	0.078
Arterial hypertension	6 (26.1)	12 (52.2)	0.130	11 (35.5)	16 (51.6)	0.306	7 (19.4)	12 (33.3)	0.285	11 (37.9)	21 (72.4)	**0.017**

Data are expressed as number (percent) or median [interquartile range-IQR].

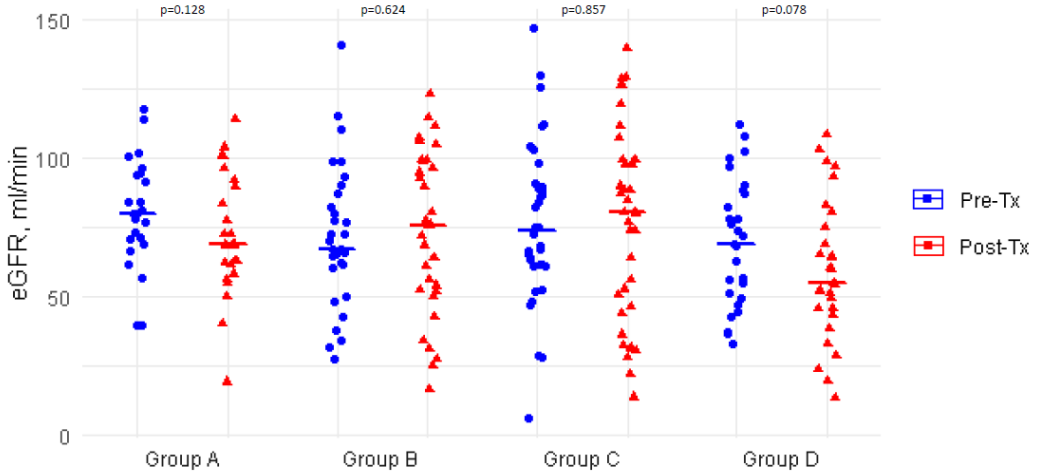

Figure 2. Column scatter plot showing changes in the estimated glomerular filtration rate from pre-transplant to post-transplant assessment in patients grouped according to changes in glucose metabolic state. Group A: worsened, including PTDM (N = 23); group B: improved (N = 31); group C: persistently normal glucose metabolism (N = 36); group D: unchanged pre-diabetes/DM (N = 29).

Mortality was significantly different according to post-transplant glucose metabolic changes. In particular, early mortality was lower in group C patients (stably normal), whereas improvement of glucose metabolic state after transplant (group B) favorably affected mid-term mortality, which was indeed better than in group D where glucose metabolism remained altered (log-rank $p = 0.028$; Figure 3). Survival in the overall study sample (all subgroups) was also analysed in a logistic regression model in relation to all major clinical risk factors before and after transplant, as well as all variables related to glucose metabolism (Supplementary Table S2). As shown, none of the evaluated factors was an independent predictor of mortality in the multivariable analysis.

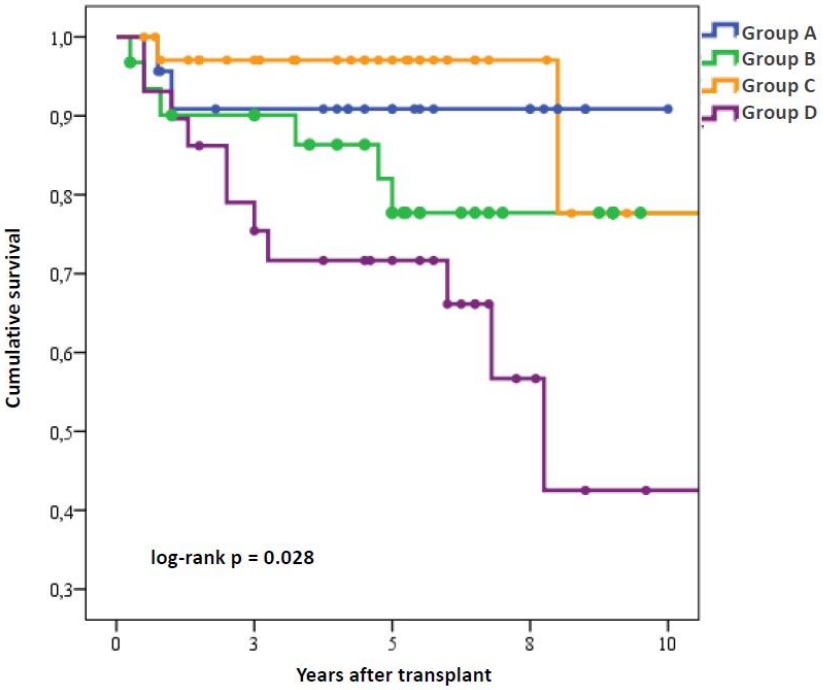

Figure 3. Kaplan-Meier survival curves of patients belonging to the 4 study subgroups: Group A: worsened, including PTDM (N = 23); group B: improved (N = 31); group C: persistently normal glucose metabolism (N = 36); group D: unchanged pre-diabetes/DM (N = 29).

No differences were observed across the 4 groups regarding risk of infections and cancer development (not shown).

4. Discussion

Since the update of criteria for PTDM diagnosis, little evidence was generated regarding PTDM after HT [5]. In our study, observed incidence was substantially lower than previously described [2,28–30]. Stringent exclusion of pre-transplant DM and of transient post-transplant hyperglycemia likely explain the difference. Also, our evaluations were done in stable patients while on maintenance immune suppression.

HT had a clear impact on recipients' metabolic function, associating with BMI increase, dyslipidemiam and raised MetS. In line with these data, overall DM prevalence slightly increased too. Interestingly, however, an association emerged between MetS and worsening glucose metabolism. Among patients who showed PTDM onset and any worsening of glycemic condition, a significant increase of BMI and MetS prevalence occurred, which was not observed in the other groups. This suggests that PTDM, or more broadly, glucose metabolic changes after HT are more likely linked to body composition changes rather than the effects of immune suppressive drugs. Indeed, in group B, showing improvement in glucose profiles, an inverse trend of reduction in MetS was observed.

Concurrent administration of multiple immune suppressors makes it difficult to analyse their possible role as inducers of glucose metabolic derangement [13–17]. PTDM pathophysiological mechanisms include factors that are specific to the post-transplant setting. Corticosteroids can promote PTDM through various mechanisms, inducing or worsening insulin resistance, increasing hepatic gluconeogenesis, reducing insulin secretion and, in the longer term, causing weight gain and visceral fat redistribution [2]. Calcineurin inhibitors reduce insulin secretion by acting on pancreatic beta cells, with tacrolimus showing a greater effect than cyclosporine [2,13]. Inhibitors of m-TOR, including everolimus, may also be implicated in the pathogenesis of PTDM, as they exert negative effects on both pancreatic beta cell function and insulin sensitivity [14–16]. In contrast, mycophenolic acid does not appear to affect glucose metabolism and the development of PTDM. Based on our data, we hypothesise immune suppressive agents increase overall recipient risk to develop glucose metabolic changes, with the latter manifesting phenotypically only among those characterised by an additional risk factor, e.g., when weight gain or development/worsening of MetS occurs. Immune suppressive treatment might therefore play a secondary/complementary role, as among our study subjects, these were homogeneously prescribed. Also, patient subgroups were consistent in terms of follow-up duration and, in turn, overall exposure to immune suppressive treatment.

Another interesting yet unexpected finding of our study was the positive effect HT had on glucose metabolism in a substantial subgroup of study subjects (N = 31, 26%—group B). Here, no weight gain and a trend for MetS prevalence reduction were observed. It is likely that these cases, previously affected by decompensated heart failure, recover metabolically as a consequence of improved functional capacity and more intense physical activity. Consistent with this hypothesis is the observed increase of HDL-cholesterol levels, observed in all groups, but less pronounced in those with worsening glucose metabolism. Unfortunately, we did not collect data regarding patient physical activity.

Our data suggest an impact of glucose metabolic changes on HT recipient outcomes. Diabetics who remain in this condition (group D) have a lower overall survival, whilst those showing persistently normal glucose status have the best outcome. Furthermore, an improved glucose metabolic state translates into a better mid-term survival. In contrast, and at variance with prior studies [18], there was no apparent association between PTDM or worsening glycemia and an increased occurrence of infections or malignancies.

Chronic kidney disease is a major issue in HT recipients. In our study, there were some clues to the association between this complication and a worse glucose metabolic state. Indeed, a trend for a greater reduction in the glomerular filtration rate was evident in group A, as well as in group D patients. In contrast, a role for PTDM and glucose metabolic

changes in the development of HT rejection and specifically cardiac allograft vasculopathy was not evident from this study, in line with prior data [19].

In conclusion, mechanisms underlying glucose metabolic changes after HT deserve further study. Our data suggest that avoidance of weight gain and MetS development could represent a viable strategy to prevent PTDM onset. This is likely pursued by low calorie diet and physical exercise throughout the post-transplant follow-up.

Supplementary Materials: The following supporting information can be downloaded at: https://www.mdpi.com/article/10.3390/biomedicines10112704/s1, Table S1: Immune suppressive drug regimens in use in the 4 subgroups of patients divided according to glucose metabolic changes before and after transplant; Table S2: Univariate and multivariable regression analysis of factors associated with mortality in the 119 patients studied.

Author Contributions: Conceptualization, E.D.-M. and D.I.; Methodology, C.M. and R.Z.; Formal Analysis, D.I., V.I. and E.D.-M.; Investigation, I.M., U.M., D.P., R.A.; Writing—Original Draft Preparation, V.I., D.I.; Writing—Review & Editing, E.D.-M.; Supervision, C.M. and R.Z.; Funding Acquisition, E.D.-M. All authors made contributions to the acquisition, analysis, and interpretation of data, and to the revision of the manuscript. All authors have read and agreed to the published version of the manuscript.

Funding: Research related to this paper was supported by the grant Ricerca di Ateneo 2015 to EDM.

Institutional Review Board Statement: Data collection from heart transplant recipients' electronic records was approved by the University of Campania and AORN Ospedali dei Colli Ethics Committee (protocol n. 28/2019).

Informed Consent Statement: Patient consent was waived due to retrospective nature of the study. All subjects gave their informed consent to all clinical procedures.

Data Availability Statement: Data are available from the corresponding author upon reasonable request.

Acknowledgments: We would like to thank Fabiana D'Amico for technical support.

Conflicts of Interest: The authors declare no conflict of interest related with the content of this article.

References

1. Khush, K.K.; Hsich, E.; Potena, L.; Cherikh, W.S.; Chambers, D.C.; Harhay, M.O.; Hayes, D.; Perch, M.; Sadavarte, A.; Toll, A.; et al. International Society for Heart and Lung Transplantation. The International Thoracic Organ Transplant Registry of the International Society for Heart and Lung Transplantation: Thirty-eighth adult heart transplantation report—2021; Focus on recipient characteristics. *J. Heart Lung Transpl.* **2021**, *40*, 1035–1049. [CrossRef]
2. Ye, X.; Kuo, H.-T.; Sampaio, M.; Jiang, Y.; Reddy, P.; Bunnapradist, S. Risk factors for development of new onset diabetes mellitus in adult heart transplant recipients. *Transplantation* **2010**, *89*, 1526–1532. [CrossRef]
3. Munshi, V.N.; Saghafian, S.; Cook, C.B.; Eric Steidley, D.; Hardaway, B.; Chakkera, H.A. Incidence, Risk Factors, and Trends for Postheart Transplantation Diabetes Mellitus. *Am. J. Cardiol.* **2020**, *125*, 436–440. [CrossRef]
4. Davidson, J.; Wilkinson, A.; Dantal, J.; Dotta, F.; Haller, H.; HERNandez, D.O.; Kasiske, B.L.; Kiberd, B.; Krentz, A.; Legendre, C.; et al. New onset diabetes after transplantation: 2003 International Consensus Guidelines. *Transplantation* **2003**, *75*, SS1–SS24. [CrossRef]
5. Sharif, A.; Hecking, M.; De Vries, A.P.; Porrini, E.; Hornum, M.; Rasoul-Rockenschaub, S.; Berlakovich, G.; Krebs, M.; Kautzky-Willer, A.; Schernthaner, G.; et al. Proceedings from an international consensus meeting on post-transplantation diabetes mellitus: Recommendations and future directions. *Am. J. Transplant.* **2014**, *14*, 1992–2000. [CrossRef]
6. American Diabetes Association. Classification and Diagnosis of Diabetes: Standards of Medical Care in Diabetes-2020. *Diabetes Care* **2020**, *43* (Suppl. 1), S14–S31. [CrossRef]
7. Chowdhury, T.A.; Wahba, M.; Mallik, R.; Peracha, J.; Patel, D.; De, P.; Fogarty, D.; Frankel, A.; Karalliedde, J.; Mark, P.B.; et al. Association of British Clinical Diabetologists and Renal Association guidelines on the detection and management of diabetes post solid organ transplantation. *Diabet. Med.* **2021**, *38*, e14523. [CrossRef]
8. Dong, M.; Parsaik, A.K.; Eberhardt, N.L.; Basu, A.; Cosio, F.G.; Kudva, Y.C. Cellular and physiological mechanisms of new-onset diabetes mellitus after solid organ transplantation. *Diabet. Med.* **2012**, *29*, e1–e12. [CrossRef]
9. Sorice, G.P.; Di Pizio, L.; Sun, V.A.; Schirò, T.; Muscogiuri, G.; Mezza, T.; Cefalo, C.M.; Prioletta, A.; Pontecorvi, A.; Giaccari, A. Metabolic syndrome in transplant patients: An updating point of view. *Minerva Endocrinol.* **2012**, *37*, 211–220.
10. ISTAT. Years 2000–2016: The Diabetes in Italy. *Stat. Rep.* **2017**.

11. Bodziak, K.A.; Hricik, D.E. New-onset diabetes mellitus after solid organ transplantation. *Transpl. Int.* **2009**, *22*, 519–530. [CrossRef]
12. van Raalte, D.H.; Diamant, M. Steroid diabetes: From mechanism to treatment? *Neth. J. Med.* **2014**, *72*, 62–72.
13. Subramanian, S.; Trence, D.L. Immunosuppressive agents: Effects on glucose and lipid metabolism. *Endocrinol. Metab. Clin. N. Am.* **2007**, *36*, 891–905. [CrossRef]
14. Barlow, A.D.; Nicholson, M.L.; Herbert, T.P. Evidence for rapamycin toxicity in pancreatic β-cells and a review of the underlying molecular mechanisms. *Diabetes* **2013**, *62*, 2674–2682. [CrossRef]
15. Johnston, O.; Rose, C.L.; Webster, A.C.; Gill, J.S. Sirolimus Is Associated with New-Onset Diabetes in Kidney Transplant Recipients. *J. Am. Soc. Nephrol.* **2008**, *19*, 1411–1418. [CrossRef]
16. Murakami, N.; Riella, L.V.; Funakoshi, T. Risk of metabolic complications in kidney transplantation after conversion to mTOR inhibitor: A systematic review and meta-analysis. *Am. J. Transplant.* **2014**, *14*, 2317–2327. [CrossRef]
17. Pirsch, J.D.; Henning, A.K.; First, M.R.; Fitzsimmons, W.; Gaber, A.O.; Reisfield, R.; Shihab, F.; Woodle, E.S. New-Onset Diabetes After Transplantation: Results From a Double-Blind Early Corticosteroid Withdrawal Trial. *Am. J. Transplant.* **2015**, *15*, 1982–1990. [CrossRef]
18. Cho, M.S.; Choi, H.I.; Kim, I.O.; Jung, S.H.; Yun, T.J.; Lee, J.W.; Kim, M.S.; Kim, J.J. The clinical course and outcomes of post-transplantation diabetes mellitus after heart transplantation. *J. Korean Med. Sci.* **2012**, *27*, 1460–1467. [CrossRef]
19. Sobieszczańska-Małek, M.; Korewicki, J.; Komuda, K.; Karczmarz, M.; Szymańska, S.; Cicha-Mikołajczyk, A.; Bekta, P.; Parulski, A.; Pronicki, M.; Grajkowska, W.; et al. Heart Transplantation and Risk of Cardiac Vasculopathy Development: What Factors Are Important? *Ann. Transplant.* **2017**, *22*, 682–688. [CrossRef]
20. Jenssen, T.; Hartmann, A. Post-transplant diabetes mellitus in patients with solid organ transplants. *Nat. Rev. Endocrinol.* **2019**, *15*, 172–188. [CrossRef]
21. Valderhaug, T.G.; Hjelmesæth, J.; Hartmann, A.; Røislien, J.; Bergrem, H.A.; Leivestad, T.; Line, P.D.; Jenssen, T. The association of early posttransplant glucose levels with long-term mortality. *Diabetologia* **2011**, *54*, 1341–1349. [CrossRef]
22. Hackman, K.L.; Snell, G.I.; Bach, L.A. Poor glycemic control is associated with decreased survival in lung transplant recipients. *Transplantation* **2017**, *101*, 2200–2206. [CrossRef]
23. Roccaro, G.A.; Goldberg, D.S.; Hwang, W.T.; Judy, R.; Thomasson, A.; Kimmel, S.E.; Forde, K.A.; Lewis, J.D.; Yang, Y.X. Sustained posttransplantation diabetes is associated with long-term major cardiovascular events following liver transplantation. *Am. J. Transplant.* **2018**, *18*, 207–215. [CrossRef]
24. Dos Santos, Q.; Hornum, M.; Terrones-Campos, C.; Geisler Crone, C.; Wareham, N.E.; Soeborg, A.; Rasmussen, A.; Gustafsson, F.; Perch, M.; Soerensen, S.S.; et al. Posttransplantation Diabetes Mellitus Among Solid Organ Recipients in a Danish Cohort. *Transpl. Int.* **2022**, *35*, 10352. [CrossRef]
25. Kim, H.J.; Jung, S.H.; Kim, J.J.; Yun, T.J.; Kim, J.B.; Choo, S.J.; Chung, C.H.; Jae Won Lee, J.W. New-onset diabetes mellitus after heart transplantation- incidence, risk factors and impact on clinical outcome. *Circ. J.* **2017**, *81*, 806–814. [CrossRef]
26. Williams, B.; Mancia, G.; Spiering, W.; Agabiti Rosei, E.; Azizi, M.; Burnier, M.; Clement, D.L.; Coca, A.; De Simone, G.; Dominiczak, A.; et al. 2018 ESC/ESH Guidelines for the management of arterial hypertension: The Task Force for the management of arterial hypertension of the European Society of Cardiology and the European Society of Hypertension. *J. Hypertens.* **2018**, *36*, 1953–2041. [CrossRef]
27. Expert Panel on Detection, Evaluation, and Treatment of High Blood Cholesterol in Adults. Executive Summary of The Third Report of The National Cholesterol Education Program (NCEP) Expert Panel on Detection, Evaluation, and Treatment of High Blood Cholesterol in Adults (Adult Treatment Panel III). *JAMA* **2001**, *285*, 2486–2497. [CrossRef]
28. Saraiva, J.; Sola, E.; Prieto, D.; Antunes, M.J. Diabetes as an outcome predictor after heart transplantation. *Interact Cardiovasc. Thorac. Surg.* **2011**, *13*, 499–504. [CrossRef]
29. Marchetti, P. New onset diabetes after transplantation. *J. Heart Lung Transplant.* **2004**, *23* (Suppl. 5), S194–S201. [CrossRef]
30. Depczynski, B.; Daly, B.; Campbell, L.V.; Chisholm, D.J.; Keogh, A. Predicting the occurrence of diabetes mellitus in recipients of heart transplants. *Diabet. Med.* **2000**, *17*, 15–19. [CrossRef]

biomedicines

MDPI

Review

Role of the Endocannabinoid System in Metabolic Control Processes and in the Pathogenesis of Metabolic Syndrome: An Update

Gabriella Dörnyei [1], Zsolt Vass [1], Csilla Berta Juhász [1], György L. Nádasy [2], László Hunyady [2,3] and Mária Szekeres [1,2,*]

[1] Department of Morphology and Physiology, Faculty of Health Sciences, Semmelweis University, Vas Street 17, 1088 Budapest, Hungary
[2] Department of Physiology, Faculty of Medicine, Semmelweis University, Tűzoltó Street 37-47, 1094 Budapest, Hungary
[3] Institute of Enzymology, Eötvös Loránd Research Network, Research Centre for Natural Sciences, Piarista Street 4, 1052 Budapest, Hungary
* Correspondence: szekeres.maria@med.semmelweis-univ.hu

Abstract: Metabolic syndrome is a complex disease state, which appears mostly as a consequence of an unhealthy, sedentary lifestyle. Metabolic complications include insulin resistance (IR), diabetes, dyslipidemia, hypertension, and atherosclerosis, impairing life standards and reducing life expectancy. The endocannabinoid system (ECS) has an important role in signalization processes, not only in the central nervous system, but also in the peripheral tissues. Several physiological functions are affected, and overexpression or downregulation contributes to several diseases. A better understanding of the functions of cannabinoid (CB) receptors may propose potential therapeutic effects by influencing receptor signaling and enzymes involved in downstream pathways. In this review, we summarize recent information regarding the roles of the ECS and the CB_1 receptor signaling in the physiology and pathophysiology of energy and metabolic homeostasis, in the development of obesity by enhancing food intake, upregulating energy balance and fat accumulation, increasing lipogenesis and glucose production, and impairing insulin sensitivity and secretion. By analyzing the roles of the ECS in physiological and pathophysiological mechanisms, we introduce some recently identified signaling pathways in the mechanism of the pathogenesis of metabolic syndrome. Our review emphasizes that the presence of such recently identified ECS signaling steps raises new therapeutic potential in the treatment of complex metabolic diseases such as diabetes, insulin resistance, obesity, and hypertension.

Keywords: endocannabinoid system; CB_1 cannabinoid receptor; diabetes; metabolic disease; metabolic syndrome

Citation: Dörnyei, G.; Vass, Z.; Juhász, C.B.; Nádasy, G.L.; Hunyady, L.; Szekeres, M. Role of the Endocannabinoid System in Metabolic Control Processes and in the Pathogenesis of Metabolic Syndrome: An Update. *Biomedicines* **2023**, *11*, 306. https://doi.org/10.3390/biomedicines11020306

Academic Editors: Alfredo Caturano and Raffaele Galiero

Received: 14 December 2022
Revised: 14 January 2023
Accepted: 18 January 2023
Published: 21 January 2023

1. Introduction

Obesity and concomitant diseases such as diabetes, atherosclerosis, and other cardiovascular diseases (CVDs), as well as their consequences, now comprise a worldwide problem representing the highest entries in mortality statistics. The term metabolic syndrome has been introduced as a complex metabolic disorder accompanied by obesity and multiple cardiovascular risk factors for chronic diseases such as atherosclerosis, hypertension, and diabetes mellitus. The development of metabolic syndrome and metabolic pathologic disorders can be attributed to lifestyle, environmental, and genetic factors. A sedentary lifestyle and an unhealthy diet are the most obvious reasons [1–8].

It has been revealed that the endocannabinoid system (ECS) plays an important role in several physiologic regulatory mechanisms. Cannabinoid receptors were first identified in the nervous system as contributing to retrograde synaptic signaling [9,10]. Since then, the role of cannabinoid receptors has also been revealed in several tissues, such as in

the cardiovascular, endocrine, and gastrointestinal systems [2,11]. Among their multiple roles, ECS and cannabinoid receptor signaling also play a regulatory role in food intake and energy metabolism. Activation of the cannabinoid type 1 receptor (CB_1R) signaling pathway may upregulate food uptake, while inhibition of ECS signaling may depress food uptake mechanisms to develop weight loss [6,12,13]. Other studies have demonstrated a significant role of the ECS in lipid homeostasis [14–16]. Thus, investigation of the specific role of the ECS and cannabinoid signaling mechanisms can reveal important means for future therapeutic interventions.

Based on previous observations, in the present review, we aimed to summarize novel ECS signaling mechanisms with promising potential in the treatment of complex metabolic diseases such as diabetes, insulin resistance (IR), obesity, and hypertension.

2. Metabolic Syndrome

Metabolic syndrome, as a complex disorder, involves the disturbance of glucose metabolism, dyslipidemias, central obesity, and elevated blood pressure, promoting further cardiovascular morbidities such as atherosclerosis [2–8,17–20]. An earlier term has also been used, "syndrome X" or IR syndrome with hyperinsulinemia [6,17,21]. Clinical and metabolic studies have revealed the link between IR/hyperinsulinemia with dyslipidemia, elevations in triglyceride (TG) levels, reduced high-density lipoprotein (HDL), and elevated low-density lipoprotein (LDL) and total cholesterol levels. These in turn contribute to cardiovascular pathologies such as hypertension and atherosclerosis. Cardiovascular risk factors, which frequently occur in obesity and metabolic syndrome in populations of middle-aged adults independently of age, gender, ethnicity, and body mass index (BMI), include elevated TGs, low HDL cholesterol, and elevated LDL cholesterol [5,6,11,17,18,21]. According to previous observations, metabolic syndrome often involves the following components: high fasting glucose, IR with hyperinsulinemia, dyslipidemia, high blood pressure, and high BMI [3,5,6,19].

Obesity and Insulin Resistance

Obesity often accompanies metabolic syndrome. An unhealthy diet (Western-type diet) in combination with a sedentary (inactive) lifestyle promotes the development of obesity and other symptoms of metabolic syndrome. The extent of obesity is often measured with BMI [1,5,6,11,22].

Obesity is often accompanied by IR, hyperinsulinemia, and dyslipidemia, which constitute further risks for CVDs. Neurohumoral activation also plays a role in the pathogenesis of obesity and metabolic syndrome through the production of adipokines such as adiponectin and leptin. Leptin produced by adipose tissue regulates hypothalamic appetite control mechanisms involving feeding behavior and hunger. Adiponectin is an anti-inflammatory hormone considered to be a protective factor against diabetes and IR. Obesity increases leptin levels and reduces adiponectin production, activating the renin–angiotensin system and inflammatory pathways such as TNF-α and NF-$_K$B [6,23,24]. Visceral obesity, IR, and activation of neuroendocrine and inflammatory metabolites induce a metabolic inflammatory state, which leads to the development of complex metabolic disease with further cardiovascular risks [6,18,25]. The role of the opioid system in the development of obesity has also been described [26]. Infusions of beta-endorphins increased plasma levels of the pancreatic hormones insulin, C peptide, and glucagon and also elevated plasma glucose levels in young patients with obese relatives, which suggests the involvement of opioid peptides in metabolic events related to obesity [26].

Obesity and IR often develop into type 2 (non-insulin-dependent) diabetes (T2D). Patients diagnosed as type 2 diabetics are treated with antidiabetic drugs; in serious cases, they also may receive insulin. Among the prescriptions of treatment, it is important to improve patients' lifestyle, maintain a special diet and perform regular activities. Type 2 diabetes (contrary to type 1) is often accompanied by obesity and metabolic syndrome. Thus,

by organizing a healthy lifestyle and nutrition, progression of the disease and worsening of the condition of the patient can be prevented [3,6,14,15,18].

3. Endocannabinoid System and Its Physiological Roles

It is known that endogenously produced cannabinoids exert their physiological role by activating cannabinoid receptors. Cannabinoid receptors were originally named after their affinity for 9-tetrahydrocannabinol (THC), the main active ingredient of the extracts of *Cannabis sativa*. Endocannabinoids (eCBs) serve as endogenous ligands for cannabinoid receptors and participate in tissue-specific paracrine regulatory mechanisms first discovered in the nervous system [9,27]. The components of the ECS are the endocannabinoids, their receptors and intracellular signaling pathways, and enzymes that modulate their production and degradation [15,28–31]. The most important endocannabinoids can be listed as arachidonoyl ethanolamide (anandamide (AEA)), 2-arachidonoylglycerol (2-AG), noladin ether, O-arachidonoyl ethanolamine (virodhamine), and N-arachidonoyl dopamine [28,31–33]. AEA was isolated from pig brain tissue in 1992 by Devan [34]; later, 2-AG was discovered [35]. Production of 2-AG endocannabinoid is catalyzed by diacylglycerol (DAG) lipase (DAGL), and its degradation is due to monoacylglycerol (MAG) lipase (MAGL). Degradation of AEA is catalyzed by fatty acid amide hydrolase (FAAH) [11,31].

Endocannabinoids exert their actions on cannabinoid receptors. These include CB_1Rs, which are characteristically present in neural tissues, and type 2 cannabinoid receptors (CB_2R), which occur mostly in immune cells [9]. Cannabinoid receptors belong to the G-protein-coupled receptor (GPCR) family [28]. Cannabinoid-binding receptors were first characterized from brain tissue [34,36]. Since then, in addition to CB_1Rs and CB_2Rs, some other receptors have also been identified to respond to cannabinoid stimuli, such as GPR55 and $TRPV_1$ [2,11,37]. CB_1Rs are characteristically present in the central nervous system (CNS), typically with presynaptic neuronal location modulating the synaptic transmission [9,28]. During neuronal stimulation by neurotransmitters such as glutamate and acetylcholine, endocannabinoid-mediated CB_1R presynaptic activation mediates the important function of depolarization-induced retrograde synaptic inhibition [9]. Signal transduction of CB_1Rs is through heterotrimeric G proteins of the $G_{i/o}$ type, inhibiting adenylyl cyclase and thus regulating calcium and potassium channels. In the case of depolarizing neurotransmitters (e.g., glutamate, acetylcholine), the concomitant release of endocannabinoids during cell signaling and the modulation of ionic channel activity will be an important neuromodulator action [30,38,39]. Several endocannabinoid compounds have been identified until now, including AEA and 2-AG [9,28,30]. 2-AG production has also been detected in the vascular smooth muscle cells of rat aorta [30,35]. AEA is a partial agonist of CB_1Rs and has less affinity to CB_2Rs, while 2-AG has been shown to have an affinity to both cannabinoid receptor subtypes [28,34,35]. CB_2Rs have been found most of all on the immune cells and peripheral nerve endings controlling inflammatory and immune processes. They have been found to be located in the spleen, tonsils, and in hematopoietic tissues, as well as in cardiac and vascular tissues [2,11,32].

In addition to the earlier recognized key functions of endocannabinoids in the CNS, their roles in peripheral tissues have also raised interest [9,19,28,30,40–42]. It has been shown that the cannabinoid system plays a role in several important physiological mechanisms, in the field of cardiovascular, inflammatory, gastrointestinal, and endocrine regulations [19,28,30,40,43]. What is important now for us, their role in metabolic control processes, energy balance, and appetite regulation has been proven [44,45]. For a better understanding of the events in metabolic syndrome, we have to take into consideration the direct cardiovascular effects of endocannabinoids: negative inotropic, vasodilatator, and hypotensive actions have been reported [19,30,46,47]. With the growing number of studies on compounds modulating the ECS, new therapies for frequently combined metabolic–cardiovascular disorders appear on the horizon [11,43,46].

Physiological Roles of CB_1 Cannabinoid Receptors

CB_1R was first discovered by its role in the CNS [36] and has been described to participate in retrograde synaptic signaling [9,10]. Later on, CB_1Rs were detected in other tissues, such as in the peripheral nervous system, in the endothelium, and smooth muscle cells of vascular tissue; in fat tissue; in splanchnic organs; in the liver; and in skeletal muscle tissue as well [19,28,30,38,40,48]. There is growing evidence that endocannabinoids via CB_1R play a role in a variety of physiological functions, such as maintenance of homeostasis and controlling the functions of several organs, such as vasoregulation, cardiac function, gastrointestinal and endocrine functions, energy metabolism, and appetite [19,28,30,40,43,46,47,49,50]. CB_1R function can be activated by agonists and synthetic agonists, such as THC, WIN 55212, and HU210, and inhibition can be achieved by selective CB_1R antagonists such as SR141716 (rimonabant), inverse agonist AM251, or neutral antagonist O2050 [11,28,30,40,47,49,51]. Activation of CB_1R produces acute and chronic effects in tissues. In the cardiovascular system, vasodilation and cardiac depression with hypotensive action have been observed [11,49]. It has been reported previously in cell-expressing systems that activation of certain GPCRs such as the type 1 angiotensin receptor (AT_1R) and calcium signaling may activate the DAGL enzyme to release 2-AG, which further mediates the paracrine transactivation of CB_1Rs [40,42]. Angiotensin II (Ang II)-induced CB_1R coactivation was inhibited by inhibitors of DAGL, which suggests that DAG generated from phosphoinositides during the AT_1R signaling pathway is converted to 2-AG by DAGL [41,42]. In concert with this observation, we have found that in vascular tissue, Ang II-induced vasoconstriction is augmented by inhibition of CB_1R and also of DAGL, whereas it is attenuated by inhibition of MAGL, suggesting that locally produced 2-AG activates vascular CB_1Rs attenuating Ang II-induced vasoconstriction [30]. In recent studies, we have also found that endocannabinoid signaling moderates the tone of coronary arterioles [47,49]. CB_1R signaling mechanisms due to locally released endocannabinoids are also involved in several metabolic processes, such as lipogenesis and altered glucose homeostasis. CB_1R-induced lipogenesis is augmented in adipose tissue by stimulation of TG synthesis in the liver. Activation of CB_1R-signaling also augments plasma TG and total cholesterol levels with depression of HDL. Related to carbohydrate homeostasis, CB_1R activation can lead to gluconeogenesis, IR, and impaired glucose tolerance [2,11,15,52].

4. Role of Endocannabinoid System in the Metabolic Control Processes

The ECS has a significant role in several metabolic control processes. The ECS is present in the CNS, affecting appetite, food consumption, eating motivation, and energy homeostasis. The ECS can influence feeding control both in the CNS and in the periphery by influencing cell signaling pathways and the production and degradation of hormones and enzymes. The ECS promotes energy intake and storage, which favors overnutrition and the development of obesity and metabolic syndrome. The ECS and overactive cannabinoid CB_1R signaling promote overnutrition, increases lipogenesis, and the risk of obesity and metabolic syndrome, including IR and dyslipidemia [14–16,18,20,28,43,44].

4.1. Effects of Endocannabinoid System on Fat Metabolism

The ECS influences fat metabolism by stimulating lipogenesis [11,14,16,28,53,54]. Activation of CB_1R signaling stimulates lipogenesis and results in weight gain. Central CB_1Rs located in the hypothalamus and limbic system are involved in the regulation of feeding. The ECS has important physiological regulatory functions not only in the CNS, but also in the periphery. Endocannabinoids and CB_1R activation at the peripheral sites influence the metabolism of adipose tissue, liver, and skeletal muscle to promote lipogenesis. CB_1Rs are expressed in both adipocytes and in hepatocytes; their activation increases lipogenesis while decreasing fatty acid oxidation in adipose tissue and the liver. Thus, endocannabinoids by peripheral CB_1R activation contribute to diet-induced obesity and hepatic steatosis [11,28,51,54–56].

Endocannabinoid-induced lipogenesis involves several pathways. In hepatic tissue, endocannabinoids via the activation of CB_1R increase expression of the lipogenic transcription factor SREBP-1c and its target genes such as acetyl-CoA carboxylase-1 and fatty acid synthase [55]. Endocannabinoids and CB_1R activation also enhance preadipocyte maturation and trigger the peroxisome proliferator-activated receptor group, which in turn increases fat cell size and TG content by activation of TG synthesis from consumed fatty acids by inhibiting lipid breakdown and oxidation of fatty acids. Meanwhile, fatty-acid-synthesizing enzymes forming de novo fatty acids will be stimulated. Elevated 2-AG levels in skeletal muscle and adipose tissue cells activate CB_1Rs and induce lipogenesis, but on the other hand, anti-lipogenic pathways will also be activated via $TRPV_1$ receptors modulating visceral fat accumulation and adiponectin production [15]. Activation of CB_1Rs by CB_1R agonists increases lipogenesis in the liver also from non-fat-origin resources activating lipogenic enzymes in mice [56]. To prove the link between diet and the ECS, it was found that a high-fat diet (HFD) in mice increased endocannabinoid levels and expression of ECS enzymes in adipose tissue [57]. By detecting eCB levels in obese patients, it was found that although diet and obesity had no influence on eCB levels, expression of DAGL was upregulated, while mRNA expressions of MAGL and FAAH were downregulated in subcutaneous adipose tissue. However, interestingly, dietary fat intake reduced skeletal muscle CB_1R and MAGL mRNA expressions, suggesting that a HFD influences ECS expression with tissue specificity [58].

4.2. Effects of Endocannabinoid System on Hunger and Appetite

Endocannabinoids and their receptors are involved at multiple levels in the control of energy homeostasis, food intake, and appetite by stimulating orexigenic pathways in the hypothalamus [6,11,51]. Endocannabinoids are orexigenic mediators and are part of the leptin-regulated central neural circuits that control energy intake [51]. Endocannabinoids via CB_1R activation modulate the activity of hypothalamic neurons and the release of orexigenic and anorexigenic neuropeptides regulating energy metabolism to stimulate hunger [6,16,50,59,60]. These actions are mediated partly by leptin and ghrelin pathways, which modulate hypothalamic eCB levels. These pathways become deregulated during obesity with elevated hypothalamic eCB tone [6,16,61,62].

In some countries, cannabis-based drugs were used for improving appetite, mood, and ameliorating nausea in the 19th century. Cannabis-based therapy is still used nowadays for enhancing appetite or reducing nausea and pain in patients having chemotherapy and cancer [7,28,29,63]. CB_1R activation increases appetite through actions on the CNS. A network of CB_1R can be found in several nuclei of the hypothalamus, including the arcuate nucleus, paraventricular nucleus (PVN), ventromedial hypothalamus (VMH), and dorsomedial hypothalamus. These areas and their pathways have an important role in regulating the body's homeostasis and several neuroendocrine functions [13,64]. To prove the direct link between cannabinoids and appetite control, it was observed in animal studies that injection of exogenous AEA (also an endocannabinoid) or THC into the VMH, or injection of AEA into PVN, significantly elevated the appetite of satiated animals [13,64].

Leptin is an important mediator in the control of food intake. Leptin, secreted by adipose tissue cells, is known to decrease food consumption by stimulating an anorexigenic pathway in the hypothalamus affecting the satiety–appetite system. Absence of leptin signaling elevated endocannabinoid levels in the hypothalamus, inducing hunger and overeating. After leptin treatment, hypothalamic AEA and 2-AG levels have been significantly reduced [16,61]. Defective leptin signaling is associated with elevated hypothalamic endocannabinoids in obese db/db and ob/ob mice and Zucker rats [61]. Leptin also stimulates the secretion and activation of FAAH, thereby decreasing the level of AEA. Leptin resistance has been found to reduce satiety, leading to obesity and secondary hyperleptinemia in several obese patients [45].

Components of the ECS located in the mesolimbic areas, the nucleus accumbens shell (NAcS) and the ventral tegmental area (VTA), participate in rewarding and motivational

processes. Dopamine elicits a pleasure feeling in several places of the CNS; levels can also be enhanced by reward-related conditioning stimuli. Absence of CB_1Rs reduces the stimulating effect on dopamine secretion, thereby preventing the development of addiction and rewarding traits [60]. The CB_1R antagonist rimonabant inhibits dopamine secretion in the NAcS after food intake. However, in the NAcS, eCB levels increase during starvation and decrease during feeding. Dopamine regulates eCB levels with a negative feedback mechanism. The need to consume delicious food increases after food withdrawal, and a more rewarding sensation will be produced after food consumption. If an imbalance of the negative feedback occurs, an elevated ECS tone enhances food enjoyment resulting in hyperphagia [60].

Signals of gastric saturation enter the brainstem. After food intake, peptides such as ghrelin are released in the stomach, which is an important regulator peptide of appetite control. Another regulator peptide, cholecystokinin (CCK), is present in areas of the brain where nutrition and behavioral functions are regulated; in the cortical and limbic areas, it is coexpressed with CB_1Rs. CCK reduces CB_1R expression with a negative feedback mechanism, thereby reducing the number of CB_1Rs after a meal. Food deprivation increases the number of CB_1Rs, while the release of ghrelin attenuates the inhibition effect of CCK on CB_1R. In the case of decreased CCK levels, the opioid signaling pathway is stimulated, which also has a major impact on the reward system [53]. The peripheral CB_1R antagonist AM6545 in diet-induced obese mice induces an hypophagic effect. This can be reversed by inhibition of CCK receptors, indicating that obesity-associated hyperphagia is mediated by the mechanism including CB_1R-mediated inhibition of gut–brain satiation signaling [44].

Motivational aspects of feeding include pathways involving the ghrelin-activated reward system in relation to dopamine, opioid, and endocannabinoid pathways [65]. Cannabinoid agonists stimulate the activity of VTA dopamine neurons, which enhances the release of dopamine in the NAcS, while antagonists of CB_1R reduce dopamine release. Thus, ghrelin-activated dopamine release is regulated by the signaling processes of the ECS. Activation of the ECS promotes energy storage, generating fat accumulation and increasing caloric intake by stimulating appetite and the consumption of delicious food. In addition, administration of low-dose THC induces gluttony due to its appetite-stimulating effect. In experimental animals, after injecting AEA into the ventromedial nucleus of the hypothalamus, hyperphagia appears. In addition, the injection of endocannabinoids into the NAcS affected eating habits by reducing eating motivation [13].

4.3. Role of Endocannabinoid System in the Pathogenesis of Obesity

Obesity is a condition that contributes to the development of several metabolic comorbidities. In obesity, the balance between food intake and metabolism shifts, and excessive fat storage will be typical. General availability of cheap energy- and fat-rich diets available results in what can be called a pandemic of obesity. It has been proven that the levels of endocannabinoids, the number of cannabinoid receptors, and the availability of arachidonic and linoleic acids are all increased in obese patients. Linoleic acid is found in large amounts in the Western-type diet, which contains excessive fat, and it facilitates endocannabinoid synthesis. An overreaction of the ECS plays a role in the pathogenesis of obesity, IR, and atherosclerosis [2]. Activation of CB_1Rs by endocannabinoids increases appetite, lipogenesis, and weight gain and results in obesity with metabolic complications [3,11,15,16,28,53,55]. The ECS plays a role in the regulation of energy turnover by stimulating both the CNS and peripheral nervous system to elevate food intake, fat storage, and lipogenesis, which in turn result in obesity and metabolic diseases [3,28,52]. It was found by Ruiz de Azua and Lutz that an increase in fat intake even without increasing caloric consumption in mice resulted in increased body weight compared to control mice fed on a conventional diet [16]. ECBs increase adiponectin secretion and fat storage by increasing the amount of newly produced fatty acids and TG synthesis in adipose tissue cells, while at the same time degradation of fatty acids is decreased. Activation of CB_1Rs in the liver also increases the production of fatty acids, so increased plasma cannabinoid

levels can lead to the formation of nonalcoholic liver steatosis. All the above-mentioned mechanisms contribute to obesity [3,11,14,15].

CB_1R signal pathways activate orexigenic ones in the hypothalamus, stimulating appetite and promoting obesity [6,54,60]. At the periphery, cannabinoid CB_1Rs are important participants in obesity-induced metabolic inflammation, IR, and dyslipidemia [18]. It was found that AEA administration into VMH increased food consumption and induced significant hyperphagia resulting in obesity, which was attenuated by pretreatment with selective CB_1R antagonist SR141716 in rats [13]. Stimulation of CB_1 cannabinoid receptors increased the amount of consumed food, and on the other hand, inhibiting the receptors resulted in an improvement of insulin sensitivity and also decreased body weight and improved metabolic parameters [6,11,28]. Further, to verify the role of CB_1R in obesity and metabolic processes, CB_1R knockout (CB_1R-KO) mice have been applied [66]. The role of CB_1Rs in appetite and weight gain could be verified by the fact that CB_1R-KO mice had a more moderate risk of obesity and weighed less than their wild-type counterparts, which could be attributed to a mild deficit in adipose tissue mass [28,53,67]. It is even more important that CB_1R-KO mice were resistant to fatty-diet-induced obesity with similar caloric inputs to their wild-type mates. This suggests the presence of an additional peripheral CB_1R contribution to the development of obesity. CB_1R-KO mice are also resistant to obesity-accompanied changes in metabolic parameters, including hyperlipidemia and elevated plasma insulin and leptin levels that consequently appear in obese wild-type (WT) mice. CB_1R-KO mice have lower leptin levels and enhanced sensitivity to the anorectic effect of leptin [28,55,67]. These metabolic changes observed in CB_1R-KO mice could also be initiated by treatment with CB_1R antagonist SR141716 [67,68].

In obesity, ECS and CB_1Rs are also characteristically found upregulated in liver and adipose tissue. In WT mice, 3 weeks of a HFD increased hepatic fatty acid synthesis. These mice developed hepatic steatosis. This liver steatogenic effect of HFD was partly reversed by SR141716 [55]. These findings indicate that a HFD activates eCBs, which contributes to lipogenesis and hepatic steatosis and thus the development of obesity [28]. CB_1R-dependent metabolic effects in relation to appetite and obesity are summarized in Table 1.

Since endogenous cannabinoids by acting on CB_1Rs stimulate appetite and lipogenesis, CB_1R antagonists seem to form a promising treatment for obesity. Treatment with CB_1R antagonists (such as rimonabant) caused a decrease in food intake and produced a sustained weight loss in animals with diet-induced obesity [11,18,51,68]. In animal experiments, HFD-induced obesity could be prevented in the absence of CB_1Rs in CB_1R-KO mice. CB_1R KO mice are detected to have less body weight, decreased body fat, and improved glucose homeostasis and plasma lipid profile compared to their wild-type mates [16]. The CB_1R blockade also improves glucose tolerance, insulin and leptin sensitivity, and lipid profile in diet-induced or genetically obese animals [11,68]. CB_1R-KO mice were resistant to HFD-induced hepatic steatosis. In addition, in HFD-fed WT mice, administration of the CB_1R antagonist decreased fatty acid production in the liver [56].

Clinical trials with rimonabant involving obese patients with metabolic syndrome suggest beneficial effects of chronic CB_1R blockade in reducing body weight and also in improving glucose tolerance and lipid profile. CB_1R antagonist rimonabant also reduced plasma leptin and insulin levels, while it increased plasma adiponectin levels [11,69,70]. In a recent study, however, decreasing the level of 2-AG by inhibiting its degrading enzyme MAGL attenuated HFD-induced obesity. Surprisingly, MAGL-deficient mice fed a HFD gained less body weight than wild-type mice and were also protected from IR and hepatic steatosis. Experiments on double MAGL-CB_1R-KO mice then indicated that these mechanisms could be independent of CB_1R signaling, suggesting other functions of the enzyme [71].

Table 1. Effects of endocannabinoid system and cannabinoids on appetite and obesity. Analysis from references. Original and review articles discussing CB receptor-dependent methods (KO mice, agonists, antagonists) are emphasized. CBR, cannabinoid receptors, CB_1R and CB_2R, cannabinoid receptors type 1 and 2, CCK, cholecystokinin, KO, knockout, HFD, high-fat diet, eCB, endocannabinoid, ECS, endocannabinoid system, DAGL, diacylglycerol lipase, MAGL, monoacylglycerol lipase, FAAH, fatty acid amide hydrolase, 2-AG, 2-arachidonoylglycerol, THC, tetrahydrocannabinol, Glu, glutamatergic.

Ref.	Article Type	Animal Model	Diet	Receptors, Agonist/Antagonist	Short Summary	Studied Mechanism and Disease
Jamshidi and Taylor, 2001 [13]	Animal study	Rats		CBR agonist AEA, CB_1R antagonist rimonabant	In presatiated rats, intrahypothalamic injection of AEA increases appetite by hypothalamic CB_1R activation.	Appetite
Argueta, Perez, Makriyannis, and DiPatrizio, 2019 [44]	Animal study	Mice	High-fat diet and sucrose diet	CBR agonist WIN55212, peripheral CBR antagonist AM6545	AM6545 decreases appetite in diet-induced obesity mice, which is reversed by CCK receptor antagonist. The mechanism of hyperphagia-associated obesity includes CB_1R-mediated inhibition of gut–brain satiety signaling.	Appetite, diet-induced obesity
Osei-Hyiaman et al., 2005 [55]	Animal study	CB_1R-KO mice	High-fat diet	CBR agonist HU210, CBR antagonist SR141716 (rimonabant)	CB_1R-KO mice are resistant to diet-induced obesity. CBR agonist increases hepatic fatty acid synthesis. HFD increases liver eCB levels.	Diet-induced obesity
Engeli et al., 2014 [58]	Clinical study		High-fat diet		HFD does not influence eCB levels, but tissue-specific DAGL is upregulated, and FAAH and MAGL are downregulated in obese patients. HFD reduces skeletal muscle CB_1R and MAGL expression.	Obesity
Bellocchio et al., 2010 [59]	Animal study	Glu-CB_1R-KO mice		CBR agonist THC	THC-inducedhyperphagia is completely blunted in Glu-CB_1R-KO mice. Ventral striatal CB_1Rs exert a hypophagic action through inhibition of GABAergic transmission.	Appetite, obesity, and obesity-related disorders
Di Marzo et al., 2001 [61]	Animal study	CB_1R-KO mice, leptin-deficient ob/ob and db/db mice		CBR antagonist rimonabant	CB_1R-KO mice eat less, and CB_1R antagonist reduces food intake in wild-type mice. Defective leptin signaling elevates hypothalamic eCBs in obese ob/ob and db/db mice that show a hyperphagic phenotype.	Appetite, obesity, and obesity-related disorders
Ravinet Trillou, Delgorge, Menet, Arnone, and Soubrié, 2004 [67]	Animal study	CB_1R-KO mice	High-fat diet	CBR antagonist SR141716 (rimonabant)	CB_1R-KO mice are hypophagic with less body weight and do not develop obesity. CB_1R inhibition reduces plasma insulin and leptin levels. CB_1R activation is a key factor in diet-induced obesity.	Diet-induced obesity

Table 1. *Cont.*

Ref.	Article Type	Animal Model	Diet	Receptors, Agonist/Antagonist	Short Summary	Studied Mechanism and Disease
Poirier et al., 2005 [68]	Animal study		High-fat diet	CBR antagonist rimonabant	Obese mice demonstrate abnormal serum lipid profile. Rimonabant treatment decreases body weight and improves lipid profile in obese mice.	Diet-induced obesity
Després, Golay, and Sjöström, 2005 [69]	Clinical study			CBR antagonist rimonabant	Rimonabant treatment decreases body weight and improves lipid profile in obese patients.	Obesity and obesity-induced disorders
Di Marzo, 2008 [15]	Review (animal/clinical studies)	CB_1R-KO mice, obese Zucker rats	High-fat diet	CB_1R, CB_2R, TRPV1; CBR agonists (AEA, 2-AG), CBR antagonists (rimonabant, taranabant)	The ECS becomes dysregulated and overactivated in energy imbalance, contributing to fat accumulation and reduced adiponectin release. CB_1R antagonists/inverse agonists improve glucose and lipid status with weight reduction in obesity and type 2 diabetes.	Obesity and related disorders
Han and Kim, 2021 [18]	Review (animal/clinical studies)			CB_1R antagonists (2nd, 3rd generation), dual-targeting drugs (CB_1R-CB_2R)	CB_1R has a crucial role in obesity-induced inflammation and in the development of metabolic syndrome. Second- and third-generation CB_1R antagonists reduce metabolic inflammation with peripheral actions.	Obesity, obesity-induced inflammation
Scheen and Paquot, 2009 [25]	Review (clinical studies)			CB_1R antagonists (rimonabant, taranabant)	CB_1R blockade reduces body weight and insulin resistance, improves lipid profile and glucose tolerance, and reduces blood pressure in nondiabetic and diabetic obese patients.	Obesity, metabolic disorders

4.4. Role of Endocannabinoid System in the Pathogenesis of Insulin Resistance

IR is a disorder of the carbohydrate metabolism, an important component of the metabolic syndrome family, often called the "ante-room of T2D". In IR, by decreased cellular insulin sensitivity, metabolic regulation of glucose homeostasis is damaged in peripheral tissues and blood. According to novel data, we can state that the ECS has an important role in the regulation of insulin signaling pathways. Activation of CB_1Rs stimulates appetite, metabolic disorders such as lipogenesis, dyslipidemia, and obesity, and disorders of carbohydrate metabolism developing IR and T2D [52].

Endocannabinoids are orexigenic hormones, so an elevated ECS tone increases appetite and food intake, resulting in obesity, which is a major risk factor in developing IR and T2D. AEA via CB_1R increases the craving for delicious meals and enhancement of energy storage, but this effect could not be observed in CB_1R-KO mice. High levels of AEA and 2-AG are associated with IR, elevated levels of visceral fat, and dyslipidemia [33].

During obesity, dysregulation of the ECS contributes to visceral fat accumulation and suppresses the synthesis of adiponectin, decreasing insulin sensitivity and fatty acid oxidation. Thus, further several cardiometabolic risk factors may develop that are associated with T2D and obesity [15]. In the skeletal muscle, eCBs disrupt the insulin signaling pathway, and stimulation of CB_1Rs in the liver depresses insulin sensitivity and insulin production. In addition, eCB signaling excites endoplasmic reticulum stress levels, which increases the levels of long-chain ceramides in the liver, inhibiting insulin signaling [52]. In patients with T2D, higher circulating levels of endocannabinoids, as well as AEA or other eCBs, can be detected than in patients without diabetes with similar body mass [33,72,73]. This observation was further supported by decreased endocannabinoid levels measured during successful therapeutic (dietary) interventions to induce weight loss and improve insulin sensitivity [33,74,75].

Stimulating CB_1R with specific agonists increases the secretion of insulin, somatostatin, and glucagon; it increases fat storage by stimulating lipoprotein lipase and release of adiponectin, and as a result, hepatic steatosis and IR develop. CB_1R-induced activation inhibits insulin signaling mechanisms by inhibiting insulin receptor substrate-1 and protein kinase B (AKT) phosphorylation, depressing pancreatic beta cell function, which mechanisms contribute to IR. Conversely, lack of CB_1Rs or inhibition of CB_1Rs improves insulin signaling, thus improving IR and pancreatic beta cell function and reducing hepatic steatosis and obesity [52,76,77]. In addition, in the mouse beta cell line and in human islets, CB_1R agonists diminished insulin secretion, whereas silencing CB_1Rs in the beta cell line increased the expression of proinsulin, glucokinase, and glucose transporter 2 (GLUT2), which was also observed in the beta cells of CB_1R-KO mice [78]. On the other hand, in adipocytes, it was found that activation of CB_1R by 2-AG promoted insulin sensitivity by increasing insulin-stimulated AKT phosphorylation, which was attenuated by the CB_1R antagonist. This mechanism may serve CB_1R-dependent lipid accumulation [79]. Targeting ECS-dependent lipid signaling in the peripheral tissues can be a potential therapeutic means to treat IR and T2D. Applying CB_1R antagonists or inverse agonists as adjuvant therapy to lifestyle modulation by weight reduction, exercise, and glycemic and lipemic control in obese and T2D patients seems to be beneficial [15,33,52]. CB_1R-dependent metabolic effects in relation to IR and T2D are summarized in Table 2.

Table 2. Effects of endocannabinoid system and cannabinoids on carbohydrate and lipid metabolism and a relationship with insulin resistance and type 2 diabetes mellitus. Analysis from references. Original and review articles discussing CB receptor-dependent methods (KO mice, agonists, antagonists) are emphasized. CBR, cannabinoid receptors, CB_1R and CB_2R, cannabinoid receptors type 1 and 2, KO, knockout, 2-AG, 2-arachidonoylglycerol, THC, tetrahydrocannabinol, AEA, anandamide, ACEA, arachidonyl-2-chloroethyl amide, IR, insulin resistance, AKT, protein kinase B, GLUT2, glucose transporter 2, HFD, high-fat diet.

Ref.	Article Type	Animal Model	Diet	Receptors, Agonist/Antagonist	Short Summary	Studied Mechanism and Disease
Després et al., 2005 [69]	Clinical study			CBR antagonist rimonabant	Rimonabant treatment decreases insulin levels and improves glucose tolerance in obese patients.	Obesity, IR
Kim et al., 2011 [76]	Cells, animal study	Isolated human/mouse islets, beta cell line, db/db and CB_1R-KO mice		CBR agonists AEA, 2-AG, CBR antagonists AM251, AM630	Inhibition of CB_1Rs enhances pancreatic beta cell signaling and proliferation in isolated islets, and also improves glucose tolerance and insulin sensitivity (in db/db mice).	IR
Liu et al., 2012 [77]	Cells, animal study	CB_1R-KO mice, human/mouse hepatocytes	high-fat diet	CBR agonist anandamide	HFD induces hepatic IR in wild-type but not in CB_1R-KO mice. CB_1R activation contributes to diet-induced IR via hepatic CB_1R-mediated inhibition of insulin signaling.	Obesity, IR
Shin et al., 2018 [78]	Cell/animal study	CB_1R-KO mice, mouse beta cell line, human islet		CBR agonist 2-AG, ACEA, WIN55212, CBR antagonist AM251	CB_1R agonists diminishes insulin secretion in β cell line and islets, whereas silencing CB_1Rs in β cells increases expression of proinsulin, glucokinase and GLUT2 glucose transporter, which is also observed in CB_1R-KO mice.	IR, type 2 diabetes
Motaghedi and McGraw, 2008 [79]	Cells	Adipocytes		CBR agonist 2-AG, CBR antagonist SR141716	Activation of CB_1R by 2-AG promotes insulin sensitivity by increasing insulin-stimulated AKT phosphorylation in adipocytes, which is attenuated by CB_1R antagonist.	IR

Table 2. *Cont.*

Ref.	Article Type	Animal Model	Diet	Receptors, Agonist/Antagonist	Short Summary	Studied Mechanism and Disease
Hirsch and Tam, 2019 [3]	Review (animal/ clinical studies)			CB_1R antagonists	CB_1R blockade decreases food intake and body weight, and ameliorates obesity, type 2 diabetes, fatty liver, and IR in animals. It also decreases body weight and improves glucose homeostasis in obese individuals.	Obesity, metabolic syndrome, type 2 diabetes
Di Marzo, 2008 [15]	Review (animal/ clinical studies)	CB_1R-KO mice, obese Zucker rats		CB_1R, CB_2R, TRPV1; CBR agonists (AEA, 2-AG), CBR antagonists (rimonabant, taranabant)	CB_1R antagonists reduce hyperglycemia and dyslipidemia, improving insulin resistance and glucose tolerance in obesity and type 2 diabetes.	Obesity and type 2 diabetes
Nagappan, Shin, and Jung, 2019 [52]	Review (animal/ clinical studies)			CB_1R agonists/overexpression CB_1R antagonists	CB_1R activation modulates insulin signaling pathway and leads to insulin resistance.	Obesity, IR, type 2 diabetes

4.5. Role of Endocannabinoid System in Hypertension

The endocannabinoid system is involved in the regulation of cardiovascular function. Complex mechanisms of cardiovascular effects of cannabinoids involve modulation of autonomic outflow in both central and peripheral nervous systems and also the direct effects on myocardium and vasculature. CB_1R-induced effects have been reported to exert vasodilatory, negative inotropic, and hypotensive actions [11,19,30,38,49,50]. Though CB_1R stimulation exerts vasodilatory action, in CB_1R-KO mice, blood pressure and heart rate are described to be normal [38,50,80]. Elevated blood pressure was observed to be effectively reduced by elevating eCB levels in a hypertensive rat model; however, systemic cannabinoids induced only a mild hypotensive action in normotensive animals [46,50]. We previously observed that inhibition of CB_1R by O2050 augmented Ang II-induced vasoconstriction in wild-type mice, whose effect was not observed in CB_1R-KO mates. In addition, acute Ang II infusion-induced pressure rise was further augmented with CB_1R inhibitor O2050 in vivo in mice containing CB_1Rs, which suggests a role of CB_1Rs in the control of vascular tone and blood pressure [30]. Previously, in a human study, THC was demonstrated to reduce blood pressure [81], while in marijuana users, a higher prevalence of elevated blood pressure has been reported [50,82]. Though CB_1R stimulation has been shown to be beneficial in hypertensive animal models [46,50], CB_1R antagonism improved cardiac function after experimental myocardial infarction and metabolic syndrome [50,83]. In addition, elevated levels of CB_1R and eCB tone may be beneficial in CVD, or it may also be an adaptive compensatory mechanism [50]. Thus, the role of the ECS in blood pressure regulation and its therapeutic potential in hypertension still need further clarification.

4.6. Summary of the Role of Endocannabinoid System in Metabolic Control Processes

The mechanisms leading to metabolic syndrome via the activation/overactivation of CB_1Rs are summarized in Figure 1. Exogenous and endogenous cannabinoids via stimulation of CB_1Rs activate hypothalamic orexigenic pathways, increasing appetite; promoting fat, liver, and muscle tissue lipogenesis and energy uptake; body weight elevation; and obesity development. CB_1R activation also induces alteration of lipid homeostasis, elevating TG and plasma cholesterol levels and thus increasing the risk for the development of atherogenesis, hypertension, and liver steatosis. In addition, CB_1R activation may induce the risk of T2D by developing IR and stimulating gluconeogenesis.

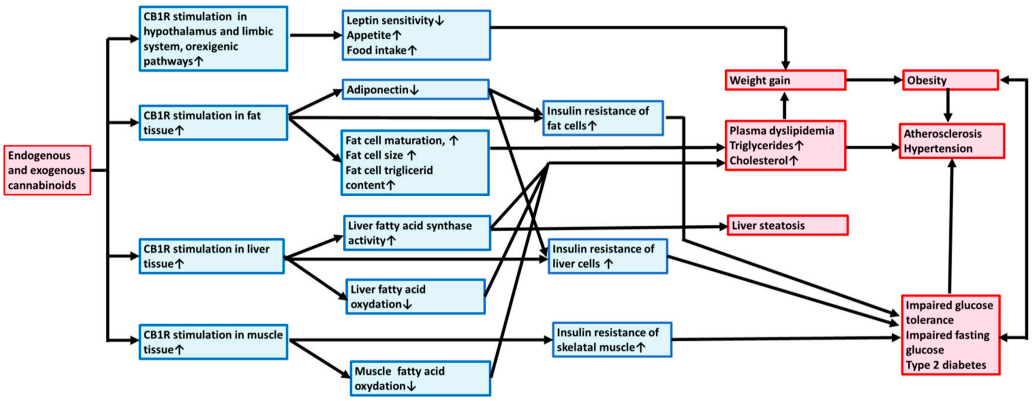

Figure 1. Exogenous and endogenous cannabinoids promote metabolic syndrome and atherosclerosis through central and peripheral type 1 cannabinoid receptors. Mechanism of action. Exogenous and endogenous cannabinoids via stimulation of CB_1Rs activate orexigenic pathway, increasing appetite and stimulating fat, liver, and muscle tissues to promote lipogenesis, weight gain, and obesity. CB_1R activation also induces alteration of lipid homeostasis elevating plasma triglyceride and cholesterol levels and thus increasing the risk for the development of atherogenesis, hypertension, and liver steatosis. In addition, CB_1R activation by developing insulin resistance and gluconeogenesis may induce the risk for type 2 diabetes mellitus. CB_1R, type 1 cannabinoid receptor.

Increased expression of the components of the ECS and elevated levels of endocannabinoids increase food intake and produce hunger due to the activation of orexigen pathways in the hypothalamus. Several brain regions are involved in regulating food intake and are upregulated by the ECS. In addition, reward-related stimuli are conditioned by endocannabinoids in some brain regions. The ECS increases the anabolic processes; tonic enhancement causes hyperphagia, reduces energy expenditure, and increases glucose uptake and lipogenesis. It also suppresses the production of adiponectin, decreasing insulin sensitivity and fat oxidation [52]. Furthermore, CB_1R activation enhances fat cell maturation, increases adipose storage capacity, stimulates fatty acid and TG synthesis, and inhibits fatty acid oxidation. Activation of CB_1Rs in the liver can cause nonalcoholic hepatic steatosis with increased fat production [15]. All these mechanisms contribute to the development of obesity and worsen existing overweight. Inhibition of CB_1R activity improves the peripheral lipid profile and may start recovery from metabolic syndrome by decreasing body weight and appetite, thus also improving glucose and lipid homeostasis and preventing atherosclerosis [15,20,52].

5. Therapeutic Potential of Endocannabinoid System in Complex Diseases of Metabolic Syndrome

Recently, the therapeutic application of cannabidiol, a cannabinoid derivative supposedly without central actions, has been raised and is under investigation.

Cannabinoids and endocannabinoids have been shown to play a role in modulating pathological conditions in inflammatory, neurodegenerative, gastrointestinal, metabolic, and cardiovascular diseases and in cancer. Cannabidiol-based drugs may be used for therapy of several pathological situations, such as pain, sleep disorders, neurodegenerative and psychiatric diseases, etc. [7,11,12,28,29,37]. We can state that modulating the ECS may have and will have therapeutic potential. Targeting the ECS may provide a novel option for the management of obesity and obesity-related diseases, type 2 diabetes, and several CVDs as well [3,14,20,28,29,51]. The sites of pharmacological interventions can be most of all the modulation of CB_1R activity and signaling, as well as the modulation of enzymes responsible for the synthesis and degradation of endocannabinoids, especially FAAH and MAGL. Inhibition of FAAH and MAGL elevates endocannabinoid levels [11,46]. In addition, inhibition of MAGL or FAAH in vivo or in vitro may exert vasodilatory and hypotensive actions [30,46,47]. CB_1R stimulation by its vasodilatory action may be beneficial in hypertension. Thus, CB_1R agonism or elevation of eCB levels may exert certain therapeutic effects, such as antinociceptive, anti-inflammatory, vasodilatator, hypotensive, and anticancer actions [11,29,46].

Under normal conditions, the production of leptin increases the activity and amount of FAAH, thereby reducing endocannabinoid levels in the body. FAAH is responsible for breaking down AEA and therefore suppresses food intake. Upon suppression/inhibition of the FAAH or MAGL enzymes, endocannabinoid levels are elevated, and hyperphagia, leptin resistance, and obesity may develop. Suppression or absence of endocannabinoid-degrading enzymes is clearly associated with an increased risk of obesity [45].

As we could see earlier, CB_1R has a crucial role in obesity-induced proinflammation and metabolic syndrome, including IR and dyslipidemia. Targeting the receptors this way can be a promising therapeutic strategy in obesity and metabolic syndrome. Inhibition of the CB_1R may have a beneficial effect in the prevention and treatment of metabolic syndrome, improving glucose homeostasis and IR [11,18,51]. CB_1R antagonists successfully targeted obesity-induced metabolic disease; among them, rimonabant was proven to be a promising treatment in obesity to induce weight loss and improve dyslipidemia [11,25,51,69,70]. Rimonabant has been subjected to several clinical trials, including patients being obese, overweight, dyslipidemic, or suffering from hypertension or metabolic syndrome and type 2 diabetes. Rimonabant medication significantly decreased body weight and hip circumference, while it increased HDL levels and reduced LDL cholesterol, TG, and HbA1c levels in obese patients in contrast to the control group. Rimonabant, by its actions of

reducing body weight and improving dyslipidemia and glucose homeostasis, significantly reduced the chance of having CVDs and metabolic syndrome. However, bad mood and nausea were the most common side effects. In several cases, even withdrawal of the therapy has been implemented because of its inconvenient psychotic side effects. Development of medication with specific therapeutic effects and with fewer side effects is now the focus of pharmacological research [6,11,25,37,51,69,70,84].

The beneficial actions of CB_1R antagonism have been further investigated with new generations of CB_1R antagonists. Since increased tissue fibrosis may accompany CB_1R activity, due to an interplay between the ECS and inflammatory mechanisms, the antifibrotic efficacy of CB_1R antagonism can form a new therapeutic potential. Second- or third-generation CB_1R antagonists may have therapeutic potential in pulmonary or liver fibrosis [12]. In animal experiments, the development of diabetes-induced cardiomyopathy and fibrosis has been attenuated and prevented by treatment with the CB_1R antagonist, which was observed also in CB_1R-KO mice [85]. Similarly to CB_1R inhibition, a decrease in eCB levels by inhibition of DAG lipase may be beneficial in some chronic diseases, such as neurodegenerative and metabolic disorders [86].

On the other hand, the therapeutic potential of FAAH inhibition is still controversial. A previous pharmacology model showed that complete inhibition of FAAH was insufficient to raise the endogenous ligands enough to produce significantly increased pharmacological activity [87]. Pharmacodynamic and pharmacokinetic studies have been performed on different FAAH inhibitor components (e.g., BIA 10-2474, PF-04457845, and JNJ-42165279). BIA 10-2474 was a less potent FAAH inhibitor than PF-04457845 in humans, but it was effective in mouse FAAH enzymes [88]. Although BIA 10-2474 was released to clinical trials, it has been retrieved due to its serious side effects [87,88].

To summarize ECS-related therapeutic potential, it is suggested that moderate activation of CB_1Rs by selective agonists or by endocannabinoids, as well as the elevation of eCB levels by inhibition of degrading enzymes MAGL or FAAH, may have acute beneficial therapeutic actions such as pain relief and antipsychotic effects, beneficial outcomes in some neuropsychiatric diseases, and potential beneficial effects in hypertension by a CB_1R-dependent vasodilatory effect.

However, long-term antagonism of CB_1Rs has been proven to be beneficial in obesity-related disorders, improving glucose and lipid homeostasis and inducing weight loss. In addition, CB_1R antagonism has been shown to be beneficial in the prevention of chronic inflammation and fibrosis. Similar effects can be produced by inhibition of 2-AG-producing DAG lipase [3,6,11,12,14,20,28,29,37,43,86]. Recently, reports on new generations of CB_1R antagonists have been published with limited neurobehavioral and psychiatric side effects [12,18]. CB_1R antagonists/inverse agonists are potential beneficial adjuvants to lifestyle modification and weight reduction in the control of carbohydrate and lipid homeostasis to prevent dyslipidemia and hyperglycemia in obese and T2D patients.

We can conclude that this complex lipid signaling system can serve as a potential therapeutic source in metabolic syndrome, pathologic obesity, and even T2D [1,15,33]. Modulation of the ECS can serve as part of a complex therapy for obesity-related metabolic disorders, such as IR and diabetes mellitus [1,11,15,29].

6. Summary and Conclusions

In the present review, we summarized the role of the ECS and CB_1R activation in energy homeostasis and metabolism and in the development of metabolic syndrome involving obesity, IR, type 2 diabetes, and dyslipidemia. The metabolic regulatory role of the ECS is manifested partly centrally through brain regions (mostly hypothalamic) controlling the nutritional and metabolic processes of the body with the involvement of neural CB_1R activation influencing neuroendocrine functions. Central endocannabinoids increase appetite by stimulating orexigenic pathways, changing the homeostatic balance toward energy storage, and weight gain. Their direct and indirect peripheral actions increase glucose uptake and lipogenesis in adipose tissue and stimulate the de novo synthesis of

fatty acids and glucose in the liver. Elevated endocannabinoid activation promotes obesity and obesity-linked disorders such as metabolic syndrome, glucose intolerance and type 2 diabetes, and dyslipidemia, with the subsequent risk of atherosclerosis and further CVDs. These ECS-dependent effects are attributed mainly to CB_1R activation and its signaling mechanisms. Inhibition of CB_1Rs has been shown to exert beneficial therapeutic effects improving metabolic conditions by decreasing obesity and inducing weight loss, improving glucose homeostasis and lipid profile, and reducing fibrosis in several chronic diseases of different parenchymal organs. Based on these observations, it can be stated that modulation of the ECS may provide novel therapeutic strategies, especially after developing a new generation of CB_1R antagonists with limited psychologizing effects.

Thus, pharmacological modulation of the ECS forms a promising therapy for complex treatment of obesity-related metabolic diseases, IR, and diabetes mellitus. Modulation of eCB activity, using new-generation CB_1R antagonists and also improvement of lifestyle factors, may serve as complex therapy for obesity-related metabolic disorders, such as IR and diabetes mellitus.

Author Contributions: Conceptualization, G.D. and M.S.; Data curation, G.D., Z.V., C.B.J., M.S.; Funding acquisition, G.D., L.H. and Z.V.; Investigation, Project administration, L.H. and M.S.; Supervision, G.L.N. and L.H.; Visualization, G.L.N., Z.V. and M.S.; Writing—original draft, G.D., Z.V., M.S. and C.B.J.; Writing—review and editing, G.D., Z.V., C.B.J., G.L.N., L.H. and M.S. All authors have read and agreed to the published version of the manuscript.

Funding: This work was supported by grants from the Semmelweis University Faculty of Health Sciences: PhD grants, ÚNKP-22-3-II-SE-6 and ÚNKP-20-1-SE-12 grants, and Hungarian National Grants OTKA K116954 and K139231 (to L.H.).

Institutional Review Board Statement: Not applicable.

Informed Consent Statement: Not applicable.

Data Availability Statement: Not applicable.

Acknowledgments: The authors are thankful to Gábor Turu and Andras Balla (Semmelweis University, Budapest, Hungary) for helpful advice and support.

Conflicts of Interest: The authors declare no conflict of interest. The funders had no role in the design of the study; in the collection, analyses, or interpretation of data; in the writing of the manuscript, or in the decision to publish the results.

Abbreviations

AEA	anandamide
2-AG	2-arachidonoylglycerol
AKT	protein kinase B
Ang II	angiotensin II
AT_1R	type 1 angiotensin receptor
BMI	body mass index
CB	cannabinoid
CB_1R	type 1 cannabinoid receptor
CB_2R	type 2 cannabinoid receptor
CB_1R-KO	type 1 cannabinoid receptor knockout ($CB_1R -/-$)
CCK	cholecystokinin
CNS	central nervous system
CVD	cardiovascular disease
DAG	diacylglycerol
DAGL	diacylglycerol lipase
eCB	endocannabinoid
ECS	endocannabinoid system

FAAH	fatty acid amide hydrolase
GLUT2	glucose transporter 2
GPCR	G-protein-coupled receptor
HDL	high-density lipoprotein
HFD	high-fat diet
IR	insulin resistance
KO	knockout
LDL	low-density lipoprotein
MAG	monoacylglycerol
MAGL	monoacylglycerol lipase
NAcS	nucleus accumbens
PVN	paraventricular nucleus
T2D	type 2 diabetes mellitus
TG	triglyceride
THC	tetrahydrocannabinol
VMH	ventromedial hypothalamus
VTA	ventral tegmental area
WT	wild type

References

1. Di Marzo, V.; Silvestri, C. Lifestyle and Metabolic Syndrome: Contribution of the Endocannabinoidome. *Nutrients* **2019**, *11*, 1956. [CrossRef] [PubMed]
2. Guillamat-Prats, R.; Rami, M.; Herzig, S.; Steffens, S. Endocannabinoid Signalling in Atherosclerosis and Related Metabolic Complications. *Thromb. Haemost.* **2019**, *119*, 567–575. [CrossRef] [PubMed]
3. Hirsch, S.; Tam, J. Cannabis: From a Plant That Modulates Feeding Behaviors toward Developing Selective Inhibitors of the Peripheral Endocannabinoid System for the Treatment of Obesity and Metabolic Syndrome. *Toxins* **2019**, *11*, 275. [CrossRef] [PubMed]
4. Laaksonen, D.E.; Lakka, H.M.; Niskanen, L.K.; Kaplan, G.A.; Salonen, J.T.; Lakka, T.A. Metabolic syndrome and development of diabetes mellitus: Application and validation of recently suggested definitions of the metabolic syndrome in a prospective cohort study. *Am. J. Epidemiol.* **2002**, *156*, 1070–1077. [CrossRef] [PubMed]
5. Liese, A.D.; Mayer-Davis, E.J.; Haffner, S.M. Development of the multiple metabolic syndrome: An epidemiologic perspective. *Epidemiol. Rev.* **1998**, *20*, 157–172. [CrossRef]
6. Mastinu, A.; Premoli, M.; Ferrari-Toninelli, G.; Tambaro, S.; Maccarinelli, G.; Memo, M.; Bonini, S.A. Cannabinoids in health and disease: Pharmacological potential in metabolic syndrome and neuroinflammation. *Horm. Mol. Biol. Clin. Investig.* **2018**, *36*, 20180013. [CrossRef]
7. Navarrete, C.; Garcia-Martin, A.; DeMesa, J.; Muñoz, E. Cannabinoids in Metabolic Syndrome and Cardiac Fibrosis. *Curr. Hypertens. Rep.* **2020**, *22*, 98. [CrossRef]
8. Takamiya, T.; Zaky, W.R.; Edmundowics, D.; Kadowaki, T.; Ueshima, H.; Kuller, L.H.; Sekikawa, A. World Health Organization-Defined Metabolic Syndrome Is a Better Predictor of Coronary Calcium Than the Adult Treatment Panel III Criteria in American Men Aged 40–49 Years. *Diabetes Care* **2004**, *27*, 2977–2979. [CrossRef]
9. Freund, T.F.; Katona, I.; Piomelli, D. Role of endogenous cannabinoids in synaptic signaling. *Physiol. Rev.* **2003**, *83*, 1017–1066. [CrossRef]
10. Katona, I.; Freund, T.F. Endocannabinoid signaling as a synaptic circuit breaker in neurological disease. *Nat. Med.* **2008**, *14*, 923–930. [CrossRef]
11. Pacher, P.; Mukhopadhyay, P.; Mohanraj, R.; Godlewski, G.; Bátkai, S.; Kunos, G. Modulation of the endocannabinoid system in cardiovascular disease: Therapeutic potential and limitations. *Hypertension* **2008**, *52*, 601–607. [CrossRef] [PubMed]
12. Cinar, R.; Iyer, M.R.; Kunos, G. The therapeutic potential of second and third generation CB(1)R antagonists. *Pharmacol. Ther.* **2020**, *208*, 107477. [CrossRef] [PubMed]
13. Jamshidi, N.; Taylor, D.A. Anandamide administration into the ventromedial hypothalamus stimulates appetite in rats. *Br. J. Pharmacol.* **2001**, *134*, 1151–1154. [CrossRef] [PubMed]
14. Cota, D. Role of the endocannabinoid system in energy balance regulation and obesity. *Front. Horm. Res.* **2008**, *36*, 135–145. [CrossRef]
15. Di Marzo, V. The endocannabinoid system in obesity and type 2 diabetes. *Diabetologia* **2008**, *51*, 1356–1367. [CrossRef]
16. Ruiz de Azua, I.; Lutz, B. Multiple endocannabinoid-mediated mechanisms in the regulation of energy homeostasis in brain and peripheral tissues. *Cell Mol. Life Sci.* **2019**, *76*, 1341–1363. [CrossRef]
17. Haffner, S.M.; Valdez, R.A.; Hazuda, H.P.; Mitchell, B.D.; Morales, P.A.; Stern, M.P. Prospective analysis of the insulin-resistance syndrome (syndrome X). *Diabetes* **1992**, *41*, 715–722. [CrossRef]
18. Han, J.H.; Kim, W. Peripheral CB1R as a modulator of metabolic inflammation. *Faseb. J.* **2021**, *35*, e21232. [CrossRef]

19. Pacher, P.; Bátkai, S.; Kunos, G. Cardiovascular pharmacology of cannabinoids. *Handb. Exp. Pharmacol.* **2005**, *168*, 599–625. [CrossRef]
20. Steffens, S.; Pacher, P. The activated endocannabinoid system in atherosclerosis: Driving force or protective mechanism? *Curr. Drug Targets* **2015**, *16*, 334–341. [CrossRef]
21. Reaven, G.M. Why Syndrome X? From Harold Himsworth to the insulin resistance syndrome. *Cell Metab.* **2005**, *1*, 9–14. [CrossRef] [PubMed]
22. Rosenheck, R. Fast food consumption and increased caloric intake: A systematic review of a trajectory towards weight gain and obesity risk. *Obes. Rev.* **2008**, *9*, 535–547. [CrossRef] [PubMed]
23. Lindsay, R.S.; Funahashi, T.; Hanson, R.L.; Matsuzawa, Y.; Tanaka, S.; Tataranni, P.A.; Knowler, W.C.; Krakoff, J. Adiponectin and development of type 2 diabetes in the Pima Indian population. *Lancet* **2002**, *360*, 57–58. [CrossRef] [PubMed]
24. Wallace, A.M.; McMahon, A.D.; Packard, C.J.; Kelly, A.; Shepherd, J.; Gaw, A.; Sattar, N. Plasma leptin and the risk of cardiovascular disease in the west of Scotland coronary prevention study (WOSCOPS). *Circulation* **2001**, *104*, 3052–3056. [CrossRef] [PubMed]
25. Scheen, A.J.; Paquot, N. Use of cannabinoid CB1 receptor antagonists for the treatment of metabolic disorders. *Best Pract. Res. Clin. Endocrinol. Metab.* **2009**, *23*, 103–116. [CrossRef]
26. Cozzolino, D.; Sessa, G.; Salvatore, T.; Sasso, F.C.; Giugliano, D.; Lefebvre, P.J.; Torella, R. The involvement of the opioid system in human obesity: A study in normal weight relatives of obese people. *J. Clin. Endocrinol. Metab.* **1996**, *81*, 713–718. [CrossRef]
27. Di Marzo, V.; Melck, D.; Bisogno, T.; De Petrocellis, L. Endocannabinoids: Endogenous cannabinoid receptor ligands with neuromodulatory action. *Trends Neurosci.* **1998**, *21*, 521–528. [CrossRef]
28. Pacher, P.; Bátkai, S.; Kunos, G. The endocannabinoid system as an emerging target of pharmacotherapy. *Pharmacol. Rev.* **2006**, *58*, 389–462. [CrossRef]
29. Pacher, P.; Kunos, G. Modulating the endocannabinoid system in human health and disease—Successes and failures. *Febs. J.* **2013**, *280*, 1918–1943. [CrossRef]
30. Szekeres, M.; Nádasy, G.L.; Turu, G.; Soltész-Katona, E.; Benyó, Z.; Offermanns, S.; Ruisanchez, É.; Szabó, E.; Takáts, Z.; Bátkai, S.; et al. Endocannabinoid-mediated modulation of Gq/11 protein-coupled receptor signaling-induced vasoconstriction and hypertension. *Mol. Cell Endocrinol.* **2015**, *403*, 46–56. [CrossRef]
31. Ueda, N.; Tsuboi, K.; Uyama, T.; Ohnishi, T. Biosynthesis and degradation of the endocannabinoid 2-arachidonoylglycerol. *Biofactors* **2011**, *37*, 1–7. [CrossRef] [PubMed]
32. De Petrocellis, L.; Cascio, M.G.; Di Marzo, V. The endocannabinoid system: A general view and latest additions. *Br. J. Pharmacol.* **2004**, *141*, 765–774. [CrossRef] [PubMed]
33. Veilleux, A.; Di Marzo, V.; Silvestri, C. The Expanded Endocannabinoid System/Endocannabinoidome as a Potential Target for Treating Diabetes Mellitus. *Curr. Diab. Rep.* **2019**, *19*, 117. [CrossRef] [PubMed]
34. Devane, W.A.; Hanus, L.; Breuer, A.; Pertwee, R.G.; Stevenson, L.A.; Griffin, G.; Gibson, D.; Mandelbaum, A.; Etinger, A.; Mechoulam, R. Isolation and structure of a brain constituent that binds to the cannabinoid receptor. *Science* **1992**, *258*, 1946–1949. [CrossRef]
35. Mechoulam, R.; Fride, E.; Ben-Shabat, S.; Meiri, U.; Horowitz, M. Carbachol, an acetylcholine receptor agonist, enhances production in rat aorta of 2-arachidonoyl glycerol, a hypotensive endocannabinoid. *Eur. J. Pharmacol.* **1998**, *362*, R1–R3. [CrossRef]
36. Devane, W.A.; Dysarz, F.A., III; Johnson, M.R.; Melvin, L.S.; Howlett, A.C. Determination and characterization of a cannabinoid receptor in rat brain. *Mol. Pharmacol.* **1988**, *34*, 605–613.
37. Aizpurua-Olaizola, O.; Elezgarai, I.; Rico-Barrio, I.; Zarandona, I.; Etxebarria, N.; Usobiaga, A. Targeting the endocannabinoid system: Future therapeutic strategies. *Drug Discov. Today* **2017**, *22*, 105–110. [CrossRef]
38. Szekeres, M.; Nádasy, G.L.; Turu, G.; Soltész-Katona, E.; Tóth, Z.E.; Balla, A.; Catt, K.J.; Hunyady, L. Angiotensin II induces vascular endocannabinoid release, which attenuates its vasoconstrictor effect via CB1 cannabinoid receptors. *J. Biol. Chem.* **2012**, *287*, 31540–31550. [CrossRef]
39. Turu, G.; Hunyady, L. Signal transduction of the CB1 cannabinoid receptor. *J. Mol. Endocrinol.* **2010**, *44*, 75–85. [CrossRef]
40. Gyombolai, P.; Pap, D.; Turu, G.; Catt, K.J.; Bagdy, G.; Hunyady, L. Regulation of endocannabinoid release by G proteins: A paracrine mechanism of G protein-coupled receptor action. *Mol. Cell Endocrinol.* **2012**, *353*, 29–36. [CrossRef]
41. Turu, G.; Simon, A.; Gyombolai, P.; Szidonya, L.; Bagdy, G.; Lenkei, Z.; Hunyady, L. The role of diacylglycerol lipase in constitutive and angiotensin AT1 receptor-stimulated cannabinoid CB1 receptor activity. *J. Biol. Chem.* **2007**, *282*, 7753–7757. [CrossRef] [PubMed]
42. Turu, G.; Várnai, P.; Gyombolai, P.; Szidonya, L.; Offertaler, L.; Bagdy, G.; Kunos, G.; Hunyady, L. Paracrine transactivation of the CB1 cannabinoid receptor by AT1 angiotensin and other Gq/11 protein-coupled receptors. *J. Biol. Chem.* **2009**, *284*, 16914–16921. [CrossRef] [PubMed]
43. Kunos, G.; Osei-Hyiaman, D.; Bátkai, S.; Sharkey, K.A.; Makriyannis, A. Should peripheral CB(1) cannabinoid receptors be selectively targeted for therapeutic gain? *Trends Pharmacol. Sci.* **2009**, *30*, 1–7. [CrossRef] [PubMed]
44. Argueta, D.A.; Perez, P.A.; Makriyannis, A.; DiPatrizio, N.V. Cannabinoid CB(1) Receptors Inhibit Gut-Brain Satiation Signaling in Diet-Induced Obesity. *Front Physiol.* **2019**, *10*, 704. [CrossRef]

45. Balsevich, G.; Sticht, M.; Bowles, N.P.; Singh, A.; Lee, T.T.Y.; Li, Z.; Chelikani, P.K.; Lee, F.S.; Borgland, S.L.; Hillard, C.J.; et al. Role for fatty acid amide hydrolase (FAAH) in the leptin-mediated effects on feeding and energy balance. *Proc. Natl. Acad. Sci. USA* **2018**, *115*, 7605–7610. [CrossRef]
46. Bátkai, S.; Pacher, P.; Osei-Hyiaman, D.; Radaeva, S.; Liu, J.; Harvey-White, J.; Offertáler, L.; Mackie, K.; Rudd, M.A.; Bukoski, R.D.; et al. Endocannabinoids acting at cannabinoid-1 receptors regulate cardiovascular function in hypertension. *Circulation* **2004**, *110*, 1996–2002. [CrossRef]
47. Szekeres, M.; Nádasy, G.L.; Soltész-Katona, E.; Hunyady, L. Control of myogenic tone and agonist induced contraction of intramural coronary resistance arterioles by cannabinoid type 1 receptors and endocannabinoids. *Prostaglandins Other Lipid Mediat.* **2018**, *134*, 77–83. [CrossRef]
48. Gyires, K.; Rónai, A.Z.; Zádori, Z.S.; Tóth, V.E.; Németh, J.; Szekeres, M.; Hunyady, L. Angiotensin II-induced activation of central AT1 receptors exerts endocannabinoid-mediated gastroprotective effect in rats. *Mol. Cell Endocrinol.* **2014**, *382*, 971–978. [CrossRef]
49. Miklós, Z.; Wafa, D.; Nádasy, G.L.; Tóth, Z.E.; Besztercei, B.; Dörnyei, G.; Laska, Z.; Benyó, Z.; Ivanics, T.; Hunyady, L.; et al. Angiotensin II-Induced Cardiac Effects Are Modulated by Endocannabinoid-Mediated CB(1) Receptor Activation. *Cells* **2021**, *10*, 724. [CrossRef]
50. Haspula, D.; Clark, M.A. Cannabinoid Receptors: An Update on Cell Signaling, Pathophysiological Roles and Therapeutic Opportunities in Neurological, Cardiovascular, and Inflammatory Diseases. *Int. J. Mol. Sci.* **2020**, *21*, 7693. [CrossRef]
51. Kunos, G.; Osei-Hyiaman, D. Endocannabinoids and liver disease. IV. Endocannabinoid involvement in obesity and hepatic steatosis. *Am. J. Physiol. Gastrointest. Liver Physiol.* **2008**, *294*, G1101–G1104. [CrossRef] [PubMed]
52. Nagappan, A.; Shin, J.; Jung, M.H. Role of Cannabinoid Receptor Type 1 in Insulin Resistance and Its Biological Implications. *Int. J. Mol. Sci.* **2019**, *20*, 2109. [CrossRef] [PubMed]
53. Cota, D.; Marsicano, G.; Lutz, B.; Vicennati, V.; Stalla, G.K.; Pasquali, R.; Pagotto, U. Endogenous cannabinoid system as a modulator of food intake. *Int. J. Obes.* **2003**, *27*, 289–301. [CrossRef] [PubMed]
54. Cota, D.; Marsicano, G.; Tschöp, M.; Grübler, Y.; Flachskamm, C.; Schubert, M.; Auer, D.; Yassouridis, A.; Thöne-Reineke, C.; Ortmann, S.; et al. The endogenous cannabinoid system affects energy balance via central orexigenic drive and peripheral lipogenesis. *J. Clin. Investig.* **2003**, *112*, 423–431. [CrossRef]
55. Osei-Hyiaman, D.; DePetrillo, M.; Pacher, P.; Liu, J.; Radaeva, S.; Bátkai, S.; Harvey-White, J.; Mackie, K.; Offertáler, L.; Wang, L.; et al. Endocannabinoid activation at hepatic CB1 receptors stimulates fatty acid synthesis and contributes to diet-induced obesity. *J. Clin. Investig.* **2005**, *115*, 1298–1305. [CrossRef]
56. Tibiriça, E. The multiple functions of the endocannabinoid system: A focus on the regulation of food intake. *Diabetol. Metab. Syndr.* **2010**, *2*, 5. [CrossRef]
57. Kuipers, E.N.; Kantae, V.; Maarse, B.C.E.; Van Den Berg, S.M.; Van Eenige, R.; Nahon, K.J.; Reifel-Miller, A.; Coskun, T.; De Winther, M.P.J.; Lutgens, E.; et al. High Fat Diet Increases Circulating Endocannabinoids Accompanied by Increased Synthesis Enzymes in Adipose Tissue. *Front. Physiol.* **2018**, *9*, 1913. [CrossRef]
58. Engeli, S.; Lehmann, A.C.; Kaminski, J.; Haas, V.; Janke, J.; Zoerner, A.A.; Luft, F.C.; Tsikas, D.; Jordan, J. Influence of dietary fat intake on the endocannabinoid system in lean and obese subjects. *Obesity* **2014**, *22*, E70–E76. [CrossRef]
59. Bellocchio, L.; Lafenêtre, P.; Cannich, A.; Cota, D.; Puente, N.; Grandes, P.; Chaouloff, F.; Piazza, P.V.; Marsicano, G. Bimodal control of stimulated food intake by the endocannabinoid system. *Nat. Neurosci.* **2010**, *13*, 281–283. [CrossRef]
60. Di Marzo, V.; Ligresti, A.; Cristino, L. The endocannabinoid system as a link between homoeostatic and hedonic pathways involved in energy balance regulation. *Int. J. Obes.* **2009**, *33*, S18–S24. [CrossRef]
61. Di Marzo, V.; Goparaju, S.K.; Wang, L.; Liu, J.; Bátkai, S.; Járai, Z.; Fezza, F.; Miura, G.I.; Palmiter, R.D.; Sugiura, T.; et al. Leptin-regulated endocannabinoids are involved in maintaining food intake. *Nature* **2001**, *410*, 822–825. [CrossRef] [PubMed]
62. Monteleone, P.; Maj, M. Dysfunctions of leptin, ghrelin, BDNF and endocannabinoids in eating disorders: Beyond the homeostatic control of food intake. *Psychoneuroendocrinology* **2013**, *38*, 312–330. [CrossRef] [PubMed]
63. Pisanti, S.; Bifulco, M. Modern History of Medical Cannabis: From Widespread Use to Prohibitionism and Back. *Trends Pharm. Sci.* **2017**, *38*, 195–198. [CrossRef]
64. Verty, A.N.; McGregor, I.S.; Mallet, P.E. Paraventricular hypothalamic CB(1) cannabinoid receptors are involved in the feeding stimulatory effects of Delta(9)-tetrahydrocannabinol. *Neuropharmacology* **2005**, *49*, 1101–1109. [CrossRef] [PubMed]
65. Al Massadi, O.; Nogueiras, R.; Dieguez, C.; Girault, J.A. Ghrelin and food reward. *Neuropharmacology* **2019**, *148*, 131–138. [CrossRef] [PubMed]
66. Zimmer, A.; Zimmer, A.M.; Hohmann, A.G.; Herkenham, M.; Bonner, T.I. Increased mortality, hypoactivity, and hypoalgesia in cannabinoid CB1 receptor knockout mice. *Proc. Natl. Acad. Sci. USA* **1999**, *96*, 5780–5785. [CrossRef]
67. Ravinet Trillou, C.; Delgorge, C.; Menet, C.; Arnone, M.; Soubrié, P. CB1 cannabinoid receptor knockout in mice leads to leanness, resistance to diet-induced obesity and enhanced leptin sensitivity. *Int. J. Obes. Relat. Metab. Disord.* **2004**, *28*, 640–648. [CrossRef]
68. Poirier, B.; Bidouard, J.P.; Cadrouvele, C.; Marniquet, X.; Staels, B.; O'Connor, S.E.; Janiak, P.; Herbert, J.M. The anti-obesity effect of rimonabant is associated with an improved serum lipid profile. *Diabetes Obes. Metab.* **2005**, *7*, 65–72. [CrossRef]
69. Després, J.P.; Golay, A.; Sjöström, L. Effects of rimonabant on metabolic risk factors in overweight patients with dyslipidemia. *N. Engl. J. Med.* **2005**, *353*, 2121–2134. [CrossRef]

70. Ruilope, L.M.; Després, J.P.; Scheen, A.; Pi-Sunyer, X.; Mancia, G.; Zanchetti, A.; Van Gaal, L. Effect of rimonabant on blood pressure in overweight/obese patients with/without co-morbidities: Analysis of pooled RIO study results. *J. Hypertens.* **2008**, *26*, 357–367. [CrossRef]
71. Yoshida, K.; Kita, Y.; Tokuoka, S.M.; Hamano, F.; Yamazaki, M.; Sakimura, K.; Kano, M.; Shimizu, T. Monoacylglycerol lipase deficiency affects diet-induced obesity, fat absorption, and feeding behavior in CB(1) cannabinoid receptor-deficient mice. *Faseb J.* **2019**, *33*, 2484–2497. [CrossRef] [PubMed]
72. Grapov, D.; Adams, S.H.; Pedersen, T.L.; Garvey, W.T.; Newman, J.W. Type 2 diabetes associated changes in the plasma non-esterified fatty acids, oxylipins and endocannabinoids. *PLoS ONE* **2012**, *7*, e48852. [CrossRef] [PubMed]
73. Matias, I.; Petrosino, S.; Racioppi, A.; Capasso, R.; Izzo, A.A.; Di Marzo, V. Dysregulation of peripheral endocannabinoid levels in hyperglycemia and obesity: Effect of high fat diets. *Mol. Cell Endocrinol.* **2008**, *286*, S66–S78. [CrossRef]
74. Di Marzo, V.; Côté, M.; Matias, I.; Lemieux, I.; Arsenault, B.J.; Cartier, A.; Piscitelli, F.; Petrosino, S.; Alméras, N.; Després, J.P. Changes in plasma endocannabinoid levels in viscerally obese men following a 1 year lifestyle modification programme and waist circumference reduction: Associations with changes in metabolic risk factors. *Diabetologia* **2009**, *52*, 213–217. [CrossRef] [PubMed]
75. Van Eyk, H.J.; Van Schinkel, L.D.; Kantae, V.; Dronkers, C.E.A.; Westenberg, J.J.M.; De Roos, A.; Lamb, H.J.; Jukema, J.W.; Harms, A.C.; Hankemeier, T.; et al. Caloric restriction lowers endocannabinoid tonus and improves cardiac function in type 2 diabetes. *Nutr. Diabetes* **2018**, *8*, 6. [CrossRef]
76. Kim, W.; Doyle, M.E.; Liu, Z.; Lao, Q.; Shin, Y.K.; Carlson, O.D.; Kim, H.S.; Thomas, S.; Napora, J.K.; Lee, E.K.; et al. Cannabinoids inhibit insulin receptor signaling in pancreatic β-cells. *Diabetes* **2011**, *60*, 1198–1209. [CrossRef]
77. Liu, J.; Zhou, L.; Xiong, K.; Godlewski, G.; Mukhopadhyay, B.; Tam, J.; Yin, S.; Gao, P.; Shan, X.; Pickel, J.; et al. Hepatic cannabinoid receptor-1 mediates diet-induced insulin resistance via inhibition of insulin signaling and clearance in mice. *Gastroenterology* **2012**, *142*, 1218–1228. [CrossRef] [PubMed]
78. Shin, H.; Han, J.H.; Yoon, J.; Sim, H.J.; Park, T.J.; Yang, S.; Lee, E.K.; Kulkarni, R.N.; Egan, J.M.; Kim, W. Blockade of cannabinoid 1 receptor improves glucose responsiveness in pancreatic beta cells. *J. Cell Mol. Med.* **2018**, *22*, 2337–2345. [CrossRef]
79. Motaghedi, R.; McGraw, T.E. The CB1 endocannabinoid system modulates adipocyte insulin sensitivity. *Obesity* **2008**, *16*, 1727–1734. [CrossRef] [PubMed]
80. Ledent, C.; Valverde, O.; Cossu, G.; Petitet, F.; Aubert, J.F.; Beslot, F.; Böhme, G.A.; Imperato, A.; Pedrazzini, T.; Roques, B.P.; et al. Unresponsiveness to cannabinoids and reduced addictive effects of opiates in CB1 receptor knockout mice. *Science* **1999**, *283*, 401–404. [CrossRef]
81. Crawford, W.J.; Merritt, J.C. Effects of tetrahydrocannabinol on arterial and intraocular hypertension. *Int. J. Clin. Pharmacol. Biopharm.* **1979**, *17*, 191–196. [PubMed]
82. Vidot, D.C.; Prado, G.; Hlaing, W.M.; Florez, H.J.; Arheart, K.L.; Messiah, S.E. Metabolic Syndrome Among Marijuana Users in the United States: An Analysis of National Health and Nutrition Examination Survey Data. *Am. J. Med.* **2016**, *129*, 173–179. [CrossRef] [PubMed]
83. Slavic, S.; Lauer, D.; Sommerfeld, M.; Kemnitz, U.R.; Grzesiak, A.; Trappiel, M.; Thöne-Reineke, C.; Baulmann, J.; Paulis, L.; Kappert, K.; et al. Cannabinoid receptor 1 inhibition improves cardiac function and remodelling after myocardial infarction and in experimental metabolic syndrome. *J. Mol. Med.* **2013**, *91*, 811–823. [CrossRef] [PubMed]
84. Sam, A.H.; Salem, V.; Ghatei, M.A. Rimonabant: From RIO to Ban. *J. Obes.* **2011**, *2011*, 432607. [CrossRef] [PubMed]
85. Rajesh, M.; Bátkai, S.; Kechrid, M.; Mukhopadhyay, P.; Lee, W.S.; Horváth, B.; Holovac, E.; Cinar, R.; Liaudet, L.; Mackie, K.; et al. Cannabinoid 1 receptor promotes cardiac dysfunction, oxidative stress, inflammation, and fibrosis in diabetic cardiomyopathy. *Diabetes* **2012**, *61*, 716–727. [CrossRef] [PubMed]
86. Janssen, F.J.; Van der Stelt, M. Inhibitors of diacylglycerol lipases in neurodegenerative and metabolic disorders. *Bioorg. Med. Chem. Lett.* **2016**, *26*, 3831–3837. [CrossRef] [PubMed]
87. Peck, R.W.; Holstein, S.A.; Van Der Graaf, P.H. BIA 10-2474: Some Lessons are Clear but Important Questions Remain Unanswered. *Clin. Pharmacol. Ther.* **2022**, *111*, 343–345. [CrossRef] [PubMed]
88. Bonifácio, M.J.; Sousa, F.; Aires, C.; Loureiro, A.I.; Fernandes-Lopes, C.; Pires, N.M.; Palma, P.N.; Moser, P.; Soares-da-Silva, P. Preclinical pharmacological evaluation of the fatty acid amide hydrolase inhibitor BIA 10-2474. *Br. J. Pharmacol.* **2020**, *177*, 2123–2142. [CrossRef]

biomedicines

MDPI

Article

Association of N-Acetyl Asparagine with QTc in Diabetes: A Metabolomics Study

Giacomo Gravina [1,2], Melissa Y. Y. Moey [3], Edi Prifti [4,5], Farid Ichou [6], Olivier Bourron [7], Elise Balse [8], Fabio Badillini [9], Christian Funck-Brentano [2] and Joe-Elie Salem [2,*,†]

1 Institute of Neuroscience and Physiology, Sahlgrenska Academy, University of Gothenburg, 41390 Gothenburg, Sweden
2 Department of Pharmacology and Clinical Investigation Centre (CIC-1901), Pitié-Salpêtrière Hospital, AP-HP, Sorbonne Université, INSERM, F-75013 Paris, France
3 Department of Cardiovascular Sciences, East Carolina University (ECU) Health Medical Center, East Carolina University, Greenville, NC 27834, USA
4 IRD, Unité de Modélisation Mathématique et Informatique des Systèmes Complexes, Sorbonne Université, UMMISCO, F-93143 Bondy, France
5 Nutrition et Obesities, Systemic Approaches, NutriOmique, Hôpital Pitié-Salpêtrière, AP-HP, Sorbonne Université, INSERM, F-75013 Paris, France
6 ICAN Omics, Foundation for Innovation in Cardiometabolism and Nutrition (ICAN), Hôpital Pitié-Salpêtrière, F-75013 Paris, France
7 Sorbonne Université Médecine, Assistance Publique Hôpitaux de Paris (APHP), Service de Diabétologie, Hôpital Pitié-Salpêtrière, INSERM UMRS_1138, Centre de Recherche des Cordeliers, Institute of Cardiometabolisme and Nutrition (ICAN), F-75013 Paris, France
8 Institute of Cardiometabolism and Nutrition (ICAN), INSERM, Sorbonne Université, UMR_S1166, F-75013 Paris, France
9 AMPS LLC, New York, NY 10041, USA
* Correspondence: joe-elie.salem@aphp.fr; Tel.: +33-1-42-17-85-31; Fax: +33-1-42-17-85-32
† Current address: Centre d'Investigation Clinique Paris-Est, CIC-1901, Hôpital Pitié-Salpêtrière, Bâtiment Antonin Gosset, 47-83 Bld de l'hôpital, F-75013 Paris, France.

Citation: Gravina, G.; Moey, M.Y.Y.; Prifti, E.; Ichou, F.; Bourron, O.; Balse, E.; Badillini, F.; Funck-Brentano, C.; Salem, J.-E. Association of N-Acetyl Asparagine with QTc in Diabetes: A Metabolomics Study. *Biomedicines* **2022**, *10*, 1955. https://doi.org/10.3390/biomedicines10081955

Academic Editors: Alfredo Caturano and Raffaele Galiero

Received: 6 July 2022
Accepted: 11 August 2022
Published: 12 August 2022

Abstract: Changes in the cardio-metabolomics profile and hormonal status have been associated with long QT syndrome, sudden cardiac death and increased mortality. The mechanisms underlying QTc duration are not fully understood. Therefore, an identification of novel markers that complement the diagnosis in these patients is needed. In the present study, we performed untargeted metabolomics on the sera of diabetic patients at a high risk of cardiovascular disease, followed up for 2.55 [2.34–2.88] years (*NCT02431234*), with the aim of identifying the metabolomic changes associated with QTc. We used independent weighted gene correlation network analysis (WGCNA) to explore the association between metabolites clusters and QTc at T1 (baseline) and T2 (follow up). The overlap of the highly correlated modules at T1 and T2 identified N-Acetyl asparagine as the only metabolite in common, which was involved with the urea cycle and metabolism of arginine, proline, glutamate, aspartate and asparagine. This analysis was confirmed by applying mixed models, further highlighting its association with QTc. In the current study, we were able to identify a metabolite associated with QTc in diabetic patients at two chronological time points, suggesting a previously unrecognized potential role of N-Acetyl asparagine in diabetic patients suffering from long QTc.

Keywords: metabolomics; diabetes; N-Acetyl asparagine; QTc

1. Introduction

Cardio-metabolomic and hormonal conditions including diabetic patients have been associated with increased cardiovascular (CV) mortality from cardiomyopathies, ischemic events and sudden cardiac death (SCD) [1]. The pathophysiology of SCD in diabetic patients has been shown to be multifactorial secondary to hypo- and hyperglycemia with associated disorders of potassium abnormalities, autonomic neuropathy and inflammatory

and fibrotic changes of the ventricular myocardium [2]. Malignant ventricular arrhythmias (VAs) stemming from a prolonged QT interval occur more frequently in diabetic patients compared to the general population [3]. QT is the time interval between QRS start and T-wave end, reflecting overall cardiac repolarization time [4,5]. When corrected for heart rate (QTc), a prolonged QTc above 480 ms (and even more if >500 ms) is a risk marker for a peculiar form of life-threatening polymorphic VA, called torsade de pointes [6,7]. Determinants of QTc are not fully elucidated and the identification of new markers and pathways is needed to better delineate the pathophysiology of QT dynamics in the diabetic population.

Metabolomics, which involves the study of metabolomes (characteristic set of metabolites or low-molecular-weight components) from a variety of biological samples in a particular condition [8], is an emerging field that can complement clinical diagnostics, identify prognostic indicators to reveal new potential mechanisms associated with specific diseases and assess targeted therapies. In CV disease (CVD), metabolomics has been applied to identify risk factors and understand molecular mechanisms in cardiomyopathies and coronary artery disease (CAD) [9]. The use of metabolomics to assess the risk of QTc prolongation is currently limited to only two studies in the published literature, which assessed the metabolic profiles in an animal model exposed to a fluroquinolone [10] and in a small study of patients who were shift workers [11].

To the best of our knowledge, there are no metabolomic studies that assessed the metabolic profile associated with prolonged QTc in diabetic patients. We used an untargeted metabolomics analysis on the sera of study participants with type 2 diabetes mellitus (T2DM) [12], to identify the metabolomic changes associated with QTc. Employing metabolomics analyses, we were able to identify N-Acetyl asparagine as a common molecule in both time points.

2. Materials and Methods

2.1. Study Design

Our study is a sub-analysis of the *Diabète et Calcification Arterielle* (DIACART) study, a single-center prospective observational cohort study among French patients with T2DM (ClinicalTrials.gov: NCT02431234). The participants were prospectively enrolled at Pitié-Salpêtrière Hospital (Paris, France) and included type 2 diabetic patients (T2DM), at high risk for CVD [13]. A total of 170 patients at baseline visit (T1) and 139 patients at T2 (follow-up for 2.55 years [IQR 2.34–2.88 years]) were included in the study. Patients were excluded if they had severe chronic kidney disease or end-stage renal failure (estimated glomerular filtration rate < 30 mL/min using the Modification of Diet in Renal Disease equation). As QTc becomes unreliable in conditions with prolonged QRS (>130 ms), multiple premature ventricular contractions, ventricular pacing and supraventricular tachycardia, these conditions were excluded from this study [13]. All patients provided written consent and the study was approved by the institutional ethics committee. The data concerning the progression of their peripheral limb arterial disease have recently been published elsewhere [14].

2.2. Metabolomics Study

2.2.1. Reference Compounds and Reagents

All liquid chromatography mass spectrometry (LC-MS) grade reference solvents, acetonitrile (ACN) and methanol (MeOH) were from VWR International (Plainview, NY, USA). LC grade ammonium formate and formic acid were from Sigma-Aldrich (Saint Quentin Fallavier, France). Stock solutions of stable isotope-labeled mix (Algal amino acid mixture-13C, 15N) for the metabolomic approach were purchased from Sigma-Aldrich (Saint Quentin Fallavier, France).

2.2.2. Sera Preparation for Metabolomic Analyses

Eight volumes of frozen (−20 °C) acetonitrile containing the internal standards (12.5 µg/mL labeled amino acid mixture) were added to 100 µL of serum samples and vortexed. The samples were sonicated for 15 min and centrifuged for 2 min at 10,000× *g* at 4 °C. The centrifuged samples were then incubated at 4 °C for 1 h to precipitate the proteins. The samples were centrifuged at 20,000× *g* at 4 °C and the supernatants were transferred to another set of tubes to be dried-up and frozen at −80 °C. Samples were reconstituted with the starting mobile phase composition of the chromatographic column and transferred to vials prior to LC-MS analyses.

2.2.3. Ultra-Performance Liquid Chromatography-Mass Spectrometry (UPLC-MS) Analyses of Serum Samples

Metabolomic preparation of samples for analyses was detailed previously [15]. In brief, LC-MS experiments were performed using PFPP, Discovery HS F5-PFPP column, 5 µm, 2.1 × 150 mm (Sigma, Saint Quentin Fallavier, France) on a UPLC® Waters Acquity (Waters Corp, Saint-Quentin-en-Yvelines, France) and Q-Exactive mass spectrometer (Thermo Scientific, San Jose, CA, USA). LC-MS raw data were first converted into mzXML format using MSconvert tool [16]. Peak detection, correction, alignment and integration were processed using the XCMS R package with CentWave algorithm [17] and workflow4metabolomics platforms [18]. The resulting dataset was Log−10 normalized, filtered and cleaned based on quality control (QC) samples [19]. Features were annotated based on their mass over charge ratio (m/z) and retention time using a local database including commercial standards as described previously [20]. The remaining unknown features were discarded from the dataset.

2.3. Weighted Gene Co-Expression Network Analysis and Visualization

Standard WGCNA procedure was followed to create unsigned gene co-expression networks from the WGCNA R-package v1.68 [21]. Gene cluster dendrogram was constructed with a power value = 3. A total of 132 metabolites were imported for the WGCNA analysis. The modules identified by WGCNA analysis were further associated, using Spearman correlation, with QTc independently at T1 and T2. The results identified at T1 and T2 were overlapped using Venn diagrams in R software and visualized using MetScape [22] in Cytoscape software [23].

2.4. Electrocardiography Acquisition and QTc Analysis

Electrocardiograms were recorded using a digital electrocardiograph by trained personnel, with a sampling rate of 1000 Hz and a filter of 150 Hz. The methodology for QTc assessment (CalECG software®, New York City, NY, USA) on 10 s triplicated digitized ECG, Bazett's heart rate correction) has been extensively detailed elsewhere. Inter- and intra-observer variability assessment for QTc measurement was also performed as has been previously described [4].

2.5. Statistical Analysis

Statistical analyses were performed in R-software (version 1.4.1106, RStudio) using "nlme" package, random effect = subjects; fixed effects: age, sex and N-Acetyl asparagine). Correlation with *p*-values < 0.05 were considered significant.

3. Results

3.1. Baseline Demographics and Clinical Characteristics

Demographic and clinical characteristics of diabetic patients included in this study are shown in Table 1 and were published in a previous study [13]. The mean age and QTc were 63.9 ± 8.4 years and 422 ± 24.9 ms, respectively, at the baseline visit (T1) and 132/170 subjects were male (77.7%). Mean age and QTc at follow-up visit (T2) were

66.8 ± 8.4 years and 424.9 ± 24.3 ms, respectively, and 112/139 subjects were male (80.6%). A total of 8/139 (5.8%) patients developed an acute coronary syndrome during follow up.

Table 1. Baseline demographics, clinical and electrocardiographic characteristics (adapted from [13]. No statistical differences were identified between T1 and T2, except for age.

	Measurement at T1 (N = 170)	**Measurement at T2 (N = 139)**
General Characteristics		
Age, years (mean ± SD)	63.9 ± 8.4	66.8 ± 8.4
Male, n (%)	132 (77.7)	112 (80.6)
Weight, kg (mean ± SD)	83.4 ± 15.3	83.2 ± 15.8
Height, m (median [IQR])	1.71 (1.65–1.76)	1.71 (1.65–1.76)
BMI, kg/m^2 (mean ± SD)	28.9 ± 4.7	28.8 ± 4.9
History of CAD [a], n (%)	110 (64.7)	90 (64.7)
Hypertension, n (%)	137 (80.6)	119 (85.7)
Metabolic Biochemistry Profile		
HbA1c, % (median [IQR])	7.5 (7.0–8.3)	7.6 (6.9–8.3)
Blood glucose, mmol/L (median (IQR))	7.8 (6.4–9.3)	8.1 (6.6–10.4)
Triglycerides, mmol/L (median (IQR))	1.2 (0.8–2.0)	1.4 (0.9–2.0)
Total cholesterol, mmol/L(median (IQR))	3.7 (3.2–4.4)	3.8 (3.4–4.4)
HDL cholesterol, mmol/L(median (IQR))	1.1 (0.9–1.3)	1.1 (0.9–1.3)
LDL cholesterol, mmol/L (median (IQR))	1.9 (1.5–2.4)	1.9 (1.6–2.4)
QT Prolonging Drugs [b]		
Present, n (%)	8 (4.7)	8 (5.8)
Basic Metabolic Profile		
Calcium [c], mmol/L (mean ± SD)	2.3 ± 0.1	2.3 ± 0.1
Potassium, mmol/L (mean ± SD)	4.7 ± 0.4	4.6 ± 0.4
Creatinine, mmol/L (median [IQR])	84 (74–101)	87 (76–105)
Albumin, g/L (median [IQR])	42.5 (39.8–44.4)	43 (40.5–45)
Electrocardiogram Variables		
Heart rate, beats/min (mean ± SD)	69.7 ± 11.1	69.1 ± 11.8
QTc, ms (mean ± SD)	422 ± 24.9	424.9 ± 24.3

Abbreviations: BMI = body mass index; CAD = coronary artery disease; HbA1c = hemoglobin A1c; HDL = high density lipoprotein; IQR = interquartile range; LDL = low density lipoprotein; QTc = Bazett's QTc; [a] CAD defined as a history of myocardial infarction; coronary angioplasty or bypass grafting; [b] Patients taking a drug at known risk of torsades de pointes (www.crediblemeds.org [24]: at T1, these drugs included amiodarone (n = 3), domperidone (n = 1), escitalopram (n = 1) and sotalol (n = 3); at T2, all 8 patients were taking amiodarone. [c] Corrected for albumin concentrations.

3.2. Untargeted Metabolomics Analysis Using Weighted Gene Correlation Network Analysis (WGCNA)

To capture the full extent of the metabolomics expression profiles, we performed a weighted gene co-expression network analysis (WGCNA). WGCNA is a useful method to tightly link co-expressed gene modules to phenotypic traits (e.g., QTc) [21]. The full dataset of 170 patients at T1 and 139 patients at T2 was used for WGCNA analysis. No outliers were identified; therefore, all samples were included in the study analyses. At T1, there were a total of ten clusters of metabolites identified (Figure 1A, left panel). Correlations between clusters of metabolites and QTc were evaluated through Spearman's correlation analysis. QTc was significantly correlated with the dark grey and the pink clusters (r = 0.25, *p*-value = 0.0008 and r = −0.21, *p*= 0.005, respectively) (Figure 1B, left panel). Similarly, at T2, seven clusters of metabolites were identified (Figure 1A, right panel), among which only the red cluster was correlated with QTc (r = −0.26 and *p* = 0.002) (Figure 1B, right panel).

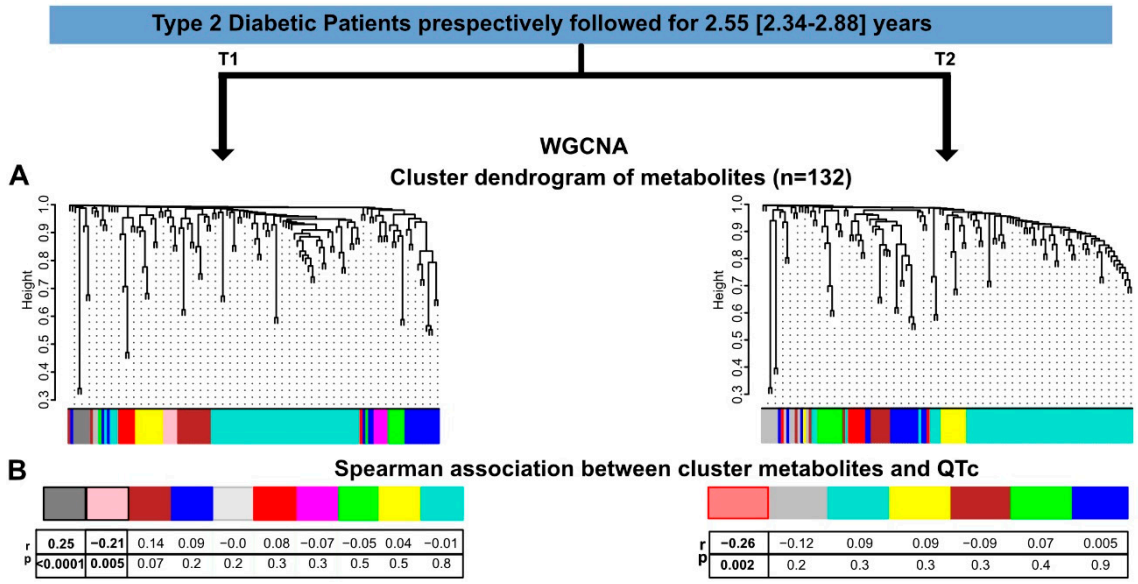

Figure 1. Untargeted metabolomics analysis using weight gene correlation network analysis (WGCNA). Type 2 diabetic patients from the DIACART study were prospectively enrolled and followed up over 2.55 [IQR 2.34–2.88] years. There were 10 clusters of metabolites identified at T1 (**A**, **left panel**) with the dark grey and pink clusters significantly correlated with QTc (**B**, **left panel**). At T2, there were 7 clusters of metabolites identified (**A**, **right panel**) with the light red cluster correlated with QTc (**B**, **right panel**).

3.3. Identification of N-Acetyl Asparagine

These clusters identified by the WGCNA analysis were then compared to identify the common metabolites that correlate with QTc at both time-points (Figure 2A). The intersection of the significant clusters identified N-Acetyl asparagine as the only metabolite in common, pointing to a potential significant involvement of this amino acid in QTc dynamics (Figure 2A). Using the MetScape Cytoscape plugin, we identified the N-Acetyl asparagine enzymatic pathway (including its precursor L-asparagine), as illustrated in Figure 2B. Other pathways associated with N-Acetyl asparagine include the urea cycle and metabolism of arginine, proline, glutamate, aspartate and asparagine.

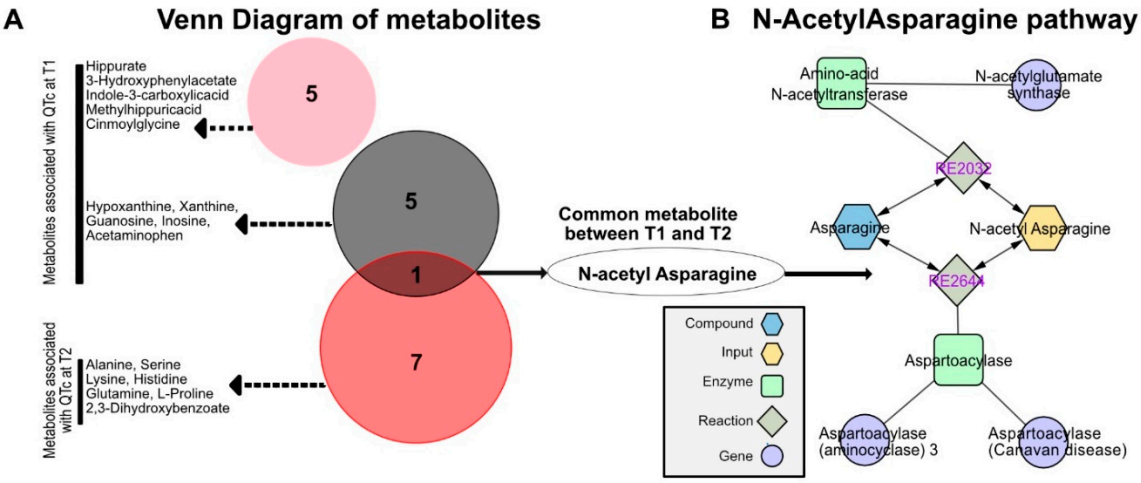

Figure 2. Identification of individual metabolites at T1 and T2. (**A**) A total of 10 metabolites were identified at T1 and 7 metabolites were identified at T2 associated with QTc. The intersection of the significant clusters identified N-Acetyl asparagine as the only metabolite in common. (**B**) N-Acetyl asparagine enzymatic pathway.

3.4. N-Acetyl Asparagine Positively Correlates with QTc

To evaluate the potential involvement of N-Acetyl asparagine with QTc, we performed Spearman correlation analysis to evaluate the actual relationship between QTc and N-Acetyl asparagine. We found that in both T1 and T2, N-Acetyl asparagine was positively correlated with QTc (r = 0.19, p = 0.01 and r = 0.23, p = 0.007, respectively) (Figure 3A). In contrast, L-asparagine was negatively correlated with QTc at T2 (r = −0.18, p = 0.03) (Figure 3A). We further confirmed the association of N-Acetyl asparagine with QTc in this cohort by applying mixed models (R-software, package 'nlme', random effect = subjects; fixed effects: sex and N-Acetyl asparagine) integrating the evolution over time of N-Acetyl asparagine circulating levels in the same subject (Figure 3B).

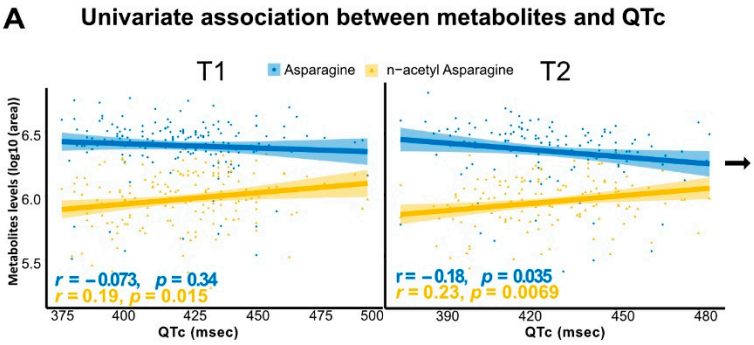

B Multivariate mixed model showing association between N-Acetyl Asparagine and QTc

	Estimate	Standard Error	P-value
(Intercept)	335.416	36.136	$<2^{-16}$
N-acetyl Asparagine	17.258	5.986	0.00422
Sex Male	-18.718	3.913	3.7^{-06}

Figure 3. Association between metabolites and QTc. (**A**) N-Acetyl asparagine was positively corrected with QTc at both T1 and T2. L-asparagine was negatively correlated with QTc at T2. (**B**) Multivariate mixed model showed a significant correlation with N-Acetyl asparagine and QTc.

4. Discussion

To the best of our knowledge, our study was the first to explore metabolomic pathways as potential determinants of QTc in diabetic patients, demonstrating a significant association between N-Acetyl asparagine and QTc.

Metabolomics is a powerful approach at the forefront of scientific discoveries in CVD with its role emphasized in a scientific statement by the American Heart Association [25]. Metabolomics has the potential to reflect the molecular processes more proximal to a disease state by measuring the final downstream products of biological pathways and thereby crucial for the identification of novel biomarkers for risk prognostication and specific therapeutic targets in cardiomyopathies, dyslipidemia treatments and CAD [9,26].

In comparison to CAD, heart failure and diabetes, for which metabolomics has been frequently applied to understand the pathophysiology and prognostic risk factors, there are limited metabolomic studies in QTc prolongation and the risk of SCD. On the pathophysiological basis of ischemic changes resulting in metabolic derangements in the cardiomyocyte with decreased ATP and increased reactive oxygen species, Wang and colleagues used proton nuclear magnetic resonance (H^1-NMR-based) and gas chromatography–mass spectrometry (GC-MS) myocardial tissue metabolic profiling to identify the metabolic alterations in a rat animal model that developed SCD after myocardial infarction [27]. Among 34 rats, 13 developed lethal ventricular arrhythmias (VA, ventricular tachycardia/fibrillation) and 7 developed atrioventricular blocks (AVB) resulting in SCD. There were higher levels of isoleucine, lactate, glutamate, choline, phosphorylcholine, taurine and asparagine, and decreased levels of alanine, urea, phenylalanine, linoleic acid, elaidic acid and stearic acid associated with VA-related SCD. In comparison, only glutamate was elevated and urea was lowered in AVB-related SCD [27]. These metabolic changes were felt to be a result of the detrimental effects of ischemia leading to a depletion in myocardial energy stores and the dysfunction of myocardial membranes altering the cardiac ion channels.

In the current study, using WGCNA analysis, we identified a significant association between N-acetyl asparagine with QTc in diabetic patients at two distinct chronological

time points, which was further confirmed using multivariate mixed models. Using a similar metabolomics approach, in two cohorts of CAD patients, Mehta et al. identified the asparagine pathway as 1 of 7 metabolic pathways in two cohorts of CAD patients. It was an independent predictor of mortality, which was further translated into a prognostic biomarker for all-cause death [28]. Among the different metabolites previously identified in myocardial energetics and inflammation, the aspartate/asparagine pathway exerts a crucial role as anaplerotic substrates in the Krebs cycle during anoxia [29]. Asparagine is converted to aspartate that is then transaminated to oxaloacetate, a critical early metabolite in gluconeogenesis, and plays a key role in the regulation of Krebs cycle intermediates [30]. The appropriate regulation of these metabolites is especially important during ischemia, in which imbalance in the aspartate/asparagine pathway and the inhibition of aspartate has been shown to increase the susceptibility to ischemic damage [31].

In a non-diabetic study cohort, a metabolomics study which assessed metabolomic patterns associated with QTc in small population of 32 male shift-workers from Italy demonstrated a positive correlation between QTc, obesity and hyperglycemia [11]. There were also higher lactate and glucose metabolite levels associated with prolonged QTc while lysine, pyroglutamate, 3-hydroxybutyrate, acetate and glutamine were inversely correlated. Their clinical and metabolomic findings associated with prolonged QTc were suggestive of a metabolic imbalance shift towards anaerobic metabolism or ketosis that can be observed with metabolic syndrome, diabetes and insulin resistance.

The identification of early metabolic markers and strategies to prevent the development of CV complications (heart failure, CAD and SCD) in diabetic patients is of particular importance, as patients may often not manifest any symptoms of these CV comorbidities. In a large cohort study of 14,294 deaths in Denmark, SCD was found to be 8–9 times higher among young diabetic patients aged 1–35 years old and approximately 6 times higher among those aged 36–49 years old with diabetes than non-diabetic patients [1]. Importantly, within the younger group of diabetic patients, the common cause of SCD was due to 'sudden arrhythmic death syndrome' while CAD or ischemia was more common in the older patient population [1]. Previous studies have demonstrated hypo- and hyperglycemia [32], autonomic neuropathy [33], electrolyte abnormalities and ventricular inflammation [2] as contributors to alterations in the cardiac ion channels and increased risk for SCD in the diabetic population. These biochemical and physiologic changes are typically not manifested as symptoms in the disease process and thus the use of metabolomics would be crucial for early recognition of the risk of developing prolonged QTc and subsequent SCD. An upcoming and highly anticipated study, the Recognition of Sudden Cardiac Arrest Vulnerability in Diabetes (RESCUED) project, plans to assess the metabolomic profiles of Dutch patients with T2DM and SCD from the Amsterdam Resuscitation Studies (ARREST) Registry, the Hoorn Diabetes Care System (DCS) and local family practitioner electronic health records to further elucidate the clinical and metabolic factors to prognosticate the risk of SCD in these patients [34].

There are limitations to our study which first include that this was a single-center, observational study and thus, a causal relationship cannot be established. While our study identified a particular metabolomic pathway associated with prolonged QTc, future studies involving in vitro experiments such as with cardiomyocytes derived from pluripotent stem cells [5] as well as in vivo interventional studies may be useful to further assess the underlying mechanisms of these findings. Additionally, relatively few subjects had abnormal QTc values in our cohort; which may have limited the discovery of potential associations between other metabolites beyond N-acetyl asparagine and QTc. As our study cohort was limited to a single center of patients in France and with diabetes, the relevance of our findings beyond the geographical location and diabetic population needs to be further evaluated.

5. Conclusions

In conclusion, our study employed an untargeted metabolomics approach and identified an association between N-acetyl asparagine with prolonged QTc in diabetic patients. Our findings further highlight the potential role of asparagine metabolism in cardio-metabolic disease and deserve further validation and investigation.

Author Contributions: Conceptualization, G.G. and J.-E.S.; methodology, G.G. and J.-E.S.; software, validation and formal analysis, G.G.; F.B.; investigation, E.P., F.I., O.B. and J.-E.S.; resources, F.I., O.B. and J.-E.S.; data curation, O.B.; writing—original draft preparation, G.G., M.Y.Y.M., E.B., C.F.-B. and J.-E.S.; writing—review and editing, all authors; visualization, G.G. and J.-E.S.; supervision, E.P. and J.-E.S.; project administration, J.-E.S.; funding acquisition, O.B. and J.-E.S. All authors have read and agreed to the published version of the manuscript.

Funding: DIACART study was funded by the French Ministry of Health grant (PHRC Code project: P111105; N○ID RCB: 2013-A00896-39).

Institutional Review Board Statement: This study was conducted according to the guidelines of the Declaration of Helsinki, and approved by the Institutional Review Board of Assistance Publique—Hôpitaux de Paris.

Informed Consent Statement: Informed consent was obtained from all subjects involved in the study.

Data Availability Statement: The data that support the findings of this study are available from the authors upon request.

Conflicts of Interest: The authors declare no conflict of interest.

References

1. Lynge, T.H.; Svane, J.; Pedersen-Bjergaard, U.; Gislason, G.; Torp-Pedersen, C.; Banner, J.; Risgaard, B.; Winkel, B.G.; Tfelt-Hansen, J. Sudden cardiac death among persons with diabetes aged 1-49 years: A 10-year nationwide study of 14 294 deaths in Denmark. *Eur. Heart J.* **2020**, *41*, 2699–2706. [CrossRef] [PubMed]
2. Rana, B.S.; Band, M.M.; Ogston, S.; Morris, A.D.; Pringle, S.D.; Struthers, A.D. Relation of QT interval dispersion to the number of different cardiac abnormalities in diabetes mellitus. *Am. J. Cardiol.* **2002**, *90*, 483–487. [CrossRef]
3. Aune, D.; Schlesinger, S.; Norat, T.; Riboli, E. Diabetes mellitus and the risk of sudden cardiac death: A systematic review and meta-analysis of prospective studies. *Nutr. Metab. Cardiovasc. Dis.* **2018**, *28*, 543–556. [CrossRef] [PubMed]
4. Saque, V.; Vaglio, M.; Funck-Brentano, C.; Kilani, M.; Bourron, O.; Hartemann, A.; Badilini, F.; Salem, J.E. Fast, accurate and easy-to-teach QT interval assessment: The triplicate concatenation method. *Arch. Cardiovasc. Dis.* **2017**, *110*, 475–481. [CrossRef] [PubMed]
5. Salem, J.E.; Yang, T.; Moslehi, J.J.; Waintraub, X.; Gandjbakhch, E.; Bachelot, A.; Hidden-Lucet, F.; Hulot, J.S.; Knollmann, B.C.; Lebrun-Vignes, B.; et al. Androgenic Effects on Ventricular Repolarization: A Translational Study from the International Pharmacovigilance Database to iPSC-Cardiomyocytes. *Circulation* **2019**, *140*, 1070–1080. [CrossRef]
6. Roden, D.M. Drug-induced prolongation of the QT interval. *N. Engl. J. Med.* **2004**, *350*, 1013–1022. [CrossRef]
7. De Bruin, M.L.; Pettersson, M.; Meyboom, R.H.; Hoes, A.W.; Leufkens, H.G. Anti-HERG activity and the risk of drug-induced arrhythmias and sudden death. *Eur. Heart J.* **2005**, *26*, 590–597. [CrossRef]
8. Nicholson, J.K. Global systems biology, personalized medicine and molecular epidemiology. *Mol. Syst. Biol.* **2006**, *2*, 52. [CrossRef]
9. McGarrah, R.W.; Crown, S.B.; Zhang, G.F.; Shah, S.H.; Newgard, C.B. Cardiovascular Metabolomics. *Circ. Res.* **2018**, *122*, 1238–1258. [CrossRef]
10. Park, J.; Noh, K.; Lee, H.W.; Lim, M.S.; Seong, S.J.; Seo, J.J.; Kim, E.J.; Kang, W.; Yoon, Y.R. Pharmacometabolomic approach to predict QT prolongation in guinea pigs. *PLoS ONE* **2013**, *8*, e60556. [CrossRef]
11. Campagna, M.; Locci, E.; Piras, R.; Noto, A.; Lecca, L.I.; Pilia, I.; Cocco, P.; d'Aloja, E.; Scano, P. Metabolomic patterns associated to QTc interval in shiftworkers: An explorative analysis. *Biomarkers* **2016**, *21*, 607–613. [CrossRef] [PubMed]
12. Bourron, O.; Aubert, C.E.; Liabeuf, S.; Cluzel, P.; Lajat-Kiss, F.; Dadon, M.; Komajda, M.; Mentaverri, R.; Brazier, M.; Pierucci, A.; et al. Below-knee arterial calcification in type 2 diabetes: Association with receptor activator of nuclear factor kappaB ligand, osteoprotegerin, and neuropathy. *J. Clin. Endocrinol. Metab.* **2014**, *99*, 4250–4258. [CrossRef]
13. Madhukar, R.; Jagadeesh, A.T.; Moey, M.Y.Y.; Vaglio, M.; Badilini, F.; Leban, M.; Hartemann, A.; Dureau, P.; Funck-Brentano, C.; Bourron, O.; et al. Association of thyroid-stimulating hormone with corrected QT interval variation: A prospective cohort study among patients with type 2 diabetes. *Arch. Cardiovasc. Dis.* **2021**, *114*, 656–666. [CrossRef] [PubMed]

14. Bourron, O.; Phan, F.; Diallo, M.H.; Hajage, D.; Aubert, C.E.; Carlier, A.; Salem, J.E.; Funck-Brentano, C.; Kemel, S.; Cluzel, P.; et al. Circulating Receptor Activator of Nuclear Factor kB Ligand and triglycerides are associated with progression of lower limb arterial calcification in type 2 diabetes: A prospective, observational cohort study. *Cardiovasc. Diabetol.* **2020**, *19*, 140. [CrossRef] [PubMed]
15. Nguyen, L.S.; Prifti, E.; Ichou, F.; Leban, M.; Funck-Brentano, C.; Touraine, P.; Salem, J.E.; Bachelot, A. Effect of congenital adrenal hyperplasia treated by glucocorticoids on plasma metabolome: A machine-learning-based analysis. *Sci. Rep.* **2020**, *10*, 8859. [CrossRef]
16. Kessner, D.; Chambers, M.; Burke, R.; Agus, D.; Mallick, P. ProteoWizard: Open source software for rapid proteomics tools development. *Bioinformatics* **2008**, *24*, 2534–2536. [CrossRef]
17. Smith, C.A.; Want, E.J.; O'Maille, G.; Abagyan, R.; Siuzdak, G. XCMS: Processing mass spectrometry data for metabolite profiling using nonlinear peak alignment, matching, and identification. *Anal. Chem.* **2006**, *78*, 779–787. [CrossRef]
18. Giacomoni, F.; Le Corguille, G.; Monsoor, M.; Landi, M.; Pericard, P.; Petera, M.; Duperier, C.; Tremblay-Franco, M.; Martin, J.F.; Jacob, D.; et al. Workflow4Metabolomics: A collaborative research infrastructure for computational metabolomics. *Bioinformatics* **2015**, *31*, 1493–1495. [CrossRef]
19. Dunn, W.B.; Broadhurst, D.; Begley, P.; Zelena, E.; Francis-McIntyre, S.; Anderson, N.; Brown, M.; Knowles, J.D.; Halsall, A.; Haselden, J.N.; et al. Procedures for large-scale metabolic profiling of serum and plasma using gas chromatography and liquid chromatography coupled to mass spectrometry. *Nat. Protoc.* **2011**, *6*, 1060–1083. [CrossRef]
20. Boudah, S.; Olivier, M.F.; Aros-Calt, S.; Oliveira, L.; Fenaille, F.; Tabet, J.C.; Junot, C. Annotation of the human serum metabolome by coupling three liquid chromatography methods to high-resolution mass spectrometry. *J. Chromatogr. B Anal. Technol. Biomed. Life Sci.* **2014**, *966*, 34–47. [CrossRef]
21. Langfelder, P.; Horvath, S. WGCNA: An R package for weighted correlation network analysis. *BMC Bioinform.* **2008**, *9*, 559. [CrossRef]
22. Karnovsky, A.; Weymouth, T.; Hull, T.; Tarcea, V.G.; Scardoni, G.; Laudanna, C.; Sartor, M.A.; Stringer, K.A.; Jagadish, H.V.; Burant, C.; et al. Metscape 2 bioinformatics tool for the analysis and visualization of metabolomics and gene expression data. *Bioinformatics* **2012**, *28*, 373–380. [CrossRef] [PubMed]
23. Shannon, P.; Markiel, A.; Ozier, O.; Baliga, N.S.; Wang, J.T.; Ramage, D.; Amin, N.; Schwikowski, B.; Ideker, T. Cytoscape: A software environment for integrated models of biomolecular interaction networks. *Genome Res.* **2003**, *13*, 2498–2504. [CrossRef] [PubMed]
24. Woosley, R.L.; Heise, C.W.; Gallo, T.; Tate, J.; Woosley, D.; Romero, K.A. QTdrugs List [Internet]. Available online: https://crediblemeds.org/ (accessed on 3 May 2020).
25. Cheng, S.; Shah, S.H.; Corwin, E.J.; Fiehn, O.; Fitzgerald, R.L.; Gerszten, R.E.; Illig, T.; Rhee, E.P.; Srinivas, P.R.; Wang, T.J.; et al. Potential Impact and Study Considerations of Metabolomics in Cardiovascular Health and Disease: A Scientific Statement from the American Heart Association. *Circ. Cardiovasc. Genet.* **2017**, *10*, e000032. [CrossRef] [PubMed]
26. Vieira-Silva, S.; Falony, G.; Belda, E.; Nielsen, T.; Aron-Wisnewsky, J.; Chakaroun, R.; Forslund, S.K.; Assmann, K.; Valles-Colomer, M.; Nguyen, T.T.D.; et al. Statin therapy is associated with lower prevalence of gut microbiota dysbiosis. *Nature* **2020**, *581*, 310–315. [CrossRef]
27. Wang, D.; Wang, X.; Wu, J.; Su, R.; Kong, J.; Yu, X. Metabolic risk factors associated with sudden cardiac death (SCD) during acute myocardial ischemia. *Forensic Sci. Res.* **2017**, *2*, 126–131. [CrossRef]
28. Mehta, A.; Liu, C.; Nayak, A.; Tahhan, A.S.; Ko, Y.A.; Dhindsa, D.S.; Kim, J.H.; Hayek, S.S.; Sperling, L.S.; Mehta, P.K.; et al. Untargeted high-resolution plasma metabolomic profiling predicts outcomes in patients with coronary artery disease. *PLoS ONE* **2020**, *15*, e0237579. [CrossRef]
29. Holmes, E.; Wilson, I.D.; Nicholson, J.K. Metabolic phenotyping in health and disease. *Cell* **2008**, *134*, 714–717. [CrossRef]
30. Owen, O.E.; Kalhan, S.C.; Hanson, R.W. The key role of anaplerosis and cataplerosis for citric acid cycle function. *J. Biol. Chem.* **2002**, *277*, 30409–30412. [CrossRef]
31. Julia, P.; Young, H.H.; Buckberg, G.D.; Kofsky, E.R.; Bugyi, H.I. Studies of myocardial protection in the immature heart. II. Evidence for importance of amino acid metabolism in tolerance to ischemia. *J. Thorac. Cardiovasc. Surg.* **1990**, *100*, 888–895. [CrossRef]
32. Zhang, Y.; Han, H.; Wang, J.; Wang, H.; Yang, B.; Wang, Z. Impairment of human ether-a-go-go-related gene (HERG) K+ channel function by hypoglycemia and hyperglycemia. Similar phenotypes but different mechanisms. *J. Biol. Chem.* **2003**, *278*, 10417–10426. [CrossRef] [PubMed]
33. Vinik, A.I.; Ziegler, D. Diabetic cardiovascular autonomic neuropathy. *Circulation* **2007**, *115*, 387–397. [CrossRef] [PubMed]
34. van Dongen, L.H.; Harms, P.P.; Hoogendoorn, M.; Zimmerman, D.S.; Lodder, E.M.; M't Hart, L.M.; Herings, R.; van Weert, H.; Nijpels, G.; Swart, K.M.A.; et al. Discovery of predictors of sudden cardiac arrest in diabetes: Rationale and outline of the RESCUED (REcognition of Sudden Cardiac arrest vUlnErability in Diabetes) project. *Open Heart* **2021**, *8*, e001554. [CrossRef] [PubMed]

biomedicines

MDPI

Article

Relationship between Arterial Calcifications on Mammograms and Cardiovascular Events: A Twenty-Three Year Follow-Up Retrospective Cohort Study

Natalia González Galiano [1,2], Noemi Eiro [2], Arancha Martín [2,3], Oscar Fernández-Guinea [4], Covadonga del Blanco Martínez [4] and Francisco J. Vizoso [2,5,*]

1 Department of Internal Medicine, Fundación Hospital de Jove, Av. Eduardo Castro, 161, 33290 Gijón, Spain
2 Research Unit, Fundación Hospital de Jove, Av. Eduardo Castro, 161, 33290 Gijón, Spain
3 Department of Emergency, Hospital Universitario de Cabueñes, Los Prados, 395, 33394 Gijón, Spain
4 Department of Radiology, Fundación Hospital de Jove, Av. Eduardo Castro, 161, 33290 Gijón, Spain
5 Department of Surgery, Fundación Hospital de Jove, Av. Eduardo Castro, 161, 33290 Gijón, Spain
* Correspondence: investigacion@hospitaldejove.com; Tel.: +34-985-320050 (ext. 84216); Fax: +34-985-315710

Abstract: Purpose: Breast arterial calcifications (BAC) have been associated with cardiovascular diseases. We aimed to examine whether the presence of BAC could predict the development of cardiovascular events in the very long term, as evidence has suggested. Patients and Methods: We conducted a 23-year follow-up retrospective cohort study considering women specifically studied for breast cancer. After reviewing the mammograms of 1759 women, we selected 128 patients with BAC and an equal number of women without BAC. Results: Women with BAC had higher relative risk (RR) for cardiovascular events, globally 1.66 (95% CI): 1.31–2.10 vs. 0.53 (0.39–0.72), and individually for ischemic heart disease 3.25 (1.53–6.90) vs. 0.85 (0.77–0.94), hypertensive heart disease 2.85 (1.59–5.09) vs. 0.79 (0.69–0.89), valvular heart disease 2.19 (1.28–3.75) vs. 0.83 (0.73–0.94), congestive heart failure 2.06 (1.19–3.56) vs. 0.85 (0.75–0.96), peripheral vascular disease 2.8 (1.42–5.52) vs. 0.85 (0.76–0.94), atrial fibrillation 1.83 (1.09–3.08) vs. 0.86 (0.76–0.98), and lacunar infarction 2.23 (1.21–4.09) vs. 0.86 (0.77–0.96). Cox's multivariate analysis, also considering classical risk factors, indicated that this BAC was significantly and independently associated with survival (both cardiovascular event-free and specific survival; 1.94 (1.38–2.73) and 6.6 (2.4–18.4)). Conclusions: Our data confirm the strong association of BAC on mammograms and the development cardiovascular events, but also evidence the association of BAC with cardiovascular event-free and specific survival.

Keywords: breast arterial calcifications; cardiovascular risk; mammograms; risk assessment; prevention; cost effectiveness

Citation: Galiano, N.G.; Eiro, N.; Martín, A.; Fernández-Guinea, O.; Martínez, C.d.B.; Vizoso, F.J. Relationship between Arterial Calcifications on Mammograms and Cardiovascular Events: A Twenty-Three Year Follow-Up Retrospective Cohort Study. *Biomedicines* **2022**, *10*, 3227. https://doi.org/10.3390/biomedicines10123227

Academic Editors: Alfredo Caturano and Raffaele Galiero

Received: 9 November 2022
Accepted: 7 December 2022
Published: 12 December 2022

1. Introduction

Medicine needs to optimize health resources. In this way, mammograms represent the most valid test for detecting breast cancer, with good acceptance, minimal adverse effects, and low economic costs. Moreover, mammograms can recognize other morphological findings, such as breast arterial calcifications (BAC), the presence of which could predict cardiovascular risk [1]. BAC are a common finding on mammograms, seen as parallel radiopaque structures or tubular tracts frequently involving the entire circumference of the artery and easy to detect. The prevalence of BAC is estimated to be between 8.2% and 12% among women over 50 [1].

BAC correspond to the calcification of the arterial middle layer, or Mönckeberg's arteriosclerosis, an early histological change where vascular smooth muscle cells are similar to matrix bone, without macrophages and lipids [2,3].

As some studies have shown, there is an association between the presence of BAC and renal disease [4], stroke [5], peripheral vascular disease, low bone mass, carotid artery

narrowing and, mainly, coronary artery disease [6–10]. Several studies have shown a strong association between the presence of BAC and cardiovascular mortality [1,11–13]. It has been reported that the finding of BAC on mammograms of women under 59 years could be an additional risk factor for cardiovascular diseases [14], especially in diabetic patients [13]. Cardiovascular mortality increased by a 40% in women with BAC compared to women without BAC, reaching the 90% in diabetic women [1,12]. More recent studies confirm the evidence of a relationship between the presence of BAC and coronary disease in asymptomatic women [15,16].

We previously reported an association between BAC and biochemical markers of endothelial injury (higher serum levels of triglycerides, homocysteine, hs-CRP and an elevated LDL-C/HDL-C ratio (coronary risk index > 2)) [17] and between BAC and aged-related macular degeneration [18]. However, despite all of these data concerning the relationship between BAC and the occurrence of cardiovascular risk factors and cardiovascular disease, there is little information between this radiographic finding and the subsequent development of cardiovascular events and the associated mortality. Hence, the aim of the present study was to evaluate these clinical associations in a cohort of women after a long period of time.

2. Methods

2.1. Patient Selection

We conducted a retrospective cohort study in a regional hospital. Considering that BAC were not a commonly described finding in mammographic reports many years ago, we were able to carry out the present study with such a long follow-up period thanks to our previous works about the relationship between BAC and biochemical markers of endothelial injury [17]. In this prior study, we reviewed the mammograms of 1759 women, made between June 1996 and June 2004, in a screening breast cancer program. We detected BAC in 147 women. We contacted these patients between January and March 2021. A total of 19 cases were lost in the BAC female population; 10 women refused to communicate because of the anxiety caused by the pandemic circumstances, and 9 other candidates could not be located. Finally, a cohort of 128 women with BAC in the baseline mammograms or their families were contacted and agreed to participate in the present study, and they form the main study group. Due to difficulties in following up all initially studied subjects, an equal number of women without BAC were completed and selected from the initial population (1615 remaining women without BAC). There was an exact coincidence for mean age (the women without BAC age matched to the women with BAC) and a similar distribution for baseline clinical characteristics, such as hypertension, diabetes mellitus (DM), dyslipidemia (DL), or smoking, between both women groups. We investigated the evolution of all the women in terms of the development of cardiovascular events and their associated mortality over such a long time (a mean of 23 years of follow up, range 16–26 years, from June 1996 to March 2021).

2.2. Data Collection

BAC were identified as breast tissue opacities affecting all of circumference or seen as parallel tubular opacities. BAC was classified as present or absent, as recommended by the American College of Radiology for breast cancer screening [19]. None of these patients showed changes in the BAC status with regard to the latest mammogram, performed either 1 or 2 years earlier. Considering the long time of the study, we evaluate the initial analog mammography for classifying women as having BAC and not. Senographe 600T and Senographe 800T (0.3 mm focal spot and 0.1 mm for magnification) and Mamoray films, screens, and cassettes (18 cm $\times$ 24 cm) were used to perform mammography. To reduce scatter radiation, a grid was used to make a vigorous breast compression. Two basic projections (mediolateral oblique and craniocaudal views), on semiautomatic to automatic exposure mode applying 27 to 30 keV were performed. Additional projections and accessory magnification images were performed when needed. The mammography image was

reviewed by two expert radiologists (O.F.-G. and C.d.B.M.), independently, with extensive experience in this area. The reading was blinded for both of them; they had no knowledge about any clinical data. The concordance was greater than 95%. When there was a disagreement in their interpretation (present vs. absent), authors revised the image together to reach an agreement.

The baseline variables recovered were the age and clinical-pathological characteristics: hypertension, diabetes mellitus (DM), hypercholesterolemia (DL), smoking, cardiovascular diseases among first-degree relatives, weight, height, and body mass index. These same clinical variables were recorded from the medical health records of each woman at the end of the follow-up period. Hypertension was defined as a systolic blood pressure greater than 140 and diastolic blood pressure greater than 90 mmHg. The diagnostic criteria for DM were: random venous blood glucose greater than 200 mg/dL, associated with classic symptoms such as polyuria, polydipsia, polyphagia, weight loss, and asthenia; fasting venous blood glucose greater than 125 mg/dL; a glycosylated hemoglobin (HbA1c) greater than 6.5%, and a blood glucose level two hours after an oral glucose stress test greater than 200 mg/dL. A history of DL was considered if total blood cholesterol values were greater than 250 mg/dl and/or triglyceride values were greater than 200 mg/dl. We consider date on therapies. A history of cardiovascular risk or cardiovascular disease was considered as present if a woman was taking any medical treatment for that. Body mass index (BMI) was calculated as body weight in kilograms divided by height in squared meters (BMI = weight/height [2] (kg/m^2). Women were considered obese if BMI calculation was equal or greater than 30 kg/m^2. Women who smoke every day or stopped smoking less than 6 weeks before the study began were considered smokers.

The occurrence of cardiovascular diseases, such as ischemic, hypertensive, and valvular heart diseases, congestive heart failure, peripheral vascular disease (PVD), and cerebrovascular accident (ischemic, hemorrhagic, and lacunar infarction), were confirmed from the patient's medical history and considered as events during all the follow up period. The development of atrial fibrillation was also registered and included as an endpoint in consideration of its importance in the risk of sudden cardiac death [20]. We considered the date of the initial prescription. Both the events and the causes of death were extracted manually from the medical records where they are coded by the ICD-10 nomenclature.

2.3. Statistical Analysis

Statistical analysis was performed by N.E. using the SPSS for Windows software, version 25 (Chicago, Illinois). The sample size was calculated from the established population of women specifically studied for early breast cancer screening. The Kolmogorov–Smirnov test was used to determine data distribution. Non-normally distributed data are expressed as median-range, whereas categorical variables are displayed as numbers and percentages. There were no missing data. Non-parametric Mann–Whitney U tests were used to determine the differences between mean values for non-normally distributed variables. Since this is a cohort study, the risk ratio was used to comparatively evaluate the development of events in each group. For survival analysis Cox's univariate method was used. In the case of cardiovascular event-free survival analysis, the first cardiovascular event in each woman was considered as end-point, and we considered the time to event since the first mammography was performed. Cox's regression model was used to examine interactions of different risk factors in a multivariate analysis. Only factors that achieve statistical significance in the univariate analysis were included in the multivariate analysis (Cox's regression model). $p \leq 0.05$ was considered as significant. The significance level was stablished at level $p < 0.05$. The PASW (Predictive Analytics Software) statistics 18 program (SPSS Inc., Chicago, IL, USA) was used for all calculations.

2.4. Ethical Aspects

Following the guidelines of the Ethics Committee of our institution, in accordance with the Declaration of Helsinki, informed consent was obtained from each participant. The

family was contacted to sign the informed consent if the patient had cognitive impairment or had died. Accurate and complete information was gathered from interconnected electronic health records between the hospital and general primary care centers, preserving their confidentiality in accordance with institutional regulations. N.G.-G. was authorized to consult these records.

3. Results

3.1. Baseline Clinical Characteristics of the Patients and at the End of the Follow-Up Period

Table 1 shows clinical-pathological characteristics of 128 women in each group. The mean age at the baseline mammogram was 59 years (44–74) in the BAC group and 59.5 years (44–70) in the control group. Both groups displayed a similar distribution of classical cardiovascular risk factors, such as hypertension, DM, DL, obesity, and smoking.

Table 1. Clinical- pathological characteristics of the 128 patients in each group at the beginning and the end of the follow-up period.

	At the Beginning			**At the End of the Follow-Up Period**		
	Women with BAC (n = 128)	**Women without BAC (n = 128)**	***p* Value ***	**Women with BAC (n = 128)**	**Women without BAC (n = 128)**	***p* Value ***
Hypertension	38 (29.7%)	31 (24.2%)	0.398	101 (78.9%)	86 (67.2%)	0.049
Diabetes mellitus	9 (7%)	4 (3.1%)	0.255	36 (28.6%)	35 (27.3%)	0.938
Dyslipidemia	23 (18%)	34 (26.6%)	0.133	81 (63.3%)	81 (63.3%)	1.000
Obesity	35 (27.3%)	22 (17.2%)	0.071	47 (36.8%)	46 (35.9%)	1.000
Tobacco	3 (2.3%)	7 (5.5%)	0.333	n.a	n.a	-

BAC, breast arterial calcifications; Data are reported as number of cases (%) * Chi-squared test. n.a: not available.

Regarding the number of cardiovascular risk factors recorded between the two groups at the end of the 23-year follow-up period, no significant differences were found, except for hypertension (Table 1).

3.2. Development of Cardiovascular Events during the Follow-Up Period

Table 2 shows the number of cardiovascular events during the follow-up period of 23 years for each group. The identification of BAC in the baseline mammogram (Figure 1) was strongly associated with the incidence of cardiovascular events. Thus, a total of 88 (68.8%) women with BAC developed at least one of these events compared to 53 (41.4%) women in the BAC-free group. In addition, our data also shows significant differences between cardiovascular events-free survival curves calculated for both groups ($p < 0.0001$) (Figure 2A). Globally, over the follow-up period, the BAC group had a higher global incidence of cardiovascular events than women without BAC (total number: 232 vs. 102) ($p < 0.0001$) (Table 2). In the BAC group, 19 (14.8%) women had one event, 28 (21.9%) two events, 22 (17.2%) three events, and 21 (16.4%) four or five events, whereas in the BAC-free group, 21 (16.4%) women had one event, 22 (17.2%) two events, seven (5.5%) three events; and four women (3.1%) four events. In addition, as can be seen in Table 2, women with BAC had a higher relative risk (RR) of global cardiovascular events compared with women without BAC, as well as specifically for each event type. Women with BAC have a higher RR of developing ischemic heart disease, hypertensive heart disease, valvular heart disease, congestive heart failure, atrial fibrillation, PVD, and lacunar infarction, as well as higher mortality due to cardiovascular events (RR: 13.13 (1.84–238) vs. 0.61 (0.47–0.79)). However, we found no significant difference between the groups for ischemic or hemorrhagic cerebral events.

Table 2. Relative risk of the occurrence of cardiovascular events during the follow-up period in women with or without BAC.

	Women with BAC (n = 128)		**Women without BAC (n = 128)**	
Cardiovascular Events	**Nº (%) of Events (*)**	**RR (95% CI)**	**Nº (%) of Events (*)**	**RR (95% CI)**
Ischemic heart disease	26 (20.3)	3.25 (1.53–6.90)	8 (6.3)	0.85 (0.77–0.94)
Hypertensive heart disease	35 (27.3)	2.85 (1.59–5.09)	16 (12.5)	0.79 (0.69–0.89)
Valvular heart disease	37 (28.9)	2.19 (1.28–3.75)	13 (10.2)	0.83 (0.73–0.94)
Congestive heart failure	33 (25.8)	2.06 (1.19–3.56)	16 (12.5)	0.85 (0.75–0.96)
Atrial fibrillation	33 (25.8)	1.83 (1.09–3.08)	18 (14.1)	0.86 (0.76–0.98)
Peripheral vascular disease	28 (21.9)	2.8 (1.42–5.52)	10 (7.8)	0.85 (0.76–0.94)
Ischemic stroke	9 (7)	1.5 (0.55–4.09)	6 (4.7)	0.98 (0.92–1.04)
Hemorrhagic stroke	2 (1.6)	1.0 (0.14–6.99)	2 (1.6)	1.0 (0.97–1.03)
Lacunar infarction	29 (22.7)	2.23 (1.21–4.09)	13 (10.2)	0.86 (0.77–0.96)
Total events	232	1.66 (1.31–2.1)	102	0.53 (0.39–0.72)

BAC, Breast arterial calcification; Nº: number of events; RR, relative risk; CI; confidence interval. (*) Note that a woman may have had more than one event during the follow-up period.

Figure 1. Mammogram showing breast arterial calcifications (rows).

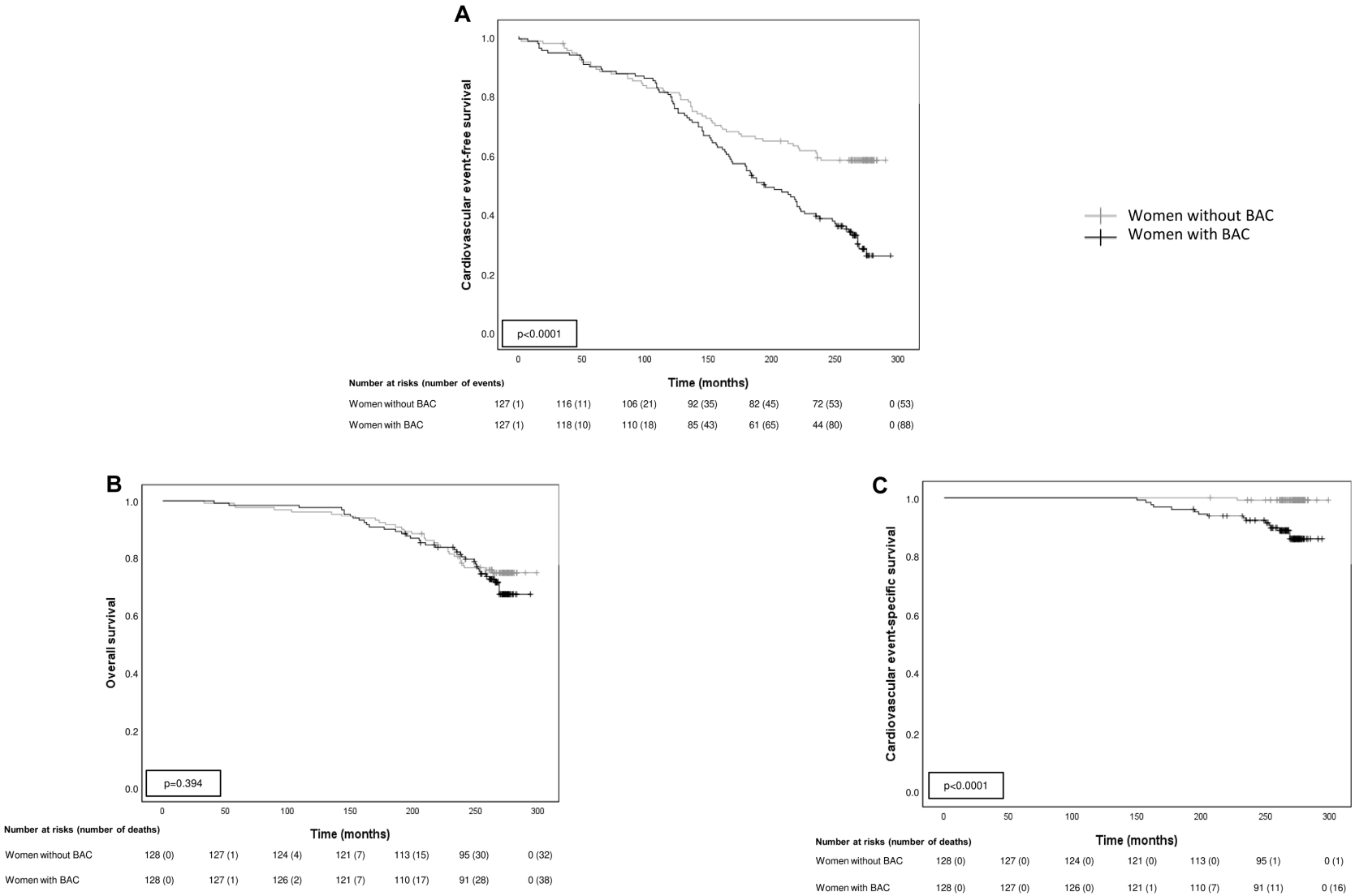

Figure 2. Kaplan-Meier survival curves. (**A**) Kaplan-Meier cardiovascular events-free survival curve as a function of patients with or without BAC. Kaplan-Meier survival curve as a function of patients with or without BAC. (**B**) overall survival and (**C**) cardiovascular event-specific survival.

3.3. BAC Influence on Survival

During the study period, there were 38 deaths (29.7%) in the BAC group and 32 (25%) in the BAC-free group (Figure 2B-overall survival curve). Nevertheless, as illustrated in Figure 2C, there were significant differences between cardiovascular event-specific survival curves calculated for both patient groups ($p < 0.0001$). There was a higher number of deaths because of cardiovascular events in women with BAC (16 (42.1%) vs. 1 (3.1%)) (Figure 3). There were no statistically significant differences between the age of death in both groups ($p = 0.706$).

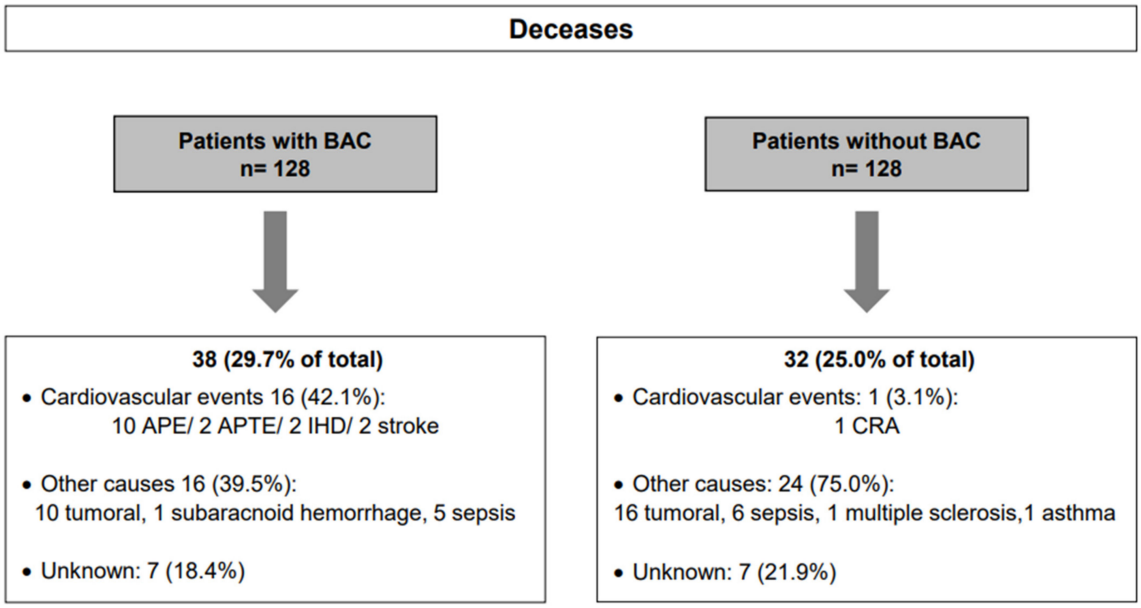

Figure 3. Overview of deceases and causes in patients with or without BAC. BAC: Breast arterial calcification, APE: Acute pulmonary edema; APTE: Acute pulmonary thromboembolism; IHD: Ischemic heart disease; CRA: Cardiorespiratory arrest.

Table 3 shows Cox's multivariate (hazard ratio) analysis of the relationship between classical cardiovascular risk factors present at the baseline study, cardiovascular event-free survival, and cardiovascular event-specific survival. The results show that DM and BAC were significantly and independently associated with both survival analysis, whereas hypertension was also significantly and independently associated with event-specific survival. This analysis also demonstrated that BAC was a significant and independent factor to predict both survival variables.

Table 3. Multivariate analysis of the relationship of classical risk factors at the beginning of the study and BAC with cardiovascular event-free and cardiovascular event-specific survival.

		Cardiovascular Event-Free Survival		Cardiovascular Event-Specific Survival	
Risk Factors	**N° of Women**	**Event Frecuency**	**HR (95% CI)**	**Event Frecuency**	**HR (95% CI)**
BAC/no BAC	128/128	88/53	1.9 (1.3–2.7) ***	16/1	14.1 (1.9–107.6) **
Hypertension/ no Hypertension	69/187	38/103	-	11/6	6.6 (2.4–18.4) ***
DL/no DL	57/199	30/111	-	2/15	-
DM/no DM	13/243	12/129	2.6 (1.4–4.8) **	3/14	4.9 (1.4–17.9) *
Obesity/no Obesity	57/199	33/108	-	4/13	-
Tobacco/no tobacco	10/246	7/134	-	0/17	-

BAC, breast arterial calcifications; DL, dyslipidemia; DM, diabetes mellitus; HR, hazard ratio; CI, confidence interval. Only the first event was considered for every woman. * $p < 0.05$; ** $p < 0.005$; *** $p < 0.0001$.

4. Discussion

This is one of the first studies evaluating, over such a long period of time, the impact of BAC for the development of cardiovascular events and their associated mortality in a cohort of women studied specifically for its radiological finding. Our results, showing a very strong and positive association between BAC, cardiovascular events and associated mortality, are consistent with previous studies [21,22]. Even the association between BAC and coronary artery disease was stronger compared with traditional Framinghan risk factors [23]. In accordance with this, Chadashvili et al. found out that BAC predicted a coronary artery calcium score over 11, which indicates a moderate or severe risk of developing coronary artery disease [7]. In addition, recent data from over 45-year-old women show a significant correlation between the severity of BAC and the extent of coronary artery disease (verified by coronary angiography defined by the SYNTAX classification) [24]. On the other hand, in our study, the presence of BAC at the baseline mammogram was also very positively and strongly associated with other cardiovascular events, such as valvular disease, heart failure, PVD, and cerebral lacunar infarction, as well as atrial fibrillation, compared to the control group. All these events in the group of women with BAC were not influenced by the emergence of new risk factors throughout the 23 years of follow-up, except for hypertension. In accordance with these findings, our results indicate that BAC was an independent prognostic factor to predict not only the development of cardiovascular events, but also a higher probability of derived death.

Recently, Iribarren et al. reported the results of a similar study but after a mean follow-up of 6.5 years [16]. They noticed a higher global cardiovascular events among women with BAC than those without BAC, statistically significantly ($p \leq 0.04$) for ischemic stroke, cardiovascular death, cerebrovascular disease, cardiomyopathy, deep venous thrombosis/pulmonary embolism, peripheral arterial disease, and retinal vascular occlusion. However, while in their study there was no clear separation of survival curves between the two groups, we found significant differences ($p < 0.0001$), with a higher number of deaths from cardiovascular outcomes in women with BAC (16 (42.1%) vs. 1 (3.1%)), probably due to the longer follow-up period. On the other hand, although women without BAC had similar baseline classical risk factors compared with women with BAC, our data show that they develop less frequently hypertension at the end of the follow-up period ($p = 0.049$) compared with women with BAC. This finding could contribute to some protection against cardiovascular events. Nevertheless, further investigation might to identify other protective factors in these women without BAC.

The findings of the present study are particularly relevant considering that cardiovascular diseases are the leading cause of mortality worldwide. It is estimated that by 2030, approximately 23.3 million people will die from cardiovascular diseases. In addition, it is relevant to consider that coronary disease is the main cause of death among women, as well as this process has a worse prognosis than for men [21]. Therefore, quantifying the importance of cardiovascular diseases and their main risk factors is an essential aspect of proper planning of existing health resources, since nearly 50% of cardiovascular mortality reductions are due to the control of its major risk factors. However, the problem is that many patients ignore that they suffer from any of these disorders, such as 50% of hypercholesterolemic, a third of hypertensive, or 20% of diabetics. Therefore, the BAC detected by mammography could represent a diagnostic axis on which to focus cardiovascular disease prevention policies.

Mammography, reflecting the composition of a part of the human tissues, offers us the possibility to use this diagnostic platform to recognize another morphological finding of interest that is not usually recorded in mammographic reports, such as BAC. In addition, there are data which support a stronger association between BAC and cardiovascular mortality, compared to arterial calcification in other locations, such as aortic, splenic, internal and external iliac, detected by computed tomography [8]. Millions of women worldwide undergo a mammogram annually or biannually. Correspondingly, there is a large amount of available data in digital files from studies which could be already

conducted. The tools of current computer applications and modern artificial intelligence makes easier to manage all these massive digital data. Combined with clinical data, it could help us to create different universal algorithms to identify women who may benefit from therapeutic or preventive health measures. On the other hand, there are other possibilities for using resources based on the associations previously described for BAC, such as the possibility of identifying women with low bone mass [24], predicting the course of chronic kidney disease [25], or the cardiotoxic effect of anthracycline- derived agents, trastuzumab, and radiotherapy in the treatment of breast cancer [26].

Limitations of our study are its retrospective design and the use of historical analog mammography, which prevented us from refining tiny details of the calcifications evaluated by the radiologist. However, these circumstances allowed us to track women time enough to properly assess the impact of BAC on the development of cardiovascular events. Futures studies with higher number of women and new technologies, such as digital mammograms or tomosynthesis, may contribute to improving BAC evaluation, e.g., in terms of bilaterality, number, and intensity (mild, moderate or severe). On the other hand, to avoid depending only on radiologists and their eye-observation, we need new methods of BAC quantification in order to perform a better radiological identification [27]. In this way, we could predict exactly the risk of cardiovascular disease and define better individualized preventive actions [27]. Along the same lines, AlGhamdi et al. [28] recently presented a model of deep neural network (deep learning) capable of accurately detecting BAC in mammograms, which can be used to automatically mark calcifications on the original image. The results exhibit a more accurate assessment of BAC than expert radiologists, with fewer mistakes.

Our results point to the importance of BAC on mammograms to identify women with increased cardiovascular risk and death. This may bring us the opportunity to improve preventive cardiovascular measures.

Author Contributions: F.J.V. conceptualized, designed, and supervised the study, N.G.-G. collected the data. N.G.-G. and N.E. analyzed the data and completed the statistical analysis. F.J.V. wrote the original draft. N.G.-G., A.M., and N.E. translated, reviewed, and edited the manuscript. All authors have read and accepted the final version of the manuscript. O.F.-G. and C.d.B.M. were responsible for executing and evaluating mammograms. All authors have read and agreed to the published version of the manuscript.

Funding: This study had no source of funding. The corresponding author had complete access to all data and the ultimate responsibility of submitting them for publication.

Institutional Review Board Statement: The study was conducted in accordance with the Declaration of Helsinki, and approved by the Ethics Committee of Fundación Hospital de Jove (PI06-2020; approved on 20 January 2021).

Informed Consent Statement: Informed consent was obtained from all subjects involved in the study.

Data Availability Statement: Data available on request.

Acknowledgments: The authors are enormously grateful to the study participants. Thanks to our previously published works on the subject, we have been able to carry out this study with such a long follow-up, so we are also grateful for the previous work of our colleagues of the Research Unit.

Conflicts of Interest: The author reports no conflict of interest in this work.

Abbreviations

A.M., Arancha Martín; APE, Acute pulmonary edema; APTE, Acute pulmonary thromboembolism; BAC, Breast arterial calcification; BMI, Body mass index; C.d.B.M., Covadonga del Blanco Martínez; COVID-19, Coronavirus Disease-2019; CRA, Cardiorespiratory arrest; CVRF, Cardiovascular risk factors; DL, Dyslipidemia; DM, Diabetes Mellitus; HBP, High blood pressure; IHD, Ischemic heart disease; LDL-C, Low-density lipoprotein cholesterol; N.E., Noemi Eiro; N.G.-G., Natalia González-Galiano; O.F.-G., Oscar Fernández-Guinea; PVD, Peripheral vascular disease; SPSS, Statistical Package for the Social Sciences.

References

1. Kemmeren, J.M.; van Noord, P.A.; Beijerinck, D.; Fracheboud, J.; Banga, J.D.; van der Graaf, Y. Arterial calcification found on breast cancer screening mammograms and cardiovascular mortality in women: The DOM Project. Doorlopend Onderzoek Morbiditeit en Mortaliteit. *Am. J. Epidemiol.* **1998**, *147*, 333–341. [CrossRef]
2. Wallin, R.; Wajih, N.; Greenwood, G.T.; Sane, D.C. Arterial calcification: A review of mechanisms, animal models, and the prospects for therapy. *Med. Res. Rev.* **2001**, *21*, 274–301. [CrossRef]
3. Wang, Q.; Jin, L.; Wang, H.; Tai, S.; Liu, H.; Zhang, D. AWRK6, A Synthetic Cationic Peptide Derived from Antimicrobial Peptide Dybowskin-2CDYa, Inhibits Lipopolysaccharide-Induced Inflammatory Response. *Int. J. Mol. Sci.* **2018**, *19*, 600. [CrossRef]
4. Abou-Hassan, N.; Tantisattamo, E.; D'Orsi, E.T.; O'Neill, W.C. The clinical significance of medial arterial calcification in end-stage renal disease in women. *Kidney Int.* **2015**, *87*, 195–199. [CrossRef]
5. Ahn, K.J.; Kim, Y.J.; Cho, H.J.; Yim, H.W.; Kang, B.J.; Kim, S.H.; Kim, H.S.; Kim, K.T.; Lee, J.H.; Whang, I.Y. Correlation between breast arterial calcification detected on mammography and cerebral artery disease. *Arch. Gynecol. Obstet.* **2011**, *284*, 957–964. [CrossRef]
6. Jiang, X.; Clark, M.; Singh, R.K.; Juhn, A.; Schnatz, P.F. Association of breast arterial calcification with stroke and angiographically proven coronary artery disease: A meta-analysis. *Menopause* **2015**, *22*, 136–143. [CrossRef] [PubMed]
7. Chadashvili, T.; Litmanovich, D.; Hall, F.; Slanetz, P.J. Do breast arterial calcifications on mammography predict elevated risk of coronary artery disease? *Eur. J. Radiol.* **2016**, *85*, 1121–1124. [CrossRef]
8. Soylu, A.; Soylu, K.; Aydın, R.; Uzunkaya, F.; Aslan, K.; Polat, A.V. Calcification of breast artery as detected by mammography: Association with coronary and aortic calcification. *Turk. J. Med. Sci.* **2019**, *49*, 190–197. [CrossRef]
9. McLenachan, S.; Camilleri, F.; Smith, M.; Newby, D.E.; Williams, M.C. Breast arterial calcification on mammography and risk of coronary artery disease: A SCOT-HEART sub-study. *Clin. Radiol.* **2019**, *74*, 421–428. [CrossRef]
10. Fathala, A.L.; Alabdulkarim, F.M.; Shoukri, M.; Alanazi, M. Association between breast arterial calcifications found on mammography and coronary artery calcifications in asymptomatic Saudi women. *Ann. Saudi. Med.* **2018**, *38*, 433–438. [CrossRef] [PubMed]
11. van Noord, P.A.; Beijerinck, D.; Kemmeren, J.M.; van der Graaf, Y. Mammograms may convey more than breast cancer risk: Breast arterial calcification and arterio-sclerotic related diseases in women of the DOM cohort. *Eur. J. Cancer Prev.* **1996**, *5*, 483–487. [PubMed]
12. Kemmeren, J.M.; Beijerinck, D.; van Noord, P.A.; Banga, J.D.; Deurenberg, J.J.; Pameijer, F.A.; van der Graaf, Y. Breast arterial calcifications: Association with diabetes mellitus and cardiovascular mortality. Work in progress. *Radiology* **1996**, *201*, 75–78. [CrossRef] [PubMed]
13. Moshyedi, A.C.; Puthawala, A.H.; Kurland, R.J.; O'Leary, D.H. Breast arterial calcification: Association with coronary artery disease. Work in progress. *Radiology* **1995**, *194*, 181–183. [CrossRef]
14. de Waard, F.; Collette, H.J.; Rombach, J.J.; Baanders-van Halewijn, E.A.; Honing, C. The DOM project for the early detection of breast cancer, Utrecht, The Netherlands. *J. Chronic. Dis.* **1984**, *37*, 1–44. [CrossRef]
15. Gennarelli, M.; Jedynak, A.; Forman, L.; Wold, E.; Newman, R.B.; Dhand, A.; Kapoor, A.; Jafri, F.; Pal, S.; Pandav, J.; et al. The potential impact of mammographic breast arterial calcification on physician practices in a primary care setting. *Future Cardiol.* **2021**, *17*, 7. [CrossRef]
16. Iribarren, C.; Chandra, M.; Lee, C.; Sanchez, G.; Sam, D.L.; Azamian, F.F.; Cho, H.M.; Ding, H.; Wong, N.D.; Molloi, S. Breast Arterial Calcification: A Novel Cardiovascular Risk Enhancer Among Postmenopausal Women. *Circ. Cardiovasc. Imaging* **2022**, *15*, e013526. [CrossRef]
17. Pidal, D.; Sánchez Vidal, M.T.; Rodríguez, J.C.; Corte, M.D.; Pravia, P.; Guinea, O.; Pidal, I.; Bongera, M.; Escribano, D.; González, L.O.; et al. Relationship between arterial vascular calcifications seen on screening mammograms and biochemical markers of endothelial injury. *Eur. J. Radiol.* **2009**, *69*, 87–92. [CrossRef]
18. Saá, J.; Fernández-Guinea, O.; García-Pravia, P.; Fernandez-Garcia, B.; Eiró, N.; del Casar, J.M.; Venta, R.; Baamonde, B.; Vizoso, F.J. Relationship between breast arterial calcifications seen on screening mammograms and age-related macular degeneration. *Acta Ophthalmol.* **2014**, *92*, e582–e584. [CrossRef]
19. Brown, A.L.; Wahab, R.A.; Zhang, B.; Smetherman, D.H.; Mahoney, M.C. Reporting and Perceptions of Breast Arterial Calcification on Mammography: A Survey of ACR Radiologists. *Acad Radiol* **2022**, *29* (Suppl. 1), S192–S198. [CrossRef]
20. Chen, L.Y.; Sotoodehnia, N.; Buzkova, P.; Lopez, F.L.; Yee, L.M.; Heckbert, S.R.; Prineas, R.; Soliman, E.Z.; Adabag, S.; Konety, S.; et al. Atrial fibrillation and the risk of sudden cardiac death: The atherosclerosis risk in communities study and cardiovascular health study. *JAMA Intern. Med.* **2013**, *173*, 29–35. [CrossRef]
21. Coronado, B.E.; Griffith, J.L.; Beshansky, J.R.; Selker, H.P. Hospital mortality in women and men with acute cardiac ischemia: A prospective multicenter study. *J. Am. Coll. Cardiol.* **1997**, *29*, 1490–1496. [CrossRef] [PubMed]
22. Margolies, L.; Salvatore, M.; Hecht, H.S.; Kotkin, S.; Yip, R.; Baber, U.; Bishay, V.; Narula, J.; Yankelevitz, D.; Henschke, C. Digital Mammography and Screening for Coronary Artery Disease. *JACC Cardiovasc. Imaging* **2016**, *9*, 350–360. [CrossRef] [PubMed]
23. Ružičić, D.; Dobrić, M.; Vuković, M.; Hrnčić, D.; Đorđević, S.; Ružičić, M.; Aleksandrić, S.; Đorđević-Dikić, A.; Beleslin, B. The correlation of SYNTAX score by coronary angiography with breast arterial calcification by digital mammography. *Clin. Radiol.* **2018**, *73*, 454–459. [CrossRef] [PubMed]

24. Yoon, Y.E.; Kim, K.M.; Han, J.S.; Kang, S.H.; Chun, E.J.; Ahn, S.; Kim, S.M.; Choi, S.I.; Yun, B.; Suh, J.W. Prediction of Subclinical Coronary Artery Disease With Breast Arterial Calcification and Low Bone Mass in Asymptomatic Women: Registry for the Women Health Cohort for the BBC Study. *JACC Cardiovasc. Imaging* **2019**, *12*, 1202–1211. [CrossRef] [PubMed]
25. Disthabanchong, S.; Boongird, S. Role of different imaging modalities of vascular calcification in predicting outcomes in chronic kidney disease. *World J. Nephrol.* **2017**, *6*, 100–110. [CrossRef] [PubMed]
26. Gernaat, S.A.M.; van Velzen, S.G.M.; Koh, V.; Emaus, M.J.; Išgum, I.; Lessmann, N.; Moes, S.; Jacobson, A.; Tan, P.W.; Grobbee, D.E.; et al. Automatic quantification of calcifications in the coronary arteries and thoracic aorta on radiotherapy planning CT scans of Western and Asian breast cancer patients. *Radiother. Oncol.* **2018**, *127*, 487–492. [CrossRef] [PubMed]
27. Trimboli, R.M.; Codari, M.; Guazzi, M.; Sardanelli, F. Screening mammography beyond breast cancer: Breast arterial calcifications as a sex-specific biomarker of cardiovascular risk. *Eur. J. Radiol.* **2019**, *119*, 108636. [CrossRef] [PubMed]
28. AlGhamdi, M.; Abdel-Mottaleb, M.; Collado-Mesa, F. DU-Net: Convolutional Network for the Detection of Arterial Calcifications in Mammograms. *IEEE Trans. Med. Imaging* **2020**, *39*, 3240–3249. [CrossRef]

biomedicines

MDPI

Review

Novel Therapies for the Treatment of Cardiac Fibrosis Following Myocardial Infarction

Kamila Raziyeva, Yevgeniy Kim, Zharylkasyn Zharkinbekov, Kamila Temirkhanova and Arman Saparov *

Department of Medicine, School of Medicine, Nazarbayev University, Nur-Sultan 010000, Kazakhstan
* Correspondence: asaparov@nu.edu.kz

Abstract: Cardiac fibrosis is a common pathological consequence of most myocardial diseases. It is associated with the excessive accumulation of extracellular matrix proteins as well as fibroblast differentiation into myofibroblasts in the cardiac interstitium. This structural remodeling often results in myocardial dysfunctions such as arrhythmias and impaired systolic function in patients with heart conditions, ultimately leading to heart failure and death. An understanding of the precise mechanisms of cardiac fibrosis is still limited due to the numerous signaling pathways, cells, and mediators involved in the process. This review article will focus on the pathophysiological processes associated with the development of cardiac fibrosis. In addition, it will summarize the novel strategies for anti-fibrotic therapies such as epigenetic modifications, miRNAs, and CRISPR technologies as well as various medications in cellular and animal models.

Keywords: cardiac fibrosis; scar tissue; anti-fibrotic therapies; cardiovascular diseases; myofibroblasts

Citation: Raziyeva, K.; Kim, Y.; Zharkinbekov, Z.; Temirkhanova, K.; Saparov, A. Novel Therapies for the Treatment of Cardiac Fibrosis Following Myocardial Infarction. *Biomedicines* **2022**, *10*, 2178. https://doi.org/10.3390/biomedicines10092178

Academic Editors: Alfredo Caturano and Raffaele Galiero

Received: 12 July 2022
Accepted: 22 August 2022
Published: 2 September 2022

1. Introduction

Cardiovascular diseases (CVDs) include all heart and vessel related disorders such as coronary heart disease, cerebrovascular disease, rheumatic heart disease, peripheral artery diseases, and other conditions. Currently, CVDs are among the major causes of death worldwide [1]. According to the World Health Organization, approximately eighteen million people die from cardiac disorders every year, which is equivalent to 39% and 45% of all deaths in the male and female populations, respectively [2]. Recent data from Public Health England shows that high-income countries spend GBP 7.4 billion yearly on CVD treatment. Overall, the forecast for the impact of CVDs on the economy worldwide is disappointing. In the U.S. alone, costs for CVDs are predicted to rise from USD 555 billion in 2015 to USD 1.1 trillion in 2035 [2]. Therefore, developing new advanced approaches and therapies to treat CVDs is of great demand. Importantly, the majority of CVDs result in myocardial fibrosis, which in turn impairs heart function and drastically aggravates cardiac morbidity and mortality.

The term "fibrosis" describes the pathological reparative process occurring in all tissues in the body. It is characterized by the excessive deposition and impaired degradation of extracellular matrix (ECM) proteins, leading to tissue thickness and abnormal tissue remodeling [3]. The main outcomes of fibrosis are rapid wound healing and the reduction in adverse immune responses following injury and infection as well as re-epithelialization and the protection of injured tissue from contaminants. However, fast repair results in the loss of proper anatomy and thus proper functions of the tissue [4]. The formed scar area in the heart is not functional, as cells that replace cardiomyocytes lack a contractile function.

The leading cause of cardiac fibrosis is myocardial infarction (MI) because an adult mammalian heart has limited regenerative capacity following a myocardial injury [5,6]. During MI, dying cardiomyocytes are substituted with a collagen scar, resulting in impaired contractile and mechano-electric functions [7]. Apart from MI, several other pathological cardiac dysfunctions also induce excessive collagen deposition [8]. For example, progressive fibrosis is observed in elderly people and is associated with the development

of diastolic heart failure. Myocardial fibrosis can also be formed as a result of persistent pressure load caused by hypertensive heart disease. In addition, hypertrophic cardiomyopathy, idiopathic dilated cardiomyopathy, and metabolic failures are also associated with fibrosis in human and animal models [9–11]. Nevertheless, regardless of the nature of the injury, any damage to the heart causes a fibrotic response, which results in cardiac tissue remodeling and dysfunction.

The process of scar formation is orchestrated by a number of cells such as cardiomyocytes, cardiac fibroblasts, endothelial cells, and immune cells [12–14]. These cells and their secreted products activate a series of pathways and induce the secretion of paracrine factors, resulting in collagen deposition and myofibroblast transdifferentiation, the two major pathological hallmarks of cardiac fibrosis [15]. Overall, scar formation at the place of necrotic cardiomyocytes leads to myocardial dysfunction and arrhythmia, which increases the risk of tissue rupture and the death of patients with various cardiac conditions [16]. At this time, the precise mechanisms of cardiac fibrosis are still not fully deciphered. The process is complex and requires additional knowledge of the exact mechanisms of cardiac fibroblast activation and their interaction with other cells to understand whether there is a possibility of disabling these cells or modifying their functions during fibrosis [12,17]. Another challenge is the limited potential of the heart to self-regenerate. For example, as much as 25% of cardiomyocytes in the left ventricle die due to acute myocardial injury [18,19]. The inability of cardiomyocytes to proliferate in an adult heart makes it impossible to use therapies directed to totally block scar formation, as there will be no cardiac cells to replenish the lost muscle mass. In addition, the environment after heart injury is highly reactive with a large number of dying cardiac cells and infiltrating immune cells that also make the use of anti-fibrotic drugs challenging.

Overall, the consequences of fibrotic tissue formation on myocardial functions are severe, therefore, understanding the mechanisms of cardiac fibrosis and discovering new potential targets for its therapy may introduce new perspectives for the clinical treatment of heart failure. This manuscript will review the molecular mechanism of scar formation and will focus on novel therapies including epigenetic, clustered regularly interspaced short palindromic repeats (CRISPR), microRNAs (miRNAs), and recent medications directed to treat cardiac fibrosis.

2. Cardiac Fibrosis

Cardiac fibrosis is a condition acquired as a result of various heart diseases, including MI, myocarditis, hypertrophy, hypertension, and dilated cardiomyopathy [20,21]. Cellular mechanisms and molecular pathways are common for cardiac fibrosis caused by various disorders. However, their contributions are relatively different due to the specific alterations occurring in cells during various injuries. Overall, the development of fibrosis in the heart is similar to other tissues in the body. It is characterized by the overproduction and impaired degradation of ECM proteins and the accumulation of myofibroblasts [22]. This, in turn, leads to a change in normal cardiac morphology and functions as well as mechano-electric coupling, resulting in increased left ventricular stiffness, delayed systole–diastole cycle, and arrhythmias [13].

There are three types of cardiac fibrosis: replacement fibrosis, when fibrotic tissue substitutes dead cardiomyocytes; reactive fibrosis, featured by the diffuse distribution of collagen in the ECM; and infiltrative fibrosis, presented by the induced deposition of insoluble amyloid, iron, or glycosphingolipids in the heart [23,24]. Replacement fibrosis, which is associated with the loss of healthy cardiomyocytes, keeps the anatomical integrity of the ventricles. In contrast, reactive fibrosis is not related to the death of cardiomyocytes and is rather stimulated by chronic forces such as hemodynamic stress and inflammation, resulting in mechanical stiffness of the myocardial tissue [25]. Thus, although reactive fibrosis is a protective mechanism against raised wall stress, it leads to consequences such as cardiac systolic and diastolic dysfunction, arrhythmias and metabolic impairment, and is associated with a pathological state of fibrosis [26]. Cardiac amyloids, which induces the

formation of infiltrative fibrosis in the heart, are pathological extracellular proteins with a stable and fibrous structure. Amyloid fibrils are formed in multiple tissues in the body including the liver, eyes, kidney, and heart [27]. Among all of them, the most important amyloids in the myocardium are transthyretin (TTR) and immunoglobulin light chains [28]. Their deposition into cardiac tissue damages the heart functions by reducing myocardial contractile function and electrical conduction [24].

There are pro- and anti-fibrotic factors that include cytokines, chemokines, hormones, growth factors, and proteases that shift the balance in ECM component production by activating and stimulating myofibroblasts [29]. In turn, secretomes released from myofibroblasts in a paracrine manner stimulate cardiomyocyte hypertrophy, which also leads to decreased capillary density [20]. In particular, massive cardiomyocyte death leads to fibroblast proliferation and differentiation either via direct activation by cell signaling proteins such as miRNAs and matrix metalloproteinases (MMPs) or indirect activation by pro-fibrotic factors produced by endothelial, epithelial, and inflammatory cells [23]. After the death of cardiomyocytes, three overlapping stages, namely, the inflammatory, the proliferative, and the maturation phases, are activated (Figure 1) [30]. Thus, within the first few hours after heart injury, the process of inflammation is initiated: damage-associated molecular pattern (DAMP) signals from dying necrotic cardiomyocytes activate innate immune pathways such as nuclear factor kappa B (NF-kB), leading to the secretion of cytokines and chemokines including IL-1, IL-8, CCL2/MCP-1, and CXCL8 by resident myocardial cells and the infiltration of leukocytes to the damaged area [31]. When the injury is cleared from phagocytosing dead cells and matrix debris, the process is followed by the termination of leukocyte infiltration and their apoptosis in a wound area as well as the secretion of anti-inflammatory molecules such as interleukin-10 (IL-10) and transforming growth factor-β (TGF-β) by macrophages and lymphocytes, which is required for proper transition to the next step and is crucial to avoid left ventricular dilatation [32,33]. The hallmark of the end of the inflammatory phase is the infiltration of the infarct zone with fibroblasts and endothelial cells.

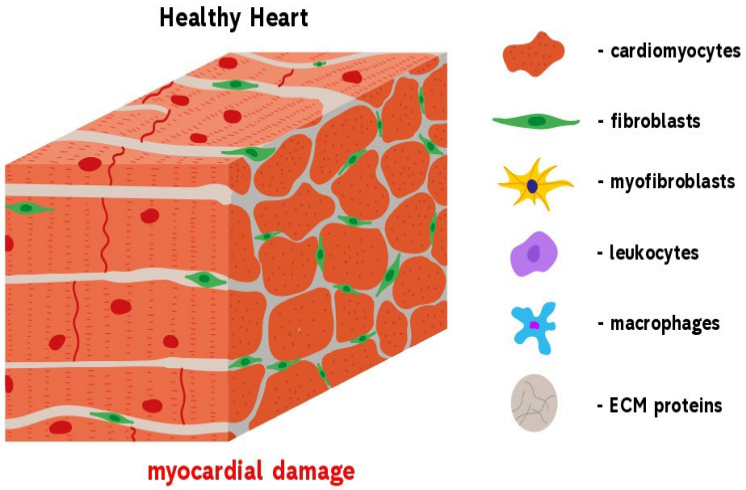

Figure 1. *Cont.*

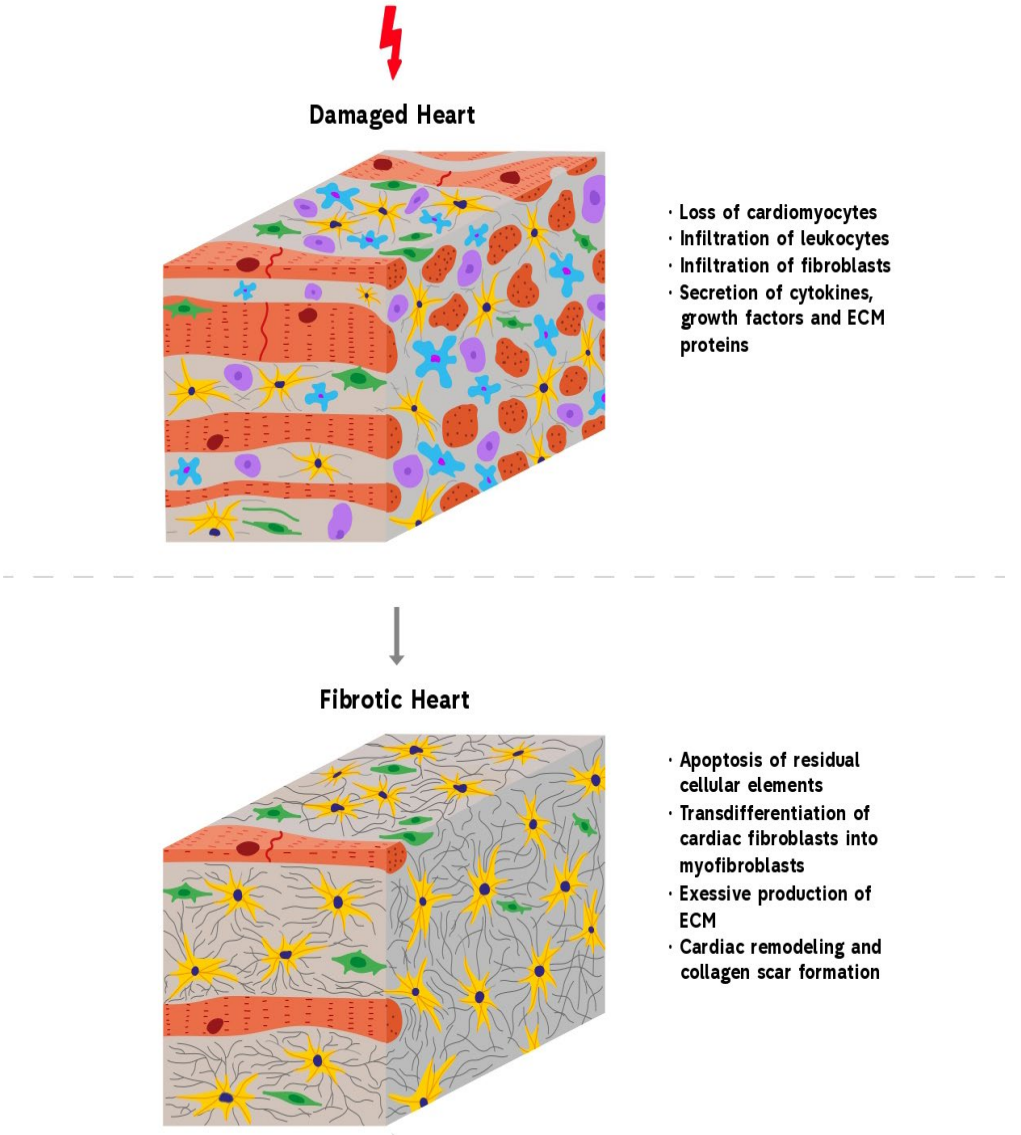

Figure 1. Development of reparative fibrosis in the heart. A healthy heart contains cardiomyocytes that are mainly involved in the contractile function of the heart. An injury to the heart results in myocardial damage. This activates repair mechanisms, leading to the formation of fibrosis. Heart trauma causes the death of cardiomyocytes that express DAMP molecules and by this induce the infiltration of leukocytes and fibroblasts into the damaged area. At the same time, cardiac fibroblasts begin to trans-differentiate into pathological myofibroblasts which, in turn, begin the over-production of ECM proteins. When the wound is cleared from phagocytosing dead cells and matrix debris, resident cells undergo apoptosis and the collagen-based scar is formed.

In the next proliferative phase, which usually lasts from a few days to a month, the immune cells such as macrophages, mast cells, and lymphocytes are recruited [34]. They secrete mediators including cytokines, growth factors, and matricellular proteins that initiate transdifferentiation of cardiac fibroblasts into myofibroblasts, whose functions include the change in cell proliferation and migration, the expression of ECM proteins, and the secretion of bioactive molecules [35].

In normal conditions, the heart is composed of endothelial cells, vascular smooth muscle cells, fibroblasts, and cardiomyocytes. The number and proportion of these cells depend on gender, age, and species [20]. For example, a murine heart contains 45% of endothelial cells, 30% of cardiomyocytes, 11% of fibroblasts, 8% of pericytes, and 6% of immune cells [36]. However, an injury can cause the transdifferentiation of cardiac

fibroblasts into myofibroblasts. Myofibroblasts have features of both fibroblasts and smooth muscle cells and are normally absent in healthy myocardium [36]. They regulate the production of ECM such as collagen types I and III [37,38]. An excessive production of ECM by myofibroblasts leads to cardiac remodeling [37]. Furthermore, myofibroblasts replace cardiomyocytes that irreversibly die within a few days after the damage, and form scar tissue in the place of injury [17]. Myofibroblast transdifferentiation is a multi-step process, consisting of the development of proto-myofibroblasts, their delivery into the site of lesion, and finally, complete maturation into myofibroblasts [20]. The key feature of mature myofibroblasts is the secretion of α-SMA [37]. The differentiation process is regulated by various cytokines and other signaling molecules such as TGF-β, tumor necrosis factor-α (TNF-α), connective tissue growth factor (CTGF), renin–angiotensin–aldosterone system (RAAS), galectin-3 (Gal-3), endothelin, and IL-11 [23]. Aside from cardiac fibroblasts, other cell types including hematopoietic progenitor cells, pericytes, endothelial, and epithelial cells also show an ability to transdifferentiate into myofibroblasts, however, their role in fibrosis development is unclear [36].

Other cell types including endothelial cells, pericytes, smooth muscle cells, and cardiomyocytes are also involved in the proliferative phase [39]. Activated and proliferated fibroblasts initiate the angiogenic processes by supplying the injured area with oxygen and nutrients and form an extensive vascular network. The proliferation phase is terminated by the release of anti-fibrotic mediators such as IFN-γ, angiotensin AT2-receptor, and CXCL10 to terminate the fibrotic tissue formation [40].

In the final maturation phase, the residual cellular elements including fibroblasts and vascular cells undergo apoptosis in the injured area and the collagen-based scar itself is fully formed (Figure 1). The surrounding tissue is filled with local fibroblasts that constantly respond to morphologically altered infarct zones, where the pressure and volume loads produce activation signals, resulting in the additional production of ECM proteins by local fibroblasts [41]. Over time, myofibroblasts, which secrete ECM proteins to form the scar, transform into matrifibrocytes. Matrifibrocytes secrete cartilage oligomeric matrix proteins and thus support mature scars [42]. Overall, scar formation is a multistep process that involves various cells including infiltrated macrophages, endothelial cells, and lymphocytes as well as transdifferentiated cardiac fibroblasts.

3. Molecular Mechanisms of Cardiac Fibrosis

A number of molecular pathways are involved in the pathogenesis of myocardial fibrosis [43]. This, in turn, creates obstacles in the full understanding of the precise mechanisms occurring in this pathological process. Various tools are now implicated in the understanding of the nature of fibrosis including high-throughput genomic and transcriptomic strategies and studies on cell and animal models.

A number of molecular pathways are involved in the pathogenesis of myocardial fibrosis [43]. The TGF-β and WNT signaling pathways, which act as pro-fibrotic mediators in fibrosis formation, are activated in myofibroblasts [20]. Platelet-derived growth factor is also involved in the activation of fibroblasts via the regulation of matrix deposition, pericyte recruitment, and vascular migration [44]. The two critical fibrotic mediators are TGF-β and angiotensin. They stimulate transdifferentiation of cardiac fibroblasts into myofibroblasts and promote the synthesis of collagen in the infarct zone, resulting in repair of the injured site.

3.1. The Role of TGF-β in Cardiac Fibrosis

Two main features of cardiac fibrosis include the breakdown of a normal myocardial structure and the overproduction of ECM proteins [45]. The modulation of several growth factor expressions by silencing genes responsible for their production or using neutralizing antibodies can change the progression of fibrotic tissue formation. Thus, the downregulation of TGF-β reduces fibrotic development [46]. This is because TGF-β, together with WNT, which act as pro-fibrotic mediators in cardiac fibrosis formation, are the key regulators of

myofibroblast functions [20,47]. TGF-β stimulates the activation of pro-fibrotic genes by increasing Smad2/3 while decreasing the inhibitory Smad 6/7 in myofibroblasts [20]. Smad 2/3, in turn, was reported to be activated in fibroblasts infiltrating the remodeling hearts after injury [48]. TGF-β also increases the deposition of collagens I, III, and VI, and enhances the expression of matrix proteins such as ED-A fibronectin in myofibroblasts through the regulation of plasminogen activator inhibitor, tissue inhibitor of metalloproteinases, and pro-fibrotic cytokine expression [20,49]. In addition, TGF-β suppresses the degradation of ECM proteins by controlling the expression of plasminogen activator inhibitor (PAI)-1 and TIMPs. Moreover, as TGF-β receptors are found in almost all inflammatory cells, TGF-β itself regulates the function of those cells during fibrosis [13].

3.2. The Role of RAAS in Cardiac Fibrosis

Following cardiac injury, pro-fibrotic mediators including the components of RAAS activate myofibroblast differentiation, leading to their proliferation and migration as well as the deposition of ECM proteins, which results in the formation of fibrosis [50]. Angiotensin II is generated by macrophages and fibroblasts that migrate into the injured heart area and produce renin and angiotensin-converting enzymes [51]. Once released, angiotensin II stimulates cardiac fibroblast differentiation via either direct activation or through TGF-β1-mediated effects [33]. In particular, angiotensin II causes the generation of reactive oxygen species (ROS), which induce the pro-fibrotic TGF-β1-Smad2/3 signaling pathway activation, collagen type I and III synthesis, and transdifferentiation of cardiac fibroblasts into myofibroblasts. Aldosterone mediates its pro-fibrotic effect via several mechanisms including the stimulation of cytokine and chemokine expression by vascular cells, the induction of macrophage differentiation into fibroblasts, the activation of cardiomyocyte-derived fibrogenic signals, and the stimulation of collagen synthesis [33]. Thus, the inhibition of RAAS facilitates an improvement in the heart functions and prevents further complications of CVDs [52].

Thus, the development of cardiac fibrosis involves numerous molecular processes including hormonal, mechanical, and inflammatory mechanisms such as the activation of RAAS and the expression of fibrogenic growth factors. Their relative significance depends on the nature of fibrosis.

4. Anti-Fibrotic Therapies

Novel anti-fibrotic therapies target various levels of myocardial fibrosis including epigenetic enzymes, genes, translation machinery, and signaling molecules. These therapies are overviewed in Figure 2 and are discussed in detail below.

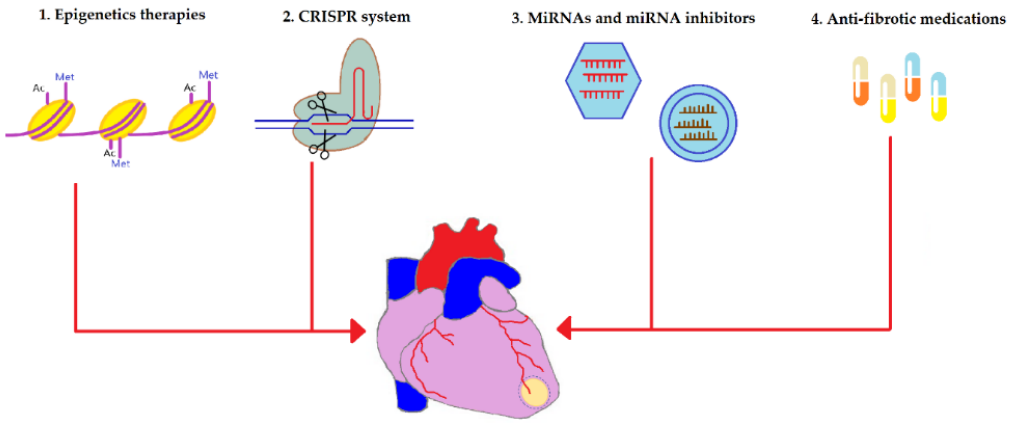

Figure 2. An overview of the novel strategies utilized to alleviate fibrotic remodeling after cardiac diseases. Multiple cardiac pathologies tend to terminate in the replacement of contractile myocardium with the fibrous tissue, one of these diseases is myocardium infarction (infarction area is depicted in yellow). Novel anti-fibrotic therapies target various levels of the pathogenesis of cardiac fibrosis:

(1) Epigenetics-based therapies such as histone deacetylase (HDAC) and histone methyltransferases (HMT) have been shown to regulate the gene expression of many fibrosis-associated proteins such as TGF-β1, collagen type I, collagen type III, fibronectin, and many others. Consequently, HDAC inhibitors and HMT inhibitors have been applied to suppress the expressions of those proteins and downregulate fibrosis. (2) Clustered regularly interspaced short palindromic repeats (CRISPR) technology has been used to silence pro-fibrotic genes as well as to introduce "useful" genes into stem cells to enhance their therapeutic potential for myocardial fibrosis. (3) Anti-fibrotic microRNAs (miRNAs) can be utilized to repress the gene expression of fibrosis-mediating genes at the level of mRNA whereas miRNA inhibitors interact with pro-fibrotic miRNA and inhibit them. Viral vectors (shown as hexagons) are generally used to deliver miRNAs while miRNA inhibitors can be transferred using liposomes (depicted as circles). (4) Anti-fibrotic medications such as pirfenidone, angiotensin receptor blockers, and NLRP3 inflammasome inhibitors work by inhibiting enzymes and signaling molecules involved in the pathophysiology of cardiac fibrosis.

4.1. Epigenetics

Epigenetics-based therapeutic strategies have been successfully utilized to alleviate fibrosis in pre-clinical trials of cardiac, pulmonary, hepatic, and renal diseases [53–55]. Epigenetic drugs were shown to reduce fibrosis and improve cardiac function in animal models of MI, ischemia-reperfusion, hypertension, and cardiac hypertrophy [56,57]. However, due to space limitations, we will provide an overview of the use of epigenetic therapies for cardiac fibrosis after MI only. Several groups have demonstrated the importance of epigenetic modifications in the pathogenesis of MI-related fibrosis and proposed novel anti-fibrotic therapies that would target epigenetic regulators [58]. For instance, in a number of studies, targeting histone deacetylases (HDACs) was reported to prevent adverse cardiac remodeling and fibrosis following MI. Wang and colleagues demonstrated that daily intraperitoneal injections of the HDAC inhibitor trichostatin A (TSA) for 8 weeks significantly reduced fibrosis after MI in mice [59]. They also found an improvement in the left ventricular systolic and diastolic functions in the TSA group compared to the controls. It was reported that the cardioprotective effects of TSA were mediated via restoration of autophagosome clearance. Specifically, TSA treatment resulted in a higher expression of LAMP2, an important regulator of autophagosome-lysosome fusion, but decreased levels of autophagic proteins LC3-II, P62, and beclin 1. In contrast, clearance of the autophagosomes was impaired in the control group, which was confirmed by a more than two-fold reduction in LAMP2 expression and 2.5–4.5-fold elevations in the LC3-II, P62, and beclin 1 levels. Importantly, the authors demonstrated that the aforementioned molecular events also happened at the level of the fibroblasts during the cell culture experiments. Thus, TSA repaired autophagosome–lysosome fusion in the neonatal rat ventricular fibroblast primary culture after 4 h of hypoxia treatment.

Another potential target for epigenetics-based therapy of post-MI fibrosis is HDAC4, which was reported by Zhang and colleagues [60]. Using transgenic mice with HDAC4 overexpression, the researchers identified the role of this protein in cardiac development and, most importantly, in MI-induced fibrosis. Compared with the control mice, HDAC4-transgenic mice suffered from substantial interstitial fibrosis, enhanced apoptotic signaling, weakened cardiac function, and reduced capillary density, among other detrimental effects, 3 weeks after MI. Due to its significant role in the pathogenesis of adverse cardiac remodeling following MI, it could be reasonably suggested that the inhibition of HDAC4 might have therapeutic effects on the infarcted myocardium. In particular, the suppression of HDAC4 might potentially decrease fibrosis, prevent apoptosis of cardiomyocytes, increase angiogenesis, and enhance ventricular function after MI overall. In another study, Rhein, a novel class I and II histone deacetylase inhibitor, was demonstrated to block TGF-β1-stimulated fibroblast-to-myofibroblast transition and the transcription of pro-fibrotic genes in primary human ventricular cardiac fibroblasts under sustained hypoxia for four days [61]. Taking into consideration the significant role of TGF-β1 in the pathogenesis of

myocardial fibrosis, it can be suggested that the HDAC inhibitor Rhein could become a potential therapeutic approach for MI-induced cardiac fibrosis.

Another group of epigenetic regulators that has been targeted to alleviate post-MI fibrosis is the methyltransferases. In a recent paper, Li and colleagues demonstrated that knockdown of histone methyltransferase DOT1L attenuates fibrosis and improves cardiac function in a murine model of MI [62]. Thus, the degree of post-MI fibrosis was significantly lower in the DOT1L-knockdown group compared to the control group, which was confirmed by the expression levels of collagen type I alpha1 and fibronectin 1 fibrosis markers and Masson's trichrome staining. Moreover, in the DOT1L-deficient mice, left ventricular function was preserved 4 weeks after MI in contrast to the controls. The authors further reported the important role of DOT1L epigenetic regulation in the progression of fibrosis following MI. First, DOT1L expression was significantly increased in the MI group in comparison to the sham-surgery group. Next, the TGF-β1/Smad3 pathway, which is classically described to be involved in tissue fibrosis, was activated in response to higher levels of DOT1L expression but was suppressed in DOT1L-knockdown cells. Furthermore, it was found that DOT1L methylates lysine-79 of histone H3 (H3K79me2) of the promoter region of the spleen tyrosine kinase (SYK). The latter protein was reported to be elevated in tissue fibrosis. In MI mice, H3K79me2 methylation of the SYK promoter was higher before DOT1L inhibition, whereas DOT1L knockdown reduced this epigenetic modification. Finally, the overexpression of SYK by lentiviral transduction terminated the anti-fibrotic effects of DOT1L inhibition. Thus, it enhanced the expression of fibrosis markers and stimulated the TGF-β1/Smad3 pathway in the fibroblast culture and in DOT1L-deficient MI mice. All of the aforementioned findings indicate the significance of DOT1L epigenetic modifications in the pathogenesis of MI-induced fibrosis as well as provide potential targets for the anti-fibrotic therapies.

Another histone methyltransferase that has been studied as a potential target for anti-fibrotic therapy after MI is G9a. Sung and colleagues reported that suppression of G9a with the UNC0638 inhibitor resulted in a decreased expression of several fibrosis markers, namely, fibronectin, Smad3, and TGF-β as well as reduced fibrotic area, increased angiogenesis, and preserved heart function in a rat model of MI [63]. Interestingly, the amelioration of fibrosis as well as other beneficial effects were synergistically enhanced when G9a suppression was combined with erythropoietin treatment. Erythropoietin itself has been reported to mediate anti-fibrotic effects in myocardial fibrosis. For instance, Liu and colleagues have recently shown that erythropoietin overexpression attenuated cardiac fibrosis in rats with abdominal aortic constriction [64]. The authors revealed that beneficial actions of erythropoietin were generated via the activation of the PI3K/Akt signaling pathway and by lowering Toll-like receptor (TLR) 4 expression, which in turn downregulated the levels of TGF-β1, TNF-α, IL-6, IL-1β, IL-17A, MMP-2, and MMP-9. In summary, certain HDAC and methyltransferases have been identified as potential mediators of fibrotic cardiac remodeling after MI and other CVDs. The obtained data are summarized in Table 1. It was, therefore, reasonably suggested that the inhibition of these epigenetic regulators might present a promising approach to treat fibrosis after MI, which was indeed demonstrated by recent studies. Nevertheless, it should be mentioned that complete inhibition of fibrotic response after MI and other cardiac diseases might have detrimental consequences rather than therapeutic effects due to the fact that fibrosis has important protective effects, namely, it helps maintain the heart's structural integrity and secures the organ from rupture [39].

4.2. CRISPR

CRISPR technology has been demonstrated to attenuate liver, renal, and pulmonary fibrosis in animal models [65–68]. Although CRISPR has been utilized to model and treat CVD caused by genetic mutations, the use of this approach as a therapy for acquired diseases associated with cardiac fibrosis is quite limited [69,70]. Nevertheless, the latest studies report encouraging results of CRISPR technology for the treatment of fibrotic cardiac remodeling

after MI. In a recent study by Park and colleagues [70], a CRISPR/Cas9 system-based on in vivo genome editing was used to treat MI in a murine model. Specifically, CRISPR was designed to mediate inactivation of the miR34a gene, whose deletion has been shown to reduce cardiomyocyte death and myocardial fibrosis. In order to ensure more efficient targeted delivery, the researchers created CRISPR/Cas9-conjugated magnetic nanoparticles that could be directed to the heart using an external magnetic field following intravenous injection. Treatment with CRISPR/Cas9-combined magnetic nanoparticles resulted in decreased fibrosis two weeks after MI, which was demonstrated by Masson trichrome staining and expression levels of fibrosis marker genes, namely, TGF-β2, FN, CTGF, COL1, COL3, and Postn. Moreover, the treatment significantly increased the proliferation of cardiomyocytes and overall improved contractile function of the left ventricle. In another study, Jiang and colleagues used CRISPR to reprogram fibroblasts into cardiovascular progenitor cells, which ameliorated heart function and reduced myocardial fibrosis after transplanting them into mice with MI [71]. In particular, mouse extracardiac fibroblasts were reprogrammed into cardiovascular progenitor cells in vitro by activating *Gata4*, *Nkx2.5*, and *Tbx5* genes using lentiviral transduction with the CRISPR activation system. After injection into the infarction area of the mouse heart, these cardiovascular progenitor cells differentiated into the cells of the cardiac tissue. In particular, 39% of the engrafted cells differentiated into CD31+ endothelial cells, 36% of the cells became cTnT+ cardiomyocytes, and 24% of the cells gave rise to α-SMA+ smooth muscle cells. Importantly, treatment with CRISPR-induced cardiovascular progenitor cells significantly reduced the post-infarction scar area and recovered cardiac function, indicating that this therapeutic strategy has the potential to become one of the novel anti-fibrotic and regenerative therapies for MI.

The CRISPR system has also been used indirectly to optimize cellular therapy for MI. Cho and colleagues utilized CRISPR/Cas9 to integrate the LEF1 gene into human umbilical cord blood-derived mesenchymal stem cells (hUCB-MSCs) in order to enhance their therapeutic efficiency [72]. The LEF1 gene, which is involved in cellular proliferation, survival, and differentiation, was introduced into hUCB-MSCs using transfection with Lipofectamine 3000 and then inserted into an adeno-associated virus integration site 1 with the help of CRISPR/Cas9 tools. As the authors state, CRISPR/Cas9 was chosen over viral gene editing techniques to avoid potential off-target effects and tumorigenesis. It was found that the LEF1 gene was precisely integrated into the targeted site and continuously expressed by the genetically modified cells. Importantly, CRISPR/Cas9-edited hUCB-MSCs showed greater survival after implantation into the infarcted hearts of rat models using the UpCell cardiac patch system. Furthermore, compared with the non-engineered hUCB-MSCs and no treatment groups, therapy with LEF1-knockin cells resulted in improved overall survival, enhanced cardiac function, increased vessel density, and reduced fibrosis after MI. Specifically, infarction of the myocardium and the formation of fibrotic tissue happened 52% less in the LEF1-expressing hUCB-MSCs-treated animals versus only 21% less in the non-modified hUCB-MSCs in comparison to the control group. In another interesting study, CRISPR engineering was employed to improve the survival and the therapeutic potential of bone marrow-derived mesenchymal stem cells (BM-MSCs) for the treatment of MI in the context of diabetes mellitus [73]. To be specific, the researchers used the CRISPR/dCas9 activation system to induce the overexpression of IL-10 in BM-MSCs. Transcription activation of IL-10 was successfully accomplished by CRISPR/dCas9, which was demonstrated by a high and stable expression of this cytokine in vitro as well as after BM-MSC transplantation to a murine model of MI. Moreover, IL-10 overexpressing BM-MSCs mediated regenerative and reparative effects on the infarcted myocardium by reducing scar tissue, bettering post-infarction heart function, inhibiting apoptosis, and enhancing angiogenesis. It is important to point out that one of the findings in this study was the suppression of inflammation by the IL-10-engineered BM-MSCs. Namely, the transplanted cells caused decreased recruitment of the CD68+ immune cells and suppressed the expression of IL-1β, TNF-α, IL-6, and MCP-1 pro-inflammatory cytokines. Since inflammation is believed to be a critical contributor to fibrotic remodeling after MI, it could

be suggested that in this study, IL-10-engineered BM-MSCs reduced fibrosis due to their anti-inflammatory actions [74].

Overall, there is some hesitancy in implementing CRISPR technology for the treatment of cardiac fibrosis due to numerous challenges such as the postmitotic nature of cardiomyocytes, difficulties in achieving targeted delivery, restricted cargo capacity of delivery systems, possible off-target mutagenesis, and others [69,75]. Despite the above-mentioned limitations, data from several studies are quite encouraging. In particular, the CRISPR system was utilized to directly edit genes involved in MI and fibrosis as well as to enhance the efficiency of cell mediated therapy for MI, which is summarized in Table 1.

Table 1. The epigenetics and clustered regularly interspaced short palindromic repeats (CRISPR) used for the treatment of cardiac fibrosis.

Strategy	Treatment	Outcome	Reference
Epigenetics	Histone deacetylase inhibitor trichostatin A	Reduced fibrosis and improved systolic and diastolic functions a murine MI model	[59]
	Class I and II Histone deacetylase inhibitor Rhein	Inhibited TGF-β1-induced fibroblast-to-myofibroblast transition and transcription of pro-fibrotic genes in primary human ventricular cardiac fibroblasts culture under sustained hypoxia	[61]
	Histone methyltransferase DOT1L inhibition	Alleviated fibrosis, reduced expression of collagen type I alpha1 and fibronectin 1 and improved cardiac function in mice with MI	[62]
	Histone methyltransferase G9a inhibition	Decreased expression of several fibrosis markers such as fibronectin, Smad3, and TGF-ß; reduced fibrotic area; increased angiogenesis; and preserved heart function in a rat model of MI	[63]
CRISPR	CRISPR-Cas9-mediated inactivation of miR34a gene	Decreased fibrosis, enhanced proliferation cardiomyocytes, and improved heart function	[70]
	CRISPR-mediated reprogramming of fibroblasts to cardiovascular progenitor cells	Differentiation of reprogrammed fibroblasts to endothelial cells, cardiomyocytes, and smooth muscle cells; reduced scar size; and restored cardiac function in a mouse model of MI	[71]
	CRISPR/Cas9-mediated integration of LEF1 gene into human umbilical cord blood-derived mesenchymal stem cells	Improved survival, enhanced cardiac function, increased vessel density, and decreased fibrosis after MI	[72]
	CRISPR/dCas9 activation system-induced overexpression of IL-10 in bone marrow-derived mesenchymal stem cells	Reduced scar tissue, improved heart function, suppresses cardiomyocyte apoptosis, and enhanced angiogenesis	[73]

4.3. miRNAs

MiRNAs are small (about 22 nucleotides), single-stranded, non-coding RNA molecules involved in the post-transcriptional regulation of genes implicated in various biological processes [76]. A considerable amount of evidence points that miRNAs are extensively involved in the regulation of cardiac remodeling after different CVDs [77,78]. Depending on the effects of fibrosis, miRNAs could be classified into pro-fibrotic and anti-fibrotic, and each of the two and the associated pathways that could be targeted to alleviate cardiac remodeling will be reviewed below.

4.3.1. Pro-Fibrotic miRNAs

Pro-fibrotic miRNAs promote the increased expression of ECM components and other fibrosis-related proteins in different tissues, and therefore, could serve as an attractive target for therapeutic modifications in cardiac diseases such as MI, atrial fibrillation, cardiac

ischemia, and others [79–82]. One of the first examples to be considered was miR-27b, which has been shown to stimulate hypertrophy and promote heart failure, whereas its inhibition alleviates cardiac dysfunction [83,84]. Further findings have indicated that a TGF-β1/Smad signaling pathway plays a key role in the regulation of miR-27b, since TGF-β1 interfered with the activity of the miR-27b promoter and reduced the growth of hypertrophic cells, while smad4 knockout, in contrast, stimulated hypertrophy [85]. Later, another study identified a different pathway, FBW7/Snail, regulated by the same miRNA [86]. The results suggest that miR-27b may target the FBW7 ubiquitin ligase and suppress Snail degradation, which promotes cardiac fibroblast proliferation and ECM synthesis, leading to myocardial fibrosis. In particular, miR-27b transfection of cardiac fibroblasts substantially lowered the expression of FBW7 at 2, 6, and 12 days in the peri-infarct area of rats with MI when compared with the sham-operated animals. In addition, the same manipulations were shown to suppress the luciferase activity of FBW7, which, in turn, was restored upon the inhibition of miR-27b by its antagonist, suggesting that miR-27b suppresses FBW7. Furthermore, it was reported that FBW7 expression in the cardiac fibroblasts inhibited Snail induction, collagen I and III, and MMP-9. Experiments performed using antagomir-27b also showed that downregulation of miR-27b has beneficial effects on cardiac remodeling as it leads to a highly significant reduction in fibrotic tissue in rat MI models [86]. Similarly, miR-96 has been reported to have a pro-fibrogenic function in the context of atrial fibrosis [87]. Thus, Su and colleagues demonstrated that its inhibition was able to suppress Ang-II-induced proliferation, migration, and collagen production by mouse cardiac fibroblasts, as evidenced by CCK-8 and Transwell migration assays, reduced inflammatory infiltration, and decreased deposition of collagen I and III. Through analysis of a publicly available database, the authors were able to identify a potential gene target of miR-96, Kruppel-like factor 13 (Klf13), which has previously been shown to be associated with heart development and cardiomyocyte protection against DNA damage and apoptosis. According to the luciferase reporter assay results, HEK293T cells cotransfected with the Wt-3′UTR reporter and miR-96 had significantly lower luciferase activity compared to the negative controls, whereas the activity of the mutant reporter gene was not affected. Additionally, the overexpression of miR-96 has been shown to suppress Klf13 expression, whereas knockdown had the opposite effect. Collectively, these results suggest that Klf13 is a functional target of miR-96 and that the effects of miR-96 on atrial fibrosis are mediated by Klf13 downregulation [87].

Another miRNA involved in fibrogenesis after CVD is miR-99b-3p. Recent work showed that miR-99b-3p was upregulated in a cardiac fibrosis model induced by angiotensin II [88]. Moreover, forced overexpression of this miRNA led to an increase in the expression of pro-fibrotic biomarkers (fibronectin, collagen I, vimentin, and α-SMA) and the proliferation of cardiac fibroblasts and migration, whereas its inhibition had the opposite effect. In addition, target prediction software revealed a negative correlation between miR-99b-3p and GSK-3 beta, serine threonine kinase implicated in the pathogenesis of diabetes, cancer, inflammation, and CVDs. A quantitative real-time polymerase chain reaction analysis showed that the level of GSK-3β mRNA in cardiac fibroblasts was not affected by miR-99b-3p. However, at the protein level, GSK-3β expression was markedly reduced by the miR-99b-3p mimic, which implies its regulatory effect by suppressing translation. Importantly, other studies have demonstrated that GSK-3β exerts its anti-fibrotic effect by interacting with Smad3 and inhibiting its activation [13]. In agreement with this, the administration of the miR-99b-3p mimic led to enhanced levels of phosphorylated smad3. The same effect was observed upon the inactivation of GSK-3β. Overall, it could be proposed that miR-99b-3p can promote cardiac fibrosis by downregulating GSK-3β, and therefore can lead to the activation of the downstream pro-fibrotic effector Smad3 [88].

MiR-1202 is yet another miRNA that has been reported to have pro-fibrotic properties. In a recent work by Xiao and colleagues, it was reported that TGF-β1-stimulated human cardiac fibroblasts had a high expression of miR-1202, which was time and dose dependent [89]. According to their observations, transfection of the fibroblasts with the miR-1202

mimic increased the levels of collagen I and III, α-SMA, and the Smad2/3 protein as well as promoted Smad2/3 phosphorylation, subsequently leading to the deposition of ECM. Next, using the TargetScan software, the 3′-UTR region of the nitric oxide synthase gene was identified as a target site for miR-1202. As a proof-of-concept, the miR-1202 mimic was shown to reduce the luciferase activity of the NOS1 WT 3′-UTR relative to that of the control group. Moreover, the nNOS protein expression in human cardiac fibroblasts was also shown to be inhibited by miR-1202 mimic transfection and TGF-β1 treatment, but this trend was reversed when the miR-1202 inhibitor was used. In summary, due to their pro-fibrotic effects, the aforementioned miRNAs could be considered as attractive targets for anti-fibrotic therapies of various heart diseases.

4.3.2. Anti-Fibrotic miRNAs

Anti-fibrotic miRNAs can also be considered as therapeutic targets for CVDs as their overexpression was reported to suppress fibrosis-associated cardiac remodeling [90,91]. For instance, miR-150 is involved in the suppression of fibrosis after MI. In a recent study by Tian and colleagues, miR-150 significantly inhibited the expression of myocardial fibrosis-related proteins such as col1α1, col1α2, col3, and α-SMA in the border zone of MI [92]. In addition, miR-150 treatment improved survival and suppressed apoptosis of cardiomyocytes. In a related study, the mechanism by which miR-150-5p prevents the progression of myocardial fibrosis was described [93]. First, miR-150-5p was shown to have inhibitory effects on the expression of fibrosis-related proteins such as MMP-13, collagen I and III, and to induce apoptosis of human myocardial fibrosis cells generated by Trypanosoma cruzi infection. In contrast, another known fibrosis regulator, namely, early growth response 1 (EGR1), was found to improve cell proliferation and enhance the expression of three fibrosis-related proteins, MMP-13, collagen I, and collagen III, in the myocardial fibrosis cell culture. Next, the upregulation of miR-150-5p reversed the effect of EGR1, pointing to the possible mechanism through which they directly interacted with each other. At the same time, EGR1 knockdown retarded myocardial fibrosis while silencing miR-150-5p exacerbated fibrotic expansion, as evidenced by H&E and Masson's trichrome staining. Putting all of this together, it was concluded that the inhibition of EGR1 by miR-150 might become an effective method for cardiac fibrosis therapy [93]. Similarly, miR-1954 has also been determined to play a critical role in cardiac fibrogenesis [94]. Specifically, heart-specific overexpression of miR-1954 was demonstrated to be protective in a mouse model of cardiac hypertrophy and remodeling generated by angiotensin II infusion. Namely, miR-1954 attenuated cardiac remodeling, reduced systolic blood pressure, and decreased the expression of cardiac hypertrophy (NppA, NppB, beta-MHC) and fibrotic marker genes (col1a1, col3a1, and col4) [94]. The investigators further proposed the potential target of miR-1954, namely, thombospondin 1 (THBS1), since cardiac fibroblasts transfected with miR-1954 had lower expression levels of THBS1, whereas the inhibition of miR-1954 had the opposite effect. Thus, it was suggested that the enhancement of miR-1954 levels could be another promising treatment strategy, as it targets the THBS1 gene involved in the promotion of cardiac fibrosis [94]. Yang and colleagues reported a different miRNA type that could negatively regulate cardiac fibrosis [95]. In their study, miR-489 suppressed isoproterenol induced cardiac fibrosis in rats. To be specific, miR-489 downregulated pro-fibrotic markers such as col1a1, α-SMA, and HDAC2 and inhibited the viability and differentiation of cardiac fibroblasts. Importantly, HDAC2 was identified as a direct target of miR-489 by using the computational prediction software, TargetScan. This was further confirmed by a reverse transcription-quantitative polymerase chain reaction analysis, which demonstrated a decrease in the HDAC2 expression in cells transfected with the miR-489 mimic and a corresponding increase in cells transfected with the miR inhibitor. They also determined a reduction in the colA1 and α-SMA levels with HDAC2 silencing in the siHDAC-transfected group compared to siNC, providing additional clues to the mechanism of action of miR-489. Another anti-fibrotic miRNA that was recently investigated in the context of CVDs is miR-30d. In a murine model of MI, overexpression

of miR-30d in the heart ameliorated left ventricular function, reduced cardiac fibrosis, and downregulated fibrotic markers such as α-SMA [96]. It is important to mention that miR-30d overexpression was also associated with inhibitory effects on apoptosis. Further investigations revealed that integrin α5 was a direct target of miR-30d, which is involved in the regulation of fibrogenesis. Similarly, miR-145 has also been identified as a suppressor of MI-induced cardiac fibrosis in rat models [97]. Thus, the injection of adenovirus expressing miR-145 in the infarcted zone significantly reduced fibrous tissue formation and collagen synthesis. Moreover, improvement in left ventricular functions was observed upon treatment with miR-145. Regarding the mechanism of action of miR-145, it was found that SOX9, which plays a role in cardiac fibrogenesis, was directly repressed by miR-145. Furthermore, the study showed that SOX9 negatively regulated PTEN and promoted PI3K, AKT, and GSK-3beta signaling and collagen I/III secretion, whereas a contrary effect was observed after miR-145 overexpression, suggesting an inhibitory role of miR-145 on SOX9 and its downstream PI3K/AKT pathway. Overall, this study provided evidence for the involvement of SOX9 and miR-145 in cardiac fibrogenesis, which can be further used to develop new strategies to combat cardiac fibrosis [97]. Summarizing all of the data, some miRNAs have been identified as potential mediators of cardiac fibrosis, while others have been shown to have the opposite effect. Taking this into account, the up- and downregulation of these miRNAs may provide novel strategies for CVDs associated with fibrotic cardiac remodeling. We summarize some of the related studies in Table 2.

Table 2. The pro- and anti-fibrotic microRNAs used for the treatment of cardiac fibrosis.

Class of Micro-RNA	Example	Treatment	Outcome	Reference
Pro-fibrotic	MiR-27b	Inhibition	Lowered expression of collagen I and III, and MMP9; significantly reduced fibrotic tissue formation in rat MI model	[86]
	MiR-96	Inhibition	Suppressed angiotensin II-induced proliferation of, migration of and collagen production by murine cardiac fibroblasts; decreased inflammatory cells infiltration; and reduced collagen I and III deposition in atrial tissue	[87]
	MiR-1202	Inhibition	Decreased expression of collagen I and III, α-SMA, and Smad2/3	[89]
	MiR-150	Inhibition	Reduced expression of col1α1, col1α2, col3, and α-SMA; improved survival of cardiomyocytes in rat model of MI	[92]
Anti-fibrotic	MiR-150-5p	Use of miRNA mimic	Suppressed the expression of MMP-13, collagen I and III; induced apoptosis of human myocardial fibrosis cells after Trypanosoma cruzi infection	[93]
	MiR-1954	Overexpression	Alleviated fibrotic cardiac remodeling, reduced systolic blood pressure, and decreased the expression of cardiac hypertrophy (NppA, NppB, beta-MHC) and fibrotic marker genes (col1a1, col3a1 and col4) in angiotensin II-induced model of cardiac hypertrophy in mice	[94]
	MiR-489	Use of miRNA mimic	Downregulated pro-fibrotic markers such as col1a1, α-SMA, and HDAC2 in an isoproterenol-induced rat model of cardiac fibrosis and inhibited the viability and differentiation of cardiac fibroblasts in vitro	[95]
	MiR-30d	Overexpression	Reduced cardiac fibrosis, downregulated fibrosis marker genes such as α-SMA, inhibited cardiomyocyte apoptosis, and improved left ventricular function in a murine model of MI	[96]
	MiR-145	Overexpression	Reduced fibrous tissue formation and collagen synthesis; enhanced left ventricular function in rat model of MI	[97]

4.4. Anti-Fibrotic Medications

Differentiation of pathological myofibroblasts from cardiac fibroblasts is the major hallmark of cardiac fibrosis [98]. Thus, controlling this process is crucial for attenuating the pathology of fibrosis. CTGF, TGF-β, RAAS, Gal-3, TNF-α, endothelin, and IL-11 are either directly or indirectly involved in the differentiation of fibroblasts into myofibroblasts. Therefore, the current therapies are mainly focused on targeting these pro-fibrotic agents in order to attenuate the development of cardiac fibrosis in damaged hearts. These therapies include, but are not limited to, drugs focused on the inhibition of RAAS, TGF-β, CTGF, Gal-3, and NLRP3 expression and production.

4.4.1. Renin–Angiotensin–Aldosterone System (RAAS) Inhibitors

RAAS inhibitors are widely used to target cardiac fibrosis. Drugs such as lisinopril, losartan, amlodipine, and spironolactone have proven their anti-fibrotic effect on cardiomyocytes [23,99,100]. A recent study demonstrated that a new first-in-class angiotensin receptor inhibitor, sacubitril/valsartan, can suppress the effect of RAAS during cardiac remodeling by blocking angiotensin II type 1 receptors and activating vasoactive peptides through the inhibition of the neprilysin enzyme, which is responsible for their degradation [101]. Sacubitril/valsartan prevented maladaptive cardiac fibrosis and dysfunction by blocking cardiac fibroblast activation and proliferation in a mouse model of pressure overload–induced hypertrophy [102]. Moreover, the effects on exosome production and content isolated from human induced pluripotent stem cell-derived cardiomyocytes by sacubitril/valsartan demonstrated that it decreases myocardial fibrosis via the downregulation of exosomal miR-181a, resulting in the attenuation of myocardial fibrosis and hypertrophy in a rodent model of chronic MI [103]. Another recently identified RAAS inhibitor, alamandine, demonstrated that it could decrease the density of cardiac fibrosis and reduce the expression of fibrotic proteins (CTGF, collagen I (COL1A1), and MMP-9) in a spontaneous hypertensive rat model [104]. Furthermore, alamandine blocks the increase in ERK1/2 phosphorylation and restores the level of 5′-adenosine monophosphate-activated protein kinase (AMPK) α phosphorylation, preventing cardiac hypertrophy and fibrosis in a mouse model of cardiac remodeling induced by transverse aortic constriction [105]. Additionally, a novel hormone like polypeptide, irisin, can be involved in the protection of cardiac tissues during cardiac hypertension, coronary artery disease, MI, and myocardial ischemia-reperfusion injury through the inhibition of the RAAS system [106,107]. Chen and colleagues demonstrated that irisin could decrease the angiotensin II-induced cardiac fibrosis via activating the Nrf2-antioxidant signaling pathway and inhibiting pro-fibrotic TGF-β1-Smad3 signaling [107]. In a mouse model of DOX-induced cardiotoxicity, irisin ameliorated cardiac perivascular fibrosis through the inhibition of endothelial-to-mesenchymal transition by regulating ROS accumulation and autophagy disorder in endothelial cells [108]. In addition, irisin was shown to suppress ROS generation induced by angiotensin II, leading to the inhibition of its pro-fibrotic effect [107]. Furthermore, cardiac tissue fibrosis induced by angiotensin II-stimulated TGF-β enhances the binding of IL-33 to sST2 but not to ST2L, which normally provides cardioprotection against fibrotic formation. This again leads to the overproduction of angiotensin II and the subsequent progression of fibrosis formation. The inhibition of angiotensin II by angiotensin converting enzyme inhibitors reduces the inflammatory response and the level of sST2. In the absence of sST2, IL-33 interacts with ST2L [109]. Moreover, in vitro studies have shown that angiotensin II treatment significantly elevated the level of circHIPK3 in the cardiac fibroblasts and surrounding heart tissue. Thus, silencing circHIPK3 reduced the proliferation of fibroblasts and the expression of α-SMA as well as improved the diastolic functions [37]. The pathological effect of angiotensin II can be inhibited by quercetin dehydrate, which is involved in the suppression of collagen production and fibroblast proliferation and differentiation [110]. Another potential target for anti-fibrotic therapy is SNHG20, a long non-coding RNA, which is upregulated in the angiotensin II-treated murine heart. Its downregulation eliminated the angiotensin II effects on fibrosis such as the expression of fibrotic and apoptosis-related

proteins by directly targeting the miR-335/Gal-3 axis [111]. In addition, the infusion of IGF-1 can improve angiotensin II-caused myocardial fibrosis via the regulation of the Akt pathway and downregulation of α-SMA expression mediated by ho-associated coiled-coil containing kinases (ROCK)2, leading to the suppression of fibroblast differentiation and proliferation [112].

Overall, despite the various previously known drugs, it seems that new RAAS inhibitors such as sacubitril/valsartan, alamandine, irisin, angiotensin converting enzyme inhibitors, and quercetin dihydrate can provide new opportunities for the treatment of cardiac fibrosis.

4.4.2. TGF-β and CTGF Inhibitors

As another strategy, targeting different pro-inflammatory mediators such as TGF-β and CTGF can be utilized in order to prevent the development of cardiac fibrosis by decreasing myofibroblast activation, which results in the reduced expression of integrins by the cells, preventing further deposition of pathological ECM [29,113,114]. Recently, it was shown that the treatment of mice with CTGF monoclonal antibody, pamrevlumab, in a mouse model of MI enhanced cardiac repair and reduced adverse post-MI left ventricle remodeling [115]. The study showed a reduction in the MI-induced fibrosis in the remote, non-ischemic myocardium in mice treated with pamrevlumab compared with MI mice treated with the control IgG. Moreover, pamrevlumab reduced the basal and TGF-β1–induced α-SMA and collagen I expression, possibly through regulating the JNK signaling pathway and genes related to fibrosis and/or inflammation and cardiac repair. Another drug called pirfenidone, which was previously approved for the treatment of idiopathic pulmonary fibrosis, demonstrated promising results in the treatment of cardiac fibrosis in animal models due to its similarity to the mechanisms of myocardial and pulmonary fibrosis [116]. Several groups have reported that pirfenidone blunts TGF-β signaling, which is a crucial determinant of pulmonary and cardiac fibrosis [117]. The expansion of cardiac fibrosis following MI is thought to affect viable tissue adjacent to the infarcted area, predisposing to impulse fragmentation and the development of ventricular arrhythmias. In a rat model, pirfenidone treatment was initiated one week after ischemia-reperfusion injury and continued for four weeks. Pirfenidone caused a reduction in the scar size and myocardial fibrosis in the border zone, with better preserved left ventricle systolic function and lower rates of ventricular tachycardia inducibility [118].

In rats subjected to ligation of the left anterior descending coronary artery, pirfenidone reduced cardiac fibrosis and scar size and slowed down progression toward heart failure [119]. Moreover, pirfenidone attenuated left ventricle remodeling and improved survival in mice with diphtheria toxin-mediated acute myocardial injury and closed-chest ischemia-reperfusion injury [120]. The authors observed a reduced percentage of B lymphocytes in mice treated with pirfenidone and the depletion of B lymphocytes abolished the beneficial effects of pirfenidone. Moreover, activation of B lymphocytes that were stimulated with lipopolysaccharide and extracts of necrotic cells were attenuated by pirfenidone through a TIRAP-dependent pathway. The authors then postulated that the cardioprotective effects of pirfenidone depended at least partially on the modulation of myocardial B lymphocytes [120].

A recent study revealed that the activation of TGF-β in cardiac fibroblasts, which resulted in their transdifferentiation into myofibroblasts, is induced by the overexpression of ADAMTS16, an extracellular enzyme that is associated with ECM protein degradation and remodeling. ADAMTS16 activates the latency-associated peptide (LAP)-(TGF)-β (LAP-TGF-β) signaling pathway through the RRFR motif [121]. Another study focused on the relationship between the TGF-β/Smad2/3 signaling pathways and the Smad7 molecule. They revealed that Smad7 had an inhibitory effect on TGF-β expression in fibroblasts by promoting TβR and R-Smad turnover, leading to the downregulation of Smad2 and Smad3 molecules. This resulted in reduced myofibroblastic activity and decreased synthesis of EMPs [122]. Additionally, the TGF-β1/Smad signaling pathways are regulated by Slit2. The

Slit2–Robo1 signaling pathway interferes with the functions of TGF-β1/Smad, leading to the increased production of Periostin, Robo1, and collagen I. Thus, silencing the Slit2–Robo1 pathway may open a window to a new therapy for the treatment of cardiac fibrosis [45].

The TGF-β1/Smads signaling pathway can be suppressed by tissue nonspecific alkaline phosphatase (TNAP). TNAP is overproduced in patients with MI, and the suppression of its production reduces the expression of collagen-related genes. A study on rats with MI-induced fibrosis showed that this effect was partially caused by the deactivation of the TGF-β1/Smads pathway [123]. In addition, baicalin, a natural polyphenol that has been used in traditional Chinese medicine to treat inflammation and hypertension, has recently received attention for its protective effects on CVDs such as its inhibition of the progression of atherosclerosis, against myocardial ischemia-reperfusion injury and the suppression of endothelial dysfunction. Xiao and colleagues revealed that baicalin inhibits cell proliferation, collagen synthesis, fibronectin, and CTGF protein expression in cardiac fibroblasts induced by angiotensin II in the model of abdominal aortic constriction ameliorating cardiac fibrosis in rats [124]. Moreover, baicalin inhibited the TGF-β/Smads signaling pathway stimulated with Ang II through the activation of AMPK, providing evidence that its effect against cardiac fibrosis may be attributed to its regulation in AMPK/TGF-β/Smads signaling. Finally, a recent in vivo and ex vivo study found that CTRP9 (C1q/tumor necrosis factor-related protein-9), a secreted glycoprotein highly expressed in the heart, can also be effective in reducing arterial inflammation and fibrosis, possibly via its inhibitory effects on TGF-β and collagen deposition, in the early phase of MI. It attenuated left atrial fibrosis by reducing the expressions of collagen types I and III, α-SMA, and TGF-β1 seven days after MI, possibly through depressing the Toll-like receptor 4/nuclear factor-κB and Smad2/3 signaling pathways [125].

Taken together, the inhibition of CTGF and TGF-β with their inhibitors such as CTGF mAb, pirfenidone, TNAP inhibitor, baicalin, and CTRP9 can be a promising strategy for the treatment of cardiac fibrosis due to their effects on different signaling pathways involved in the development of fibrosis in cardiac tissue.

4.4.3. Gal-3 and NLRP3 Inflammasome Inhibitors

Gal-3 is a soluble β-galactosidase-binding glycoprotein. Activated macrophages and pathologically damaged cardiomyocytes are the source of their high expression in blood serum in various cardiac and cerebrovascular diseases including acute ischemic stroke, atrial fibrillation, myocardial fibrosis, and HF [126]. A recent study on rabbits revealed that treatment with Gal-3 inhibitor, modified citrus pectin (MCP), can decrease myocardial fibrosis, resulting in relatively regular and neatly arranged non-fibrotic myocardial cells with scattered nuclei in the infarct zone. In addition, myocardial Gal-3, collagen type I, the collagen type III gene, and the protein expression levels were also decreased in the MCP treatment group [127]. Moreover, in a mouse model of isoproterenol induced HF, MCP ameliorated myocardial fibrosis via the inhibition of the TLR4/MyD88/NF-κB signaling pathway and decreased expression of IL-1β, IL-18, and TNF-α, which is involved in the pathogenesis of HF [128]. On the other hand, the formation of inflammasome in the mouse MI heart can lead to an additional loss of functional myocardium, resulting in the development of HF [129]. Particularly, the NLRP3 inflammasome plays a pivotal role in the identification of danger signals and the further induction of sterile inflammatory responses after MI. Furthermore, MI-induced myocardial injury initiates the assembly of NLRP3 inflammasome, leading to the secretion of various inflammatory factors including IL-1β and IL-18. This aggravates myocardial damage and the further development of systolic dysfunction [130]. Therefore, NLRP3 inflammasome inhibitors can serve as another approach to control the development of cardiac remodeling and fibrosis. A recent study revealed that MCC950, a specific inhibitor of the NLRP3 inflammasome, can attenuate myocardial fibrosis and improve cardiac remodeling in a mouse model of MI [131]. In this study, myocardial fibrosis was reduced in the MCC950-treated animals (MCC950, 23.2 ± 3.0 vs. PBS, 36.2 ± 3.7; $p < 0.05$). Moreover, histological and molecular analysis

revealed a decrease in the level of inflammatory cells in the treated group, and cardiac function was preserved compared to that in the control group. In vitro, MCC950 also inhibited NLRP3 and reduced caspase-1 activity with further downregulation of IL-1β and IL-18. Another NLRP3 inhibitor, oridonin, which is an active ingredient of medicinal herb *rabdosia rubescens*, also has an anti-inflammatory effect and suppresses NLPR3 activation by forming a covalent bond with NACHT's cysteine 279 and preventing NEK7–NLRP3 interaction [132]. Recently, Gao and colleagues demonstrated that oridonin treatment can preserve ejection fraction and fractional shortening of the left ventricle, and notably reduce myocardial fibrosis in the treated mice. Furthermore, oridonin decreased the expression of IL-1β and IL-18 as well as myocardial macrophage and neutrophil influxes [133]. Overall, the application of Gal-3 and NLRP3 inhibitors in the treatment of cardiac fibrosis can be a promising alternative therapy in addition to the methods discussed above due to their negative effect on pro-inflammatory cytokines and pro-fibrotic genes and proteins.

4.4.4. β-Adrenergic Receptor Inhibitors

β-adrenergic receptors (βARs) are members of the G-protein-coupled receptor family and consist of three subtypes: β1AR, β2AR, and β3AR. It is probable that the β3AR isoform expression in cardiac myocytes influences the cardiovascular physiology and pathology due to its lack of G protein–coupled receptor kinase recognition sites, which protect the receptor from desensitization. Receptor desensitization, in turn, is one of the pathogenetic mechanisms of chronic cardiac disease progression. Therefore, the β3AR isoform, which is resistant to desensitization, appears as a promising target for the therapy of various cardiac conditions [134,135]. Particularly, β3AR may play different roles in the regulation of cardiac contractility, relaxation, vasodilatation, and metabolism [134]. Moreover, β3AR can demonstrate protective effects against myocardial interstitial fibrosis in response to hemodynamic stress through modulating nitric oxide and oxidant stress-dependent paracrine signaling to the fibroblasts [135]. In the mouse model of MI, Niu and colleagues showed that stimulation of β3AR with its agonist BRL37344 (BRL) significantly attenuated fibrosis and decreased the scar area [136]. Further analysis revealed that BRL treatment altered the phosphorylation of endothelial nitric oxide synthase (NOS) and increased neuronal NOS expression, suggesting that the activation of both endothelial and neuronal NOS can be associated with cardioprotective effects of the receptor. However, a recent study with mirabegron, the first-in-class β3AR agonist approved for the treatment of overactive bladder in humans, demonstrated that it does not reduce infarct size and LV fraction in the swine model of reperfused MI [137]. Overall, the stimulation of β3AR can be another new approach for the treatment of myocardial fibrosis, but its agonists should be further investigated.

Thus, CTGF, TGF-β, RAAS, Gal-3, and βARs have been identified as potential mediators of fibrotic cardiac remodeling. In addition, the role of NLRP3 inflammasome in the progression of myocardial fibrosis has also been demonstrated in in vitro and in vivo studies. Hence, it is reasonable to suggest that targeting these pro-fibrotic factors with CTGF, TGF-β, RAAS, Gal-3, NLRP3, and βAR inhibitors can be a promising approach for the treatment of myocardial fibrosis after cardiac tissue damage/remodeling. Table 3 summarizes the various medications for the therapy of cardiac fibrosis.

Table 3. The anti-fibrotic medications.

Group of Inhibitors	Drugs/Inhibitors	Outcome	Reference
RAAS inhibitors	Sacubitril/Valsartan	Blocked cardiac fibroblasts activation and proliferation via downregulation of exosomal miR-181a	[101–103]
	Alamandine	Decreased the density of cardiac fibrosis and reduced expression of fibrotic proteins, increased of ERK1/2 phosphorylation and restored the level of AMPKα phosphorylation preventing cardiac hypertrophy and fibrosis	[104,105]
	Irisin	Ameliorated cardiac perivascular fibrosis via regulating ROS accumulation and activating Nrf2-antioxidant signaling pathway and inhibiting pro-fibrotic TGFβ1-Smad3 signaling	[107,108]
	Angiotensin converting enzyme inhibitors	Reduced the proliferation of fibroblasts and expression of a-SMA as well as improved diastolic functions, reduced the inflammatory response and the level of sST2 providing cardioprotection against fibrosis	[37,109]
TGF-beta and CTGF inhibitors	Pamrevlumab	Reduced MI-induced fibrosis in in the remote, nonischemic myocardium, reduced basal and TGF-β1–induced αSMA and collagen-1 expression, and genes related to fibrosis	[115]
	Pirfenidone	Reduced scar size and myocardial fibrosis in the border zone, with better preserved LV systolic function and slowed down the progression toward HF	[118,119]
	Tetramisole	Reduced the expression of collagen-related genes and MI-induced fibrosis	[123]
	Baicalin	Inhibited cell proliferation, collagen synthesis, fibronectin, and CTGF protein expression in cardiac fibroblasts through reduction of TGF-β/Smads signaling pathway	[124]
	C1q/tumor necrosis factor-related protein-9	Reduced atrial inflammation and fibrosis via inhibition of TLR4/MyD88/NF-κB signaling pathway, TGF-β, collagen deposition, in early phase of MI, decreased the expression of IL-1β, IL-18 and TNF-α	[127,128]
Galectin-3 and NLRP3 inflammasome Inhibitor	Modified citrus pectin	Decreased myocardial fibrosis, myocardial Gal-3, collagen type I, and collagen type III gene and protein expressions via inhibiting TLR4/MyD88/NF-κB signaling pathway, decreased expression of IL-1β, IL-18, and TNF-α	[127,128]
	MCC950	Attenuated myocardial fibrosis and improved cardiac remodeling as well as inhibited NLRP3 and reduced caspase-1 activity with further downregulation of IL-1β and IL-18	[131]
	Oridonin	Reduced myocardial fibrosis, decreased expression of IL-1β and IL-18 as well as infiltration by myocardial macrophages and neutrophils	[133]
β3AR inhibitors	BRL37344 Agonist	Attenuated fibrosis, decreased scar area, altered the phosphorylation of endothelial NOS, and increased neuronal NOS expression	[136]

5. Conclusions

Fibrosis is a pathogenetic process that leads to heart failure and increased morbidity and mortality after MI and other CVD. Unfortunately, there are no approved therapies that would specifically target cardiac fibrosis. Nevertheless, a variety of novel treatments have demonstrated encouraging results in pre-clinical studies. For instance, miRNAs and epigenetic regulators such as HDAC and methyltransferases have been shown to control fibrotic cardiac remodeling and have therefore been tested as potential candidates or targets for anti-fibrosis therapy for a number of heart conditions. CRISPR technology has been utilized to silence fibrosis-related genes as well as to genetically engineer stem cells to enhance their efficiency. Anti-fibrotic medications such as pirfenidone, angiotensin receptor blockers, NLRP3 inflammasome inhibitors, and others have either been approved or are being evaluated in clinical trials for the treatment of fibrosis-related diseases. Although their use to address cardiac fibrosis is still limited, a number of pre-clinical studies have demonstrated compelling evidence of their efficiency.

Despite promising results in pre-clinical studies, there are multiple challenges that can compromise the clinical translation of the aforementioned novel treatments. Some of these challenges, namely, low concentration at the target site, feasible route of delivery, appropriate time of administration, and the limitations of existing animal models also pertain to other known cardiac therapies. Additional hurdles concern specific therapies such as potential off-target effects in the case of CRISPR and miRNA. Possible solutions to these issues include the synergistic use of several therapeutic approaches together, the establishment of more rigorous administration protocols, the utilization of human organoids for CVD models, in silico testing, and bioinformatics tools to prevent off-site mutagenesis and many others.

Author Contributions: Conceptualization and editing, A.S.; Writing—original draft preparation, K.R., Y.K., Z.Z. and K.T. All authors have read and agreed to the published version of the manuscript.

Funding: This research was funded by a Collaborative Research grant from Nazarbayev University (021220CRP0722).

Institutional Review Board Statement: Not applicable.

Informed Consent Statement: Not applicable.

Conflicts of Interest: The authors declare no conflict of interest.

References

1. Virani, S.S.; Alonso, A.; Benjamin, E.J.; Bittencourt, M.S.; Callaway, C.W.; Carson, A.P.; Chamberlain, A.M.; Chang, A.R.; Cheng, S.; Delling, F.N. Heart disease and stroke statistics—2020 update: A report from the American Heart Association. *Circulation* **2020**, *141*, e139–e596. [CrossRef] [PubMed]
2. Timmis, A.; Vardas, P.; Townsend, N.; Torbica, A.; Katus, H.; De Smedt, D.; Gale, C.P.; Maggioni, A.P.; Petersen, S.E.; Huculeci, R. European Society of Cardiology: Cardiovascular disease statistics 2021. *Eur. Heart J.* **2022**, *43*, 716–799. [CrossRef] [PubMed]
3. Weiskirchen, R.; Weiskirchen, S.; Tacke, F. Organ and tissue fibrosis: Molecular signals, cellular mechanisms and translational implications. *Mol. Asp. Med.* **2019**, *65*, 2–15. [CrossRef] [PubMed]
4. Klinkhammer, B.M.; Floege, J.; Boor, P. PDGF in organ fibrosis. *Mol. Asp. Med.* **2018**, *62*, 44–62. [CrossRef]
5. Hashimoto, H.; Olson, E.N.; Bassel-Duby, R. Therapeutic approaches for cardiac regeneration and repair. *Nat. Rev. Cardiol.* **2018**, *15*, 585–600. [CrossRef]
6. Raziyeva, K.; Smagulova, A.; Kim, Y.; Smagul, S.; Nurkesh, A.; Saparov, A. Preconditioned and genetically modified stem cells for myocardial infarction treatment. *Int. J. Mol. Sci.* **2020**, *21*, 7301. [CrossRef]
7. Kim, Y.; Zharkinbekov, Z.; Sarsenova, M.; Yeltay, G.; Saparov, A. Recent Advances in Gene Therapy for Cardiac Tissue Regeneration. *Int. J. Mol. Sci.* **2021**, *22*, 9206. [CrossRef]
8. Hinderer, S.; Schenke-Layland, K. Cardiac fibrosis—A short review of causes and therapeutic strategies. *Adv. Drug Deliv. Rev.* **2019**, *146*, 77–82. [CrossRef]
9. De Boer, R.A.; Heymans, S.; Backs, J.; Carrier, L.; Coats, A.J.; Dimmeler, S.; Eschenhagen, T.; Filippatos, G.; Gepstein, L.; Hulot, J.S. Targeted therapies in genetic dilated and hypertrophic cardiomyopathies: From molecular mechanisms to therapeutic targets. A position paper from the Heart Failure Association (HFA) and the Working Group on Myocardial Function of the European Society of Cardiology (ESC). *Eur. J. Heart Fail.* **2022**, *24*, 406–420.

10. Raafs, A.G.; Verdonschot, J.A.; Henkens, M.T.; Adriaans, B.P.; Wang, P.; Derks, K.; Abdul Hamid, M.A.; Knackstedt, C.; van Empel, V.P.; Díez, J. The combination of carboxy-terminal propeptide of procollagen type I blood levels and late gadolinium enhancement at cardiac magnetic resonance provides additional prognostic information in idiopathic dilated cardiomyopathy–A multilevel assessment of myocardial fibrosis in dilated cardiomyopathy. *Eur. J. Heart Fail.* **2021**, *23*, 933–944.
11. Zhao, X.; Kwan, J.Y.Y.; Yip, K.; Liu, P.P.; Liu, F.-F. Targeting metabolic dysregulation for fibrosis therapy. *Nat. Rev. Drug Discov.* **2020**, *19*, 57–75. [CrossRef] [PubMed]
12. Park, S.; Nguyen, N.B.; Pezhouman, A.; Ardehali, R. Cardiac fibrosis: Potential therapeutic targets. *Transl. Res.* **2019**, *209*, 121–137. [CrossRef]
13. Ma, Z.G.; Yuan, Y.P.; Wu, H.M.; Zhang, X.; Tang, Q.Z. Cardiac fibrosis: New insights into the pathogenesis. *Int. J. Biol. Sci.* **2018**, *14*, 1645–1657. [CrossRef]
14. Kim, Y.; Nurakhayev, S.; Nurkesh, A.; Zharkinbekov, Z.; Saparov, A. Macrophage Polarization in Cardiac Tissue Repair following Myocardial Infarction. *Int. J. Mol. Sci.* **2021**, *22*, 2715. [CrossRef] [PubMed]
15. Gibb, A.A.; Lazaropoulos, M.P.; Elrod, J.W. Myofibroblasts and fibrosis: Mitochondrial and metabolic control of cellular differentiation. *Circ. Res.* **2020**, *127*, 427–447. [CrossRef] [PubMed]
16. Disertori, M.; Masè, M.; Ravelli, F. Myocardial fibrosis predicts ventricular tachyarrhythmias. *Trends Cardiovasc. Med.* **2017**, *27*, 363–372. [CrossRef]
17. Hall, C.; Gehmlich, K.; Denning, C.; Pavlovic, D. Complex relationship between cardiac fibroblasts and cardiomyocytes in health and disease. *J. Am. Heart Assoc.* **2021**, *10*, e019338. [CrossRef]
18. Park, T.-J.; Park, J.H.; Lee, G.S.; Lee, J.-Y.; Shin, J.H.; Kim, M.W.; Kim, Y.S.; Kim, J.-Y.; Oh, K.-J.; Han, B.-S. Quantitative proteomic analyses reveal that GPX4 downregulation during myocardial infarction contributes to ferroptosis in cardiomyocytes. *Cell Death Dis.* **2019**, *10*, 1–15. [CrossRef]
19. Giacca, M. Cardiac regeneration after myocardial infarction: An approachable goal. *Curr. Cardiol. Rep.* **2020**, *22*, 1–8. [CrossRef]
20. Yousefi, F.; Shabaninejad, Z.; Vakili, S.; Derakhshan, M.; Movahedpour, A.; Dabiri, H.; Ghasemi, Y.; Mahjoubin-Tehran, M.; Nikoozadeh, A.; Savardashtaki, A. TGF-β and WNT signaling pathways in cardiac fibrosis: Non-coding RNAs come into focus. *Cell Commun. Signal.* **2020**, *18*, 1–16. [CrossRef]
21. Bacmeister, L.; Schwarzl, M.; Warnke, S.; Stoffers, B.; Blankenberg, S.; Westermann, D.; Lindner, D. Inflammation and fibrosis in murine models of heart failure. *Basic Res. Cardiol.* **2019**, *114*, 1–35. [CrossRef] [PubMed]
22. Kurose, H. Cardiac fibrosis and fibroblasts. *Cells* **2021**, *10*, 1716. [CrossRef] [PubMed]
23. Webber, M.; Jackson, S.P.; Moon, J.C.; Captur, G. Myocardial fibrosis in heart failure: Anti-fibrotic therapies and the role of cardiovascular magnetic resonance in drug trials. *Cardiol. Ther.* **2020**, *9*, 363–376. [CrossRef] [PubMed]
24. Karamitsos, T.D.; Arvanitaki, A.; Karvounis, H.; Neubauer, S.; Ferreira, V.M. Myocardial tissue characterization and fibrosis by imaging. *Cardiovasc. Imaging* **2020**, *13*, 1221–1234. [CrossRef] [PubMed]
25. Tanaka, R.; Umemura, M.; Narikawa, M.; Hikichi, M.; Osaw, K.; Fujita, T.; Yokoyama, U.; Ishigami, T.; Tamura, K.; Ishikawa, Y. Reactive fibrosis precedes doxorubicin-induced heart failure through sterile inflammation. *ESC Heart Fail.* **2020**, *7*, 588–603. [CrossRef]
26. Hara, H.; Takeda, N.; Komuro, I. Pathophysiology and therapeutic potential of cardiac fibrosis. *Inflamm. Regen.* **2017**, *37*, 1–10. [CrossRef]
27. Kyriakou, P.; Mouselimis, D.; Tsarouchas, A.; Rigopoulos, A.; Bakogiannis, C.; Noutsias, M.; Vassilikos, V. Diagnosis of cardiac amyloidosis: A systematic review on the role of imaging and biomarkers. *BMC Cardiovasc. Disord.* **2018**, *18*, 221. [CrossRef]
28. Bonderman, D.; Pölzl, G.; Ablasser, K.; Agis, H.; Aschauer, S.; Auer-Grumbach, M.; Binder, C.; Dörler, J.; Duca, F.; Ebner, C. Diagnosis and treatment of cardiac amyloidosis: An interdisciplinary consensus statement. *Wien. Klin. Wochenschr.* **2020**, *132*, 742–761. [CrossRef]
29. Heymans, S.; González, A.; Pizard, A.; Papageorgiou, A.P.; López-Andrés, N.; Jaisser, F.; Thum, T.; Zannad, F.; Díez, J. Searching for new mechanisms of myocardial fibrosis with diagnostic and/or therapeutic potential. *Eur. J. Heart Fail.* **2015**, *17*, 764–771. [CrossRef]
30. Frangogiannis, N.G. Cardiac fibrosis: Cell biological mechanisms, molecular pathways and therapeutic opportunities. *Mol. Asp. Med.* **2019**, *65*, 70–99. [CrossRef]
31. Scharf, G.M.; Kilian, K.; Cordero, J.; Wang, Y.; Grund, A.; Hofmann, M.; Froese, N.; Wang, X.; Kispert, A.; Kist, R.; et al. Inactivation of Sox9 in fibroblasts reduces cardiac fibrosis and inflammation. *JCI Insight* **2019**, *5*, e126721. [CrossRef] [PubMed]
32. Wen, H.; Peng, L.; Chen, Y. The effect of immune cell-derived exosomes in the cardiac tissue repair after myocardial infarction: Molecular mechanisms and pre-clinical evidence. *J. Cell. Mol. Med.* **2021**, *25*, 6500–6510. [CrossRef] [PubMed]
33. Kong, P.; Christia, P.; Frangogiannis, N.G. The pathogenesis of cardiac fibrosis. *Cell. Mol. Life Sci.* **2014**, *71*, 549–574. [CrossRef] [PubMed]
34. Raziyeva, K.; Kim, Y.; Zharkinbekov, Z.; Kassymbek, K.; Jimi, S.; Saparov, A. Immunology of acute and chronic wound healing. *Biomolecules* **2021**, *11*, 700. [CrossRef] [PubMed]
35. Ceauşu, Z.; Socea, B.; Costache, M.; Predescu, D.; Şerban, D.; Smarandache, C.G.; Pacu, I.; Alexandru, H.H.; Daviţoiu, A.M.; Jacotă-Alexe, F. Fibroblast involvement in cardiac remodeling and repair under ischemic conditions. *Exp. Ther. Med.* **2021**, *21*, 1. [CrossRef]

36. Talman, V.; Ruskoaho, H. Cardiac fibrosis in myocardial infarction—from repair and remodeling to regeneration. *Cell Tissue Res.* **2016**, *365*, 563–581. [CrossRef] [PubMed]
37. Ni, H.; Li, W.; Zhuge, Y.; Xu, S.; Wang, Y.; Chen, Y.; Shen, G.; Wang, F. Inhibition of circHIPK3 prevents angiotensin II-induced cardiac fibrosis by sponging miR-29b-3p. *Int. J. Cardiol.* **2019**, *292*, 188–196. [CrossRef]
38. Krenning, G.; Zeisberg, E.M.; Kalluri, R. The origin of fibroblasts and mechanism of cardiac fibrosis. *J. Cell. Physiol.* **2010**, *225*, 631–637. [CrossRef]
39. Frangogiannis, N.G. Cardiac fibrosis. *Cardiovasc. Res.* **2021**, *117*, 1450–1488. [CrossRef]
40. Aujla, P.K.; Kassiri, Z. Diverse origins and activation of fibroblasts in cardiac fibrosis. *Cell. Signal.* **2021**, *78*, 109869. [CrossRef]
41. Dobaczewski, M.; de Haan, J.J.; Frangogiannis, N.G. The extracellular matrix modulates fibroblast phenotype and function in the infarcted myocardium. *J. Cardiovasc. Transl. Res.* **2012**, *5*, 837–847. [CrossRef] [PubMed]
42. Cakir, S.N.; Whitehead, K.M.; Hendricks, H.K.; de Castro Brás, L.E. Novel Techniques Targeting Fibroblasts after Ischemic Heart Injury. *Cells* **2022**, *11*, 402. [CrossRef] [PubMed]
43. Sygitowicz, G.; Maciejak-Jastrzębska, A.; Sitkiewicz, D. A review of the molecular mechanisms underlying cardiac fibrosis and atrial fibrillation. *J. Clin. Med.* **2021**, *10*, 4430. [CrossRef] [PubMed]
44. Hamid, T.; Xu, Y.; Ismahil, M.A.; Rokosh, G.; Jinno, M.; Zhou, G.; Wang, Q.; Prabhu, S.D. Cardiac mesenchymal stem cells promote fibrosis and remodeling in heart failure: Role of PDGF signaling. *JACC Basic Transl. Sci.* **2022**, *7*, 465–483. [CrossRef]
45. Liu, Y.; Yin, Z.; Xu, X.; Liu, C.; Duan, X.; Song, Q.; Tuo, Y.; Wang, C.; Yang, J.; Yin, S. Crosstalk between the activated Slit2–Robo1 pathway and TGF-β1 signalling promotes cardiac fibrosis. *ESC Heart Fail.* **2021**, *8*, 447–460. [CrossRef] [PubMed]
46. Noskovicova, N.; Schuster, R.; van Putten, S.; Ezzo, M.; Koehler, A.; Boo, S.; Coelho, N.M.; Griggs, D.; Ruminski, P.; McCulloch, C.A. Suppression of the fibrotic encapsulation of silicone implants by inhibiting the mechanical activation of pro-fibrotic TGF-β. *Nat. Biomed. Eng.* **2021**, *5*, 1437–1456. [CrossRef]
47. Działo, E.; Czepiel, M.; Tkacz, K.; Siedlar, M.; Kania, G.; Błyszczuk, P. WNT/β-catenin signaling promotes TGF-β-mediated activation of human cardiac fibroblasts by enhancing IL-11 production. *Int. J. Mol. Sci.* **2021**, *22*, 10072. [CrossRef]
48. Hanna, A.; Humeres, C.; Frangogiannis, N.G. The role of Smad signaling cascades in cardiac fibrosis. *Cell. Signal.* **2021**, *77*, 109826. [CrossRef]
49. Vallée, A.; Lecarpentier, Y. TGF-β in fibrosis by acting as a conductor for contractile properties of myofibroblasts. *Cell Biosci.* **2019**, *9*, 1–15. [CrossRef]
50. Parichatikanond, W.; Luangmonkong, T.; Mangmool, S.; Kurose, H. Therapeutic targets for the treatment of cardiac fibrosis and cancer: Focusing on TGF-β signaling. *Front. Cardiovasc. Med.* **2020**, *7*, 34. [CrossRef]
51. AlQudah, M.; Hale, T.M.; Czubryt, M.P. Targeting the renin-angiotensin-aldosterone system in fibrosis. *Matrix Biol.* **2020**, *91*, 92–108. [CrossRef] [PubMed]
52. Jia, G.; Aroor, A.R.; Hill, M.A.; Sowers, J.R. Role of renin-angiotensin-aldosterone system activation in promoting cardiovascular fibrosis and stiffness. *Hypertension* **2018**, *72*, 537–548. [CrossRef] [PubMed]
53. Lyu, X.; Hu, M.; Peng, J.; Zhang, X.; Sanders, Y.Y. HDAC inhibitors as antifibrotic drugs in cardiac and pulmonary fibrosis. *Ther. Adv. Chronic Dis.* **2019**, *10*, 2040622319862697. [CrossRef]
54. Yoon, S.; Kang, G.; Eom, G.H. HDAC inhibitors: Therapeutic potential in fibrosis-associated human diseases. *Int. J. Mol. Sci.* **2019**, *20*, 1329. [CrossRef]
55. Fernández-Barrena, M.G.; Arechederra, M.; Colyn, L.; Berasain, C.; Avila, M.A. Epigenetics in hepatocellular carcinoma development and therapy: The tip of the iceberg. *JHEP Rep.* **2020**, *2*, 100167. [CrossRef] [PubMed]
56. Prasher, D.; Greenway, S.C.; Singh, R.B. The impact of epigenetics on cardiovascular disease. *Biochem. Cell Biol.* **2020**, *98*, 12–22. [CrossRef]
57. Soler-Botija, C.; Forcales, S.V.; Genís, A.B. Spotlight on epigenetic reprogramming in cardiac regeneration. *Semin. Cell Dev. Biol.* **2020**, *97*, 26–37. [CrossRef]
58. Li, X.; Yang, Y.; Chen, S.; Zhou, J.; Li, J.; Cheng, Y. Epigenetics-based therapeutics for myocardial fibrosis. *Life Sci.* **2021**, *271*, 119186. [CrossRef]
59. Wang, Y.; Chen, P.; Wang, L.; Zhao, J.; Zhong, Z.; Wang, Y.; Xu, J. Inhibition of histone deacetylases prevents cardiac remodeling after myocardial infarction by restoring autophagosome processing in cardiac fibroblasts. *Cell. Physiol. Biochem.* **2018**, *49*, 1999–2011. [CrossRef]
60. Zhang, L.X.; Du, J.; Zhao, Y.T.; Wang, J.; Zhang, S.; Dubielecka, P.M.; Wei, L.; Zhuang, S.; Qin, G.; Chin, Y.E. Transgenic overexpression of active HDAC4 in the heart attenuates cardiac function and exacerbates remodeling in infarcted myocardium. *J. Appl. Physiol.* **2018**, *125*, 1968–1978. [CrossRef]
61. Barbosa, D.M.; Fahlbusch, P.; Herzfeld de Wiza, D.; Jacob, S.; Kettel, U.; Al-Hasani, H.; Krüger, M.; Ouwens, D.M.; Hartwig, S.; Lehr, S. Rhein, a novel Histone Deacetylase (HDAC) inhibitor with antifibrotic potency in human myocardial fibrosis. *Sci. Rep.* **2020**, *10*, 4888. [CrossRef] [PubMed]
62. Li, F.; Li, L.; Zhang, J.; Yang, X.; Liu, Y. Histone methyltransferase DOT1L mediates the TGF-β1/Smad3 signaling pathway through epigenetic modification of SYK in myocardial infarction. *Hum. Cell* **2022**, *35*, 98–110. [CrossRef] [PubMed]
63. Sung, P.-H.; Luo, C.-W.; Chiang, J.Y.; Yip, H.-K. The combination of G9a histone methyltransferase inhibitors with erythropoietin protects heart against damage from acute myocardial infarction. *Am. J. Transl. Res.* **2020**, *12*, 3255.

64. Liu, F.; Wen, Y.; Kang, J.; Wei, C.; Wang, M.; Zheng, Z.; Peng, J. Regulation of TLR4 expression mediates the attenuating effect of erythropoietin on inflammation and myocardial fibrosis in rat heart. *Int. J. Mol. Med.* **2018**, *42*, 1436–1444. [CrossRef] [PubMed]
65. Yu, L.; Wang, L.; Yi, H.; Wu, X. LRP6-CRISPR prevents activation of hepatic stellate cells and liver fibrogenesis in rats. *Am. J. Transl. Res.* **2020**, *12*, 397.
66. Yu, L.; Wang, L.; Wu, X.; Yi, H. RSPO4-CRISPR alleviates liver injury and restores gut microbiota in a rat model of liver fibrosis. *Commun. Biol.* **2021**, *4*, 230. [CrossRef] [PubMed]
67. Xu, X.; Tan, X.; Tampe, B.; Wilhelmi, T.; Hulshoff, M.S.; Saito, S.; Moser, T.; Kalluri, R.; Hasenfuss, G.; Zeisberg, E.M. High-fidelity CRISPR/Cas9-based gene-specific hydroxymethylation rescues gene expression and attenuates renal fibrosis. *Nat. Commun.* **2018**, *9*, 3509. [CrossRef]
68. Tan, Q.; Link, P.A.; Meridew, J.A.; Pham, T.X.; Caporarello, N.; Ligresti, G.; Tschumperlin, D.J. Spontaneous lung fibrosis resolution reveals novel antifibrotic regulators. *Am. J. Respir. Cell Mol. Biol.* **2021**, *64*, 453–464. [CrossRef]
69. Nishiga, M.; Liu, C.; Qi, L.S.; Wu, J.C. The use of new CRISPR tools in cardiovascular research and medicine. *Nat. Rev. Cardiol.* **2022**, *19*, 505–521. [CrossRef]
70. Park, H.; Kim, D.; Cho, B.; Byun, J.; Kim, Y.S.; Ahn, Y.; Hur, J.; Oh, Y.-K.; Kim, J. In vivo therapeutic genome editing via CRISPR/Cas9 magnetoplexes for myocardial infarction. *Biomaterials* **2022**, *281*, 121327. [CrossRef]
71. Jiang, L.; Liang, J.; Huang, W.; Ma, J.; Park, K.H.; Wu, Z.; Chen, P.; Zhu, H.; Ma, J.-J.; Cai, W. CRISPR activation of endogenous genes reprograms fibroblasts into cardiovascular progenitor cells for myocardial infarction therapy. *Mol. Ther.* **2022**, *30*, 54–74. [CrossRef] [PubMed]
72. Cho, H.-M.; Lee, K.-H.; Shen, Y.-M.; Shin, T.-J.; Ryu, P.-D.; Choi, M.-C.; Kang, K.-S.; Cho, J.-Y. Transplantation of hMSCs genome edited with LEF1 improves cardio-protective effects in myocardial infarction. *Mol. Ther. Nucleic Acids* **2020**, *19*, 1186–1197. [CrossRef] [PubMed]
73. Meng, X.; Zheng, M.; Yu, M.; Bai, W.; Zuo, L.; Bu, X.; Liu, Y.; Xia, L.; Hu, J.; Liu, L. Transplantation of CRISPRa system engineered IL10-overexpressing bone marrow-derived mesenchymal stem cells for the treatment of myocardial infarction in diabetic mice. *J. Biol. Eng.* **2019**, *13*, 1–12. [CrossRef] [PubMed]
74. Liu, Y.; Xu, J.; Wu, M.; Kang, L.; Xu, B. The effector cells and cellular mediators of immune system involved in cardiac inflammation and fibrosis after myocardial infarction. *J. Cell. Physiol.* **2020**, *235*, 8996–9004. [CrossRef] [PubMed]
75. Rezaei, H.; Farahani, N.; Hosseingholi, E.Z.; Sathyapalan, T.; hossein Sahebkar, A. Harnessing CRISPR/Cas9 technology in cardiovascular disease. *Trends Cardiovasc. Med.* **2020**, *30*, 93–101. [CrossRef]
76. Dexheimer, P.J.; Cochella, L. MicroRNAs: From Mechanism to Organism. *Front. Cell Dev. Biol.* **2020**, *8*, 409. [CrossRef]
77. Ferrari, S.; Pesce, M. Cell-Based Mechanosensation, Epigenetics, and Non-Coding RNAs in Progression of Cardiac Fibrosis. *Int. J. Mol. Sci.* **2019**, *21*, 28. [CrossRef]
78. Varzideh, F.; Kansakar, U.; Donkor, K.; Wilson, S.; Jankauskas, S.S.; Mone, P.; Wang, X.; Lombardi, A.; Santulli, G. Cardiac Remodeling After Myocardial Infarction: Functional Contribution of microRNAs to Inflammation and Fibrosis. *Front. Cardiovasc. Med.* **2022**, *9*, 863238. [CrossRef]
79. O'Reilly, S. MicroRNAs in fibrosis: Opportunities and challenges. *Arthritis Res. Ther.* **2016**, *18*, 11. [CrossRef]
80. Ghafouri-Fard, S.; Abak, A.; Talebi, S.F.; Shoorei, H.; Branicki, W.; Taheri, M.; Dilmaghani, N.A. Role of miRNA and lncRNAs in organ fibrosis and aging. *Biomed. Pharmacother.* **2021**, *143*, 112132. [CrossRef]
81. Liu, X.; Xu, Y.; Deng, Y.; Li, H. MicroRNA-223 regulates cardiac fibrosis after myocardial infarction by targeting RASA1. *Cell. Physiol. Biochem.* **2018**, *46*, 1439–1454. [CrossRef] [PubMed]
82. Liu, Y.; Song, J.-W.; Lin, J.-Y.; Miao, R.; Zhong, J.-C. Roles of microRNA-122 in cardiovascular fibrosis and related diseases. *Cardiovasc. Toxicol.* **2020**, *20*, 463–473. [CrossRef] [PubMed]
83. Peters, L.J.F.; Biessen, E.A.L.; Hohl, M.; Weber, C.; van der Vorst, E.P.C.; Santovito, D. Small Things Matter: Relevance of MicroRNAs in Cardiovascular Disease. *Front. Physiol.* **2020**, *11*, 793. [CrossRef] [PubMed]
84. Li, G.; Shao, Y.; Guo, H.C.; Zhi, Y.; Qiao, B.; Ma, K.; Lai, Y.Q.; Du, J.; Li, Y. MicroRNA-27b-3p downregulates FGF1 and aggravates pathological cardiac remodelling. *Cardiovasc. Res.* **2021**, *118*, 2139–2151. [CrossRef] [PubMed]
85. Chatterjee, E.; Das, S. Non-coding RNAs in cardiac remodeling: Diversity in composition and function. *Curr. Opin. Physiol.* **2022**, *26*, 100534. [CrossRef]
86. Fu, Q.; Lu, Z.; Fu, X.; Ma, S.; Lu, X. MicroRNA 27b promotes cardiac fibrosis by targeting the FBW7/Snail pathway. *Aging* **2019**, *11*, 11865–11879. [CrossRef] [PubMed]
87. Su, L.; Yao, Y.; Song, W. Downregulation of miR-96 suppresses the profibrogenic functions of cardiac fibroblasts induced by angiotensin II and attenuates atrial fibrosis by upregulating KLF13. *Hum. Cell* **2020**, *33*, 337–346. [CrossRef]
88. Yu, Y.H.; Zhang, Y.H.; Ding, Y.Q.; Bi, X.Y.; Yuan, J.; Zhou, H.; Wang, P.X.; Zhang, L.L.; Ye, J.T. MicroRNA-99b-3p promotes angiotensin II-induced cardiac fibrosis in mice by targeting GSK-3β. *Acta Pharmacol. Sin.* **2021**, *42*, 715–725. [CrossRef]
89. Xiao, J.; Zhang, Y.; Tang, Y.; Dai, H.; OuYang, Y.; Li, C.; Yu, M. MiRNA-1202 promotes the TGF-β1-induced proliferation, differentiation and collagen production of cardiac fibroblasts by targeting nNOS. *PLoS ONE* **2021**, *16*, e0256066. [CrossRef]
90. Chen, C.; Ponnusamy, M.; Liu, C.; Gao, J.; Wang, K.; Li, P. MicroRNA as a Therapeutic Target in Cardiac Remodeling. *BioMed Res. Int.* **2017**, *2017*, 1278436. [CrossRef]

91. Yuan, J.; Liu, H.; Gao, W.; Zhang, L.; Ye, Y.; Yuan, L.; Ding, Z.; Wu, J.; Kang, L.; Zhang, X.; et al. MicroRNA-378 suppresses myocardial fibrosis through a paracrine mechanism at the early stage of cardiac hypertrophy following mechanical stress. *Theranostics* **2018**, *8*, 2565–2582. [CrossRef]
92. Tian, H.B.; Li, S.H.; Hu, K.Q.; Zan, Y.S.; Zhang, X.L.; Su, G.H. MicroRNA-150 alleviates acute myocardial infarction through regulating cardiac fibroblasts in ventricular remodeling. *Eur. Rev. Med. Pharmacol. Sci.* **2019**, *23*, 7611–7618. [CrossRef]
93. Shen, J.; Xing, W.; Gong, F.; Wang, W.; Yan, Y.; Zhang, Y.; Xie, C.; Fu, S. MiR-150-5p retards the progression of myocardial fibrosis by targeting EGR1. *Cell Cycle* **2019**, *18*, 1335–1348. [CrossRef]
94. Chiasson, V.; Takano, A.P.C.; Guleria, R.S.; Gupta, S. Deficiency of MicroRNA miR-1954 Promotes Cardiac Remodeling and Fibrosis. *J. Am. Heart Assoc.* **2019**, *8*, e012880. [CrossRef]
95. Yang, X.; Yu, T.; Zhang, S. MicroRNA-489 suppresses isoproterenol-induced cardiac fibrosis by downregulating histone deacetylase 2. *Exp. Ther. Med.* **2020**, *19*, 2229–2235. [CrossRef]
96. Li, J.; Salvador, A.M.; Li, G.; Valkov, N.; Ziegler, O.; Yeri, A.; Yang Xiao, C.; Meechoovet, B.; Alsop, E.; Rodosthenous, R.S.; et al. Mir-30d Regulates Cardiac Remodeling by Intracellular and Paracrine Signaling. *Circ. Res.* **2021**, *128*, e1–e23. [CrossRef]
97. Cui, S.; Liu, Z.; Tao, B.; Fan, S.; Pu, Y.; Meng, X.; Li, D.; Xia, H.; Xu, L. miR-145 attenuates cardiac fibrosis through the AKT/GSK-3β/β-catenin signaling pathway by directly targeting SOX9 in fibroblasts. *J. Cell. Biochem.* **2021**, *122*, 209–221. [CrossRef]
98. Liu, M.; de Juan Abad, B.L.; Cheng, K. Cardiac fibrosis: Myofibroblast-mediated pathological regulation and drug delivery strategies. *Adv. Drug Deliv. Rev.* **2021**, *173*, 504–519. [CrossRef]
99. Leader, C.J.; Moharram, M.; Coffey, S.; Sammut, I.A.; Wilkins, G.W.; Walker, R.J. Myocardial global longitudinal strain: An early indicator of cardiac interstitial fibrosis modified by spironolactone, in a unique hypertensive rat model. *PLoS ONE* **2019**, *14*, e0220837. [CrossRef]
100. Kovács, Z.Z.; Szűcs, G.; Freiwan, M.; Kovács, M.G.; Márványkövi, F.M.; Dinh, H.; Siska, A.; Farkas, K.; Kovács, F.; Kriston, A. Comparison of the antiremodeling effects of losartan and mirabegron in a rat model of uremic cardiomyopathy. *Sci. Rep.* **2021**, *11*, 17495. [CrossRef]
101. Khder, Y.; Shi, V.; McMurray, J.J.V.; Lefkowitz, M.P. Sacubitril/Valsartan (LCZ696) in Heart Failure. *Handb. Exp. Pharmacol.* **2017**, *243*, 133–165. [CrossRef]
102. Burke, R.M.; Lighthouse, J.K.; Mickelsen, D.M.; Small, E.M. Sacubitril/Valsartan Decreases Cardiac Fibrosis in Left Ventricle Pressure Overload by Restoring PKG Signaling in Cardiac Fibroblasts. *Circ. Heart Fail.* **2019**, *12*, e005565. [CrossRef]
103. Vaskova, E.; Ikeda, G.; Tada, Y.; Wahlquist, C.; Mercola, M.; Yang, P.C. Sacubitril/Valsartan Improves Cardiac Function and Decreases Myocardial Fibrosis Via Downregulation of Exosomal miR-181a in a Rodent Chronic Myocardial Infarction Model. *J. Am. Heart Assoc.* **2020**, *9*, e015640. [CrossRef]
104. Wang, L.; Liu, C.; Chen, X.; Li, P. Alamandine attenuates long-term hypertension-induced cardiac fibrosis independent of blood pressure. *Mol. Med. Rep.* **2019**, *19*, 4553–4560. [CrossRef]
105. Silva, M.M.; de Souza-Neto, F.P.; Jesus, I.C.G.; Gonçalves, G.K.; Santuchi, M.C.; Sanches, B.L.; de Alcântara-Leonídio, T.C.; Melo, M.B.; Vieira, M.A.R.; Guatimosim, S.; et al. Alamandine improves cardiac remodeling induced by transverse aortic constriction in mice. *Am. J. Physiol. Heart Circ. Physiol.* **2021**, *320*, H352–H363. [CrossRef]
106. Fu, J.; Li, F.; Tang, Y.; Cai, L.; Zeng, C.; Yang, Y.; Yang, J. The Emerging Role of Irisin in Cardiovascular Diseases. *J. Am. Heart Assoc.* **2021**, *10*, e022453. [CrossRef]
107. Chen, R.R.; Fan, X.H.; Chen, G.; Zeng, G.W.; Xue, Y.G.; Liu, X.T.; Wang, C.Y. Irisin attenuates angiotensin II-induced cardiac fibrosis via Nrf2 mediated inhibition of ROS/ TGFβ1/Smad2/3 signaling axis. *Chem. Biol. Interact.* **2019**, *302*, 11–21. [CrossRef]
108. Pan, J.A.; Zhang, H.; Lin, H.; Gao, L.; Zhang, H.L.; Zhang, J.F.; Wang, C.Q.; Gu, J. Irisin ameliorates doxorubicin-induced cardiac perivascular fibrosis through inhibiting endothelial-to-mesenchymal transition by regulating ROS accumulation and autophagy disorder in endothelial cells. *Redox Biol.* **2021**, *46*, 102120. [CrossRef]
109. Ambari, A.M.; Setianto, B.; Santoso, A.; Radi, B.; Dwiputra, B.; Susilowati, E.; Tulrahmi, F.; Doevendans, P.A.; Cramer, M.J. Angiotensin Converting Enzyme Inhibitors (ACEIs) Decrease the Progression of Cardiac Fibrosis in Rheumatic Heart Disease Through the Inhibition of IL-33/sST2. *Front. Cardiovasc. Med.* **2020**, *7*, 115. [CrossRef]
110. Wang, L.; Tan, A.; An, X.; Xia, Y.; Xie, Y. Quercetin Dihydrate inhibition of cardiac fibrosis induced by angiotensin II In Vivo and In Vitro. *Biomed. Pharm.* **2020**, *127*, 110205. [CrossRef]
111. Li, M.; Qi, C.; Song, R.; Xiong, C.; Zhong, X.; Song, Z.; Ning, Z.; Song, X. Inhibition of Long Noncoding RNA SNHG20 Improves Angiotensin II-Induced Cardiac Fibrosis and Hypertrophy by Regulating the MicroRNA 335/Galectin-3 Axis. *Mol. Cell Biol.* **2021**, *41*, e0058020. [CrossRef]
112. Ock, S.; Ham, W.; Kang, C.W.; Kang, H.; Lee, W.S.; Kim, J. IGF-1 protects against angiotensin II-induced cardiac fibrosis by targeting αSMA. *Cell Death Dis.* **2021**, *12*, 688. [CrossRef] [PubMed]
113. Lipson, K.E.; Wong, C.; Teng, Y.; Spong, S. CTGF is a central mediator of tissue remodeling and fibrosis and its inhibition can reverse the process of fibrosis. *Fibrogenesis Tissue Repair* **2012**, *5*, S24. [CrossRef] [PubMed]
114. Meagher, P.B.; Lee, X.A.; Lee, J.; Visram, A.; Friedberg, M.K.; Connelly, K.A. Cardiac fibrosis: Key role of integrins in cardiac homeostasis and remodeling. *Cells* **2021**, *10*, 770. [CrossRef] [PubMed]

115. Vainio, L.E.; Szabó, Z.; Lin, R.; Ulvila, J.; Yrjölä, R.; Alakoski, T.; Piuhola, J.; Koch, W.J.; Ruskoaho, H.; Fouse, S.D.; et al. Connective Tissue Growth Factor Inhibition Enhances Cardiac Repair and Limits Fibrosis After Myocardial Infarction. *JACC Basic Transl. Sci.* **2019**, *4*, 83–94. [CrossRef]
116. Aimo, A.; Cerbai, E.; Bartolucci, G.; Adamo, L.; Barison, A.; Lo Surdo, G.; Biagini, S.; Passino, C.; Emdin, M. Pirfenidone is a cardioprotective drug: Mechanisms of action and preclinical evidence. *Pharmacol. Res.* **2020**, *155*, 104694. [CrossRef]
117. Graziani, F.; Varone, F.; Crea, F.; Richeldi, L. Treating heart failure with preserved ejection fraction: Learning from pulmonary fibrosis. *Eur. J. Heart Fail.* **2018**, *20*, 1385–1391. [CrossRef]
118. Nguyen, D.T.; Ding, C.; Wilson, E.; Marcus, G.M.; Olgin, J.E. Pirfenidone mitigates left ventricular fibrosis and dysfunction after myocardial infarction and reduces arrhythmias. *Heart Rhythm.* **2010**, *7*, 1438–1445. [CrossRef]
119. Li, C.; Han, R.; Kang, L.; Wang, J.; Gao, Y.; Li, Y.; He, J.; Tian, J. Pirfenidone controls the feedback loop of the AT1R/p38 MAPK/renin-angiotensin system axis by regulating liver X receptor-α in myocardial infarction-induced cardiac fibrosis. *Sci. Rep.* **2017**, *7*, 40523. [CrossRef]
120. Adamo, L.; Staloch, L.J.; Rocha-Resende, C.; Matkovich, S.J.; Jiang, W.; Bajpai, G.; Weinheimer, C.J.; Kovacs, A.; Schilling, J.D.; Barger, P.M.; et al. Modulation of subsets of cardiac B lymphocytes improves cardiac function after acute injury. *JCI Insight* **2018**, *3*, e120137. [CrossRef]
121. Yao, Y.; Hu, C.; Song, Q.; Li, Y.; Da, X.; Yu, Y.; Li, H.; Clark, I.M.; Chen, Q.; Wang, Q.K. ADAMTS16 activates latent TGF-β, accentuating fibrosis and dysfunction of the pressure-overloaded heart. *Cardiovasc. Res.* **2020**, *116*, 956–969. [CrossRef] [PubMed]
122. Humeres, C.; Shinde, A.V.; Hanna, A.; Alex, L.; Hernández, S.C.; Li, R.; Chen, B.; Conway, S.J.; Frangogiannis, N.G. Smad7 effects on TGF-β and ErbB2 restrain myofibroblast activation and protect from postinfarction heart failure. *J. Clin. Investig.* **2022**, *132*, e146926. [CrossRef] [PubMed]
123. Gao, L.; Wang, L.Y.; Liu, Z.Q.; Jiang, D.; Wu, S.Y.; Guo, Y.Q.; Tao, H.M.; Sun, M.; You, L.N.; Qin, S.; et al. TNAP inhibition attenuates cardiac fibrosis induced by myocardial infarction through deactivating TGF-β1/Smads and activating P53 signaling pathways. *Cell Death Dis.* **2020**, *11*, 44. [CrossRef] [PubMed]
124. Xiao, Y.; Ye, J.; Zhou, Y.; Huang, J.; Liu, X.; Huang, B.; Zhu, L.; Wu, B.; Zhang, G.; Cai, Y. Baicalin inhibits pressure overload-induced cardiac fibrosis through regulating AMPK/TGF-β/Smads signaling pathway. *Arch. Biochem. Biophys.* **2018**, *640*, 37–46. [CrossRef]
125. Liu, M.; Li, W.; Wang, H.; Yin, L.; Ye, B.; Tang, Y.; Huang, C. CTRP9 Ameliorates Atrial Inflammation, Fibrosis, and Vulnerability to Atrial Fibrillation in Post-Myocardial Infarction Rats. *J. Am. Heart Assoc.* **2019**, *8*, e013133. [CrossRef]
126. Cao, Z.Q.; Yu, X.; Leng, P. Research progress on the role of gal-3 in cardio/cerebrovascular diseases. *Biomed. Pharm.* **2021**, *133*, 111066. [CrossRef]
127. Li, S.; Li, S.; Hao, X.; Zhang, Y.; Deng, W. Perindopril and a Galectin-3 Inhibitor Improve Ischemic Heart Failure in Rabbits by Reducing Gal-3 Expression and Myocardial Fibrosis. *Front. Physiol.* **2019**, *10*, 267. [CrossRef]
128. Xu, G.R.; Zhang, C.; Yang, H.X.; Sun, J.H.; Zhang, Y.; Yao, T.T.; Li, Y.; Ruan, L.; An, R.; Li, A.Y. Modified citrus pectin ameliorates myocardial fibrosis and inflammation via suppressing galectin-3 and TLR4/MyD88/NF-κB signaling pathway. *Biomed. Pharm.* **2020**, *126*, 110071. [CrossRef]
129. Mezzaroma, E.; Toldo, S.; Farkas, D.; Seropian, I.M.; Van Tassell, B.W.; Salloum, F.N.; Kannan, H.R.; Menna, A.C.; Voelkel, N.F.; Abbate, A. The inflammasome promotes adverse cardiac remodeling following acute myocardial infarction in the mouse. *Proc. Natl. Acad. Sci. USA* **2011**, *108*, 19725–19730. [CrossRef]
130. Zhou, W.; Chen, C.; Chen, Z.; Liu, L.; Jiang, J.; Wu, Z.; Zhao, M.; Chen, Y. NLRP3: A Novel Mediator in Cardiovascular Disease. *J. Immunol. Res.* **2018**, *2018*, 5702103. [CrossRef]
131. Gao, R.; Shi, H.; Chang, S.; Gao, Y.; Li, X.; Lv, C.; Yang, H.; Xiang, H.; Yang, J.; Xu, L.; et al. The selective NLRP3-inflammasome inhibitor MCC950 reduces myocardial fibrosis and improves cardiac remodeling in a mouse model of myocardial infarction. *Int. Immunopharmacol.* **2019**, *74*, 105575. [CrossRef] [PubMed]
132. He, H.; Jiang, H.; Chen, Y.; Ye, J.; Wang, A.; Wang, C.; Liu, Q.; Liang, G.; Deng, X.; Jiang, W.; et al. Oridonin is a covalent NLRP3 inhibitor with strong anti-inflammasome activity. *Nat. Commun.* **2018**, *9*, 2550. [CrossRef] [PubMed]
133. Gao, R.F.; Li, X.; Xiang, H.Y.; Yang, H.; Lv, C.Y.; Sun, X.L.; Chen, H.Z.; Gao, Y.; Yang, J.S.; Luo, W.; et al. The covalent NLRP3-inflammasome inhibitor Oridonin relieves myocardial infarction induced myocardial fibrosis and cardiac remodeling in mice. *Int. Immunopharmacol.* **2021**, *90*, 107133. [CrossRef] [PubMed]
134. Cannavo, A.; Koch, W.J. Targeting β3-Adrenergic Receptors in the Heart: Selective Agonism and β-Blockade. *J. Cardiovasc. Pharmacol.* **2017**, *69*, 71–78. [CrossRef]
135. Michel, L.Y.; Farah, C.; Balligand, J.-L. The beta3 adrenergic receptor in healthy and pathological cardiovascular tissues. *Cells* **2020**, *9*, 2584. [CrossRef]
136. Niu, X.; Zhao, L.; Li, X.; Xue, Y.; Wang, B.; Lv, Z.; Chen, J.; Sun, D.; Zheng, Q. β3-Adrenoreceptor stimulation protects against myocardial infarction injury via eNOS and nNOS activation. *PLoS ONE* **2014**, *9*, e98713. [CrossRef]
137. Rossello, X.; Piñero, A.; Fernández-Jiménez, R.; Sánchez-González, J.; Pizarro, G.; Galán-Arriola, C.; Lobo-Gonzalez, M.; Vilchez, J.P.; García-Prieto, J.; García-Ruiz, J.M. Mirabegron, a Clinically Approved β3 adrenergic receptor agonist, does not reduce infarct size in a swine model of reperfused myocardial infarction. *J. Cardiovasc. Transl. Res.* **2018**, *11*, 310–318. [CrossRef]

biomedicines

MDPI

Review

Direct Oral Anticoagulants for Stroke Prevention in Special Populations: Beyond the Clinical Trials

Andreina Carbone [1], Roberta Bottino [1], Antonello D'Andrea [2] and Vincenzo Russo [1,3,*]

[1] Department of Cardiology, University of Campania "Luigi Vanvitelli", 80131 Naples, Italy
[2] Unit of Cardiology and Intensive Coronary Care, "Umberto I" Hospital, 84014 Nocera Inferiore, Italy
[3] Monaldi Hospital, P.zzale Ettore Ruggeri, 80131 Naples, Italy
* Correspondence: v.p.russo@libero.it; Tel.: +39-081-5665144

Abstract: Currently, direct oral anticoagulants (DOACs) are the first-line anticoagulant strategy in patients with non-valvular atrial fibrillation (NVAF). They are characterized by a more favorable pharmacological profile than warfarin, having demonstrated equal efficacy in stroke prevention and greater safety in terms of intracranial bleeding. The study population in the randomized trials of DOACs was highly selected, so the results of these trials cannot be extended to specific populations such as obese, elderly, frail, and cancer patients, which, on the other hand, are sub-populations widely represented in clinical practice. Furthermore, due to the negative results of DOAC administration in patients with mechanical heart valves, the available evidence in subjects with biological heart valves is still few and often controversial. We sought to review the available literature on the efficacy and safety of DOACs in elderly, obese, underweight, frail, cancer patients, and in patients with bioprosthetic heart valves with NVAF to clarify the best anticoagulant strategy in these special and poorly studied subpopulations.

Keywords: direct oral anticoagulant; stroke prevention; atrial fibrillation; elderly; frail; malignancy; extreme weight; bioprosthetic valve

Citation: Carbone, A.; Bottino, R.; D'Andrea, A.; Russo, V. Direct Oral Anticoagulants for Stroke Prevention in Special Populations: Beyond the Clinical Trials. *Biomedicines* **2023**, *11*, 131. https://doi.org/10.3390/biomedicines11010131

Academic Editor: Bart De Geest

Received: 17 November 2022
Revised: 19 December 2022
Accepted: 29 December 2022
Published: 4 January 2023

1. Introduction

Atrial fibrillation (AF) is the most common arrhythmia in clinical practice, and it is associated with an increased risk of ischemic stroke and mortality [1]. The estimated prevalence of AF in adults is between 2% and 4%, increasing in view of the progressive increase in life expectancy [1].

The European Society of Cardiology (ESC) guidelines recommend the assessment of stroke risk using the CHA2DS2-VASc score, considering oral anticoagulation (OAC) prescription for scores of $\geq$1 in males and $\geq$2 in females [1]. OAC with vitamin K antagonists (VKAs) decrease the risk of stroke by 68% [2], but at the cost of routine monitoring of anticoagulation levels [International Normalized Ratio (INR) determination], due to their pharmacokinetic variability and frequent food and drug interactions [2,3].

Direct oral anticoagulants (DOACs) have emerged as an alternative to VKAs as they have demonstrated comparable efficacy in stroke prevention with less major bleeding than warfarin in patients with non-valvular AF [4]. Moreover, DOACs do not require routine monitoring of anticoagulation parameters as they are characterized by a predictable pharmacokinetic and few drug and food interactions [4]. Dabigatran etexilate is the first established factor IIa (thrombin) inhibitor. It is a prodrug converted into the active form of dabigatran by microsomal carboxylesterases in the liver [1,3]. The mechanism of action of rivaroxaban, apixaban, and edoxaban is the inhibition of prothrombinase complex-bound and clot-associated factor Xa, resulting in a reduction of the thrombin burst during the propagation phase of the coagulation cascade [1].

For special populations, such as elderly and frail patients, subjects with extreme body weight, cancer, and bioprosthetic heart valves (BHV), the indications and the choice of

the optimal OAC therapy are a challenge because of the poor representation of these populations in major randomized clinical trials (RCTs). This review aims to summarize the current relevant literature regarding the use of DOACs in the special populations mentioned above.

2. DOACs in Elderly Patients

Older age increases both ischemic (especially stroke events) and bleeding risk [5,6]. In older patients with AF, VKAs prevent stroke with increased bleeding risk and the need for frequent INR monitoring [7,8]. Likewise, the elderly often present with multiple comorbidities, so an integrated approach to prevent stroke events, including tailored therapy and careful drug-dose monitoring, is mandatory [9–11]. To date, DOACs are the first-line therapy for stroke prevention and are characterized by a more favorable pharmacological profile than VKA. The efficacy and safety profile of DOACs in patients >75 years have been analyzed in various studies, but their use in octogenarians and frail patients is still poorly explored. Table 1 summarizes the main characteristics of principal DOAC trials and outcomes in patients ≥75 years.

In a sub-analysis of the RE-LY (Randomized Evaluation of Long-Term Anticoagulation Therapy) trial [12,13], both dabigatran 110 mg BID and 150 mg BID were found comparable to VKAs for the combined endpoint of stroke/systemic embolism and major bleeding. However, comparing dabigatran dosages with warfarin showed a lower risk of intracranial bleeding but similar or higher extracranial bleeding events [13]. These results were confirmed for stroke and systemic embolism events in both patients ≥80 years [dabigatran 110 mg bid (HR = 0.75; p = non-significant [NS]) and 150 mg bid (HR = 0.67; p = NS)] and ≥85 years old [dabigatran 110 mg bid (HR = 0.52, p = NS) and 150 mg bid (HR = 0.70; p = NS)] [14].

Finally, compared to warfarin, the use of dabigatran in women aged 75 years and older seems to be related to an increased risk of major gastrointestinal bleeding (HR 1.50; $p < 0.05$) as well as in men aged 85 years and older (HR 1.55; $p < 0.05$) [15]. In women ≥85 years, no effect on mortality was found using the dabigatran [15].

A sub-analysis of ROCKET-AF (Rivaroxaban Once-daily oral direct factor Xa inhibition Compared with vitamin K antagonism for Prevention of Stroke and Embolism Trial in Atrial Fibrillation) trial found that in elderly patients (≥75 years old; n = 6229), rivaroxaban had similar efficacy in reducing stroke and systemic embolism (HR = 0.88; $p < 0.05$) with a lower rate of intracranial bleeding (HR = 0.80; $p < 0.05$) when compared with warfarin [16]. Anyway, patients on rivaroxaban showed a higher risk of the combined bleeding endpoint due to more frequent non-major gastrointestinal bleeding (2.81% versus 1.66%/100 patient years; HR 0.70; p: 0.0002) [16].

The ARISTOTLE (Apixaban for Reduction in Stroke and Other Thromboembolic Events in Atrial Fibrillation) trial included 5678 patients ≥75 years (31%) and 2436 patients (18%) ≥80 years at baseline [17]. Apixaban showed absolute clinical benefits in the older population with a significant reduction of stroke or systemic embolism (HR 0.81; $p < 0.05$), major bleeding (HR: 0.66; $p < 0.05$), and intracranial hemorrhage (HR 0.36; $p < 0.05$) in patients ≥80 years compared to warfarin [17].

In a study cohort of 14,214 AF patients (mean age 78.1), the risk of stroke/systemic embolism (HR: 0.65, $p < 0.001$), major bleeding (HR: 0.53, $p < 0.001$), and gastro-intestinal bleeding (HR: 0.53, $p < 0.001$) was lower in the apixaban group when compared with the same number of elderly patients on warfarin (7107 patients in each group) [18]. These results were later confirmed by Yao et al. in a cohort of AF patients with a median age of 73 years old, in which apixaban patients showed a 33% lower risk of stroke/systemic embolism (HR = 0.67 $p = 0.04$) and 55% lower risk of major bleeding (HR 0.45, $p < 0.001$) compared to VKAs [19].

In the ENGAGE AF-TIMI 48 (Effective Anticoagulation with Factor Xa Next Generation in Atrial Fibrillation–Thrombolysis in Myocardial Infarction 48), 40.2% of the enrolled patients were aged over 75 years old and 17% over 80 years old (8474 and 1440 patients, re-

spectively). While the incidence of stroke/systemic embolism in AF patients aged ≥75 years was similar between edoxaban and warfarin (1.5% per year in warfarin group; 1.18% per year in edoxaban group; HR vs. warfarin, HR 0.79; $p < 0.001$ for noninferiority, $p = 0.02$ for superiority), the incidence of major bleeding was lower in the edoxaban group (3.43% per year in warfarin group and 2.75% in edoxaban group) [20].

In a meta-analysis of the randomized controlled trial (RCT), DOACs were associated with equal or greater efficacy than VKAs, without relevant bleeding among patients of ≥75 years [21].

The ELDERCARE-AF (Edoxaban Low-Dose for ElderR CARE AF patients) compared the safety and efficacy of once-daily edoxaban 15 mg versus placebo in AF Japanese patients aged ≥80 years for whom standard oral anticoagulants were contraindicated [22,23]. Edoxaban 15 mg was superior to a placebo in reducing stroke or systemic embolism, but the study was limited by race clustering (all patients were Asian) and by a low mean of the body weight of the cohort (about 50 kg).

The safety profile of DOACs is also maintained in patients aged ≥90 years, as shown by the analysis of 15,756 AF patients sourced from the Taiwan National Health Insurance Research Database (NHIRD) [24]. Indeed, while the risk of ischemic stroke was found to be comparable between VKAs and DOAC users among elderly patients (4.07%/y versus 4.59%/y; HR: 1.16; $p = 0.654$), the DOAC group showed a lower risk of intracranial hemorrhage (0.42%/year versus 1.63%/year; HR 0.32; $p = 0.044$) [24].

In addition, it is worth mentioning that inappropriate DOAC dosage prescription affects up to 15% of AF patients [25], especially older patients [1,25].

In a multicenter study of AF patients aged ≥80 years who received DOAC treatment ($n = 253$), Carbone et al. showed that nearly one-third of octogenarians with AF received an inappropriate dose of DOACs [26]. Several clinical factors were associated with DOAC overdosing [diabetes mellitus type II (OR 18; $p < 0.001$), previous bleeding (OR 6.4; $p = 0.03$)] or underdosing [male gender (OR 3.15; $p < 0.001$), coronary artery disease (OR 3.60; $p < 0.001$), and higher body mass index (OR 1.27; $p < 0.001$)] [26]. Octogenarians with inappropriate DOAC underdosing showed less survival ($p < 0.001$) [26].

Table 1. Characteristics of DOAC principal trials and outcomes in patients aged ≥75 years.

	RE-LY [12]	**ROCKET-AF [16]**	**ARISTOTLE [17]**	**ENGAGE [20]**
DOACs vs. VKAs	dabigatran	rivaroxaban	apixaban	edoxaban
Dose	150 mg bid	20 mg qd	5 mg bid	60 mg qd
Reduced dose	110 mg bid	15 mg qd	2.5 mg bid	30 mg qd
Patients (n)	18,113	14,264	18,201	14,071
Age (mean in years)	72	73	70	72
Patients ≥ 75 years, n (%)	7258 (40)	6229 (44)	5678 (31)	5668 (40)
ClCr in ≥75 years at baseline	• ≥80 mL/min: 12% • 50–79 mL/min: 57% • <50 mL/min: 26%	Median 55 mL/min (IQR 44, 68).	• >80 mL/min: 10.5% • 51–80 mL/min: 51.5% • 31–50 mL/min: 33.6% • ≤30 mL/min: 3.9%	• >80 mL/min: 12% • 51–80 mL/min: 52% • ≤50 mL/min: 37%
Stroke or systemic embolism in patients ≥75 years				
Event rates (DOACs vs. VKAs %/years)	1.9 (110 mg bid) vs. 2.1 1.4 (150 mg bid) vs. 2.1	2.3 vs. 2.9	1.6 vs. 2.2	1.9 vs. 2.3
HR (or RR for dabigatran) (IC 95%)	0.88 (0.66–1.17) (110 bid) 0.67 (0.49–0.90) (150 bid)	0.80 (0.63–1.02)	0.71 (0.53–0.95)	0.83 (0.67–1.04)
Major bleedings in patients ≥75 years				
Event rates (DOACs vs. VKAs %/years)	4.4 (110 mg bid) vs. 4.4 5.1 (150 mg bid) vs. 4.4	4.9 vs. 4.4	3.3 vs. 5.2	4.0 vs. 4.8
HR (or RR for dabigatran) (IC 95%)	1.01 (0.83–1.23) (110 bid) 1.18 (0.98–1.42) (150 bid)	1.11 (0.92–1.34)	0.64 (0.52–0.79)	0.83 (0.70–0.89)
Gastrointestinal bleedings in patients ≥75 years				
Event rates (DOACs vs. VKAs %/years)	2.2 (110 mg bid) vs. 1.6 2.8 (150 mg bid) vs. 1.6	2.8 vs. 1.7	1.3 vs. 1.3	2.2 vs. 1.7
HR (or RR for dabigatran) (IC 95%)	1.39 (1.03–1.98) (110 bid) 1.79 (1.35–2.37) (150 bid)	1.69 (1.19–2.39)	0.99 (0.69–1.42)	1.32 (1.01–1.72)
Intracranial bleeding in patients ≥75 years				
Event rates (DOACs vs. VKAs %/years)	0.37 (110 mg bid) vs. 1 0.41 (150 mg bid) vs. 1	0.66 vs. 0.83	0.43 vs. 1.29	0.5 vs. 1.2
HR (or RR for dabigatran) (IC 95%)	0.37 (0.21–0.64) (110 bid) 0.42 (0.25–0.70) (150 bid)	0.80 (0.50–1.28)	0.34 (0.20–0.57)	0.40 (0.26–0.62)

3. DOACs and Frailty

"Frailty" is defined as a vulnerability to infectious processes and physical and emotional stresses [27]. The prevalence of such a condition increases with age and ranges from 9% in 75–79-year-old patients to 26% in patients ≥85 years [28].

Frail subjects are less likely to receive OAC despite evidence supporting the use of OAC in this population [15,29]. According to the results of RCTs [30,31], meta-analyses [4,21], and large registries [15,24,32], when compared to warfarin, DOACs demonstrate a better risk-benefit profile in frail patients [11,24,30,33,34]. The prescription of a reduced dose of OAC is less effective in preventing adverse outcomes [35–37].

In the systematic review by Oqab et al. [38], it was highlighted that 40% of hospitalized elderly patients with AF (over the age of 80) were classified as frail, and the rate of OAC prescription was lower in these patients than in non-frail patients (OR 0.49, 95% CI 0.32–0.74) [38]. Among frailty characteristics, cognitive impairment, malnutrition risk, depression, and falls were recognized as the main reasons for the under-prescription of oral anticoagulants [38].

The FRAIL-AF study [39] showed that severely frail patients are much less likely to be prescribed with DOACs than non-frail, mildly or moderately frail patients (OR 3.4), regardless of the individual patient's thrombotic and bleeding risk. This evidence suggests that frailty, in clinical practice, significantly influences the prescription of DOACs [39].

Thus, the best antithrombotic therapeutic strategy in frail AF patients remains unclear at present. Moreover, comparison studies between different DOACs are still not available. Anyhow, apixaban seems to have a good risk/benefit profile in older patients, especially in those with renal failure [40–42]. On the other hand, it could be reasonable to avoid dabigatran and rivaroxaban because of the increased risk of gastrointestinal bleeding described in patients aged ≥75 years [43].

4. DOACs in Patients with AF and Active Cancer

AF is commonly diagnosed in the setting of active cancer [44]. Antithrombotic prevention against the risk of cerebral stroke and systemic embolism in patients with AF and cancer disease is essential [45], and the risk of bleeding also depends on the type of tumor [46].

Due to the low life expectancy and high bleeding risk of cancer patients, the major RCTs of DOACs have included few patients with AF and cancer [12,17,47,48]. Therefore, data on this sub-population remain lacking and uncertain. In this regard, several observational studies and meta-analyses have investigated the efficacy and safety of DOACs in this population [49–52], assessing their viability when compared to warfarin [49,51,52] (Table 2).

Russo et al. published a systematic review of the literature of six eligible studies, founding that the efficacy and safety of DOACs in cancer patients are similar to that of the general population [49]. In particular, authors found a low annual incidence of bleeding and thrombotic events in cancer patients treated with DOACs compared to those treated with warfarin. Moreover, the risk of such events was comparable to non-cancer patients regardless of the treatment used (DOACs or VKAs) [49].

A systematic review and metanalysis of three sub-studies of ARISTOTLE [53], ROCKET-AF [54], and ENGAGE-TIMI 48 trials [55] showed no significant differences in safety and efficacy outcomes between cancer and non-cancer patients in OAC therapy (all $p < 0.05$) [51]. Moreover, DOAC therapy resulted in a significantly lower risk of stroke/systemic embolism ($p = 0.04$), venous thromboembolism ($p < 0.0001$), and a decreased risk of intracranial or gastrointestinal bleeding compared with warfarin ($p = 0.04$) [51].

Yang et al., in a network meta-analysis [52], showed that in AF patients with cancer, apixaban was associated with the lowest risk of stroke/systemic embolism (OR 0.12, 95% confidence interval [CI] 0.05–0.52), followed by rivaroxaban, dabigatran, edoxaban, and warfarin. Apixaban was also the best treatment option to avoid major bleeding, followed by dabigatran and edoxaban (OR 0.39, 95% CI 0.18–0.79) [52].

A large meta-analysis (46,424 DOAC users and 182,797 VKA users) comparing the efficacy and safety of DOACs and VKAs in cancer patients has shown that DOACs are more effective in preventing strokes in the course of the AF [56]. Indeed, DOACs, compared to VKAs, significantly reduced the risk of both ischemic (RR 0.84; $p = 0.007$) and hemorrhagic stroke (RR 0.61, $p < 0.00001$) [56]. Moreover, the risk of major bleeding was significantly reduced by up to 32% (RR 0.68, $p = 0.01$) and the risk of systemic embolism or any type of stroke by 35% with DOACs compared with VKA (RR 0.65, $p < 0.0001$) [56]. Similarly, the use of DOACs versus VKAs significantly reduced the risk of intracranial or gastrointestinal bleeding (RR 0.64, $p = 0.006$) [56].

Furthermore, in a study of 16,096 patients with AF and active cancer [57], the bleeding rate was similar with rivaroxaban and dabigatran but significantly lower with apixaban (HR 0.37; $p = 0.002$). None of the anticoagulants showed greater efficacy in reducing the incidence of ischemic stroke [57].

The Scientific and Standardization Committee (SSC) of the International Society on Thrombosis and Haemostasis (ISTH) recommends that individual decisions should be made for a patient with cancer and AF, considering the risk of stroke and bleeding [58]. In patients who had initiated anticoagulation before anti-cancer treatment, therapy should not be modified if there are no significant interactions with oncological drugs. In the case of newly diagnosed AF during chemotherapy, DOACs should be preferred over VKAs or low-molecular-weight heparin (LMWH) if no significant drug–drug interactions are found. The exception is patients with gastrointestinal neoplasms or other gastrointestinal tract diseases predisposing to bleeding, where the OAC prescription should be strongly individualized. LMWH in therapeutic doses should only be recommended when the patient cannot take oral anticoagulants. VKAs are recommended in patients with mechanical heart valves or moderate-to-severe mitral stenosis.

In conclusion, several preliminary pieces of evidence suggest that DOACs are effective and safe in cancer patients with AF, but RCTs should improve these findings. The choice of the DOAC should be individualized, considering the prothrombotic risk related to cancer disease and the risk of bleeding.

Table 2. Results of the main studies exploring the efficacy and safety of direct oral anticoagulants in cancer patients with atrial fibrillation.

Authors, Reference	Main Study Characteristics	Ischemic Events	Major Bleeding	Conclusions
Russo et al. [49]	Systematic Review of retrospective studies (6 studies included) DOACs in AF cancer patients Cancer Vs. Non-cancer patients	Annual incidence range 0 to 4.9% versus 1.3 to 5.1%	Annual incidence range 1.2 to 4.4% versus 1.215 to 3.1%	No significant differences in safety and efficacy outcomes between cancer and no-cancer patients with AF on DOACs
Deng et al. [51]	Systematic Review and Meta-Analysis (5 studies included) DOACs Vs. Warfarin	SSE RR = 0.52 95% CI, 0.28–0.99 $p = 0.04$ VTE RR = 0.37 95% CI, 0.22–0.63 $p < 0.0001$ IS RR = 0.63 95% CI, 0.40–1.00 $p = 0.05$ MI RR = 0.75 95% CI, 0.45–1.25 $p = 0.26$	Intracranial or GI RR = 0.65 95% CI, 0.42–0.98 $p = 0.04$ MB RR = 0.73 95% CI, 0.53–1.00 $p = 0.05$ MB or CRNMB RR = 1.00 95% CI, 0.86–1.17 $p = 0.96$ Any bleeding RR = 0.93; 95% CI, 0.78–1.10 $p = 0.39$	In cancer patients, DOACs have similar rates or lower rates of ischemic and bleeding events and a reduced risk of venous thromboembolism compared with warfarin.

Table 2. *Cont.*

Authors, Reference	Main Study Characteristics	Ischemic Events	Major Bleeding	Conclusions
Mariani et al. [56]	Meta-analysis (9 studies included) DOACs versus Warfarin	SSE RR 0.65 95% CI, 0.52–0.81 $p = 0.001$ IS RR 0.84 95% CI 0.74–0.95 $p = 0.007$ MI RR 0.71 95% CI 0.48–1.04 $p = 0.08$	HS RR 0.61 95% CI 0.52–0.71 $p = 0.00001$ MB RR 0.68 95% CI 0.50–0.92 $p = 0.01$ Intracranial or GI RR 0.64 95% CI 0.47–0.88 $p = 0.006$ MB or CRNMB RR 0.94; 95% CI 0.78–1.13; p 0.50 Any bleeding RR 0.91 95% CI 0.78–1.06 $p = 0.24$	In patients with cancer and non-valvular AF, the use of DOACs is associated with a significant reduction of thromboembolic and bleeding events in patients when compared to warfarin

DOACs: direct oral anticoagulants; AF: atrial fibrillation; SSE: stroke/systemic embolism; VTE: venous thromboembolism; IS: ischemic stroke; MI: myocardial infarction; GI: gastrointestinal; MB: major bleeding; CRNMB: clinically relevant non-major bleeding; HS: hemorrhagic stroke.

5. DOAC Treatment in Obese Patients

In both ENGAGE AF-TIMI [48] and ARISTOTLE [17] trials, an important amount of the enrolled subjects were overweight, and approximately 40% of patients were obese (BMI $\geq$ 30 kg/m^2).

According to the European Society of Cardiology guidelines for the management of the AF [1], obesity is a comorbidity that needs to be corrected as part of the ABC-integrated approach. At the extreme of the distribution of obese patients, there are underweight patients, whose prevalence is higher in Asia [59–61], with a limited representation in multicenter trials that validated DOACs [62,63].

Studies that have investigated the efficacy and safety of DOACs in obese patients are summarized in Table 3.

Table 3. Main studies that investigated the efficacy and safety of DOACs in obese patients.

First Author	Study Design	Patients (*n*)	BMI (kg/m^2)	Stroke/SE HR (CI 95%)	Major Bleeding HR (CI 95%)	Follow-Up (Mean in Years)
Sandhu et al. [61]	RCT Apixaban * vs. Warfarin (ARISTOTLE sub-analysis)	17,913	18–<25 (n = 4052) 25–30 (n = 6702) $\geq$30 (n = 7159)	0.86 (0.68–1.08) 0.79 (0.61–1.02)	0.82 (0.68–0.99) 0.91 (0.74–1.10)	1.8 **
Boriani et al. [62]	RCT Edoxaban * vs. Warfarin (ENGAGE-TIMI 48 sub-analysis)	21,105	18–25 (n = 4491) 25–<30 (n = 7903) 30–<35 (n = 5209) 35–40 (n = 2099) $\geq$40 (n = 1149)	0.91 (0.78–1.07) 0.82 (0.68–1.00) 0.68 (0.52–0.89) 0.54 (0.35–0.83)	1.03 (0.88–1.20) 1.12 (0.94–1.34) 1.18 (0.94–1.48) 1.28 (0.96–1.70)	2.8 **
Balla et al. [63]	RCT Rivaroxaban * vs. Warfarin (ROCKET-AF post-hoc analysis)	14,264	18.5–24.99 (n = 3289) 24–29.99 (n = 5535) $\geq$30 (n = 5206)	0.78 (0.64–0.96) 0.65 (0.52–0.80)	0.99 (0.82–1.18) 0.91 (0.75–1.10)	2
Kido et al. [64]	Meta-analysis of 6 studies DOACs vs. Warfarin.	8732	>40	0.85 (0.60–1.19)°	0.63 (0.43–0.94)°	-

DOACs = direct oral anticoagulants; ClCr = clearance of creatinine; HR = Hazard ratio; CI = confidence interval; SE = systemic embolism; BMI = body mass index. ** median; °ODDS RATIO. * reduced dose for apixaban: age $\geq$ 80 years, body weight $\leq$ 60 kg, or serum creatinine level $\geq$ 1.5 mg/dL; reduced dose for edoxaban: CrCl $\leq$ 50 mL/min, a body weight $\leq$ 60 kg use of P-glycoprotein inhibitors; reduced dose for rivaroxaban: ClCr 30–49 mL/min.

The post-hoc analysis of the ROCKET-AF trial evaluated patients with normal BMI (BMI from 18.5 to <25 kg/m^2), overweight (BMI 25 to <30 kg/m^2), or obese (BMI $\geq$ 30 kg/m^2), and overall, 36.5% of subjects enrolled were classifiable as obese [64]. The risk of stroke was statistically significantly lower for obese patients with BMI $\geq$ 35 kg/m^2 than that for normal-weight patients in both the rivaroxaban and warfarin group [63].

The post-hoc analysis of the ARISTOTLE trial found that 39.4% of enrolled patients had a BMI $\geq$ 30 kg/m^2. In these patients, the comparison between apixaban and warfarin showed no differences in terms of stroke or major bleeding [61].

In the ENGAGE AF-TIMI 48 trial, a higher BMI value was associated with a lower risk of stroke or thromboembolism and better survival but with an increased risk of bleeding [62]. The efficacy and safety profile of edoxaban was comparable among BMI categories ranging from 18.5 to >40 kg/m^2, indicating the reliability of edoxaban treatment also in patients with obesity [62].

A systematic review and meta-analysis based on trials about various levels of BMI showed that in patients with soft or morbid obesity (class III, with BMI 40–49 kg/m^2), there are limited data on the efficacy and safety of dabigatran and rivaroxaban, while more data are available for edoxaban and apixaban [64].

In extremely obese (BMI $\geq$ 50 kg/m^2), data are very limited for all DOACs [65]. The assessment of DOAC plasma levels, as well as the evaluation of the effect on coagulation parameters, could improve the management in obese patients [66–70]. According to the International Society of Thrombosis and Haemostasis, VKAs should be the treatment of choice in morbidly obese patients [71]. Both the International Society of Thrombosis and Haemostasis and the European Heart Rhythm Association suggest that if a DOAC is administered in morbidly obese patients with AF, drug-specific peak and trough levels (anti-FXa for apixaban, edoxaban, and rivaroxaban, ecarin time or dilute-thrombin time with appropriate calibrators for dabigatran, or mass spectrometry drug level for any of the DOACs) should be checked to switch to VKAs if any drug level is found below the expected range [71,72].

In the ENGAGE AF-TIMI 48 trial, the concentration of edoxaban and the anti-factor Xa activity at baseline after one month of treatment was assessed in a large number of patients [4]. A sub-analysis of ENGAGE AF-TIMI 48 study showed that the concentrations of edoxaban and anti-factor Xa activity did not vary significantly between underweight, normal BMI, and obesity categories [62]. The data of the ENGAGE AF-TIMI 48 trials were also analyzed in ratio to weight in a study that evaluated patients with weight $\leq$ 55 kg and $\geq$120 kg in comparison with patients weighing 80–84 kg, highlighting that the concentrations of edoxaban, the activity anti-factor Xa, and factor Xa inhibition rates were comparable between the three groups [73].

The peak concentrations of DOACs (apixaban, dabigatran, and rivaroxaban) were measured in a cohort of 38 obese patients (median weight, 135.5 kg) with venous thromboembolism or AF by Piran et al. [74]. Results showed that the peak drug concentration was higher than the expected median trough level in the majority of patients (79%); however, a considerable part of the study population (21%) still had a peak plasma concentration below the usual on-therapy range of peak concentration for the corresponding DOACs [74].

In a cohort of 100 patients with AF or venous thromboembolism and weight > 120 kg receiving apixaban or rivaroxaban, Martin et al. found no significant relationship between DOAC concentrations at peak or trough, weight, BMI, or renal function [72].

In the study of Russo et al. [67], among 58 patients with extreme obesity (BMI $\geq$ 40 kg/m^2) and AF, nine patients (15.5%) showed that DOAC plasma concentrations were out of the expected ranges. Among these patients, according to the multivariate logistic analysis, the only independent predictor of DOAC plasma levels out of the expected ranges was the inappropriate prescription of low-dose DOACs (hazard ratio = 29.37; p = 0.0002) [67]. According to these results, extreme obesity does not significantly impact DOAC plasma levels [67].

6. DOAC Use in Patients with Low Body Weight

In the RE-LY trial, the study population was stratified according to groups of body weight to analyze the safety and efficacy of dabigatran in each subgroup of patients [12]. Both dabigatran 150 mg BID and 110 mg BID showed greater efficacy and similar safety compared to warfarin in patients < 50 kg (n = 376) [12].

Even if low body weight increases the exposure to rivaroxaban, in a single-blind, placebo-controlled study, no differences in plasma levels, nor the incidence of adverse events related to the body weight (range 45–173 kg), were found in healthy volunteers of both genders with the use of a fixed dose of rivaroxaban (10 mg, half the dose recommended for stroke prevention in AF) [75].

In the ARISTOTLE trial, despite a higher risk of stroke or systemic embolism and major bleeding, patients with isolated body weight < 60 kg (or age > 80, or serum creatinine > 1.5 mg/dL) showed better outcomes with apixaban 5 mg BID versus warfarin when compared with patients without these characteristics [17].

In both phase III studies, edoxaban half standard dose (30 mg) was administered to participants weighing $\leq$ 60 kg [48,76] because of the risk of an increased drug plasma level in these patients [48].

Underweight patients (BMI < 18.5 kg/m^2) suffer from a higher risk of bleeding and all-cause death, as demonstrated in a recent survey from Korea (underweight patients vs. normal weight patients: adjusted HR 4.135 p = 0.008; adjusted HR 10.524, p < 0.001) [77]. However, there was no significant difference in the risk of thromboembolism among these groups [77].

Russo et al. [78] conducted a propensity score-matched study on elderly AF patients (>75 years) with a low body weight (<60 kg) sourced from the Italian cohorts of PREFER in AF and PREFER in AF PROLONGATION registries to compare the safety and effectiveness of DOACs versus VKA therapy (213 patients in each group). No statistically significant differences were found in any analyzed outcome (DOACs vs. VKAs; thromboembolic events: 3.76% vs. 4.69%, p = 0.63; major bleeding events: 1.88% vs. 4.22%, p = 0.15; hospitalizations: 9.9% vs. 16.9%, p = 0.06) [78]. However, a net clinical benefit (+1.6) of DOACs vs. VKAs was demonstrated [78].

Furthermore, an analysis of 279 AF patients aged $\geq$ 80 years and weighed $\leq$ 60 kg (136 in DOAC vs. 143 in VKA group) showed a lower incidence of all-cause of mortality in the DOAC group (14.91 per 100 person-years in DOAC vs. 37.94 per 100 person-years in VKA group, adjusted HR 0.43; p = 0.003) with no significant differences in major bleeding events (9 in DOAC vs. 13 in VKA group, p = 0.6), suggesting the safety and efficacy of the use of DOACs in octogenarians with low weight [79].

In conclusion, patients with low body weight (<60 kg) were poorly included in RCTs. In each RCT, subgroup analyses showed that the efficacy and safety of DOACs demonstrated in patients weighing >60 kg is maintained in patients with low body weight, with edoxaban requiring a dose reduction, as well as apixaban, if at least one other clinical criterion is met. Anyway, monitoring drug levels is a prudent strategy in very low body weight patients.

7. DOACs in Patients with AF and BHV

To date, it is still unclear which is the best treatment option for AF patients with BHVs [80]. Current guidelines recommend lifelong OAC therapy in this subgroup of patients with a class IC of evidence [81], with VKAs preferred to DOACs for the first three months after the procedure [81,82]. ESC/EACTS guidelines [82] admit the use of rivaroxaban directly after surgical BHV implantation in the mitral position (class IIb C) due to the results of the Rivaroxaban for Valvular heart disease and atRial fibrillation (RIVER) trial [83].

Some experiences with DOACs are available in clinical practice in this setting.

Yadlapti et al. registered almost no thrombotic events (one transient ischemic attack) but a higher risk of bleeding (five major bleedings, six minor bleedings, and one hem-

orrhagic stroke) in a cohort of 73 AF patients treated with DOACs (dabigatran, n = 44; rivaroxaban, n = 25; apixaban, n = 4) after aortic (n = 61) or mitral (n = 12) BHV replacement [84]. However, 72% of patients were on antiplatelet treatment, possibly causing a bias in the incidence of bleeding outcomes [85].

Indeed, in a larger, multicenter observational study, Russo et al. [84] recorded two thromboembolic events and only four major bleedings in a cohort of 122 AF patients with a prior BHV replacement or valve repair, treated with apixaban (53.1%), dabigatran (31%), or rivaroxaban (15.5%), with only 20% treated with antiplatelet therapy also [86]. Table 4 summarizes the results of these studies.

Table 4. Observational studies on the clinical performance of Direct oral anticoagulants after bioprosthetic heart valve replacement in atrial fibrillation patients.

First Author, Reference	Study Characteristics (Design, Included patients, Procedure Included)	DOAC n, (%)	Ischemic Events (%)	Bleeding Events (%)
Yadlapati et al. [85]	Single center Retrospective Observational 73 patients included ABHV; MBHV	Dabigatran 44, (60.3) Rivaroxaban 25, (34.2) Apixaban 4, (5.5)	1 TIA (1.4)	5 MB (6.9) 6 mB (8.2), 2 ICH (2.7)
Russo et al. [84]	Multicenter Retrospective Observational 122 patients included ABHV; MBHV; VR	Dabigatran 38, (31) Rivaroxaban 19, (15.5) Apixaban 65, (53.3)	TE 2 (1,7) M.A.I: 0.8%	4 (3.3) M.A.I: 1.3%

DOACs: direct oral anticoagulant; ABHV: aortic bioprosthetic heart valve; MBHV: mitral bioprosthetic heart valve; TIA: transient ischemic attack; MB: major bleeding: mB: minor bleeding; VR: valve repair; TE: thromboembolic events; M.A.I: mean annual incidence.

Of the four major RCTs comparing DOACs to warfarin [12,17,47,77], only the ENGAGE AF-TIMI 48 trial and the ARISTOTLE trial included AF patients with BHV replacement. In a post-hoc analysis from the ENGAGE AF-TIMI 48, the analysis of 191 AF patients with aortic (31.4%) or mitral (68.6%) BHV replacement, edoxaban showed a comparable rate of stroke/systemic embolism (HR, 0.37; p = 0.15) and major bleeding (HR, 0.5; p = 0.26) [86] but lower rates of myocardial infarction, stroke, or cardiovascular death (HR, 0.36; p = 0.03) when compared to warfarin [86].

Moreover, in the ARISTOTLE trial, no significant differences were found in safety or efficacy outcomes between apixaban and warfarin in the included cohort of 156 patients with AF and BHVs or valve repair [83].

These results were consistent with those of two multicenter observational studies [87,88], in which DOACs also showed a lower rate of major bleeding compared to warfarin. Table 5 displays the results of the aforementioned observational studies.

Regarding RCTs, the DAWA (Dabigatran Versus Warfarin After Mitral and/or Aortic Bioprosthesis Replacement and Atrial Fibrillation Postoperatively) pilot study was the first RCT designed to compare efficacy and safety outcomes of dabigatran 110 mg BID to warfarin in patients with mitral and aortic BHV replacement [89]. In a follow-up period of 90 days, no differences in the measured outcomes were recorded between the two treatments, but the trial was prematurely terminated because of the low enrollment (34 patients) [89].

Table 5. Overview of the study characteristics comparing Direct oral anticoagulants with Vitamin K antagonist oral anticoagulants in AF patients with bioprosthetic valves or prior surgical valve repair.

Author, Reference	Study Characteristics (Design, Number of Patients, Procedure Included)	DOAC n, (%)	Results
Carnicelli et al. [86]	Post-hoc analysis phase III trial 191 patients included ABHV; MBHV	Edoxaban 121 (63.4)	Efficacy outcome
			S/SE HDE vs. warfarin: HR 0.37 95% CI, 0.10–1.42 $p = 0.15$ LDE vs. warfarin: HR 0.53 95% CI, 0.16–1.78 $p = 0.31$
			Safety outcome
			MB HDE vs. warfarin: HR 0.5, 95% CI 0.15–1.67 $p = 0.26$ LDE vs. warfarin HR 0.12, 95% CI 0.01–0.95 $p = 0.045$
			Primary net clinical outcome (S/SE, MB, death)
			HDE vs. warfarin: HR 0.46 (95% CI, 0.23–0.91) $p = 0.03$ LDE vs. warfarin HR (0.43, 95% CI, 0.21–0.88) $p = 0.02$
Guimarães et al. [83]	Post-hoc analysis phase III trial 156 patients included ABHV; MBHV; VR	Apixaban 87 (55.8)	Efficacy outcomes
			S/SE HR 1.714 (95% CI 0.313–9.372) $p = 0.53$ ACS HR 1.714 (95% CI 0.313–9.372) $p = 0.53$ IS HR 3.286 (95% CI 0.37–29.4) $p = 0.29$ MI HR 0.825 (95% CI 0.367–29.40) $p = 0.29$
			Safety outcome
			MB HR 0.882 (95% CI 0.309–2.519) $p = 0.82$ MB/CRNMB HR 0.781 (95% CI 0.317–1.925) $p = 0.59$ ICH HR 0.467 (95% CI 0.042–5.187) $p = 0.54$ GI bleeding HR 1.244 (95% CI 0.208–7.448) $p = 0.81$ Any bleeding HR 0.866 (95% CI 0.517–1.451) $p = 0.59$

Table 5. *Cont.*

Author, Reference	Study Characteristics (Design, Number of Patients, Procedure Included)	DOAC n, (%)	Results
Russo et al. [85]	Retrospective Propensity Score matched 130 for each group ABHV; MBHV	Apixaban 72 (55.4) Rivaroxaban 39 (30.0) Dabigatran 17 (13.1) Edoxaban 2 (1.4)	Efficacy outcome S/SE-TIA HR 0.49 (95% CI, 0.19–1.22) $p = 0.14$ Safety outcome MB HR 0.59 (95% CI, 0.15–2.4) $p = 0.47$ ICH HR 0.33 (95% CI, 0.05–2.34) $p = 0.3$
Duan et al. [87]	Retrospective cohort study 2672 patients included ABHV; MBHV	Dabigatran 362 (13.5) Apixaban 60 (2.2) Rivaroxaban 17 (0.6)	Efficacy outcome Composite of IS/TIA/SE HR 1.19 (95% CI, 0.96–1.48), $p = 0.106$ Safety outcome Composite of MB [1] HR 0.69 (95% CI 0.56–0.85) $p < 0.001$

DOACs: direct oral anticoagulant; ABHV: aortic bioprosthetic heart valve; MBHV: mitral bioprosthetic heart valve; S/SE: stroke/systemic embolism; HDE: high-dose edoxaban; LDE: low-dose edoxaban; VR: valve repair; HR: hazard ratio; CI: confidential interval; MB: major bleeding; CRNMB: clinically relevant non-major bleeding; ACS all-cause stroke; IS: ischemic stroke; MI: myocardial infarction; ICH: intracranial hemorrhage; GI: gastrointestinal; TIA: transient ischemic attack; [1]: Gastrointestinal bleeding, intracranial hemorrhage and bleeding from other sites.

In a recent small trial on 50 AF patients undergoing aortic BHV replacement, apixaban ($n = 25$) and warfarin ($n = 25$) were compared for adverse events in three months following surgery. Only one CV death due to massive pericardial effusion was recorded nine days after surgery in the warfarin group. At the end of the follow-up period, three patients experienced a major bleeding event in the warfarin group, with no such events in the apixaban one. In light of these pieces of evidence, authors concluded that apixaban is proven safer than warfarin early after aortic BHV replacement with comparable efficacy in preventing valvular dysfunction (no event recorded in either group) [90].

Recently, 1005 AF patients were enrolled in The RIVER trial [91] to randomly receive rivaroxaban or warfarin after surgical mitral BHV replacement. No differences in ischemic and bleeding events or death occurred between rivaroxaban versus warfarin at the end of the follow-up (12 months follow-up; stroke, 3% vs. 2.4; major bleeding, 1.4% vs. 2.6%; death, 4% vs. 4%). Table 6 summarizes the results of these latter RCTs.

Data on DOAC clinical profiles in patients with transcatheter aortic valve implantation (TAVI) and AF are still lacking. According to the results of the propensity score-matched study of Jochheim et al. [91], DOAC safety was comparable to warfarin at the cost of a higher incidence of the composite efficacy endpoint (all-cause mortality, myocardial infarction, and any cerebrovascular events; 21.2% vs. 15%; HR, 1.44; $p = 0.05$) in a cohort of 962 TAVI patients with AF discharged on DOACs ($n = 326$; 53.7% rivaroxaban, 39.2% apixaban, and 7.1% dabigatran) or warfarin ($n = 626$), and followed-up for 12 months [91] (Table 7).

Table 6. Characteristics of the randomized clinical trials comparing Direct oral anticoagulants with vitamin K antagonist oral anticoagulants in AF patients with bioprosthetic valves or surgical valve repair.

Author, Reference	Study Design	Number of Patients (DOACs/VKAs)	Results
Durães et al. [92]	Phase 2 RCT pilot study Dabigatran 110 mg Vs. Warfarin ABHV; MBHV	27 patients included Dabigatran = 15 Warfarin = 12	New intracardiac thrombus Warfarin = 1 Dabigatran = 0 RR 1.1, CI 95% 0.9–1.3 $p = 0.42$
Piepiorka-Broniecka et al. [89]	Prospective RCT Apixaban Vs. Warfarin ABHV	50 patients included Apixaban = 25 Warfarin = 25	Cumulative Death Warfarin = 1 Apixaban = 0 $p = 0.31$ Cumulative Bleeding Warfarin = 3 Apixaban = 0 $p = 0.07$ Valve dysfunction Warfarin = 0 Apixaban = 0
Guimarães et al. [90]	Multicenter RCT Rivaroxaban Vs. Warfarin MBHV	1005 patients included Rivaroxaban = 500 Warfarin = 505	Efficacy outcome [1] Composite of Death/MACE [2]/MB [3] Warfarin = 340.1 Rivaroxaban = 347.5 RMST difference: 7.4 days (−1.4–16.3) $p < 0.001$ for noninferiority $p = 0.10$ for superiority Safety outcome MB Warfarin = 13 Rivaroxaban = 7 HR 0.54 (0.21–1.35) p = N/A ICH Warfarin = 5 Rivaroxaban = 0 N/A Fatal bleeding Warfarin = 2 Rivaroxaban = 0 N/A

DOACs: direct oral anticoagulants; VKAs: vitamin K antagonists oral anticoagulant; ABHV: aortic bioprosthetic heart valve; MBHV: mitral bioprosthetic heart valve; RCT: randomized clinical trial; RR: relative risk; MB: major bleeding; ICH: intracranial hemorrhage; RMST: restricted mean survival time; [1]: mean time until a primary-outcome event in days; [2]: ischemic attack, valve thrombosis, systemic embolism not related to the central nervous system, or hospitalization for heart failure; [3]: according to the criteria of the Rivaroxaban Once Daily Oral Direct Factor Xa Inhibition Compared with Vitamin K Antagonism for Prevention of Stroke and Embolism Trial in Atrial Fibrillation (ROCKET AF): Any bleeding; Major bleeding; Intracranial bleeding; Fatal bleeding; Clinically relevant nonmajor bleeding; Minor bleeding; N/A: not available.

Table 7. Characteristics and results of the studies comparing Direct oral anticoagulants with vitamin K antagonist oral anticoagulants in AF patients after TAVI.

Author, Reference	Study Design	Number of Patients (NOACs/VKAs)	Results
Jochheim et al. [91]	Prospective Observational Multicenter study DOACs Vs. VKAs	962 patients included DOACs = 326 VKAs = 636	All-cause mortality/MI/CVE DOACs = 63/326 VKAs = 87/636 1.44, CI 95% 1.00–2.07 p = 0.050 All-cause death DOACs = 47/326 VKAs = 70/636 1.36, CI 95% 0.90–2.06 p = 0.136 MB DOACs = 67/326 VKAs = 144/636 0.9, CI 95% 0.64–1.26 p = 0.548 MACCE DOACs = 30/326 VKAs = 42/636 1.43, CI 95% 0.85–2.43 p = 0.173
Kawashima et al. [93]	Prospective observational Multicenter DOACs Vs. VKAs	403 patients included DOACs = 227 VKAs = 127	All-cause mortality 10.3% vs. 23.3%; HR: 0.391, CI 95% 0.204–0.749; p = 0.005
Butt et al. [94]	Retrospective Observational Cohort study DOACs Vs. VKAs	735 patients included DOACs = 219 VKAs = 516	Arterial thromboembolism [1] HR, 1.23; 95% CI, 0.58–2.59 Bleeding HR, 1.14; p = 0.63–2.06 All-cause mortality HR, 0.93, 95% CI, 0.61–1.4
Van Mieghem et al. [95]	RCT Edoxaban Vs. VKAs	1426 patients included Edoxaban = 713 VKAs = 713	Composite primary efficacy outcome [2] HR, 1.05, 95% CI, 0.85 to 1.31; p = 0.01 for noninferiority MB HR, 1.40; 95% CI, 1.03 to 1.91 p = 0.93 for noninferiority
Collet et al. [96]	RCT (stratum 1—with indication for OAC) Apixaban Vs. VKAs	451 included patients In stratum 1 Apixaban = 223 VKAs = 228	Primary efficacy outcome [3] HR, 1.02; 95% CI, 0.68 to 1.51 Primary safety outcome [4] HR, 0.91; 95% CI, 0.52 to 1.60

DOACs: direct oral anticoagulants; VKAs: vitamin K antagonist oral anticoagulant; MI: myocardial infarction; CVE: cerebrovascular events; MB: major bleeding; MACCE: major adverse cardiac and cerebrovascular events; RCT: randomized clinical trial; OAC: oral anticoagulant; HR: hazard ratio; CI: confidential interval; [1] composite of ischemic stroke, transient cerebral ischemia, and thrombosis or embolism in peripheral arteries); [2] death from any cause, myocardial infarction, ischemic stroke, systemic thromboembolic event, valve thrombosis, or major bleeding; [3] composite of death, myocardial infarction, stroke or transient ischemic attack, systemic embolism, intracardiac or bioprosthetic thrombosis, deep vein thrombosis or pulmonary embolism, and life-threatening, disabling, or major bleeding over 1-year follow-up; [4] major disabling, or life-threatening bleeding.

The prospective multicenter observational Optimized Transcatheter Valvular Intervention (OCEAN) study [93] showed a low incidence of all-cause mortality in DOAC patients

(n = 227) compared to VKAs (n = 176) in TAVI patients with AF (10.3% vs. 23.3%; HR, 0.391; p = 0.005) during a median follow-up of 568 days [93] (Table 7). The same conclusions were applied in the three-year follow-up study of Butt et al. [94] for the incidence of arterial thromboembolism, bleeding, or mortality. The study included 219 (29.8%) AF patients treated with DOACs and 516 (70.2%) treated with VKAs following TAVI (Table 7).

Regarding RCTs, in the ENVISAGE trial [95], when compared to VKAs, edoxaban was non-inferior for the composite endpoint of death from any cause, myocardial infarction, ischemic stroke, systemic thromboembolism, and valve thrombosis (HR, 1.05; p = 0.01), as well as for major bleeding (HR, 1.05; p = 0.01), but the rate of major bleeding events was found higher in the DOAC group (HR, 1.40; p = 0.93), because of a higher rate of gastrointestinal bleeding [95] (Table 7).

Also, in the AF cohort of the ATLANTIS trial (stratum 1) (Anti-Thrombotic Strategy to Lower All cardiovascular and Neurologic Ischemic and Hemorrhagic Events after Trans-Aortic Valve Implantation for Aortic Stenosis), apixaban 5 mg BID compared to warfarin was not superior for both the primary and safety outcomes (primary efficacy outcome: HR, 1.02; 95% CI, 0.68 to 1.51; primary safety outcome: HR, 0.91; 95% CI, 0.52 to 1.60) [97] (Table 7).

In conclusion, guidelines recommend OAC alone therapy in AF patients undergoing BHV replacement [82]. Several studies highlight the favorable role of DOACs over VKAs among AF patients undergoing surgical BHV replacement. However, those studied are limited by a large use of concomitant antiplatelet therapy, which implies biases both for thromboembolic and bleeding outcomes. Except for mitral valve replacement, about the early use of DOACs after BHV replacement (first three months), data are scarce to draw definitive conclusions. Among AF patients undergoing TAVI, OAC alone is preferred over OAC plus clopidogrel [81,94,96,98], but conclusions on the DOAC profile are unclear at this point.

8. Conclusions

OAC therapy in patients with AF should be based on the risk of thromboembolism, stroke, and bleeding but also on the patient's preference. Special populations require careful evaluation and personalized therapy, considering the evidence regarding the pathology, comorbidities, and the risk–benefit ratio of long-term OAC. Many studies have been performed to test the efficacy and safety of DOACs, but special populations—elderly, frail, patients with extreme weight, cancer patients, and subjects with BHV—are underrepresented in the pivotal RCTs. "Real-world-setting" studies help to shed light on the OAC management of these patients; however, there is a need for further studies in this area.

Author Contributions: V.R. and A.C. designed the research; A.C. and R.B. wrote the paper; A.D. reviewed the paper. All authors have read and agreed to the published version of the manuscript.

Funding: This research received no external funding.

Institutional Review Board Statement: Not applicable.

Informed Consent Statement: Not applicable.

Data Availability Statement: Not applicable.

Conflicts of Interest: The authors declare no conflict of interest.

References

1. Hindricks, G.; Potpara, T.; Dagres, N.; Arbelo, E.; Bax, J.J.; Blomström-Lundqvist, C.; Boriani, G.; Castella, M.; Dan, G.-A.; Dilaveris, P.E.; et al. 2020 ESC Guidelines for the Diagnosis and Management of Atrial Fibrillation Developed in Collaboration with the European Association for Cardio-Thoracic Surgery (EACTS): The Task Force for the Diagnosis and Management of Atrial Fibrillation of the European Society of Cardiology (ESC) Developed with the Special Contribution of the European Heart Rhythm Association (EHRA) of the ESC. *Eur. Heart J.* **2021**, *42*, 373–498. [CrossRef] [PubMed]
2. Ageno, W.; Gallus, A.S.; Wittkowsky, A.; Crowther, M.; Hylek, E.M.; Palareti, G. Oral Anticoagulant Therapy. *Chest* **2012**, *141*, e44S–e88S. [CrossRef] [PubMed]

3. Eriksson, B.I.; Quinlan, D.J.; Eikelboom, J.W. Novel Oral Factor Xa and Thrombin Inhibitors in the Management of Thromboembolism. *Annu. Rev. Med.* **2011**, *62*, 41–57. [CrossRef]
4. Ruff, C.T.; Giugliano, R.P.; Braunwald, E.; Hoffman, E.B.; Deenadayalu, N.; Ezekowitz, M.D.; Camm, A.J.; Weitz, J.I.; Lewis, B.S.; Parkhomenko, A.; et al. Comparison of the Efficacy and Safety of New Oral Anticoagulants with Warfarin in Patients with Atrial Fibrillation: A Meta-Analysis of Randomised Trials. *Lancet* **2014**, *383*, 955–962. [CrossRef]
5. Lip, G.Y.H.; Nieuwlaat, R.; Pisters, R.; Lane, D.A.; Crijns, H.J.G.M. Refining Clinical Risk Stratification for Predicting Stroke and Thromboembolism in Atrial Fibrillation Using a Novel Risk Factor-Based Approach. *Chest* **2010**, *137*, 263–272. [CrossRef] [PubMed]
6. Pisters, R.; Lane, D.A.; Nieuwlaat, R.; de Vos, C.B.; Crijns, H.J.G.M.; Lip, G.Y.H. A Novel User-Friendly Score (HAS-BLED) to Assess 1-Year Risk of Major Bleeding in Patients with Atrial Fibrillation. *Chest* **2010**, *138*, 1093–1100. [CrossRef] [PubMed]
7. Perera, V.; Bajorek, B.V.; Matthews, S.; Hilmer, S.N. The Impact of Frailty on the Utilisation of Antithrombotic Therapy in Older Patients with Atrial Fibrillation. *Age Ageing* **2008**, *38*, 156–162. [CrossRef]
8. Zimetbaum, P.J.; Thosani, A.; Yu, H.-T.; Xiong, Y.; Lin, J.; Kothawala, P.; Emons, M. Are Atrial Fibrillation Patients Receiving Warfarin in Accordance with Stroke Risk? *Am. J. Med.* **2010**, *123*, 446–453. [CrossRef]
9. Andreotti, F.; Rocca, B.; Husted, S.; Ajjan, R.A.; ten Berg, J.; Cattaneo, M.; Collet, J.-P.; De Caterina, R.; Fox, K.A.A.; Halvorsen, S.; et al. Antithrombotic Therapy in the Elderly: Expert Position Paper of the European Society of Cardiology Working Group on Thrombosis. *Eur. Heart J.* **2015**, *36*, 3238–3249. [CrossRef]
10. Russo, V.; Carbone, A.; Rago, A.; Golino, P.; Nigro, G. Direct Oral Anticoagulants in Octogenarians with Atrial Fibrillation: It Is Never Too Late. *J. Cardiovasc. Pharmacol.* **2019**, *73*, 207–214. [CrossRef]
11. Russo, V.; Attena, E.; Mazzone, C.; Melillo, E.; Rago, A.; Galasso, G.; Riegler, L.; Parisi, V.; Rotunno, R.; Nigro, G.; et al. Real-Life Performance of Edoxaban in Elderly Patients with Atrial Fibrillation: A Multicenter Propensity Score–Matched Cohort Study. *Clin. Ther.* **2019**, *41*, 1598–1604. [CrossRef] [PubMed]
12. Connolly, S.J.; Ezekowitz, M.D.; Yusuf, S.; Eikelboom, J.; Oldgren, J.; Parekh, A.; Pogue, J.; Reilly, P.A.; Themeles, E.; Varrone, J.; et al. Dabigatran versus Warfarin in Patients with Atrial Fibrillation. *N. Engl. J. Med.* **2009**, *361*, 1139–1151. [CrossRef] [PubMed]
13. Eikelboom, J.W.; Wallentin, L.; Connolly, S.J.; Ezekowitz, M.; Healey, J.S.; Oldgren, J.; Yang, S.; Alings, M.; Kaatz, S.; Hohnloser, S.H.; et al. Risk of Bleeding with 2 Doses of Dabigatran Compared with Warfarin in Older and Younger Patients with Atrial Fibrillation: An Analysis of the Randomized Evaluation of Long-Term Anticoagulant Therapy (RE-LY) Trial. *Circulation* **2011**, *123*, 2363–2372. [CrossRef] [PubMed]
14. Lauw, M.N.; Eikelboom, J.W.; Coppens, M.; Wallentin, L.; Yusuf, S.; Ezekowitz, M.; Oldgren, J.; Nakamya, J.; Wang, J.; Connolly, S.J. Effects of Dabigatran According to Age in Atrial Fibrillation. *Heart* **2017**, *103*, 1015–1023. [CrossRef] [PubMed]
15. Graham, D.J.; Reichman, M.E.; Wernecke, M.; Zhang, R.; Southworth, M.R.; Levenson, M.; Sheu, T.-C.; Mott, K.; Goulding, M.R.; Houstoun, M.; et al. Cardiovascular, Bleeding, and Mortality Risks in Elderly Medicare Patients Treated with Dabigatran or Warfarin for Nonvalvular Atrial Fibrillation. *Circulation* **2015**, *131*, 157–164. [CrossRef] [PubMed]
16. Halperin, J.L.; Hankey, G.J.; Wojdyla, D.M.; Piccini, J.P.; Lokhnygina, Y.; Patel, M.R.; Breithardt, G.; Singer, D.E.; Becker, R.C.; Hacke, W.; et al. Efficacy and Safety of Rivaroxaban Compared with Warfarin Among Elderly Patients with Nonvalvular Atrial Fibrillation in the Rivaroxaban Once Daily, Oral, Direct Factor Xa Inhibition Compared with Vitamin K Antagonism for Prevention of Stroke and Embolism Trial in Atrial Fibrillation (ROCKET AF). *Circulation* **2014**, *130*, 138–146. [CrossRef] [PubMed]
17. Granger, C.B.; Alexander, J.H.; McMurray, J.J.V.; Lopes, R.D.; Hylek, E.M.; Hanna, M.; Al-Khalidi, H.R.; Ansell, J.; Atar, D.; Avezum, A.; et al. Apixaban versus Warfarin in Patients with Atrial Fibrillation. *N. Engl. J. Med.* **2011**, *365*, 981–992. [CrossRef]
18. Deitelzweig, S.; Luo, X.; Gupta, K.; Trocio, J.; Mardekian, J.; Curtice, T.; Lingohr-Smith, M.; Menges, B.; Lin, J. Comparison of Effectiveness and Safety of Treatment with Apixaban vs. Other Oral Anticoagulants among Elderly Nonvalvular Atrial Fibrillation Patients. *Curr. Med. Res. Opin.* **2017**, *33*, 1745–1754. [CrossRef]
19. Yao, X.; Abraham, N.S.; Sangaralingham, L.R.; Bellolio, M.F.; McBane, R.D.; Shah, N.D.; Noseworthy, P.A. Effectiveness and Safety of Dabigatran, Rivaroxaban, and Apixaban Versus Warfarin in Nonvalvular Atrial Fibrillation. *J. Am. Heart Assoc.* **2016**, *5*, e003725. [CrossRef]
20. Kato, E.T.; Giugliano, R.P.; Ruff, C.T.; Koretsune, Y.; Yamashita, T.; Kiss, R.G.; Nordio, F.; Murphy, S.A.; Kimura, T.; Jin, J.; et al. Efficacy and Safety of Edoxaban in Elderly Patients with Atrial Fibrillation in the ENGAGE AF–TIMI 48 Trial. *J. Am. Heart Assoc.* **2016**, *5*, e003432. [CrossRef]
21. Sardar, P.; Chatterjee, S.; Chaudhari, S.; Lip, G.Y.H. New Oral Anticoagulants in Elderly Adults: Evidence from a Meta-Analysis of Randomized Trials. *J. Am. Geriatr. Soc.* **2014**, *62*, 857–864. [CrossRef] [PubMed]
22. Okumura, A.; Araki, Y.; Nishimura, Y.; Iwama, T.; Kaku, Y.; Furuichi, M.; Sakai, N. The Clinical Utility of Contrast-Enhanced 3D MR Angiography for Cerebrovascular Disease. *Neurol. Res.* **2001**, *23*, 767–771. [CrossRef] [PubMed]
23. Okumura, K.; Lip, G.Y.H.; Akao, M.; Tanizawa, K.; Fukuzawa, M.; Abe, K.; Akishita, M.; Yamashita, T. Edoxaban for the Management of Elderly Japanese Patients with Atrial Fibrillation Ineligible for Standard Oral Anticoagulant Therapies: Rationale and Design of the ELDERCARE-AF Study. *Am. Heart J.* **2017**, *194*, 99–106. [CrossRef] [PubMed]
24. Chao, T.-F.; Liu, C.-J.; Lin, Y.-J.; Chang, S.-L.; Lo, L.-W.; Hu, Y.-F.; Tuan, T.-C.; Liao, J.-N.; Chung, F.-P.; Chen, T.-J.; et al. Oral Anticoagulation in Very Elderly Patients with Atrial Fibrillation: A Nationwide Cohort Study. *Circulation* **2018**, *138*, 37–47. [CrossRef]

25. Sugrue, A.; Sanborn, D.; Amin, M.; Farwati, M.; Sridhar, H.; Ahmed, A.; Mehta, R.; Siontis, K.C.; Mulpuru, S.K.; Deshmukh, A.J.; et al. Inappropriate Dosing of Direct Oral Anticoagulants in Patients with Atrial Fibrillation. *Am. J. Cardiol.* **2021**, *144*, 52–59. [CrossRef]
26. Carbone, A.; Santelli, F.; Bottino, R.; Attena, E.; Mazzone, C.; Parisi, V.; D'Andrea, A.; Golino, P.; Nigro, G.; Russo, V. Prevalence and Clinical Predictors of Inappropriate Direct Oral Anticoagulant Dosage in Octagenarians with Atrial Fibrillation. *Eur. J. Clin. Pharmacol.* **2022**, *78*, 879–886. [CrossRef]
27. Clegg, A.; Young, J.; Iliffe, S.; Rikkert, M.O.; Rockwood, K. Frailty in Elderly People. *Lancet* **2013**, *381*, 752–762. [CrossRef]
28. Collard, R.M.; Boter, H.; Schoevers, R.A.; Oude Voshaar, R.C. Prevalence of Frailty in Community-Dwelling Older Persons: A Systematic Review. *J. Am. Geriatr. Soc.* **2012**, *60*, 1487–1492. [CrossRef]
29. Singh, P.; Arrevad, P.S.; Peterson, G.M.; Bereznicki, L.R. Evaluation of Antithrombotic Usage for Atrial Fibrillation in Aged Care Facilities: Antithrombotic Usage for Atrial Fibrillation. *J. Clin. Pharm. Ther.* **2011**, *36*, 166–171. [CrossRef]
30. Mant, J.; Hobbs, F.R.; Fletcher, K.; Roalfe, A.; Fitzmaurice, D.; Lip, G.Y.; Murray, E. Warfarin versus Aspirin for Stroke Prevention in an Elderly Community Population with Atrial Fibrillation (the Birmingham Atrial Fibrillation Treatment of the Aged Study, BAFTA): A Randomised Controlled Trial. *Lancet* **2007**, *370*, 493–503. [CrossRef]
31. Rash, A.; Downes, T.; Portner, R.; Yeo, W.W.; Morgan, N.; Channer, K.S. A Randomised Controlled Trial of Warfarin versus Aspirin for Stroke Prevention in Octogenarians with Atrial Fibrillation (WASPO). *Age Ageing* **2007**, *36*, 151–156. [CrossRef] [PubMed]
32. Lip, G.Y.H.; Clementy, N.; Pericart, L.; Banerjee, A.; Fauchier, L. Stroke and Major Bleeding Risk in Elderly Patients Aged ≥75 Years with Atrial Fibrillation: The Loire Valley Atrial Fibrillation Project. *Stroke* **2015**, *46*, 143–150. [CrossRef] [PubMed]
33. Alnsasra, H.; Haim, M.; Senderey, A.B.; Reges, O.; Leventer-Roberts, M.; Arnson, Y.; Leibowitz, M.; Hoshen, M.; Avgil-Tsadok, M. Net Clinical Benefit of Anticoagulant Treatments in Elderly Patients with Nonvalvular Atrial Fibrillation: Experience from the Real World. *Heart Rhythm.* **2019**, *16*, 31–37. [CrossRef] [PubMed]
34. Russo, V.; Attena, E.; Di Maio, M.; Mazzone, C.; Carbone, A.; Parisi, V.; Rago, A.; D'Onofrio, A.; Golino, P.; Nigro, G. Clinical Profile of Direct Oral Anticoagulants versus Vitamin K Anticoagulants in Octogenarians with Atrial Fibrillation: A Multicentre Propensity Score Matched Real-World Cohort Study. *J. Thromb. Thrombolysis* **2020**, *49*, 42–53. [CrossRef] [PubMed]
35. Nieuwlaat, R.; Olsson, S.B.; Lip, G.Y.H.; Camm, A.J.; Breithardt, G.; Capucci, A.; Meeder, J.G.; Prins, M.H.; Lévy, S.; Crijns, H.J.G.M. Guideline-Adherent Antithrombotic Treatment Is Associated with Improved Outcomes Compared with Undertreatment in High-Risk Patients with Atrial Fibrillation. The Euro Heart Survey on Atrial Fibrillation. *Am. Heart J.* **2007**, *153*, 1006–1012. [CrossRef]
36. Dillinger, J.-G.; Aleil, B.; Cheggour, S.; Benhamou, Y.; Béjot, Y.; Marechaux, S.; Delluc, A.; Bertoletti, L.; Lellouche, N. Dosing Issues with Non-Vitamin K Antagonist Oral Anticoagulants for the Treatment of Non-Valvular Atrial Fibrillation: Why We Should Not Underdose Our Patients. *Arch. Cardiovasc. Dis.* **2018**, *111*, 85–94. [CrossRef]
37. Steinberg, B.A.; Kim, S.; Piccini, J.P.; Fonarow, G.C.; Lopes, R.D.; Thomas, L.; Ezekowitz, M.D.; Ansell, J.; Kowey, P.; Singer, D.E.; et al. Use and Associated Risks of Concomitant Aspirin Therapy with Oral Anticoagulation in Patients with Atrial Fibrillation: Insights from the Outcomes Registry for Better Informed Treatment of Atrial Fibrillation (ORBIT-AF) Registry. *Circulation* **2013**, *128*, 721–728. [CrossRef]
38. Oqab, Z. What Is the Impact of Frailty on Prescription of Anticoagulation in Elderly Patients with Atrial Fibrillation? A Systematic Review and Meta-Analysis. *J. Atr. Fibrillation* **2018**, *10*, 1870. [CrossRef]
39. Lefebvre, M.-C.D.; St-Onge, M.; Glazer-Cavanagh, M.; Bell, L.; Kha Nguyen, J.N.; Viet-Quoc Nguyen, P.; Tannenbaum, C. The Effect of Bleeding Risk and Frailty Status on Anticoagulation Patterns in Octogenarians with Atrial Fibrillation: The FRAIL-AF Study. *Can. J. Cardiol.* **2016**, *32*, 169–176. [CrossRef]
40. Diener, H.-C.; Aisenberg, J.; Ansell, J.; Atar, D.; Breithardt, G.; Eikelboom, J.; Ezekowitz, M.D.; Granger, C.B.; Halperin, J.L.; Hohnloser, S.H.; et al. Choosing a Particular Oral Anticoagulant and Dose for Stroke Prevention in Individual Patients with Non-Valvular Atrial Fibrillation: Part 2. *Eur. Heart J.* **2016**, *38*, 860–868. [CrossRef]
41. The FORTA authors/expert panel members; Kuhn-Thiel, A.M.; Weiß, C.; Wehling, M. Consensus Validation of the FORTA (Fit fOR The Aged) List: A Clinical Tool for Increasing the Appropriateness of Pharmacotherapy in the Elderly. *Drugs Aging* **2014**, *31*, 131–140. [CrossRef] [PubMed]
42. Pazan, F.; Weiss, C.; Wehling, M. The FORTA (Fit fOR The Aged) List 2015: Update of a Validated Clinical Tool for Improved Pharmacotherapy in the Elderly. *Drugs Aging* **2016**, *33*, 447–449. [CrossRef] [PubMed]
43. By the 2019 American Geriatrics Society Beers Criteria® Update Expert Panel American Geriatrics Society 2019 Updated AGS Beers Criteria® for Potentially Inappropriate Medication Use in Older Adults: 2019 AGS BEERS CRITERIA® UPDATE EXPERT PANEL. *J. Am. Geriatr. Soc.* **2019**, *67*, 674–694. [CrossRef]
44. Mann, D.L.; Krone, R.J. Cardiac Disease in Cancer Patients: An Overview. *Prog. Cardiovasc. Dis.* **2010**, *53*, 80–87. [CrossRef]
45. Yun, J.P.; Choi, E.-K.; Han, K.-D.; Park, S.H.; Jung, J.-H.; Park, S.H.; Ahn, H.-J.; Lim, J.-H.; Lee, S.-R.; Oh, S. Risk of Atrial Fibrillation According to Cancer Type. *JACC CardioOncol.* **2021**, *3*, 221–232. [CrossRef] [PubMed]
46. Pastori, D.; Marang, A.; Bisson, A.; Menichelli, D.; Herbert, J.; Lip, G.Y.H.; Fauchier, L. Thromboembolism, Mortality, and Bleeding in 2,435,541 Atrial Fibrillation Patients with and without Cancer: A Nationwide Cohort Study. *Cancer* **2021**, *127*, 2122–2129. [CrossRef] [PubMed]
47. Patel, M.R.; Mahaffey, K.W.; Garg, J.; Pan, G.; Singer, D.E.; Hacke, W.; Breithardt, G.; Halperin, J.L.; Hankey, G.J.; Piccini, J.P.; et al. Rivaroxaban versus Warfarin in Nonvalvular Atrial Fibrillation. *N. Engl. J. Med.* **2011**, *365*, 883–891. [CrossRef]

48. Giugliano, R.P.; Ruff, C.T.; Braunwald, E.; Murphy, S.A.; Wiviott, S.D.; Halperin, J.L.; Waldo, A.L.; Ezekowitz, M.D.; Weitz, J.I.; Špinar, J.; et al. Edoxaban versus Warfarin in Patients with Atrial Fibrillation. *N. Engl. J. Med.* **2013**, *369*, 2093–2104. [CrossRef]
49. Russo, V.; Bottino, R.; Rago, A.; Micco, P.; D' Onofrio, A.; Liccardo, B.; Golino, P.; Nigro, G. Atrial Fibrillation and Malignancy: The Clinical Performance of Non–Vitamin K Oral Anticoagulants—A Systematic Review. *Semin. Thromb. Hemost.* **2018**, *45*, 205–214. [CrossRef]
50. Russo, V.; Rago, A.; Papa, A.A.; Meo, F.D.; Attena, E.; Golino, P.; D'Onofrio, A.; Nigro, G. Use of Non-Vitamin K Antagonist Oral Anticoagulants in Atrial Fibrillation Patients with Malignancy: Clinical Practice Experience in a Single Institution and Literature Review. *Semin. Thromb. Hemost.* **2018**, *44*, 370–376. [CrossRef]
51. Deng, Y.; Tong, Y.; Deng, Y.; Zou, L.; Li, S.; Chen, H. Non–Vitamin K Antagonist Oral Anticoagulants Versus Warfarin in Patients with Cancer and Atrial Fibrillation: A Systematic Review and Meta-Analysis. *J. Am. Heart Assoc.* **2019**, *8*, e012540. [CrossRef]
52. Yang, P.; Zhu, D.; Xu, X.; Shen, W.; Wang, C.; Jiang, Y.; Xu, G.; Wu, Q. Efficacy and Safety of Oral Anticoagulants in Atrial Fibrillation Patients with Cancer—A Network Meta-Analysis. *Heart Fail. Rev.* **2020**, *25*, 823–831. [CrossRef] [PubMed]
53. Melloni, C.; Dunning, A.; Granger, C.B.; Thomas, L.; Khouri, M.G.; Garcia, D.A.; Hylek, E.M.; Hanna, M.; Wallentin, L.; Gersh, B.J.; et al. Efficacy and Safety of Apixaban Versus Warfarin in Patients with Atrial Fibrillation and a History of Cancer: Insights from the ARISTOTLE Trial. *Am. J. Med.* **2017**, *130*, 1440–1448.e1. [CrossRef] [PubMed]
54. Chen, S.T.; Hellkamp, A.S.; Becker, R.C.; Berkowitz, S.D.; Breithardt, G.; Fox, K.A.A.; Hacke, W.; Halperin, J.L.; Hankey, G.J.; Mahaffey, K.W.; et al. Efficacy and Safety of Rivaroxaban vs. Warfarin in Patients with Non-Valvular Atrial Fibrillation and a History of Cancer: Observations from ROCKET AF. *Eur. Heart J.-Qual. Care Clin. Outcomes* **2019**, *5*, 145–152. [CrossRef] [PubMed]
55. Fanola, C.L.; Ruff, C.T.; Murphy, S.A.; Jin, J.; Duggal, A.; Babilonia, N.A.; Sritara, P.; Mercuri, M.F.; Kamphuisen, P.W.; Antman, E.M.; et al. Efficacy and Safety of Edoxaban in Patients with Active Malignancy and Atrial Fibrillation: Analysis of the ENGAGE AF-TIMI 48 Trial. *J. Am. Heart Assoc.* **2018**, *7*, e008987. [CrossRef] [PubMed]
56. Mariani, M.V.; Magnocavallo, M.; Straito, M.; Piro, A.; Severino, P.; Iannucci, G.; Chimenti, C.; Mancone, M.; Rocca, D.G.D.; Forleo, G.B.; et al. Direct Oral Anticoagulants versus Vitamin K Antagonists in Patients with Atrial Fibrillation and Cancer a Meta-Analysis. *J. Thromb. Thrombolysis* **2021**, *51*, 419–429. [CrossRef] [PubMed]
57. Shah, S.; Norby, F.L.; Datta, Y.H.; Lutsey, P.L.; MacLehose, R.F.; Chen, L.Y.; Alonso, A. Comparative Effectiveness of Direct Oral Anticoagulants and Warfarin in Patients with Cancer and Atrial Fibrillation. *Blood Adv.* **2018**, *2*, 200–209. [CrossRef]
58. Delluc, A.; Wang, T.; Yap, E.; Ay, C.; Schaefer, J.; Carrier, M.; Noble, S. Anticoagulation of Cancer Patients with Non-valvular Atrial Fibrillation Receiving Chemotherapy: Guidance from the SSC of the ISTH. *J. Thromb. Thrombolysis* **2019**, *17*, 1247–1252. [CrossRef]
59. Boriani, G.; Huisman, M.V.; Teutsch, C.; Marler, S.; França, L.R.; Lu, S.; Lip, G.Y.H. Influence of BMI and Geographical Region on Prescription of Oral Anticoagulants in Newly Diagnosed Atrial Fibrillation: The GLORIA-AF Registry Program. *Eur. J. Intern. Med.* **2020**, *80*, 35–44. [CrossRef]
60. De Caterina, R.; Kim, Y.-H.; Koretsune, Y.; Wang, C.-C.; Yamashita, T.; Chen, C.; Reimitz, P.-E.; Unverdorben, M.; Kirchhof, P. Safety and Effectiveness of Edoxaban in Atrial Fibrillation Patients in Routine Clinical Practice: One-Year Follow-Up from the Global Noninterventional ETNA-AF Program. *J. Clin. Med.* **2021**, *10*, 573. [CrossRef]
61. Sandhu, R.K.; Ezekowitz, J.; Andersson, U.; Alexander, J.H.; Granger, C.B.; Halvorsen, S.; Hanna, M.; Hijazi, Z.; Jansky, P.; Lopes, R.D.; et al. The 'obesity paradox' in atrial fibrillation: Observations from the ARISTOTLE (Apixaban for Reduction in Stroke and Other Thromboembolic Events in Atrial Fibrillation) trial. *Eur. Heart J.* **2016**, *37*, 2869–2878. [CrossRef] [PubMed]
62. Boriani, G.; Ruff, C.T.; Kuder, J.F.; Shi, M.; Lanz, H.J.; Rutman, H.; Mercuri, M.F.; Antman, E.M.; Braunwald, E.; Giugliano, R.P. Relationship between Body Mass Index and Outcomes in Patients with Atrial Fibrillation Treated with Edoxaban or Warfarin in the ENGAGE AF-TIMI 48 Trial. *Eur. Heart J.* **2019**, *40*, 1541–1550. [CrossRef]
63. Balla, S.R.; Cyr, D.D.; Lokhnygina, Y.; Becker, R.C.; Berkowitz, S.D.; Breithardt, G.; Fox, K.A.A.; Hacke, W.; Halperin, J.L.; Hankey, G.J.; et al. Relation of Risk of Stroke in Patients with Atrial Fibrillation to Body Mass Index (from Patients Treated with Rivaroxaban and Warfarin in the Rivaroxaban Once Daily Oral Direct Factor Xa Inhibition Compared with Vitamin K Antagonism for Prevention of Stroke and Embolism Trial in Atrial Fibrillation Trial). *Am. J. Cardiol.* **2017**, *119*, 1989–1996. [CrossRef] [PubMed]
64. Kido, K.; Shimizu, M.; Shiga, T.; Hashiguchi, M. Meta-Analysis Comparing Direct Oral Anticoagulants Versus Warfarin in Morbidly Obese Patients with Atrial Fibrillation. *Am. J. Cardiol.* **2020**, *126*, 23–28. [CrossRef] [PubMed]
65. Wang, S.Y.; Giugliano, R.P. Non-Vitamin K Antagonist Oral Anticoagulant for Atrial Fibrillation in Obese Patients. *Am. J. Cardiol.* **2020**, *127*, 176–183. [CrossRef]
66. Russo, V.; Rago, A.; Laezza, N.; Di Micco, P.; Giannetti, L.; Atripaldi, L.; D'Onofrio, A.; Golino, P.; Nigro, G. Edoxaban in Elderly Patient with Morbid Obesity and Atrial Fibrillation: The Role of Plasma Levels Evaluation for Selecting the Appropriate Dose. *Monaldi Arch. Chest Dis.* **2020**, *90*, 1224. [CrossRef]
67. Russo, V.; Cattaneo, D.; Giannetti, L.; Bottino, R.; Laezza, N.; Atripaldi, U.; Clementi, E. Pharmacokinetics of Direct Oral Anticoagulants in Patients with Atrial Fibrillation and Extreme Obesity. *Clin. Ther.* **2021**, *43*, e255–e263. [CrossRef]
68. Renon, F.; Rago, A.; Liccardo, B.; D'Andrea, A.; Riegler, L.; Golino, P.; Nigro, G.; Russo, V. Direct Oral Anticoagulants Plasma Levels Measurement: Clinical Usefulness from Trials and Real-World Data. *Semin. Thromb. Hemost.* **2021**, *47*, 150–160. [CrossRef]
69. Russo, V.; Bottino, R.; Rago, A.; Papa, A.A.; Liccardo, B.; D'Onofrio, A.; Golino, P.; Nigro, G. Clinical Performance of Nonvitamin K Antagonist Oral Anticoagulants in Real-World Obese Patients with Atrial Fibrillation. *Semin. Thromb. Hemost.* **2020**, *46*, 970–976. [CrossRef]

70. Russo, V.; Paccone, A.; Rago, A.; Maddaloni, V.; Iafusco, D.; Proietti, R.; Atripaldi, U.; D'Onofrio, A.; Golino, P.; Nigro, G. Apixaban in a Morbid Obese Patient with Atrial Fibrillation: A Clinical Experience Using the Plasmatic Drug Evaluation. *J. Blood Med.* **2020**, *11*, 77–81. [CrossRef]
71. Martin, K.; Beyer-Westendorf, J.; Davidson, B.L.; Huisman, M.V.; Sandset, P.M.; Moll, S. Use of the Direct Oral Anticoagulants in Obese Patients: Guidance from the SSC of the ISTH. *J. Thromb. Haemost.* **2016**, *14*, 1308–1313. [CrossRef] [PubMed]
72. Steffel, J.; Collins, R.; Antz, M.; Cornu, P.; Desteghe, L.; Haeusler, K.G.; Oldgren, J.; Reinecke, H.; Roldan-Schilling, V.; Rowell, N.; et al. 2021 European Heart Rhythm Association Practical Guide on the Use of Non-Vitamin K Antagonist Oral Anticoagulants in Patients with Atrial Fibrillation. *EP Eur.* **2021**, *23*, 1612–1676. [CrossRef] [PubMed]
73. Boriani, G.; Ruff, C.T.; Kuder, J.F.; Shi, M.; Lanz, H.J.; Antman, E.M.; Braunwald, E.; Giugliano, R.P. Edoxaban versus Warfarin in Patients with Atrial Fibrillation at the Extremes of Body Weight: An Analysis from the ENGAGE AF-TIMI 48 Trial. *Thromb. Haemost.* **2021**, *121*, 140–149. [CrossRef] [PubMed]
74. Piran, S.; Traquair, H.; Chan, N.; Bhagirath, V.; Schulman, S. Peak Plasma Concentration of Direct Oral Anticoagulants in Obese Patients Weighing over 120 Kilograms: A Retrospective Study. *Res. Pract. Thromb. Haemost.* **2018**, *2*, 684–688. [CrossRef] [PubMed]
75. Kubitza, D.; Becka, M.; Zuehlsdorf, M.; Mueck, W. Body Weight Has Limited Influence on the Safety, Tolerability, Pharmacokinetics, or Pharmacodynamics of Rivaroxaban (BAY 59-7939) in Healthy Subjects. *J. Clin. Pharmacol.* **2007**, *47*, 218–226. [CrossRef]
76. Lip, G.Y.H.; Agnelli, G. Edoxaban: A Focused Review of Its Clinical Pharmacology. *Eur. Heart J.* **2014**, *35*, 1844–1855. [CrossRef] [PubMed]
77. Park, C.S.; Choi, E.-K.; Kim, H.M.; Lee, S.-R.; Cha, M.-J.; Oh, S. Increased Risk of Major Bleeding in Underweight Patients with Atrial Fibrillation Who Were Prescribed Non-Vitamin K Antagonist Oral Anticoagulants. *Heart Rhythm.* **2017**, *14*, 501–507. [CrossRef]
78. Russo, V.; Attena, E.; Baroni, M.; Trotta, R.; Manu, M.C.; Kirchhof, P.; De Caterina, R. Clinical Performance of Oral Anticoagulants in Elderly with Atrial Fibrillation and Low Body Weight: Insight into Italian Cohort of PREFER-AF and PREFER-AF Prolongation Registries. *J. Clin. Med.* **2022**, *11*, 3751. [CrossRef] [PubMed]
79. Russo, V.; Attena, E.; Di Maio, M.; Carbone, A.; Parisi, V.; Rago, A.; Grieco, F.V.; Buonauro, A.; Golino, P.; Nigro, G. Non-vitamin K vs Vitamin K Oral Anticoagulants in Patients Aged > 80 Year with Atrial Fibrillation and Low Body Weight. *Eur. J. Clin. Investig.* **2020**, *50*, e13335. [CrossRef]
80. Bottino, R.; Carbone, A.; Liccardo, B.; Imbalzano, E.; D'Andrea, A.; Russo, V. Optimal Anticoagulation in Patients with Atrial Fibrillation and Bioprosthetic Heart Valves. *Kardiol. Pol.* **2022**, *80*, 137–150. [CrossRef]
81. Vahanian, A.; Beyersdorf, F.; Praz, F.; Milojevic, M.; Baldus, S.; Bauersachs, J.; Capodanno, D.; Conradi, L.; De Bonis, M.; De Paulis, R.; et al. 2021 ESC/EACTS Guidelines for the Management of Valvular Heart Disease. *Eur. Heart J.* **2022**, *43*, 561–632. [CrossRef] [PubMed]
82. Otto, C.M.; Nishimura, R.A.; Bonow, R.O.; Carabello, B.A.; Erwin, J.P.; Gentile, F.; Jneid, H.; Krieger, E.V.; Mack, M.; McLeod, C.; et al. 2020 ACC/AHA Guideline for the Management of Patients with Valvular Heart Disease: A Report of the American College of Cardiology/American Heart Association Joint Committee on Clinical Practice Guidelines. *Circulation* **2021**, *143*, e35–e71. [CrossRef]
83. Guimarães, P.O.; Pokorney, S.D.; Lopes, R.D.; Ms, D.M.W.; Gersh, B.J.; Ms, A.G.; Carnicelli, A.; Lewis, B.S.; Hanna, M.; Wallentin, L.; et al. Efficacy and safety of apixaban vs warfarin in patients with atrial fibrillation and prior bioprosthetic valve replacement or valve repair: Insights from the ARISTOTLE trial. *Clin. Cardiol.* **2019**, *42*, 568–571. [CrossRef] [PubMed]
84. Russo, V.; Attena, E.; Mazzone, C.; Esposito, F.; Parisi, V.; Bancone, C.; Rago, A.; Nigro, G.; Sangiuolo, R.; D' Onofrio, A. Nonvitamin K Antagonist Oral Anticoagulants Use in Patients with Atrial Fibrillation and Bioprosthetic Heart Valves/Prior Surgical Valve Repair: A Multicenter Clinical Practice Experience. *Semin. Thromb. Hemost.* **2018**, *44*, 364–369. [CrossRef]
85. Yadlapati, A.; Groh, C.; Malaisrie, S.C.; Gajjar, M.; Kruse, J.; Meyers, S.; Passman, R. Efficacy and Safety of Novel Oral Anticoagulants in Patients with Bioprosthetic Valves. *Clin. Res. Cardiol.* **2015**, *105*, 268–272. [CrossRef] [PubMed]
86. Carnicelli, A.P.; De Caterina, R.; Halperin, J.L.; Renda, G.; Ruff, C.T.; Trevisan, M.; Nordio, F.; Mercuri, M.F.; Antman, E.; Giugliano, R.P. Edoxaban for the Prevention of Thromboembolism in Patients with Atrial Fibrillation and Bioprosthetic Valves. *Circulation* **2017**, *135*, 1273–1275. [CrossRef] [PubMed]
87. Duan, L.; Doctor, J.N.; Adams, J.L.; Romley, J.A.; Nguyen, L.-A.; An, J.; Lee, M.-S. Comparison of Direct Oral Anticoagulants Versus Warfarin in Patients with Atrial Fibrillation and Bioprosthetic Heart Valves. *Am. J. Cardiol.* **2021**, *146*, 22–28. [CrossRef]
88. Russo, V.; Carbone, A.; Attena, E.; Rago, A.; Mazzone, C.; Proietti, R.; Parisi, V.; Scotti, A.; Nigro, G.; Golino, P.; et al. Clinical Benefit of Direct Oral Anticoagulants Versus Vitamin K Antagonists in Patients with Atrial Fibrillation and Bioprosthetic Heart Valves. *Clin. Ther.* **2019**, *41*, 2549–2557. [CrossRef]
89. Piepiorka-Broniecka, M.; Michalski, T.A.; Figatowski, T.; Wojtowicz, A.; Jurowiecki, J.; Stanska, A.; Rogowski, J.; Jaguszewski, M.J. NOAC versus warfarin in the treatment of atrial fibrillation during the first three months after bioprosthetic aortic valve replacement. *Cardiol. J.* **2022**, *29*, 355–357. [CrossRef]
90. Guimarães, H.P.; Lopes, R.D.; de Barros e Silva, P.G.; Liporace, I.L.; Sampaio, R.O.; Tarasoutchi, F.; Hoffmann-Filho, C.R.; de Lemos Soares Patriota, R.; Leiria, T.L.; Lamprea, D.; et al. Rivaroxaban in Patients with Atrial Fibrillation and a Bioprosthetic Mitral Valve. *N. Engl. J. Med.* **2020**, *383*, 2117–2126. [CrossRef]

91. Jochheim, D.; Barbanti, M.; Capretti, G.; Stefanini, G.G.; Hapfelmeier, A.; Zadrozny, M.; Baquet, M.; Fischer, J.; Theiss, H.; Todaro, D.; et al. Oral Anticoagulant Type and Outcomes After Transcatheter Aortic Valve Replacement. *JACC Cardiovasc. Interv.* **2019**, *12*, 1566–1576. [CrossRef] [PubMed]
92. Durães, A.R.; de Souza Roriz, P.; de Almeida Nunes, B.; Albuquerque, F.P.E.; de Bulhões, F.V.; de Souza Fernandes, A.M.; Aras, R. Dabigatran Versus Warfarin After Bioprosthesis Valve Replacement for the Management of Atrial Fibrillation Postoperatively: DAWA Pilot Study. *Drugs R&D* **2016**, *16*, 149–154. [CrossRef]
93. Kawashima, H.; Watanabe, Y.; Hioki, H.; Kozuma, K.; Kataoka, A.; Nakashima, M.; Nagura, F.; Nara, Y.; Yashima, F.; Tada, N.; et al. Direct Oral Anticoagulants Versus Vitamin K Antagonists in Patients with Atrial Fibrillation After TAVR. *JACC Cardiovasc. Interv.* **2020**, *13*, 2587–2597. [CrossRef] [PubMed]
94. Butt, J.H.; De Backer, O.; Olesen, J.B.; Gerds, T.A.; Havers-Borgersen, E.; Gislason, G.H.; Torp-Pedersen, C.; Søndergaard, L.; Køber, L.; Fosbøl, E.L. Vitamin K Antagonists vs. Direct Oral Anticoagulants after Transcatheter Aortic Valve Implantation in Atrial Fibrillation. *Eur. Heart J.-Cardiovasc. Pharmacother.* **2021**, *7*, 11–19. [CrossRef] [PubMed]
95. Van Mieghem, N.M.; Unverdorben, M.; Hengstenberg, C.; Möllmann, H.; Mehran, R.; López-Otero, D.; Nombela-Franco, L.; Moreno, R.; Nordbeck, P.; Thiele, H.; et al. Edoxaban versus Vitamin K Antagonist for Atrial Fibrillation after TAVR. *N. Engl. J. Med.* **2021**, *385*, 2150–2160. [CrossRef]
96. Nijenhuis, V.J.; Brouwer, J.; Delewi, R.; Hermanides, R.S.; Holvoet, W.; Dubois, C.L.F.; Frambach, P.; De Bruyne, B.; van Houwelingen, G.K.; Van Der Heyden, J.A.S.; et al. Anticoagulation with or without Clopidogrel after Transcatheter Aortic-Valve Implantation. *N. Engl. J. Med.* **2020**, *382*, 1696–1707. [CrossRef] [PubMed]
97. Collet, J.P.; Van Belle, E.; Thiele, H.; Berti, S.; Lhermusier, T.; Manigold, T.; Neumann, F.J.; Gilard, M.; Attias, D.; Beygui, F.; et al. Apixaban vs. standard of care after transcatheter aortic valve implantation: The ATLANTIS trial. *Eur. Heart J.* **2022**, *43*, 2783–2797. [CrossRef] [PubMed]
98. ten Berg, J.; Sibbing, D.; Rocca, B.; Van Belle, E.; Chevalier, B.; Collet, J.-P.; Dudek, D.; Gilard, M.; Gorog, D.A.; Grapsa, J.; et al. Management of Antithrombotic Therapy in Patients Undergoing Transcatheter Aortic Valve Implantation: A Consensus Document of the ESC Working Group on Thrombosis and the European Association of Percutaneous Cardiovascular Interventions (EAPCI), in Collaboration with the ESC Council on Valvular Heart Disease. *Eur. Heart J.* **2021**, *42*, 2265–2269. [CrossRef]

biomedicines

MDPI

Article

Associations of Warfarin Use with Risks of Ischemic Cerebrovascular Events and Major Bleeding in Patients with Hyperthyroidism-Related Atrial Fibrillation

Sian-De Liu [1,2,†], Shwu-Jiuan Lin [1,3,†], Chin-Ying Ray [4,5], Fang-Tsyr Lin [6], Weei-Chin Lin [6,7] and Li-Hsuan Wang [1,8,*]

1 School of Pharmacy, Taipei Medical University, Taipei 110, Taiwan
2 Department of Pharmacy, New Taipei Municipal TuCheng Hospital (Built and Operated by Chang Gung Medical Foundation), New Taipei City 236, Taiwan
3 PhD Program in Clinical Drug Development of Herbal Medicine, College of Pharmacy, Taipei Medical University, Taipei 110, Taiwan
4 Department of Clinical Pharmacy, Chang Gung Memorial Hospital, Linkou, Taoyuan 333, Taiwan
5 Heart Failure Center, Chang Gung Memorial Hospital, Linkou, Taoyuan 333, Taiwan
6 Section of Hematology/Oncology, Department of Medicine, Baylor College of Medicine, Houston, TX 77030, USA
7 Department of Molecular and Cellular Biology, Baylor College of Medicine, Houston, TX 77030, USA
8 Department of Pharmacy, Taipei Medical University Hospital, Taipei 110, Taiwan
* Correspondence: shiuan@tmu.edu.tw
† These authors contributed equally to this work.

Citation: Liu, S.-D.; Lin, S.-J.; Ray, C.-Y.; Lin, F.-T.; Lin, W.-C.; Wang, L.-H. Associations of Warfarin Use with Risks of Ischemic Cerebrovascular Events and Major Bleeding in Patients with Hyperthyroidism-Related Atrial Fibrillation. *Biomedicines* **2022**, *10*, 2670. https://doi.org/10.3390/biomedicines10112670

Academic Editors: Alfredo Caturano and Juan Sahuquillo

Received: 24 August 2022
Accepted: 20 October 2022
Published: 22 October 2022

Abstract: The use of oral anticoagulants for patients with new-onset hyperthyroidism-related atrial fibrillation (AF) is controversial. We aimed to evaluate the clinical benefits of warfarin therapy in this population. This retrospective cohort study used a data-cut of Taiwan Health and Welfare Database between 2000 and 2016. We compared warfarin users and nonusers among AF patients with hyperthyroidism. We used 1:2 propensity score matching to balance covariates and Cox regression model to calculate hazard ratios (HRs). The primary outcome was risk of ischemic stroke/transient ischemic attack (TIA), and the secondary outcome was major bleeding. After propensity score matching, we defined 90 and 168 hyperthyroidism-related AF patients with mean (SD) age of 59.9 ± 13.5 and 59.2 ± 14.6 in the warfarin-treated group and untreated group separately. The mean (SD) CHA2DS2-VASc scores for the two groups were 2.1 ± 1.6 and 1.8 ± 1.5, respectively. Patients with hyperthyroidism-related AF receiving warfarin had no significant risk of ischemic stroke/TIA (adjusted HR: 1.16, 95% confidence interval [CI]: 0.52–2.56, $p = 0.717$) compared to nonusers. There was a comparable risk of major bleeding between those receiving warfarin or not (adjusted HR: 0.91, 95% CI: 0.56–1.47, $p = 0.702$). The active-comparator design also demonstrated that warfarin use had no significant association with the risk of stroke/TIA versus aspirin use (adjusted HR: 2.43; 95% CI: 0.68–8.70). In conclusion, anticoagulation therapy did not have a statistically significant benefit on ischemic stroke/TIA nor risk of bleeding, among patients with new-onset hyperthyroidism-related AF under a low CHA2DS2-VASc score, by comparing those without use.

Keywords: atrial fibrillation; hyperthyroidism; warfarin; ischemic stroke; transient ischemic attack

1. Introduction

Atrial fibrillation (AF) is a common sustained cardiac arrhythmia in adults worldwide, and it is associated with substantial mortality and risk of ischemic stroke [1]. AF contributes to an overall five-fold higher risk of stroke [2]. It is well recognized that hyperthyroidism is associated with a risk of heart disease progression, but by itself can cause cardiac disease [3,4]. Hyperthyroidism is consistently reported as a risk factor for AF [5,6]. Thyroid hormones modulate the transcription rate of multiple genes, the production of

sarcoplasmic reticulum proteins, calcium-activated ATPase and phospholamban in cardiac myocytes [3,7]. Furthermore, the hormones increase in systolic depolarization and diastolic repolarization, decreasing the action potential duration and the refraction period of the atrial myocardium, as well as the atrial nodal refraction period [7]. Elevated thyroid hormones activate arrhythmogenic foci and increase supraventricular ectopic activity, which is considered a significant causal link between hyperthyroidism and AF [7–9]. Additionally, to identify those at high risk for incident AF, hyperthyroidism was proposed as a variable involved in the C2HEST score (coronary artery disease or chronic obstructive pulmonary disease (1 point each), hypertension (1 point), elderly (aged $\geq$ 75 years, 2 points), systolic heart failure (2 points), thyroid disease (hyperthyroidism, 1 point)) [2,6,10]. However, its correlation with thromboembolic stroke among patients with hyperthyroidism-related AF is still unclear [3,11–14]. Prophylactic treatment with oral anticoagulants for stroke prevention in this population is still controversial.

A previous prospective study in hyperthyroid patients with new-onset AF reported an increased risk of ischemic stroke clustering during the presentation phase [11]. Those authors suggested prompt early use of anticoagulation therapy in such patients with hyperthyroidism-related AF [11]. Another study showed that warfarin was beneficial compared to aspirin or no-treatment in stroke prevention in these patients with a CHA2DS2-VASc score of $\geq$1 and persistent AF [12]. However, the presence of hyperthyroidism did not confer an additional risk of ischemic stroke compared to that with non-hyperthyroid AF [12]. Recent research suggested that thromboprophylaxis with direct oral anticoagulants (DOACs) may be an effective and safer alternative to warfarin and should be considered for patients with AF concomitant with hyperthyroidism [15].

Current guidelines present limited evidence on management of AF in these settings [1,2,16]. Some studies revealed that hyperthyroidism is not an independent higher risk factor for stroke or systemic embolic events compared to non-hyperthyroid patients [12–14]. There are currently no recommendations focusing on AF patients with hyperthyroidism. However, Canadian guidelines suggest anticoagulation therapy during thyrotoxicosis with low-quality evidence [17]. To the present, no randomized controlled trial has specifically focused on these patients in relation to the efficacy and safety of anticoagulation therapy. Given the lack of clear evidence, a recommendation to initiate anticoagulation appears to be warranted. Therefore, the aim of our study was to investigate the association between warfarin therapy and risks of ischemic stroke/transient ischemic attack (TIA) and bleeding among patients with hyperthyroidism-related AF.

2. Materials and Methods

2.1. Source of Data

This retrospective cohort study used a subset of the Health and Welfare Database (HWD) from Health and Welfare Data Science Center of Taiwan. The HWD consists of medical claim data of the National Health Insurance which covers 99.99% of Taiwan's population. We used data from the 2000 Longitudinal Generation Tracking Database (LGTD 2000), which contains the information of 2 million beneficiaries randomly sampled from the HWD. Details of the HWD and the subset were documented in previous studies [18–21]. The subset contains all anonymized and deidentified personal information, medical records, procedures, and diagnoses, which were recorded using the International Classification of Diseases, 9th Revision, Clinical Modification (ICD-9-CM) codes from 1997 through 2015 and the International Classification of Diseases, 10th Revision, Clinical Modification (ICD-10-CM) codes since 2016. This study obtained ethical approval from the Taipei Medical University Joint Institutional Review Board (no. N201908068; 31 August 2019) and followed the Strengthening the Reporting of Observational Studies in Epidemiology (STROBE) guidelines.

2.2. Study Population

We extracted data on patients who aged ≥20 years and had one discharge nonvalvular AF diagnosis or two or more records in an outpatient department [18,20]. Patients with hyperthyroidism were identified by having two consecutive records of a diagnosis [22]. Individuals were all from January 2002 through December 2012 with at least a 2-year washout period to define newly diagnosed cases. Among these patients, those whose first nonvalvular AF diagnosed with hyperthyroidism was within 1 year were defined as hyperthyroidism-related nonvalvular AF.

Exclusion criteria for the study were patients (1) who had a stroke or TIA; (2) who had previous major bleeding; or (3) who had a diagnosis of hypothyroidism before the date of the hyperthyroidism diagnosis to maximize specificity for a diagnosis of hyperthyroidism. Details of the study design flowchart and patient numbers are given in Figure 1.

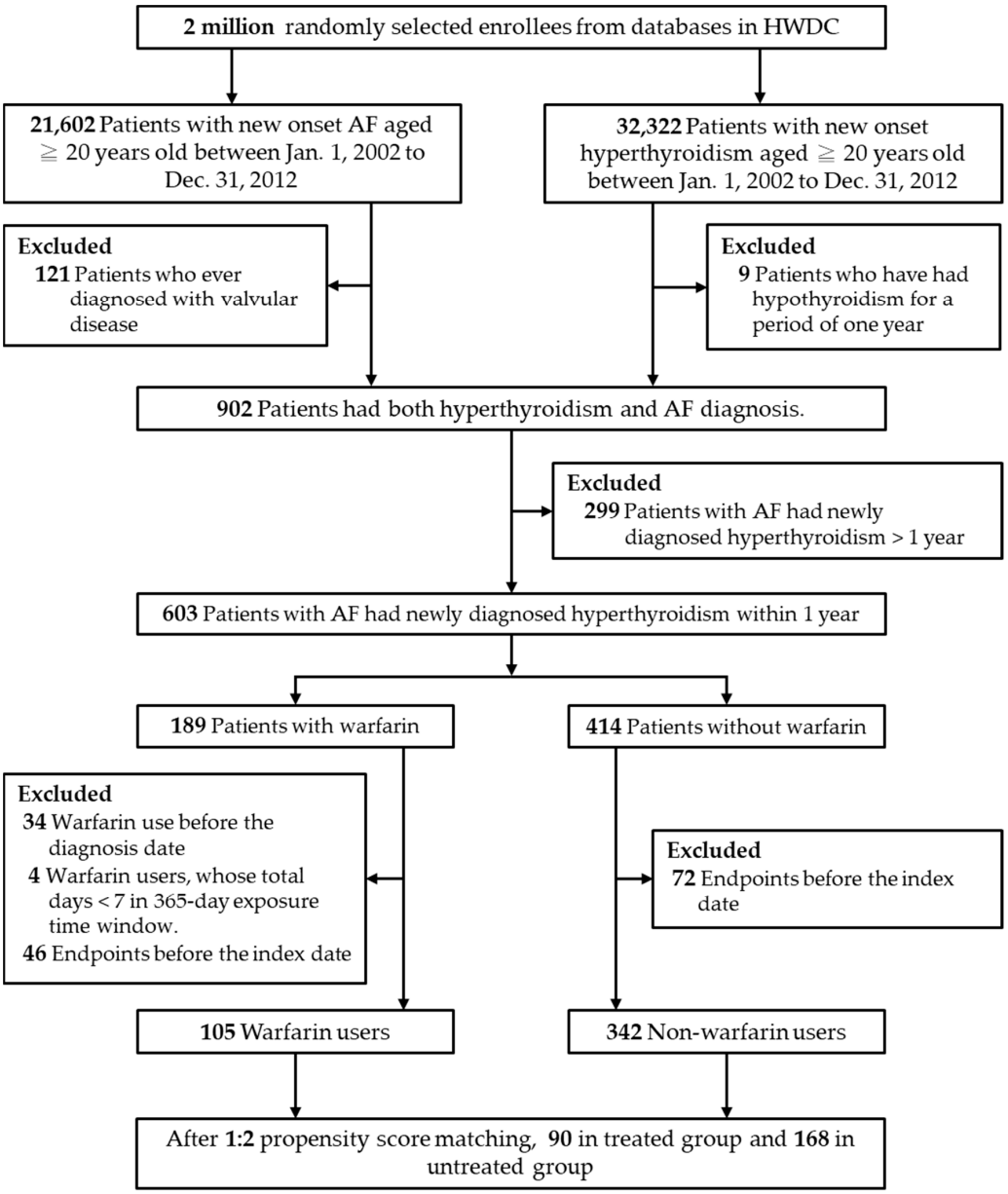

Figure 1. Flowchart of the study and analysis. Abbreviations: AF, atrial fibrillation; HWDC, Health and Welfare Data Science Center.

2.3. Medication Exposure and Covariates

We defined patients with hyperthyroidism-related nonvalvular AF who received warfarin within 365 days after the first nonvalvular AF diagnosis as the exposed group. The index date was defined as the first date on which warfarin was prescribed. A total prescription length of 7 days or longer was applied. We excluded patients who had previously used anticoagulants. All enrolled patients were followed up from the index date until the occurrence of any study outcome independently, or until the end date of the study (31 December 2016), whichever came first.

Patient demographics, comorbidities (hypertension, myocardial infarction, congestive heart failure, peripheral vascular disease, cerebrovascular disease, diabetes mellitus, chronic obstructive pulmonary disease, rheumatic disease, chronic kidney disease, hyperlipidemia, cardiomyopathy, pulmonary embolism, deep vein thrombosis, atherosclerosis, and any malignancy including leukemia) were identified as covariates. The CHA2DS2-VASc score was calculated as a measure of stroke risk. Relevant medications (amiodarone, aspirin, P2Y12 inhibitors, nonsteroidal anti-inflammatory drugs, and statins) were also assessed. The code lists of these covariates are shown in Supplementary Table S1.

2.4. Outcomes

The primary outcome was a composite of ischemic stroke and TIA. The diagnostic accuracy of ischemic stroke in the HWD is high [23–25]. We designated events first occurring after 14 days following the index date as outcomes, because the occurrence of events within the first few days of a diagnosis of AF was most likely related to the initial presentation of AF rather than a new event. The secondary outcome was major bleeding, defined as intracranial hemorrhage, or bleeding at gastrointestinal or other sites requiring hospitalization. We included only one major bleeding event occurring after the index date [20]. The code lists of these outcomes are shown in Supplementary Table S1.

2.5. Patient and Public Involvement

Patients or the public were not involved in the design, or conduct, or reporting or dissemination plans of our research.

2.6. Statistical Analysis

Continuous variables are expressed as the mean (±standard deviation (SD)), and categorical variables are expressed as proportions. Differences between continuous values were compared using a two-tailed *t*-test, and differences between nominal variables were compared using a Chi-squared test. We used a propensity score (PS) matching method to balance covariates across the warfarin-treated and untreated groups [26]. The PS was estimated using a multivariable logistic regression model based on various patient baseline characteristics which are listed in Table 1. We applied the greedy nearest neighbor 1:2 PS matching with a caliper of 0.2 on the PS scale, and an exact match was made for the index year [26]. The balance of baseline characteristics was evaluated using the standardized mean difference (SMD). Characteristics with an absolute SMD of >0.2 following PS matching were considered imbalanced between the two groups [27]. After PS matching, Cox proportional hazard modeling with a robust sandwich variance estimator analysis was performed to compare rates of clinical events [28].

We performed the first sensitivity analysis to examine the impacts of DOACs and new antiplatelet medication users on outcomes, because the approval date for the first DOACs in Taiwan was June 2012. Second, to reduce potential unmeasured confounding, we performed an active comparator design with warfarin versus aspirin. All statistical analyses were conducted by using SAS 9.4 (version 9.4, SAS Institute, Cary, NC, USA). Statistical significance was defined as a two-tailed p value of < 0.05.

Table 1. Baseline characteristics of the study population.

Characteristic (*n*, %)	Before PSM				After PSM			
	Warfarin Users *N* = 105	Warfarin Nonusers *N* = 342	*p* Value	SMD	Warfarin Users *N* = 90	Warfarin Nonusers *N* = 168	*p* Value	SMD
Age, years (mean ± SD)	60.1 ± 12.9	57.4 ± 14.5	0.088	0.197	59.9 ± 13.5	59.2 ± 14.6	0.699	0.051
Aged ≥ 65 years	40 (38.1)	111 (32.5)	0.285	0.118	36 (40.0)	64 (38.1)	0.765	0.039
Gender: Male	48 (45.7)	124 (36.3)	0.082	0.118	38 (42.2)	75 (44.6)	0.709	0.039
CHA2DS2-VASc (mean ± SD)	2.0 ± 1.6	1.7 ± 1.4	0.080	0.205	2.1 ± 1.6	1.8 ± 1.5	0.171	0.178
Hypertension	38 (36.2)	93 (27.2)	0.076	0.194	32 (35.6)	43 (25.6)	0.093	0.218
Diabetes mellitus	22 (21.0)	44 (12.9)	0.041	0.217	18 (20.0)	27 (16.1)	0.428	0.102
Hyperlipidemia	9 (8.6)	36 (10.5)	0.560	−0.067	9 (10.0)	20 (11.9)	0.644	−0.061
Chronic kidney disease	3 (2.9)	17 (5.0)	0.433	−0.109	2 (2.2)	4 (2.4)	0.936	−0.011
Congestive heart failure	38 (36.2)	58 (17.0)	<0.0001	0.446	35 (38.9)	44 (26.2)	0.035	0.274
Myocardial infarction	0	10 (2.9)	0.126	−0.245	0	0	NA	NA
Peripheral vascular disease	4 (3.8)	4 (1.2)	0.092	0.170	3 (3.3)	4 (2.4)	0.698	0.057
Chronic obstructive pulmonary disease	14 (13.3)	37 (10.8)	0.478	0.077	13 (14.4)	21 (12.5)	0.660	0.057
Rheumatic disease	0	3 (0.9)	1.000	−0.133	0	2 (1.2)	0.544	−0.155
Thromboembolism	0	1 (0.3)	1.000	−0.077	0	0	NA	NA
Cardiomyopathy	4 (3.8)	5 (1.5)	0.224	0.147	4 (4.4)	3 (1.8)	0.243	0.154
Any malignancy including leukemia	0	5 (1.5)	0.596	−0.172	0	3 (1.8)	0.554	−0.191
Cerebrovascular disease	2 (1.9)	4 (1.2)	0.629	0.060	2 (2.2)	3 (1.8)	1.000	0.031
Amiodarone	20 (19.1)	50 (14.6)	0.275	0.119	19 (21.1)	24 (14.3)	0.161	0.180
Aspirin	38 (36.2)	105 (30.7)	0.292	0.117	35 (38.9)	50 (29.8)	0.137	0.193
Clopidogrel	3 (2.9)	9 (2.6)	1.000	0.014	3 (3.3)	2 (1.2)	0.346	0.145
NSAIDs	10 (9.5)	34 (9.9)	0.900	−0.014	9 (10.0)	18 (10.7)	0.858	−0.023
Statins	6 (5.7)	16 (4.7)	0.668	0.047	6 (6.7)	9 (5.4)	0.668	0.055

Abbreviations: NA, not applicable; NSAIDs, non-steroid anti-inflammatory drugs; PSM, propensity score matching; SD, standard deviation; SMD, standardized mean difference.

3. Results

3.1. Baseline Characteristics

From a total of 447 eligible patients included in the study, 105 (23.5%) were new warfarin users, and 342 individuals (76.5%) were nonusers. Table 1 shows characteristics of the unmatched and matched cohorts. Before PS matching, warfarin users had significantly higher CHA2DS2-VASc scores than did the untreated group. In addition, warfarin users were significantly more likely to have a history of comorbidities (diabetes mellitus, heart failure, myocardial infarction). After PS matching, 258 patients were included in the final analysis, with 90 patients in the treated group (mean (SD) age, 59.9 (13.5) years; 38 males (42.2%)) and 168 patients in the untreated group (mean (SD) age, 59.2 (14.6) years; 75 males (44.6%)). The mean (SD) CHA2DS2-VASc scores were 2.1 (1.6) and 1.8 (1.5) in the warfarin-treated and untreated groups, respectively. Most patient characteristics were comparable between the two groups after PS matching (SMD < 0.2), except the history of hypertension and heart failure, which were further added in the regression model.

3.2. Risks of an Ischemic Stroke and Transient Ischemic Attack

The primary study outcome is summarized in Table 2. In the matched cohort, there were 19 events (21.1%) in the warfarin-treated group and 21 events (12.5%) in the untreated group. Mean follow-up times of stroke/TIA occurrence were 6.7 years among warfarin users and 7.2 years among nonusers. In terms of stroke/TIA events, the annual cumulative incidence was 1.74% per year in hyperthyroidism-related AF among nonusers. Results from the robust Cox regression model with multiple covariates are presented in Supplementary Table S2. The risk of stroke/TIA among warfarin users did not significantly differ from that of nonusers (adjusted hazard ratio (aHR): 1.16, 95% confidence interval (CI): 0.52–2.56). Compared to the warfarin-untreated group, congestive heart failure (aHR: 4.30, 95% CI: 1.15–16.09), peripheral vascular disease (aHR: 6.01, 95% CI: 1.56–23.11) and a history of taking aspirin (aHR: 3.42, 95% CI: 1.37–8.54) were significantly associated with an increased risk of stroke/TIA.

Table 2. Number of events and adjusted hazard ratios between warfarin users and nonusers among patients with hyperthyroidism-related atrial fibrillation.

	After PSM		
	Warfarin Users N **= 90**	**Warfarin Nonusers** N **= 168**	p **Value**
Stroke/TIA			
Events (%)	19 (21.1)	21 (12.5)	0.069
Mean follow-up time (months, SD)	79.8 (43.1)	86.0 (41.1)	0.254
aHR (95% CI) [a]	1.16 (0.52–2.56)	Reference	0.717
Major bleeding			
Events (%)	39 (43.3)	64 (38.1)	0.413
Mean follow-up time (months, SD)	65.0 (45.5)	65.3 (43.7)	0.958
aHR (95% CI) [b]	0.91 (0.56–1.47)	Reference	0.702

Abbreviations: CI, confidence interval; PSM, propensity score matching; SD, standard deviation; TIA, transient ischemic attack. [a] Adjusted for age, gender, CHA2DS2-VASc, hypertension, congestive heart failure, peripheral vascular disease, diabetes mellitus, and aspirin. [b] Adjusted for age, gender, CHA2DS2-VASc, hypertension, congestive heart failure, diabetes mellitus, chronic obstructive pulmonary disease, hyperlipidemia, aspirin, and statins.

3.3. Risk of Major Bleeding

The secondary study outcome is summarized in Table 2. In the matched cohort, there were 39 events (43.3%) in the warfarin-treated group and 64 events (38.1%) in the untreated group. Mean follow-up times of major bleeding occurrence among both groups were about 5.4 years. Results of the robust Cox regression model with multiple covariates are presented in Supplemental Table S3. The risk of major bleeding among warfarin users did not significantly differ from that of nonusers (aHR: 0.91, 95% CI: 0.56–1.47). Compared to the warfarin-untreated group, hypertension (aHR: 2.11, 95% CI: 1.15–3.88) and a history of taking aspirin (aHR: 1.85, 95% CI: 1.20–2.85) were significantly associated with an increased risk of major bleeding.

3.4. Sensitivity Analyses

The results of the first sensitivity analysis revealed consistency in the findings even when we excluded DOACs and new antiplatelet medication users after the index date. After multivariate adjustment, the risk of the occurrence of stroke/TIA did not significantly differ between the warfarin users and nonusers (Supplementary Table S4, aHR, 1.18, 95% CI: 0.53–2.64). The risk of the occurrence of bleeding had no significant association in the warfarin users (aHR: 0.95, 95% CI: 0.58–1.55). To reduce selection bias, we repeated our analysis with use of warfarin versus aspirin (Supplementary Figure S1). The results are in accordance with our earlier observations. It demonstrated that warfarin use had no significant association with the risk of stroke/TIA, even comparing with aspirin use (aHR: 2.43, 95% CI: 0.68–8.70).

4. Discussion

This is the first retrospective cohort study that compares risks of ischemic stroke/TIA and major bleeding associated with warfarin users vs. nonusers among patients with hyperthyroidism-related AF. In the clinical reality, new onset disease might not require anticoagulation therapy. Our results showed that the use of warfarin was not associated with a statistically significantly lower risk of ischemic stroke/TIA nor a higher risk of major bleeding. The sensitivity analysis which excluded new DOAC users showed similar results.

In our study, 2.8% of patients referred to the hospital with AF also had hyperthyroidism. This rate is compatible with other studies in Taiwan and other countries [14,29,30], and female patients were predominant [12,15,30]. The annual stroke/TIA incidence of 1.74% per year among nonusers with a mean CHA2DS2-VASc score of 1.8 was numerically lower in Taiwanese and in a Swedish cohort which had a CHA2DS2-VASc score of 2 [13,31].

The reason could be that patients with hyperthyroidism-related AF are not at a higher risk of ischemic stroke than those with non-thyroid AF [12,30]. In most AF patients with hyperthyroidism, spontaneous reversion to sinus rhythm often occurs after restoration of thyroid function [2,29]. Antithyroid therapy were prescribed to decrease the arrhythmogenic activity under the guidance of Taiwan National Health Insurance program [9,16,30]. However, a national cohort study demonstrated the incidence of thromboembolic events may be not influenced by antithyroid therapies among patients with hyperthyroidism-related AF [30]. Another study used a Cox proportional hazard model to predict that over 60% of patients who cardioverted even after 4 to 10 years of AF will remain in sinus rhythm when so treated [29]. Consistent with our data, the duration of stroke/TIA was compatible. This result probably implies that hyperthyroidism in new onset AF patients with a CHA2DS2-VASc score of <2 would have less influence on short-term outcomes.

Most studies showed that hyperthyroidism per se did not confer an additional risk of thromboembolic events among patients with AF compared to non-hyperthyroidism patients [14,30,32]. Our study was conducted to determine the role of anticoagulation therapy in patients with hyperthyroidism-related AF through a mimic clinical controlled trial. The finding of no association between warfarin use (users vs. nonusers) and ischemic stroke/TIA is also consistent with several previous observational studies conducted with other study designs and in other populations [12,14,30,32]. An early study with age-matched controls found that the risk of cerebrovascular events in thyrotoxicosis patients with AF did not significantly increase compared to those in sinus rhythm [14]. However, the mean ages of the two groups were markedly different at 56 and 39 years, respectively. Moreover, a recent single-center observational study demonstrated that in hyperthyroidism patients with non-paroxysmal AF, warfarin therapy was associated with a reduced risk of ischemic stroke via Kaplan-Meier estimate. However, no statistical association was found in univariate analysis [12]. Nevertheless, those studies did not adjust for amiodarone use, [12,14,32], and those positive results were based on the patients with old age and a vary-high risk of thromboembolism (high CHA2DS2-VASc score) [12,15,33,34].

Conversely, our population was less severe in terms of both new onset of AF and hyperthyroidism with mean CHA2DS2-VASc scores of around 2, which is close to clinical practice, when the first diagnosis and a decision as to whether to initiate anticoagulation therapy are made. The two groups in our study had comparable ages, genders, and mean CHA2DS2-VASc scores, and other different baseline comorbidities were included in the Cox model for adjustment. In addition, a cohort study showed that DOAC use was associated with a comparable risk of thromboembolisms and a significantly lower risk of major bleeding compared to warfarin use [15]. So, we excluded DOAC use in the two groups, and thus there was no association with outcome risks and warfarin use compared to nonusers.

The results of the study have clinical implications. We demonstrated that anticoagulation therapy did not have a statistically significant benefit among patients with new-onset AF that occurred with new-onset hyperthyroidism compared to those with no anticoagulation therapy. Annual cerebral thromboembolic event rates in the untreated group were lower than those in Taiwanese and Swedish cohorts [13,31]. Therefore, oral anticoagulation might not be required in terms of cerebral thromboprophylaxis, especially in patients with a first episode and who are younger than 65 years. Our data support the gap of current guidelines [2,35], and the initiation of oral anticoagulants was based on the CHA2DS2-VASc score despite hyperthyroidism.

Our study has some limitations. First, this is not a prospective randomized study. Second, the cohort study was based on ICD codes that could be limited by coding errors. However, diagnoses of AF, hyperthyroidism, stroke, bleeding, and other comorbidities in the HWD are well validated [18,20,22–25]. Third, information on different types of AF is not available in the HWD. Forth, we had no data of antithyroid medications and the exact timing of recovery to sinus rhythms. However, a national retrospective cohort study found that different antithyroid medications did not influence the incidence of thromboembolic

events in this population [30]. This supports our study results that antithyroid medications had little impact on our outcomes. Fifth, we did not apply an active comparator design and might have experienced confounding by indications (high stroke/TIA rates). Nevertheless, there is no other appropriate active drug used in clinical practice in terms of oral anticoagulants, and most patients realistically receive no anticoagulants in Taiwan [30]. Although some selection bias might remain, we adjusted for confounding biases as far as was possible, even accounting for different baseline comorbidities between the two groups. We used PS matching and tried to adjust for baseline differences using variant multivariable Cox proportional hazard regression analyses to minimize the bias. Sixth, data for different types of AF are not available in the HWD. However, hyperthyroidism-related AF has a higher chance of paroxysmal AF, and previous studies have indicated that patients with paroxysmal AF might suffer fewer thromboembolic events when compared with patients with non-paroxysmal AF [36]. Seventh, HWD did not have laboratory data on international normalized ratios (INRs). However, up to 99.99% of Taiwan's population was enrolled under National Health Insurance Program. Patients had good access to health care, and their physicians prescribed warfarin based on the clinical presentation and INR monitoring. Therefore, we assumed that the individual differences in the INR were minimal. Finally, the actual drug consumption could not be determined from the database. Therefore, our conclusion was based on reasonable therapeutic adherence.

5. Conclusions

Among patients with hyperthyroidism-related AF, oral anticoagulation therapy was not associated with benefits in terms of ischemic cerebrovascular events or with major bleeding. The findings suggest that patients who are younger than 65 years with new-onset hyperthyroidism-related AF do not require an oral anticoagulant under a CHA2DS2-VASc score <2. The initiation of oral anticoagulants should be based on CHA2DS2-VASc scores according to current guidelines. Healthcare providers should consider periodic reassessment of the AF and thyroid statuses. Future large controlled studies of oral anticoagulants for preventing stroke in such patients are required to confirm these findings.

Supplementary Materials: The following supporting information can be downloaded at: https://www.mdpi.com/article/10.3390/biomedicines10112670/s1, Table S1: definitions and codes of comorbidities and outcomes; Table S2: results of univariable and multivariable Robust Cox proportional hazards regression analyses for the outcome of stroke/TIA; Table S3: results of univariable and multivariable Robust Cox proportional hazards regression analyses for the outcome of major bleeding; Table S4: sensitivity analysis for new medications after index date; Figure S1: study flowchart and sensitivity analysis (warfarin versus aspirin users); Table S5: results of univariable and multivariable Robust Cox proportional hazards regression analyses for the outcome of stroke/TIA among warfarin versus aspirin users.

Author Contributions: S.-D.L., S.-J.L. and L.-H.W. conceptualized the research aims, designed the study, and wrote the manuscript. S.-D.L., S.-J.L. and C.-Y.R. collected and analyzed the data. F.-T.L. and W.-C.L. provided suggestions for the research design and data interpretation from a clinical perspective. S.-J.L., F.-T.L., W.-C.L. and L.-H.W. reviewed and revised the paper. All authors have read and agreed to the published version of the manuscript.

Funding: This research was funded by the New Taipei Municipal TuCheng Hospital (built and operated by the Chang Gung Medical Foundation) (grant number CFRPVVL0011), the Ministry of Science and Technology of Taiwan (grant number MOST 110-2511-H-038-005), and Taipei Medical University Hospital (grant number 111TMUH-MOST-07).

Institutional Review Board Statement: The study was conducted in accordance with the Declaration of Helsinki and approved by the Joint Institutional Review Board of Taipei Medical University (no. N201908068; 31 August 2019). The identification numbers for all the entries in the HWD are encrypted to ensure privacy.

Informed Consent Statement: Not applicable.

Data Availability Statement: We must follow the Computer-Processed Personal Data Protection Law and related regulations in Taiwan. The datasets for this manuscript are not publicly available because of the HWD protection policy.

Acknowledgments: The author thanks Shu-Fu Lin, Division of Endocrinology and Metabolism, Department of Internal Medicine, New Taipei Municipal TuCheng Hospital, New Taipei City, Taiwan, for valuable information and comments. This work was financially supported by the New Taipei Municipal TuCheng Hospital (built and operated by the Chang Gung Medical Foundation) (grant no. CFRPVVL0011), the Ministry of Science and Technology of Taiwan (MOST 110-2511-H-038-005) and Taipei Medical University Hospital (111TMUH-MOST-07).

Conflicts of Interest: The authors declare no conflict of interest.

References

1. Virani, S.S.; Alonso, A.; Aparicio, H.J.; Benjamin, E.J.; Bittencourt, M.S.; Callaway, C.W.; Carson, A.P.; Chamberlain, A.M.; Cheng, S.; Delling, F.N.; et al. Heart Disease and Stroke Statistics—2021 Update: A Report From the American Heart Association. *Circulation* **2021**, *143*, e254–e743. [CrossRef]
2. Hindricks, G.; Potpara, T.; Dagres, N.; Arbelo, E.; Bax, J.J.; Blomström-Lundqvist, C.; Boriani, G.; Castella, M.; Dan, G.-A.; Dilaveris, P.E.; et al. 2020 ESC Guidelines for the diagnosis and management of atrial fibrillation developed in collaboration with the European Association for Cardio-Thoracic Surgery (EACTS): The Task Force for the diagnosis and management of atrial fibrillation of the European Society of Cardiology (ESC) Developed with the special contribution of the European Heart Rhythm Association (EHRA) of the ESC. *Eur. Heart J.* **2021**, *42*, 373–498. [CrossRef]
3. Klein, I.; Ojamaa, K. Thyroid Hormone and the Cardiovascular System. *N. Engl. J. Med.* **2001**, *344*, 501–509. [CrossRef]
4. Frost, L.; Vestergaard, P.; Mosekilde, L. Hyperthyroidism and Risk of Atrial Fibrillation or Flutter: A population-based study. *Arch. Intern. Med.* **2004**, *164*, 1675–1678. [CrossRef]
5. Baumgartner, C.; da Costa, B.R.; Collet, T.-H.; Feller, M.; Floriani, C.; Bauer, D.C.; Cappola, A.R.; Heckbert, S.R.; Ceresini, G.; Gussekloo, J.; et al. Thyroid Function Within the Normal Range, Subclinical Hypothyroidism, and the Risk of Atrial Fibrillation. *Circulation* **2017**, *136*, 2100–2116. [CrossRef]
6. Guo, Y.; Tian, Y.; Wang, H.; Si, Q.; Wang, Y.; Lip, G.Y. Prevalence, Incidence, and Lifetime Risk of Atrial Fibrillation in China: New insights into the global burden of atrial fibrillation. *Chest* **2015**, *147*, 109–119. [CrossRef]
7. Bielecka-Dabrowa, A.; Mikhailidis, D.P.; Rysz, J.; Banach, M. The mechanisms of atrial fibrillation in hyperthyroidism. *Thyroid. Res.* **2009**, *2*, 4. [CrossRef]
8. Wustmann, K.; Kucera, J.P.; Zanchi, A.; Burow, A.; Stuber, T.; Chappuis, B.; Diem, P.; Delacrétaz, E. Activation of Electrical Triggers of Atrial Fibrillation in Hyperthyroidism. *J. Clin. Endocrinol. Metab.* **2008**, *93*, 2104–2108. [CrossRef]
9. Chen, Y.-C.; Chen, S.-A.; Chen, Y.-J.; Chang, M.-S.; Chan, P.; Lin, C.-I. Effects of thyroid hormone on the arrhythmogenic activity of pulmonary vein cardiomyocytes. *J. Am. Coll. Cardiol.* **2002**, *39*, 366–372. [CrossRef]
10. Li, Y.-G.; Pastori, D.; Farcomeni, A.; Yang, P.-S.; Jang, E.; Joung, B.; Wang, Y.-T.; Guo, Y.-T.; Lip, G.Y. A simple clinical risk score (c2hest) for predicting incident atrial fibrillation in asian subjects: Derivation in 471,446 Chinese Subjects, with internal validation and external application in 451,199 Korean subjects. *Chest* **2018**, *155*, 510–518. [CrossRef]
11. Siu, C.-W.; Pong, V.; Zhang, X.; Chan, Y.-H.; Jim, M.-H.; Liu, S.; Yiu, K.-H.; Kung, A.W.; Lau, C.-P.; Tse, H.-F. Risk of ischemic stroke after new-onset atrial fibrillation in patients with hyperthyroidism. *Heart Rhythm* **2009**, *6*, 169–173. [CrossRef] [PubMed]
12. Chan, P.-H.; Hai, J.; Yeung, C.-Y.; Lip, G.Y.; Lam, K.S.-L.; Tse, H.F.; Siu, C.-W. Benefit of Anticoagulation Therapy in Hyperthyroidism-Related Atrial Fibrillation. *Clin. Cardiol.* **2015**, *38*, 476–482. [CrossRef] [PubMed]
13. Friberg, L.; Rosenqvist, M.; Lip, G.Y. Evaluation of risk stratification schemes for ischaemic stroke and bleeding in 182,678 patients with atrial fibrillation: The Swedish Atrial Fibrillation cohort study. *Eur. Heart J.* **2012**, *33*, 1500–1510. [CrossRef] [PubMed]
14. Petersen, P.; Hansen, J.M. Stroke in thyrotoxicosis with atrial fibrillation. *Stroke* **1988**, *19*, 15–18. [CrossRef] [PubMed]
15. Chan, Y.-H.; Wu, L.-S.; See, L.-C.; Liu, J.-R.; Chang, S.-H.; Chao, T.-F.; Yeh, Y.-H.; Kuo, C.-T.; Lee, H.-F.; Lip, G.Y.H. Direct Oral Anticoagulants in Atrial Fibrillation Patients With Concomitant Hyperthyroidism. *J. Clin. Endocrinol. Metab.* **2020**, *105*, 2893–2904. [CrossRef]
16. Gorenek, B.; Boriani, G.; Dan, G.-A.; Fauchier, L.; Fenelon, G.; Huang, H.; Kudaiberdieva, G.; Lip, G.Y.H.; Mahajan, R.; Potpara, T.; et al. European Heart Rhythm Association (EHRA) position paper on arrhythmia management and device therapies in endocrine disorders, endorsed by Asia Pacific Heart Rhythm Society (APHRS) and Latin American Heart Rhythm Society (LAHRS). *Eur.* **2018**, *20*, 895–896. [CrossRef]
17. Andrade, J.G.; Aguilar, M.; Atzema, C.; Bell, A.; Cairns, J.A.; Cheung, C.C.; Cox, J.L.; Dorian, P.; Gladstone, D.J.; Healey, J.S.; et al. The 2020 Canadian Cardiovascular Society/Canadian Heart Rhythm Society Comprehensive Guidelines for the Management of Atrial Fibrillation. *Can. J. Cardiol.* **2020**, *36*, 1847–1948. [CrossRef]
18. Chao, T.-F.; Lip, G.Y.; Liu, C.-J.; Lin, Y.-J.; Chang, S.-L.; Lo, L.-W.; Hu, Y.-F.; Tuan, T.-C.; Liao, J.-N.; Chung, F.-P.; et al. Relationship of Aging and Incident Comorbidities to Stroke Risk in Patients With Atrial Fibrillation. *J. Am. Coll. Cardiol.* **2018**, *71*, 122–132. [CrossRef]
19. Chan, W.S.H. Taiwan's healthcare report 2010. *EPMA J.* **2010**, *1*, 563–585. [CrossRef]

20. Chang, S.-H.; Chou, I.-J.; Yeh, Y.-H.; Chiou, M.-J.; Wen, M.-S.; Kuo, C.-T.; See, L.-C.; Kuo, C.-F. Association Between Use of Non–Vitamin K Oral Anticoagulants With and Without Concurrent Medications and Risk of Major Bleeding in Nonvalvular Atrial Fibrillation. *JAMA* **2017**, *318*, 1250–1259. [CrossRef]
21. Tsai, C.-T.; Liao, J.-N.; Chiang, C.-E.; Lin, Y.-J.; Chang, S.-L.; Lo, L.-W.; Hu, Y.-F.; Tuan, T.-C.; Chung, F.-P.; Chao, T.-F.; et al. Association of Ischemic Stroke, Major Bleeding, and Other Adverse Events with Warfarin Use vs Non–vitamin K Antagonist Oral Anticoagulant Use in Patients with Atrial Fibrillation With a History of Intracranial Hemorrhage. *JAMA Netw. Open* **2020**, *3*, e206424. [CrossRef] [PubMed]
22. Man, K.-M.; Chen, K.-B.; Chen, H.-Y.; Chiang, J.-H.; Su, Y.-C.; Man, S.S.; Xie, D.-D.; Wang, Y.; Zhang, Z.-Q.; Bi, L.-K.; et al. Hyperthyroidism is not a significant risk of benign prostatic hyperplasia: A nationwide population-based study. *Medicine* **2018**, *97*, e12459. [CrossRef] [PubMed]
23. Hsieh, C.-Y.; Chen, C.-H.; Li, C.-Y.; Lai, M.-L. Validating the diagnosis of acute ischemic stroke in a National Health Insurance claims database. *J. Formos. Med. Assoc.* **2015**, *114*, 254–259. [CrossRef] [PubMed]
24. Sung, S.-F.; Hsieh, C.-Y.; Lin, H.-J.; Chen, Y.-W.; Yang, Y.-H.K.; Li, C.-Y. Validation of algorithms to identify stroke risk factors in patients with acute ischemic stroke, transient ischemic attack, or intracerebral hemorrhage in an administrative claims database. *Int. J. Cardiol.* **2016**, *215*, 277–282. [CrossRef]
25. Cheng, C.-L.; Kao, Y.-H.Y.; Lin, S.-J.; Lee, C.-H.; Lai, M.L. Validation of the national health insurance research database with ischemic stroke cases in Taiwan. *Pharmacoepidemiol. Drug Saf.* **2011**, *20*, 236–242. [CrossRef]
26. Austin, P.C. Optimal caliper widths for propensity-score matching when estimating differences in means and differences in proportions in observational studies. *Pharm. Stat.* **2011**, *10*, 150–161. [CrossRef]
27. Austin, P.C. Balance diagnostics for comparing the distribution of baseline covariates between treatment groups in propensity-score matched samples. *Stat. Med.* **2009**, *28*, 3083–3107. [CrossRef]
28. Lin, D.Y.; Wei, L.J. The Robust Inference for the Cox Proportional Hazards Model. *J. Am. Stat. Assoc.* **1989**, *84*, 1074–1078. [CrossRef]
29. Nakazawa, H.; Lythall, D.; Noh, J.; Ishikawa, N.; Sugino, K.; Ito, K.; Hardman, S. Is there a place for the late cardioversion of atrial fibrillation?. A long-term follow-up study of patients with post-thyrotoxic atrial fibrillation. *Eur. Heart J.* **2000**, *21*, 327–333. [CrossRef]
30. Lin, Y.-S.; Tsai, H.-Y.; Lin, C.-Y.; Wu, V.C.-C.; Chen, T.-H.; Yang, T.-Y.; Aboyans, V.; Chen, M.-C. Risk of Thromboembolism in Non-Valvular Atrial Fibrillation With or Without Clinical Hyperthyroidism. *Glob. Heart* **2021**, *16*, 45. [CrossRef]
31. Chiang, C.-E.; Wu, T.-J.; Ueng, K.-C.; Chao, T.-F.; Chang, K.-C.; Wang, C.-C.; Lin, Y.-J.; Yin, W.-H.; Kuo, J.-Y.; Lin, W.-S.; et al. 2016 Guidelines of the Taiwan Heart Rhythm Society and the Taiwan Society of Cardiology for the management of atrial fibrillation. *J. Formos. Med. Assoc.* **2016**, *115*, 893–952. [CrossRef] [PubMed]
32. Kim, K.; Yang, P.-S.; Jang, E.; Yu, H.T.; Kim, T.-H.; Uhm, J.-S.; Kim, J.-Y.; Sung, J.-H.; Pak, H.-N.; Lee, M.-H.; et al. Increased risk of ischemic stroke and systemic embolism in hyperthyroidism-related atrial fibrillation: A nationwide cohort study. *Am. Heart J.* **2021**, *242*, 123–131. [CrossRef] [PubMed]
33. Zhang, J.; Bisson, A.; Fauchier, G.; Bodin, A.; Herbert, J.; Ducluzeau, P.H.; Lip, G.Y.H.; Fauchier, L. Yearly Incidence of Stroke and Bleeding in Atrial Fibrillation with Concomitant Hyperthyroidism: A National Discharge Database Study. *J. Clin. Med.* **2022**, *11*, 1342. [CrossRef] [PubMed]
34. Bang, O.Y.; On, Y.K.; Lee, M.-Y.; Jang, S.-W.; Han, S.; Han, S.; Won, M.-M.; Park, Y.-J.; Lee, J.-M.; Choi, H.-Y.; et al. The risk of stroke/systemic embolism and major bleeding in Asian patients with non-valvular atrial fibrillation treated with non-vitamin K oral anticoagulants compared to warfarin: Results from a real-world data analysis. *PLoS ONE* **2020**, *15*, e0242922. [CrossRef] [PubMed]
35. January, C.T.; Wann, L.S.; Calkins, H.; Chen, L.Y.; Cigarroa, J.E.; Cleveland, J.C., Jr.; Ellinor, P.T.; Ezekowitz, M.D.; Field, M.E.; Furie, K.L.; et al. 2019 AHA/ACC/HRS Focused Update of the 2014 AHA/ACC/HRS Guideline for the Management of Patients With Atrial Fibrillation: A report of the American College of Cardiology/American Heart Association task force on clinical practice guidelines and the Heart Rhythm Society. *J. Am. Coll. Cardiol.* **2019**, *74*, 104–132. [CrossRef]
36. Hohnloser, S.H.; Pajitnev, D.; Pogue, J.; Healey, J.S.; Pfeffer, M.A.; Yusuf, S.; Connolly, S.J. Incidence of Stroke in Paroxysmal Versus Sustained Atrial Fibrillation in Patients Taking Oral Anticoagulation or Combined Antiplatelet Therapy: An ACTIVE W Substudy. *J. Am. Coll. Cardiol.* **2007**, *50*, 2156–2161. [CrossRef]

MDPI
St. Alban-Anlage 66
4052 Basel
Switzerland
Tel. +41 61 683 77 34
Fax +41 61 302 89 18
www.mdpi.com

Biomedicines Editorial Office
E-mail: biomedicines@mdpi.com
www.mdpi.com/journal/biomedicines

Academic Open
Access Publishing

www.mdpi.com

ISBN 978-3-0365-7878-1